# SYNTHETIC STUDIES ON A POTENTIAL ANTITUMOUR COMPOUND

A thesis submitted in partial fulfillment
of the requirements
for the degree of
**Doctor of Philosophy in Chemistry**
at the University of Canterbury,
Christchurch, New Zealand.

**by Andrew M. Thompson**

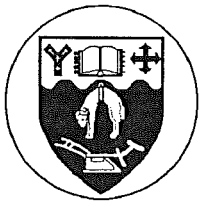

**University of Canterbury**

**1991**

In memory of my mother, Iris Nancy Thompson, who died on the 19th of May, 1990 of bowel and liver cancer. This thesis is dedicated to my family and friends and is to the glory of God.

*And if I understand all truths and mysteries and possess all knowledge but have not love (God's love in me) I am nothing.*

1 Cor. 13:2 (Amplified Version)

*For since the creation of the world God's invisible qualities - his eternal power and divine nature - have been clearly seen, being understood from what has been made, so that men are without excuse...*

Rom. 1:20 (New International Version)

# CONTENTS

# ACKNOWLEDGEMENTS

I would like to extend my sincere thanks to my supervisors, Drs. John Blunt and Murray Munro, for their guidance, help and encouragement during this project. I particularly thank Dr. John Blunt for his patience, suggestions and editing of this manuscript. I also wish to thank Dr. Nigel Perry for his background work in the isolation and characterisation of the mycalamides and subsequent collaboration and advice in early derivatisations and conformational studies of the mycalamides, pederin and pederin dibenzoate.

The financial assistance provided by the University Grants Committee and, subsequently, the University of Canterbury in the form of postgraduate scholarships is gratefully acknowledged. The collaboration and financial support of Harbor Branch Oceanographic Institute and Seapharm Incorporated in this project is acknowledged, particularly the supply of purified mycalamides for these synthetic studies, provision of equipment and early biological assays. I also acknowledge the collaboration of Dr. F. Matsuda in supplying samples of pederin and pederin dibenzoate for comparative assays and conformational studies.

I sincerely thank Bruce Clark (U.O.C.) and Dr. Lewis Pannell (National Institutes of Health, U.S.A.) for their exhaustive mass spectrometric analyses, together with Gill Barns, the Christchurch Hospital Board and the National Cancer Institute for biological assays. Thanks also to Quentin McDonald and Dr. Coxon for their assistance with molecular modelling calculations and to the other academic and technical staff of the Chemistry Department for their help. I also thank my lab-mates, particularly Dr. Michele Prinsep, Dr. Brent Copp and Dr. Peter Northcote, for their friendship and contributions to our research group. Finally I would like to thank my friends at the New Life Centre and Garden City Church for their encouragement and support throughout this research.

# ABSTRACT

Mycalamides A and B, isolated recently from a marine sponge of the genus *Mycale*, show strong *in vitro* and *in vivo* antiviral and antitumour properties. In this research, the chemistry of the mycalamides was explored and structure-activity relationships were determined, with the overall objective of producing analogues with better, or more selective biological activities. Along with this, the conformational behaviour of the mycalamides and a related compound, pederin, was examined.

Simple esters, silyl and alkyl ethers of the hydroxyl and amide functionalities were prepared during initial studies. While many of these proved to be inactive, they were still useful as protected intermediates for use in acid and base catalysed hydrolysis reactions. In the course of the acid catalysed reactions, the acetal groups were partially or completely hydrolysed, eliminated, or exchanged and cleavage fragments were isolated. The exocyclic double bond was hydrogenated, epoxidised and rearranged in further studies. Base catalysed hydrolysis, elimination and rearrangement reactions were examined extensively and many interesting and unexpected products were obtained, including epimers and further cleavage fragments. Reduction and oxidation reactions also provided a source of important and potentially useful derivatives.

In all, more than one hundred and ten derivatives of mycalamides A and B were prepared, characterised and tested for biological activity. The central portion of the structure, including the α-hydroxy amide and neighbouring groups, was shown to be crucial for the biological activity. A simple model structure was prepared containing some of these elements. The structure-activity relationships described in this work, combined with a better knowledge of the chemistry and conformational behaviour of these

compounds, should together provide renewed stimulus for the ongoing study and development of these potential antitumour compounds.

# INTRODUCTION

## 0.1 OVERVIEW

Nature, particularly terrestrial plants and animals, has long been realised to be the source of substances exhibiting various medicinal properties for the treatment of disease in mankind. However, the isolation and structure determination of the active constituents of various plants and animals has occurred only comparatively recently in our history. In particular, the treatment of diseases with specific drugs, chemotherapy, has made substantial progress only over the past fifty years[1-3], partly as a result of this expanding natural products research. Of the large number of antibiotics and other drugs available in today's society, a high proportion arise from natural sources or represent a modification of compounds from such sources[4,5]. An interesting feature of most naturally occurring biologically active compounds is that they are secondary metabolites, that is, they have no clearly recognisable function for the host organism, although there are cases where they could serve as weapons of defence[6-12].

The search for new and effective antiviral and anticancer agents has recently been extended to the consideration of marine sources, which represent a vast, new and relatively untapped resource. Prominent amongst the organisations involved in such investigations is the National Cancer Institute (NCI) in the United States of America, which has initiated large scale systematic bioactivity-directed screening programs of extracts and natural products worldwide, in an attempt to discover new compounds for the development of anti-HIV and anticancer drugs[1,13]. The success of these and other initiatives worldwide can, at least to some extent, be measured by the large numbers of novel compounds reported in marine natural products

reviews[7-13], some of which are notable as much for the uniqueness or complexity of their chemical structure as for their cytotoxicity. (Note that the terms 'antitumour' or 'antineoplastic' refer to *in vivo* biological activity and the term 'cytotoxicity' is best used to describe similar activities against cells cultured *in vitro*[13]). These include such compounds as palytoxin, a complex polyhydroxy structure containing sixty-four chiral centres, the didemnins, cyclic peptides with varying potency as anticancer and immunosuppresive agents, the bryostatins, containing a unique bryopyran ring structure, and the halichondrins, to name a few[13].

Unfortunately, the limited natural abundance of some compounds has limited their further investigation and evaluation, at least until synthetic routes can be established. Furthermore, while many compounds show some *in vitro* biological activity, few have shown significant *in vivo* antitumour or antiviral activity, and it is of course the latter which is vital if the compound is to be clinically useful[1]. Moreover, even those that show good *in vivo* activity may be relatively unselective in their action. This illustrates an important aspect, that to be an effective drug the compound must display selective toxicity against the tumour or virus, yet leave the normal cells of the host organism unaffected[2]. In particular, few antiviral agents have been developed because of the similarity between cells infected by a virus and normal cells[3,13,14].

Most success in the anticancer field has been confined to inhibiting the cell growth or cell division of tumours with rapidly dividing cells and to the treatments of various leukemias[2]. This may reflect the extensive early use of primary screening assays based on the mouse leukemia models, L1210 and P388, and similar models, which represent rapidly dividing cell lines. These systems have some advantages, as they are fast and convenient in the *in vitro* stage, and results for the P388 assay can be readily compared with *in vivo* results, while the P388 test has been found to be predictive of over 95% of all

the known, clinically effective antitumour drugs[13]. However, less progress has been made against solid tumours containing slowly dividing cells, which develop in the lungs, colon, breast and brain[1,2]. A recently developed screening protocol by the NCI, involving a large panel of various human tumour cell lines cultured *in vitro*, places more emphasis on solid tumour growth inhibition, so that progress in this area is expected in the future[2,13]. Compounds displaying selective *in vivo* activity against any one tumour may be advanced for human clinical trials, where both maximum and optimum dosages are determined. Didemnin B was the first marine natural product to be tested in such trials[13], but, in reality, few compounds ever reach this stage.

Evidence from the pharmaceutical industry has shown that the most effective drug may not be the isolated compound, but some analogue of it[4]. This highlights the importance of performing chemical modifications on such compounds to obtain the therapeutically most useful derivatives, which may, for example, be more potent, more selective, less toxic, or give less side effects. In this process structure-activity relationships[1,15] may be elucidated, which can provide some insight into the essential structural and conformational requirements[16] for the biological activity of the natural compound. This can ultimately lead to the design of more simple analogues[4] and an understanding of the active site geometry.

## 0.2 STUDIES AT THE UNIVERSITY OF CANTERBURY AND BACKGROUND TO THE ISOLATION OF THE MYCALAMIDES

### 0.2.1 GENERAL APPROACHES AND EARLY RESULTS OF THE MARINE CHEMISTRY GROUP

Since its founding in 1975, the Marine Chemistry Group at the University of Canterbury has been involved in the search for new, biologically

active molecules. From 1982, in conjunction with the NCI and various pharmaceutical companies, this group has been involved in the collection of organisms from a variety of locations around New Zealand and other places, ranging from Western Samoa to Antarctica[6,17]. These organisms were identified, and small extracts tested for antifungal, antibacterial and antiviral activity and for cytotoxicity (P388 antileukemic assay). An additional useful outcome of these collections was the generation of information on the incidence and disposition of biological activity within the marine phyla. A marine natural products literature database was also set up to allow fast and convenient access to information on various organisms and compounds.

The most interesting and suitable candidates from this screening programme were extracted in larger quantity, leading to the isolation and structure determination of their active constituents. More recently, a second, chemical prescreening method has been implemented prior to this step, to reduce the chance of re-isolating known compounds. One early lead led to a series of antiviral compounds from an ascidian, *Ritterella sigillinoides*, that were the same or similar to the eudistomins and also proved to have effective antitumour activity[6]. A series of cytotoxic sponge pigments, named the discorhabdins A (**0.1**) to E, were isolated from various species of *Latrunculia*, and one of these had significant antitumour activity[6,17]. Other recently isolated compounds included some new β-carboline (**0.2**) derivatives and a cytotoxic trithiane[17] (**0.3**).

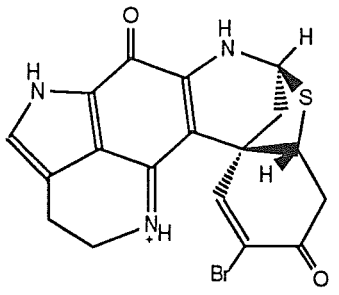


Discorhabdin A (**0.1**)

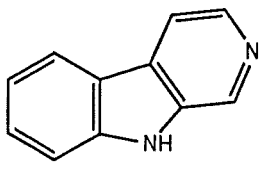


β-Carboline (**0.2**)

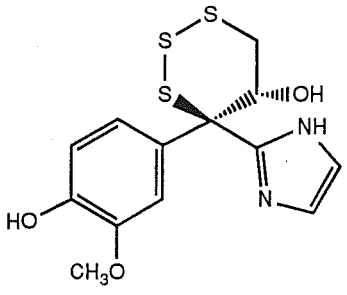


Trithiane A (**0.3**)

One of the most significant discoveries, however, arose from the investigation of a sponge of the genus *Mycale*, which led to the isolation and structural determination of two new compounds, mycalamides A[18] (**0.4**) and B[19] (**0.5**). These compounds were found to have potent antiviral and antitumour activity and a collaborative effort was set up, involving this group and two pharmaceutical agencies in the United States, Harbor Branch Oceanographic Institution (Incorporated) and SeaPharm Incorporated, to develop the potential of these compounds. An investigation of these novel compounds and their derivatives forms the major basis for the work described in this thesis and outlined in following sections. Before considering these compounds further, the biological assay systems employed in this work will be discussed, along with a review of compounds isolated from *Mycale* sponges worldwide.

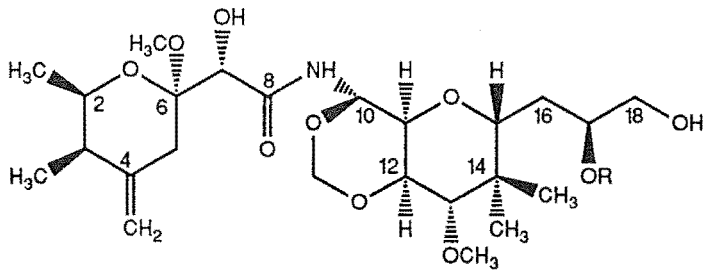


R=H: Mycalamide A (**0.4**)
R=$CH_3$: Mycalamide B (**0.5**)

## 0.2.2 BIOLOGICAL ASSAY SYSTEMS

Three *in vitro* biological assay systems have been employed in the initial screening of extracts from marine organisms, as well as for testing routine samples. These include antifungal/antibacterial, antileukemic and antiviral assays, and enzyme inhibition assays have also recently become available, although these will not be discussed here.

### 0.2.2.1 ANTIFUNGAL/ANTIBACTERIAL ASSAYS

Three bacteria were available for testing in this assay, *Bacillus subtilis, Pseudomonas aeruginosa* and *Escherichia coli*, along with three fungi, *Candida albicans*, *Trichophyton mentagrophytes* and *Cladosporium resinae.* The antibacterial or antifungal activity of compounds is tested by placing a paper disc (6 mm diameter), impregnated with the test solution, onto the surface of an agar plate which has been incubated with the microorganism in question. Solvent and antibiotic controls are prepared in a similar manner and the set of dishes incubated at 37°C for at least 24 hours. Antibacterial or antifungal activity is determined by measuring the size (in mm) of any inhibition zone from the edge of the central sample disc.

### 0.2.2.2 P388 ANTILEUKEMIC ASSAY

The *in vitro* P388 mouse leukemia assay system is used as an indication of potential antitumour activity, as discussed above. The sample solution, and up to eight successive two-fold sample dilutions, are added to wells containing the leukemia cells and these, along with media, solvent, cell and positive controls, are incubated at 35°C for three days. The number of healthy leukemia cells present in each well is determined by the addition of a yellow dye, MTT tetrazolium (3-(4,5-dimethylthiazol-2-yl)-2,5-diphenyltetrazolium bromide), which is reduced to a purple MTT formazan derivative by such cells. The amount of MTT formazan is then determined spectrophotometrically, by recording the absorbance at 540 nm, and this absorbance is then expressed as a percentage of the absorbance of the cell control. By plotting these percentages against the logarithm of the sample concentration, the concentration at which the number of healthy cells is reduced by 50% over the control (the $IC_{50}$) may be interpolated. For crude

extracts, an $IC_{50}$ of less than 30 µg/ml is considered to represent an active sample and thus to be of potential interest[13].

0.2.2.3 ANTIVIRAL/CYTOTOXICITY ASSAY

The antiviral/cytotoxicity assay system was employed on a BSC monkey kidney cell line, using two viruses, *Herpes simplex virus* Type I (a DNA virus) and *Poliovirus* Type I (an RNA virus). Assay wells (13 mm diameter) were prepared, containing a cellular monolayer infected with virus and overlaid with methyl cellulose, and sample-impregnated paper discs (6 mm diameter) were introduced to lie directly upon the virus-infected cells. Following incubation at 35°C for 24 hours, the sizes of the viral inhibition and/or cytotoxic zones (measured from the central disc) were determined by microscopic examination.

The antiviral assay result was presented on a scale, ranging from no discernible antiviral effect (-) to an effect over the whole well (WW), with intermediate zone sizes being classified as + (1-2 mm), ++ (2-4 mm) and +++ (4-6 mm). The cytotoxic effect of the sample on the BSC cells was also recorded on the same scale. This effect was further described according to the appearance of the affected cells, which would generally fall into one of twelve categories (C1-C12). All the compounds discussed in later chapters of this thesis displayed a single light cytotoxicity, type C7*, in which there were indistinct individual cells throughout the antiviral zone, with a misty appearance. The antiviral/cytotoxicity results will be reported in the form x (HSV result), y (PV result), z (cytotoxicity result), m (mass of the sample loaded onto the disc, in nanograms).

## 0.2.3 COMPOUNDS ISOLATED FROM *MYCALE* SPONGES

Marine sponges of the genus *Mycale* have been the source of several diverse structures (selected structures from each class of compounds have been depicted below). Extracts of the sponge *Mycale rotalis*, from the Mediterranean Sea, yielded two diterpenoid compounds[20], which were given the trivial names, rotalin A (**0.6**) and rotalin B. A Japanese *Mycale* sponge yielded two nucleosides[21], mycalisines A (**0.7**) and B, which inhibited the cell division of fertilised starfish eggs (an *in vitro* assay determining antitumour potential[13]), although it was asserted that these compounds were likely to be produced by symbiotic microorganisms. Three trisoxazole macrolides, mycalolides A (**0.8**), B and C, which were isolated from another Japanese *Mycale* sponge[22], were cytotoxic and antifungal, although possibly also of microbial origin. An Australian sponge, *Mycale ancorina*, was the source of a norsesterterpene cyclic peroxide (**0.9**), displaying antimicrobial activity[23]. Further investigations of this sponge also gave two more isomers of this compound[24]. Finally, various steroid glycosides (structures not given) were found from a Russian sponge, *Mycale purpurea*[25].

As an appendix to this review, it should be noted that amongst the most recent work in our group was the further study of *Mycale* sponges, this time in the Fiordland area, which yielded another new biologically active compound and no mycalamides. This compound, a macrolide containing thiazole and amine functionalities and named pateamine (**0.10**), was also very cytotoxic and had other very promising biological activities[26]. The local regional variation in the active constituents of *Mycale* sponges of the same species is not yet understood and will be the subject of further investigations in the future.

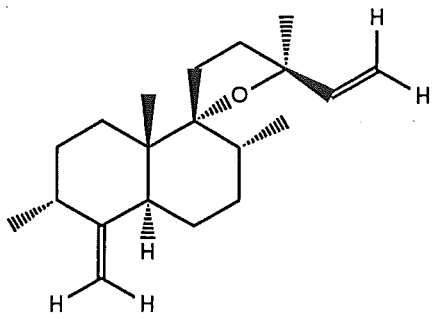

Rotalin A (**0.6**)

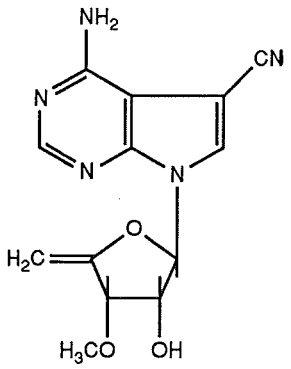

Mycalisine A (**0.7**)

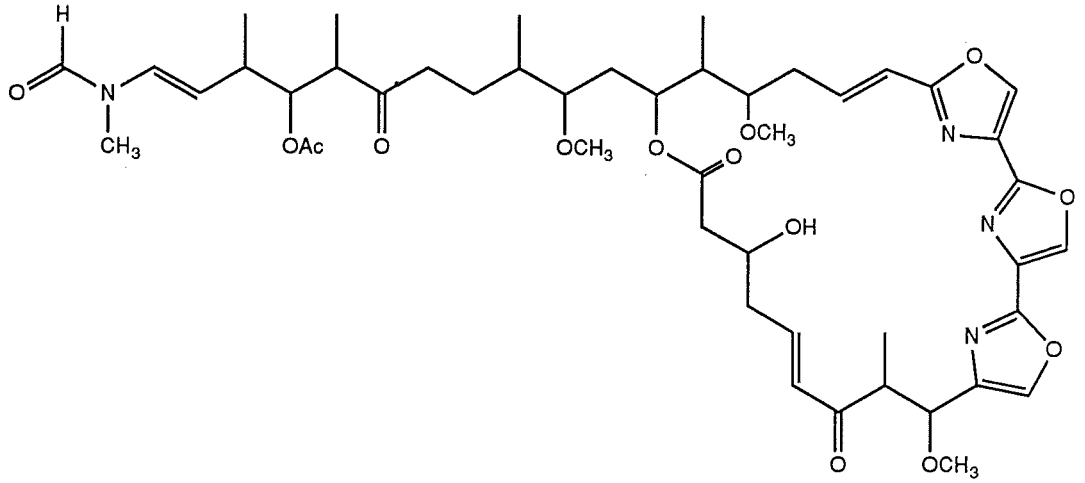

Mycalolide A (**0.8**)

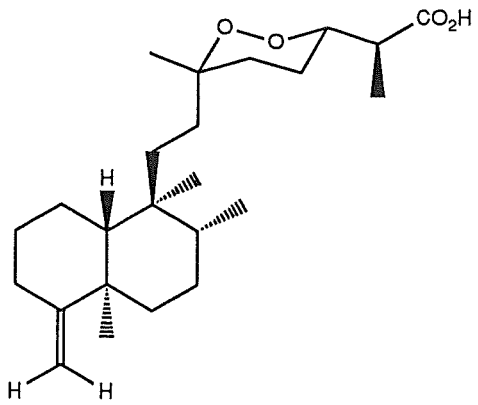

Cyclic peroxide (**0.9**)

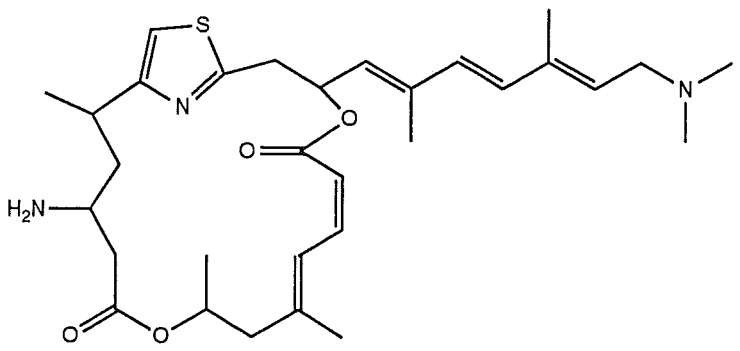

Pateamine (**0.10**)

## 0.3 THE ANTIVIRAL AND ANTITUMOUR AGENTS, MYCALAMIDES A AND B, PEDERIN AND ONNAMIDE A

### 0.3.1 ISOLATION OF MYCALAMIDES A AND B

The routine screening of extracts of marine organisms determined that an extract of a marine sponge of the genus *Mycale*, collected from the Otago Harbour, had significant *in vitro* antiviral activity. Subsequent bioactivity-directed chromatography on a larger extract (reproduced from reference 18 in the Experimental section) led to the isolation of mycalamide A (**0.4**), a new compound with strong antiviral and antileukemic activity[18]. In our assay system, mycalamide A gave a whole-well antiviral zone at 5 ng/disk for both test viruses, with only very light cytotoxicity, and had a P388 $IC_{50}$ of 0.5 ng/ml (Table 0.1). By comparison, mycalamide A showed no antibacterial activity against the three bacteria listed above at 30 μg/disk, and only weak growth reductions in the fungi *Candida albicans* and *Trichophyton mentagrophytes* for the same sample loading.

The structure of mycalamide A was solved primarily using results from one- and two-dimensional NMR spectroscopy experiments, supported by infrared and high resolution mass spectroscopic analyses. It was also facilitated by a Chemical Abstracts on-line substructure search, which retrieved references to a remarkably similar structure, pederin (**0.11**), and its derivatives[27,28]. Pederin was isolated from a terrestrial blister beetle[29,30] (see below) and was initially the only known compound with comparable structure to mycalamide A. However, within weeks of the characterisation of mycalamide A, the isolation and structure of onnamide A (**0.12**), a closely related structure from a Japanese sponge of the genus *Theonella*, was independently established[31].

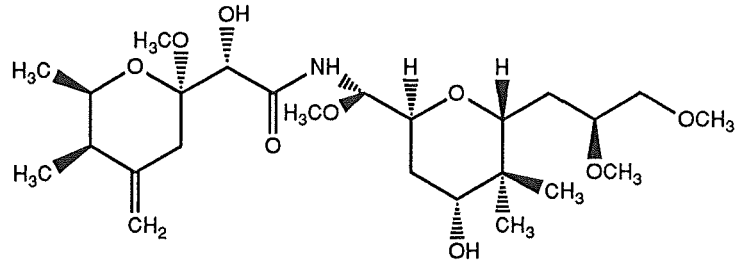

Pederin (**0.11**)

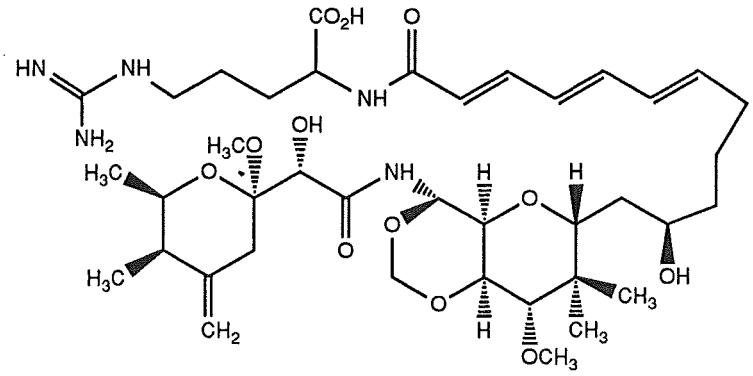

Onnamide A (**0.12**)

Further extractions of *Mycale* sponge, in order to obtain a larger quantity of mycalamide A for extensive biological testing, led to the isolation and structure determination of mycalamide B (**0.5**), the 17-*O*-methyl derivative of mycalamide A[19]. Mycalamide B was a less abundant compound than mycalamide A (3-4 times less abundant), but displayed stronger biological activities, giving a whole-well antiviral response at between 1 and 2 ng/disk and having a P388 $IC_{50}$ of about 0.1 ng/ml in our assays (Table 0.1). Recently a sample of pederin (**0.11**) was also obtained and assayed for comparative purposes. This was found to give a whole-well antiviral response at between 0.5 and 1 ng/ml and a P388 $IC_{50}$ of 0.07 ng/ml (Table 0.1), so that it was possibly slightly more active than mycalamide B (**0.5**). In view of the similar structures and *in vitro* biological activities of mycalamides A and B and pederin, it is useful to review the extensive amount of literature describing the known biological properties of pederin.

## 0.3.2 THE BIOLOGICAL ACTIVITY OF PEDERIN

Pederin (**0.11**) was the active constituent of an East African beetle, *Paederus fuscipes* (known as the Nairobi eye fly), which secretes a vesicating fluid causing eye closure and red weals followed by severe blisters on the skin of human sufferers[32]. Although first isolated in 1952[29,33], the structure of pederin was not solved conclusively until 1968[34]. To albino mice, pederin was reported to cause permanent hair loss, swelling to the head, and dermititis to the back[33]. However, by 1962 the first therapeutic uses of pederin had been reported[35], including its use in the treatment of human bed sores, ulcers and gangrene, as well as its use against parasites. Several recent reports have been published[36-38] which record the success of these dermatological applications, with 35% complete cures and 46% partial improvements reported in the treatment of human ulcers to the skin[38].

Pederin was found to be remarkably toxic to animals and plants. The $LD_{50}$ (lethal dose for 50% of animals) for mice, rats and guinea pigs was about 2 μg per 100 g of body weight[32,39]. On *in vitro* cultures of HeLa (mouse tumoural) cells, concentrations around 1 ng/ml caused marked inhibition of cellular growth and severe cytological alterations[40]. Minimum inhibitory concentrations (MIC) of 1.5 ng/ml were later reported for a wider range of different strains and cell lines[39]. Also, levels of 0.5 μg/ml of pederin inhibited the germination of seeds of *Lupinus albus* and blocked cell division in root-tip meristems of *Allium cepa*[35,39]. The growth of tumours, induced by chemical agents in *Lupinus albus* and in Sarcoma 180 (mice), was also slowed or prevented[40,41]. However, pederin had no antibacterial power[41].

This striking toxicity of pederin prompted numerous studies into its mechanism of action. An analysis of DNA, RNA and protein synthesis in cellular systems, using radioactive precursors, established that pederin caused an almost immediate block in protein and DNA synthesis, without such

an effect on RNA synthesis[39]. In cell-free systems, the compound inhibited protein synthesis only, so that this was its major mechanism of action and the effect on DNA synthesis was secondary[39]. More detailed studies[42-45] strongly suggested that pederin inhibits the translocation of the peptidyl-tRNA from the amino-acyl (A) site to the peptidyl (P) site on the ribosome[46-49]. It was proposed that pederin binds to a ribosomal site[42,47], causing inhibition of protein synthesis by steric hindrance, or by the inactivation of a specific protein involved in the translocation, or the inactivation of some other ribosomal function[50]. Further studies[44,51] showed that pederin did not affect peptide bond formation or the binding of the aminoacyl-tRNA to the ribosome.

The site of action of pederin and other protein synthesis inhibitors has been further investigated[52]. There is evidence that inhibitors such as cryptopleurine, emetine (**0.13**) and tubulosine may have a common or overlapping binding site, differing from the action and binding sites of pederin and cycloheximide (**0.14**) (a glutarimide antibiotic), which are believed to be more similar but non-identical[47,52,53].

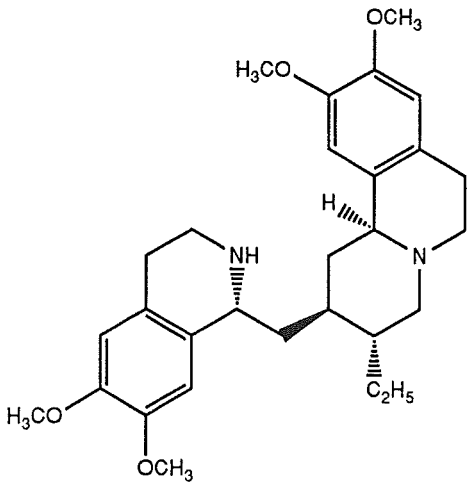


Emetine (**0.13**)

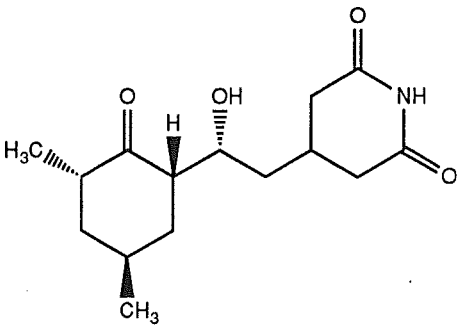


Cycloheximide (**0.14**)

Pederin has been reported to induce cell fusion in human skin fibroplasts[54], but this did not occur in ascidian eggs[55]. The cytological action

of pederin has also been studied[41,56]. Thus a great deal of information on the biological properties and action of pederin has been amassed.

### 0.3.3 THE BIOLOGICAL ACTIVITIES OF MYCALAMIDES A AND B AND ONNAMIDE A

#### 0.3.3.1 ANTITUMOUR PROPERTIES

The antiproliferative effects of mycalamides A and B (**0.4**, **0.5**), pederin (**0.11**) and onnamide A (**0.12**) against four *in vitro* cell lines[57] have been compared in Table 0.1. Note that P388 and HL-60 are mouse and human leukemia cell lines, respectively, HT-29 is a human colon carcinoma cell line and A549 is a human lung carcinoma cell line. The results show that mycalamide B is the most potent inhibitor, although the mycalamide A results were also in the nanomolar range. Onnamide A (**0.12**) showed strong P388 activity, but reduced activity in the other assays. A sample of pederin was about twice as active as mycalamide B in the same assay[58].

These compounds were also tested for *in vivo* P388 antileukemic activity[57], using tumour-infected mice. Mycalamides A and B showed moderate activity, giving 40% and 50% increases in lifespan after applying a schedule of daily injection for nine days at doses of 10 μg/kg and 2.5 μg/kg, respectively. Onnamide A was inactive in the *in vivo* P388 assay. Since mycalamide A displayed significant *in vivo* activity against P388 leukemia, it was also tested against other *in vivo* tumour models[57]. Good responses were observed against the models B16 melanoma and M5076 ovarian carcinoma (Table 0.2), but less activity was shown against colon 26 carcinoma, although this activity was still considered to be significant. Mycalamide A was also particularly active against solid tumour cultures. The growth of Lewis lung, M5076 and Burkitt's lymphoma tumours were markedly inhibited by administration of mycalamide A and moderate activity was observed against

MX-1 and CX-1 human tumour xenografts. Thus mycalamide A was active against nine of the eleven tumour models tested. Mycalamide B was active against six of eight tumour models, with similar levels of response to mycalamide A, but onnamide A was active in only three of seven such assays.

In view of this impressive *in vitro* and *in vivo* antitumour activity, further work was performed to establish the mechanism of action of these compounds[57]. It was found that these compounds were potent inhibitors of protein synthesis, with DNA synthesis but not RNA synthesis also being affected in cellular systems, just as was found for pederin. (It was noted that mycalamide A did not intercalate into DNA or disrupt deoxynucleoside synthesis). Thus inhibition of protein synthesis was a probable cytotoxic mechanism for this class of compounds.

0.3.3.2 ANTIVIRAL ACTIVITY

Further testing of the *in vitro* antiviral properties of mycalamides A and B[6] showed that mycalamide B was more active than mycalamide A against *Vesicular stomatitis virus* (VSV) and against *Coronovirus* A59, a mouse hepatitis (RNA) virus (Table 0.2). Mycalamide A was quite active against human *Cytomegalovirus*[14] (CMV), without any associated cytotoxicity[59]. However mycalamides A and B displayed no anti-HIV (anti-AIDS) activity[58].

A partially purified extract of mycalamide A (~2%) was also found to have significant *in vivo* activity against *Coronovirus* A59[6,18]. All infected mice which had been administered 0.1 mg/kg of this sample daily for nine days remained alive after fourteen days, whereas the control group had died after eight days. However, it was noted that the toxicity level of this sample was not ideal and no result was obtained with pure mycalamide A.

Mycalamides A and B were also able to cause *Harvey sarcoma virus*-transformed[60] NRK (mouse) cells to change their morphology from the

transformed shape to the normal one[61] (at concentrations of 10 and 1 ng/ml, respectively). Cycloheximide (**0.14**) and its acetyl derivative also showed this type of activity[62] and all four compounds were found to inhibit the biosynthesis of a p21 protein preferentially[61,62]. The concentrations required for morphological change were similar or higher than those required for inhibition of protein synthesis so that this was probably the mechanism of action. However some other protein synthesis inhibitors did not display this activity[61,62].

0.3.3.3 OTHER BIOLOGICAL ACTIVITIES

Mycalamides A and B were both found to be strongly immunosuppressive. (There is current interest in new immunosuppressants such as FK506[63-66] for use use in preventing graft rejection, following bone marrow and organ transplants). This immunosuppressive property was observed in skin grafting experiments on mice[58], where mycalamide A appeared to be more useful than mycalamide B in that it gave good acceptance of grafts with less toxicity. In one animal treated with mycalamide A, complete graft tolerance was achieved, resulting in hair growth from the grafted skin. However, there was significant reduction in bone marrow cell numbers and there were some additional complications. Mycalamide A did not have activity in topical skin models such as wound healing or burns[58].

Mycalamide A was also active *in vitro* against a strain of malarial parasite *Plasmodium falciparum* with an $IC_{50}$ of 0.9 ng/ml, but apparently did not have any *in vivo* activity[58]. Other protein synthesis inhibitors, including emetine (**0.13**), cycloheximide (**0.14**), anisomycin and pederin also show some activity against various parasites[35,53,58,67].

Thus the biological activities of mycalamides A and B, along with pederin and onnamide A, are evidently related to their inhibition of protein

synthesis. The antiviral and antitumour properties of protein synthesis inhibitors have been known for some time. In particular, Grollman[53] stated that all inhibitors of protein synthesis in eukaryotes possessed some degree of *in vivo* antitumour activity, but that the chemotherapeutic usefulness of these compounds was always limited by their cytotoxic action. Emetine (**0.13**), for example, which has been successfully used for over three hundred years in the treatment of amoebiasis, has a cardiotoxic action[53], as has diptheria toxin. Protein synthesis inhibitors were also noted to manifest antiviral activity in cell cultures, and in some cases *in vivo*, by inhibiting the formation of enzymes used by the virus, or by inhibiting the synthesis of proteins required for the synthesis of viral RNA[53]. However, protein synthesis in the host cell is also usually affected, which is certainly not ideal for an antiviral agent[2,13]. Thus protein synthesis inhibitors in general have not been useful as antiviral agents, although several are either in use, or remain of interest as antitumour agents. Therefore, although mycalamides A and B were originally isolated as antiviral agents[18], they have also been patented as potential antitumour agents[68,69], which probably reflects the more likely property considered for their ongoing development and possible therapeutic usefulness.

## 0.4 SYNTHETIC STUDIES ON MYCALAMIDES A AND B

### 0.4.1 OVERALL OBJECTIVES AND PROPOSALS

The work in this thesis will describe primarily the synthetic modifications of mycalamides A and B, including an exploration of the chemistry of these compounds and the preparation and characterisation of a range of derivatives to be tested for their biological activity. There were several specific aims to be considered in this work. Firstly, the ultimate aim was to produce analogues with better antitumour properties, that is, compounds which could be

therapeutically more useful, whether for their improved potency, reduced toxicity, or reduced side effects[2,4]. Secondly, it was hoped to discover the structural requirements for antitumour activity by determining overall structure-activity relationships[1,15]. Another, third, important consideration was to determine the conformational features of the active compounds[16,70,71]. A fourth objective was to obtain a crystalline heavy atom mycalamide derivative for x-ray structural analysis, since this would enable a confirmation of the absolute stereochemistry and a comparison of the solid state and solution conformations[70,72]. The potential to incorporate isotopic labels, such as deuterium, was also a consideration for possible future pharmacokinetic studies[73]. Finally, the data obtained from these investigations would be used in the synthesis of some simple model compounds, which would incorporate some essential structural features of the mycalamides.

There are numerous examples in the literature[74,75] of the derivatisation of biologically active molecules to elucidate structure-activity relationships, and these will not be discussed here. However, in considering the structure of the mycalamides, it is apparent that these are quite complex compounds, containing several functional groups. Thus it was proposed that initial reactions should concentrate on the preparation of simple ethers and esters for the protection of the hydroxyl groups[76-78] of mycalamides A and B. The size, polarity, stability and position of these substituents were factors which could be varied in initial studies[75,76]. These protected intermediates would then become the substrates for acid and base catalysed substitution, elimination, rearrangement and hydrolysis reactions, as required. The potential cleavage of the molecule into various fragments[79], which could be tested for their biological activities was a further aim of this work. Reduction and oxidation reactions would also be considered in this investigation and,

where possible, the results compared with those from similar studies on pederin.

### 0.4.2 MATERIALS AND METHODS

A limited supply of purified mycalamides A and B (~250 mg mycalamide A, 120 mg mycalamide B) was available from a large scale commercial extraction of *Mycale* sponge (mycalamide A was present at about 5 mg/kg of sponge). This supply was both very valuable and very toxic (adverse skin reactions, including acute dermatitis - rashes to the skin which led to extensive blistering and swelling to the eyes, were encountered several times during this work with the mycalamides). Therefore most reactions were performed on the milligram scale, typically 0.5-5 mg, using small scale equipment. High-yielding and accurate chromatographic separation techniques were also employed, including analytical and preparative silica gel thin layer chromatography (TLC) and reverse phase high performance liquid chromatography (HPLC).

A strong emphasis was placed on the use of one- and two-dimensional nuclear magnetic resonance (NMR) spectroscopy experiments for the structure determination and characterisation of derivatives, supported by high resolution mass spectroscopy measurements wherever possible. In particular, homonuclear correlation spectroscopy (COSY) experiments[80,81] were routinely performed to unambiguously assign the coupled resonances in the $^1$H NMR spectra, together with nuclear Overhauser enhancement (NOE) experiments[82] to determine the stereochemistry and solution conformations of derivatives in various solvents[19,72,83,84]. (Some molecular modelling techniques were also investigated as methods to probe the conformational behaviour of various mycalamide derivatives and related compounds). A $^1$H-detected heteronuclear multiple quantum coherence (HMQC) experiment[85], a

$^{1}$H-detected heteronuclear multiple bond connectivity (HMBC) experiment[86,87], and a reverse detection probe, were recent additions to the software and hardware of the Varian XL-300 NMR spectrometer available in this department and these proved invaluable for the correlation of $^{1}$H and $^{13}$C resonances for several mycalamide derivatives. The main advantage of these experiments over the analogous $^{13}$C-detected HETCOR[88] and XCORFE[87,89] (long range HETCOR) experiments was the large increase in sensitivity, enabling successful results for only 1-3 mg of sample. In some cases these experiments even enabled the accumulation of $^{13}$C NMR spectral data where the sample was too small to record a $^{13}$C NMR spectrum directly.

In all, more than 110 derivatives of mycalamides A or B were synthesised during the course of this research and each was characterised and tested for its biological activity, enabling some useful structure-activity relationships to be elucidated. Part of the structure of mycalamides A and B which seemed to be essential for the biological activity was then targeted for synthesis, based on procedures developed for the synthesis of pederin[90]. This led to the synthesis of some simple model compounds. Unfortunately no x-ray crystal structure determination of a mycalamide derivative was achieved during the course of this work. However, the recently reported total synthesis of mycalamides A and B[91] has enabled the relative and absolute stereochemistries of these structures to be verified. Hopefully this achievement and the work described here will stimulate a more complete assessment of the potential of these compounds and their derivatives as antitumour agents.

**Table 0.1** Biological activities[a] of mycalamides A and B, onnamide A and pederin against various *in vitro* cell lines.

| | | $IC_{50}$ (ng/ml) | | | |
|---|---|---|---|---|---|
| Compound | P388 (UOC) | P388 | HL-60 | HT-29 | A549 |
| Mycalamide A | 0.5 | 2.6 | 1.5 | 1.4 | 1.8 |
| Mycalamide B | 0.1 | 0.7 | 0.8 | 0.8 | 0.3 |
| Onnamide A | | 1.9 | 20 | 140 | 140 |
| Pederin | 0.07 | 0.3 | | | |

[a]Results from reference 47, except UOC values (results from our assays).

**Table 0.2** Antitumour activities of mycalamide A (*in vivo*)[a].

| Tumour type | Site | Dose schedule | Best response | Dose (µg/kg) |
|---|---|---|---|---|
| P388 leukemia | i.p.[b] | daily (9 doses)[c] | 56% ILS[d] | 10 |
| B16 melanoma | i.p. | every 4 days (9 doses) | 145% ILS (40%[d]) | 30 |
| M5076 reticulum cell | i.p. | every 4 days (3 doses) | 133% ILS (40%) | 60 |
| Colon 26 carcinoma | i.p. | every 4 days (3 doses) | 49% ILS (20%) | 60 |
| B16 melanoma | s.c.[b] | every 4 days (9 doses) | 0.77 T/C TWI[d] | 3.8 |
| B16 melanoma | s.c. | every 4 days (9 doses) | 43% ILS | 7.5 |
| Lewis lung | s.c. | daily (9 doses) | 0.15 T/C TWI | 20 |
| M5076 reticulum cell | s.c. | every 4 days (3 doses) | 0.15 T/C TWI | 120 |
| MX-1 mammary xeno. | s.c. | every 4 days (3 doses) | 0.21 T/C TWI | 80 |
| CX-1 colon xenograft | s.c. | every 4 days (3 doses) | 0.29 T/C TWI | 60 |
| LX-1 lung xenograft | s.c. | every 4 days (3 doses) | 0.76 T/C TWI | 7.5 |
| Burkitt's lymphoma | s.c. | every 4 days (3 doses) | 0.19 T/C TWI | 20 |

[a]Results from reference 57. [b]Site of tumour, i.p.=intraperitoneal , s.c=subcutaneous, injected one day prior to treatment, except the last four tumours, inoculated 2-3 days prior to treatment [c]Site of injection of mycalamide A was i.p. except M5076 s.c. tumour when it was i.v. [d]ILS=increase in life span compared to control experiment. Values in brackets refer to % cures T/C TWI=tumour weight index, based on a ratio of tumour volumes of test versus control samples.

**Table 0.3** Antiviral activities[a] of mycalamides A and B and pederin (*in vitro*) and their cytotoxicities.

| Compound | mass (ng) | PV1 (UOC) | HSV (UOC) | A59 | HSV | VSV | CMV |
|---|---|---|---|---|---|---|---|
| Mycalamide A | 10 | | | ++, + | | | |
| | 5 | WW, + | WW, + | | | | |
| | 2 | +, + | +, + | | ++, - | +, + | |
| | 0.5 | | | | | | +++, - |
| Mycalamide B | 2 | WW, + | WW, + | ++, - | ++, - | ++, + | |
| | 1 | +++, + | +++, + | | | | |
| Pederin | 1 | WW, + | WW, + | | | | |
| | 0.5 | +++, + | | | | | |

[a]Results listed in the order antiviral result, cytotoxicity, where -,+,++,+++,WW=antiviral zone size or cytotoxic effect (see text) for a given sample mass loaded onto an assay disk. Note that UOC refers to a result in our assays, the remaining results were from references 6, 58 and 59. For a description of the viruses, see text.

# CHAPTER 1
# STRUCTURES AND SOLUTION CONFORMATIONS OF MYCALAMIDES A AND B, PEDERIN AND PEDERIN DIBENZOATE

## 1.1 INTRODUCTION

The structural similarities between mycalamides A and B, onnamide A and pederin were noted in the Introduction. These compounds are all strong inhibitors of protein synthesis[47,57], a property which is thought to be the basis of the biological activities of these compounds. Therefore it is likely that some common substructure in these compounds is involved in interactions with the same active site[15]. These structures consist of various flexible chains and six-membered rings which would appear to permit many different conformations. However, it is likely that only one conformer is involved in specific receptor binding to generate the biological response[70,71]. This is important because conformationally restricted analogues of biologically active compounds can show higher levels of activity or selectivity than the original compound[70,92]. The main aim of this study was to establish the major solution conformations of mycalamides A and B and pederin, using a combination of NMR spectroscopic techniques with molecular mechanics calculations, to determine whether there were similarities in overall shape. The solid state conformation of pederin di-p-bromobenzoate (**1.1**), as found by x-ray crystallography[93], has also been compared with the major solution conformations of pederin dibenzoate (**1.2**) to illustrate the influence of intermolecular forces.

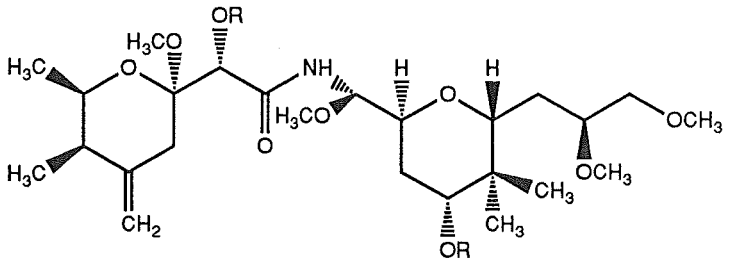


R=$COC_6H_4Br$: Pederin di-p-bromobenzoate (**1.1**)
R=$COC_6H_5$: Pederin dibenzoate (**1.2**)

The isolation and structure determination of mycalamides A and B[18,19] were not part of this research. However, the assignment of the $^1H$ and $^{13}C$ NMR spectra of both compounds in various solvents, using two-dimensional correlation and NOE experiments, forms an important part of the conformational analysis described here and is therefore considered in detail. This also serves as a useful background to the use of molecular modelling and various NMR spectroscopic techniques, and in particular to the results obtained for mycalamides A and B, which form some basis for work performed on various derivatives, as described in subsequent chapters. Infrared (IR) and mass spectroscopic (MS) results for mycalamides A and B are also analysed in this chapter.

The structure of pederin[27,94,95] was initially based simply on the analysis of signals in the $^1H$ NMR spectrum, coupled with chemical evidence, and on the results from various other analyses, such as infrared and mass spectroscopies and elemental analysis. The structure was later completely solved by an x-ray crystallographic study[34]. However, there had not been a complete assignment of the $^1H$ NMR spectral data, nor had any assignment of the $^{13}C$ NMR spectral data been reported. These assignments are described here as the first step in analysing the solution conformations of pederin and pederin dibenzoate (a collaborative effort), which complemented work on mycalamides A and B.

## 1.2 STRUCTURE OF MYCALAMIDES A AND B

### 1.2.1 INFRARED AND MASS SPECTROSCOPIC ANALYSES

#### 1.2.1.1 INFRARED SPECTRA OF MYCALAMIDES A AND B

The infrared (IR) spectrum of mycalamide A was recorded initially[18] as a film. The major features of this spectrum were:-

i) a carbonyl stretching band at 1690 $cm^{-1}$, and a weaker band at 1540$cm^{-1}$ indicative of a (secondary) amide group[96],

ii) a broad band between 3100 and 3700 $cm^{-1}$ indicating NH and OH stretches broadened by hydrogen bonding, and

iii) several bands from 1040 to 1100 $cm^{-1}$, representing C-O-C stretches.

There were also bands around 2960, 1470 and 1390 $cm^{-1}$, indicative of various C-H stretching and bending vibrational modes, respectively[96]. The film IR spectrum of mycalamide B[19] was almost identical, as expected from the similarity of their structures.

The IR spectra of mycalamides A and B were also recorded in chloroform solution. The spectrum of mycalamide A showed a sharper peak at 3420 $cm^{-1}$, probably due to the amide NH stretch, superimposed on a broader band, and the amide carbonyl stretch was at 1680 $cm^{-1}$. Otherwise this spectrum was similar to the one described above. Similarly, the solution IR spectrum of mycalamide B showed a sharp peak at 3380 $cm^{-1}$, superimposed on a broader band. Note that in both spectra the characteristic C=C band for the terminal alkene was not observed, being weak and hidden by the large amide carbonyl band.

Thus the major focus of these IR spectra of mycalamides A and B was the position of the amide carbonyl stretch. This was of reasonably high frequency in both the solution and film IR spectra, and this could be caused by

the presence of neighbouring oxygenated carbons, competing for some electron density from this group[96].

1.2.1.2 MASS SPECTRA OF MYCALAMIDES A AND B

Mycalamides A and B were analysed by several modes of mass spectroscopy. High resolution electron impact mass spectroscopy (HREIMS) of mycalamide A gave a weak molecular ion at *m/z* 503.27220 daltons, corresponding to a molecular formula of $C_{24}H_{41}NO_{10}$. However, under these ionisation conditions there was a facile loss of 32 mass units, corresponding to a loss of methanol from the C6 acetal (Scheme 1.1), as reported for pederin and its derivatives[97]. This elimination, forming a double bond between C5 and C6, would be assisted by the presence of the exocyclic double bond. Thus for mycalamide A the peak at *m/z* 471 was dominant. Similarly, for mycalamide B, a strong ion at *m/z* 485.2634 daltons was the dominant high mass peak under these conditions, giving a molecular formula for the parent compound of $C_{25}H_{45}NO_{10}$.

Although an analysis of the fragmentation pattern of pederin under analogous EIMS conditions was reported[97], this was rather complex, and so a complete analysis of the mycalamide A and B spectra was not attempted. However, there was a common dominant peak at *m/z* 155 in the spectra of all three compounds, corresponding to a fragment obtained by a cleavage of the C6-C7 bond, and a smaller peak at *m/z* 123, corresponding to a loss of methanol from this fragment (Scheme 1.1). Another common peak in these spectra was at *m/z* 208, reported to represent a rearranged fragment, involving the left hand portion to C10 and containing an oxazolidinone ring. In the DEIMS spectrum of mycalamide A, there were other significant low mass ions at *m/z* 147, 215 and 226 which were not assigned, and an *m/z* 229 ion in the spectrum of mycalamide B.

**Scheme 1.1** EI mass spectroscopy fragmentation of mycalamides A and B.

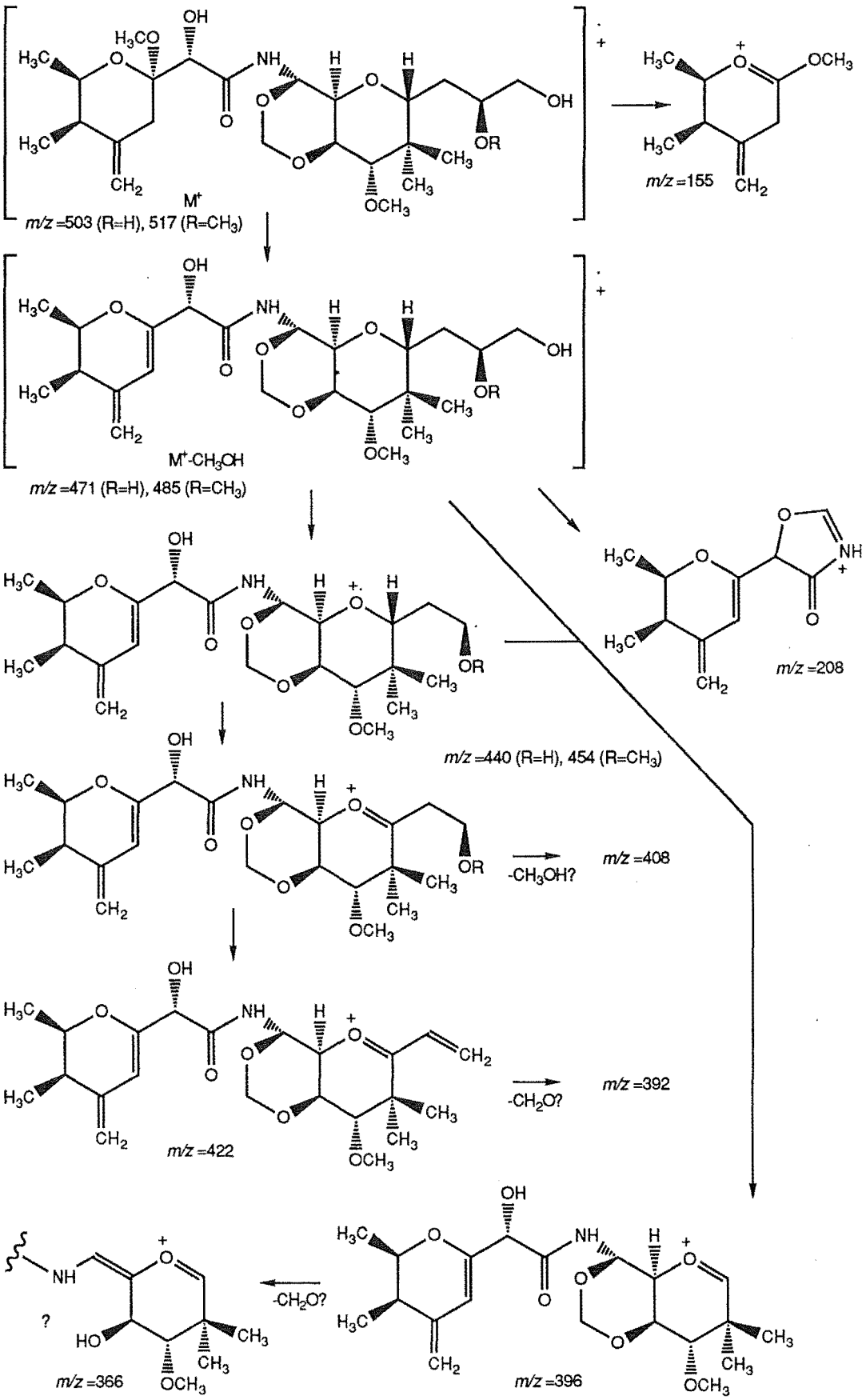

The fragmentation pattern near to the parent ion was better understood, being assigned on the basis of high resolution results and by comparison with similar results for pederin[97]. For mycalamide A, there were peaks at *m/z* 440 and 422, which probably represented successive cleavages along the C16-C18 sidechain (Scheme 1.1) from the major $M^+$-$CH_3OH$ ion (*m/z* 471). In particular, cleavage of C17-C18 would give an *m/z* 440 ion, then a loss of $H_2O$ across C16-C17 could give rise to the *m/z* 422 ion. Similarly, for mycalamide B, peaks at *m/z* 454 and 422 would correspond to a cleavage of the C17-C18 bond from the major $M^+$-$CH_3OH$ ion (*m/z* 485), then a loss of $CH_3OH$ across C16-C17, as above. There were also further peaks for mycalamide B at *m/z* 396, 366 and 348, which could be accounted for by cleavages of the C15-C16 bond and cleavages of the C10-C12 methylene acetal. However, there were also likely to be other combinations which could account for some of these smaller ions, so that these fragmentations were not studied further.

The mass spectrum of mycalamide A under DCI (desorption chemical ionisation) conditions, using ammonia ($NH_3$) as the reagent gas, gave an adduct peak of low intensity at *m/z* 521 ($MNH_4^+$) and a much stronger peak at *m/z* 489, corresponding to a loss of methanol, as above ($MNH_4^+$-$CH_3OH$). If the reagent gas was deuterated ammonia ($ND_3$), then the adduct ions maximised in intensity at *m/z* 529 and 497, so that this indicated the presence of four exchangeable protons in mycalamide A. For mycalamide B, DCIMS, using $NH_3$ as the reagent gas, gave peaks at *m/z* 535 ($MNH_4^+$), 503 ($MNH_4^+$-$CH_3OH$) and 486 ($MH^+$-$CH_3OH$). With $ND_3$ as the reagent gas these peaks shifted to *m/z* 542, 510 and 490, requiring the presence of three exchangeable protons for this compound. If the reagent gas was methane ($CH_4$) then little low mass material was obtained and no adduct ions were observed, so that the $MH^+$-$CH_3OH$ peak was dominant in the spectra of mycalamides A and B.

Mass spectroscopy under fast atom bombardment (FAB) ionisation conditions seemed to be most useful for these compounds, since sodium or potassium adduct ions ($MNa^+$, $MK^+$) were found in good intensity, in addition to other peaks showing loss of methanol. Therefore FABMS was probably the method of choice for the mass spectroscopic analysis of mycalamide derivatives.

### 1.2.2 ASSIGNMENT OF THE $^1H$ NMR SPECTRA OF MYCALAMIDES A AND B IN DEUTEROCHLOROFORM

The $^1H$ NMR spectrum of mycalamide A, as recorded in $CDCl_3$, is shown in Figure 1.1, while the data obtained are listed in Table 1.1. The broad doublet at δ7.49 ppm was assignable to the proton attached to the secondary amide nitrogen, since this resonance was removed slowly on addition of $D_2O$ to the sample[98]. The remaining three exchangeable protons were necessarily hydroxyl protons from the molecular formula, but their resonances were not observed in this $^1H$ NMR spectrum.

A homonuclear correlation spectroscopy (COSY) experiment[80,81] was performed to assign the coupled resonances, and the spectrum obtained is shown in Figure 1.2. There was a connectivity from the amide NH resonance to the triplet at δ5.87 ppm, and from the latter to a doublet of doublets at δ3.86 ppm, so that these were assignable to the H10 and H11 protons respectively. This series of connectivities continued through to H12 and H13. A similar series of connectivities established the linkage of resonances from H15 to H18, and the assignment of the H16 resonances was obvious from their chemical shifts, thus locating the remaining resonances in this chain. There were three remaining coupled networks in the COSY spectrum. One involved the methyl doublets at δ1.19 and 0.99 ppm, being coupled to resonances at δ3.98 and 2.23 ppm respectively. These represented the C2 and C3 methyl

groups being coupled to the H2 and H3 protons, but the expected correlation between the H2 and H3 resonances was absent in the COSY spectrum, probably because the coupling constant was small (2.7 Hz)[81,99]. A second spin system involved the multiplets at δ4.84 and 4.72 ppm, which were weakly coupled to a two proton multiplet at δ2.36 ppm. These multiplets were assigned to the exocyclic methylene and C5 methylene protons respectively, which were in an allylic relationship. The remaining isolated spin system involved the coupled resonances at δ5.13 and 4.87 ppm, which corresponded to signals for the methylene acetal protons contained in the C10-C12 dioxan ring.

The assignments of the two methoxyl resonances and the stereochemistry associated with the exocyclic methylene resonances were achieved by NOE experiments. In particular, irradiation of the H7 resonance (the singlet at δ4.31 ppm) enhanced the methoxyl resonance at δ3.29 ppm, whereas irradiation of one of the two methyl singlets (assigned to groups at C14) enhanced the resonance at δ3.55 ppm, so that these resonances could be assigned to groups at C6 and C13, respectively (Table 1.2). Similarly, irradiation of the H3 resonance gave an enhancement of the more downfield 4=CH resonance, at δ4.84 ppm, and irradiation of the $H_2$5 multiplet enhanced the resonance at δ4.72 ppm, so that these were designated *Z* and *E*, respectively. (These assignments represent an application of the sequence rules for prochirality to the double bond substituents[100]). The stereochemistry associated with the C14 methyl and 10-$OCH_2$ methylene proton resonances is discussed in a following subsection describing the solution conformations of the trioxadecalin ring system. Thus the complete assignments of the $^1$H NMR spectrum of mycalamide A have been listed in Table 1.1.

**Figure 1.1** $^{1}H$ NMR spectrum of mycalamide A in $CDCl_3$ solution

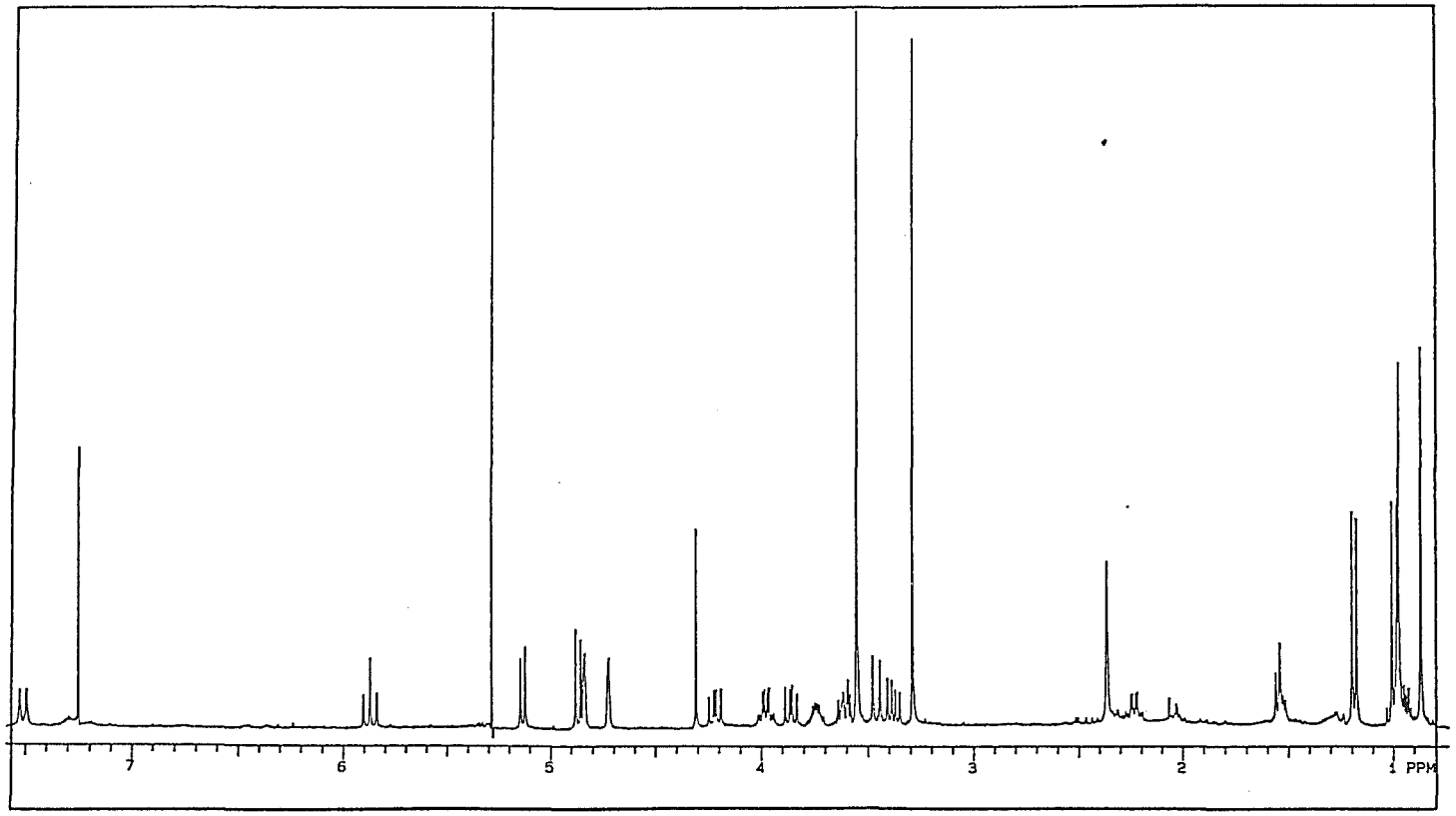

**Figure 1.2** Homonuclear correlation spectroscopy (COSY) spectrum of mycalamide A in $CDCl_3$ solution

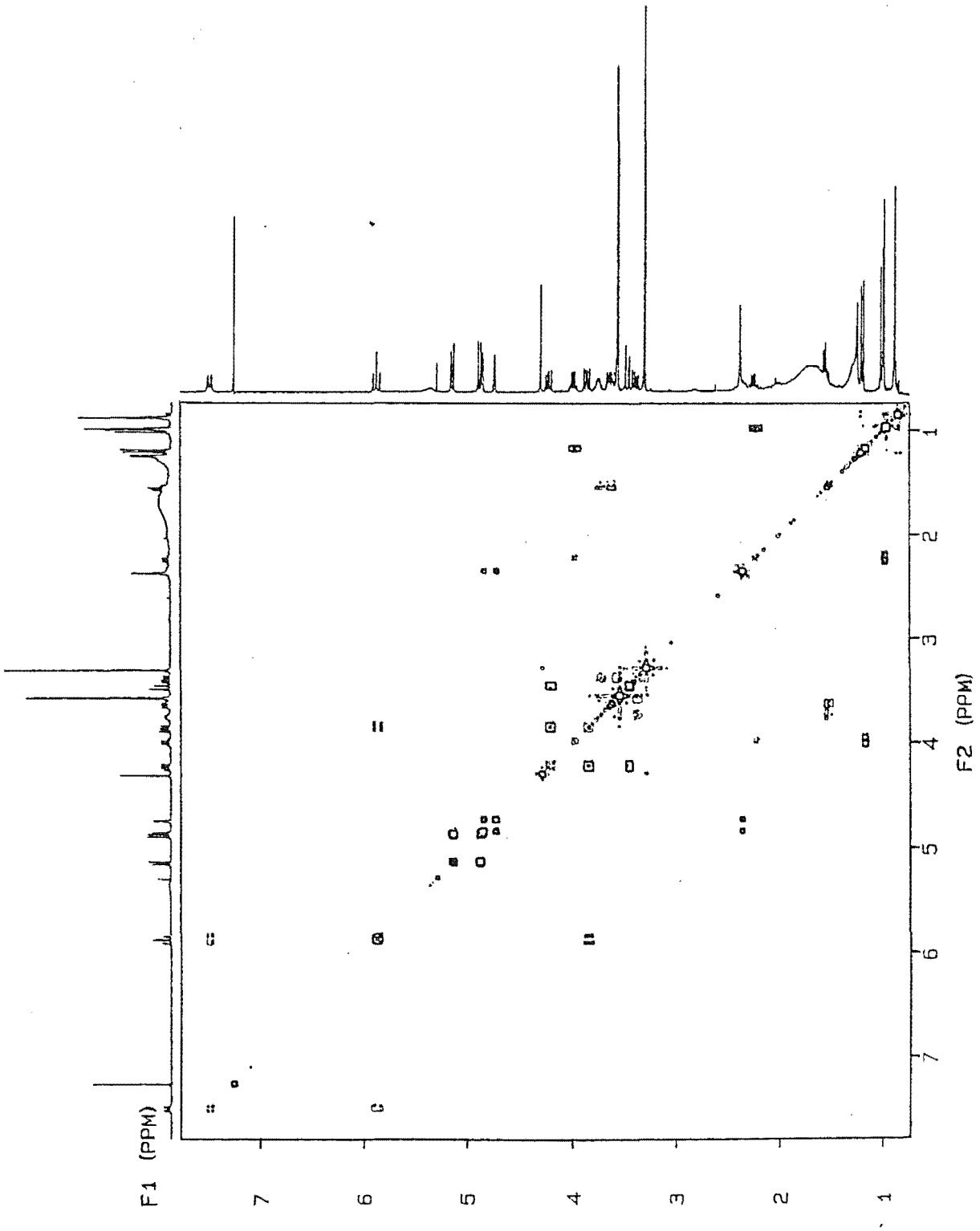

The $^1H$ NMR spectrum of mycalamide B was similar to that of mycalamide A, but contained three methoxyl resonances. A COSY experiment was performed, which enabled assignments of all the coupled resonances (Table 1.1), and this indicated that there were significant shifts (in ppm) in the H5 (-0.1), H15 (-0.2) and H17 (-0.5) proton resonances, compared to data for mycalamide A. However, the observed chemical shifts of the other resonances were all within 0.1 ppm of data recorded for mycalamide A. These chemical shifts were consistent with the location of the third methoxyl group at C17, since methylation of an hydroxyl group is known to cause an upfield shift in the α-proton resonance[101]. The assignments of the three methoxyl resonances were obtained from the results of NOE experiments, as described above for mycalamide A. Irradiation of the third methoxyl resonance, at δ3.24 ppm, in an NOE experiment gave enhancements of the $H_2$16 and H18 resonances (Table 1.2), further confirming the location of this methoxyl group in the mycalamide B structure. Interestingly, the resonances for the two H5 methylene protons were resolved in the $^1H$ NMR spectrum of mycalamide B, and only one of the two protons showed allylic coupling to the exocyclic methylene protons. These points will be considered further in the following conformational analysis.

### 1.2.3 ANALYSIS OF THE SOLUTION CONFORMATIONS OF MYCALAMIDES A AND B BY $^1H$ NMR SPECTROSCOPY

The solution conformations of mycalamides A and B (in $CDCl_3$) have been examined initially by combining an analysis of the vicinal proton-proton coupling constants with the results of extensive NOE experiments. The basis for the former analysis stems from the well known relationship relating the size of the three-bond coupling constants to the dihedral angle between the protons, as documented in the Karplus equation[102]. Recently, the precision of

this equation has been enhanced by an empirical generalisation, which includes correction terms for the electronegativities of substituents in the α and β positions and for the orientations of these substituents[103]. This calculation lends itself to computer programming and is a feature of many molecular modelling programs.

The solution conformation of the O1-C6 tetrahydropyran ring of mycalamides A and B was elucidated mainly from the results of NOE experiments (Table 1.2). In particular, irradiation of the H2 resonance of mycalamide A caused an enhancement of the C6 methoxyl resonance and irradiation of the C3 methyl resonance enhanced the $H_2$5 multiplet, and vice versa. These NOE interactions suggested that H2, 6-$OCH_3$, 3-$CH_3$ and one H5 proton were axial substituents, so that this ring was required to be in a chair conformation, as shown in Figure 1.3.

**Figure 1.3** $^1$H-$^1$H NOE interactions and solution conformation of the O1-C6 tetrahydropyran ring in mycalamides A and B

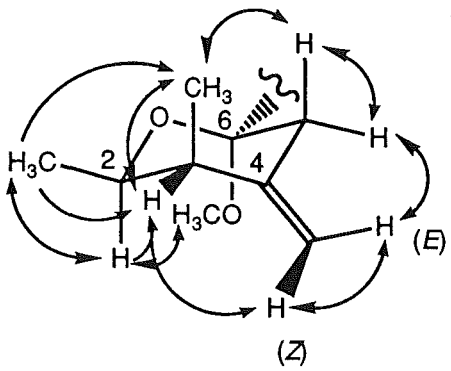


Other NOE interactions between substituents of this O1-C6 ring in both mycalamides A and B were supportive of this proposed conformation (Table 1.2). In mycalamide B, where the two H5 resonances were resolved, it was the more upfield H5 resonance which was enhanced on irradiation of the C3 methyl resonance, so that this could be assigned to the axial H5 proton (H5a). Only H5a showed significant coupling to the 4=CH protons, and this was

consistent with the dependence of the size of the allylic coupling constant[102] on the angle $\phi$ in Figure 1.4. In particular, the magnitude of this coupling constant is zero for $\phi$=0 or 180°, and maximum (~3 Hz) for $\phi$=90°, since it is related to the degree of $\sigma$-$\pi$ orbital overlap, and is similar for both the cisoid and transoid coupling paths[104].

**Figure 1.4** Angular dependence of the allylic coupling constant

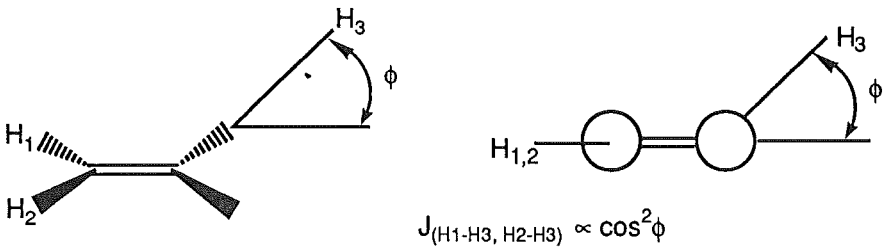


The proposed chair conformation for the O1-C6 ring is favoured by two factors. Firstly, the bulky C7 sidechain is in the favoured equatorial position to minimise unfavourable steric interactions and, secondly, the C6 acetal methoxyl oxygen is axial, as favoured by the anomeric effect[105,106]. The anomeric effect is the unexpected preference displayed by polar substituents, X, at the 2 position of tetrahydropyran ring systems, to adopt an axial orientation, and is believed to result mainly from unfavourable polar effects operating in the equatorial form which destabilise that orientation[106]. However, there is also believed to be significant stabilisation of the axial form by overlap of the antibonding orbital of the C-X bond with the lone pair orbital on the ring oxygen atom[105,106]. The exo-anomeric effect[105], which describes the general preference for a methoxyl group in this position to adopt a conformation in which the O-$CH_3$ bond lies anti-coplanar to the C2-C3 bond of a general tetrahydropyran ring, is probably also effective in the present system. There is evidence for such a conformation of the C6 methoxyl group (Figure 1.5a) from the observed strong NOE interactions between this

methoxyl group and both H2 and H7, whereas there was only a very weak interaction between this group and the equatorial H5 proton.

**Figure 1.5** Newman projections for the major staggered conformers about the C6-C7 bond in mycalamides A and B

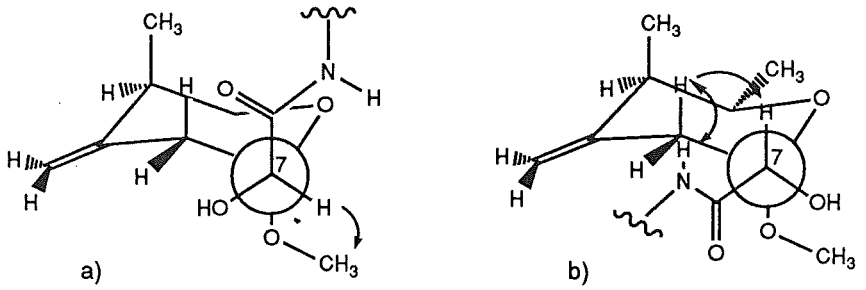


The conformations of the C7-N9 chain portion were less clearly defined. However, there was a strong NOE interaction between the H7 and NH protons which suggested that these protons were mainly in a gauche relationship and that the conformation about the amide C-N bond was mainly *Z* (a *trans* relationship of the alkyl substituents)[100]. In fact, this *Z* conformation about the amide bond has been reported to be strongly preferred over the *E* conformation for *N*-monosubstituted amides in general[107]. The conformations about the C6-C7 bond could also be deduced from NOE interactions. It was noted above that there was a strong interaction between the H7 and C6 methoxyl protons. Irradiation of H5a (in mycalamide B) gave enhancements of the H7 and NH resonances, whereas these resonances were not significantly enhanced on irradiation of H5e. These data required the presence of two of the three staggered rotamers about the C6-C7 bond, as shown in Figure 1.5. At the other end of this chain, the N9-C10 bond was required to be approximately fixed, with the NH and H10 protons in an anti relationship, since the H10-H11 vicinal coupling constant was sufficiently large (9.8 Hz)[102,108]. There was no significant NOE interaction between these protons. Therefore,

although this portion of the structure was potentially rather flexible, this study has shown that it consists of only a few major solution conformations.

The trioxadecalin ring system of mycalamides A and B was required to be *cis*-fused[109-111], with the two rings in chair conformations, as in Figure 1.6a, in order to satisfy the observed NOE interactions across these rings, H10-10-OCH, H10-H13, H10-H15, 10-OCH-H13, H12-14-$CH_3$ and H13-H15 (Table 1.2). These NOE interactions required that the downfield 10-OCH resonance (enhanced) be assigned to the axial pro-*R* proton and that the more upfield 14-$CH_3$ resonance be assigned to the axial pro-*S* methyl group[112]. These assignments were confirmed by further NOE interactions, such as from H13, 13-$OCH_3$ and H15 to the 14-$CH_3$*R* group only. Also, irradiation of 10-OCH*S* gave an enhancement of the 10-OCH*R* resonance only. Irradiation of H11 gave strong enhancements of the NH and H12 proton resonances, but not H10 or H16, consistent with the proposed anti relationships between NH and H10 and between H10 and H11 and the proposed chair conformation of the C11-C16 ring.

**Figure 1.6** $^1$H-$^1$H NOE interactions and possible chair-chair conformations of the trioxadecalin ring system in mycalamide A

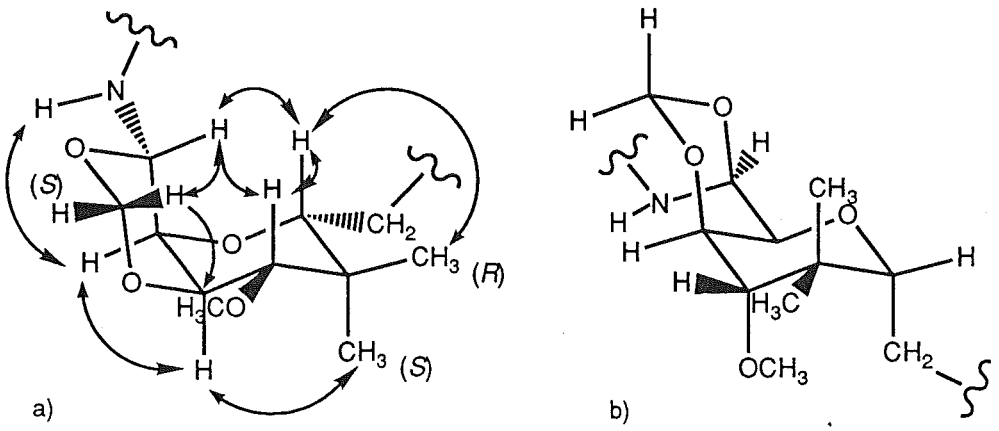


These results were in good agreement with the geometric requirements obtained from an analysis of the vicinal proton-proton coupling constants

between C10 and C13. In particular, the values (in Hz) for H10-H11 (9.8), H11-H12 (6.7) and H12-H13 (10.3) (Table 1.1) required that there be anti, gauche, and anti relationships[102], repectively, between these proton pairs, as found in the proposed conformation (Figure 1.6a).

Significantly, in the stated conformation of the trioxadecalin ring system (Figure 1.6a) both the N9 and C16 sidechains (at C10 and C15 respectively) were equatorial substituents, and this preference appeared to be reasonable, since it would minimise unfavourable steric interactions involving these chains. However, while the C12 and C13 oxygen substituents were equatorial to the C11-C15 ring, C10 was axial, so that there were unfavourable gauche interactions between C10 and C13, C10 and C15, and 10-$OCH_2$ and C13. Such a conformation has been described as an 'O-outside' conformation for derivatives of *cis* 1,3-dioxadecalane[109,111], and the alternate chair-chair conformation is termed 'O-inside'. An alternate chair-chair conformation for the trioxadecalin ring system of mycalamide A has been depicted in Figure 1.6b. This conformation has the N9 and C16 chain atoms axial (introducing unfavourable gauche interactions between C11 and C16, and C13 and C16 for example) and the C12 and C13 oxygen substituents axial to the C11-C15 ring. There was no evidence from NOE experiments or from an analysis of the vicinal coupling constants to suggest the presence of this second chair-chair conformation for mycalamides A or B in $CDCl_3$ solution. However, various studies describing the chemical and conformational equilibration of derivatives of *cis* 1,3-dioxadecalane[109,111] and related compounds[113] have been reported, and in one case[109] both $^1H$ and $^{13}C$ NMR spectroscopy were used to probe their conformations. There have also been several studies of the conformational behaviour of various *cis*-decalins using $^{13}C$ NMR spectroscopy[114,115]. Therefore this discussion is continued in a following

subsection, where the results from $^{13}C$ NMR spectroscopy on mycalamides A and B are presented.

The conformations of the C16-C18 chain portion of mycalamides A and B were not able to be determined from these data, due to the overlap of the two H16 resonances and the close proximity of the H15, H17 and H18 and other resonances in the $^{1}H$ NMR spectra. However, there was clearly a difference in the relative populations of various rotamers about the C15-C16 bonds in these two compounds, based on the observed coupling constants recorded for their respective H15 resonances (Table 1.1). These values were not consistent with the presence of a single conformation about the C15-C16 bond, although those for mycalamide B suggested that there was one major conformation, probably having C17 anti to C14[102,116]. The coupling constants recorded for the two H18 resonances were similar for mycalamides A and B, but also indicative of some combination of rotamers about the C17-C18 bond. Thus this substructure appeared to be quite conformationally flexible.

There were several long range NOE interactions which were indicative of major overall solution conformations of the mycalamide A and B structures. There were NOE interactions between the C3 methyl protons and the NH and H11 protons (strong for mycalamide B), and possibly from the C3 methyl protons to H17 (weak), in addition to an interaction between the H5 axial proton and H17 (strongest for mycalamide B). These results suggested that the mycalamide molecule was folded around in a roughly circular shape, and this possibility will be discussed in more detail in relation to molecular modelling results, presented in a subsequent section.

Therefore, to summarise the results of these analyses, it has been shown that the three rings of mycalamides A and B were almost entirely in single chair conformations, that the central amide chain portion C7-N9 has

some conformational rigidity, but that the C15-C18 sidechain was rather flexible.

### 1.2.4 ASSIGNMENT OF THE $^{13}C$ NMR SPECTRA OF MYCALAMIDES A AND B IN DEUTEROCHLOROFORM

The $^{13}C$ NMR spectrum of mycalamide A is shown in Figure 1.7, while the data obtained are listed in Table 1.3. The resonance at δ171.82 ppm clearly belonged to the C8 amide carbonyl, and resonances at δ145.65 and 110.55 ppm were assignable to the carbons of the exocyclic double bond[117]. A coupled $^{1}H$-detected heteronuclear multiple quantum coherence (HMQC) experiment[85] was performed to assign the protonated carbon signals of mycalamide A. The increased sensitivity of this HMQC experiment over the standard $^{13}C$-detected HETCOR experiment[88] was very apparent, in that a 2.5 hour acquisition on a 9 mg sample of mycalamide A gave an almost complete set of correlations, whereas a HETCOR experiment on the same sample for an equivalent time period gave almost no real correlations. Of interest from the $^{13}C$ assignments obtained (Table 1.3) was the chemical shift of the C10 resonance, δ73.74 ppm, which was lower than expected for a methine carbon having oxygen and nitrogen substituents[117]. This carbon was therefore probably affected by shielding affects associated with the adjacent carbonyl oxygen functionality[117,118]. Also, the methyl groups at C14 were of quite different chemical shift, but the upfield position of the 14-$CH_3$*S* resonance was entirely consistent with standard gauche shielding effects for axial ring substituents[117,119,120], and was similarly observed for the 3-$CH_3$ and, possibly, the 6-$OCH_3$ resonances.

**Figure 1.7** $^{13}C$ NMR spectrum of mycalamide A in $CDCl_3$ solution

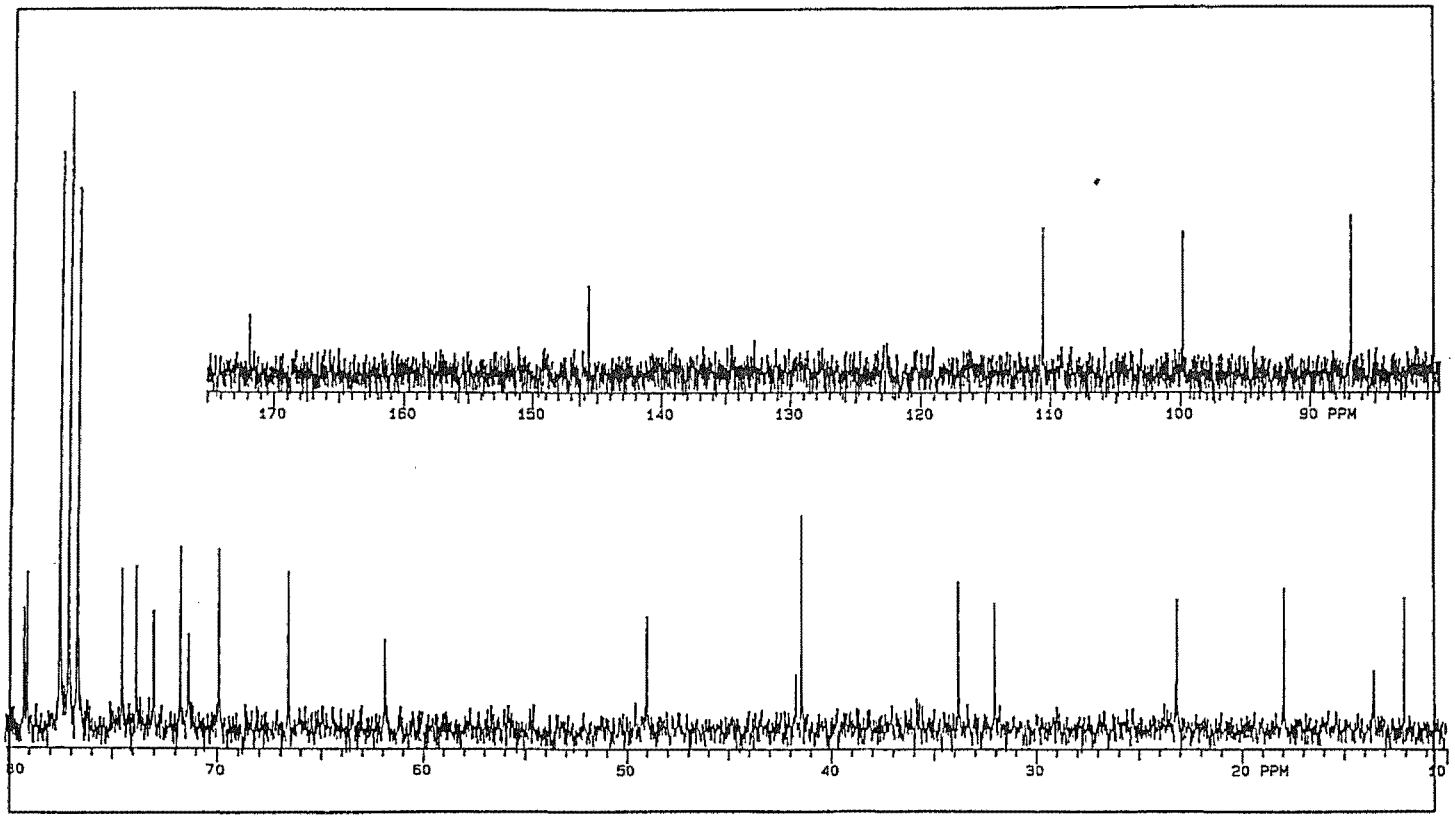

**Figure 1.8** Heteronuclear multiple bond correlation (HMBC) spectrum of mycalamide A in $CDCl_3$ solution

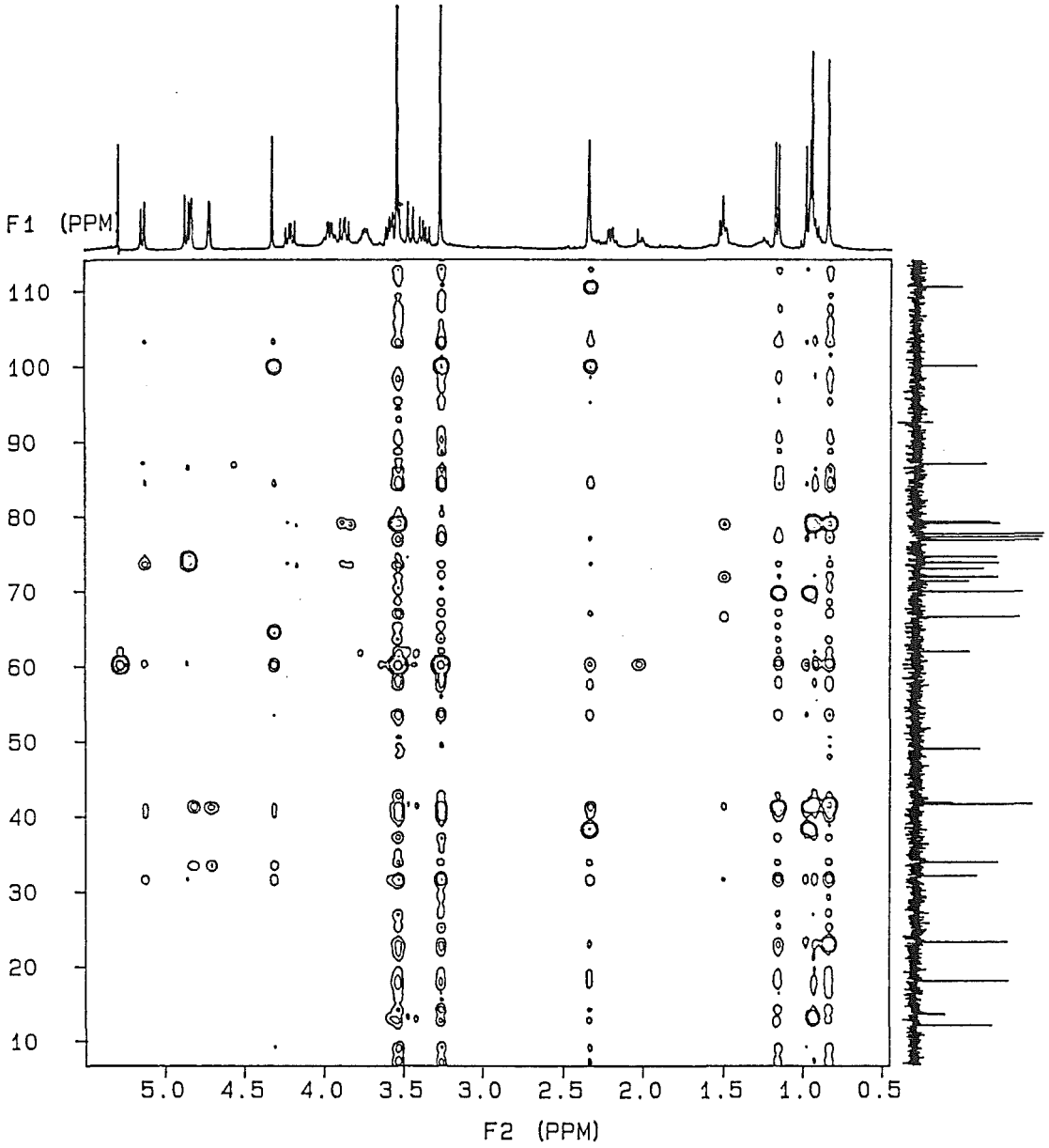

A $^{1}H$-detected heteronuclear multiple bond connectivity (HMBC) experiment[86] was performed to assign the quaternary carbon signals of mycalamide A and to provide further evidence for the above assignments. This experiment was effective for obtaining two or three bond $^{1}H$-$^{13}C$ correlations and was found to be much more sensitive than the corresponding $^{13}C$-detected long range HETCOR (XCORFE) experiment[87,89]. Results obtained from the two experiments have been compared in Table 1.4, and the HMBC spectrum has been reproduced in Figure 1.8. It can be seen that many more correlations were observed in the HMBC experiment, although this was performed on a larger sample. Both experiments were less sensitive in detecting correlations involving proton resonances of high multiplicity, because the correlation was spread over a greater frequency range, leading to a poorer signal to noise ratio in the two-dimensional spectrum. Here both experiments provided effective assignment of the quaternary carbon resonances, C4, C6, C8 and C14, and proved the location of the C6 and C13 methoxyl groups.

The $^{13}C$ NMR spectrum of mycalamide B was similar to that of mycalamide A, but there was a third methoxyl resonance at δ56.65 ppm, and there were shifts in the C7 (-1.2), C15 (+3.5), C16 (-2.3), C17 (+7.2) and C18 (-3.0) carbon resonances, as previously assigned by a HETCOR experiment[19]. The shifts in the C15-C18 resonances were in accordance with standard substituent effects[117] for the methylation of the C17 hydroxyl group of mycalamide A, providing further strong evidence for the structure of mycalamide B.

### 1.2.5 VARIABLE TEMPERATURE $^{13}C$ NMR STUDY ON MYCALAMIDE A

Further to the above analyses, it was noticed that the linewidths of some of the $^{13}C$ NMR signals in the spectra of mycalamides A and B that were

assigned to substituents of the trioxadecalin ring system were larger than normally observed. The C11 and 14-$CH_3S$ resonances appeared to be most affected. (A similar line broadening behaviour was also observed in the $^{13}C$ NMR spectrum of onnamide A[19]). This behaviour was suggestive of the occurrence of some conformational exchange[121], although the evidence from analyses of NOE interactions and proton-proton coupling constants for mycalamides A and B required the presence of one major solution conformation for this trioxadecalin ring system.

The line broadening of the $^{13}C$ NMR signals of some *cis*-decalins[114,115] has been extensively studied and is reported to arise from conformational exchange between two chair-chair conformations. The line broadening of such signals is a function of the temperature and the spacing (in Hz) between resonances for the same carbons in the two conformations, and these data can be used to calculate thermodynamic parameters for the conformational inversion process[114,121]. In considering the exchange process, there are three key spectral forms[114] and these have been simulated in Figure 1.9 for two conformations in a population ratio of 95:5. Firstly, at low temperature, the kinetic exchange is slowed to the extent that separate, reasonably sharp signals are observed for individual carbons in the two conformations (Figure 1.9a). Secondly, at the coalescence temperature, peaks for the two conformations merge (due to kinetic averaging on the NMR time scale), but the peak widths may be very broad (Figure 1.9b). Thirdly, at temperatures above coalescence, the merged peaks also become reasonably sharp (Figure 9.1c). However, neither the low temperature nor the high temperature resonances are as sharp as those resonances not involved in the exchange process due to residual kinetic effects[114].

**Figure 1.9** Computer simulation of the three key spectral forms for conformational exchange involving two conformations in a population ratio of 95:5.

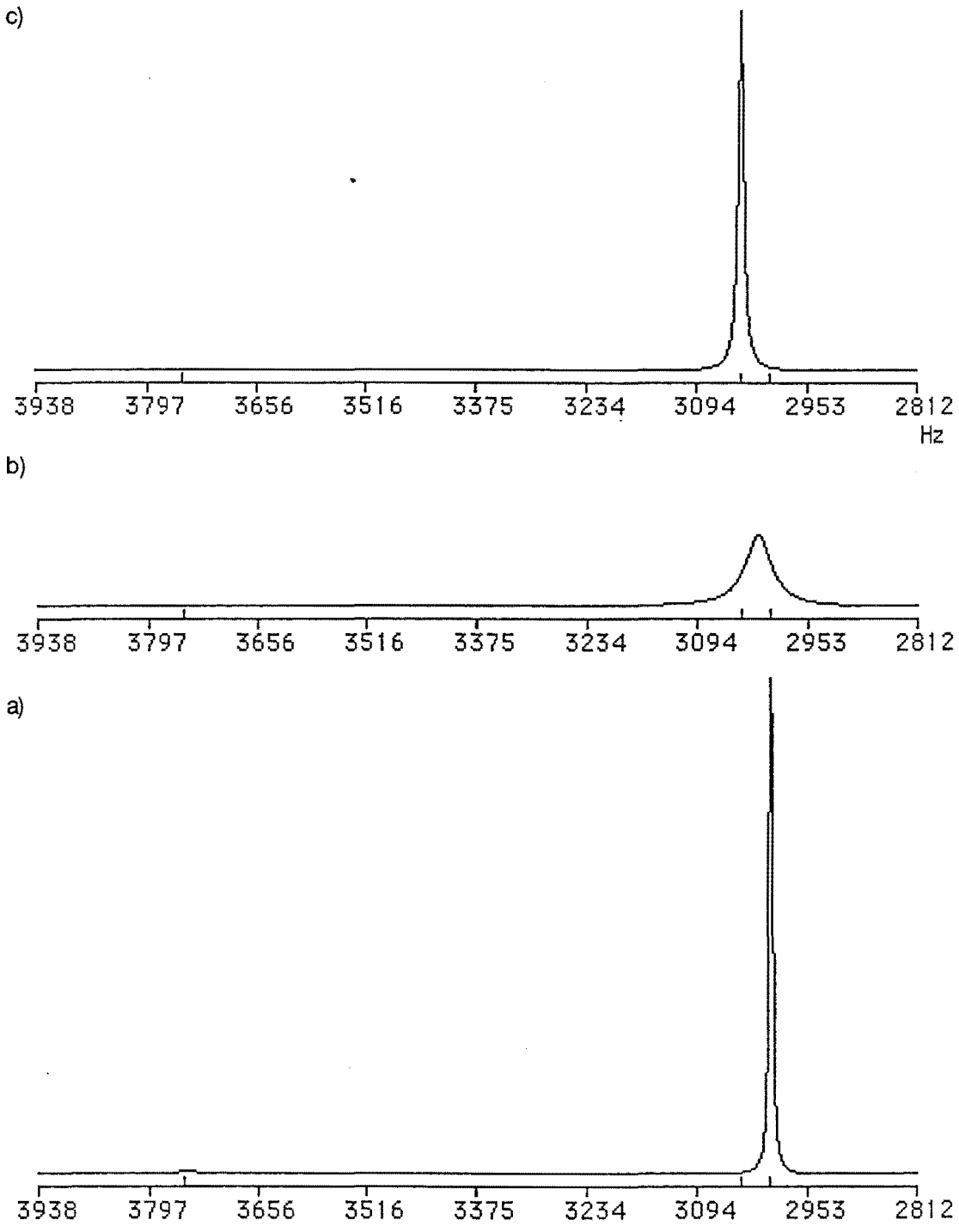

A variable temperature $^{13}C$ NMR study was therefore performed to investigate the nature of this proposed conformational exchange in mycalamide A. $^{13}C$ NMR spectra were recorded at intervals of 25°C, for a temperature range of -50°C to +50°C. The spectrum at 50°C contained resonances for substituents of the trioxadecalin ring system that were significantly sharper than those recorded at 23°C, and this was particularly obvious for the C11 and 14-$CH_3S$ resonances. At 0°C these resonances were broader, as was the C16 resonance, and this was even more pronounced at -25°C. However, at -50°C, the 14-$CH_3R$, 14-$CH_3S$ and some resonances of the trioxadecalin ring system were again sharper, although the C16 resonance was broad.

To account for this behaviour, it is proposed that the trioxadecalin ring system is undergoing conformational exchange between two chair-chair conformations[114,115,121], where the coalescence temperature for the C14 methyl resonances must lie between -50°C and -25°C. The fact that the C16 and other resonances did not necessarily show similar linewidths at particular temperatures merely reflects the dependence of the coalescence temperature on the δ separation of a particular pair of resonances from a single carbon in the two conformations[114]. Note also that the slight variation of the chemical shifts of some resonances with temperature did not allow unambiguous assignment of all the resonances between δ70 to 80 ppm in these spectra. The spectrum at -50°C did not seem to contain any new resonances, so that the proportion of the proposed alternate chair-chair conformation of the trioxadecalin ring system was comparatively small, probably less than 10% from the signal to noise ratio of this spectrum. In fact, the simulation in Figure 1.9 shows that as little as 5% of the alternate chair-chair conformation could give rise to the observed line broadening behaviour of the 14-$CH_3S$ resonance. (This simulation was constructed with a δ separation of 10 ppm

between the two resonances and an activation energy of 54 kJ $mol^{-1}$, which are reasonable values for such systems[114,121]). This population distribution was consistent with the lack of direct evidence for the minor conformation from NOE experiments or analyses of the vicinal proton-proton coupling constants.

## 1.3 SOLUTION CONFORMATIONS OF MYCALAMIDES A AND B IN OTHER SOLVENTS AND MOLECULAR MODELLING

It has been shown above that, despite the potential flexibility of the mycalamide A and B structures, there were a limited number of major solution conformations present in chloroform solution. One probe for the variation in the population distributions of these and other conformations with changes in their environment is to observe the distribution of conformations in a range of solvents of varying polarity by $^1H$ NMR spectroscopy[72]. The conservation of shape for particular structural portions has been considered to be some indication that similar conformations may be involved in binding to a receptor[15], since every conformational change must be repaid by binding energy[70]. (This obviously still allows higher energy conformations to be considered[16,70,122]). Therefore it was of interest to study the conformations of mycalamides A and B in a range of other solvents, and to attempt to model the resulting conformations, in order to obtain some insights into their overall shape.

### 1.3.1 SOLUTION CONFORMATIONS OF MYCALAMIDE A IN $D_4$-METHANOL

The $^1H$ NMR spectrum of mycalamide A in $CD_3OD$ was very similar to that recorded in $CDCl_3$ and the spectral assignments (Table 1.1) were confirmed by the results of a COSY experiment. (These data were also similar to those recorded for onnamide A[31] in the same solvent (Table 1.7)). The

major differences between the data recorded for mycalamide A in this solvent, compared with those in $CDCl_3$, were in the chemical shifts of the H2 (-0.1), H11 (+0.1), H13 (+0.2), H15 (-0.1) and H16 (+0.1) proton resonances. The two H5 and two H16 resonances were also resolved in this solvent. Analysis of the vicinal proton-proton coupling constants showed that the only significant differences between data in the two solvents were in the magnitude of the H15-H16 constants, although the H16-H17 values could not be extracted from data recorded in $CDCl_3$ due to the overlap of the H16 resonances. These results suggested that the solution conformations of the ring structures of mycalamide A were similar in the two solvents, but that those of the C16-C18 sidechain could be different.

This was investigated further by a series of NOE experiments and the results of these have been listed in Table 1.5. Irradiation of H5a gave an enhancement of the 3-$CH_3$, H5e and H7 resonances, but irradiation of H5e gave only a very weak enhancement of H7, along with stronger enhancements of the 4=CH*E* and H5a resonances. There was also a strong NOE interaction between 6-$OCH_3$ and both H2 and H7. Therefore the conformations of the O1-C6 ring and the C6 methoxyl group were the same in both solvents, as were the conformations about the C6-C7 bond. No data regarding the conformations about the C7-C8 and N9-C10 bonds could be obtained since the NH proton was fully exchanged in this solvent.

As indicated above, the two H16 resonances were resolved in this solvent, enabling some analysis of the solution conformations of the C16-C18 portion of mycalamide A. Irradiation of the more downfield H16 resonance gave an enhancement of the 14-$CH_3$*R*, H15 and H17 resonances, whereas irradiation of the upfield H16 resonance enhanced the 14-$CH_3$*S* and H17 resonances. These results suggested that there was only one major conformation about the C15-C16 bond of mycalamide A in this solvent, such

that C17 was anti to C14[116], as shown in Figure 1.10. Also, the observed vicinal coupling constants between H15 and the two H16 protons, of 2.3 and 10.3 Hz, were indicative of gauche and anti relationships, respectively, between these protons[102], consistent with the proposed conformation. The coupling constants between the two H16 protons and H17, of 5.6 and 7.0 Hz, and those between H17 and the two H18 protons, of 3.8 and 6.3 Hz, were suggestive of combinations of several conformations about the C16-C17 and C17-C18 bonds, so that the solution conformations of this portion of the structure were not well defined. Therefore the only detected difference in the solution conformations of mycalamide A in $CD_3OD$, compared to those in $CDCl_3$, was in the conformation about the C15-C16 bond. This difference was probably indicative of the different properties of these solvents, where $CDCl_3$ is relatively non-polar and favours intramolecular hydrogen bonding, whereas methanol is more polar and is itself a good hydrogen bond donor and acceptor, so that intramolecular hydrogen bonding is disrupted. (The hydroxyl groups would also be more solvated in $CD_3OD$).

**Figure 1.10** $^1H$-$^1H$ NOE interactions and proposed solution conformation about the C15-C16 bond of mycalamide A in $CD_3OD$ solution

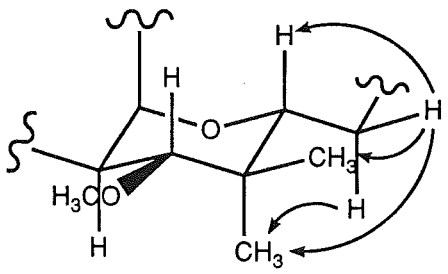


The $^{13}C$ NMR spectrum of mycalamide A in $CD_3OD$ was also similar to that recorded in $CDCl_3$, although many of the resonances were slightly more downfield. The C11, C12, C13, 14-$CH_3$*R* and 14-$CH_3$*S* resonances were also

broader, so that a similar conformational exchange process was occurring for the trioxadecalin ring system to that found in $CDCl_3$.

### 1.3.2 SOLUTION CONFORMATIONS OF MYCALAMIDE A IN DMSO

The $^1H$ NMR spectrum of mycalamide A in DMSO showed the presence of all four exchangeable protons. The NH and 7-OH doublets were located at δ8.37 and 5.76 ppm respectively, suggesting that these protons were involved in intramolecular hydrogen bonding interactions[98,101]. The 18-OH and 17-OH resonances appeared as broad singlets at δ4.37 and 3.27 ppm, or as a triplet and doublet, respectively, depending on the temperature and state of the sample. Unfortunately, the large $H_2O$ peak, at δ3.4 ppm, obscured some of the C15-C18 proton resonances. A COSY experiment was performed, which was very useful in locating these hidden resonances and in assigning the remainder of the $^1H$ NMR data (Table 1.1).

Compared to data recorded in $CD_3OD$, there were significant shifts in only the H13 (+0.1), H17 (-0.1) and H18 (-0.1) proton resonances. However, the vicinal proton-proton coupling constants, H10-H11 (8.9), H11-H12 (6.1) and H12-H13 (9.5) were significantly less than those recorded in $CDCl_3$ solution, suggesting that there was a higher proportion of the alternate chair conformation of the trioxadecalin ring system of mycalamide A in this solvent. Furthermore, the H11, H13 and H16 resonances were broad in the $^1H$ NMR spectrum. A variable temperature $^1H$ NMR study was therefore performed to investigate these results.

The $^1H$ NMR spectra at 45, 65 and 85°C showed successively sharper resonances for the H11, H13 and H16 protons, but the exchangeable proton resonances became broader due to an increased rate of exchange. Also the $H_2O$ peak was shifted to higher fields in these spectra, enabling the resonances between δ3.3 and 3.5 ppm to be directly observed. Thus the H15

resonance was a doublet of doublets (2.2, 9.8), as were the H18 resonances (3.8, 11.3) and (5.7, 11.1), and the upfield H16 resonance became a doublet of doublet of doublets (5.1, 9.8, 14.2) (coupling constants in Hz). Note that the couplings between H15 and the two H16 protons were indicative of the presence of one major C15-C16 rotamer, having C17 anti to C14 (Figure 1.10), as for mycalamide A in $CD_3OD$.

NOE experiments were performed to further analyse the solution conformations of mycalamide A in this solvent. There were weak NOE interactions between the NH and the 10-OCH*S* and H12 protons, between the H10 and H11 protons, between the H13 and 14-$CH_3$*S* protons and between the H11 and one of the H16 protons (Table 1.5), giving direct evidence for the presence of the minor chair-chair conformation for the trioxadecalin ring system of mycalamide A. The remaining NOE interactions were similar to those observed in $CDCl_3$ and $CD_3OD$ solution so that, overall, the major solution conformations of mycalamide A were conserved in all three solvents.

A $^{13}C$ NMR spectrum was also recorded and assigned with the assistance of an HMQC experiment (Table 1.3). Even greater linewidths were observed for some of these $^{13}C$ resonances than those found above, consistent with earlier proposals of a higher proportion of the minor chair-chair conformation of the trioxadecalin ring system[114]. To illustrate this point, the largest linewidths were (in Hz), C10/C12 (8), C11 (>>20), C13 (10), 14-$CH_3$*R* (16) and 14-$CH_3$*S* (>>20), whereas those of 'normal' $^{13}C$ resonances were 2-2.5 Hz. Thus this conformational exchange process was most obvious in DMSO, due to the different population distribution of the two chair-chair conformations in this solvent.

### 1.3.3 NMR ASSIGNMENTS OF MYCALAMIDE B IN $D_6$-BENZENE

The $^1H$ NMR spectrum of mycalamide B in $d_6$-benzene displayed some very different chemical shifts to those recorded in $CDCl_3$, which was expected, due to the anisotropic shielding effects associated with aromatic rings[98,123]. A COSY experiment was performed which enabled complete assignments to be performed (Table 1.1). Despite the unusual chemical shifts, the vicinal proton-proton coupling constants were very similar in both solvents, except for the magnitude of the NH-H10 constant (6.5 Hz), which was significantly smaller than that normally observed (~9.8 Hz), and was suggestive of a mixture of conformations having gauche and anti relationships between these protons[102,108]. However, no NOE experiments were performed to investigate these conformations further. The $^{13}C$ NMR spectral data (Table 1.3) appeared to very similar to those recorded in $CDCl_3$, including both the chemical shifts and the linewidths of the observed resonances. Thus it was likely that the conformations of the ring structures of mycalamides A and B, at least, were the same in all these solvents, with only minor changes in the conformations of the flexible chain portions.

### 1.3.4 MOLECULAR MODELLING STUDIES

The major aim of initial molecular modelling studies on the structure of mycalamide A was to produce model structures for the proposed solution conformations discussed in previous sections, which could be crudely minimised in energy. Note that there were too many rotatable bonds in mycalamide A to perform a full conformational search to find global energy minima[122,124]. The starting structure of mycalamide A was derived from the structure of pederin di-p-bromobenzoate (**1.1**), which was specified by its x-ray crystal structure coordinates[93]. This was achieved by modifying the substituents at C7, C10, C12, C13, C17 and C18, setting the H10 and H11

protons and the N-C10 and O-$CH_2$ bonds in anti relationships, and then introducing the third ring[19]. This gave a structure in which the trioxadecalin ring system was in the major observed chair-chair conformation discussed above, and which had H7 anti to C5 and gauche to the C6 methoxyl group about the C6-C7 bond and had C17 anti to C14 about the C15-C16 bond. Energy minimisation, using a modified MODEL program[125] with MM2 parameters, gave the conformation displayed in Figure 1.11a, which, as stated above, was not necessarily a global minimum, since rotations had not been performed about other bonds in the molecule. However, note that in this conformation the H17 proton was only 2.2 Å from the H5a proton and 2.5 Å from the closest C3 methyl proton, and that the NH and H11 protons were both only 3.6 Å from the closest C3 methyl proton, consistent with long range NOE interactions specified earlier for mycalamides A and B and shown on this figure, suggesting that this was a valid low energy conformation of mycalamide A. This conformation also displayed hydrogen bonds between the NH proton and O1 and between the C7-OH proton and the C8 carbonyl oxygen.

Rotation about the C6-C7 bond and reminimisation gave a second conformation, of 3.5 kJ $mol^{-1}$ higher energy (Figure 1.11b), which satisfied the observed NOE interaction between H7 and H5a and between H5a and NH. This structure contained a single hydrogen bond only, between the C7-OH proton and the C8 carbonyl oxygen. Note that the energies of these conformations could not be used to predict relative populations since the remaining rotatable bonds had not been considered.

**Figure 1.11** Long range $^1H$-$^1H$ NOE interactions and proposed overall solution conformations of mycalamide A as derived from molecular modelling (methyl protons are not shown)

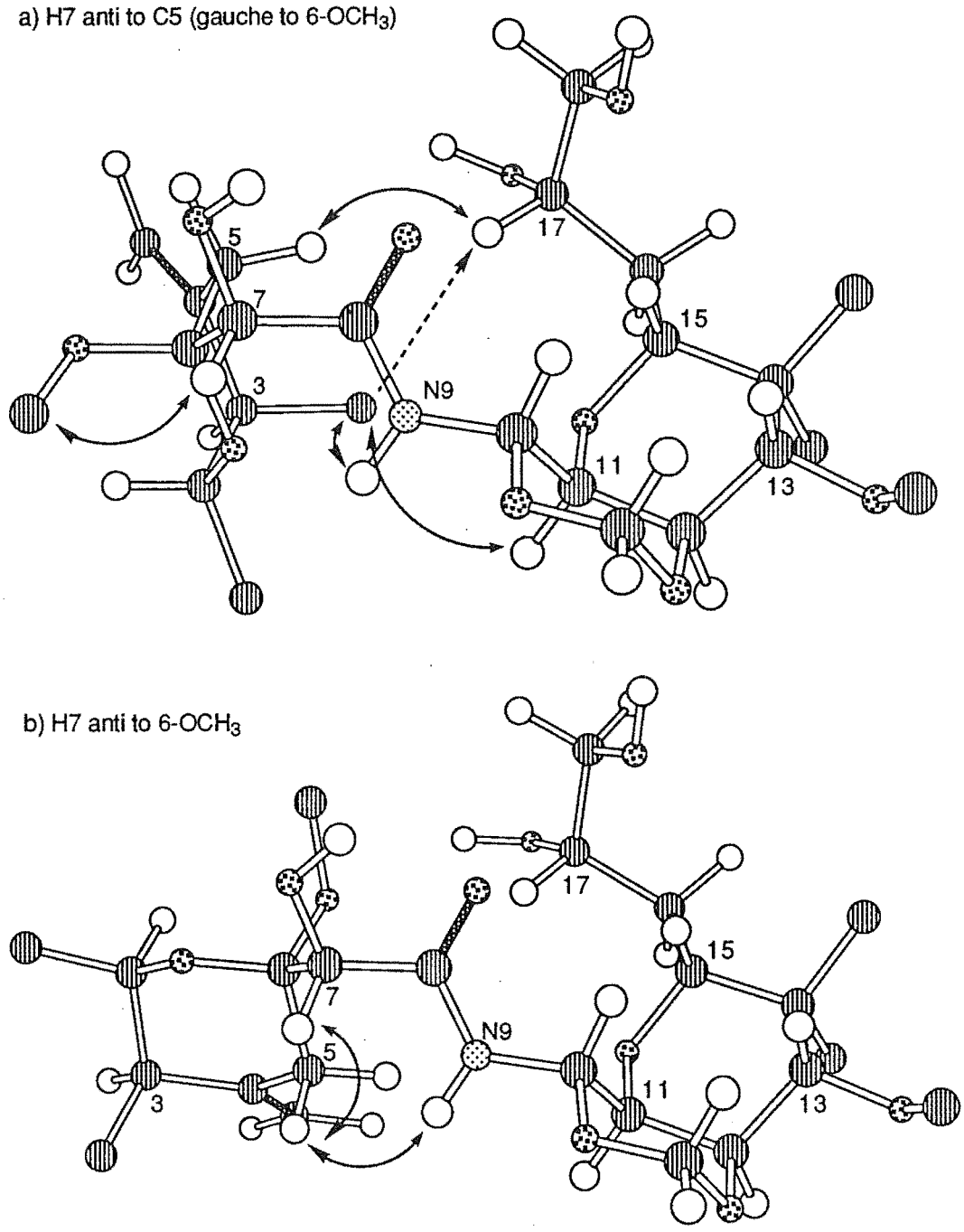


The two chair-chair conformations of the trioxadecalin ring system were modelled independently, by entering the two simplified structures **1.3A** and **1.3B** (shown in Figure 1.12), having N9 terminating as $NH_2$ and C16

terminating as $CH_3$. Energy minimisation was performed and the resulting structure, containing the alternate chair-chair conformation, was only 1.7 kJ $mol^{-1}$ higher in energy than the minimised structure containing the normal chair-chair conformation. Thus both conformations were relatively similar in energy and were therefore both likely to be accessible for mycalamides A and B. The coupling constants for the two conformations were calculated using Haasnoot's generalisation of the Karplus equation[103] and have been shown in Table 1.6. Those for the alternate chair conformation were (in Hz), H10-H11 (1.7), H11-H12 (1.4) and H12-H13 (2.2). The values for structure **1.3A** were closest to the experimental values recorded for mycalamides A and B, agreeing with other NMR evidence that this was the major solution conformation of the trioxadecalin ring system. However, these calculated values were all significantly lower than the experimental values[102], so that these results were not sufficiently accurate to allow the calculation of a precise ratio of the two conformations.

**Figure 1.12** Starting structures for preliminary molecular modelling of the trioxadecalin ring system of mycalamides A and B

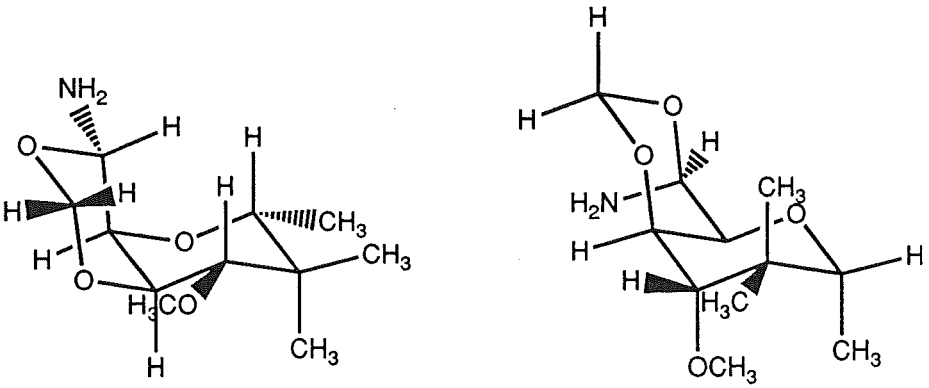


**1.3A** **1.3B**

Thus these molecular modelling results were clearly useful in providing further support for the proposed major solution conformations of mycalamide A and in depicting the overall shape of the molecule, in agreement with NOE

results. The following sections describe similar studies on pederin and pederin dibenzoate which will be compared with the results above. (The collaboration of Dr F. Matsuda in supplying samples of these compounds and of Dr N. Perry in performing some of the NMR and molecular modelling work[84] is specifically acknowledged here).

## 1.4 NMR ASSIGNMENTS AND SOLUTION CONFORMATIONS OF PEDERIN

### 1.4.1 ASSIGNMENT OF THE $^{1}H$ AND $^{13}C$ NMR SPECTRA OF PEDERIN

The $^{1}H$ NMR spectrum of pederin in $CDCl_3$ showed some similarities to those of mycalamides A and B, as expected, and the coupled resonances were unambiguously assigned using the results obtained from a COSY experiment (Table 1.7). Interestingly, the C7 hydroxyl proton resonance was observed in this spectrum, at δ3.92 ppm, coupled to H7 (2.2 Hz), but the C13 hydroxyl proton resonance was not observed. The NH resonance was also shifted slightly upfield of its position in mycalamides A and B, possibly reflecting the different environment at C10. The assignments of two of the four methoxyl resonances were obtained from the results of selective NOE experiments. Irradiation of the H10 signal gave a strong enhancement of the methoxyl resonance at δ3.380 ppm, whereas irradiation of the H7 signal enhanced the resonance at δ3.326 ppm, so that these resonances could be assigned to the methoxyl groups at C10 and C6, respectively. The remaining two methoxyl resonances were due to the groups at C17 and C18, but NOE experiments could not distinguish these because of the similarity in the chemical shifts of these and the H17 and H18 resonances. The stereochemistries associated with the two 4=CH resonances and the two C14 methyl resonances were assigned by comparison with data obtained for

mycalamides A and B and were confirmed by NOE experiments as discussed below. (Note that, because of the different substituents at C12 and C13 in mycalamides A and B, pederin and pederin dibenzoate, the true prochiral assignments[112] for the C14 methyl groups would be different only for pederin. To avoid confusion, this has been disregarded, so that the C14 methyl groups have been assigned the same labels as for mycalamides A and B in all cases). Similar assignments for the two H12 and H16 methylene proton resonances are also presented in a following analysis of the solution conformations of pederin. Note that the complete $^{1}H$ NMR spectral assignments for pederin presented here agreed well with previous partial assignments[94,95,126-128], and that the data for the left hand portion to the amide were very similar for mycalamides A and B and pederin, as expected.

The $^{13}C$ NMR spectral data of pederin had been reported[128,129], but not assigned. Hence a $^{13}C$ NMR spectrum was recorded on this sample and HMQC and HMBC experiments were performed to permit an assignment of the data obtained. The HMQC experiment gave correlations for all the protonated carbon resonances but could not allow an assignment of the C17 and C18 methoxyl resonances since the $^{1}H$ NMR signals were not yet assigned. However, results from the HMBC experiment resolved this ambiguity, since there were three-bond correlations between all the methoxyl protons and the chain or ring carbon atoms bonded to the methoxyl oxygen atoms, including from 17-$OCH_3$ to C17 and from 18-$OCH_3$ to C18 (Table 1.4). The HMBC experiment also allowed the assignment of the four quaternary carbon resonances, but these were obvious from their chemical shifts and by comparison with data for mycalamides A and B. The $^{13}C$ NMR data for the C2 to C8 portion of pederin were all within 0.4 ppm of those recorded for mycalamide A and the differences for the remaining data were consistent with normal substituent effects[117] (Table 1.3). The 14-$CH_3S$ (axial) and C11

resonances were broad, as in mycalamide A, suggesting that a similar conformational exchange process was occurring in this compound. This is investigated further in the following conformational analysis.

### 1.4.2 CONFORMATIONAL ANALYSIS OF PEDERIN

The results of all the NOE experiments on pederin are listed in Table 1.8. The NOE interactions between H5a and 3-$CH_3$, H7 and 6-$OCH_3$ and between the H5a and H7 protons, indicated that the O1-C6 ring was in the same chair conformation and that the same two staggered rotamers about C6-C7 as found for mycalamide A (Figure 1.5) were present for pederin, as expected. There were additional NOE interactions between C7-OH and the H5e, 6-$OCH_3$, H7 and NH protons, as well as between the NH proton and both the H5a and H7 protons, which supported these conformations and required the presence of at least two conformations about C7-C8 which had the H7 and/or C7-OH protons in gauche relationships with the NH proton.

The observed vicinal proton-proton coupling constants, NH-H10 (9.7) and H10-H11 (8.0), required that these protons be in predominantly anti relationships (Figure 1.13a), although the 8 Hz value also suggested the presence of a minor conformation having the H10 and H11 protons in a gauche relationship[102], such as in Figure 1.13b. These conformations were supported by a strong NOE interaction between the H11 and NH protons, and weaker interactions between NH and H10 and between H10 and H11. The interaction between 10-$OCH_3$ and both NH and H10, but not H11 or H12, indicated that the C10 methoxyl group was anti to C11 and gauche to H10, as shown in Figure 1.13. Therefore, despite the absence of the C10-C12 dioxan ring of mycalamides A and B in the structure of pederin, it was apparent that the major conformation of the N9-C11 chain portion was similar in these compounds.

**Figure 1.13** $^{1}H$-$^{1}H$ NOE interactions and proposed solution conformations for the N9-C16 portion of pederin

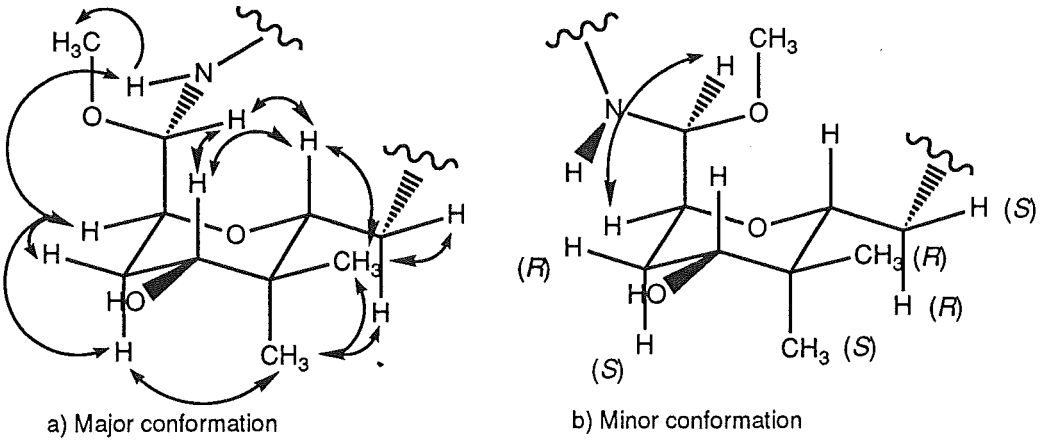


There were NOE interactions between H10 and both H13 and H15 and between H13 and H15 which required the C11-C15 ring to be the same major chair conformation as observed for mycalamides A and B (Figure 1.13). Irradiation of H13 caused an enhancement of the more downfield H12 and 14-$CH_3$ resonances, so that these could be assigned to the equatorial H12*R* and 14-$CH_3$*R* protons, respectively. Other NOE interactions between H12*S* and 14-$CH_3$*S* and between H15 and 14-$CH_3$*R* supported the proposed major chair conformation. However, there were weaker interactions between 14-$CH_3$*S* and the H13 and H15 protons which indicated the presence of a minor alternate chair conformation, although the 11.2 Hz vicinal coupling constant between the H12*S* and H13 protons required that the normal chair conformation be very dominant[101,102]. Thus this portion of the structure of pederin was also displaying very similar conformational behaviour to that found for mycalamides A and B, despite the different substituents at C12 and C13.

The coupling constants between H15 and the two H16 protons, of 2.0 and 10.1 Hz, required predominantly gauche and anti relationships between these protons, so that there was one major staggered rotamer about the C15-

C16 bond having C17 anti to C14 (compare Figure 1.10). This was supported by the observation of NOE interactions between the H16*S* proton (which had the smaller coupling constant to H15) and the 14-$CH_3$*R* protons, and between the H16*R* and the 14-$CH_3$*S* protons (Figure 1.13). This behaviour was similar to that found for mycalamide B, but not mycalamide A, in $CDCl_3$ solution, and was also similar to that found for various *C*-glycosides[116]. The coupling constants from H17 to H16*R* (3.4) and H16*S* (9.4) were also indicative of mainly gauche and anti relationships, respectively, between these protons, although there were probably also other minor conformations contributing to these values. The remainder of this sidechain portion was not analysed.

Thus it was found that the major solution conformations of pederin and mycalamide B, and, to a slightly lesser extent, mycalamide A, were very similar. This was consistent with the similarity in the chemical shifts of resonances in their NMR spectra which corresponded to equivalent structural features. This was also further supported by comparing molecular mechanics models of the two major C6-C7 rotamers of pederin (not shown) with those obtained for mycalamide A, and noting the similarities in the overall shape of the proposed major conformations of the two molecules[58,84]. The differences in the substituents at the C10, C12, C13, C17 and C18 positions in these compounds evidently did not affect the (unknown) active conformation, or interactions at the active site, since these molecules displayed such similar biological activities. The synthesis of analogues of these structures could lead to a better understanding of the essential structural and conformational features required for these biological activities and such is the aim of work in subsequent chapters.

## 1.5 SOLID STATE CONFORMATION OF PEDERIN DI-P-BROMO-BENZOATE AND SOLUTION CONFORMATIONS OF PEDERIN DIBENZOATE

The aim of this study was to determine the solution conformations of pederin dibenzoate (**1.2**) and to compare them, firstly with those of pederin and the mycalamides, and secondly with the solid state conformation of pederin di-p-bromobenzoate (**1.1**). The rationale behind these comparisons was to illustrate the relative influences of intermolecular forces, in addition to those of intramolecular forces, on the (low energy) conformations of these molecules[70,84]. In particular, conformational studies of some other biologically active molecules, including cyclosporin[72] and cycloheximide[83] (**0.14**) have revealed distinct differences between their solid and solution state conformations, which have been considered to be important for the potential understanding of the binding of these molecules to their receptors. Such studies also form a basis for observing correlations between the conformations of derivatives of these molecules and their biological activity[16,70,71], in addition to comparing differences in structure[1,15].

### 1.5.1 CRYSTAL STRUCTURE OF PEDERIN DI-P-BROMOBENZOATE

Two independent x-ray crystallographic studies were reported for pederin di-p-bromobenzoate[34,93] (**1.1**). The crystal structure of this compound is displayed in Figure 1.14. In this conformation, the O1-C6 ring had the usual chair conformation, as found for the mycalamides and pederin, and H7 was gauche to the C6 methoxyl group. The central amide chain, C7-C10, was planar, with some $\pi$-delocalisation of the amide reported. The C10 methoxyl group was anti to the C10-C11 bond, with NH anti to H10, as in a proposed solution conformation of pederin (Figure 1.13 above). However, the

conformation about the C10-C11 bond was such that the H10 and H11 protons were in a gauche relationship, rather than the mainly anti relationship which was the proposed major solution conformation of pederin[130]. The C11-C15 ring was in the usual chair conformation, having the ester and sidechain substituents at C13 and C15 equatorial, and the amide chain axial at C11. The latter caused some considerable distortion in the dihedral angles about the C11-O and C11-C12 bonds[93], a fact which is illustrated by the calculated vicinal coupling constants[103] between the H11-H12*R* (0.9) and H11-H12*S* (8.3) protons, which are in distorted gauche relationships. The C16-C18 sidechain was such that C17 was anti to C14 and 17-O was anti to C15, about the C15-C16 and C16-C17 bonds, respectively. The space group was $P2_1$, and the structure contained two molecules in the unit cell, which were linked together by a single co-crystallised alcohol molecule (methanol or ethanol) via hydrogen bonds involving the amide NH and C=O groups, to form a zig-zag chain.

**Figure 1.14** X-ray crystal structure of pederin di-p-bromobenzoate (**1.1**). Note that no hydrogen atoms were located so these have not been shown.

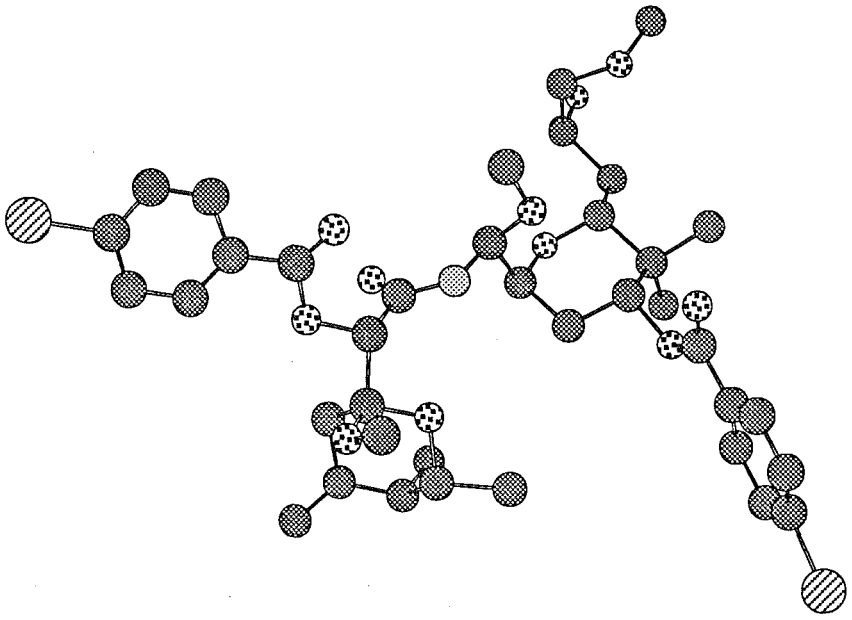

Thus the only unusual feature of this structure was the conformation about the C10-C11 bond. This conformation was reported to be favoured by an attractive O/O gauche effect[130]. However, it was likely that intermolecular forces, including Van der Waals and hydrogen bonding interactions between molecules packed in the crystal, were important factors in this solid state conformation[70]. It was therefore of interest to determine whether such a conformation was present in solution.

### 1.5.2 ASSIGNMENT OF THE $^{1}H$ AND $^{13}C$ NMR SPECTRA OF PEDERIN DIBENZOATE IN DEUTEROCHLOROFORM

The $^{1}H$ NMR spectrum of a sample of pederin dibenzoate (**1.2**) in $CDCl_3$ showed large downfield shifts (>1 ppm) in the H7 and H13 proton resonances, compared to data recorded for pederin, consistent with this esterification of the C7 and C13 hydroxyl groups of pederin[98,101]. The coupled resonances were unambiguously assigned with the assistance of a COSY experiment (Table 1.7). There were further shifts in the H5a (+0.4), NH (-0.4), H11 (+0.2), H15 (+0.4) and H16 (+0.4) proton resonances, which suggested that the solution conformations of this derivative could be slightly different from those of pederin. NOE experiments enabled an assignment of the C6 and C10 methoxyl proton resonances, but not the C17 and C18 methoxyl resonances. Assignments of the stereochemistries associated with the C12 and C16 methylene and the C14 methyl resonances were also achieved by NOE experiments, but these are described with an analysis of the solution conformations below.

A $^{13}C$ NMR spectrum of pederin dibenzoate (**1.2**) was recorded and the protonated carbon resonances were assigned by an HMQC experiment (Table 1.3). The C17 and C18 methoxyl resonances and the quaternary carbon resonances were assigned by comparison with data recorded for

pederin. There were shifts in the C8 (-4.3), C10 (+2.3), C11 (-2.5), C12 (-3.0), C13 (+3.1), C14 (-1.5), 14-$CH_3R$ (+1.8), 14-$CH_3S$ (+4.4), C16 (-1.0) and C18 (-1.0) carbon resonances, compared to data recorded for pederin, which were also suggestive of changes in the solution conformations, since, of these, only the C8 and C12-C14 carbons would be appreciably affected by the esterification[117]. The C11 and 14-$CH_3S$ resonances were also significantly broader than those in pederin, suggestive of the occurrence of some conformational exchange process for the C11-C15 tetrahydropyran ring.

### 1.5.3 SOLUTION CONFORMATIONS OF PEDERIN DIBENZOATE IN DEUTEROCHLOROFORM

An extensive series of NOE experiments was performed to examine the solution conformations of pederin dibenzoate (**1.2**) and the results of these have been detailed in Table 1.8. The solution conformations of the left hand portion of the structure to the amide were found to be the same as for pederin and mycalamides A and B, as evidenced by the similarity in the chemical shifts and NOE interactions for these structures. The observed vicinal coupling constant between the NH and H10 protons, of 9.8 Hz, was also indicative of a predominantly anti relationship between these protons[102,108], as in pederin.

The coupling constants (in Hz) between H10 and H11 (4.2), H11 and the two H12 protons (5.6, 6.1), and between H13 and the two H12 protons (4.1,7.9), were rather different to those recorded for pederin. The small H10-H11 constant was also noted for derivatives of pederin dibenzoate during synthetic studies[127,130] and had been ascribed to the presence of a similar conformation to that observed for pederin di-p-bromobenzoate in the solid state. However, this conformation could not explain the differences in the sizes of the C11 to C13 vicinal proton-proton coupling constants for the benzoates compared to those of pederin (Table 1.9), nor the observed

broadening of the 14-$CH_3S$ and the C11 carbon resonances. It was therefore more likely, based on results for mycalamide A, that there was a significant population of both chair conformations of the C11-C15 ring.

This proposal was confirmed by NOE results (Table 1.8). There were strong NOE interactions between H10 and H15 and between H13 and H15 suggestive of a significant contribution from the major chair conformation observed for pederin to the overall conformations of this C11-C15 ring. Irradiation of the more downfield H12 resonance gave strong enhancements of the NH, H11 and H13 resonances, whereas irradiation of the more upfield H12 resonance strongly enhanced the H11 and the more downfield 14-$CH_3$ resonances. This provided further support for this chair conformation and allowed an assignment of the stereochemistry associated with the two H12 and 14-$CH_3$ resonances. However, irradiation of H11 gave strong enhancements of the H10 and the more downfield H16 resonances, and there were weak interactions between H12*R* and 14-$CH_3R$, H12*S* and H13, H13 and 14-$CH_3S$, for example, which required the (minor) presence of an alternate chair conformation for the C11-C15 ring. Thus it is proposed that this ring was involved in conformational exchange between these two chair conformations. Molecular mechanics calculations to determine approximate relative proportions of these conformations are described in a following subsection.

The vicinal proton-proton coupling constants from C15 to C18 were very similar to those observed for pederin, implying a similar mixture of solution conformations for this substructure in both compounds. Thus C17 was predominantly anti to C14 about the C15-C16 bond, so that the stereochemistry associated with the H16 resonances could also be assigned, as for pederin.

### 1.5.4 SOLUTION CONFORMATIONS OF PEDERIN DIBENZOATE IN $D_4$-METHANOL

In order to compare the conformations above more conclusively with the solid state conformation of pederin di-p-bromobenzoate (**1.1**), it was appropriate to also consider the conformations of pederin dibenzoate (**1.2**) in methanol, which was the crystallisation solvent in the first reported crystal structure analysis[34]. The $^1H$ NMR spectrum of pederin dibenzoate in $CD_3OD$ was readily assigned by comparison with the data recorded in $CDCl_3$ and these assignments were confirmed by the results of a COSY experiment (Table 1.7). A $^{13}C$ NMR spectrum was also recorded and assigned by comparison with the data recorded in $CDCl_3$ (Table 1.3). Note that the C11 and 14-$CH_3$*S* resonances were slightly broad in this spectrum also.

Selected NOE experiments were performed and the results are shown in Table 1.8. There were similar NOE interactions observed to those found above for $CDCl_3$ solution, including H10-H15, H13-H15, H11-H16*R* and H10-H11. These results indicated that the same two chair conformations of the C11-C15 ring were also present in this solvent as in $CDCl_3$. This was confirmed by an analysis of the vicinal proton-proton coupling constants from C10 to C13. The H10-H11 constant, 3.4 Hz, was smaller than in $CDCl_3$, suggesting a higher contribution from a conformer having the H10-H11 protons in a gauche relationship[102,127]. By comparison, the remaining coupling constants for this portion of the structure were all within 0.5 Hz of the values recorded in $CDCl_3$, so that there was likely to be a similar ratio of the chair conformations of this ring in both solvents. Also the coupling constants for the C15-C18 portion were fairly similar. Thus it appeared that a similar set of solution conformations of this compound were present in both $CDCl_3$ and $CD_3OD$.

## 1.5.5 MOLECULAR MECHANICS CALCULATIONS AND CONCLUSIONS

Modification of the x-ray structure of pederin di-p-bromobenzoate (**1.1**), by removal of the bromine atoms and adding hydrogen atoms throughout the structure, provided a starting structure of pederin dibenzoate (**1.2**). Energy minimisation thus gave a conformation which had the H10 and H11 protons in a gauche relationship. Rotation about the C10-C11 bond and reminimisation gave a slightly higher energy conformation[58], having the H10 and H11 protons in an anti relationship, as shown in Figure 1.15a. An alternate chair conformation was also generated[84] and the minimised conformation is shown in Figure 1.15b. The calculated coupling constants for these conformations (designated **1.2A** and **1.2B**, respectively) have been listed in Table 1.9, and it is readily apparent that the experimental values required a combination of the two proposed conformations. Equal contributions from these conformations gave averaged values that were all within 2 Hz of the experimental values, so this would seem to a reasonable approximation given the inevitable inaccuracies in the calculated values[102,103]. This result was not quite in accordance with the observed NOE results, which appeared to indicate a major 'normal' chair conformation, but was reasonable. Note that the calculated energies could not be used to predict ratios of these conformations since a full conformational search involving all the rotatable bonds in the molecule had not been performed.

Thus it has been shown that the solution state conformations of pederin dibenzoate (**1.2**) were indeed different to the solid state conformations of pederin di-p-bromobenzoate (**1.1**). This illustrates the importance of intermolecular forces, as well as intramolecular forces, in determining the favoured conformation, and similar forces are likely to be involved in interactions with the unknown active site. Therefore any one of several low energy solution conformations may be the active conformation[16,70,71,122].

With large flexible structures such as pederin and the mycalamides, the design and biological testing of conformationally restricted analogues[70,92] could lead to a more conclusive understanding of the active site geometry. The synthetic modifications of the mycalamides are a first step in such a direction.

**Figure 1.15** Alternate chair conformations (**1.2A** and **1.2B**, respectively) for the C11-C15 ring of pederin dibenzoate (**1.2**), as calculated by molecular modelling (methyl and aromatic protons not shown).

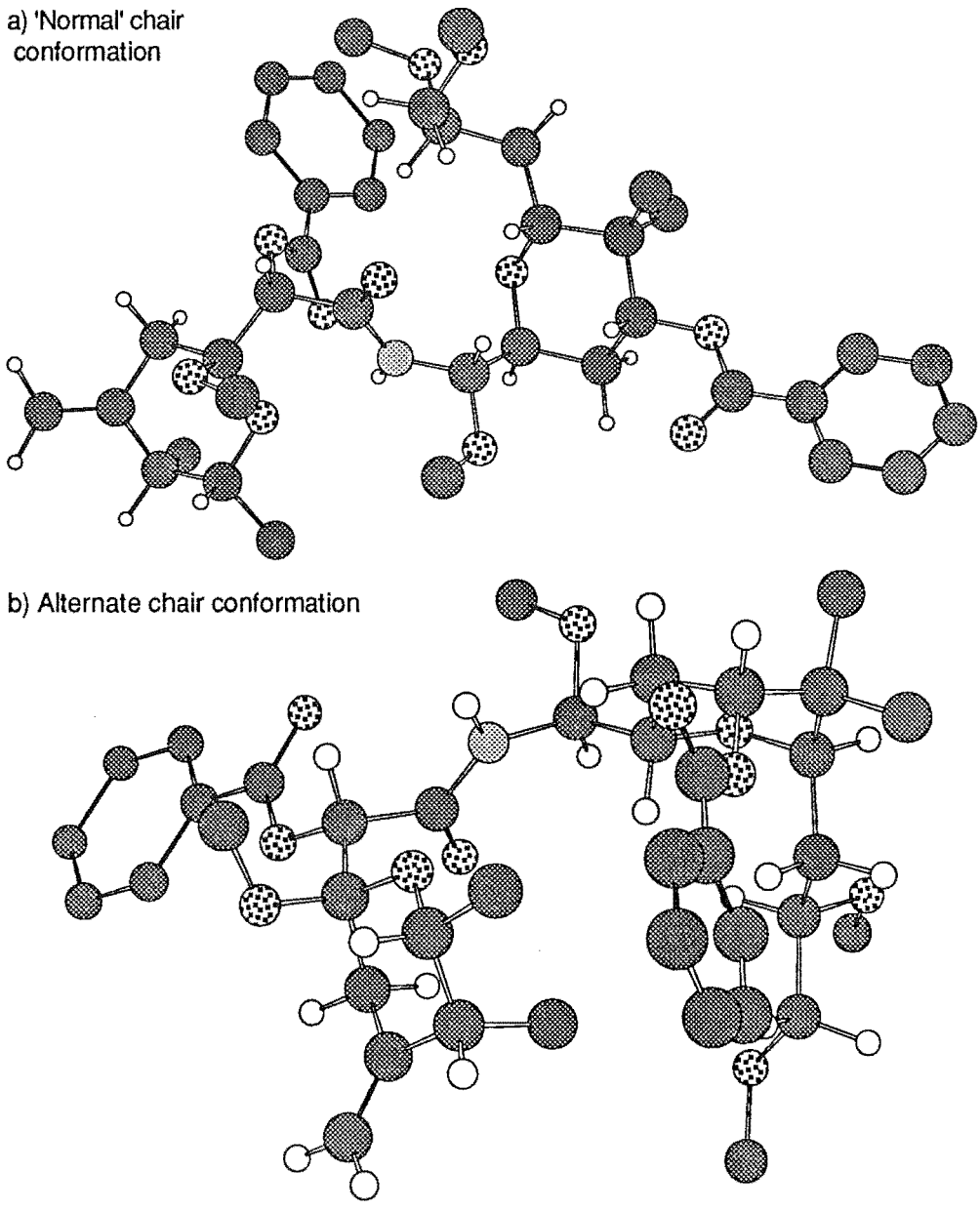

**Table 1.1** $^1$H NMR data[a] for mycalamides A and B in various solvents.

| Proton[b] | Typical[c] multiplicity | Mycalamide A ($CDCl_3$) | Mycalamide A ($CD_3OD$) | Mycalamide A ($d_6$-DMSO) | Mycalamide B ($CDCl_3$) | Mycalamide B ($C_6D_6$) |
|---|---|---|---|---|---|---|
| H2 | dq | 3.98 (2.7,6.6) | 3.88 (2.6,6.6) | 3.83 (2.4,6.5) | 4.02 (2.8,6.6) | 3.98 (2.8,6.6) |
| 2-$CH_3$ | d | 1.19 (6.6) | 1.16 (6.6) | 1.16 (6.6) | 1.19 (6.6) | 0.99 (6.6) |
| H3 | dq | 2.23 (2.7,7.0) | 2.19 (2.7,7.1) | 2.24 (2.1,6.9) | 2.25 (2.8,7.0) | 2.04 (2.7,7.3) |
| 3-$CH_3$ | d | 0.99 (7.0) | 0.96 (7.1) | 0.97 (7.0) | 1.01 (7.1) | 1.10 (7.2) |
| 4=CH*Z* | t or m | 4.84 (m) | 4.79 (2.1) | 4.84 (m) | 4.85 (1.9) | 4.89 (2.0) |
| 4=CH*E* | t or m | 4.72 (m) | 4.65 (2.2) | 4.67 (m) | 4.71 (1.8) | 4.84 (2.1) |
| H5a | td | 2.36 (m) | 2.41 (2.1,14.3) | 2.49 (m,14.5) | 2.23 (1.9,14.0) | 2.59 (2.0,14.1) |
| H5e | d | 2.36 (m) | 2.30 (14.2) | 2.29 (14.4) | 2.36 (14.0) | 2.78 (14.0) |
| 6-$OCH_3$ | s | 3.29 | 3.24 | 3.22 | 3.29 | 3.34 |
| H7 | s or d | 4.31 | 4.29 | 4.20 (4.4) | 4.28 | 4.37 |
| 7-OH | s or d | | | 5.76 (4.5) | | |
| NH9 | d | 7.51 (9.7) | | 8.37 (9.3) | 7.53 (9.6) | 6.91 (6.5) |
| H10 | t or dd | 5.87 (9.7) | 5.81 (9.5) | 5.80 (9.0) | 5.78 (9.6) | 6.03 (6.5,10.0) |
| 10-OCH*R* | d | 5.13 (6.9) | 5.21 (6.9) | 5.24 (7.0) | 5.11 (7.0) | 4.77 (6.9) |
| 10-OCH*S* | d | 4.87 (6.9) | 4.80 (6.9) | 4.85 (6.9) | 4.84 (6.9) | 4.71 (6.9) |
| H11 | dd | 3.86 (6.8,9.7) | 3.98 (6.5,9.4) | 4.02 (6.0,8.8)[d] | 3.78 (6.8,9.7) | 3.87 (6.9,10.1) |
| H12 | dd | 4.22 (6.8,10.3) | 4.17 (6.6,9.9) | 4.14 (6.2,9.5) | 4.20 (6.8,10.4) | 4.41 (7.0,10.6) |
| H13 | d | 3.46 (10.3) | 3.66 (10.1) | 3.77 (9.4)[d] | 3.43 (10.3) | 3.17 (10.6) |
| 13-$OCH_3$ | s | 3.55 | 3.56 | 3.54 | 3.54 | 3.41 |
| 14-$CH_3$*R* | s | 0.97 | 1.00 | 1.03 | 0.97 | 0.97 |
| 14-$CH_3$*S* | s | 0.87 | 0.86 | 0.86 | 0.85 | 0.94 |
| H15 | d | 3.62 (5.5,7.1) | 3.49 (2.4,10.6) | 3.47 (m) | 3.41 (3.3,8.7) | 3.58 (m) |
| H16 | ddd or m | 1.54 (m) | 1.66 (2.3,7.0,14.2) | 1.68 (1.9,8.1,14.3) | 1.54 (m) | 1.73 (m) |
| H16 | ddd or m | 1.54 (m) | 1.49 (5.6,10.4,14.2) | 1.41 (m)[d] | 1.54 (m) | 1.73 (m) |
| H17 | m | 3.74 (m) | 3.69 (m) | 3.56 (m) | 3.20 (m) | 3.51 (m) |
| 17-$OCH_3$ | s | | | | 3.24 | 3.21 |
| H18 | dd | 3.57 (3.5,11.3) | 3.50 (3.8,11.3) | 3.39 (4.0,11.4) | 3.65 (3.3,11.9) | 4.00 (3.6,11.9) |
| H18 | dd | 3.38 (6.2,11.3) | 3.38 (6.3,11.4) | 3.32 (5.2,11.4) | 3.46 (5.7,11.9) | 3.88 (5.3,11.8) |

[a]All data were recorded in the stated solvents, with chemical shifts in ppm relative to $CHCl_3$, δ7.25, $CHD_2OD$, δ3.30, $CHD_2SOCD_3$, δ2.60, $C_6HD_5$, δ7.27 (coupling constants in Hz). [b]Methylene proton or methyl group prochiral stereochemistries were assigned by NOE experiments.
[c]Appearance of signal: s=singlet, d=doublet, t=triplet, m=multiplet [d]Resonances showed unusual line broadening.

**Table 1.2** $^{1}H$-$^{1}H$ NOE interactions[a] for mycalamides A and B.

| Compound | Signal(s) irradiated | Signals enhanced (% enhancement) |
|---|---|---|
| Mycalamide A | H2 | 2-$CH_3$(2), H3(7), 6-$OCH_3$(2) |
| | 2-$CH_3$ | H2(9), H3(2) |
| | H3 | H2(9), 3-$CH_3$(2), 4=CH*Z*(6) |
| | 3-$CH_3$ (14-$CH_3$*R*) | H3(6), $H_2$5(1), NH(1), H11(1), H13(4)[b], 13-$OCH_3$(0.8)[b], H15(3)[b], $H_2$16(3)[b] |
| | 4=CH*Z* | H3(6), 4=CH*E*(21), 10-OCH*R*(6)[b] |
| | 4=CH*E* | 4=CH*Z*(21), $H_2$5(1) |
| | $H_2$5 | 3-$CH_3$(0.9), 4=CH*E*(6)[b], 6-$OCH_3$(0.4), H7(2), NH(3) H17(1) |
| | 6-$OCH_3$ | H2(7), $H_2$5(0.5), H7(7) |
| | H7 | 6-$OCH_3$(3), NH(2) |
| | NH | H7(3), H11(6) |
| | H10 | 10-OCH*R*(4), H13(3), H15(6) |
| | 10-OCH*R* | H10(5), 10-OCH*S*(19), H13(5), 13-$OCH_3$(0.7) |
| | 10-OCH*S* (4=CH*Z*) | H3(3)[b], 4=CH*E*(7)[b], 10-OCH*R*(14) |
| | H11 | NH(4), H12(10) |
| | H12 | H11(9), 14-$CH_3$*S*(1) |
| | H13 (H18u[c]) | H10(5), 10-OCH*R*(5), 13-$OCH_3$(1), 14-$CH_3$*R*(0.9), H15(4), H18d(4)[b,c] |
| | 13-$OCH_3$ (H18d[c]) | 10-OCH*R*(2), H12(1), H13(3), 14-$CH_3$*R*(0.5), H17(4)[b], H18u(3)[b,c] |
| | 14-$CH_3$*R* (3-$CH_3$) | H3(3)[b], H5(1)[b], H13(5), 13-$OCH_3$(1), H15(4), $H_2$16(3) |
| | 14-$CH_3$*S* | H12(10), $H_2$16(2) |
| | H15 (13-$OCH_3$, H18d[c]) | H10(10), H13(3), 14-$CH_3$*R*(1), $H_2$16(2), H17(6), H18u(8)[b,c] |
| | $H_2$16 | 14-$CH_3$*R*(2), 14-$CH_3$*S*(1), H15(2), H17(5), H18u(1)[c] |
| | H17 | $H_2$16(1) |
| | H18d[c] (H15, 13-$OCH_3$) | H10(10)[b] ,H13(3)[b], 14-$CH_3$*R*(1)[b], $H_2$16(2), H17(6), H18u(8)[c] |
| | H18u[c] | $H_2$16(1), H17(2), H18d(1)[c] |
| Mycalamide B | 3-$CH_3$ (14-$CH_3$*R*) | 2-$CH_3$(1), H3(5), H5a(3), NH(2), H11(3), H13(1)[b], H15(1)[b], $H_2$16(0.5)[b], H17(0.8), 17-$OCH_3$(0.5) |
| | H5a (H3) | H2(5)[b], 2-$CH_3$(0.4)[b], 3-$CH_3$(2), 4=CH*Z*(4)[b], H5e(14), H7(2), NH(1), H17(3) |
| | H5e | 4=CH*E*(5), H5a(12), H7(0.4) |
| | 6-$OCH_3$ (H13, H15) | H2(5), H7(9), H10(0.9)[b], 10-OCH*R*(0.5)[b] |
| | H7 (H12) | H5a(0.4), 6-$OCH_3$(3), NH(3), H11(0.8)[b] |
| | NH | H5a(0.8), H7(4), H11(7) |
| | H10 | NH(1), 10-OCH*R*(4), H13(5), H15(5) |
| | H11 | 3-$CH_3$(0.7), NH(5), H10(1), H12(10) |
| | 14-$CH_3$*R* (3-$CH_3$) | H3(2)[b], H5a(1)[b], H13(6), 13-$OCH_3$(1), H15(6), $H_2$16(3), 17-$OCH_3$(0.3) |
| | 14-$CH_3$*S* | H12(4), $H_2$16(2) |
| | $H_2$16 | 14-$CH_3$*R*(2), 14-$CH_3$*S*(2), H15/H18u(5)[c], H17(5), H18d(2)[c] |
| | H17 (17-$OCH_3$) | H5a(2), $H_2$16(1), H18d(2)[c] |
| | 17-$OCH_3$ (H17, 6-$OCH_3$) | H5a(0.5)[b], H7(0.8)[b], $H_2$16(2), H18d(1)[c] |

[a]All were data recorded in $CDCl_3$ [b]Enhancement interpreted as being due to the irradiation of an overlapping signal [c]Higher field (u) or lower field (d) signal of a geminal pair.

**Table 1.3** $^{13}C$ NMR data[a,b] for mycalamides A and B, pederin, and pederin dibenzoate in various solvents.

| | Myc.A ($CDCl_3$) | Myc.A ($CD_3OD$) | Myc.A ($d_6$-DMSO) | Myc.B ($CDCl_3$) | Myc.B ($C_6D_6$) | Pederin ($CDCl_3$) | Pederin dibenzoate (**1.2**) ($CDCl_3$) | ($CD_3OD$) |
|---|---|---|---|---|---|---|---|---|
| **C2** | 69.81 | 71.14 | 69.09 | 69.63 | 69.93 | 69.57 | 69.68 | 71.03 |
| **2-$CH_3$** | 17.88 | 18.40 | 18.61 | 19.94 | 18.36 | 17.92 | 17.91 | 18.56 |
| **C3** | 41.37 | 43.33 | 41.86 | 41.27 | 42.25 | 41.32 | 41.35 | 43.12 |
| **3-$CH_3$** | 12.02 | 12.59 | 12.50 | 12.15 | 12.89 | 12.07 | 11.98 | 12.66 |
| **C4** | 145.65 | 148.51 | 148.24 | 145.10 | 146.33 | 145.72 | 145.67 | 147.98 |
| **4=$CH_2$** | 110.55 | 110.32 | 109.88 | 111.03 | 111.24 | 110.62 | 110.48 | 110.70 |
| **C5** | 33.75 | 34.80 | 34.21 | 33.66 | 34.74 | 34.14 | 34.09 | 34.90 |
| **C6** | 99.83 | 101.67 | 100.58 | 99.92 | 100.94 | 99.74 | 99.36 | 110.84 |
| **6-$OCH_3$** | 48.94 | ? | 48.53 | 48.59 | 48.86 | 49.04 | 48.62 | ? |
| **C7** | 72.92 | 73.93 | 72.97 | 71.75 | 72.80 | 72.84 | 72.64 | 74.42 |
| **C8** | 171.82 | 175.11 | 172.31 | 171.79 | 172.75 | 171.77 | 167.44 | 170.60 |
| **C10** | 73.74 | 75.24 | 74.28 | 73.93 | 74.70 | 79.43 | 81.71 | 84.70 |
| **10-$OCH_2$** | 86.84 | 88.02 | 86.69 | 86.49 | 86.94 | | | |
| **10-$OCH_3$** | | | | | | 56.41 | 56.43 | 56.95 |
| **C11** | 71.26 | 71.32[c] | 69.23[c] | 70.94 | 72.42 | 72.77 | 70.25[c] | 71.52[c] |
| **C12** | 74.42 | 75.95 | 74.28 | 74.44 | 75.68 | 29.59 | 26.62 | 26.86 |
| **C13** | 79.15 | 80.88 | 79.77 | 79.30 | 79.32 | 71.98 | 75.07 | 77.00 |
| **13-$OCH_3$** | 61.81 | 62.25 | 61.59 | 61.77 | 61.86 | | | |
| **C14** | 41.66 | 42.63 | ? | 41.46 | 42.15 | 38.60 | 37.10 | 38.43 |
| **14-$CH_3$*R*** | 23.11 | 23.82 | 24.13 | 23.17 | 23.40 | 23.00 | 24.75 | 25.63 |
| **14-$CH_3$*S*** | 13.49 | 14.50[c] | 15.20[c] | 13.35 | 13.78 | 12.93 | 17.36[c] | 18.29[c] |
| **C15** | 78.99 | 78.67 | 76.54 | 75.51 | 76.15 | 75.85 | 76.72 | 78.31 |
| **C16** | 31.99 | 33.68 | 33.31 | 29.68 | 31.00 | 30.09 | 29.14 | 30.75 |
| **C17** | 71.64 | 72.32 | 70.24 | 78.80 | 79.62 | 77.69 | 77.53 | 79.72 |
| **17-$OCH_3$** | | | | 56.65 | 57.08 | 56.81 | 56.88 | 57.58 |
| **C18** | 66.49 | 66.62 | 65.24 | 63.45 | 64.41 | 73.81 | 72.82 | 74.02 |
| **18-$OCH_3$** | | | | | | 59.17 | 59.21 | 59.75 |

[a]All data were recorded in the stated solvents, with chemical shifts in ppm relative to $CDCl_3$, δ77.01, $CD_3OD$, δ49.30, $(CD_3)_2SO$, δ40.5, or $C_6D_6$, δ128.40.
[b]Benzoate ester carbon resonances are listed in the Experimental section. [c]These signals were unusually broad.

**Table 1.4** $^{2}J_{CH}$ and $^{3}J_{CH}$ HMBC and XCORFE correlations[a] for mycalamide A and pederin.

| Compound (Expt) | Detected signal | Correlated resonances |
|---|---|---|
| Mycalamide A (HMBC) | H2 | 3-$CH_3$ |
| | 2-$CH_3$ | C2, C3 |
| | H3 | 3-$CH_3$,C4, 4=$CH_2$ |
| | 3-$CH_3$ | C2, C3, C4 |
| | 4=CH*E/Z* | C3, C5 |
| | $H_2$5 | C3, C4, 4=$CH_2$, C6 |
| | 6-$OCH_3$ | C6 |
| | H7 | C6, C8 |
| | NH9 | C8, C10 (weak) |
| | H10 | C8 (weak) |
| | 10-OCH*R/S* | C10, C12 |
| | H11 | C10, C12, C13 |
| | H12 | C10, 10-$OCH_2$, C11, C13 |
| | H13 | C12, 13-$OCH_3$, C14, 14-$CH_3$*R*, 14-$CH_3$*S* |
| | 13-$OCH_3$ | C13 |
| | 14-$CH_3$*R* | C13, C14, 14-$CH_3$*S*, C15 |
| | 14-$CH_3$*S* | C13, C14, 14-$CH_3$*R*, C15 |
| | H15 | 14-$CH_3$*S*, C16 |
| | $H_2$16 | C14, C15, C17, C18 |
| | H18 | C16 |
| Mycalamide A (XCORFE) | C2 | 2-$CH_3$, 3-$CH_3$ |
| | C4 | 3-$CH_3$, $H_2$5 |
| | 4=$CH_2$ | $H_2$5 |
| | C6 | H2, $H_2$5, 6-$OCH_3$, H7 |
| | C8 | H7, H10 |
| | C10 | NH9 |
| | 10-$OCH_2$ | H12 |
| | 13-$OCH_3$ | H13 |
| | C14 | 14-$CH_3$*S* |
| | 14-$CH_3$*R* | 14-$CH_3$*S* |
| Pederin (HMBC) | H2 | 3-$CH_3$ |
| | 2-$CH_3$ | C2, C3 |
| | H3 | 3-$CH_3$,C4, 4=$CH_2$, C5 |
| | 3-$CH_3$ | C2, C3, C4 |
| | 4=CH*E/Z* | C3, C5 |
| | H5a/e | C3, C4, 4=$CH_2$, C6 |
| | 6-$OCH_3$ | C6 |
| | H7 | C6, C8 |
| | NH | C8 (weak) |
| | H10 | C8, 10-$OCH_3$ |
| | 10-$OCH_3$ | C10 |
| | H11 | C10, C12, C13, C15 |
| | H12*R/S* | C10, C13, C14 |
| | 14-$CH_3$*R* | C13, C14, 14-$CH_3$*S*, C15 |
| | 14-$CH_3$*S* | C13, C14, 14-$CH_3$*R*, C15 |
| | H16*R/S* | C17, C18 |
| | 18-$OCH_3$ | C18 |

[a]All data were recorded in $CDCl_3$

**Table 1.5** $^1$H-$^1$H NOE interactions[a] for mycalamide A in other solvents.

| Compound | Signal(s) Irradiated | Signals enhanced (% enhancement) |
|---|---|---|
| Mycalamide A ($CD_3OD$) | H2 | 2-$CH_3$(2), H3(8), 6-$OCH_3$(2) |
| | H3 | H2(8), 2-$CH_3$(1), 3-$CH_3$(2), 4=C*H**Z***(6) |
| | 3-$CH_3$ (14-$CH_3$*R*) | 2-$CH_3$(2), H3(8), H5a(4), H11(1) |
| | 4=C*H**E*** | 4=C*H**Z***(19), H5e(4) |
| | H5a | 3-$CH_3$(2), H5e(15), H7(4) |
| | H5e | 4=C*H**E***(7), H5a(18), H7(0.8) |
| | 6-$OCH_3$ | H2(8), H7(10) |
| | H7 | 6-$OCH_3$(3) |
| | 13-$OCH_3$ | 14-$CH_3$*R*(1) |
| | H16d[c] | 14-$CH_3$*R*(2), 14-$CH_3$*S*(0.6), H15/H18d(2)[c], H16u(8)[c], H17(3), H18u(1)[c] |
| | H16u[c] | 14-$CH_3$*S*(1), H16d(12)[c], H17(3) |
| | H18u[c] | H17(5), H18d(9)[c] |
| Mycalamide A ($d_6$-DMSO) | H5a | 3-$CH_3$(1), H5e(9), H7(2), NH(0.9) |
| | H5e (H3) | H2(5)[b], 2-$CH_3$(0.3)[b], 3-$CH_3$(0.8)[b], 4=C*H**E***(3), 4=C*H**Z***(3)[b], H5a(10), H7(0.3), 7-OH(0.5) |
| | H7 | H5a(0.9), 6-$OCH_3$(2), 7-OH(1), NH(2) |
| | NH | H5a(0.9), H7 (3), 10-OC*H**S***(0.9), H11(4), H12(0.8) |
| | H10 (7-OH) | H7(3)[b], NH(2)[b], 10-OC*H**R***(2), H11(0.8), H13(2) |
| | H11 | NH(3), H10(0.7) |
| | H12 (H7) | 6-$OCH_3$(0.4)[b], NH(1)[b], 10-OC*H**S***(0.8), 13-$OCH_3$(0.5), 14-$CH_3$*S*(1) |
| | H13 (H2) | 2-$CH_3$(0.6)[b], H3(2)[b], 6-$OCH_3$(0.6)[b], H10(2), 10-OC*H**R***(4), 14-$CH_3$*R*(1), 14-$CH_3$*S*(0.3) |
| | 14-$CH_3$*R* | H13(3), 13-$OCH_3$(1), 14-$CH_3$*S*(0.8), H16d(3)[c] |
| | 14-$CH_3$*S* | H12(4), 13-$OCH_3$(0.4), 14-$CH_3$*R*(0.5), H16u(1)[c] |
| | H16d[c] | 14-$CH_3$*R*(0.5), 14-$CH_3$*S*(0.3), H16u(4)[c], H17(2) |
| | H16u[c] | H11(1), 14-$CH_3$*S*(0.4), H16d(6)[c], H17(3) |

[a]All data were recorded in the stated solvents, $CD_3OD$ and $d_6$-DMSO
[b]Enhancement interpreted as being due to the irradiation of an overlapping signal
[c]Higher field (u) or lower field (d) signal of a geminal pair.

**Table 1.6** Comparison of calculated vicinal proton-proton coupling constants for the model structures, **1.3A** and **1.3B**, with experimental values recorded for mycalamide A[a].

| Protons | Experimental (Myc.A) | Calculated values (dihedral angles) **1.3A** | **1.3B** |
|---|---|---|---|
| H10-H11 | 9.7 | 8.4 (176) | 1.7 (71) |
| H11-H12 | 6.8 | 6.1 (45) | 1.4 (53) |
| H12-H13 | 10.3 | 9.1 (172) | 2.2 (73) |

[a]Coupling constants measured in Hz; experimental values recorded in $CDCl_3$ solution.

**Table 1.7** $^{1}H$ NMR data[a,b] for onnamide A, pederin and pederin dibenzoate.

| | Onnamide A | Pederin | Pederin dibenzoate (**1.2**) ($CDCl_3$) | ($CD_3OD$) |
|---|---|---|---|---|
| **H2** | 3.87 (2.4,6.5) | 3.99 (2.7,6.6) | 3.96 (2.6,6.6) | 3.81 (2.5,6.5) |
| **2-$CH_3$** | 1.17 (6.5) | 1.18 (6.6) | 1.11 (6.6) | 0.94 (6.6) |
| **H3** | 2.18 (m) | 2.24 (2.6,7.1) | 2.21 (2.5,7.3) | 2.12 (2.4,7.1) |
| **3-$CH_3$** | 0.96 (6.9) | 1.00 (7.1) | 0.96 (7.3) | 0.86 (7.0) |
| **4=CH*Z*** | 4.79 (m) | 4.85 (1.8) | 4.86 (1.8) | 4.80 (7.0) |
| **4=CH*E*** | 4.63 (m) | 4.73 (1.8) | 4.79 (1.8) | 4.71 (2.2) |
| **H5a** | 2.40 (m,14.4) | 2.32 (1.9,14.3) | 2.76 (1.8,14.4) | 2.87 (2.2,14.5) |
| **H5e** | 2.32 (14.4) | 2.43 (14.2) | 2.49 (14.4) | 2.39 (14.6) |
| **6-$OCH_3$** | 3.22 | 3.33 | 3.24 | 3.21 |
| **H7** | 4.23 | 4.30 (2.2) | 5.50 | 5.47 |
| **7-OH** | | 3.92 (2.3) | | |
| **NH9** | | 7.15 (9.7) | 6.78 (9.8) | |
| **H10** | 5.79 (9.3) | 5.38 (8.0,9.7) | 5.34 (4.3,9.7) | 5.30 (3.4) |
| **10-$OCH_3$** | | 3.38 | 3.45 | 3.47 |
| **10-OCH*R*** | 5.18 (6.9) | | | |
| **10-OCH*S*** | 4.80 (6.9) | | | |
| **H11** | 3.98 (6.5,9.3) | 3.78 (2.3,6.2,8.0) | 3.95 (4.0,5.8) | 3.97 (3.4,5.5,6.5) |
| **H12*R*** | | 2.04 (2.4,4.6,13.4) | 2.15 (4.3,6.2,13.8) | 2.30 (4.3,6.6,14.0) |
| **H12*S*** | 4.16 (6.5,9.7) | 1.76 (6.2,11.2,13.3) | 1.81 (5.6,7.7,13.6) | 1.85 (5.5,7.3,14.0) |
| **H13** | 3.62 (9.6) | 3.63 (4.8,11.1) | 5.14 (4.1,7.8) | 5.25 (4.3,7.3) |
| **13-$OCH_3$** | 3.55 | | | |
| **14-$CH_3$*R*** | 1.00 | 0.93 | 0.98 | 1.05 |
| **14-$CH_3$*S*** | 0.85 | 0.86 | 1.00 | 1.01 |
| **H15** | 3.47 (3.6,8.1) | 3.23 (2.0,10.1) | 3.63 (2.4,11.2) | 3.76 (2.4,11.2) |
| **H16*R*** | 1.53 (m) | 1.68 (3.4,10.0,14.2) | 2.05 (2.4,11.2,13.5) | 2.09 (3.6,11.3,14.6) |
| **H16*S*** | 1.53 (m) | 1.57 (2.1,9.4,14.2) | 1.79 (2.4,8.6,13.6) | 1.82 (2.4,8.6,14.5) |
| **H17** | 3.64 (m) | 3.38 (m) | 3.48 (m) | 3.54 (m) |
| **17-$OCH_3$** | | 3.32 | 3.35 | 3.37 |
| **H18** | 1.49 (m) | 3.44 (1.8,9.5) | 3.53 (2.5,9.1) | 3.57 (2.4,8.7) |
| **H18** | 1.28 (m) | 3.32 (5.9,9.5) | 3.43 (3.6,9.1) | 3.51 (5.2,8.9) |
| **18-$OCH_3$** | | | 3.36 | 3.35 |

[a]Data for onnamide (in $CD_3OD$) were reproduced from reference 31, omitting data beyond C18. Data for pederin were measured in $CDCl_3$, with chemical shifts in ppm relative to $CHCl_3$, δ7.25 (coupling constants in Hz). Data for pederin dibenzoate were measured in the stated solvents, where chemical shifts in $CD_3OD$ were relative to $CHD_2OD$, δ3.30 ppm.

[b]Aromatic proton resonances are listed in the Experimental section.

**Table 1.8** $^{1}H$-$^{1}H$ NOE interactions for pederin and pederin dibenzoate (**1.2**).

| Compound | Signal(s) irradiated | Signals enhanced (% enhancement) |
|---|---|---|
| Pederin | H2 | 2-$CH_3$(2), H3(6) |
| | H5a (H3) | H2(1)[b], 3-$CH_3$(1), H5e(11), H7(3), NH(0.8) |
| | H5e | 4=CH*E*(6), H5a(10), H7(0.5) |
| | H7 | H5a(2), H5e(0.5), 6-$OCH_3$(2), 7-OH(1), NH(3) 10-$OCH_3$(0.5) |
| | 7-OH (H2, H12*S*, 2x H16) | 2-$CH_3$(0.7)[b], H3(2)[b], H5e(0.8), 6-$OCH_3$(0.8), H7(6), NH(3), 10-$OCH_3$(0.5), H13(1)[b], 14-$CH_3R$(0.5)[b], 14-$CH_3S$(0.5)[b] |
| | NH | 3-$CH_3$(0.5), H5a(0.5), 6-$OCH_3$(0.5), H7(4), H10(2), 10-$OCH_3$(0.5), H11(6) |
| | H10 | NH(1), 10-$OCH_3$(2), H11(3), H13(6), H15(7) |
| | H11 | NH(4), H10(1), H12*R*(2), H12*S*(3) |
| | H12*R* | H10(1), H11(2), H12*S*(15), H13(4) |
| | H12*S* (H16*R*) | H11(6), H12*R*(16), 14-$CH_3S$(2), H16*S*(4) |
| | H13 | H10(6), H12*R*(4), 14-$CH_3R$(2), 14-$CH_3S$(0.5), H15(4) |
| | 14-$CH_3R$ | H13(6), H15(6), H16*S*(3) |
| | 14-$CH_3S$ (14-$CH_3R$) | H12*S*(5), H13(2)[b], H15(1)[b], H16*R*(2), H16*S*(1) |
| | H15 (6-$OCH_3$, 17-$OCH_3$, H18u[c]) | H10(8), H13(6), 14-$CH_3R$(2), H16*S*(1), H18d(3)[c] |
| Pederin dibenzoate (**1.2**) | 2-$CH_3$ | H2(10), H3(4) |
| | H3 (H12*R*) | H2/H11(4), 2-$CH_3$(0.6), 3-$CH_3$(2), 4=CH*Z*(6), NH(1)[b] H12*S*(7)[b], H13(3)[b] |
| | 4=CH*Z* | H3(9), 4=CH*E*(9) |
| | 4=CH*E* | 4=CH*Z*(13), H5e(5) |
| | H5a | 3-$CH_3$(1), H5e(24), H7(2) |
| | 6-$OCH_3$ | H2(6), H7(11) |
| | H7 | 6-$OCH_3$(4), NH(6) |
| | NH | H7(11), H10(2), 10-$OCH_3$(0.3), H11(3) |
| | H10 | NH(1), 10-$OCH_3$(3), H11(3), H15(4) |
| | 10-$OCH_3$ (H17, H18u[c]) | H7(0.6), NH(1), H10(4), H15(2)[b] |
| | H11 (H2) | 2-$CH_3$(2)[b], H3(7)[b], 6-$OCH_3$(2)[b], NH(3), H10(5), H12*S*(2), H16*R*(3) |
| | H12*R* (H3) | H2/H11(4), 2-$CH_3$(0.6)[b], 3-$CH_3$(0.7)[b], 4=CH*Z*(3)[b], NH(3), H12*S*(12), H13(6), 14-$CH_3R$(0.7) |
| | H12*S* (H16*S*) | H10(1), H11(3), H12*R*(16), H13(1), 14-$CH_3S$(2), H15(4)[b], H16*R*(13)[b], H17(2)[b] |
| | H13 | H12*R*(3), H12*S*(1), 14-$CH_3R$(1), 14-$CH_3S$(0.7), H15(4) |
| | H15 | H10(5), H13(4), 14-$CH_3R$(0.8), H16*S*(1) |
| | H16*R* (H12*R*) | H11(4), H13(1)[b], 14-$CH_3S$(0.6), H16*S*(9), H17(2), 17-$OCH_3$(1) |
| Pederin dibenzoate (**1.2**) ($CD_3OD$) | H10 (H13) | 10-$OCH_3$(3), H11(6), 14-$CH_3R$(0.6)[b], H15(4) |
| | H11 | H10(8), H12*S*(3), H16*R*(2) |
| | H12*R* (H5e) | H5a(4)[b], H12*S*(10), H13(5) |
| | H13 (H10) | 10-$OCH_3$(1)[b], H11(4)[b], H12*R*(4), 14-$CH_3R$(1), H15(5) |
| | H15 (H2) | 2-$CH_3$(0.8)[b], H3(3)[b], H10(3), H13(4), 14-$CH_3R$(1) |

[a]All data were recorded in $CDCl_3$ unless otherwise stated. [b]Enhancement interpreted as due to the irradiation of an overlapping signal. [c]Higher field (u) or lower field (d) signal of a geminal pair.

**Table 1.9** Comparisons of calculated vicinal proton-proton coupling constants for pederin di-p-bromobenzoate (**1.1**) and model conformations of pederin dibenzoate (**1.2A**, **1.2B**) with experimental values for pederin dibenzoate (**1.2**)[a].

| | Experimental | Calculated values (dihedral angles) | | | 50% |
|---|---|---|---|---|---|
| Protons | **1.2** | **1.1** | **1.2A** | **1.2B** | **1.2A/1.2B** |
| H10-H11 | 4.1 | 1.7 | 8.1 | 1.5 | 4.8 |
| H11-H12*R* | 5.9 | 0.9 | 1.2 | 11.4 | 6.3 |
| H11-H12*S* | 5.7 | 8.3 | 5.8 | 1.6 | 3.7 |
| H12*R*-H13 | 4.1 | 5.0 | 4.3 | 3.6 | 4.0 |
| H12*S*-H13 | 7.8 | 10.9 | 11.2 | 2.7 | 7.0 |

[a]Coupling constants measured in Hz; experimental values recorded in $CDCl_3$ solution.

# CHAPTER 2
# ESTERS, SILYL AND ALKYL ETHERS OF MYCALAMIDES A & B

## 2.1 INTRODUCTION

The overall aims of this research project, as defined in the Introduction, were to explore the chemistry of the mycalamides and to determine structure-activity relationships which would assist in the design of analogues. In particular, it was desirable to produce mycalamide derivatives with better or more selective antiviral or antitumour activity. Another objective was to obtain a crystalline heavy atom derivative for examination by x-ray crystallography, to confirm the stereochemistry, and to compare the solid state and solution conformations, as described in Chapter 1.

The mycalamide structure has many potentially reactive functional groups. As a first step towards achieving the above goals, the syntheses of a number of esters, silyl ethers and alkyl ethers were undertaken, to provide protected intermediates for use in further reactions. This work was also performed to establish the relative reactivity of the individual hydroxyl groups so that particular groups could be protected, as required, thus allowing more selective reactions to be performed. This relative reactivity depends on a combination of steric and electronic factors[76] and could provide important information about the structure. The requirements for effective protection of a particular hydroxyl group are that the derivatisation reaction be high yielding and specific, that the protecting group be stable to the desired sequence of chemical reactions and, usually, that the original hydroxyl group be readily regenerated, specifically and in high yield[76,131]. The protecting groups presented in this chapter represent a range of size and polarity and a range of

stabilities and methods of cleavage. Note that acetals were not considered because of potential problems with acid stability of existing groups in the mycalamide structure, as found for pederin[95,130,132,133]. Acid catalysed reactions of mycalamide A and derivatives will be considered in Chapter 3. This study also represents an introduction to the application of microscale reaction chemistry for working on the milligram scale, which included the use of small scale equipment, high yielding and accurate analytical chromatographic techniques and sensitive spectroscopic methods.

There was little work of this kind performed on pederin. No ethers of pederin were reported, but various esters and acetals of fragments were prepared during its total synthesis[127,134,135]. Pederin and various derivatives were commonly acetylated as a means of structural identification in an early study[27,94]. This acetate group was removed by reduction with lithium aluminium hydride. The only other reported esters of pederin were the di-p-bromobenzoate ester (**1.1**), which was successfully examined by xray crystallography[34,93], and the related dibenzoate ester[127,129,132] (**1.2**), used for NMR spectroscopic analysis, as described in Chapter 1.

## 2.2 SILYLATION OF MYCALAMIDES A AND B

### 2.2.1 PREPARATION AND CHARACTERISATION OF MYCALAMIDE A AND B TRIMETHYLSILYL ETHERS

Silyl ethers have found wide use in synthetic organic chemistry for the protection of active hydrogen functionalities and a large series of silyl groups and reagents have become available[78]. As protecting groups, they have the advantages of being formed and cleaved readily, in high yield and under mild reaction conditions[136], while possessing a range of stabilities, which also allows the selective addition or removal of different silyl ethers[137]. The most

simple of all these are the trimethylsilyl (TMS) ethers, which are also the least stable[138], but have found good use in gas chromatography and mass spectroscopy to give improved volatility, thermal stability and chromatographic behaviour[76], and limited use in carbohydrate chemistry[77,137].

The reaction of mycalamide A with *N,O*-bis-trimethylsilyl acetamide in pyridine at room temperature readily yielded a less polar derivative (by TLC), which was a mycalamide A tris-TMS ether (**2.1**) by HREIMS. The $^1$H NMR spectrum, recorded in $CDCl_3$, showed the presence of three new signals between δ0.0 and 0.2 ppm, of correct intensity for TMS ether groups at the three hydroxyl sites of mycalamide A. The amide nitrogen was not silylated, consistent with the lower reactivity of such groups to silylation[78]. The chemical shift changes on silylation were relatively minor and the spectrum was easily assigned using the observed spin multiplicities, coupling constants and chemical shifts, compared with those of mycalamide A (Table 2.1). In particular, the α-protons were almost unaffected, with the largest differences occurring in the H5e (+0.2), H15 (-0.3) and H16 (+0.2) signals, and smaller differences in signals assigned to H2, NH, H10, H11 and H16. These are best explained by steric interactions[123] involving the new, bulky TMS ethers, which may have caused changes in the solution conformations of the chain portions.

This derivative was not stable in $CDCl_3$ solution, probably due to the trace acidity associated with this solvent[95,139], which is considered more fully in a later chapter. However, the reprepared derivative was stable in $CD_2Cl_2$, allowing both $^1$H and $^{13}$C NMR spectra to be recorded. The $^1$H NMR data were almost identical in the two solvents, therefore to avoid repetition, where data in both solvents were recorded, only data in $CDCl_3$ solution have been reported. The $^{13}$C NMR data were assigned by comparison with those for mycalamide A, although some assignments remained uncertain at this point (Table 2.2). The C5, C7 and C15 resonances were shifted most, with C16-

C18 also slightly affected. These shifts[117] would also result from changes in conformation and shielding effects associated with the proximity of the new TMS ether groups. A noticeable feature was the selective broadening of the 14-$CH_3$*S* and C11 resonances (and the other C12-C15 resonances to a lesser extent), and this was found to be a general feature of the $^{13}C$ NMR spectra of all the mycalamide A and B esters and silyl ethers. This may indicate a slightly different rate of exchange of chair-chair conformations of the trioxadecalin ring system, as discussed in Chapter 1, or a marginal change in the relative populations of the conformations[114,115]. (Note that the magnitudes of the C10-C13 vicinal proton-proton coupling constants were similar to those found in data recorded for mycalamide A).

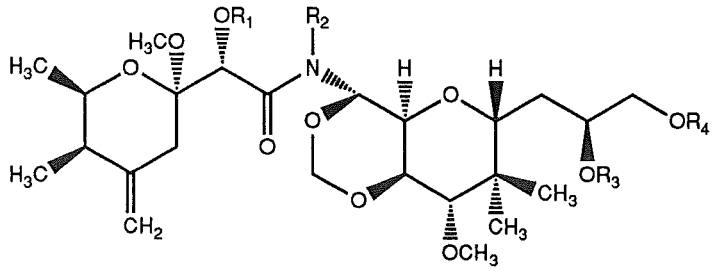


$R_1$=$R_3$=$R_4$=$Si(CH_3)_3$, $R_2$=H: Mycalamide A tris-TMS ether (**2.1**)
$R_1$=$R_4$=$Si(CH_3)_3$, $R_2$=H, $R_3$=$CH_3$: Mycalamide B bis-TMS ether (**2.2**)
$R_1$=$R_2$=H, $R_3$=$CH_3$, $R_4$=$Si(CH_3)_3$: Mycalamide B 18-mono-TMS ether (**2.3**)
$R_1$=$R_2$=H, $R_3$=$R_4$=$Si(CH_3)_3$: Mycalamide A 17,18-bis-TMS ether (**2.4**)
$R_1$=$R_2$=$R_3$=H, $R_4$=$Si(CH_3)_2C(CH_3)_3$: Myc.A 18-mono-TBDMS ether (**2.5**)
$R_1$=$R_2$=H, $R_3$=$R_4$=$Si(CH_3)_2C(CH_3)_3$: Myc.A 17,18-bis-TBDMS ether (**2.6**)
$R_1$=$R_3$=$R_4$=$Si(CH_3)_2C(CH_3)_3$, $R_2$=H: Mycalamide A tris-TBDMS ether (**2.7**)
$R_1$=$R_2$=H, $R_3$=$CH_3$, $R_4$=$Si(CH_3)_2C(CH_3)_3$: Myc.B 18-mono-TBDMS... (**2.8**)
$R_1$=$R_4$=$Si(CH_3)_2C(CH_3)_3$, $R_2$=H, $R_3$=$CH_3$: Myc.B bis-TBDMS ether (**2.9**)
$R_1$=$R_2$=$R_3$=H, $R_4$=$COC_6H_4Br$: Myc.A 18-mono-p-bromobenzoate (**2.10**)
$R_1$=$COC_6H_4Br$, $R_2$=$R_3$=$R_4$=H: Myc.A 7-mono-p-bromobenzoate (**2.11**)
$R_1$=$R_4$=$COC_6H_4Br$, $R_2$=$R_3$=H: Myc.A 7,18-di-p-bromobenzoate (**2.12**)
$R_1$=$R_2$=H, $R_3$=$R_4$=$COC_6H_4Br$: Myc.A 17,18-di-p-bromobenzoate (**2.13**)
$R_1$=$R_3$=$R_4$=$COC_6H_4Br$, $R_2$=H: Mycalamide A tri-p-bromobenzoate (**2.14**)
$R_1$=$COC_6H_4Br$, $R_2$=$R_4$=H, $R_3$=$CH_3$: Myc.B 7-mono-p-bromobenzoate (**2.15**)
$R_1$=$R_2$=H, $R_3$=$CH_3$, $R_4$=$COC_6H_4Br$: Myc.B 18-mono-p-bromobenzoate (**2.16**)

$R_1$=$R_4$=$COC_6H_4Br$, $R_2$=H, $R_3$=$CH_3$: Myc.B di-p-bromobenzoate (**2.17**)
$R_1$=$R_3$=$R_4$=$COCH_3$, $R_2$=H: Mycalamide A triacetate (**2.18**)
$R_1$=$R_4$=$COCH_3$, $R_2$=H, $R_3$=$CH_3$: Mycalamide B diacetate (**2.19**)
$R_1$=$R_2$=H, $R_3$=$CH_3$, $R_4$=$COCH_3$: Mycalamide B 18-monoacetate (**2.20**)
$R_1$=$COCH_3$, $R_2$=$R_4$=H, $R_3$=$CH_3$: Mycalamide B 7-monoacetate (**2.21**)
$R_1$=$R_3$=$R_4$=$COCH_2CH_3$, $R_2$=H: Mycalamide A tripropanoate (**2.22**)
$R_1$=$R_2$=H, $R_3$=$CH_3$, $R_4$=$SO_2CH_3$: Mycalamide B 18-monomesylate (**2.23**)
$R_1$=$R_2$=$CH_3$, $R_3$=$R_4$=H: 7-*O*-Methyl, *N*-methyl mycalamide A (**2.24**)
$R_1$=$R_2$=$R_4$=$CH_3$, $R_3$=H: 7,18-di-*O*-Methyl, *N*-methyl mycalamide A (**2.25**)
$R_1$=$R_2$=$R_3$=$R_4$=$CH_3$: 7,17,18-tri-*O*-Methyl, *N*-methyl mycalamide A (**2.26**)
$R_1$=$R_2$=$R_3$=$CH_3$, $R_4$=H: 7,17-di-*O*-Methyl, *N*-methyl mycalamide A (**2.27**)
$R_1$=$R_3$=$R_4$=$CH_3$, $R_2$=H: 7,17,18-tri-*O*-Methyl mycalamide A (**2.31**)
$R_1$=$R_4$=$CH_3$, $R_2$=$R_3$=H: 7,18-di-*O*-Methyl mycalamide A (**2.32**)
$R_1$=$R_3$=$CH_3$, $R_2$=$R_4$=H: 7,17-di-*O*-Methyl mycalamide A (**2.33**)
$R_1$=$CH_3$, $R_2$=$R_3$=$R_4$=H: 7-*O*-Methyl mycalamide A (**2.34**)
$R_1$=$R_2$=$R_3$=H, $R_4$=$CH_3$: 18-*O*-Methyl mycalamide A (**2.35**)
$R_1$=$COCH_3$, $R_2$=H, $R_3$=$R_4$=$CH_3$: 17,18-di-*O*-Methyl myc.A 7-monoacet. (**2.36**)
$R_1$=$R_3$=$CH_3$, $R_2$=H, $R_4$=$COCH_3$: 7,17-di-*O*-Methyl myc.A 18-monoacet. (**2.37**)
$R_1$=$R_2$=H, $R_3$=$R_4$=$CH_3$: 17,18-di-*O*-Methyl mycalamide A (**2.38**)
$R_1$=$CH_2Ph$, $R_2$=$R_3$=$R_4$=H: 7-*O*-Benzyl mycalamide A (**2.39**)
$R_1$=$R_4$=$CH_2Ph$, $R_2$=$R_3$=H: 7,18-di-*O*-Benzyl mycalamide A (**2.40**)
$R_1$=$R_2$=$CH_2Ph$, $R_3$=$R_4$=H: 7,18-di-*O*-Benzyl mycalamide A (**2.41**)
$R_1$=$R_2$=$R_4$=$CH_2Ph$, $R_3$=H: 7,18-di-*O*-Benzyl, *N*-benzyl mycalamide A (**2.42**)
$R_1$=$CH_2Ph$, $R_2$=$R_4$=H, $R_3$=$CH_3$: 7-*O*-Benzyl mycalamide B (**2.43**)
$R_1$=$R_4$=$CH_2Ph$, $R_2$=H, $R_3$=$CH_3$: 7,18-di-*O*-Benzyl mycalamide B (**2.44**)
$R_1$=$R_2$=$CH_2Ph$, $R_3$=$CH_3$, $R_4$=H: 7-*O*-Benzyl, *N*-benzyl mycalamide B (**2.45**)
$R_1$=$R_2$=$R_4$=$CH_2Ph$, $R_3$=$CH_3$: 7,18-di-*O*-Benzyl, *N*-benzyl myc.B (**2.46**)

The reaction of mycalamide B with the same reagent gave mycalamide B bis-TMS ether (**2.2**) by HREIMS. The $^1H$ NMR spectrum showed the presence of two TMS signals between δ0.0 and 0.2 ppm, consistent with this formulation, with similar chemical shift changes on silylation to those noted above (Table 2.1). Irradiation of the signal at δ0.2 ppm, in an NOE experiment, gave an enhancement of the H7 and 6-$OCH_3$ resonances (Table 2.3), so this was assigned to the TMS ether group located at C7. The $^{13}C$

NMR spectrum also showed a similar pattern of chemical shifts to those observed above, but with less effect at C15 and C16 (Table 2.2).

### 2.2.2 SELECTIVE TRIMETHYLSILYLATIONS OF MYCALAMIDES A AND B

It was clear that silylation of mycalamides A and B proceeded very readily, but it was proposed that cooling of the reaction might introduce some selectivity in the site of silylation. The reaction of mycalamide B with the reagent in an ice-cooled system for five minutes gave a single product by TLC which was more polar than the bis-TMS ether above, but less polar than mycalamide B. HREIMS confirmed that this was a mycalamide B mono-TMS ether. The $^{1}H$ NMR spectrum showed a single TMS resonance at $\delta$0.13 ppm, and comparison of all the chemical shifts (Table 2.1) with those for the bis-TMS ether and mycalamide B suggested that the silyl group was attached to the C18 oxygen. This was confirmed by an observed broadening of the H7 resonance due to coupling to the underivatised C7 hydroxyl group, which was removed on addition of $D_2O$ and by selective proton decoupling. The $^{13}C$ NMR data (Table 2.2) were also consistent with mono-silylation at the C18 oxygen, and were similar to those recorded for mycalamide B. Therefore this derivative was assigned the structure **2.3**.

The reaction of mycalamide A under similar conditions also gave a single product by TLC, of intermediate polarity, and HREIMS showed that it was a mycalamide A bis-TMS ether. The $^{1}H$ NMR spectrum showed the presence of two TMS signals between $\delta$0.0 and 0.2 ppm, and the H7 resonance appeared as a doublet, implying the presence of the C7 hydroxyl group. This was confirmed by addition of $D_2O$, which removed this coupling, and the doublet at $\delta$3.95 ppm, so the latter was assigned to this hydroxyl proton. This required that the product be a mycalamide A 17,18-bis-TMS ether (**2.4**) and the chemical shift data (Table 2.1) were consistent with this.

There was insufficient sample to record a $^{13}C$ NMR spectrum and attempts to repeat this reaction were unsuccessful due to the formation of either tris- or mixed mono-silylated products. Therefore the initial clean formation of this bis-TMS ether was actually rather fortuitous.

### 2.2.3 CLEAVAGE OF TMS ETHERS AND DISCUSSION

The removal of these TMS ether groups from mycalamide A tris-TMS ether was attempted using tetra-n-butyl ammonium fluoride in tetrahydrofuran (THF) at room temperature[78]. TLC and $^1H$ NMR spectroscopy showed complete hydrolysis to mycalamide A within minutes. The mechanism for this cleavage involves an attack of fluoride ion on the central silicon atom and displacement of the alkoxy group in an $S_N2$ reaction. The driving force for this cleavage is the preferential formation of the very stable silicon-fluorine bond, and is general for silyl ethers[136].

The mechanism of formation of these silyl ethers is also $S_N2$, with attack of the hydroxy oxygen on the silyl electrophile, as activated in the reagent. This explains the preferred silylation of the C18 hydroxyl group in mycalamide B, since there is an expected steric effect in such reactions which favours reaction of primary over secondary hydroxyl groups[76,140,141]. The favoured silylation of both C17 and C18 hydroxyl groups in mycalamide A over the C7 hydroxyl group was slightly more surprising, and some synergistic effect may be involved.

An example of the use of the TMS ether group as a protecting group in an acylation reaction will be given later in the chapter. However, it became apparent that this group was too readily hydrolysed to be of much use in mycalamide modifications, as the derivatives were too unstable to storage and to mild acid and base[138]. Therefore a more versatile silyl ether was considered and the t-butyldimethylsilyl ether was chosen, since it was

reported to show good acid and base stability[136,138]. This group, being of larger size, also allows greater selectivity in reaction and can be used for the selective protection of primary hydroxyl groups[142,143], as well as for secondary and tertiary groups[78,136].

### 2.2.4 PREPARATION AND CHARACTERISATION OF MYCALAMIDE A AND B T-BUTYLDIMETHYLSILYL ETHERS

The reaction of mycalamide A with t-butyldimethylchlorosilane (TBDMCS) and triethylamine in chloroform was very slow at room temperature. Silylation reactions were expected to be more rapid in polar aprotic solvents[136,142] so in this case the solvent was changed to pyridine, which could also act as a co-catalyst[142]. Also dimethylaminopyridine[142,143] (DMAP) has been reported to be an excellent catalyst for difficult silylation and acylation reactions, so this was incorporated into the present reaction. These modifications were highly successful, with two less polar derivatives being readily obtained from mycalamide A, as monitored by TLC. These products were well resolved on silica gel and were cleanly separated and purified from reagents using a small pipette column (see Experimental). HRFABMS of these products showed that the major one was a mycalamide A mono-TBDMS ether and the other a mycalamide A bis-TBDMS ether derivative.

The $^1$H NMR spectrum of the mono-silylated derivative showed the presence of two new signals, at δ0.9 and 0.1 ppm, which were assigned to the t-butyl methyl and the two methyl groups attached to silicon, respectively. The H7 resonance was coupled to a signal at δ3.8 ppm, which was assigned to the C7 hydroxyl proton, and there was a second hydroxyl resonance at δ2.8 ppm, which appeared as a doublet, so this had to arise from the hydroxyl group at C17. Both resonances were removed on addition of $D_2O$. Therefore this was a mycalamide A 18-mono-TBDMS ether (**2.5**), as expected, based on the

preferential silylation of primary hydroxyl groups by this reagent, discussed above. Full $^1H$ NMR spectral assignments are shown in Table 2.4. The major chemical shift changes occurred for the H15, two H16, H17 and H18 proton resonances, consistent with this assignment. A $^{13}C$ NMR spectrum was also recorded for this derivative, and this showed the presence of new signals at δ25.8 and -5.5 ppm for the new methyl resonances, which were similar to those shown in model compounds[144], but few chemical shift changes compared with data recorded for mycalamide A (Table 2.5).

Similarly the $^1H$ NMR spectrum of the bis-TBDMS ether derivative, recorded in $CD_2Cl_2$, showed two sets of signals for the TBDMS ether groups, and the presence of the coupled H7-C7-OH system required that these silyl ether groups be at C17 and C18, as in structure **2.6**. By adding a trace of pyridine to the sample, the compound was also found to be stable in $CDCl_3$, and the $^1H$ NMR spectrum was readily assigned to give the data in Table 2.4. The addition of a TBDMS ether at C17 had an effect on the chemical shifts of some protons which appeared to be remote, including the NH, H10, H11, H13, H15, H5a and H5e protons. This suggested that there were some changes to the solution conformations of the chain portions due to longer range steric effects. NOE experiments established the assignment of the dimethyl silyl ether resonances at C17 and C18 (Table 2.3) but the solution conformations were not investigated. The $^{13}C$ NMR spectrum of a larger sample showed shifts in the C15-C18 resonances, in addition to the new signals for the TBDMS ether groups (Table 2.5).

A second reaction of mycalamide A with the same reagents, but at 60°C for two days, gave a mixture of the mycalamide A 17,18-bis-TBDMS ether (**2.6**) above and a less polar derivative. These were separated by silica gel column chromatography and the new product was found to be the corresponding mycalamide A tris-TBDMS ether (**2.7**) by HRFABMS. The $^1H$

NMR spectrum showed shifts in the H2, two H5 and NH resonances (Table 2.4), and the new dimethyl silyl signals were resolved, suggesting a more chiral neighbouring environment[98]. Irradiation of H7 in an NOE experiment gave a strong enhancement of the H5e and 6-$OCH_3$ resonances, as well as the new dimethyl silyl signals (Table 2.3). The strong H5e-H7 interaction represents a larger population of this C6-C7 rotamer than in mycalamide A or B, as discussed in Chapter 1, and could be caused by steric effects involving the new bulky silyl ether group at C7. The $^{13}C$ NMR spectrum reflected these changes, with shifts in the C5, 6-$OCH_3$, C7 and C8 resonances (Table 2.5).

Similar results were obtained for mycalamide B, where the mycalamide B 18-mono-TBDMS ether derivative (**2.8**) was obtained from a reaction at room temperature, but the bis-TBDMS ether (**2.9**) was obtained only under forcing conditions. HRFABMS, $^1H$ and $^{13}C$ NMR spectra were obtained for both derivatives and assignments of the NMR data are shown in Tables 2.1 and 2.5. The $^{13}C$ NMR spectral assignments were confirmed by an HMQC experiment, particularly the assignment of the downfield C7 resonance, which was uncertain in other derivatives until this result[144]. The remaining shifts in both mycalamide B derivatives were similar to those observed for the mycalamide A TBDMS ethers.

### 2.2.5 CONCLUSIONS AND BIOLOGICAL ACTIVITY

In summary, the order of silylation of the hydroxyl groups in mycalamide A was C18, C17 then C7, and this was more pronounced in reactions with the more bulky TBDMCS reagent. This order of substitution would therefore allow a selective reaction at the C7 hydroxyl group, if desired. Biological assay results on these derivatives are shown in Table 2.6. It is apparent that the mycalamide A and B TMS ethers were of similar activity to the parent compounds, but this may simply reflect the ease of hydrolysis and instability of

these derivatives[138]. However, the mycalamide A and B TBDMS ethers, which were much more stable (reportedly $10^4$ times more stable to hydrolysis[136]), displayed a rapid decline in activity with increasing substitution of the hydroxyl groups of mycalamides A and B. In particular, substitution at the C18 group caused a 50-fold loss in the activity of mycalamide A and a 200-fold loss in the activity of mycalamide B. Further substitution led to effectively inactive derivatives in both assay systems. One possible factor in the loss of biological activity could be the reduced polarity of these derivatives, which could decrease their solubility[1]. Another factor could be the size[16] of these TBDMS ether groups as it has been indicated from the NMR spectroscopic work above that the solution conformations of some of the derivatives have been altered from those of mycalamides A and B. It is possible that at least some of the hydroxyl groups of mycalamides A and B are important for favourable interactions with an active site[15], although the structure of pederin and mycalamide B suggests that the C17 and C18 hydroxyl groups of mycalamide A are not essential, and this is investigated more completely in a later section of this chapter. Therefore, although these compounds could be useful protected intermediates, they did not appear to be useful analogues for their biological activity.

## 2.3 ESTERIFICATION OF MYCALAMIDES A AND B

### 2.3.1 PREPARATION AND CHARACTERISATION OF P-BROMOBENZOATE ESTERS OF MYCALAMIDES A AND B

The overall aim of this investigation was to determine the optimum conditions for the preparation of larger quantities of a mycalamide A or B p-bromobenzoate ester, which could be crystallised and subjected to analysis by x-ray crystallography. Therefore it was important to investigate the relative

reactivities of the various hydroxyl groups in mycalamides A and B under the reaction conditions required for this esterification, and to examine the physical properties of the products obtained.

Mycalamide A reacted with p-bromobenzoyl chloride and triethylamine in dichloromethane at room temperature to give a mixture of two products and starting material by TLC. This mixture was separated by reverse phase HPLC and the two products, which were white solids from methanol-water mixtures but oils from less polar solvents, were found to be mycalamide A mono-p-bromobenzoate isomers by HRFABMS. UV spectra were recorded which also confirmed the presence of this aromatic ester group.

The $^1$H NMR spectrum of the major product showed two new doublets, at δ7.89 and 7.57 ppm, due to the aromatic protons of a p-bromobenzoate ester group[101], and two hydroxyl proton doublets, at δ3.76 and 3.20 ppm, which were removed on addition of $D_2O$. The multiplicity of these latter resonances required that the underivatised hydroxyl groups be those at C7 and C17, and the complete spectrum of this mycalamide A 18-p-bromobenzoate (**2.10**) was assigned using results from a COSY experiment (Table 2.7). Note that there were shifts in the H15 (+0.1), H16 (+0.1), H17 (+0.3), H18 (+0.7) and H18 (+0.9) proton resonances which also required that the esterification be at the C18 oxygen[101].

The $^1$H NMR spectrum of the minor product contained aromatic proton resonances for the new ester group and showed a large downfield shift in the H7 resonance (+1.4 ppm), consistent with a mycalamide A 7-mono-p-bromobenzoate ester (**2.11**). There were also shifts in many of the resonances belonging to protons on the O1-C6 ring or its substituents (Table 2.7), whereas those resonances for the rest of the structure were relatively unchanged in chemical shift from those observed for mycalamide A. No $^{13}$C NMR spectra were recorded for either of these derivatives.

As with the silylation of mycalamide A using the bulky TBDMCS reagent, this p-bromobenzoylation reaction was slow. Therefore the reaction conditions were modified to include dimethylaminopyridine as a catalyst[143], pyridine as the solvent and a higher reaction temperature, in order to favour the formation of more substituted derivatives. This modified reaction on mycalamide A was successful by TLC and three new derivatives were separated by reverse phase HPLC, along with more of the 18-mono ester derivative (**2.10**). HRFABMS showed that these new products, which were white solids from methanol-water mixtures but oils from less polar solvents, were two mycalamide A di-p-bromobenzoates and one tri-p-bromobenzoate ester.

The $^{1}H$ NMR spectrum of the new compound, which had the shortest retention time on reverse phase HPLC, contained H7 and H18 proton resonances which were shifted downfield by more than 0.6 ppm, in addition to two pairs of aromatic resonances. There were also smaller shifts in the resonances of protons near to C7 and C18 (Table 2.7), consistent with a mycalamide A 7,18-di-p-bromobenzoate ester (**2.12**). A $^{13}C$ NMR spectrum was recorded which showed significant shifts in the C8 (-4.3), C17 (-2.7) and C18 (+2.0) carbon resonances (Table 2.2), consistent with normal substituent effects for acylation[117] at C7 and C18 (the C6 and C7 resonances may be otherwise influenced by changes in the solution conformations). The $^{1}H$ NMR spectrum of the second mycalamide A di-p-bromobenzoate showed the presence of the coupled H7-C7-OH system, in addition to the new aromatic signals, so that the two ester groups had to be at C17 and C18, as in structure **2.13**. The downfield shifts in the C16-C18 sidechain proton resonances were consistent with this (Table 2.7), as assigned by a COSY experiment. The $^{1}H$ NMR spectrum of the remaining tri-substituted product showed three sets of aromatic signals and large downfield shifts in the H7, H17 and H18 proton

resonances (Table 2.7), as expected for this structure (**2.14**). Some resonances were broadened, such as those assigned to H12, H15 and the two H16 protons, suggesting some conformational averaging. This was not surprising with the presence of three bulky ester groups and the high molecular weight (1052 daltons). The H10-H11, H11-H12 and H12-H13 coupling constants were significantly smaller, suggesting a higher proportion of the alternate chair-chair conformation of the trioxadecalin ring system than in mycalamides A and B, as proposed in Chapter 1, but this was not investigated further.

It was apparent that although there was a progressive reaction at the three hydroxyl groups in mycalamide A, there was no great selectivity in the reaction, so this was not ideal for the preparation of larger amounts of a single derivative. Therefore the reaction of mycalamide B was considered, since this compound had only two hydroxyl groups. The reaction of mycalamide B under the modified conditions above, at 55°C for one week, gave a mixture of unreacted material and the three possible product esters, although one was minor. Preparative reverse phase HPLC separated these compounds, which were also white solids from methanol-water mixtures, and HRFABMS confirmed that there were two mono-p-bromobenzoates (**2.15**, **2.16**) and one di-p-bromobenzoate ester (**2.17**) of mycalamide B.

The $^{1}H$ NMR spectrum of the minor product, which had eluted first by HPLC, showed that the single ester group was positioned at C7 (structure **2.15**), since there were the usual shifts in the H7 and nearby proton resonances (Table 2.4), whereas other signals were not affected. The major product, eluting second by HPLC, was mycalamide B 18-mono-p-bromobenzoate (**2.16**) by $^{1}H$ NMR spectroscopy, with the assignments (Table 2.4) being confirmed by a COSY experiment. A $^{13}C$ NMR spectrum was also recorded for this derivative, which showed only the expected shifts in the C16

(+0.9), C17 (-2.4) and C18 (+1.0) carbon resonances (Table 2.2). The $^{1}H$ and $^{13}C$ NMR spectra of the remaining product, the mycalamide B di-p-bromobenzoate ester (**2.17**), were similarly assigned (Tables 2.4 and 2.2) Biological activity results on all these esters will be discussed in a later section.

### 2.3.2 ATTEMPTS TO CRYSTALLISE MYCALAMIDE A AND B P-BROMO-BENZOATE ESTERS

Large quantities of pederin and some of its derivatives were readily crystallised from benzene-hexane mixtures, giving, invariably, needles, plates or elongated prisms[94]. Pederin di-p-bromobenzoate (**1.1**) was examined in two independent x-ray crystallographic investigations[34,93]. The crystals required for these studies were grown from methanol-ether and ethanol solutions, respectively, and were described as colourless plates or prisms[34].

Initial attempts to crystallise the small amounts of the mycalamide A and B p-bromobenzoate esters prepared above did not produce encouraging results. The samples were first dissolved in small amounts of methanol-water mixtures in Craig tubes and set aside at 4°C. Slow evaporation of these solutions eventually yielded only oils. Similar results were obtained from methanol-ether solutions, also benzene-heptane, ether-petroleum ether, and ethanol-ether-petroleum ether mixtures. One sample, mycalamide A 7-mono-p-bromobenzoate (**2.11**), gave fine, hair-like needles after slow evaporation from benzene-ether, but these were unsuitable for x-ray examinations.

The best derivative to direct a large scale reaction towards appeared to be the mycalamide B di-p-bromobenzoate ester (**2.17**), since, based on the work above, this derivative would be favoured with higher temperatures and longer reaction times, and was also the most similar in structure and polarity to

pederin di-p-bromobenzoate (**1.1**). Such a reaction was performed to give about 17 mg of this derivative after purification on silica gel. Several attempts were then made to obtain suitably crystalline material, but all were unsuccessful. From alcoholic solvents, including methanol, ethanol and iso-propyl alcohol, the material slowly oiled out of solution. From hot hexane solution the material precipitated slowly as a white, non-crystalline solid. With a few drops of ethanol added to this sample, a mixture of white solid, fine fibrous material and oil was obtained. Other solvent mixtures were also tried, but all were ineffective in producing single crystals, despite the high purity of the sample, and, regrettably, this work was eventually abandoned.

### 2.3.3 PREPARATION AND CHARACTERISATION OF MYCALAMIDE A AND B ACETATE ESTERS

The mycalamide A and B p-bromobenzoate esters were not ideal protected intermediates, since the formation reactions were slow and generally gave mixtures of several products which required chromatographic separation, while the cleavage reaction would require the use of fairly strong bases[78,138]. In contrast, acetylation was a derivatisation reaction used extensively in an early chemical and structural study of pederin[94], and was expected to be fast and high yielding, while giving products that had some mild acid stability, but would be easily removed by bases[78,138].

The reaction of mycalamide A with pyridine and acetic anhydride proceeded readily at room temperature, to give a single product by TLC, and HREIMS showed that this was mycalamide A triacetate (**2.18**). The IR spectrum, recorded in chloroform solution, showed a major carbonyl stretching band[96] at 1740 $cm^{-1}$, with shoulders at 1705 and 1690 $cm^{-1}$, while the FTIR spectrum, recorded as a film, showed these bands at 1741, 1705 and 1680

$cm^{-1}$. Also distinctive was the sharp N-H stretch at 3380 and 3370 $cm^{-1}$ in the solution and film IR spectra, respectively[96].

The $^1H$ NMR spectrum of mycalamide A triacetate (**2.18**) showed three new methyl resonances between δ2.0 and 2.2 ppm, being those for the acetate esters, and shifts in many signals as assigned by a COSY experiment (Table 2.7). In particular, the H7 (+1.2), NH (-0.2), H15 (-0.2), H16 (+0.2), H17 (+1.2), H18 (+0.7) and H18 (+0.8) resonances were shifted most, with smaller shifts in H5a, 6-$OCH_3$ and H16, consistent with acetylation of the three hydroxyl groups[101]. However, the H10, 10-OCH*R*, H11, H12 and H13 resonances were also affected, and the vicinal proton-proton coupling constants for the trioxadecalin ring system protons were slightly smaller, suggesting some changes in the relative proportions of various solution conformations. This was also found for the mycalamide A tri-p-bromobenzoate ester (**2.14**) above, but was not investigated further. A $^{13}C$ NMR spectrum showed shifts in some resonances (Table 2.2), for example those assigned to C7 (-1.1), C8 (-4.5), C11 (-1.3), C15 (-3.4), C16 (-1.9), C17 (-1.5) and C18 (-2.8), in addition to the new methyl and carbonyl resonances, consistent with acetylation[117,145] and conformational changes. Note that the shielding effect at the β carbons is stronger than the deshielding effect at the carbons α to the new acetate groups. This effect is apparently general for aliphatic esters, and is thought to arise in part from steric perturbations involving the carbonyl oxygen[118].

When the mycalamide A acetylation reaction was left for a shorter time, a 1:1 mixture of two products was obtained, including mycalamide A triacetate (**2.18**) and a more polar derivative. The $^1H$ NMR spectrum of the mixture showed that the second product was probably mycalamide A 7,18-diacetate, since there were large downfield shifts in the H7 and H18 proton resonances, two new acetyl methyl resonances between δ2.0 and 2.2 ppm, and also a new

doublet at δ3.0 ppm, which was probably the C17 hydroxyl proton resonance. However no attempt was made to isolate this product.

The acetylation of mycalamide B under analogous conditions readily gave a diacetyl derivative (**2.19**) by HREIMS and HRFABMS. The $^{1}H$ NMR spectrum was consistent with this, since there were similar shifts in the various resonances on acetylation to those found above (Table 2.8), as assigned by a COSY experiment, in addition to the two new acetyl methyl resonances. Irradiation of the three methoxyl resonances in an NOE experiment proved the assignment of these resonances, with known interactions being observed (Table 2.3). Of interest was the observed NOE interaction between the 17-$OCH_3$/H17 and the H5 protons, as found for mycalamide B (Chapter 1), which suggests that these compounds share a similar major overall solution conformation. The $^{13}C$ NMR spectrum of mycalamide B diacetate (**2.19**) was similar to that of mycalamide B, except for the new resonances, a large upfield shift in the C8 resonance, as above, and a smaller shift in C17 (Table 2.9).

### 2.3.4 SELECTIVE CLEAVAGE OF ACETATE ESTERS IN MYCALAMIDE A AND B ACETYL DERIVATIVES

The most common method for the cleavage of ester groups is base hydrolysis[77,78], although lithium aluminium hydride was successfully used to selectively remove the acetate groups of pederin diacetate[94]. Note that the standard mechanism for base catalysed ester hydrolysis is almost the reverse of the formation mechanism, and involves the attack of hydroxide ion on the carbonyl group of the ester to give a tetrahedral intermediate, then a loss of the alkoxy group to regenerate the starting alcohol and the carboxylate of the ester group[146]. Mycalamides A and B were expected to be stable to the mildly basic conditions required for such hydrolysis, which seemed preferable to reductive cleavage.

Mycalamide A triacetate (**2.18**) was stirred with a dilute solution of potassium carbonate in aqueous methanol at room temperature[78]. After two hours, TLC showed complete hydrolysis to mycalamide A. The same reaction was attempted on mycalamide B diacetate (**2.19**), monitoring by TLC. The reaction was observed to give a compound of intermediate polarity, probably a mycalamide B monoacetate, within minutes, which decomposed slowly to give mycalamide B, by TLC and $^1$H NMR spectroscopy, after twelve hours.

In order to determine the nature of this partial hydrolysis product, the reaction was repeated, but quenched after one hour. Preparative TLC purified the major product, which was a mycalamide B mono-acetate by DCIMS and HREIMS. The $^1$H NMR spectrum of this derivative showed a single methyl resonance at δ2.08 ppm, and H18 resonances that were downfield of their position in the spectrum of mycalamide B, as assigned by a COSY experiment (Table 2.8), whereas the chemical shifts of the H7 resonance and resonances of nearby protons were relatively similar for the two compounds. The H7 resonance was also broadened by coupling to the C7 hydroxyl resonance, as shown by a selective proton decoupling experiment. A $^{13}$C NMR spectrum was also recorded and this showed very similar chemical shifts to those of mycalamide B, except at C16, C17 and C18, along with the expected new acetyl methyl and carbonyl resonances (Table 2.9). Therefore this was mycalamide B 18-monoacetate (**2.20**).

The faster rate of hydrolysis of the acetate group at C7, compared with that at C18, probably reflects the greater stability of primary acetate esters over secondary ones, due to steric factors[77]. However, the presence of neighbouring electron-withdrawing entities at C6 and C8 may also cause some destabilisation of esters at C7[140], making them more susceptible to hydrolysis. Therefore it has been shown that acetyl esters of mycalamides A

and B could be easily formed and cleaved under mild reaction conditions and in high yields, making this a potentially useful protecting group[76,78].

### 2.3.5 PREPARATION OF MYCALAMIDE B 7-MONOACETATE USING A TMS ETHER PROTECTING GROUP

It was expected that the partial acetylation of mycalamide B would favour the formation of a C18 ester, as found for the p-bromobenzoylation reaction above. In order to prepare a C7 mono-acetyl derivative in good yield for use in structure-activity comparisons it was therefore considered necessary to use a protecting group, and this seemed to be a good opportunity to test the stability of the mycalamide TMS ethers. Therefore mycalamide B 18-mono-TMS ether (**2.3**) was reacted with acetic anhydride and pyridine for three hours at room temperature, before quenching by the addition of water. After workup, TLC and mass spectroscopy showed that desilylation had occurred and that there was one mono-acetyl product, along with a small amount of mycalamide B diacetate (**2.19**). Silica gel column chromatography purified this product and the $^{1}H$ NMR spectrum confirmed that this was mycalamide B 7-monoacetate (**2.21**), as shown by the characteristic shifts in the signals assigned to H7 and nearby protons, and the presence of a single new methyl resonance at δ2.20 ppm (Table 2.8). Partial $^{13}C$ NMR spectral data were obtained on the crude product (Table 2.9) and the molecular formula was confirmed by HRFABMS.

Therefore the TMS ether group was clearly useful in giving a good yield of the desired derivative, although it was not completely stable to the conditions[138] as shown by the presence of up to 25% mycalamide B diacetate in the product mixture. The observed desilylation of the major product evidently occurred during the aqueous workup procedure, and was an unexpected bonus, in that it saved an extra deprotection step. The use of the

corresponding TBDMS ether derivative would probably have eliminated the presence of mycalamide B diacetate due to the enhanced stability of these ethers[136,138], but this was not attempted.

### 2.3.6 PREPARATION AND CHARACTERISATION OF OTHER ESTERS OF MYCALAMIDES A AND B

Two other esters were also prepared, which would add to the limited structure-activity data already obtained and to the existing range of esters above, of varying size, polarity, and reactivity. Mycalamide A tripropanoate (**2.22**) was readily prepared from the reaction of mycalamide A with pyridine and propionic anhydride at room temperature, as shown by HRFABMS and NMR spectroscopy. The $^{1}H$ NMR spectrum showed very similar chemical shifts to those of mycalamide A triacetate (**2.18**) (Tables 2.7 and 2.8), but was more complex in the alkyl region, due to the presence of a small amount of reagent and the non-equivalence of the methylene protons on one of the ester groups, indicative of the chiral environment[98]. The $^{13}C$ NMR spectrum showed three carbonyl resonances between δ173 and 174 ppm for the propanoate ester groups[117], so that the assignment of the C8 resonance at δ167.2 ppm was unambiguous, and all the $^{13}C$ NMR chemical shifts for the mycalamide structure were close to those observed for mycalamide A triacetate (Table 2.2).

The preparation of methane sulphonate esters of mycalamide B was also investigated, as these were potentially reactive intermediates for substitution reactions[147]. The reaction of mycalamide B with methane sulphonyl chloride (mesyl chloride) in pyridine overnight at room temperature gave predominantly one product by TLC, with some unreacted mycalamide B. Preparative TLC purified this product and HRFABMS showed that this was a mycalamide B mono-mesylate. The $^{1}H$ NMR spectrum was assigned with the

assistance of a COSY experiment (Table 2.8), and this showed a new methyl signal at δ3.06 ppm, being the methyl group of the new sulphonate ester[101], and large downfield shifts in the H18 proton resonances. Also the C7 hydroxyl proton resonance was present, coupled to the H7 resonance, so that this product was mycalamide B 18-monomesylate (**2.23**). As expected, the $^{1}H$ NMR chemical shifts were close to those observed for mycalamide B 18-monoacetate (**2.20**). The $^{13}C$ NMR spectral data (Table 2.9) were also similar, except for the appearance of the new methyl resonance, at δ37.6 ppm, and for the chemical shift of the C18 carbon resonance, which was almost 6 ppm further downfield in the spectrum of the mesylate than in the data recorded for mycalamide B. This large downfield shift in the α carbon resonance on forming the sulphonate ester is, however, well documented for various model compounds. For example, the $^{13}C$ NMR data for both 2-mesyloxy adamantane[148] and 1-mesyloxy cyclohexane[145] show a +10-11 ppm downfield shift in the α carbon resonance, compared to data for the corresponding alcohols, whereas the shift on acetylation is only +2-3 ppm[145,148]. Therefore these data were consistent with the structures stated. However, the mycalamide B 18-mesylate derivative was unstable on storage, decomposing to a large mixture of compounds by $^{1}H$ NMR spectroscopy.

### 2.3.7 BIOLOGICAL ACTIVITY OF MYCALAMIDE A AND B ESTERS

The biological activity results obtained for the various mycalamide A and B esters described above are listed in Table 2.6. The series of p-bromobenzoates, in particular, provided some interesting results, where substitution at the C18 oxygen was significantly more deactivating for mycalamide B than for mycalamide A (the derivatives **2.16** and **2.10** were respectively 200 times and 2 times less active than the starting compounds). Assuming that this is a valid result, this therefore represents a significant

selectivity in either the size, polarity or potential conformations of the C16-C18 sidechain. Substitution at the C17 and C18 hydroxyl groups of mycalamide A gave a derivative (**2.13**) that was at least 50 times less active than the 18-mono ester (**2.10**), which was a similar pattern to that found for the mycalamide A TBDMS ethers. Mono-substitution at the C7 oxygen was strongly deactivating for both mycalamide A and B (50- and 200-fold reductions in activity). The remaining disubstituted and trisubstituted mycalamide A and B esters were even less active, but the relatively similar results observed may represent a limit in the purity achieved, rather than true activity.

Analogous results were found for the remaining esters of mycalamides A and B. Mycalamide A triacetate (**2.18**) was about 100 times less active than mycalamide A and mycamide B diacetate (**2.19**) was about 200 times less active than mycalamide B. A similar result was found for pederin dibenzoate (**1.2**) compared to data for pederin (Table 2.6). The mycalamide B 7- and 18-monoacetates (**2.21**, **2.20**) were, respectively, about 20 and 10 times less active than mycalamide B. Mycalamide A tripropanoate (**2.22**) appeared to be slightly less active than mycalamide A triacetate and mycalamide B 18-mesylate (**2.23**) only slightly less active than mycalamide B. The latter result was also interesting, since it appeared that having a methane sulphonate ester at this position was more tolerable than similar substitution with an acetate ester, but the significance of this result is uncertain.

Therefore some useful overall trends were observed in the biological activities of these esters, which would suggest that the C7 hydroxyl group is quite important for the biological activity, but that the C17 and C18 hydroxyl groups are less essential, although the size and polarity of the substituents at these positions also appeared to be important.

The above esters and silyl ethers all suffered from one major disadvantage in that they were not stable to strongly acidic or basic conditions[138]. Therefore alkylation reactions were considered as a method of further protecting the hydroxyl groups for more vigorous reaction conditions and to extend the structure-activity correlations found so far.

## 2.4 METHYLATION OF MYCALAMIDES A AND B

Mycalamides A and B have structures which are rather similar to pederin and it was shown in Chapter 1 that these compounds have very similar solution conformations. The only differences between these structures occur in the substituents at C10, C12, C13, C17 and C18. In particular, the interchange of hydroxyl and methoxyl groups at C13, C17 and C18 in these structures was of interest, in view of their similarly potent biological activities. A methylation study on mycalamides A and B was initiated to consider this, together with the effects of methylation of the C7 hydroxyl group and the amide.

### 2.4.1 REVIEW OF METHODS FOR THE METHYLATION OF HYDROXYL GROUPS

The formation of methyl ethers from hydroxyl groups can be accomplished by several methods[76-78]. The most general is the reaction of a nucleophilic oxygen group, usually an alkoxide ion formed under basic conditions, with a reagent, $CH_3X$, where X is usually halide, sulphate, or sulphonate, in an $S_N2$ reaction on the reagent. Earliest methylation methods involved the reaction of a carbohydrate with sodium in liquid ammonia, then treatment of the salt with methyl iodide. A more recent method generated the alkoxide ion with sodium hydride in aprotic solvents. Another established

method is to treat an aqueous solution of a carbohydrate with strong alkali and dimethyl sulphate (the Haworth procedure). Selective methylations have been described using two phase systems[149]. Another alternative was to use silver oxide and methyl iodide (the Purdie method). The Kuhn modification of this method uses *N,N*-dimethylformamide (DMF) as the solvent and replaces silver oxide by barium or strontium oxides or hydroxides[150]. Recently, the use of dimethylsulphoxide (DMSO) and powdered potassium hydroxide has been reported by Johnstone and coworkers[151] as a mild, rapid technique for the permethylation of hydroxyl and amide groups.

The synthesis of particular partially methylated compounds can be a problem since many protecting groups are not stable to the alkaline reaction conditions[76]. An alternative approach is the nucleophilic displacement of sulphonate esters by methoxide ion, in an $S_N2$ reaction on the substrate, or a similar ring-opening reaction on epoxides[77]. A third method of forming methyl ethers in base sensitive compounds is to use diazomethane activated by an acid catalyst, such as boron trifluoride or wet silica gel, as the methylating agent[76,78].

### 2.4.2 PREPARATION AND CHARACTERISATION OF PRODUCTS FROM THE METHYLATION OF MYCALAMIDES A AND B USING THE METHOD OF JOHNSTONE

The title reaction was chosen for initial investigation because of the mild reaction conditions, rapid reactions and high yields of permethylated products reported from reactions of alcohols and amides at room temperature[151]. It was found that none of the protecting groups above were stable to these reaction conditions, but selectivity was not a requirement for this study since the biological activities of all products were of interest, and the reaction conditions could be optimised or modified as required.

The reaction of mycalamide A with powdered potassium hydroxide and methyl iodide in DMSO for four hours at room temperature gave a mixture of two major products and a third minor product by TLC, but only two resolved peaks were apparent by reverse phase HPLC. Preparative HPLC in fact yielded only one pure fraction, representing the major, most polar product, and a second fraction, which was a mixture of two components in a 4:1 ratio, by $^1$H NMR spectroscopy. DCIMS and HREIMS showed that the first fraction consisted of a mycalamide A derivative with two new methyl groups, while the second contained tri-methylated compounds.

The $^1$H NMR spectrum of the major product showed two new $CH_3$-X resonances, at δ3.45 and 3.19 ppm. The more upfield resonance was likely to be attached to the amide nitrogen[101], as indicated by the absence of an NH resonance and the appearance of the H10 resonance as a doublet, instead of the usual triplet. There were also shifts in some resonances (Table 2.10), particularly those assigned to H5a (+0.3), H10 (+0.5) and H11 (+0.3), which suggested that the new methyl groups be located on the C7 oxygen and amide nitrogen atoms (structure **2.24**). Irradiation of H7 in an NOE experiment gave an enhancement of both of the new resonances and the C6 methoxyl resonance (Table 2.3), in accordance with this assignment. It is therefore proposed that the absence of a significant shift in the H7 resonance on methylation of the C7 hydroxyl group represents the fortuitous cancellation of two opposing effects:-

i) an expected upfield shift due to methylation of the C7 group[101], and

ii) a downfield shift due to steric deshielding effects associated with the presence of a methyl group rather than a hydrogen atom at the amide nitrogen[123].

A $^{13}$C NMR spectrum was recorded, which showed two new resonances, at δ28.8 and 58.9 ppm, which were assigned to the new *N*-methyl

and C7 methoxyl groups respectively. There were also large shifts in the C7 (+9.8), C10 (+3.6) and C11 (-4.1) resonances (Table 2.11), consistent with methylation at the positions stated[117]. Most of the resonances in the $^{1}H$ and $^{13}C$ NMR spectra were broadened, an effect which will be discussed in a conformational analysis, described below.

In order to determine the identity of the more highly substituted products, the methylation reaction was repeated on a slightly larger scale and the reaction continued until TLC showed that these products were dominant. Preparative TLC gave two fractions, where the minor one contained a tri-methylated derivative, and the major one a tetra-methylated mycalamide A, by DCIMS and HREIMS. The $^{1}H$ NMR spectrum of the more polar, tri-methylated derivative showed that this was the same compound as found in the earlier reaction, but was now pure. There were many similar features to that of the 7-*O*-methyl, *N*-methyl mycalamide A derivative (**2.24**) above, but, in addition, there was a new methoxyl resonance, at δ3.35 ppm, and further shifts in the two H16 (+0.1, -0.1), H17 (<0.1), and H18 (-0.3) proton resonances (Table 2.10), as assigned by a COSY experiment. A $^{13}C$ NMR spectrum also showed shifts in the C16 (+1.4), C17 (-1.9) and C18 (+10.0) resonances (Table 2.11). Therefore this was a 7,18-di-*O*-methyl, *N*-methyl mycalamide A derivative (**2.25**), which was also the next most likely derivative on mechanistic grounds, since the C18 primary hydroxyl group would be expected to undergo an $S_N2$ reaction faster than the secondary C17 hydroxyl group[140] (assuming prior methylation of the C7-OH and amide NH groups, as observed above).

The $^{1}H$ NMR spectrum of the major, less polar derivative was consistent with complete methylation of the amide and hydroxyl groups in mycalamide A (**2.26**), having the new *N*-methyl and methoxyl resonances of the derivative above and a new methoxyl resonance at δ3.27 ppm, which was assigned to the group at C17. There were also shifts in the H17 (-0.5) and H18 (+0.2)

resonances (Table 2.10), compared to those for the 7,18-di-*O*-methyl, *N*-methyl derivative (**2.25**), as assigned by a COSY experiment, that were indicative of this methylation[101]. Again many resonances were broad and there appeared to be some minor signals present, but this will be discussed with the results of further experiments below. The $^{13}C$ NMR spectrum was assigned with the assistance of an HMQC experiment, and this also confirmed previous assignments of the C7, N-$CH_3$ and C10 resonances. The observed shifts in the C17 and C18 resonances (+7.7 and -4.0 ppm respectively, relative to those of the 7,18-di-*O*-methyl, *N*-methyl derivative) were also in line with normal substituent effects[117] (Table 2.11).

Similarly, methylation of mycalamide B gave two products by TLC, which were separated by reverse phase HPLC. The less polar, minor product was identical by TLC, HPLC and $^{1}H$ NMR spectroscopy to that of the 7,17,18-tri-*O*-methyl, *N*-methyl mycalamide A derivative (**2.26**) above, giving further evidence that mycalamide B was the 17-*O*-methyl derivative of mycalamide A. The major, more polar derivative was therefore the expected 7-*O*-methyl, *N*-methyl mycalamide B (or 7,17-di-*O*-methyl, *N*-methyl mycalamide A, **2.27**) as shown by DCIMS, HREIMS and NMR spectroscopy. To avoid confusion in the naming of these compounds, the mycalamide B methyl ethers will be referred to as 17-*O*-methyl mycalamide A derivatives throughout this chapter. The $^{1}H$ NMR spectrum showed the same features noted above for 7-*O*-methyl, *N*-methyl mycalamide A (**2.24**), but with the usual mycalamide B C16-C18 sidechain resonances. NOE experiments were performed to confirm the assignment of the methoxyl resonances (Table 2.3). Of interest was the observation of a strong NOE interaction between the *N*-methyl and H11 protons, so that the H10 and *N*-methyl groups were in an anti relationship, just as the NH and H10 protons of mycalamide A. The $^{13}C$ NMR spectral data (Table 2.11) were also similar to those of 7-*O*-methyl, *N*-methyl mycalamide A

(**2.24**), except in the chemical shifts of the C16 sidechain resonances, as expected.

### 2.4.3 CONFORMATIONAL EXCHANGE IN *N*-METHYL MYCALAMIDES

An analysis of the vicinal proton-proton coupling constants and selected NOE interactions for all these derivatives showed that the major solution conformations of the ring structures were the same as for mycalamide A. However, the $^{1}H$ and $^{13}C$ NMR spectra of all the 7-*O*-methyl, *N*-methyl derivatives, recorded at 23°C, contained many broadened resonances, suggesting that some slow conformational exchange process was occurring[98,114,121]. A variable temperature $^{1}H$ NMR study, between -5°C and 55°C, was conducted to investigate the broadening of signals for 7,17,18-tri-*O*-methyl, *N*-methyl mycalamide A (**2.26**). Compared to the spectrum at 23°C, the spectra recorded at successive increments of 10°C higher showed an increased broadening of many signals. However, on cooling to 6°C all signals sharpened to normal resolution and linewidths, while some new signals were also observed on the baseline, which were small and broad. These new signals must arise from the presence of a minor conformation involved in an exchange process, since some saturation transfer of irradiation was observed between pairs of major and minor resonances in NOE experiments performed at room temperature[152]. For example, irradiation of the H10 resonance, at δ6.26 ppm, caused some saturation of a broad, minor signal at δ5.5 ppm, which was therefore assigned to the minor H10' resonance. The H5a', H7' and N-$CH_3$' resonances were also located in this way and integration of the resonances showed that the ratio of conformers was about 5:1. The observed NOE interaction between H7 and H10 (Table 2.3), not normally observed, required that this minor conformation involve an *E* conformation about the C-N amide bond[100,107], as shown in Figure 2.1b.

Note that the minor H10' resonance was a doublet (8.9 Hz), so that the H10 and H11 protons were in an *anti* relationship[102], suggesting that the trioxadecalin ring system had the same major solution conformation in both amide forms. The full $^1$H NMR data for the major conformer, recorded at 6°C, are listed in the Experimental section, and limited data for the minor conformer are shown in Figure 2.1b. The observed chemical shift differences between resonances for the two conformations, which was largest for the H10 resonance, could be readily explained by dipolar, anisotropic shielding effects involving the amide carbonyl, and by smaller steric effects[123].

**Figure 2.1** $^1$H-$^1$H NOE interactions and partial solution conformations of 7-*O*-methyl, *N*-methyl mycalamide A derivatives.

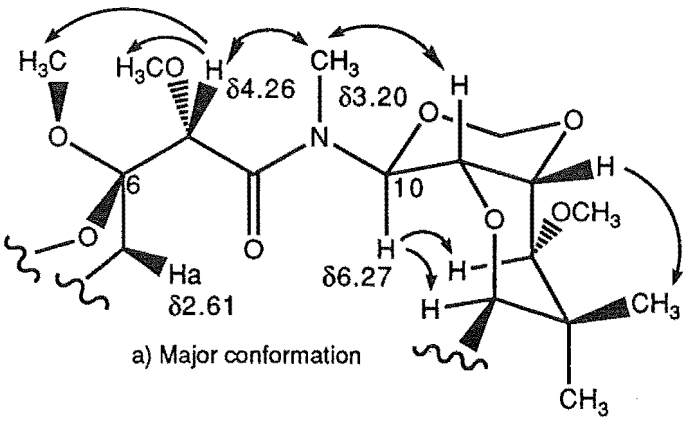


a) Major conformation

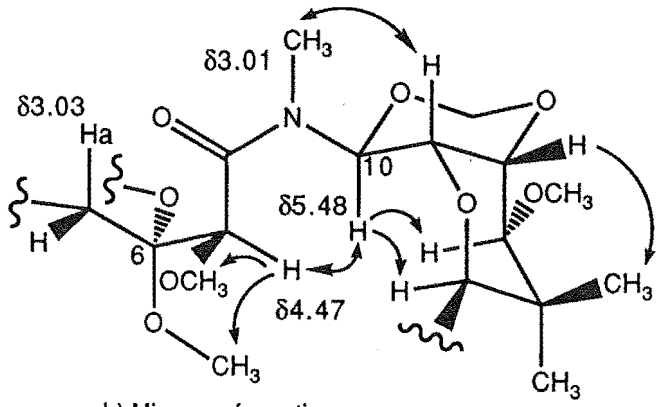


b) Minor conformation

This amide isomerism is due to the partial double bond character of the C-N bond which causes a substantial energy barrier to rotation (~80 kJ mol$^{-1}$)

and is well known in *N*,*N*-dialkyl amides and formamides[79,98,107]. Significantly, there appeared to be an increasing contribution from the minor conformation with methylation at the C17 and C18 hydroxyl groups for these 7-*O*-methyl, *N*-methyl mycalamide A derivatives. This may suggest that the sidechain substituents are sufficiently close in solution to interact with the central hydroxy amide system.

### 2.4.4 FURTHER DERIVATIVES FROM METHYLATIONS IN DMSO

Methylation experiments performed with undried DMSO were significantly slower than those with dry DMSO, as could be expected[153]. In such an experiment with mycalamide A, powdered potassium hydroxide and methyl iodide, a new product was observed in the reaction mixture, which moved faster on silica gel TLC than the tetra-methylated derivative (**2.26**) above. Preparative TLC was performed to purify this compound and DCIMS and HREIMS showed that it was an isomer of 7,17,18-tri-*O*-methyl, *N*-methyl mycalamide A (**2.26**). The $^{1}H$ NMR spectrum showed shifts in the H5a (+0.2), H5e (+0.4), H7 (-0.1), 7-$OCH_3$ (+0.1), N-$CH_3$ (-0.1), H16 (+0.1), H16 (-0.1) and H17 (-0.1) proton resonances (Table 2.10), as assigned by COSY and NOE experiments (Table 2.3). The $^{13}C$ NMR spectrum also showed shifts in the C6 (+1.0), 6-$OCH_3$ (+1.5) and C7 (-3.0) resonances (Table 2.11). These data suggested the formation of an epimer at C7 (**2.28**), which could occur through an enolisation reaction at C7-C8[154], involving the adjacent amide carbonyl group[155].

Two further experiments were performed in an attempt to prove this. Firstly, 7,17-di-*O*-methyl, *N*-methyl mycalamide A (**2.27**) was treated with a solution of sodium methoxide in methanol in a sealed vial at 90°C, monitoring by TLC. After three days, silica gel TLC showed that there was a mixture, including a minor amount of starting material and a product of higher $R_f$, so,

after workup, these were separated by preparative TLC. DCIMS and HREIMS confirmed that this was an isomer of 7,17-di-*O*-methyl, *N*-methyl mycalamide A (**2.27**), and the $^{1}H$ and $^{13}C$ NMR spectra for this derivative (Tables 2.10 and 2.11) showed similar shifts to those observed for the C7 epimer of the tetramethylated mycalamide derivative above. Therefore this was 7*S*,17-di-*O*-methyl, *N*-methyl mycalamide A (structure **2.29**). NOE experiments also showed the same interactions between the H7 proton and both the 6-$OCH_3$ and N-$CH_3$ protons (Table 2.3).

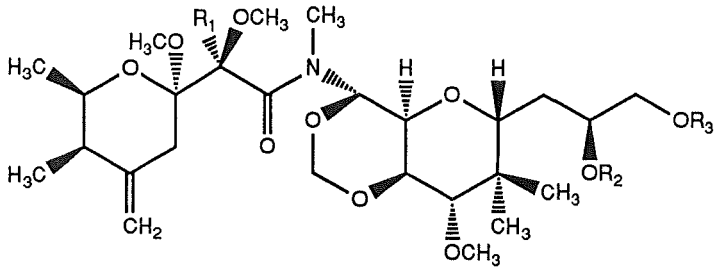


$R_1$=H, $R_2$=$R_3$=$CH_3$: 7*S*,17,18-tri-*O*-Methyl *N*-methyl mycalamide A (**2.28**)
$R_1$=$R_3$=H, $R_2$=$CH_3$: 7*S*,17-di-*O*-Methyl *N*-methyl mycalamide A (**2.29**)
$R_1$=D, $R_2$=$R_3$=H: 7-Deutero, 7*S*-*O*-methyl *N*-methyl mycalamide A (**2.30**)

In a second experiment, 7-*O*-methyl, *N*-methyl mycalamide A (**2.24**) was treated with a solution of fully deuterated sodium methoxide in methanol at 70°C, to give a similar mixture of epimers by TLC. DCIMS and HREIMS showed that a quantitative incorporation of one deuterium atom had occurred in the purified product, which was the C7 epimer of 7-*O*-methyl, *N*-methyl mycalamide A by $^{1}H$ NMR spectroscopy (structure **2.30**), having no H7 proton resonance (Table 2.10). Therefore the proposed structures of these derivatives had been confirmed.

Significantly, the observed signals in the $^{1}H$ and $^{13}C$ NMR spectra of these epimers were sharp, with no indication of conformational exchange, and no NOE interactions were observed between the H7 and H10 protons to suggest the presence of an *E* conformation of the amide. This suggests that

the normal amide conformation (*Z*) was very dominant for these C7 epimers, as for mycalamides A and B. It is possible that one factor in the different populations of the two amide conformations for these isomers could be unfavourable steric interactions[107]. The different chromatographic mobilities may also be associated with the different conformational effects, arising from the epimerisation at C7[106].

Another methylation experiment was performed on mycalamide A using barium oxide as the base[150] in place of the powdered potassium hydroxide, in a reaction conducted at 55°C. The single product obtained was found to be 7,17,18-tri-*O*-methyl, *N*-methyl mycalamide A (**2.26**) by TLC and $^1$H NMR spectroscopy. This demonstrated that the amide anion was still formed in sufficient concentration to permit amide methylation, despite the use of an apparently weaker base[156].

Finally, a reaction was performed on mycalamide B in which the amount of methyl iodide added was slightly less than usual, but still in excess. This gave an almost 1:1 ratio of 7,17-di-*O*-methyl, *N*-methyl mycalamide A (**2.27**) and a more polar compound by HPLC and $^1$H NMR spectroscopy, where the latter was not mycalamide B. The H7 resonance of the new compound was shifted upfield[101] (-0.4 ppm), whereas the H10 resonance appeared as a triplet, with a chemical shift close to that observed for the same resonance in mycalamide B, suggesting that this was a 7,17-di-*O*-methyl mycalamide A derivative (**2.33**). However, there was insufficient material from this reaction to purify this compound and, rather than repeat this reaction, it was decided to concentrate on finding alternative methods of methylation which would not affect the amide, nor be so biased towards methylation of the C7 hydroxyl group.

## 2.4.5 PREPARATION AND CHARACTERISATION OF PRODUCTS FROM THE METHYLATION OF MYCALAMIDES A AND B USING METHYL IODIDE AND SILVER OXIDE IN BENZENE

Silver(I) oxide, which is a milder base than potassium hydroxide, has been used in conjunction with methyl iodide in methylation reactions for many years[76,77] (Purdie method). It has been reported[156] that silver salts promote the *O*-alkylation of amides, which was potentially useful, although really no amide alkylation was desired. In a study on the alkylation of 2-pyridones[157] it was observed that the choice of the solvent, as well as the base, had a major effect on the methylation product obtained. For example, non-polar solvents, such as benzene, favoured *O*-alkylation. In the present study, it was reasoned that the preferential methylation of the C7 hydroxyl group for the reactions in DMSO could be a reflection of a greater ease of ionisation of this group, due to the presence of neighbouring electron-withdrawing entities at C6 and C8. A non-polar, low-ionising solvent, such as benzene[140,158], could reduce the importance of this effect, and possibly also reduce formation of the amide anion[156], so that new methylated products might be obtained. Therefore the methylation of mycalamide A was attempted with this new combination of silver oxide and methyl iodide in benzene.

### 2.4.5.1 PRODUCTS DERIVED FROM MYCALAMIDE A

The reaction of mycalamide A with the above reagents, in a sealed vial at 80°C for three days, gave a mixture of three products of higher $R_f$ by silica gel TLC, which gave light orange-brown chars on visualisation with anisaldehyde (see Experimental), similar to mycalamides A and B, whereas darker brown chars were obtained for the *N*-methylated derivatives above. A $^1$H NMR spectrum of the mixture showed that there were apparently no products arising from methylation of the amide group, since the H10

resonances were of similar chemical shift to those observed for mycalamide A and appeared as triplets, indicating the presence of coupling between the H10 protons and the adjacent NH and H11 protons. However, there were several new methoxyl resonances, confirming that methylation of some of the hydroxyl groups had occurred. Preparative TLC gave three pure fractions, which represented one trimethylated mycalamide A derivative and two dimethylated derivatives by DCIMS and HREIMS. A $^{1}H$ NMR spectrum of the least polar, major fraction showed three new methoxyl resonances, at δ3.55, 3.37 and 3.28 ppm, and there were shifts in the H7 (-0.4), NH (-0.4), H15 (-0.3), H17 (-0.4) and H18 (-0.1) proton resonances (Table 2.12), consistent with methylation of the three hydroxyl groups of mycalamide A[101] (**2.31**). Irradiation of H7 in an NOE experiment gave an enhancement of the NH resonance and the methoxyl resonances at δ3.55 and 3.28 ppm (Table 2.13), which were therefore assigned to the groups at C7 and C6, respectively, by reference to the mycalamide A data. The remaining methoxyl resonances could be assigned by comparison with data for the *N*-methylated derivatives above. The $^{13}C$ NMR spectrum of this derivative (**2.31**) also showed three new methoxyl resonances, at δ60.2, 59.19 and 56.81 ppm, which were assigned by comparison with data for derivatives above. There were also shifts in the C7 (+10.2), C8 (-1.5), C15 (-3.1), C16 (-2.1), C17 (+6.2) and C18 (+6.5) resonances (Table 2.14) which were indicative of this methylation[117].

The $^{1}H$ NMR spectrum of the second fraction showed some similar features to those discussed above for compound **2.31**, but the resonance assigned to the C17 methoxyl group was absent. Furthermore, the H15 and H17 proton resonances were shifted much less, compared to the mycalamide A data, whereas the H18 resonances were shifted further upfield (Table 2.12), as shown by a COSY experiment. The same NOE interactions were observed on irradiation of H7 as above. Therefore this evidence suggested that this

derivative was 7,18-di-*O*-methyl mycalamide A (**2.32**). The $^{13}C$ NMR spectrum confirmed this[117], since the C15 and C16 resonances were similar to those observed for mycalamide A, whereas there was a small upfield shift in the C17 resonance (-1.5) and a large downfield shift in the C18 resonance (+9.8 ppm) (Table 2.14).

The final fraction was too small to perform a full NMR spectroscopic analysis. However, a $^1H$ NMR spectrum suggested that this was a 7,17-di-*O*-methyl derivative (**2.33**), based on the chemical shifts of the H7 and new methoxyl resonances (Table 2.12) and the otherwise similarity of the spectrum to that of mycalamide B. The preparation of this compound from mycalamide B is described below.

In an attempt to prepare the remaining, less highly substituted methyl ethers, the reaction of mycalamide A with silver oxide and methyl iodide in benzene (in a sealed vial at 95°C) was stopped after 1.5 hours, when TLC showed the presence of at least two compounds of similar $R_f$ to mycalamides A and B. Careful preparative TLC separated four fractions, of which the most polar was unreacted mycalamide A by $^1H$ NMR spectroscopy. The remaining fractions contained only compounds that were isomeric with mycalamide B by DCIMS and HREIMS.

The $^1H$ NMR spectrum of the second, most polar fraction contained a new methoxyl resonance at δ3.56 ppm, which was enhanced on irradiation of H7 in an NOE experiment. The observed upfield shift in H7, and the large downfield shift of C7 in a $^{13}C$ NMR spectrum (Tables 2.12 and 2.14), were further evidence that this was 7-*O*-methyl mycalamide A (**2.34**).

The $^1H$ NMR spectrum of the least polar, major fraction contained a new methoxyl resonance at δ3.35 ppm, while the H18 resonances were shifted upfield, as confirmed by a COSY experiment. Similarly, the $^{13}C$ NMR spectrum showed similar shifts in the C16-C18 sidechain resonances to those

of the 7,18-di-*O*-methyl derivative, but was otherwise similar to that of mycalamide A. Therefore this was 18-*O*-methyl mycalamide A (**2.35**).

The $^1$H NMR spectrum of the remaining fraction showed it to be a mixture of 17-*O*-methyl mycalamide A and 18-*O*-methyl mycalamide A (**2.35**), in a ratio of about 3:2. Hence mycalamide A had been partially converted into mycalamide B, but in rather poor yield, since the major product of the reaction was clearly the 18-*O*-methyl derivative. Based on the product masses, the rate of methylation at the three hydroxyl groups, C18, C17 and C7 was about 3:1:1, which illustrates only the expected steric effect which causes $S_N2$ reactions at primary hydroxyl groups to be favoured over those at secondary hydroxyl groups[140]. Therefore this reaction had been entirely successful in obtaining a different priority for methylation of mycalamide A and thus a wider range of derivatives.

### 2.4.5.2 PRODUCTS DERIVED FROM MYCALAMIDE B AND THE USE OF AN ACETYL PROTECTING GROUP FOR OPTIMISED SEPARATIONS

The remaining derivative not obtained from the methylation of mycalamide A was the 17,18-di-*O*-methyl derivative, which was of most interest due to the similarity with pederin. Methylation of mycalamide B would seem to provide a good route to this, and the reaction of mycalamide B under analogous conditions did give a mixture of at least two components by TLC. To overcome the problem of the similarity in $R_f$ values for the different derivatives, it was decided to derivatise prior to separation. An acetylation reaction was easily performed on the crude product mixture, to give three clearly resolved components by silica gel TLC. These were separated by preparative TLC and examined by $^1$H NMR and mass spectroscopies. The $^1$H NMR spectrum of the least polar fraction showed that this was mycalamide B diacetate (**2.19**), arising from the presence of unreacted mycalamide B in the

product mixture. The remaining two fractions contained mycalamide B monoacetates, each with a new methyl group, by DCIMS and HREIMS.

The $^1$H NMR spectrum of the major monoacetate clearly showed that the ester group was at C7, since there was a large downfield shift in the H7 proton resonance and a new acetate methyl resonance at δ2.20 ppm. There was also a new methoxyl resonance at δ3.37 ppm and an upfield shift in the H18 proton resonances, consistent with methylation at the C18 hydroxyl group, giving the structure **2.36**. The $^1$H NMR spectral data were fully assigned with the assistance of a COSY experiment (Table 2.8). The $^{13}$C NMR spectral data (Table 2.9) were also consistent with these substitutions. The $^1$H NMR spectrum of the minor monoacetate similarly showed the expected downfield shifts in the H18 proton resonances, due to acetylation of the C18 hydroxyl group, and an upfield shift in the H7 resonance with methylation at the C7 group, along with the new methoxyl and acetate resonances (Table 2.8). COSY and NOE experiments were performed to prove the assignments of the $^1$H NMR data and a $^{13}$C NMR spectrum was also obtained for this compound, 7,17-di-*O*-methyl mycalamide A 18-monoacetate (**2.37**).

The pure 7,17-di-*O*-methyl (**2.33**) and 17,18-di-*O*-methyl (**2.38**) mycalamide A derivatives were obtained by deacetylation of the monoacetates (**2.37** and **2.36**) in mild base, using conditions described earlier in this chapter. TLC, DCIMS, HREIMS, $^1$H and $^{13}$C NMR spectroscopy showed complete deacetylation and the NMR data for both derivatives (Tables 2.12 and 2.14) were readily assigned by comparison with those of other derivatives. Therefore a full set of all possible partially and fully methylated derivatives of mycalamide A had been obtained from these reactions.

It was observed that, on storage, the 7,17-di-*O*-methyl derivative (**2.33**) began to form fine rosettes from the solvent evaporated oil, suggesting a

tendency towards crystallisation which none of the previous derivatives had shown. Indeed, slow evaporation from ether/petroleum ether mixtures gave fine, clear needles. Preliminary x-ray analysis of one crystal showed weak diffraction, but the size of the crystal was unfortunately too small to permit a full analysis using equipment in this department. Further crystallisation attempts from other solvent mixtures or from cooled solutions gave non-crystalline solids or oils, respectively. A subsequent attempt to repeat the results above also failed, probably because of the small sample size and contamination from solvent impurities after many attempts. It was possible that an x-ray crystallographic analysis could be performed on needles like those above on equipment not available here. However, unfortunately, there was insufficient time to repeat the synthesis and purification of this derivative for such an analysis.

### 2.4.6 BIOLOGICAL ACTIVITIES OF MYCALAMIDE METHYL ETHERS

The results obtained from tests in our assay system of the biological activities of the mycalamide methyl ethers have been listed in Table 2.6. Note that, in order to present accurate data, several derivatives were subjected to a further stage of chromatography, since the presence of trace amounts of more active derivatives may otherwise have distorted many of the results. For comparative purposes, the results for mycalamides A and B and pederin have also been listed.

It is readily apparent that alkylation of the C7 hydroxyl group leads to the greatest change in biological activity, that is a substantial deactivation by a factor of at least $10^2$-$10^3$. This loss in activity due to substitution of the C7 hydroxyl group appeared to be less dramatic for the esters, discussed in an earlier section, but just as significant for the t-butyldimethylsilyl ethers. These results confirm that the C7 hydroxyl group has a very important role in the

activity of the mycalamides. It is possible that this functionality is directly involved in binding with a receptor[15] (on a ribosome[49]) which leads to an inhibition of protein synthesis, since the latter is a known mechanism of action of the mycalamides[57] and pederin[46,47] (see Introduction). It has been shown from methylations performed in DMSO that the C7 hydroxyl group is the most nucleophilic entity in mycalamides A and B under basic conditions. This is probably due to the presence of neighbouring electron-withdrawing groups (the amide carbonyl at C8 and the acetal at C6), which may inductively promote ionisation of this hydroxyl group.

Methylation of the amide nitrogen also occurred readily, but the 7-*O*-methyl, *N*-methyl derivatives obtained appeared to be even less active than the 7-*O*-methyl derivatives above and could be considered inactive within the limits of purity attained. This result suggests the probable importance of neighbouring functional group systems to C7 for the biological activity.

Of particular interest was the biological activity of derivatives in which the C7 hydroxyl group was not methylated. Methylation of either, or both of the C17 and C18 hydroxyl groups in mycalamide A gave three different derivatives which were significantly more active than mycamide A and almost equally as potent as pederin. However, since the 17-*O*-methyl derivative (mycalamide B) is also a natural product, and the other two derivatives were approximately equal in activity to this compound, then overall this somewhat difficult sidechain methylation seems to represent no major improvement for potential analogues.

One possible factor in the increased biological activities of these derivatives, compared with mycalamide A, could be the changes in the distributions of solution conformations of this C16-C18 sidechain portion on methylation of the hydroxyl groups, as observed by $^1$H NMR spectroscopy. In particular, the H15-H16 coupling constants are 5.5 and 7.1 Hz in mycalamide

A in $CDCl_3$ solution, but 3.3 and 8.3 Hz in mycalamide B, and the smaller value is 2.9 Hz in 18-*O*-methyl mycalamide A (**2.35**). However, this portion of the molecule is undoubtedly flexible and various hydrogen bonding effects are possible. The close spatial interaction of the sidechain of mycalamide B with the O1-C6 tetrahydropyran ring has previously been shown by the observation of various NOE interactions (Chapter 1) and results from the *N*-methyl derivatives also suggest that the substituents on this sidechain have some effect on interactions at the amide site. Further reactions on this sidechain will be reported in Chapter 7.

The remaining structural differences between the mycalamides and pederin occur in the substituents at C10, C12 and C13. Evidently methylation of the C13 hydroxyl group of pederin would have no major effect on the activity, since the C13 methoxyl group is present in all the mycalamides. Also, the extra ring in mycalamides A and B and onnamide A has the effect of fixing the conformation of the C10 methoxyl group of pederin, but this too evidently has little effect on the biological activity, as illustrated by the similarity of the results for 17,18-di-*O*-methyl mycalamide A (**2.38**) and pederin. Thus these changes were not significantly affecting the active conformation[70,71] or interactions at the active site[15,16].

Further work is in progress to test these derivatives in a variety of assay systems. The mycalamide A and B methyl ethers were tested against a wide range of tumour cell lines at the National Cancer Institute (NCI) in the U.S.A. Although some were not tested at appropriate concentrations it appeared that the compounds were relatively non-selective in their action. However, the NCI has expressed further interest in some of these derivatives.

## 2.5 BENZYLATION AND RELATED ATTEMPTED ALKYLATIONS OF MYCALAMIDES A AND B

The preparation of mycalamide A and B benzyl ethers arose from the need for a protecting group that would be stable to strongly basic conditions and yet be easily added or removed under relatively neutral conditions. The methyl ethers prepared above could not be selectively cleaved, since the favoured reagent for their removal, boron trichloride[76], also attacks all ether and acetal bonds[77]. Also, the preparation and purification of these ethers was not trivial. In contrast, benzyl ethers can be cleaved under conditions in which most other groups are stable, namely by hydrogenolysis over palladium catalysts[77,78]. The reactions of mycalamides A and B under such conditions will be reported in Chapter 4, but these did not exclude this possibility. Alternatively, some substituted benzyl ethers are also removable under mild oxidising conditions[78,159]. (The lability of the benzyl group and related derivatives is due to the stability of the benzyl radical). Other advantages of benzyl ethers were their base stability[138], potential selectivity in formation, and the expected larger difference in polarity for the variously substituted mycalamide derivatives, based on results for the p-bromobenzoate esters, so that reaction products could be more easily separated and purified.

### 2.5.1 PREPARATION AND CHARACTERISATION OF MYCALAMIDE A BENZYL DERIVATIVES

Modification of the method of Johnstone[151], described for the methylation reactions above, provided a convenient starting point for preparing derivatives with a benzyl ether group at the important C7 position. Thus benzylation of mycalamide A, using benzyl bromide and potassium hydroxide in DMSO at room temperature, yielded a mixture of derivatives

within minutes by TLC. Preparative TLC gave four fractions, which consisted of one mono-benzylated, two di-benzylated, and one tri-benzylated mycalamide A derivatives by DCIMS and either HREIMS or HRFABMS.

The $^{1}H$ NMR spectrum of the most polar, mono-benzylated derivative showed the presence of a new pair of doublets, at δ4.77 and 4.68 ppm, and aromatic resonances, which were assigned to the new benzyl group. The observed shifts in the H2 (-0.1), H5a (+0.1), 6-$OCH_3$ (-0.2), H7 (-0.2) and NH (-0.3) resonances (Table 2.15), as assigned by a COSY experiment, were indicative of substitution at the C7 oxygen[101] (structure **2.39**). This substitution was confirmed by the observation of an NOE interaction between H7 and the new methylene protons of the benzyl ether group (Table 2.13). A $^{13}C$ NMR spectrum showed a large downfield shift in the C7 resonance (+8.0 ppm), consistent with this substitution[117], in addition to new resonances at δ73.24 and 128-129 ppm for the benzyl ether group (Table 2.16).

The $^{1}H$ NMR spectrum of a second fraction suggested that it was 7,18-di-*O*-benzyl mycalamide A (**2.40**), since there were additional shifts in the H16 (+0.1), H17 (+0.1) and H18 (-0.1) resonances to those observed above and there was a second set of benzyl ether proton resonances (Table 2.15). Irradiation of the H18 signals in an NOE experiment caused an enhancement of these new benzyl methylene resonances, which were also non-equivalent. The $^{13}C$ NMR spectrum further confirmed this substitution, since there was a downfield shift in the C18 resonance of 7 ppm, and there were new benzyl resonances, as expected (Table 2.16).

The $^{1}H$ NMR spectra of the remaining two derivatives contained resonances that were very broad and it was evident that both compounds contained an *N*-benzyl group, since the H10 resonances were shifted downfield and appeared as doublets. The $^{1}H$ NMR spectrum of the more polar derivative suggested that the two benzyl groups be located on the C7

oxygen and the amide nitrogen (structure **2.41**), since there were shifts in the H5a (+0.3), H5e (-0.1), 6-$OCH_3$ (-0.3), H10 (+0.5) and H11 (+0.1) proton resonances, as assigned by a COSY experiment, while the methylene resonances of the two benzyl groups were spread over a range of 1.3 ppm (Table 2.15), indicating that some shielding interactions must be involved[123]. The $^1H$ NMR spectrum of the tribenzylated derivative contained similar shifts, but the H18 resonances were shifted upfield and one of the H16 resonances downfield, as shown by a COSY experiment, so that the third benzyl ether group was located at C18 (structure **2.42**). The broadening of resonances was also apparent in a $^{13}C$ NMR spectrum of this tribenzylated derivative, which suggested that a similar conformational exchange process was occurring to that observed for the *N*-methylated derivatives above[107,121]. This was supported by the results of NOE experiments (Table 2.13), where signals for a minor conformation were saturated when the related signals for the major conformation were irradiated. This exchange is investigated in more detail below for a mycalamide B derivative.

### 2.5.2 PREPARATION, CHARACTERISATION AND SOLUTION CONFORMATIONS OF MYCALAMIDE B BENZYL DERIVATIVES

The benzylation of mycalamide B under analogous conditions gave a mixture of three products by TLC. Preparative TLC yielded three fractions, which represented one mono- and two di-benzylated mycalamide B derivatives by HRFABMS and DCIMS. The $^1H$ NMR spectra of these derivatives showed that these were 7-*O*-benzyl mycalamide B (**2.43**), 7,18-di-*O*-benzyl mycalamide B (**2.44**), and 7-*O*-benzyl, *N*-benzyl mycalamide B (**2.45**), according to the observed chemical shifts of resonances assigned by COSY experiments (Table 2.17). These structures were further confirmed by recording $^{13}C$ NMR spectra for the first two derivatives, which showed similar

substituent effects to those of the mycalamide A compounds above (Table 2.16). An NOE experiment on mycalamide B 7-*O*-benzyl ether (**2.43**) also showed the expected interaction between H7 and the new benzyl methylene protons (Table 2.13).

The benzylation of mycalamide B for longer reaction times (3 hours at room temperature) gave a mixture of two new products by TLC. Significantly, there was a difference in the colour of the spots on visualisation, with the lower $R_f$ compound giving a darker brown char and the higher $R_f$ compound an orange brown char. Preparative TLC yielded two fractions which both contained tribenzylated mycalamide B derivatives by DCIMS and HRFABMS.

The $^1$H NMR spectrum of the major fraction, which was of lower $R_f$ on silica gel TLC, showed that it contained an *N*-benzyl group, but the resonances were broad and the multiplets poorly resolved, while there appeared to be some minor signals. The data for this derivative (**2.46**) were partially assigned using results from a COSY experiment (Table 2.17). Similarly a $^{13}$C NMR spectrum showed weak, broad resonances, but was not fully assignable. A variable temperature study, from -10 to +55°C, was conducted to investigate this probable conformational exchange[98,114,121]. The $^1$H NMR spectra showed increased broadening of most resonances with increasing temperature, although some resonances of protons on the O1-C6 tetrahydropyran ring were sharper. However, on cooling to 0°C, the $^1$H NMR spectrum showed two distinct sets of sharpened resonances, in a ratio of about 5:2. Difference NOE experiments were performed which assigned some of the signals for the minor conformation. NOE interactions were observed between the H7 and H10 protons and between H7 and both sets of benzyl methylene protons (Table 2.13) which required the presence of both *E* and *Z* conformations about the C8-N amide bond[107,79], as observed for the *N*-

methylated derivatives above. The $^{1}H$ NMR data for these two conformations, recorded at -10°C, are listed in the Experimental section.

An HMQC experiment was also performed at -10°C, which enabled the $^{13}C$ NMR data to be assigned (Table 2.16), and, by comparison, the $^{13}C$ NMR data for 7,18-di-*O*-benzyl, *N*-benzyl mycalamide A (**2.42**). Some features of these data were the observed shielding of the 6-$OCH_3$, C7, 7-$OCH_2$, C11 and C18 carbon resonances on *N*-benzylation, along with the expected downfield shift of the C10 resonance[117]. The new N-$CH_2$ carbon resonance was observed at δ46.3 ppm and was correlated in the HMQC spectrum to the pair of methylene proton doublets at δ5.1 and 4.7 ppm, which had an unusually large geminal coupling constant of 17 Hz. This suggests that these *N*-benzyl methylene protons are influenced by the amide π system[102,160]. This assignment also required that the C7-*O*-benzyl methylene proton resonances be those at δ4.4 and 3.9 ppm, shifted upfield by shielding effects involving the new *N*-benzyl group[123]. Therefore the $^{1}H$ and $^{13}C$ NMR data were able to be completely assigned.

The $^{1}H$ NMR spectrum of the minor fraction from the benzylation of mycalamide B showed resonances of normal linewidths, with three sets of methylene resonances for the benzyl ethers, all with typical geminal coupling constants of about 12 Hz[102]. Therefore this compound was probably *O*-benzylated at the amide, having a double bond between C8 and the new imidate nitrogen, as in structure **2.47**. The formation of an *O*-alkylated amide derivative under these reaction conditions is unusual, since normally silver salts or strong alkylating agents under neutral conditions are required to promote *O*-alkylation of amides[156]. Here the initial preference for benzylation of the C7 hydroxyl group may leave the amide nitrogen partially hindered to benzylation, allowing some *O*-benzylation to occur.

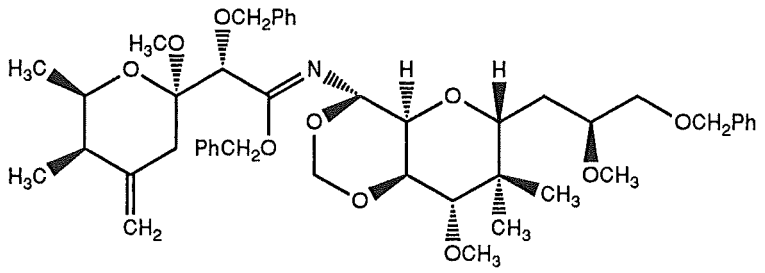

7,8,18-tri-*O*-Benzyl mycalamide B (**2.47**)

The observed $^1$H NMR chemical shifts for many resonances, particularly those relating to substituents of the trioxadecalin ring system, were very different from those observed for mycalamide B and other derivatives. To illustrate this, there were shifts (in ppm) in the H2 (-0.2), 2-$CH_3$ (-0.2), 3-$CH_3$ (-0.2), H5a (+0.8), 6-$OCH_3$ (-0.2), H7 (+0.4), H10 (-0.8), 10-OCH*R* (-0.4), 10-OCH*S* (+0.3), H11 (-0.3), H12 (-0.2), H13 (-0.6), 13-$OCH_3$ (-0.2), 14-$CH_3$*R* (+0.2), H15 (+0.1), H16 (+0.8) and H16 (+0.2) proton resonances (Table 2.17), as assigned by a combination of COSY and NOE experiments, described below. Also the vicinal proton-proton coupling constants for the C10-C13 portion were (in Hz), H10-H11 (1.5), H11-H12 (1.4) and H12-H13 (2.8), which required that the trioxadecalin ring system be in a different major solution conformation. There were certain NOE interactions, in particular H10-H11, 10-OCH*S*-H12, H12-H13, H13-14-$CH_3$*S* and H16-H11 (Table 2.13), which required that this new conformation be the alternate chair-chair conformation. Also, there was a strong NOE interaction between the H7 and H10 protons which required that the stereochemistry about the new C8=N imidate double bond be mostly *E*, and these conformations are depicted in Figure 2.2.

In this observed conformation, the new imidate nitrogen is axial to the C10-C12 dioxan ring at C10. This may suggest that the anomeric effect[105,106] is a significant factor influencing the ring conformation. However, steric effects are probably also important, since in the predominant solution conformation of mycalamide A the amide nitrogen is equatorial to this ring at C10[18,19]. Molecular modelling of the two chair-chair conformations of the

trioxadecalin ring system (Chapter 1) showed that the energy minima for both conformations were within 2 kJ $mol^{-1}$. Hence it is possible that small electronic or steric preferences may account for this change in conformation. This work thus demonstrates the availability of both chair-chair conformations for the trioxadecalin ring system, this derivative being the first to have the alternate chair-chair conformation as a major solution conformation.

The $^{13}C$ NMR spectrum also showed large changes in chemical shift for carbons involved in these new solution conformations, as assigned by an HMQC experiment. In particular, the C10 (+8.6), C11 (-6.1), C12 (-5.7), C13 (+4.7), 13-$OCH_3$ (-2.5), C14 (-5.0), 14-$CH_3$*R* (+4.5), 14-$CH_3$*S* (+8.9) and C15 (+3.1) resonances were most affected (Table 2.16). This explains the observed broadening of many of these resonances in mycalamide A and B and derivatives, where there is some conformational exchange with this alternate chair-chair conformation, since the chemical shift differences for carbons in the two conformations are substantial, especially for the 14-$CH_3$*S* resonance (C10 may be affected by the new imidate system here). The chemical shift of the new 8-$OCH_2$ resonance, at δ67.4 ppm, was consistent with the structure proposed, rather than an *N*-benzyl derivative[117], but the C8 resonance was not observed.

**Figure 2.2** $^1H$-$^1H$ NOE interactions and partial solution conformation of 7,8,18-tri-*O*-benzyl mycalamide B (**2.47**)

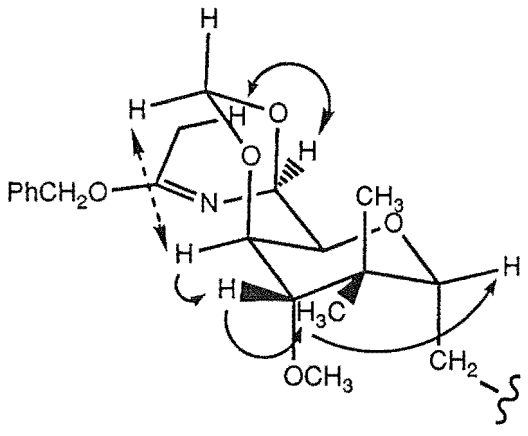

## 2.5.3 BIOLOGICAL ACTIVITY AND FURTHER ALKYLATION ATTEMPTS

The biological activity results for all the benzyl derivatives above are listed in Table 2.6. Not surprisingly, all were relatively inactive since they contained an ether group at C7. However, these derivatives were important as protected intermediates, as will be described in Chapter 6.

The presence of the double bond in mycalamides A and B meant that any attempted hydrogenolysis of the benzyl group in the derivatives above would be non-selective. An alternative method of protection was a 4-methoxy benzyl or a 3,4-dimethoxy benzyl group[159], which could be removed by very mild oxidation using 2,3-dichloro-5,6-dicyanobenzoquinone (DDQ)[161]. Before attempting the formation of these ethers, the reaction of mycalamide A with DDQ was checked by $^1$H NMR spectroscopy. Mycalamide A was observed to undergo slow decomposition in the presence of DDQ, over a period of a few hours at room temperature. This was ascribed to the known decomposition of DDQ in the presence of water and alcohols to give the acid hydrogen cyanide[161]. It was therefore of interest to note that a recent publication of the total synthesis of mycalamides A and B made successful use of this dimethoxy benzyl group for protection of the C7 hydroxyl and removed it with DDQ in a key final step[91]. This work was not pursued further.

Several attempts were made to prepare a trityl ether of mycalamide A. Trityl ethers are commonly used in carbohydrate and steroid chemistry for the selective substitution of primary hydroxyl groups[76,78]. Various methods were tried, including the use of dimethylaminopyridine (DMAP) as a catalyst in various solvents[162,143], in the presence of base and trityl chloride, but none appeared to be successful. The bulky size of both the reagent and the mycalamide A molecule may be a factor since a reaction with propan-1,2-diol was successful[58]. Therefore this reaction was also abandoned, many useful derivatives having been already synthesised above.

**Table 2.1** $^1$H NMR data[a] for mycalamide A and B trimethylsilyl (TMS) and t-butyldimethylsilyl (TBDMS) ethers.

| | Myc.A 17,18-bis-TMS ether (2.4) | Myc.A tris-TMS ether (2.1) | Myc.B 18-mono-TMS ether (2.3) | Myc.B bis-TMS ether (2.2) | Myc.B 18-mono-TBDMS ether (2.8) | Myc.B bis-TBDMS ether (2.9) |
|---|---|---|---|---|---|---|
| H2 | 3.99 (2.8,6.6) | 3.88 (2.7,6.6) | 4.05 (2.9,6.5) | 3.90 (2.7,6.6) | 4.03 (2.9,6.6) | 3.87 (2.8,6.5) |
| 2-$CH_3$ | 1.21 (6.6) | 1.18 (6.6) | 1.20 (6.6) | 1.18 (6.6) | 1.21 (6.6) | 1.17 (6.6) |
| H3 | 2.27 (2.3,6.9) | 2.19 (2.6,6.8) | 2.26 (2.6,7.1) | 2.20 (2.6,7.1) | 2.27 (2.6,7.0) | 2.19 (2.9,7.1) |
| 3-$CH_3$ | 1.02 (7.2) | 1.00 (7.0) | 1.02 (7.2) | 1.00 (7.1) | 1.02 (7.2) | 0.99 (7.0) |
| 4=CH*Z* | 4.87 (1.8) | 4.81 (2.0) | 4.86 (1.8) | 4.81 (1.9) | 4.86 (2.0) | 4.81 (2.0) |
| 4=CH*E* | 4.71 (1.8) | 4.71 (2.1) | 4.73 (1.8) | 4.71 (2.0) | 4.70 (2.0) | 4.71 (2.0) |
| H5a | 2.24 (2.0,14.0) | 2.35 (1.9,14.7) | 2.18 (2.0,13.9) | 2.34 (2.0,14.5) | 2.15 (2.1,14.2) | 2.36 (2.0,14.6) |
| H5e | 2.34 (14.0) | 2.58 (14.5) | 2.34 (13.8) | 2.50 (14.5) | 2.30 (13.8) | 2.51 (14.4) |
| 6-$OCH_3$ | 3.28 | 3.28 | 3.31 | 3.27 | 3.28 | 3.29 |
| H7 | 4.22 (2.6) | 4.25 | 4.26 | 4.26 | 4.24 (2.7) | 4.22 |
| 7-OH | 3.94 (2.6) | | 3.98 | | 3.86 (2.7) | |
| NH9 | 7.54 (9.3) | 7.38 (9.6) | 7.52 (9.6) | 7.35 (9.9) | 7.51 (9.4) | 7.27 (9.9) |
| H10 | 5.72 (9.1) | 5.76 (9.6) | 5.79 (9.4) | 5.78 (9.8) | 5.78 (9.4) | 5.76 (8.8,9.8) |
| 10-OCH*R* | 5.12 (7.0) | 5.11 (6.9) | 5.13 (6.9) | 5.13 (7.0) | 5.12 (7.0) | 5.10 (7.0) |
| 10-OCH*S* | 4.83 (7.0) | 4.81 (6.9) | 4.85 (6.9) | 4.82 (6.9) | 4.84 (7.0) | 4.82 (7.0) |
| H11 | 3.82 (6.5,9.0) | 3.77 (6.4,9.5) | 3.79 (6.6,9.3) | 3.79 (6.6,9.6) | 3.79 (6.3,9.0) | 3.74 (6.1,8.7) |
| H12 | 4.14 (6.5,9.8) | 4.17 (6.4,10.2) | 4.19 (6.4,10.2) | 4.20 (6.5,10.3) | 4.14 (6.3,9.5) | 4.14 (6.2,9.2) |
| H13 | 3.42 (10.0) | 3.42 (10.3) | 3.41 (10.3) | 3.43 (10.3) | 3.41 (9.3) | 3.38 (9.3) |
| 13-$OCH_3$ | 3.53 | 3.54 | 3.55 | 3.55 | 3.53 | 3.52 |
| 14-$CH_3$*R* | 1.01 | 0.98 | 1.00 | 0.98 | 1.02 | 1.00 |
| 14-$CH_3$*S* | 0.86 | 0.86 | 0.87 | 0.87 | 0.87 | 0.87 |
| H15 | 3.35 (2.1,10.1) | 3.34 (1.7,9.9) | 3.33 (m) | 3.25 (m) | 3.36 (1.5,9.8) | 3.35 (2.0,9.6) |
| H16 | 1.71 (2.0,9.7,14.4) | 1.74 (2.0,10.3,13.8) | 1.72 (1.8,9.8,13.8) | 1.74 (1.8,9.9,14.0) | 1.76 (2.0,9.5,14.2) | 1.79 (2.0,9.8,14.2) |
| H16 | 1.43 (m) | 1.42 (m) | 1.48 (m) | 1.52 (m) | 1.50 (m) | 1.53 (m) |
| H17 | 3.73 (m) | 3.72 (m) | 3.14 (m) | 3.18 (m) | 3.12 (m) | 3.16 (m) |
| 17-$OCH_3$ | | | 3.23 | 3.27 | 3.21 | 3.26 |
| H18 | 3.50 (4.5) | 3.53 (2.6,11.4) | 3.64 (2.6,11.4) | 3.66 (2.5,11.5) | 3.67 (2.8,11.5) | 3.70 (2.8,11.5) |
| H18 | 3.50 (4.5) | 3.47 (4.4,11.3) | 3.51 (4.2,11.6) | 3.50 (4.1,11.5) | 3.57 (4.1,11.5) | 3.57 (3.7,11.6) |
| -$OSi(CH_3)_3$ | 0.14,0.06 | 0.21,0.10,0.06 | 0.13 | 0.20,0.12 | | |
| -$OSiC(CH_3)_3$ | | | | | 0.91 | 0.94,0.88 |
| -$OSi(CH_3)_2$ | | | | | 0.09,0.08 | 0.16,0.14,0.06 |

[a]Data for compounds **2.4** and **2.8** were recorded in $CD_2Cl_2$. All other data were recorded in $CDCl_3$, with chemical shifts in ppm relative to $CHCl_3$, δ7.25, or to $CHDCl_2$, δ5.33 (coupling constants in Hz).

**Table 2.2** $^{13}C$ NMR data[a] for mycalamide A and B TMS ethers and various esters[b].

| | Myc.A tris-TMS ether (2.1) | B 18-mono-TMS ether (2.3) | Myc.B bis-TMS ether (2.2) | A 7,18-di-p-bromoBz (2.12) | B 18-mono-p-bromoBz (2.16) | B 7,18-di-p-bromoBz (2.17) | Myc.A triacetate (2.18) | Myc.A tripropanoate (2.22) |
|---|---|---|---|---|---|---|---|---|
| C2 | 69.66 | 69.69 | 69.69 | 70.18 | 69.55 | 70.04 | 69.73 | 69.61 |
| 2-$CH_3$ | 17.85 | 17.89 | 17.85 | 17.89 | 18.00 | 17.93 | 17.87 | 17.88 |
| C3 | 41.59 | 41.57 | 41.58 | 41.23 | 41.31 | 41.22 | 41.24 | 41.25 |
| 3-$CH_3$ | 11.78 | 12.31 | 11.90 | 12.14 | 12.20 | 12.19 | 12.04 | 12.03 |
| C4 | 147.37 | 145.95 | 147.32 | 144.67 | 145.01 | 144.74 | 145.08 | 145.15 |
| 4=$CH_2$ | 109.57 | 110.69 | 109.61 | 111.24 | 111.19 | 111.37 | 110.85 | 110.77 |
| C5 | 36.11 | 33.75 | 35.76 | 34.24 | 33.58 | 34.54 | 34.18 | 34.26 |
| C6 | 99.51 | 100.14 | 99.60 | 99.43 | 99.93 | 99.27 | 99.26 | 99.32 |
| 6-$OCH_3$ | 50.05 | 48.48 | 49.83 | 48.61 | 48.57 | 48.62 | 48.60 | 48.60 |
| C7 | 77.70 | 71.71 | 77.38 | 72.10 | 71.31 | 72.30 | 71.66 | 71.50 |
| C8 | 167.95 | 171.98 | 170.90 | 167.23 | 171.69 | 166.63 | 167.01 | 167.16 |
| C10 | 73.37 | 74.19 | 73.34 | 74.31 | 74.00 | 74.08 | 73.72 | 73.78 |
| 10-$OCH_2$ | 86.48 | 86.59 | 86.64 | 86.88 | 86.40 | 86.52 | 86.53 | 86.52 |
| C11 | 70.67 | 70.38 | 70.72 | 71.58 | 70.70 | 70.50 | 69.90 | 69.90 |
| C12 | 74.35 | 74.36 | 74.54 | 74.54 | 74.19 | 74.10 | 74.06 | 74.03 |
| C13 | 79.75 | 79.82 | 79.72 | 79.06 | 79.33 | 79.52 | 79.93 | 79.70 |
| 13-$OCH_3$ | 61.57 | 61.60 | 61.64 | 61.80 | 61.73 | 61.67 | 61.55 | 61.56 |
| C14 | 41.37 | 41.51 | 41.58 | 41.62 | 41.50 | 41.16 | 40.90 | ? |
| 14-$CH_3$*R* | 23.41 | 23.45 | 23.31 | 23.20 | 23.39 | 23.56 | 23.69 | 23.65 |
| 14-$CH_3$*S* | 13.89 | 13.93 | 13.70 | 13.66 | 13.78 | 14.03 | 14.40 | 14.40 |
| C15 | 75.99 | 76.25 | 76.02 | 79.03 | 75.67 | 75.78 | 75.53 | 75.45 |
| C16 | 33.36 | 29.67 | 29.59 | 32.81 | 30.49 | 30.51 | 30.08 | 30.10 |
| C17 | 70.27 | 78.92 | 78.94 | 68.82 | 76.46 | 76.48 | 70.01 | 69.96 |
| 17-$OCH_3$ | | 56.69 | 56.61 | | 57.09 | 57.01 | | |
| C18 | 65.28 | 62.17 | 62.20 | 68.45 | 64.48 | 63.68 | 63.57 | 63.25 |
| -OTMS/-OAc | 0.31,0.03, -0.39 | -0.55 | 0.29,-0.53 | | | | 170.60,21.06, 169.85,20.80, 169.64,20.65 | |

[a]Data for compounds **2.1**, **2.2** and **2.3** were recorded in $CD_2Cl_2$. All other data were recorded in $CDCl_3$, with chemical shifts in ppm relative to $CDCl_3$, δ77.01, or $CD_2Cl_2$, δ53.60 [b]Data for p-bromobenzoate and propanoate ester groups are listed in the Experimental section.

**Table 2.3** $^{1}H$-$^{1}H$ NOE interactions[a] for compounds in Sections **2.2-2.4.**

| Compound | Signal(s) irradiated | Signals enhanced (% enhancement) |
|---|---|---|
| A tris-TMS ether (**2.1**) | 7-OSi($CH_3$)$_3$ | H7(2), 6-O$CH_3$(0.2) |
| | 17/18-OSi($CH_3$)$_3$ | none |
| B bis-TMS ether (**2.2**) | 7-OSi($CH_3$)$_3$ | H7(2), 6-O$CH_3$(0.6) |
| | 17/18-OSi($CH_3$)$_3$ | 17-O$CH_3$(0.3) |
| A bis-TBDMS ether | H17 | H16u(3), 17-OSi($CH_3$)$_2$(0.3) |
| (**2.6**) | 17-OSi($CH_3$)$_2$ | H17(2), 17-OSiC($CH_3$)$_3$(0.4), H18d(1)[c] |
| | H18 (13-O$CH_3$) | 14-$CH_3$*R*(0.4)[b], 17-OSi($CH_3$)$_2$(0.2) |
| | 18-OSi($CH_3$)$_2$ | 18-OSiC($CH_3$)$_3$(0.4) |
| A tris-TBDMS et.(**2.7**) | H7 | H5e(3), 6-O$CH_3$(2), 7-OSi($CH_3$)$_2$(1) |
| Myc.B diacetate | 6-O$CH_3$ | H2(2), H7(8) |
| (**2.19**) | 13-O$CH_3$ | 10-OCH*R*(2), 14-$CH_3$*R*(0.5) |
| | 17-O$CH_3$ (H17) | $H_2$5(1)[b], H18d(2)[b,c] |
| B 18-acetate (**2.20**) | H7 | 6-O$CH_3$(2) |
| 7-*O*-Methyl, *N*-methyl | H7 (H12) | 6-O$CH_3$(2), 7-O$CH_3$(2), N-$CH_3$(2), |
| (**2.24**) | | 14-$CH_3$*S*(0.7)[b] |
| | H10 | H7(1), 10-OCH*R*(4), H13(3), H15(7) |
| 7,18-di-*O*-Methyl, | H7 (H12) | 6-O$CH_3$(1), 7-O$CH_3$(2), N-$CH_3$(3), H10(2), |
| *N*-methyl (**2.25**) | | 14-$CH_3$*S*(1)[b] |
| | H10 | H7(1), 10-OCH*R*(4), H13(2), H15(5) |
| | H15 | H10(2), 14-$CH_3$*R*(1) |
| 7,17-di-*O*-Methyl, | H2 | 2-$CH_3$(1), H3(5), 6-O$CH_3$(0.9) |
| *N*-methyl (**2.27**) | 6-O$CH_3$ (17-O$CH_3$) | H2(3), H7(4), H18d(4)[b,c] |
| | H7 (H11, H12) | 6-O$CH_3$(2), 7-O$CH_3$(2), N-$CH_3$(2), 14-$CH_3$*S*(1)[b] |
| | 7-O$CH_3$ (H13, H18) | H7(3), H10(5)[b], 10-OCH*R*(4)[b], H18d(5)[b,c] |
| | N-$CH_3$ | H7(3), H11(7) |
| | H10 | H7(3), 10-OCH*R*(3), H13/H15(4) |
| 7,17,18-tri-*O*-Methyl, | H2 | 2-$CH_3$(1), H3(5), 6-O$CH_3$(0.9) |
| *N*-methyl (**2.26**) | H5a (H5a', N-$CH_3$')[d] | 3-$CH_3$(1), H5e(19), H7(0.8) |
| | H5e | 4=CH*E*(6), H5a(24), H5a'(20)[d], 6-O$CH_3$(0.4), |
| | | H7(0.7) |
| | H7 (H7',H12)[d] | 6-O$CH_3$(2), 7-O$CH_3$(2), N-$CH_3$(2), H10(3), |
| | | 14-$CH_3$*S*(1)[b] |
| | H7' (H7)[d] | 6-O$CH_3$(1), 7-O$CH_3$(1), N-$CH_3$(0.8), |
| | | N-$CH_3$'(0.9)[d], H10(2) |
| | N-$CH_3$ (H5a', N-$CH_3$') | H5e(5)[b], H7(2), H11(4) |
| | N-$CH_3$' (H5a', N-$CH_3$) | 3-$CH_3$(0.4)[b], H5e(4)[b], H7(2), H7'(3), H11(2) |
| | H10 (H10')[d] | H7(3), 10-OCH*R*(4), H13(3), H15(10) |
| | H10' (H10)[d] | H7(1), H7'(3)[d], 10-OCH*R*(2), H13(1), H15(3) |
| | H11 (H7,H12) | N-$CH_3$(2), N-$CH_3$'(3)[d], H10(1), 14-$CH_3$*S*(1)[b] |
| | $H_2$16 | 14-$CH_3$*R*(1), 14-$CH_3$*S*(0.7), H15(4), H17(8) |
| 7*S*,17-di-*O*-Methyl, | H2 | 2-$CH_3$(1), 6-O$CH_3$(1) |
| *N*-methyl (**2.29**) | H7 | 6-O$CH_3$(1), 7-O$CH_3$(2), N-$CH_3$(3) |
| | N-$CH_3$ (H17) | H7(9), H11(9), 17-O$CH_3$(0.5)[b] |
| | H10 | 10-OCH*R*(4), H13(4), H15(6) |
| | H12 | 14-$CH_3$*S*(1) |
| | 14-$CH_3$*R* | H13(5), 13-O$CH_3$(1), H15(3) |
| 7*S*,17,18-tri-*O*-Methyl, | H7 | 6-O$CH_3$(1), 7-O$CH_3$(2), N-$CH_3$(4) |
| *N*-methyl (**2.28**) | H10 | 10-OCH*R*(3), H13(3), H15(4) |

[a]All data were recorded in $CDCl_3$ [b]Enhancement interpreted as being due to the irradiation of an overlapping signal [c]u and d have been used to designate the upfield and downfield resonances of a geminal pair [d]' used to designate signals for a minor conformation

**Table 2.4** $^1$H NMR data[a] for mycalamide A t-butyldimethylsilyl ethers and mycalamide B p-bromobenzoate esters.

| | A 18-mono-TBDMS ether (2.5) | A 17,18-bis-TBDMS ether (2.6) | A tris-TBDMS ether (2.7) | Myc.B 7-mono-p-bromoBz (2.15) | Myc.B 18-mono-p-bromoBz (2.16) | Myc.B 7,18-di-p-bromoBz (2.17) |
|---|---|---|---|---|---|---|
| H2 | 3.99 (2.8,6.6) | 4.03 (2.9,6.6) | 3.86 (2.6,6.5) | 4.09 (2.9,6.3) | 4.06 (2.8,6.5) | 4.05 (2.6,6.6) |
| 2-$CH_3$ | 1.20 (6.6) | 1.21 (6.5) | 1.17 (6.6) | 1.28 (6.5) | 1.21 (6.6) | 1.23 (6.6) |
| H3 | 2.26 (2.6,7.1) | 2.26 (2.9,7.0) | 2.19 (2.5,7.0) | 2.33 (2.5,6.9) | 2.29 (2.9,7.2) | 2.30 (2.7,6.9) |
| 3-$CH_3$ | 1.01 (7.1) | 1.02 (7.0) | 0.99 (7.1) | 1.10 (7.1) | 1.03 (7.1) | 1.07 (7.1) |
| 4=CH*Z* | 4.85 (m) | 4.88 (1.8) | 4.81 (1.9) | 4.94 (m) | 4.88 (1.7) | 4.91 (m) |
| 4=CH*E* | 4.71 (m) | 4.75 (1.8) | 4.71 (1.9) | 4.63 (m) | 4.73 (1.9) | 4.79 (m) |
| H5a | 2.30 (m) | 2.17 (1.8,14.4) | 2.36 (2.0,14.4) | 2.59 (m,14.0) | 2.17 (1.8,14.1) | 2.52 (m,13.5) |
| H5e | 2.30 (m) | 2.38 (14.1) | 2.55 (14.4) | 2.53 (13.8) | 2.36 (14.1) | 2.45 (13.9) |
| 6-$OCH_3$ | 3.28 | 3.31 | 3.29 | 3.20 | 3.30 | 3.19 |
| H7 | 4.25 (2.6) | 4.23 | 4.20 | 5.74 | 4.24 (2.1) | 5.63 |
| 7-OH | 3.79 (2.6) | | | | 3.83 (2.4) | |
| NH9 | 7.46 (9.7) | 7.58 (9.9) | 7.30 (9.7) | 7.48 (9.8) | 7.51 (9.7) | 7.28 (9.6) |
| H10 | 5.83 (9.7) | 5.74 (9.1) | 5.74 (8.5,9.7) | 5.79 (9.5) | 5.82 (9.5) | 5.79 (9.4) |
| 10-OCH*R* | 5.14 (7.0) | 5.11 (6.9) | 5.09 (6.9) | 5.11 (7.1) | 5.13 (7.0) | 5.08 (6.7) |
| 10-OCH*S* | 4.86 (7.0) | 4.84 (6.8) | 4.81 (6.8) | 4.89 (7.0) | 4.87 (6.9) | 4.87 (6.9) |
| H11 | 3.84 (6.4,9.7) | 3.77 (6.3,8.8) | 3.71 (6.1,8.5) | 3.78 (7.0,9.5) | 3.82 (6.7,9.5) | 3.80 (6.3,8.9) |
| H12 | 4.17 (6.6,10.2) | 4.15 (6.3,9.7) | 4.11 (6.0,9.3) | 4.24 (7.0,10.5) | 4.21 (6.6,10.2) | 4.17 (6.5,9.8) |
| H13 | 3.46 (10.1) | 3.38 (9.5) | 3.36 (9.2) | 3.42 (10.7) | 3.44 (10.0) | 3.38 (9.7) |
| 13-$OCH_3$ | 3.54 | 3.54 | 3.52 | 3.56 | 3.56 | 3.53 |
| 14-$CH_3$*R* | 1.01 | 1.01 | 1.01 | 0.95 | 0.98 | 0.96 |
| 14-$CH_3$*S* | 0.88 | 0.86 | 0.87 | 0.86 | 0.88 | 0.87 |
| H15 | 3.53 (2.3,10.0) | 3.41 (1.3,10.0) | 3.41 (1.6,10.2) | 3.41 (m) | 3.47 (m) | 3.46 (9.1) |
| H16 | 1.73 (2.1,5.2,14.0) | 1.80 (1.7,9.9,14.1) | 1.83 (1.7,10.2,13.8) | 1.55 (m) | 1.69 (2.0,9.6,14.8) | 1.72 (m) |
| H16 | 1.44 (m) | 1.39 (3.9,10.1,14.2) | 1.42 (4.5,10.3,13.6) | 1.55 (m) | 1.61 (m) | 1.64 (m) |
| H17 | 3.62 (m) | 3.66 (m) | 3.71 (m) | 3.20 (m) | 3.45 (m) | 3.45 (m) |
| 17-$OCH_3$ | | | | 3.28 | 3.31 | 3.31 |
| H18 | 3.53 (m) | 3.59 (4.2,10.8) | 3.64 (3.8,11.3) | 3.65 (1.9,12.2) | 4.48 (2.3,12.5) | 4.54 (3.0,12.3) |
| H18 | 3.47 (m) | 3.51 (2.5,10.7) | 3.53 (2.2,11.3) | 3.36 (6.8,12.4) | 4.36 (5.0,12.2) | 4.28 (4.2,12.4) |
| -OSIC($CH_3$)$_3$ | 0.90 | 0.89,0.83 | 0.94,0.88,0.84 | | | |
| -OSI($CH_3$)$_2$ | -0.08 | 0.06,-0.02 | 0.17,0.13,0.05,-0.01 | | | |
| 7-OBz | | | | 7.62,7.98 (8.6) | | 7.90,7.57 (8.5) |
| 18-OBz | | | | | 7.91,7.59 (8.6) | 7.85,7.54 (8.5) |

[a]Data for compound **2.5** were recorded in $CD_2Cl_2$. All other data were recorded in $CDCl_3$, with chemical shifts in ppm relative to $CHCl_3$, δ7.25, or $CHDCl_2$, δ5.33 (coupling constants in Hz).

**Table 2.5** $^{13}C$ NMR data[a] for mycalamide A and B TBDMS ethers.

| | A 18-mono-TBDMS ether (**2.5**) | A 17,18-bis-TBDMS ether (**2.6**) | Myc.A tris-TBDMS ether (**2.7**) | B 18-mono-TBDMS ether (**2.8**) | Myc.B bis-TBDMS ether (**2.9**) |
|---|---|---|---|---|---|
| C2 | 69.82 | 69.71 | 69.54 | 69.70 | 69.56 |
| 2-$CH_3$ | 17.81 | 17.98 | 17.86 | 17.90 | 17.85 |
| C3 | 41.60 | 41.10 | 41.36 | 41.57 | 41.32 |
| 3-$CH_3$ | 12.09 | 11.97 | 11.77 | 12.34 | 11.85 |
| C4 | ? | 144.91 | 146.65 | 145.88 | 146.62 |
| 4=$CH_2$ | 110.19 | 111.35 | 109.96 | 110.74 | 109.97 |
| C5 | 33.83 | 33.49 | 35.79 | 33.70 | 35.59 |
| C6 | 99.99 | 99.93 | 99.58 | 100.14 | 99.59 |
| 6-$OCH_3$ | 48.76 | 48.71 | 50.10 | 48.46 | 50.00 |
| C7 | 72.61 | 71.80 | 77.13 | 71.59 | 77.00 |
| C8 | ? | 171.34 | 170.58 | ? | 170.69 |
| C10 | 74.08 | 74.17 | 73.54 | 74.23 | 73.38 |
| 10-$OCH_2$ | 86.88 | 86.28 | 86.13 | 86.53 | 86.34 |
| C11 | ? | 70.10 | 70.03 | ? | 70.01 |
| C12 | 74.40 | 74.05 | 73.76 | 74.23 | 73.92 |
| C13 | 79.57 | 79.86 | 80.12 | 79.96 | 80.07 |
| 13-$OCH_3$ | 61.66 | 61.58 | 61.44 | 61.53 | 61.51 |
| C14 | ? | 41.10 | 40.89 | ? | 41.04 |
| 14-$CH_3$*R* | 23.27 | 23.86 | 24.06 | 23.70 | 23.89 |
| 14-$CH_3$*S* | 13.90 | 14.25 | 14.60 | ? | 14.30 |
| C15 | 79.07 | 76.15 | 76.20 | 76.49 | 76.31 |
| C16 | 32.36 | 33.31 | 33.05 | 29.91 | 29.70 |
| C17 | 71.37 | 70.38 | 70.38 | 79.09 | 78.87 |
| 17-$OCH_3$ | | | | 56.74 | 56.69 |
| C18 | 66.54 | 65.81 | 65.60 | 62.48 | 62.03 |
| -OSiC | ? | 18.45,18.05 | 18.40,18.27<br>18.04 | ? | 18.29 |
| -OSiC($CH_3$)$_3$ | 25.84 | 26.03,25.89 | 26.02,25.90 | 25.89 | 25.97,25.87 |
| -OSi($CH_3$)$_2$ | -5.48 | -5.22,-4.67<br>-4.32 | -5.27,-5.13<br>-4.84,-4.74<br>-4.43,-4.27 | -5.43 | -5.28,-4.88<br>-4.74 |

[a]Data for compounds **2.5** and **2.8** were recorded in $CD_2Cl_2$. All other data were recorded in $CDCl_3$, with chemical shifts in ppm relative to **C**$DCl_3$, δ77.01, or **C**$D_2Cl_2$, δ53.6 ppm.

**Table 2.6** Biological assay results for compounds in Chapter 2.

| Compound | P388 $IC_{50}$[a] | Antiviral Results[b] (ng/disk) | | | | | | | |
|---|---|---|---|---|---|---|---|---|---|
| Mycalamide A | 0.5 | WW | WW | +* | 5 | + | + | +* | 2 |
| Mycalamide B | 0.1 | WW | WW | +* | 2 | +++ | +++ | +* | 1 |
| Pederin | 0.07 | WW | WW | +* | 1 | | +++ | +* | 0.5 |
| Pederin dibenzoate (**1.2**) | 9 | WW | +++ | +* | 500 | + | - | +* | 200 |
| A 17,18-bis-TMS ether (**2.4**) | 1.2 | WW | WW | +* | 20 | ++ | +++ | +* | 5 |
| A tris-TMS ether (**2.1**) | 1.3 | WW | WW | +* | 20 | - | - | - | 5 |
| B 18-mono-TMS ether (**2.3**) | 0.1 | WW | WW | +* | 0.5 | | | | |
| B bis-TMS ether (**2.2**) | 0.2 | WW | WW | +* | 2 | - | - | - | 0.5 |
| A 18-TBDMS ether (**2.5**) | 28 | WW | WW | +* | 50 | - | - | - | 20 |
| A 17,18-bis-TBDMS eth.(**2.6**) | 1200 | WW | WW | +* | 20000 | - | - | - | 10000 |
| A tris-TBDMS ether (**2.7**) | >12500 | - | - | - | 40000 | | | | |
| B 18-TBDMS ether (**2.8**) | 23 | WW | WW | +* | 50 | - | - | - | 20 |
| B bis-TBDMS ether (**2.9**) | 600 | WW | WW | +* | 10000 | - | - | - | 5000 |
| | | | | | | | | | |
| A 7-mono-p-bromobenz.(**2.11**) | 23 | WW | WW | +* | 200 | - | + | +* | 50 |
| A 18-mono-p-bromobenz.(**2.10**) | 1 | +++ | WW | +* | 2 | - | - | - | 0.5 |
| A 7,18-di-p-bromobenz.(**2.12**) | 140 | WW | WW | +* | 2000 | + | ++ | +* | 500 |
| A 17,18-di-p-bromobenz.(**2.13**) | 57 | WW | WW | +* | 1000 | + | + | +* | 250 |
| A tri-p-bromobenzoate (**2.14**) | 115 | WW | WW | +* | 500 | - | - | - | 200 |
| B 7-mono-p-bromobenz.(**2.15**) | 24 | WW | WW | +* | 50 | - | - | - | 20 |
| B 18-mono-p-bromobenz.(**2.16**) | 20 | +++ | WW | +* | 20 | - | + | +* | 5 |
| B di-p-bromobenzoate (**2.17**) | 350 | WW | WW | +* | 4000 | +++ | +++ | +* | 2000 |
| | | | | | | | | | |
| Myc.A triacetate (**2.18**) | 45 | WW | WW | +* | 500 | +++ | +++ | +* | 200 |
| B 7-monoacetate (**2.21**) | 2 | WW | WW | +* | 200 | ++ | +++ | +* | 50 |
| B 18-monoacetate (**2.20**) | 0.9 | WW | WW | +* | 20 | ++ | +++ | +* | 10 |
| Myc.B diacetate (**2.19**) | 20 | WW | WW | +* | 200 | - | - | - | 50 |
| 17,18-di-*O*-Me, 7-acet.(**2.36**) | 1 | WW | WW | +* | 50 | - | - | - | 20 |
| 7,17-di-*O*-Me, 18-acet.(**2.37**) | 500 | +++ | WW | +* | 5000 | | | | |
| Myc.A tripropanoate (**2.22**) | 85 | WW | WW | +* | 500 | + | - | +* | 200 |
| B 18-monomesylate (**2.23**) | 0.13 | | WW | +* | 5 | - | - | - | 2 |
| | | | | | | | | | |
| 7-*O*-Methyl, *N*-methyl A (**2.24**) | 1000 | | WW | +* | 20000 | | +++ | +* | 10000 |
| 7,17-di-*O*-Methyl, *N*-Me (**2.27**) | 2500 | - | - | - | 5000 | | | | |
| 7,18-di-*O*-Methyl, *N*-Me (**2.25**) | 1500 | WW | WW | +* | 10000 | ++ | + | +* | 5000 |
| 7,17,18-tri-*O*-Me, *N*-Me (**2.26**) | 2000 | WW | WW | +* | 20000 | +++ | ++ | +* | 10000 |
| 7-D, 7*S*-*O*-Methyl, *N*-Me (**2.30**) | 1100 | WW | WW | +* | 20000 | ++ | ++ | +* | 10000 |
| 7*S*,17,18-tri-*O*-Me, *N*-Me (**2.28**) | 5000 | WW | WW | +* | 40000 | ++ | +++ | +* | 20000 |
| 7-*O*-Methyl myc.A (**2.34**) | 80 | WW | WW | +* | 1000 | | +++ | +* | 500 |
| 18-*O*-Methyl myc.A (**2.35**) | 0.1 | | WW | +* | 1 | | + | +* | 0.5 |
| 7,17-di-*O*-Methyl A (**2.33**) | 95 | | WW | +* | 2000 | | ++ | +* | 1000 |
| 7,18-di-*O*-Methyl A (**2.32**) | 105 | | WW | +* | 2000 | | - | - | 500 |
| 17,18-di-*O*-Methyl A (**2.38**) | 0.07 | | WW | +* | 1 | | ++ | +* | 0.5 |
| 7,17,18-tri-*O*-Methyl A (**2.31**) | 85 | | WW | +* | 2000 | | +++ | +* | 1000 |
| | | | | | | | | | |
| 7-*O*-Benzyl myc.A (**2.39**) | 90 | WW | WW | +* | 1000 | - | - | - | 500 |
| 7,18-di-*O*-Benzyl A (**2.40**) | 170 | WW | WW | +* | 5000 | ++ | +++ | +* | 2000 |
| 7-*O*-Benzyl, *N*-benzyl A (**2.41**) | 800 | +++ | WW | +* | 5000 | + | + | +* | 2000 |
| 7,18-di-*O*-Ben. *N*-ben.A (**2.42**) | 4000 | WW | WW | +* | 40000 | ++ | ++ | +* | 20000 |
| 7-*O*-Benzyl myc.B (**2.43**) | 45 | WW | WW | +* | 500 | - | - | - | 200 |
| 7,18-di-*O*-Benzyl B (**2.44**) | 75 | WW | WW | +* | 2000 | +++ | +++ | +* | 1000 |
| 7-*O*-Benzyl, *N*-benzyl B (**2.45**) | 170 | WW | WW | +* | 2000 | WW | ++ | +* | 1000 |
| 7,18-di-*O*-Ben. *N*-ben.B (**2.46**) | 1900 | WW | WW | +* | 20000 | + | + | +* | 10000 |
| 7,8,18-tri-*O*-Benzyl B (**2.47**) | 1200 | WW | +++ | +* | 40000 | - | - | - | 20000 |

[a] In ng/ml. The derivatives are estimated to be better than 95% pure, having been subjected to at least two steps of chromatographic purification in most cases.

[b] -,+,++,+++,WW=antiviral zone size. Results are listed in the order of *Herpes simplex virus*, *Polio virus*, cytotoxicity, loaded sample mass.

Table 2.7 $^1$H NMR data[a] for mycalamide A p-bromobenzoate and acetate esters.

| | Myc.A 18-mono-p-bromoBz.(2.10) | Myc.A 7-mono-p-bromoBz.(2.11) | Myc.A 17,18-di-p-bromoBz.(2.13) | Myc.A 7,18-di-p-bromoBz.(2.12) | Myc.A 7,17,18-tri-p-bromoBz.(2.14) | Mycalamide A triacetate (2.18) |
|---|---|---|---|---|---|---|
| H2 | 3.98 (2.7,6.6) | 4.05 (2.7,6.4) | 4.00 (2.9,6.6) | 4.04 (2.7,6.7) | 4.03 (2.8,6.6) | 3.99 (2.8,6.6) |
| 2-$CH_3$ | 1.18 (6.6) | 1.24 (6.5) | 1.19 (6.7) | 1.23 (6.6) | 1.23 (6.6) | 1.20 (6.6) |
| H3 | 2.23 (2.6,6.9) | 2.30 (2.8,6.9) | 2.22 (2.4,7.1) | 2.30 (2.8,7.0) | 2.28 (2.7,6.9) | 2.25 (2.7,7.0) |
| 3-$CH_3$ | 0.98 (7.0) | 1.06 (7.1) | 0.98 (7.1) | 1.05 (7.1) | 1.05 (7.0) | 1.03 (7.1) |
| 4=CH*Z* | 4.83 (m) | 4.90 (1.8) | 4.82 (1.9) | 4.88 (1.9) | 4.87 (1.8) | 4.87 (1.8) |
| 4=CH*E* | 4.68 (m) | 4.82 (1.8) | 4.70 (1.7) | 4.72 (1.8) | 4.75 (1.8) | 4.76 (1.9) |
| H5a | 2.36 (m,14.3) | 2.64 (1.8,14.4) | 2.26 (1.8,14.2) | 2.69 (1.8,14.4) | 2.58 (1.7,14.2) | 2.45 (1.8,14.4) |
| H5e | 2.31 (14.3) | 2.46 (14.4) | 2.39 (14.3) | 2.42 (14.4) | 2.51 (14.3) | 2.38 (14.4) |
| 6-$OCH_3$ | 3.27 | 3.21 | 3.28 | 3.20 | 3.20 | 3.18 |
| H7 | 4.28 (2.6) | 5.70 | 4.27 (2.9) | 5.70 | 5.64 | 5.47 |
| 7-OH | 3.76 (2.6) | | 3.93 (2.9) | | | |
| NH9 | 7.49 (9.9) | 7.40 (9.5) | 7.55 (9.6) | 7.45 (9.2) | 7.45 (9.2) | 7.32 (9.4) |
| H10 | 5.88 (9.8) | 5.83 (9.6) | 5.85 (9.2) | 5.85 (9.4) | 5.80 (8.2,9.1) | 5.76 (9.0) |
| 10-OCH*R* | 5.14 (6.9) | 5.10 (6.9) | 5.12 (6.9) | 5.11 (6.9) | 5.10 (7.0) | 5.06 (6.9) |
| 10-OCH*S* | 4.88 (6.9) | 4.89 (7.0) | 4.86 (6.8) | 4.90 (6.9) | 4.89 (7.0) | 4.86 (7.0) |
| H11 | 3.86 (6.6,9.8) | 3.79 (7.0,9.6) | 3.87 (6.1,8.8) | 3.82 (6.6,9.6) | 3.86 (5.7,8.0) | 3.79 (6.0,8.7) |
| H12 | 4.23 (6.5,10.5) | 4.21 (7.1,10.4) | 4.15 (6.0,9.5) | 4.21 (6.7,10.6) | 4.11 (5.8,8.7) | 4.10 (6.0,9.4) |
| H13 | 3.47 (10.3) | 3.41 (10.4) | 3.41 (9.5) | 3.44 (10.5) | 3.38 (9.0) | 3.36 (9.4) |
| 13-$OCH_3$ | 3.56 | 3.54 | 3.53 | 3.55 | 3.51 | 3.52 |
| 14-$CH_3$*R* | 1.00 | 0.93 | 1.01 | 0.96 | 1.03 | 1.01 |
| 14-$CH_3$*S* | 0.90 | 0.85 | 0.88 | 0.88 | 0.88 | 0.86 |
| H15 | 3.71 (2.1,9.7) | 3.60 (5.9,6.9) | 3.59 (2.2,9.9) | 3.76 (2.7,9.7) | 3.62 (1.4,10.2) | 3.45 (2.4,9.8) |
| H16 | 1.70 (2.4,3.8,14.5) | 1.49 (m) | 1.97 (2.1,9.0,14.6) | 1.68 (3.0,3.0,14.7) | 2.03 (m) | 1.77 (2.5,9.1,14.5) |
| H16 | 1.58 (7.9,9.5,14.7) | 1.49 (m) | 1.85 (3.6,10.4,14.5) | 1.55 (m) | 1.88 (m) | 1.62 (4.5,9.5,14.5) |
| H17 | 4.03 (m) | 3.70 (m) | 5.42 (m) | 4.02 (m) | 5.33 (m) | 4.98 (m) |
| H18 | 4.23 (5.5) | 3.57 (2.9,11.5) | 4.56 (4.5) | 4.23 (4.6,11.3) | 4.61 (2.6,12.5) | 4.27 (2.7,12.4) |
| H18 | 4.23 (5.5) | 3.29 (7.1,11.5) | 4.56 (4.5) | 4.17 (6.0,11.4) | 4.54 (4.9,12.6) | 4.14 (5.2,12.4) |
| 7-OBz | | 7.96,7.62 (8.8) | | 7.91,7.56 (8.5) | 7.97,7.59 (8.7) | |
| 17-OBz | | | 7.83,7.54 (8.7) | | 7.84,7.58 (8.7) | |
| 18-OBz | 7.89,7.57 (8.8) | | 7.82,7.54 (8.7) | 7.89,7.51 (8.6) | 7.84,7.56 (8.7) | |
| -$OCOCH_3$ | | | | | | 2.20,2.05,2.00 |

[a]Data for compound **2.14** were recorded in $CD_2Cl_2$. All other data were recorded in $CDCl_3$, with chemical shifts in ppm relative to $CHCl_3$, δ7.25, or $CHDCl_2$, δ5.33 (coupling constants in Hz).

**Table 2.8** $^{1}$H NMR data[a] for mycalamide B acetate and mesylate esters and a mycalamide A propanoate ester[b].

| | Mycalamide B 7-mono-acetate (2.21) | Mycalamide B 18-mono-acetate (2.20) | Mycalamide B diacetate (2.19) | 7,17-di-*O*-Me, myc.A 18-mono-acetate (2.37) | 17,18-di-*O*-Me, myc.A 7-mono-acetate (2.36) | Mycalamide B 18-mesylate (2.23) | Mycalamide A tripropanoate (2.22) |
|---|---|---|---|---|---|---|---|
| **H2** | 4.04 (2.8,6.6) | 4.05 (2.9,6.5) | 4.02 (2.8,6.7) | 3.94 (2.8,6.6) | 4.03 (2.8,6.7) | 4.05 (2.9,6.6) | 3.99 (2.8,6.6) |
| **2-CH$_3$** | 1.24 (6.7) | 1.21 (6.6) | 1.22 (6.5) | 1.17 (6.6) | 1.22 (6.6) | 1.21 (6.6) | 1.19 (6.6) |
| **H3** | 2.29 (2.9,7.1) | 2.27 (2.7,7.1) | 2.28 (2.7,7.3) | 2.21 (2.9,7.1) | 2.28 (2.9,7.2) | 2.27 (3.1,7.1) | 2.25 (m) |
| **3-CH$_3$** | 1.07 (7.1) | 1.02 (7.1) | 1.04 (7.2) | 0.98 (7.1) | 1.05 (7.1) | 1.02 (7.1) | 1.02 (7.1) |
| **4=CH*Z*** | 4.88 (m) | 4.87 (2.0) | 4.88 (m) | 4.82 (1.7) | 4.88 (1.7) | 4.87 (1.8) | 4.85 (1.7) |
| **4=CH*E*** | 4.77 (m) | 4.73 (1.9) | 4.75 (m) | 4.71 (1.8) | 4.76 (1.7) | 4.73 (1.9) | 4.75 (1.7) |
| **H5a** | 2.43 (m) | 2.17 (2.1,14.1) | 2.40 (m) | 2.41 (2.0,14.1) | 2.43 (1.8,14.2) | 2.14 (1.9,14.0) | 2.46 (m) |
| **H5e** | 2.43 (m) | 2.36 (14.0) | 2.40 (m) | 2.30 (14.3) | 2.36 (14.2) | 2.36 (13.9) | 2.38 (m) |
| **6-OCH$_3$** | 3.17 | 3.31 | 3.17 | 3.27 | 3.17 | 3.31 | 3.17 |
| **H7/7-OH** | 5.52 | 4.26 | 5.45 | 3.85 | 5.48 | 4.29/3.86 (2.3) | 5.48 |
| **NH9** | 7.46 (9.5) | 7.50 (9.6) | 7.27 (9.4) | 7.11 (9.9) | 7.38 (9.4) | 7.49 (9.4) | 7.34 (9.2) |
| **H10** | 5.77 (9.5) | 5.78 (9.5) | 5.75 (9.4) | 5.79 (9.7) | 5.78 (9.5) | 5.77 (9.5) | 5.77 (9.0) |
| **10-OCH*R*** | 5.09 (7.1) | 5.11 (7.0) | 5.07 (7.0) | 5.11 (6.9) | 5.08 (6.9) | 5.11 (7.0) | 5.06(7.0) |
| **10-OCH*S*** | 4.87 (7.1) | 4.85 (7.0) | 4.85 (6.9) | 4.83 (6.9) | 4.85 (6.9) | 4.86 (7.0) | 4.85 (6.9) |
| **H11** | 3.75 (6.6,9.6) | 3.78 (6.7,9.5) | 3.77 (6.5,9.4) | 3.81 (6.8,9.6) | 3.75 (6.4,9.3) | 3.79 (6.8,9.4) | 3.79 (6.1,8.7) |
| **H12** | 4.22 (7.1,10.2) | 4.20 (6.5,10.0) | 4.17 (6.6,10.0) | 4.20 (6.7,10.2) | 4.18 (6.5,10.0) | 4.20 (6.6,10.1) | 4.12 (6.0,9.4) |
| **H13** | 3.42 (10.4) | 3.42 (10.1) | 3.39 (9.8) | 3.43 (10.2) | 3.39 (10.1) | 3.43 (10.0) | 3.37 (9.4) |
| **13-OCH$_3$** | 3.55 | 3.55 | 3.53 | 3.54 | 3.54 | 3.55 | 3.52 |
| **14-CH$_3$*R*** | 0.96 | 0.97 | 0.97 | 0.97 | 0.98 | 1.01 | 0.99 |
| **14-CH$_3$*S*** | 0.85 | 0.86 | 0.86 | 0.87 | 0.86 | 0.87 | 0.85 |
| **H15** | 3.44 (1.7,10.0) | 3.38 (m) | 3.38 (2.5,9.2) | 3.36 (4.5,7.6) | 3.34 (m) | 3.41 (3.0,9.1) | 3.45 (2.5,9.8) |
| **H16** | 1.54 (m) | 1.60 (m) | 1.63 (m) | 1.63 (m) | 1.65 (m) | 1.67 (m) | 1.78 (2.4,9.3,14.3) |
| **H16** | 1.38 (m) | 1.60 (m) | 1.63 (m) | 1.63 (m) | 1.60 (m) | 1.63 (m) | 1.62 (m) |
| **H17** | 3.14 (m) | 3.30 (m) | 3.33 (m) | 3.37 (m) | 3.24 (m) | 3.35 (m) | 4.97 (m) |
| **17-OCH$_3$** | 3.26 | 3.24 | 3.25 | 3.28 | 3.26 | 3.25 | |
| **H18** | 3.71 (2.1,12.3) | 4.20 (2.6,12.3) | 4.28 (2.5,12.3) | 4.27 (2.5,12.1) | 3.46 (2.4,10.5) | 4.34 (2.2,11.1) | 4.28 (2.8,12.4) |
| **H18** | 3.41 (6.7,12.3) | 4.09 (5.3,12.2) | 4.07 (4.7,12.5) | 4.03 (5.3,12.1) | 3.32 (5.0,10.5) | 4.26 (4.8,11.2) | 4.16 (5.2,12.4) |
| **-OCOCH$_3$** | 2.21 | 2.08 | 2.20,2.08 | 2.08 | 2.20 | | |
| **7/18-OCH$_3$** | | | | 3.54 | /3.37 | | |
| **18-OSO$_2$CH$_3$** | | | | | | 3.06 | |

[a]All data were recorded in $CDCl_3$, with chemical shifts in ppm relative to $CHCl_3$, δ7.25 (coupling constants in Hz). [b]Propanoate ester resonances are listed in the Experimental section.

**Table 2.9** $^{13}C$ NMR data[a] for mycalamide B acetate and mesylate esters.

| | Myc.B 7-mono-acetate (2.21) | Myc.B 18-mono-acetate (2.20) | Myc.B 7,18-di-acetate (2.19) | 7,17-di-*O*-Me A 18-acetate (2.37) | 17,18-di-*O*-Me A 7-acetate (2.36) | Myc.B 18-mono-mesylate (2.23) |
|---|---|---|---|---|---|---|
| C2 | 70.30 | 69.54 | 69.95 | 69.45 | 70.00 | 69.57 |
| 2-$CH_3$ | 17.84 | 18.01 | 17.92 | 17.87 | 17.94 | 18.00 |
| C3 | 41.37 | 41.31 | 41.16 | 41.38 | 41.17 | 41.28 |
| 3-$CH_3$ | 12.20 | 12.22 | 12.19 | 11.87 | 12.26 | 12.20 |
| C4 | 145.17 | 144.95 | 144.75 | 145.95 | 144.73 | 144.94 |
| 4=$CH_2$ | 111.11 | 111.25 | 111.26 | 110.25 | 111.31 | 111.25 |
| C5 | 34.73 | 33.59 | 34.39 | 34.15 | 34.36 | 33.61 |
| C6 | 99.46 | 100.00 | 99.15 | 99.91 | 99.26 | 99.97 |
| 6-$OCH_3$ | 48.50 | 48.51 | 48.49 | 48.94 | 48.50 | 48.58 |
| C7 | 71.45 | 71.11 | 71.48 | 82.72 | 71.45 | 71.26 |
| C8 | ? | 171.69 | 166.67 | 170.87 | 166.79 | 171.68 |
| C10 | 74.29 | 74.05 | 74.02 | 73.31 | 73.79 | 74.12 |
| 10-$OCH_2$ | 86.78 | 86.43 | 86.53 | 86.45 | 86.48 | 86.51 |
| C11 | ? | 70.80 | 70.64 | 70.75 | 70.58 | 70.91 |
| C12 | 74.75 | 74.26 | 74.18 | 74.31 | 74.22 | 74.12 |
| C13 | 79.40 | 79.27 | 79.43 | 79.42 | 79.55 | 79.20 |
| 13-$OCH_3$ | 61.75 | 61.76 | 61.70 | 61.77 | 61.71 | 61.78 |
| C14 | 41.50 | 41.40 | 41.24 | 41.43 | 41.32 | ? |
| 14-$CH_3R$ | 23.13 | 23.28 | 23.38 | 23.21 | 23.46 | 23.34 |
| 14-$CH_3S$ | 13.32 | 13.60 | 13.80 | 13.55 | 13.81 | 13.60 |
| C15 | 75.86 | 75.61 | 75.68 | 75.53 | 76.08 | 75.34 |
| C16 | 30.18 | 30.29 | 30.33 | 30.20 | 30.00 | 29.73 |
| C17 | 79.91 | 76.26 | 77.93 | ? | 77.34 | 76.01 |
| 17-$OCH_3$ | 56.67 | 56.98 | 56.88 | 56.91 | 56.84 | 56.97 |
| C18 | 63.81 | 64.14 | 63.47 | 64.12 | 72.21 | 69.40 |
| 7-$OCOCH_3$ | ? | | 169.68 | | 169.60 | |
| | 20.54 | | 20.65 | | 20.63 | |
| 18-$OCOCH_3$ | | 171.04 | 170.85 | 169.69 | | |
| | | 20.97 | 20.97 | 20.95 | | |
| 7-$OCH_3$ | | | | 60.06 | | |
| 18-$OCH_3$ | | | | | 59.11 | |
| 18-$OSO_2CH_3$ | | | | | | 37.63 |

[a]Data for compound **2.21** were recorded in $CD_2Cl_2$. All other data were recorded in $CDCl_3$, with chemical shifts in ppm relative to $CDCl_3$, δ77.01, or $CD_2Cl_2$, δ53.60 ppm.

**Table 2.10** $^{1}$H NMR data[a] for mycalamide A and B methyl ethers.

| | 7-*O*-Methyl, *N*-methyl A (2.24) | 7-D,7*S*-*O*-Me, *N*-methyl A (2.30) | 7,18-di-*O*-Me, *N*-methyl A (2.25) | 7,17-di-*O*-Me, *N*-methyl A (2.27) | 7*S*,17-di-*O*-Me, *N*-methyl A (2.29) | 7,17,18-tri-*O*-Me, *N*-methyl A (2.26) | 7*S*,17,18-tri-*O*-Me, *N*-methyl A (2.28) |
|---|---|---|---|---|---|---|---|
| **H2** | 3.93 (2.6,6.3) | 3.94 (2.7,6.5) | 3.92 (2.8,6.5) | 3.94 (2.7,6.3) | 3.94 (2.6,6.6) | 3.91 (2.8,6.6) | 3.94 (2.6,6.6) |
| **2-CH$_3$** | 1.14 (6.5) | 1.13 (6.6) | 1.13 (6.4) | 1.14 (6.5) | 1.14 (6.5) | 1.12 (6.6) | 1.14 (6.6) |
| **H3** | 2.20 (2.4,6.8) | 2.21 (2.6,6.8) | 2.19 (3.0,6.9) | 2.20 (2.9,7.0) | 2.20 (2.3,7.0) | 2.18 (2.8,7.0) | 2.21 (2.4,7.2) |
| **3-CH$_3$** | 1.01 (7.0) | 1.03 (7.0) | 1.00 (6.8) | 1.00 (7.0) | 1.02 (7.0) | 0.97 (7.0) | 1.04 (7.0) |
| **4=CH*Z*** | 4.83 (2.0) | 4.84 (2.0) | 4.82 (2.0) | 4.83 (2.0) | 4.83 (2.0) | 4.81 (2.0) | 4.82 (2.0) |
| **4=CH*E*** | 4.73 (2.0) | 4.74 (2.0) | 4.72 (2.0) | 4.74 (2.0) | 4.73 (2.1) | 4.70 (2.0) | 4.73 (2.0) |
| **H5a** | 2.68 (2.0,14.5) | 2.84 (2.0,14.6) | 2.70 (2.0,14.4) | 2.71 (2.0,14.2) | 2.84 (2.0,14.9) | 2.65 (2.0,14.2) | 2.80 (2.0,14.6) |
| **H5e** | 2.29 (14.3) | 2.51 (14.5) | 2.29 (14.5) | 2.28 (14.1) | 2.54 (15.0) | 2.26 (14.2) | 2.63 (14.7) |
| **6-OCH$_3$** | 3.31 | 3.31 | 3.31 | 3.30 | 3.29 | 3.29 | 3.26 |
| **H7** | 4.27 | | 4.25 | 4.25 | 4.22 | 4.25 | 4.16 |
| **7-OCH$_3$** | 3.45 | 3.58 | 3.46 | 3.46 | 3.61 | 3.44 | 3.56 |
| **N-CH$_3$** | 3.19 | 3.14 | 3.19 | 3.22 | 3.14 | 3.20 | 3.11 |
| **H10** | 6.34 (9.9) | 6.40 (10.3) | 6.35 (9.5) | 6.26 (10.2) | 6.32 (10.3) | 6.26 (10.1) | 6.33 (10.2) |
| **10-OCH*R*** | 5.17 (6.6) | 5.15 (6.7) | 5.16 (6.7) | 5.16 (6.7) | 5.13 (6.8) | 5.15 (7.0) | 5.13 (6.7) |
| **10-OCH*S*** | 4.89 (6.7) | 4.86 (6.8) | 4.88 (6.6) | 4.87 (6.7) | 4.85 (6.8) | 4.85 (7.0) | 4.85 (6.7) |
| **H11** | 4.15 (7.2,10.0) | 4.14 (7.0,10.4) | 4.19 (7.1,9.5) | 4.16 (6.8,9.8) | 4.09 (7.1,10.2) | 4.18 (6.8,10.1) | 4.12 (6.9,10.2) |
| **H12** | 4.28 (7.1,10.6) | 4.27 (7.0,10.7) | 4.29 (7.2,10.0) | 4.29 (7.0,10.0) | 4.28 (7.0,10.7) | 4.26 (6.8,10.5) | 4.27 (6.9,10.6) |
| **H13** | 3.53 (10.7) | 3.53 (10.7) | 3.54 (10.1) | 3.48 (10.0) | 3.50 (10.8) | 3.49 (10.5) | 3.52 (10.7) |
| **13-OCH$_3$** | 3.58 | 3.56 | 3.57 | 3.57 | 3.55 | 3.55 | 3.55 |
| **14-CH$_3$*R*** | 0.99 | 0.96 | 0.99 | 0.99 | 0.96 | 0.97 | 0.97 |
| **14-CH$_3$*S*** | 0.88 | 0.87 | 0.90 | 0.87 | 0.85 | 0.87 | 0.86 |
| **H15** | 3.70 (3.2,9.8) | 3.68 (m) | 3.69 (2.5,10.0) | 3.50 (m) | 3.47 (1.6,8.6) | 3.38 (1.8,8.7) | 3.33 (9.2) |
| **H16** | 1.56 (m) | 1.53 (m) | 1.71 (m) | 1.54 (m) | 1.58 (m) | 1.70 (1.8,9.6,14.1) | 1.83 (9.4,14.3) |
| **H16** | 1.56 (m) | 1.53 (m) | 1.47 (m) | 1.54 (m) | 1.45 (m) | 1.51 (2.2,8.9,14.2) | 1.42 (2.6,9.2,14.3) |
| **H17** | 3.74 (m) | 3.67 (m) | 3.81 (m) | 3.30 (m) | 3.12 (m) | 3.33 (m) | 3.23 (m) |
| **17-OCH$_3$** | | | | 3.31 | 3.36 | 3.27 | 3.30 |
| **H18** | 3.60 (3.1,11.0) | 3.64 (3.3,11.0) | 3.28 (m) | 3.72 (2.7,11.8) | 3.72 (2.5,11.8) | 3.53 (m) | 3.49 (3.0,10.1) |
| **H18** | 3.34 (6.5,11.0) | 3.26 (6.9,11.0) | 3.28 (m) | 3.52 (5.9,11.3) | 3.54 (m) | 3.36 (m) | 3.37 (3.6,10.0) |
| **18-OCH$_3$** | | | 3.35 | | | 3.37 | 3.35 |

[a]All data were recorded in $CDCl_3$, with chemical shifts in ppm relative to $CHCl_3$, δ7.25 (coupling constants in Hz).

**Table 2.11** $^{13}C$ NMR data[a] for mycalamide A and B methyl ethers.

| | 7-*O*-Methyl, *N*-methyl A (2.24) | 7,18-di-*O*-Me, *N*-Me A (2.25) | 7,17-di-*O*-Me, *N*-Me A (2.27) | 7*S*,17-di-*O*-Me, *N*-Me A (2.29) | 7,17,18-tri-*O*-Me, *N*-Me A (2.26) | 7*S*,17,18-tri-*O*-Me, *N*-Me A (2.28) |
|---|---|---|---|---|---|---|
| **C2** | 69.39 | 69.36 | 69.52 | 69.63 | 69.40 | 69.18 |
| **2-$CH_3$** | 17.66 | 17.65 | 17.64 | 18.00 | 17.68 | 17.99 |
| **C3** | 41.39 | 41.43 | 41.38 | 41.35 | 41.35 | 41.41 |
| **3-$CH_3$** | 12.16 | 12.12 | 11.94 | 11.96 | 11.97 | 12.08 |
| **C4** | 146.76 | 147.01 | 146.62 | 146.98 | 146.76 | ? |
| **4=$CH_2$** | 109.76 | 109.52 | 109.93 | 110.10 | 109.75 | 109.72 |
| **C5** | 33.88 | 33.83 | 33.98 | 32.34 | 34.06 | 33.24 |
| **C6** | 100.82 | 100.87 | 100.86 | 102.04 | 100.74 | 101.78 |
| **6-$OCH_3$** | 48.90 | 48.90 | 48.96 | 50.55 | 48.93 | 50.48 |
| **C7** | 82.56 | 83.39 | 83.15 | 81.09 | 84.10 | 81.15 |
| **7-$OCH_3$** | 58.89 | 58.90 | 58.86 | 60.39 | 58.83 | ? |
| **C8** | ? | 171.24 | ? | ? | 170.75 | ? |
| **N-$CH_3$** | 28.75 | 28.70 | 28.74 | 29.09 | 28.79 | 28.90 |
| **C10** | 77.26 | ? | 77.27 | ? | 77.30 | ? |
| **10-$OCH_2$** | 86.49 | 86.68 | 86.15 | 86.85 | 86.37 | 87.00 |
| **C11** | 67.09 | 67.01 | 66.95 | 67.24 | 66.78 | 67.27 |
| **C12** | 74.40 | 74.40 | 74.37 | 74.74 | 74.31 | 74.69 |
| **C13** | 79.16 | 79.15 | 79.32 | 79.05 | 79.35 | 79.11 |
| **13-$OCH_3$** | 61.86 | 61.83 | 61.83 | 61.88 | 61.76 | 61.85 |
| **C14** | 41.84 | 41.90 | 41.55 | 41.66 | 41.64 | ? |
| **14-$CH_3R$** | 22.98 | 22.95 | 23.20 | 23.00 | 23.15 | 23.01 |
| **14-$CH_3S$** | 13.11 | 13.20 | 13.09 | 12.94 | 13.21 | 12.97 |
| **C15** | 78.14 | 78.64 | 75.49 | 75.84 | 75.82 | 76.10 |
| **C16** | 32.97 | 33.34 | 30.59 | 30.83 | 30.43 | 30.06 |
| **C17** | 71.07 | 69.58 | 79.00 | 79.73 | 77.30 | |
| **17-$OCH_3$** | | | 56.46 | 56.94 | 56.36 | 56.42 |
| **C18** | 66.86 | 76.44 | 64.25 | 65.70 | 72.49 | 72.01 |
| **18-$OCH_3$** | | 59.12 | | | 59.07 | 59.22 |

[a]All data were recorded in $CDCl_3$, with chemical shifts in ppm relative to $CDCl_3$, δ77.01 ppm.

**Table 2.12** $^{1}$H NMR data[a] for mycalamide A and B methyl ethers.

| | 7-*O*-Methyl myc.A (2.34) | 18-*O*-Methyl myc.A (2.35) | 7,18-di-*O*-Me myc.A (2.32) | 7,17-di-*O*-Me myc.A (2.33) | 17,18-di-*O*-Me myc.A (2.38) | 7,17,18-tri-*O*-Me myc.A (2.31) |
|---|---|---|---|---|---|---|
| **H2** | 3.90 (2.6,6.7) | 4.00 (2.7,6.5) | 3.89 (2.7,6.6) | 3.94 (2.7,6.6) | 4.05 (2.9,6.6) | 3.91 (2.7,6.5) |
| **2-CH$_3$** | 1.17 (6.6) | 1.19 (6.6) | 1.16 (6.6) | 1.17 (6.6) | 1.21 (6.6) | 1.16 (6.6) |
| **H3** | 2.19 (2.6,7.0) | 2.24 (2.6,7.1) | 2.18 (2.6,7.2) | 2.21 (2.5,7.0) | 2.27 (2.5,7.2) | 2.19 (2.6,7.2) |
| **3-CH$_3$** | 0.96 (7.0) | 1.01 (7.1) | 0.96 (7.2) | 0.98 (7.0) | 1.03 (7.1) | 0.97 (7.0) |
| **4=CH*Z*** | 4.82 (1.9) | 4.84 (1.6) | 4.81 (1.8) | 4.83 (1.9) | 4.86 (1.8) | 4.82 (1.9) |
| **4=CH*E*** | 4.71 (1.8) | 4.74 (1.5) | 4.70 (1.9) | 4.71 (2.0) | 4.74 (1.8) | 4.71 (1.9) |
| **H5a** | 2.43 (2.0,14.3) | 2.31 (1.7,14.0) | 2.44 (1.9,14.3) | 2.41 (1.9,14.3) | 2.20 (1.9,14.1) | 2.43 (2.0,14.2) |
| **H5e** | 2.32 (14.1) | 2.38 (13.9) | 2.31 (14.5) | 2.32 (14.4) | 2.37 (14.3) | 2.30 (14.2) |
| **6-OCH$_3$** | 3.28 | 3.30 | 3.28 | 3.27 | 3.32 | 3.28 |
| **H7/7-OH** | 3.88 | 4.29 | 3.88 | 3.89 | 4.28/3.92 (2.5) | 3.87 |
| **7-OCH$_3$** | 3.56 | | 3.54 | 3.57 | | 3.55 |
| **NH9** | 7.18 (10.0) | 7.49 (9.8) | 7.13 (9.9) | 7.25 (9.7) | 7.55 (9.5) | 7.13 (9.6) |
| **H10** | 5.91 (10.0) | 5.85 (9.6) | 5.90 (10.0) | 5.82 (9.7) | 5.81 (9.6) | 5.81 (9.8) |
| **10-OCH*R*** | 5.14 (6.9) | 5.13 (6.9) | 5.14 (7.0) | 5.13 (6.9) | 5.13 (6.9) | 5.13 (7.0) |
| **10-OCH*S*** | 4.85 (6.9) | 4.87 (6.9) | 4.83 (7.0) | 4.85 (7.0) | 4.86 (6.8) | 4.82 (7.0) |
| **H11** | 3.87 (6.9,10.0) | 3.84 (6.6,9.6) | 3.88 (6.7,9.8) | 3.80 (6.8,10.0) | 3.79 (6.6,9.6) | 3.84 (6.6,9.9) |
| **H12** | 4.24 (6.9,10.6) | 4.21 (6.6,10.2) | 4.23 (6.8,10.5) | 4.23 (6.8,10.5) | 4.20 (6.6,10.2) | 4.21 (6.6,10.4) |
| **H13** | 3.48 (10.6) | 3.44 (10.1) | 3.47 (10.7) | 3.45 (10.5) | 3.44 (10.3) | 3.44 (10.2) |
| **13-OCH$_3$** | 3.56 | 3.55 | 3.55 | 3.56 | 3.56 | 3.55 |
| **14-CH$_3$*R*** | 0.97 | 0.99 | 0.97 | 0.97 | 0.99 | 0.97 |
| **14-CH$_3$*S*** | 0.88 | 0.87 | 0.88 | 0.86 | 0.87 | 0.87 |
| **H15** | 3.64 (5.1,6.5) | 3.54 (m) | 3.58 (m) | 3.43 (1.7,10.0) | 3.37 (m) | 3.32 (m) |
| **H16** | 1.56 (m) | 1.60 (m) | 1.60 (m) | 1.57 (m) | 1.62 (m) | 1.62 (m) |
| **H16** | 1.56 (m) | 1.54 (m) | 1.52 (m) | 1.46 (m) | 1.57 (m) | 1.62 (m) |
| **H17** | 3.75 (m) | 3.79 (m) | 3.82 (m) | 3.22 (m) | 3.24 (m) | 3.29 (m) |
| **17-OCH$_3$** | | | | 3.30 | 3.25 | 3.29 |
| **H18** | 3.60 (3.4,11.0) | 3.32 (4.2,9.5) | 3.30 (4.6,9.6) | 3.69 (3.0,12.0) | 3.46 (2.2,10.3) | 3.45 (m) |
| **H18** | 3.38 (6.0,11.0) | 3.23 (6.2,9.6) | 3.26 (5.7,9.7) | 3.45 (m) | 3.31 (5.2,10.3) | 3.31 (m) |
| **18-OCH$_3$** | | 3.35 | 3.35 | | 3.37 | 3.37 |

[a]All data were recorded in $CDCl_3$, with chemical shifts in ppm relative to $CHCl_3$, δ7.25 (coupling constants in Hz).

**Table 2.13** $^1$H-$^1$H NOE interactions for compounds in Sections **2.4-2.5**.

| Compound | Signal(s) irradiated | Signals enhanced (% enhancement) |
|---|---|---|
| 7-*O*-Methyl myc.A (**2.34**) | H7 | 6-$OCH_3$(2), 7-$OCH_3$(1), NH(2) |
| 18-*O*-Methyl myc.A (**2.35**) | H7 | 6-$OCH_3$(2), NH(2) |
| 7,18-di-*O*-Methyl A (**2.32**) | H7 (H11) | 6-$OCH_3$(2), 7-$OCH_3$(1), H12(4)[b] |
| 7,17-di-*O*-Methyl A (**2.33**) | H7 | 6-$OCH_3$(2), 7-$OCH_3$(2) |
| 17,18-di-*O*-Me.A (**2.38**) | H7 | 6-$OCH_3$(2), 7-OH(2), NH(1) |
| 17,18-di-*O*-Me, 7-..(**2.36**) | H7 | 6-$OCH_3$(3), NH(3) |
| 7,17-di-*O*-Me, 18-..(**2.37**) | H7 | 6-$OCH_3$(2), 7-$OCH_3$(2), NH(2) |
| 7,17,18-tri-*O*-Me A (**2.31**) | H7 | 6-$OCH_3$(2), 7-$OCH_3$(2), NH(1) |
| 7-*O*-Benzyl myc.A (**2.39**) | 6-$OCH_3$ | H7(6) |
| | H7 | 6-$OCH_3$(2), 7-OCHd(2)[c], 7-OCHu(2)[c] |
| 7,18-di-*O*-Benzyl A (**2.40**) | H7 | 6-$OCH_3$(2), 7-OCHu(1)[c] |
| | $H_2$18 (H13) | H10(2)[b], 10-OCH*R*(3)[b], H17(6), 18-OCHd(3)[c] 18-OCHu(4)[c] |
| 7-*O*-Benzyl, | H7 (H7', H12)[d] | 6-$OCH_3$(2), H10(2), 14-$CH_3$*S*(2)[b] |
| *N*-benzyl A (**2.41**) | H10 (H10')[d] | H7(6), 10-OCH*R*(3), H13(2), H15(6) |
| | H11 (7-OCHu)[c] | H7(2)[b], N-CHu(2), H12(4) |
| 7,18-di-*O*-Benzyl, | H7 (H7', H12)[d] | 6-$OCH_3$(3), 6-$OCH_3$'(2)[d], 14-$CH_3$*S*(1)[b] |
| *N*-benzyl A (**2.42**) | N-CH (10-OCH*R*) | 10-OCH*S*(4)[b], H13(3)[b] |
| | H10 (H10')[d] | H7(3), 10-OCH*R*(2), H13(2), H15(7) |
| 7-*O*-Benzyl myc.B (**2.43**) | H7 | $H_2$5(1), 6-$OCH_3$(2), 7-OCHd(2)[c], 7-OCHu(3)[c], NH(2) |
| 7,18-di-*O*-Benzyl, | H5e' (H5e)[d] | H5a(2), H5a'(5)[d] |
| *N*-benzyl B (**2.46**) | 6-$OCH_3$ (H5a, H5a') | H2(4), H5e(6)[b], H5e'(5)[b,d], H7(6) |
| | H7 (H7')[d] | 6-$OCH_3$(1), 6-$OCH_3$'(1)[d], 7-OCHd(0.8)[c], 7-OCHu(2)[c], N-CHd(2)[c], N-CHu(0.8)[c], H10(0.8) |
| | H10 (H10')[d] | H7(0.9), 10-OCH*R*(2), H13(2), H15(5) |
| | H13' (H13, H5a')[d] | H5e'(1)[b,d], 10-OCH*R*(0.6), 13-$OCH_3$(0.5) |
| 7,8,18-tri-*O*-Benzyl B (**2.47**) | H2 | 2-$CH_3$(1), H3(3), 6-$OCH_3$(0.5) |
| | 3-$CH_3$ | H3(6), H5a(3) |
| | H5e (H16d[c]) | 4=CH*E*(5), H5a(23), H11(7)[b], H16u(11)[b,c] |
| | 6-$OCH_3$ (H5a) | H2(4), H5e(2)[b], H7(6) |
| | H7 (4=CH*E*, 10-OCH*R*) | 4=CH*Z*(1)[b], 6-$OCH_3$(2), 7-OCHd(1)[c], 7-OCHu(2)[c], H10(8), 10-OCH*S*(5)[b] |
| | 8-OCHd[c] | 8-OCHu(10)[c] |
| | 8-OCHu[c] | 8-OCHd(3)[c] |
| | H10 | H7(4), H11(2) |
| | 10-OCH*S* | 10-OCH*R*(6), H12(1) |
| | H12 | 10-OCH*S*(2), H11(4), H13(3), 13-$OCH_3$(1) |
| | H13 | H12(4), 13-$OCH_3$(2), 14-$CH_3$*R*(1), 14-$CH_3$*S*(0.3) |
| | 14-$CH_3$*R* | H13(7), 14-$CH_3$*S*(1), H15(5) |
| | 14-$CH_3$*S* | H13(3), 13-$OCH_3$(0.3), 14-$CH_3$*R*(1), H16d(4)[c] |
| | H16u[c] | 14-$CH_3$*S*(0.6), H15(3), H16d(10)[c] |
| | H18d[c] | H18u(6)[c] |
| | H18u[c] (H11, H15) | H10(2)[b], H12(3)[b], 14-$CH_3$*R*(0.5)[b], H16u(2)[b,c], H16d(3)[b,c], H18d(4)[c] |

[a]All data were recorded in $CDCl_3$. [b]Enhancement interpreted as being due to the irradiation of an overlapping signal. [c]u and d have been used to designate the upfield and downfield resonances of a geminal pair. [d]' has been used to designate signals for a minor conformation.

**Table 2.14** $^{13}C$ NMR data[a] for mycalamide A and B methyl ethers.

| | 7-mono-*O*-Methyl A (2.34) | 18-mono-*O*-Methyl A (2.35) | 7,18-di-*O*-Methyl A (2.32) | 7,17-di-*O*-Methyl A (2.33) | 17,18-di-*O*-Methyl A (2.38) | 7,17,18-tri-*O*-Methyl A (2.31) |
|---|---|---|---|---|---|---|
| **C2** | 69.40 | 69.48 | 69.32 | 69.52 | 69.58 | 69.39 |
| **2-$CH_3$** | 17.81 | 17.93 | 17.80 | 17.85 | 18.01 | 17.82 |
| **C3** | 41.40 | 41.35 | 41.45 | 41.36 | 41.30 | 41.42 |
| **3-$CH_3$** | 11.77 | 12.07 | 11.73 | 11.88 | 12.28 | 11.80 |
| **C4** | 146.27 | 145.50 | 146.45 | 145.77 | 145.00 | 146.20 |
| **4=$CH_2$** | 109.95 | 110.71 | 109.79 | 110.37 | 111.23 | 110.02 |
| **C5** | 34.14 | 33.72 | 34.20 | 34.19 | 33.61 | 34.16 |
| **C6** | 100.02 | 99.85 | 99.97 | 100.00 | 100.01 | 99.91 |
| **6-$OCH_3$** | 49.18 | 48.86 | 49.14 | 48.98 | 48.56 | 49.01 |
| **C7** | 82.99 | 72.52 | 83.16 | 82.39 | 71.45 | 82.98 |
| **7-$OCH_3$** | 60.50 | | 60.45 | 60.39 | | 60.20 |
| **C8** | 170.56 | 171.73 | 170.43 | 170.33 | 171.78 | 170.06 |
| **C10** | 73.22 | 73.83 | 73.07 | 73.51 | 73.94 | 73.11 |
| **10-$OCH_2$** | 86.83 | 86.72 | 86.74 | 86.61 | 86.47 | 86.49 |
| **C11** | 71.60 | 70.87 | 71.26 | 71.41 | 70.62 | 70.59 |
| **C12** | 74.55 | 74.31 | 74.47 | 74.64 | 74.33 | 74.41 |
| **C13** | 79.22 | 79.34 | 79.38 | 79.27 | 79.43 | 79.48 |
| **13-$OCH_3$** | 61.89 | 61.77 | 61.86 | 61.86 | 61.76 | 61.80 |
| **C14** | 41.81 | 41.54 | 41.81 | 41.59 | 41.47 | 41.57 |
| **14-$CH_3$*R*** | 22.98 | 23.25 | 23.03 | 23.12 | 23.34 | 23.18 |
| **14-$CH_3$*S*** | 13.24 | 13.72 | 13.35 | 13.18 | 13.66 | 13.45 |
| **C15** | 78.99 | 78.56 | 79.08 | 75.49 | 75.99 | 75.81 |
| **C16** | 32.03 | 32.49 | 32.48 | 29.94 | 29.95 | 29.83 |
| **C17** | 71.65 | 69.71 | 69.96 | 79.72 | ? | 77.66 |
| **17-$OCH_3$** | | | | 56.87 | 56.87 | 56.81 |
| **C18** | 66.68 | 76.05 | 76.19 | 64.69 | 72.63 | 72.87 |
| **18-$OCH_3$** | | 59.05 | 59.10 | | 59.20 | 59.19 |

[a]All data were recorded in $CDCl_3$, with chemical shifts in ppm relative to $CDCl_3$, $\delta$77.01 ppm.

**Table 2.15** $^1$H NMR data[a,b] for mycalamide A benzyl ethers.

| | 7-*O*-Benzyl myc.A (**2.39**) | 7,18-di-*O*-Benz. myc.A (**2.40**) | 7-*O*-Benzyl, *N*-benz.A (**2.41**) | 7,18-di-*O*-Benzyl, *N*-benz.A (**2.42**) |
|---|---|---|---|---|
| **H2** | 3.88 (2.7,6.6) | 3.86 (2.9,6.6) | 3.91 (2.9,6.5) | 3.88 |
| **2-CH$_3$** | 1.17 (6.6) | 1.16 (6.6) | 1.19 (6.5) | 1.16 (6.2) |
| **H3** | 2.19 (2.5,7.0) | 2.18 (2.9,7.1) | 2.19 (2.5,7.0) | 2.16 (2.2,7.0) |
| **3-CH$_3$** | 0.97 (7.0) | 0.95 (7.0) | 1.01 (7.0) | 1.01 (7.0) |
| **4=CH*Z*** | 4.82 (1.8) | 4.80 (m) | 4.78 (1.9) | 4.76 (m) |
| **4=CH*E*** | 4.72 (1.9) | 4.70 (m) | 4.69 (1.8) | 4.66 (m) |
| **H5a** | 2.48 (1.9,14.4) | 2.47 (m,14.5) | 2.64 (1.9,14.4) | 2.86 (m) |
| **H5e** | 2.41 (14.3) | 2.40 (14.4) | 2.28 (14.1) | 2.33 (14.0) |
| **6-OCH$_3$** | 3.14 | 3.10 | 2.96 | 2.90 |
| **H7** | 4.10 | 4.08 | 4.24 | 4.27 |
| **7-OCH** | 4.77 (11.2) | 4.75 (11.2) | 4.33 (12.0) | 4.36 (11.5) |
| **7-OCH** | 4.68 (11.2) | 4.63 (10.8) | 3.86 (12.5) | 3.90 (11.5) |
| **NH9** | 7.24 (10.0) | 7.22 (10.0) | | |
| **N-CH** | | | 5.14 (17.0) | 5.11 (17.1) |
| **N-CH** | | | 4.63 (17.1) | 4.65 (17.2) |
| **H10** | 5.93 (10.1) | 5.92 (10.0) | 6.40 (9.2) | 6.33 (9.1) |
| **10-OCH*R*** | 5.13 (7.0) | 5.13 (7.1) | 5.21 (7.0) | 5.19 (6.0) |
| **10-OCH*S*** | 4.84 (7.0) | 4.82 (7.0) | 4.90 (6.9) | 4.91 (6.0) |
| **H11** | 3.80 (6.8,10.0) | 3.81 (6.7,10.1) | 4.00 (7.0,9.2) | 4.03 (7.1,8.7) |
| **H12** | 4.23 (6.8,10.5) | 4.22 (6.8,10.5) | 4.24 (6.8,10.0) | 4.24 (6.9,10.0) |
| **H13** | 3.49 (10.5) | 3.46 (10.3) | 3.48 (10.0) | 3.47 (10.0) |
| **13-OCH$_3$** | 3.56 | 3.55 | 3.56 | 3.55 |
| **14-CH$_3$*R*** | 0.98 | 0.97 | 1.00 | 1.00 |
| **14-CH$_3$*S*** | 0.88 | 0.88 | 0.87 | 0.87 |
| **H15** | 3.68 (5.8,6.9) | 3.60 (1.8,10.4) | 3.78 (m) | 3.77 (m) |
| **H16** | 1.55 (m) | 1.70 (m) | 1.55 (m) | 1.83 (m,14.0) |
| **H16** | 1.50 (m) | 1.55 (m) | 1.55 (m) | 1.50 (m) |
| **H17** | 3.82 (m) | 3.92 (m) | 3.80 (m) | 3.92 (m) |
| **H18** | 3.62 (3.5,11.3) | 3.44 (4.7,9.6) | 3.69 (2.8,11.1) | 3.44 (m) |
| **H18** | 3.39 (6.0,11.2) | 3.39 (5.6,9.6) | 3.29 (6.5,11.0) | 3.36 (5.1,9.1) |
| **18-OCH** | | 4.59 (11.7) | | 4.56 (12.4) |
| **18-OCH** | | 4.52 (12.1) | | 4.52 (12.0) |

[a]All data were recorded in $CDCl_3$, with chemical shifts in ppm relative to $CHCl_3$, δ7.25 (coupling constants in Hz). [b]All aromatic resonances (not listed) appeared as unresolved multiplets between δ7.5-7.2 ppm.

**Table 2.16** $^{13}C$ NMR data[a,b] for mycalamide A and B benzyl ethers.

| | 7-mono-*O*-Benzyl A (2.39) | 7,18-di-*O*-Benzyl A (2.40) | 7,18-di-*O*-Benzyl, *N*-ben.A (2.42) | 7-mono-*O*-Benzyl B (2.43) | 7,18-di-*O*-Benzyl B (2.44) | 7,18-di-*O*-Benzyl, *N*-ben.B (2.46) | 7,8,18-tri-*O*-Benzyl B (2.47) |
|---|---|---|---|---|---|---|---|
| **C2** | 69.38 | 69.29 | 69.11 | 69.50 | 69.34 | 69.45 | 69.09 |
| **2-$CH_3$** | 17.80 | 17.80 | 17.70 | 17.84 | 17.83 | 17.76 | 17.67 |
| **C3** | 41.38 | 41.41 | 41.48 | 41.35 | 41.41 | 41.53 | 41.59 |
| **3-$CH_3$** | 11.76 | 11.74 | 12.46 | 11.86 | 11.82 | 12.18 | 11.73 |
| **C4** | 146.48 | 146.62 | ? | 146.00 | 146.40 | 146.97 | 147.53 |
| **4=$CH_2$** | 109.91 | 109.77 | 109.52 | 110.30 | 109.94 | 109.65 | 109.11 |
| **C5** | 34.61 | 34.65 | 34.29 | 34.53 | 34.42 | 33.46 | 33.83 |
| **C6** | 100.09 | 100.03 | ? | 100.10 | 99.95 | 101.44 | 101.32 |
| **6-$OCH_3$** | 49.22 | 49.15 | 47.92 | 48.95 | 48.94 | 47.81 | 48.24 |
| **C7** | 80.81 | 80.91 | 76.22 | 80.15 | 80.73 | 75.98 | 73.29 |
| **7-$OCH_2Ph$** | 73.24 | 73.20 | 73.32 | 73.48 | 73.25 | 71.91 | 71.71 |
| **C8** | 170.59 | 170.43 | ? | 170.52 | 170.17 | 171.63 | ? |
| **N-$CH_2Ph$/8-OCH** | | | 45.96 | | | 46.32 | /67.43 |
| **C10** | 74.19 | 74.07 | 77.80 | 74.22 | 73.98 | 79.60 | 82.56 |
| **10-$OCH_2$** | 86.86 | 86.76 | 86.23 | 86.58 | 86.42 | 86.04 | 86.40 |
| **C11** | 71.66 | 71.29 | 68.44 | 71.38 | ? | 69.05 | 64.79 |
| **C12** | 74.56 | 74.48 | 74.35 | 74.62 | 74.33 | 73.41 | 68.70 |
| **C13** | 79.24 | 79.23 | 79.84 | 79.29 | 79.55 | 80.69 | 84.03 |
| **13-$OCH_3$** | 61.88 | 61.84 | 61.67 | 61.85 | 61.75 | 61.39 | 59.32 |
| **C14** | 41.82 | 41.78 | ? | 41.59 | 41.46 | 40.46 | 36.44 |
| **14-$CH_3R$** | 22.98 | 23.06 | 23.32 | 23.14 | 23.22 | 24.11 | 27.68 |
| **14-$CH_3S$** | 13.26 | 13.41 | 13.70 | 13.22 | 13.60 | 14.84 | 22.25 |
| **C15** | 78.98 | 79.13 | 78.68 | 75.45 | 75.84 | 76.33 | 78.65 |
| **C16** | 32.02 | 32.58 | 33.60 | 29.85 | 30.11 | 30.66 | 28.46 |
| **C17** | 71.70 | 70.09 | 69.28 | 79.71 | 77.79 | 77.19 | 78.30 |
| **17-$OCH_3$** | | | | 56.86 | 57.10 | 56.44 | 56.98 |
| **C18** | 66.74 | 73.78 | 71.79 | 64.69 | 70.54 | 67.66 | 69.77 |
| **18-$OCH_2Ph$** | | 73.12 | 74.16 | | 73.13 | 73.30 | 73.32 |

[a]All data were recorded in $CDCl_3$, with chemical shifts in ppm relative to $CDCl_3$, δ77.01 ppm. [b]Aromatic carbon resonances are listed in the Experimental section.

**Table 2.17** $^{1}H$ NMR data[a,b] for mycalamide B benzyl ethers.

| | 7-mono-*O*-Benzyl B (2.43) | 7,18-di-*O*-Benzyl B (2.44) | 7-*O*-Benzyl, *N*-benzyl B (2.45) | 7,18-di-*O*-Ben, *N*-benzyl B (2.46) | 7,8,18-tri-*O*-Benzyl B (2.47) |
|---|---|---|---|---|---|
| **H2** | 3.91 (2.8,6.6) | 3.87 (2.7,6.6) | 3.89 (2.7,6.5) | 3.85 (m) | 3.75 (2.6,6.5) |
| **2-CH$_3$** | 1.17 (6.6) | 1.16 (6.6) | 1.18 (6.4) | 1.14 (7.0) | 1.02 (6.6) |
| **H3** | 2.20 (2.7,7.0) | 2.18 (2.9,7.2) | 2.17 (2.3,6.8) | 2.15 (m) | 2.12 (2.1,6.8) |
| **3-CH$_3$** | 0.98 (7.0) | 0.95 (7.1) | 0.98 (6.7) | 0.98 (7.0) | 0.84 (6.9) |
| **4=CH*Z*** | 4.82 (m) | 4.80 (1.8) | 4.78 (1.9) | 4.77 (m) | 4.76 (1.9) |
| **4=CH*E*** | 4.72 (m) | 4.69 (1.8) | 4.68 (m) | 4.66 (m) | 4.68 (1.9) |
| **H5a** | 2.43 (m) | 2.43 (1.8,14.3) | 2.59 (1.9,14.1) | 2.86 (m,14.7) | 3.07 (2.0,14.7) |
| **H5e** | 2.43 (m) | 2.35 (14.3) | 2.23 (14.2) | 2.28 (14.5) | 2.34 (14.5) |
| **6-OCH$_3$** | 3.10 | 3.06 | 2.96 | 2.89 | 3.13 |
| **H7** | 4.11 | 4.01 | 4.21 | 4.23 | 4.67 |
| **7-OCH** | 4.81 (11.5) | 4.72 (11.3) | 4.39 (11.5) | 4.37 (11.6) | 4.51 (12.1) |
| **7-OCH** | 4.64 (11.3) | 4.52 (11.3) | 3.97 (11.7) | 3.93 (11.5) | 4.39 (12.2) |
| **8-OCH** | | | | | 5.28 (12.5) |
| **8-OCH** | | | | | 5.09 (12.7) |
| **NH9** | 7.35 (9.8) | 7.22 (9.8) | | | |
| **N-CH** | | | 5.11 (17.2) | 5.07 (17.3) | |
| **N-CH** | | | 4.61 (17.4) | 4.65 (16.8) | |
| **H10** | 5.85 (9.8) | 5.81 (9.8) | 6.26 (8.9) | 6.10 (7.8) | 4.99 (1.5) |
| **10-OCH*R*** | 5.13 (6.9) | 5.11 (6.9) | 5.20 (6.8) | 5.15 (6.2) | 4.68 (6.1) |
| **10-OCH*S*** | 4.84 (7.1) | 4.81 (6.7) | 4.87 (6.6) | 4.89 (6.2) | 5.13 (6.1) |
| **H11** | 3.77 (6.7,9.9) | 3.80 (6.7,9.7) | 4.03 (7.6,8.9) | 4.07 (m) | 3.50 (1.5) |
| **H12** | 4.23 (6.9,10.6) | 4.19 (6.5,10.2) | 4.25 (7.4,9.9) | 4.25 (m) | 3.97 (1.4,2.8) |
| **H13** | 3.46 (10.4) | 3.38 (10.2) | 3.42 (9.7) | 3.31 (m) | 2.86 (2.8) |
| **13-OCH$_3$** | 3.56 | 3.54 | 3.54 | 3.51 | 3.36 |
| **14-CH$_3$*R*** | 0.98 | 0.93 | 1.02 | 0.98 | 1.20 |
| **14-CH$_3$*S*** | 0.88 | 0.87 | 0.87 | 0.85 | 0.91 |
| **H15** | 3.45 (10.0) | 3.44 (m) | 3.69 (8.4) | 3.50 (m) | 3.51 (2.5,12.5) |
| **H16** | 1.55 (m) | 1.65 (m) | 1.62 (m) | 1.85 (m) | 2.31 |
| **H16** | 1.45 (m) | 1.65 (m) | 1.56 (m) | 1.65 (m) | 1.71 |
| **H17** | 3.27 (m) | 3.28 (m) | 3.46 (m) | 3.47 (m) | 3.37 |
| **17-OCH$_3$** | 3.27 | 3.27 | 3.34 | 3.30 | 3.33 |
| **H18** | 3.71 (2.9,12.1) | 3.61 | 3.86 (3.0,11.8) | 3.71 (1.7,10.0) | 3.63 (2.8,11.2) |
| **H18** | 3.48 (6.6,11.9) | 3.45 | 3.60 (5.5,11.8) | 3.61 (3.2,10.9) | 3.52 (4.3,11.1) |
| **18-OCH** | | 4.62 (12.1) | | 4.59 (12.0) | 4.60 (12.2) |
| **18-OCH** | | 4.54 (12.0) | | 4.53 (12.0) | 4.47 (12.1) |

[a]All data were recorded in $CDCl_3$, with chemical shifts in ppm relative to $CHCl_3$, δ7.25 (coupling constants in Hz). [b]All aromatic resonances (not listed) appeared as unresolved multiplets between δ7.5-7.2 ppm.

# CHAPTER 3
# ACID CATALYSED REACTIONS OF MYCALAMIDES A & B AND DERIVATIVES

## 3.1 INTRODUCTION

Early chemical studies on pederin[27,94], which has a structure similar to mycalamides A and B, involved largely degradative chemistry, aimed at structural determination and proof of the presence of the various functional groups. These workers noted the instability of their compound to mineral acids since interaction with these gave a large number of products of 'unclear meaning' which were difficult to isolate[94]. However, some products were characterised in this and later studies and these are described briefly below as a background to similar studies on mycalamides A and B.

Hydrolysis of pederin[27] with sulphuric acid in the presence of hexane (a two-phase system) gave an α,β-unsaturated aldehyde fragment, pederenal (**3.1**), in good yield. This fragment arose from complete hydrolysis of the C10 aza-acetal functionality and involved an unusual elimination and rearrangement[163]. No other products were obtained from this reaction. Later studies of the sulphuric acid catalysed hydrolysis of pederin in methanol[164], conducted in an oxygen atmosphere, were able to show that an unusual cyclised fragment derived from the O1-C8 portion was formed, pederinolactone (**3.2**), along with a dimethyl acetal fragment from C10 onwards, meropederinacetal (**3.3**). Matsumoto[126] also gave data for an intact O1-NH9 fragment, pederamide (**3.4**), obtained by 'mild acid hydrolysis' of pederin, although the exact reaction conditions and yields were not reported.

The most useful and high-yielding modification of pederin was the hydrolysis of the C6 acetal to give a hemiacetal. The hydrolysis product,

pseudopederin (**3.5**), was obtained simply by heating pederin in water[94], so that this reaction was very facile. The reverse reaction was similarly facile, being achieved simply by heating pseudopederin in methanol[164]. Pseudopederin (**3.5**), which was also isolated during the initial extractions of pederin[29,30], probably as a degradation product[165], was itself degraded by prolonged heating in water, but into a number of products which were not isolable[94]. Partial $^1$H NMR data were reported for pseudopederin, along with other spectroscopic and analytical results, and some biological assay results were also published for this and other derivatives in a subsequent paper[40]. The assays performed measured the cytotoxicity of pederin and some of its derivatives on cultured mammalian cells, both normal and tumoural (HeLa mouse tumoural cells), and pseudopederin (**3.5**) was found to be 10-100 times less active than pederin.

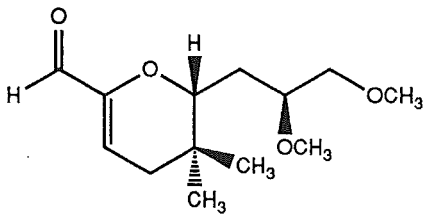

Pederenal (**3.1**)

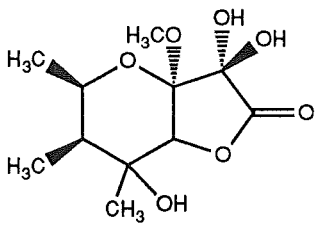

Pederinolactone (**3.2**)

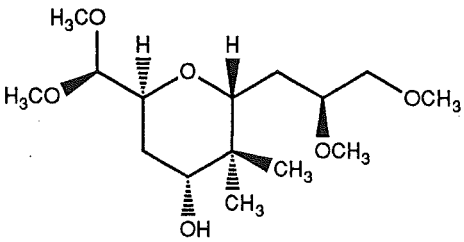

Meropederinacetal (**3.3**)

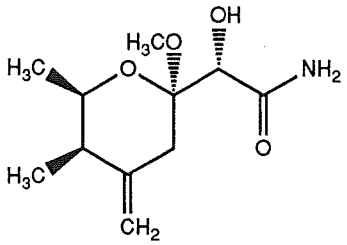

Pederamide (**3.4**)

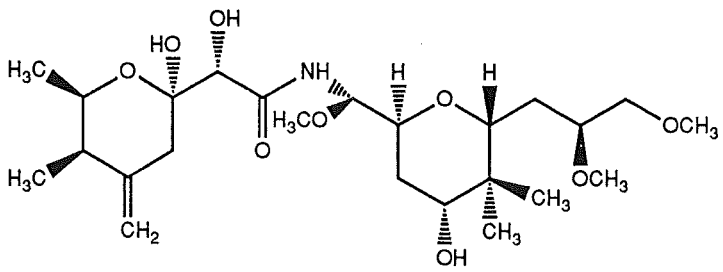

Pseudopederin (**3.5**)

The sensitivity of the pederin structure to acid was noted during various attempts at its total synthesis. For example, the acid catalysed removal of an acetonide protecting group for a C6, C7 diol was not possible in the presence of the exocyclic double bond because of an observed decomposition of the products[133]. Similarly, acid catalysed epimerisations at C10 required protection of the double bond, and exchange at C6 was always found to be faster than exchange at C10[130]. Jarowicki and coworkers[132], who performed a recent novel synthesis of pederin, summarised these results by noting that the acid lability of the homoallylic C6 acetal and N-(1-alkoxy-1-alkyl)-amide groups had necessitated delaying their introduction until the latest possible stage in the synthesis.

These same structural features are present in mycalamides A and B and preliminary work with these compounds had demonstrated their extreme acid sensitivity. Samples of mycalamides in $CDCl_3$ solution decomposed unless some base was deliberately added and this was ascribed to the presence of trace amounts of acid from the decomposition of this solvent[139]. Thus all samples for NMR spectroscopic studies in this solvent were routinely prepared and stored in the presence of pyridine (0.1%) to prevent this occurring. Note that other workers had found that a similar technique was necessary in dealing with pederin and its derivatives[95,126].

The following study summarises attempts to monitor the acid catalysed decomposition of mycalamide A, with the aim of being able to isolate products from rearrangement, cleavage or hydrolysis, which could provide further insights into the chemistry of this compound and yield some new structure-activity correlations. By careful control of the conditions it was hoped to perform acetal exchange reactions, particularly at C6. The use of an acetate protecting group in these studies is also detailed.

## 3.2 ACID CATALYSED DECOMPOSITIONS OF MYCALAMIDE A - PRELIMINARY STUDIES

### 3.2.1 EFFECT ON THE BIOLOGICAL ACTIVITY

A small amount of mycalamide A was dissolved in 10% methanol/water (1μg/ml) as a control sample. A second sample of mycalamide A was prepared in a similar manner and then heated on a steam bath for 20 minutes. A third sample of mycalamide A was dissolved in 10% methanol/aqueous hydrochloric acid (0.1M). All three samples were then assayed in the P388 system, after 2 hours and after 3 days at ambient temperature. Samples 1 and 2 showed about 90% inhibition (4+) after 3 days, but fraction 3 showed only 50% inhibition (2+) in the first assay and had no detectable activity in the second assay. Thus mycalamide A was probably fairly stable to heating in water, whereas treatment with dilute acids gave products which were substantially less active.

### 3.2.2 REACTION MONITORED BY HPLC - ISOLATION OF PEDEROLACTONE

A larger sample of mycalamide A was reacted with hydrochloric acid in methanol, as above, at ambient temperature. Aliquots were taken for analysis by reverse phase HPLC immediately after mixing, then after 10 minutes, 60 minutes, and finally 240 minutes. HPLC showed the disappearance of mycalamide A with time, and the appearance of one major new peak, which was more polar, with another minor one. Note that there was no change between one and four hours, despite the continued presence of a small amount of mycalamide A.

This reaction was repeated on a larger scale for NMR spectroscopic analysis. However, after workup, the $^1H$ NMR spectrum of the product showed

the presence of mycalamide A signals superimposed on broad humps, suggesting substantial decomposition, and one new major component which appeared to be a mycalamide fragment. The corresponding signals for this new fragment consisted simply of three methyl doublets, δ1.06 (7.2), 1.35 (6.6), 1.98 (1.5) ppm (couplings in Hz), coupled to single proton resonances at δ2.08 (doublet of quartets, 3.2, 7.2), 4.54 (doublet of quartets, 3.1, 6.6) and 5.74 (quartet, 1.5), respectively, as shown by selective decoupling experiments on the mixture. Attempts to purify this fragment were not very successful, apart from the removal of mycalamide A. However, the $^1$H NMR data obtained closely matched those reported[94,166] for pederolactone (**3.6**), a decomposition fragment of pseudopederin (**3.5**). An FTIR spectrum, also showed a strong carbonyl stretch at 1720 cm$^{-1}$, with a weak C=C stretch at about 1645 cm$^{-1}$, indicative of an α,β-unsaturated lactone[96] and in good agreement with published data for this derivative[94]. This suggested that a pseudomycalamide derivative may have been formed early in the hydrolysis, which decomposed, possibly during workup procedures. The mechanism of formation of pederolactone probably involves an allylic (air) oxidation of the C6 hemiacetal, following an acid catalysed rearrangement of the exocyclic double bond into the C4-C5 position of the O1-C6 tetrahydropyran ring, with cleavage occurring between C6 and C7. This product was later observed to be a common acid catalysed degradation product for other mycalamide derivatives.

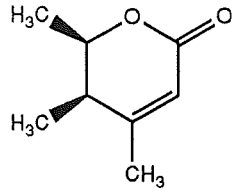


Pederolactone (**3.6**)

### 3.2.3 REACTION MONITORED BY $^1$H NMR SPECTROSCOPY - FORMATION OF PSEUDOMYCALAMIDE A?

The results of some early attempts by Perry[58] to monitor the reaction of mycalamide A with trifluoroacetic acid (0.01M) in $CDCl_3$ by $^1$H NMR spectroscopy were not very encouraging. In particular, a $^1$H NMR spectrum recorded after two hours showed a complete loss of the signals for the C6 methoxyl group and many other protons, and a rather complex mixture of components.

In a new approach, a few drops of $D_2O$ containing trifluoroacetic acid (0.01M) were added to a sample of mycalamide A in $CDCl_3$ in an NMR sample tube. The phases were mixed by shaking the sample tube vigorously, after which the sample was allowed to stand at room temperature. After one hour there was little change, but after one day there was a mixture of components. The major component was new, and appeared to have appropriate signals by $^1$H NMR spectroscopy for a pseudomycalamide A derivative (**3.7**), based on data reported for pseudopederin[94] (**3.5**). These included loss of the C6 methoxyl group resonance and shifts in the signals of some nearby protons. However, there were also other components present in this sample, including minor amounts of mycalamide A and some new compound ('UNKNOWN 1'), so that further analysis was impossible. Clearly a cleaner method of preparing pseudomycalamide A (**3.7**) was required, although the above method was the best preparation found so far.

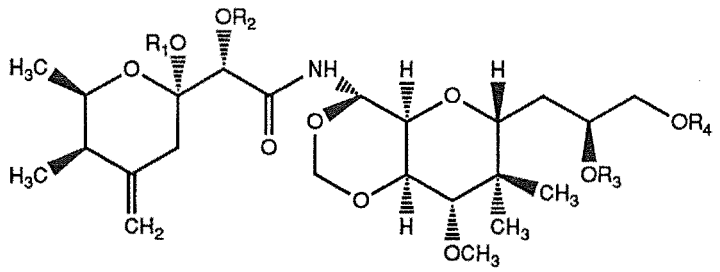

$R_1$=$R_2$=$R_3$=$R_4$=H: Pseudomycalamide A (**3.7**)
$R_1$=$R_2$=$R_4$=H, $R_3$=$CH_3$: Pseudomycalamide B (**3.8**)
$R_1$=$CD_3$, $R_2$=$R_3$=$R_4$=H: 6-Trideuteromethoxy A (**3.9**)
$R_1$=$CH_2CH_3$, $R_2$=$R_3$=$R_4$=H: 6-Ethoxy myc.A (**3.10**)
$R_1$=H, $R_2$=$R_3$=$R_4$=$COCH_3$: Pseudo A triacetate (**3.15**)

## 3.3 PREPARATION AND CHARACTERISATION OF PSEUDO-MYCALAMIDES A AND B

### 3.3.1 TWO-PHASE HYDROLYSIS REACTION

Earlier work on pederin[94], and the work above, clearly suggested that a two-phase hydrolysis system was the best method for the isolation of acid-sensitive mycalamide degradation products. The use of p-toluene sulphonic acid as a fairly mild, water soluble acetalisation catalyst[110,167] is common in synthetic chemistry. Here an aqueous solution of p-toluene sulphonic acid (0.05M) was stirred rapidly with a solution of mycalamide A in $CH_2Cl_2$ at room temperature. Reverse phase HPLC showed the gradual disappearance of mycalamide A and a slow buildup of a single, more polar peak with time, which was complete after about eight hours. Careful workup procedures gave almost pure pseudomycalamide A (**3.7**) by $^1H$ NMR and mass spectroscopies. A notable feature of the mass spectroscopy results was the ready loss of $H_2O$ from the parent or parent adduct ions in the EIMS and DCIMS spectra, consistent with the proposed structure (see Chapter 1). The reaction was successfully repeated on a larger scale and an analogous reaction on mycalamide B gave pseudomycalamide B (**3.8**).

### 3.3.2 NMR SPECTROSCOPIC CHARACTERISATIONS OF PSEUDO-MYCALAMIDES A AND B

Pseudomycalamides A and B (**3.7, 3.8**) were first analysed by $^1H$ NMR spectroscopy in $CDCl_3$ (with 0.1% pyridine added to prevent acid catalysed decomposition[139]) and these spectra were assigned with the aid of COSY and difference NOE experiments (described below) to give the data in Table 3.1. (Data for mycalamide A have also been listed for comparative purposes). The major changes in the $^1H$ NMR spectrum of pseudomycalamide A (**3.7**), compared with that of mycalamide A, were an absence of the C6-$OCH_3$ signal, a large separation in chemical shift for the two H5 proton resonances (0.6 ppm), which were coincident in mycalamide A, and minor chemical shift changes (in ppm) in the signals assigned to H2 (+0.2), 2-$CH_3$ (-0.1), H7 (-0.2), and the 4=$CH_2$, NH, H10 and H11 protons (<0.1). In the $^1H$ NMR spectrum of pseudomycalamide B (**3.8**), there were additional minor shifts in the signals assigned to the H17, 17-$OCH_3$ and H18 protons, suggesting that these protons were spatially close to the left hand portion of the molecule in solution, as for mycalamide B (Chapter 1), or that the conformations of the C16-C18 sidechain had been affected.

The separation in the two H5 signals was also found for pseudopederin (**3.5**), where it was noted that such differences were normal for structures containing different oxygenated functions whose actions were superimposed[94]. The downfield shift in the H2 resonance may result from different anisotropic long range shielding interactions[123] on replacement of the C6 methoxyl by a hydroxyl group (note that the C6-OH group is still axial, as favoured by the anomeric effect[105,106], and because the C7 chain is preferentially equatorial). However, other shifts cannot be accounted for in this way and it is more likely that these are the result of changes in the solution conformations, particularly about C6-C7, since the C8 carbonyl group, for

example, has large shielding and deshielding zones[123]. The solution conformations of mycalamides A and B have been described in detail (Chapter 1), but in the pseudomycalamides there exist new hydrogen bonding possibilities involving the new C6-OH group, which could have a significant effect on these conformations. This proposal is considered more fully in the following subsection.

The $^{13}C$ NMR spectrum of pseudomycalamide A (**3.7**) was assigned by an HMQC experiment, and the results also used to assign data for pseudomycalamide B (**3.8**) (Table 3.2). There were shifts in the signals assigned to C6 (-2), and C5, C7 and C8 (all +2 ppm), which were broadly indicative of the C6 acetal hydrolysis by the direction of the substituent effects[117] (C5, C6 and C7), although conformational changes in this area could also have some effect on the chemical shifts.

### 3.3.3 SOLUTION CONFORMATIONS OF PSEUDOMYCALAMIDES A AND B

The $^{1}H$ NMR spectrum of pseudomycalamide B (**3.8**) in $CD_2Cl_2$ solution showed that the signal assignable to the axial H5 proton was split into a broad quartet of doublets (2.0, 14 Hz) and was coupled to a broad doublet at δ4.95 ppm (2 Hz) as shown by selective proton decoupling. The latter signal was removed on addition of $D_2O$ and was therefore assigned to the C6-OH proton, which by its chemical shift must be involved in some hydrogen bonding interaction[101]. This coupling of 6-OH to the axial H5 proton was also observed for pseudopederin (**3.5**) in $d_6$-acetone[94], and requires a planar 'W' orientation of the protons for maximum long-range coupling to occur[102,104]. Several examples of such long range couplings through oxygen have been reported, including an hydroxyl proton in cycloheximide[83] (**0.14**) and hemiacetal protons in elaiophylin[152,168] and bafilomycin[169]. The latter two examples have some structural features similar to pseudomycalamides A and

B and their conformations have been studied by both x-ray crystallography and $^1H$ NMR spectroscopy. In particular, the hemiacetal proton of elaiophylin is hydrogen bonded to an oxygen on a nearby carbon, to form a 6-membered ring chair conformation. This 'locks' its position in a plane, involving the chain atoms H-O-C-C-H of the hemiacetal and an adjacent axial methylene proton, accounting for the observed 'W' coupling (1.5 Hz), as shown in Figure 3.1. The same situation occurs in bafilomycin and it was noted that the strong 'W' coupling (2.2 Hz) implied 'little or no motional freedom around the C-O(H) bond'[169].

**Figure 3.1** Structure and conformation of elaiophylin, illustrating the 'W' geometry of the hydrogen bonded hemiacetal proton with an adjacent methylene proton.

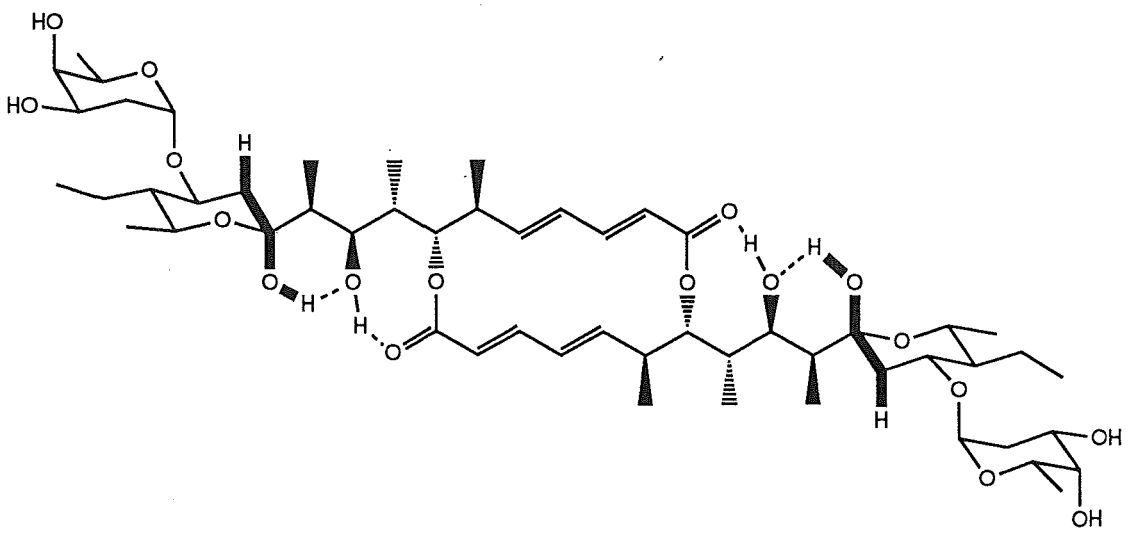


Newman projections for the three staggered conformers about the C6-C7 bond of pseudomycalamides A and B are shown in Figure 3.2. The data obtained from difference NOE experiments are shown in Table 3.3 and, where relevant, as arrows in Figure 3.2. There were NOE interactions between the C3 methyl group and H5a, which confirmed the proposed chair conformation for the O1-C6 ring, and between both H5a and H5e and H7. It is thus likely that there is some contribution from all three conformers in Figure 3.2a-c,

which each offer many hydrogen bonding possibilities, and also possibly from other conformations. In particular, the conformations in Figures 3.2c, and possibly 3.2b, are required by the observed NOE interactions between H5a and H7 and between H5e and H7, where the latter appeared to be stronger. Note, however, that the conformer in Figure 3.2c appears to be the *most* favoured, since it allows the C6-OH proton to be hydrogen bonded to the C8 carbonyl group in a 6-membered ring, with the hemiacetal proton anti to C5 about the C6-O bond, giving the observed 'W' coupling, while H7 is closest to H5e, in accordance with the strong NOE interaction observed between these protons. In the conformation depicted by Figure 3.2a, the hemiacetal proton has to be shifted out of the C5-C6-O plane to allow the same hydrogen bond with the C8 carbonyl group, which is not favourable for the observed long range coupling. This result is therefore very different from that found for mycalamide A, where the conformations in Figures 3.2a, and to a lesser extent 3.2b, were the proposed major solution conformations (Chapter 1).

**Figure 3.2** Newman projections for the staggered conformers about C6-C7 in pseudomycalamides A and B (**3.7**, **3.8**)

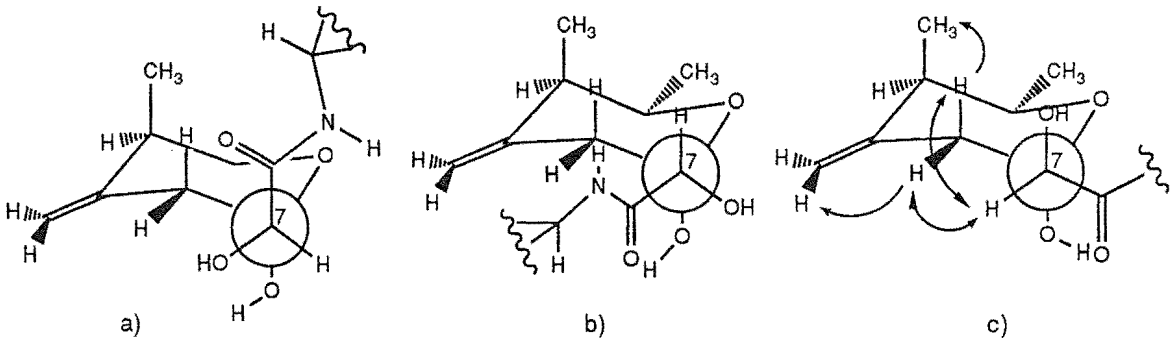


3.3.4 MECHANISM AND STEREOCHEMISTRY OF ACETAL HYDROLYSIS

The O1-C6 tetrahydropyran ring system of mycalamides A and B and pederin, containing the C6 acetal group, is analogous to that found in various glycosides. The acid catalysed hydrolysis of glycosides is known to occur with

fission of the glycosyl-oxygen bond[170,171] (shown by $^{18}O$ labelling), and involves protonation of the alkoxyl oxygen (not the ring oxygen) and cleavage to give a cyclic carbonium ion. This ion is resonance stabilised by electron donation from the ring oxygen, so that the positive charge lies mainly on the oxygen, with the acetal carbon $sp^2$ hybridised[170]. This carboxonium ion intermediate[171] is then readily attacked by $H_2O$, to give the cyclic hemiacetal in an $S_N1$ fashion[172] (Scheme 3.1).

**Scheme 3.1** Mechanism for C6 acetal hydrolysis (R=H) and exchange (R=alkyl) in mycalamide A.

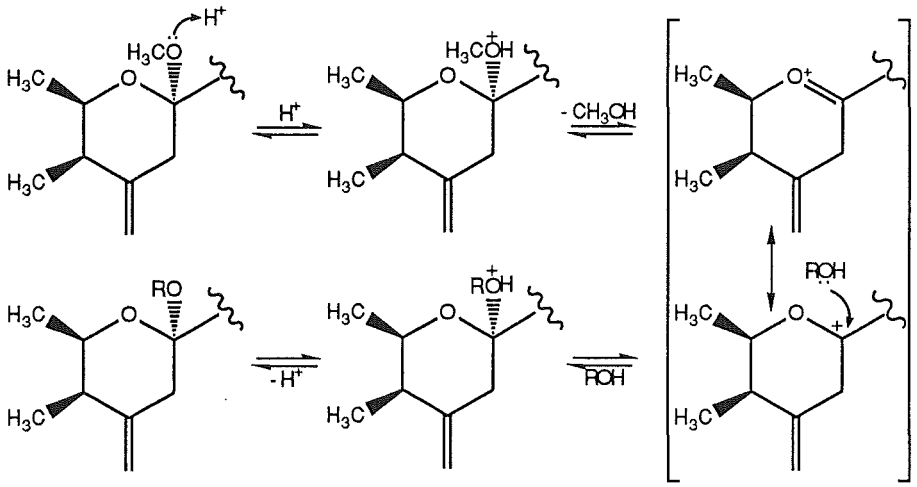


The geometry of the cyclic carboxonium ion intermediate derived from glycosides resembles a half-chair[100,170]. In mycalamide A, this conformation is only slightly modified by the presence of the exocyclic double bond (Figure 3.3). An attack of $H_2O$ from below the ring gives a product with retention of configuration at C6, whereas attack from above gives inversion. The C6 inversion product would be in a new chair conformation, having the C6-OH group axial (as favoured by the anomeric effect) and the C7 sidechain equatorial at C6 (as favoured by steric factors) (Figure 3.4). However, it would also have a 1,3-diaxial steric interaction between an axial methyl group at C2

and the C6-OH group making it less thermodynamically favourable. This thermodynamic effect causes both a stereospecific hydrolysis and a stereospecific methanolysis of the product, since these reactions are reversible. Similar results were also found for pederin[94,133,164].

**Figure 3.3** Conformation of the carboxonium ion intermediate generated from mycalamide A by acid catalysed hydrolysis.

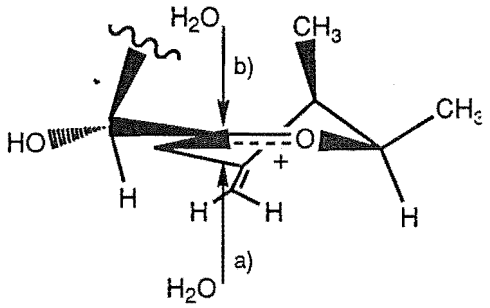


**Figure 3.4** Chair conformations for pseudomycalamides A and B (**3.7**, **3.9**) and a C6 epimer.

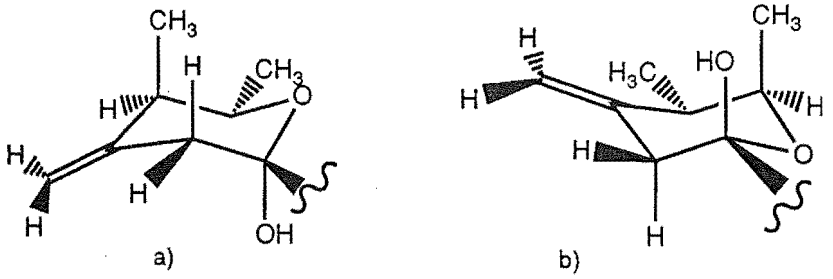


### 3.3.5 REARRANGEMENT AND DECOMPOSITION OF HEMIACETALS

In the presence of $H_2O$, free sugars (cyclic hemiacetals) undergo isomerisation between the α and β forms (mutarotation). The mechanism for this reaction[106] involves a ring opening of the hemiacetal to give an acyclic intermediate (Scheme 3.2), as shown by $^{18}O$ labelling, since the hemiacetal oxygen atoms are retained. The presence of acid-base catalysts is known to speed up this isomerisation.

**Scheme 3.2** Mechanism of epimerisation of hemiacetals, as shown for pseudomycalamide A (**3.7**).

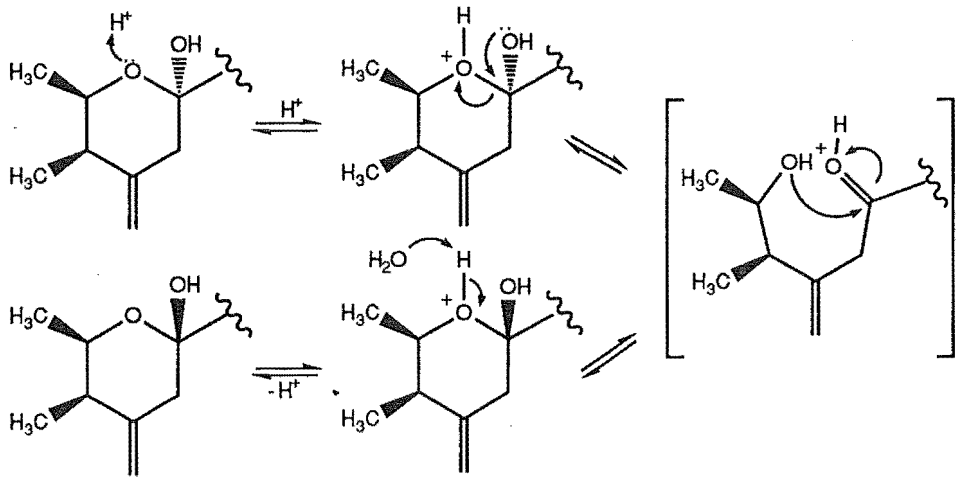

Pseudomycalamides A and B (**3.7**, **3.8**) were not very stable, as illustrated in earlier acid catalysed reactions. Attempts to purify an old sample of pseudomycalamide B (containing a new component) by preparative silica gel TLC gave two fractions which were similar, containing both pseudomycalamide B (**3.8**) and another, related compound. It is likely that the new compound was the C6 epimer, which was interconverting with pseudomycalamide B on silica gel, as discussed above. Several $^1$H NMR resonances for this epimer were significantly different in chemical shift from those observed for pseudomycalamide B. In particular, the 2-$CH_3$ (+0.1), H5a (-0.3), H5e (+0.1), H10 (+0.1) and H11 (-0.1) resonances were most affected, with smaller shifts occurring in many other resonances throughout the spectrum. These shifts would be consistent with a 'flipping' of the chair conformation of the O1-C6 ring on epimerisation at C6, thereby allowing the C6-OH group to remain in an axial orientation as favoured by the anomeric effect[106], since the remaining substituents would be in different spatial and chemical environments (Figure 3.4). Further changes in the solution conformations about the C6-C7 and C7-C8 bonds could also occur as a result. However, the separation of these isomers could not be achieved readily, and,

furthermore, these pseudomycalamide derivatives were rather unstable, so that this work was not pursued further.

### 3.3.6 CONVERSION OF PSEUDOMYCALAMIDES A AND B TO MYCALAMIDES A AND B.

Pseudomycalamide A (**3.7**) was successfully converted to mycalamide A by a reaction in methanol containing a trace of p-toluene sulphonic acid ($5x10^{-4}M$) as the acid catalyst. The reaction was monitored by reverse phase HPLC, which showed a gradual decrease in the amount of the starting compound and an increase in the intensity of a peak with an elution time identical to mycalamide A. The reaction was about 50% complete after 2 hours and at least 90% complete after 1 day at room temperature. Pseudomycalamide B (**3.8**) was treated in a similar manner to give complete reaction to mycalamide B after four hours, as determined by HPLC. TLC of the product also gave a single spot with an identical $R_f$ to that of pure mycalamide B.

This reaction occurs by an attack of $CH_3OH$ on the carboxonium ion[170], generated by loss of $H_2O$ from the protonated hemiacetal in an $S_N1$ fashion (see Scheme 3.1). Therefore this conversion of mycalamides A and B to pseudomycalamides A and B was reversible, as for pseudopederin (**3.5**). However, the reaction of pseudopederin was apparently more facile, in that it did not require the presence of an added acid catalyst[164], whereas the analogous reaction of pseudomycalamides A and B did not occur without such a catalyst.

## 3.4 C6 ALKOXY EXCHANGE AND ELIMINATION REACTIONS

### 3.4.1 D4-METHANOL EXCHANGE

The incorporation of $CD_3O$ at C6 in mycalamide A was monitored by observing changes in the $^1H$ NMR spectrum of a sample of mycalamide A in $CD_3OD$ solution containing a trace of trifluoroacetic acid (0.01M). After 45 minutes the exchange was about 40% complete, as shown by the appearance in the spectrum of a new $CH_3OH$ resonance, decrease in the intensity of the signals assigned to the 6-$OCH_3$ and H7 protons, and the appearance of a new H7 resonance, shifted slightly upfield (~2 Hz). After 15 hours the exchange was complete to give 6-trideuteromethoxy mycalamide A (**3.9**), but there appeared to be a very minor product as well, previously referred to as UNKNOWN 1. HRFABMS confirmed the quantitative inclusion of $OCD_3$ into mycalamide A at C6, in place of the $OCH_3$ group, since $CD_3OH$ was readily lost under DCI and DEI mass spectroscopy conditions. Further treatment of this product under the same reaction conditions, but using $CH_3OH$, regenerated mycalamide A. The mechanism for this and other alkoxy exchange reactions at C6 is also $S_N1$, as in Scheme 3.1, with the alcohol being the attacking nucleophile.

### 3.4.2 ETHANOL EXCHANGE

Initial attempts were made to prepare a 6-ethoxy derivative of mycalamide A by adding a trace of trifluoroacetic acid (0.01M) to a sample of mycalamide A in ethanol. However, the $^1H$ NMR spectrum of the crude product showed a mixture containing mostly pseudomycalamide A (**3.7**), with a smaller amount of a new compound, which was possibly 6-ethoxy mycalamide A (**3.10**), along with unreacted mycalamide A and a minor

amount of UNKNOWN 1. Thus hydrolysis, due to traces of $H_2O$ in the solvent, was the favoured reaction path.

A second attempt, using pyridinium p-toluene sulphonate[167,173] as the catalyst in dry ethanol, was more successful. The reaction was best monitored by reverse phase TLC or HPLC, since the new compound found above had a longer retention time than mycalamide A and pseudomycalamide A a shorter retention time, whereas on silica gel both compounds had shorter retention times than mycalamide A. The reaction was very slow, but after four days at room temperature the reaction mixture consisted of a ratio of about 2:1 in favour of a more retained product over mycalamide A, with another very minor product. Preparative HPLC was performed to purify the new major product, which was similar to mycalamide A by $^1H$ NMR spectroscopy, but lacked the C6-methoxyl group and contained a new ethoxy system (Table 3.1). These new -$OCH_2$ proton resonances were non-equivalent, with each appearing as a doublet of quartets. The more downfield -OCH resonance was enhanced most on irradiation of H7 in an NOE experiment (Table 3.3), whereas the upfield -OCH resonance was enhanced most on irradiation of H2, so that this compound was clearly 6-ethoxy mycalamide A (**3.10**). The $^{13}C$ NMR spectrum was also similar to that of mycalamide A, but contained no C6 methoxyl signal, and there were two new carbon resonances at δ56.7 and 15.2 ppm, assignable to the new ethoxy substituent (Table 3.2). The C7 resonance was only slightly shifted (+0.8 ppm) and all other signals in the $^{13}C$ NMR spectrum were within 0.2 ppm of those for mycalamide A. These results suggested that the distributions of solution conformations of this C6-ethoxy derivative were almost identical to those of mycalamide A. HRFABMS confirmed the molecular formula of this compound, which was isomeric with mycalamide B, and showed a ready loss of $CH_3CH_2OH$ from the $MH^+$ ion, as expected.

### 3.4.3 ATTEMPTED EXCHANGE WITH ISOPROPYL ALCOHOL

Little or no reaction was observed by TLC for a sample of mycalamide A in isopropyl alcohol, containing a small amount of pyridinium p-toluene sulphonate, after a period of 16 hours at room temperature, so the reaction was heated for 1 hour at 55°C. Reverse phase TLC showed the presence of some unreacted mycalamide A and other, less retained products only, so the reaction was stopped. After workup, $^1$H NMR spectroscopy showed the presence of at least four compounds, including mycalamide A, pseudomycalamide A (**3.7**), pederolactone (**3.6**), and the compound earlier designated as UNKNOWN 1. Preparative HPLC gave four fractions, but on evaporation and examination by $^1$H NMR spectroscopy only two of the four purified fractions contained recognisable signals, which belonged to mycalamide A and the unknown compound respectively.

### 3.4.4 STRUCTURE OF 'UNKNOWN 1'

The $^1$H NMR spectrum of this compound was similar to that of mycalamide A but there were no C6 methoxyl or H5 resonances apparent, although there was a new single proton singlet at δ5.64 ppm. There were also shifts in the H2 (+0.2), H3 (+0.2), 4=CH*Z* (-0.2), H7 (+0.3) and NH (-0.3) proton resonances, compared to data recorded for mycalamide A (Table 3.1). Irradiation of the new resonance in an NOE experiment gave an enhancement of the downfield 4=CH*E* and H7 signals (Table 3.3). Similarly, irradiation of these signals enhanced the singlet at δ5.64 ppm. This evidence suggested that this singlet was due to a single H5 proton on a double bond, which must be located between C5 and C6, as in structure **3.11**.

Note that the chemical shifts of the 4=$CH_2$ protons had 'swapped', compared to data for mycalamide A, with the 4=CH*E* signal now being the more downfield resonance, consistent with shielding effects due to this double

bond[123]. The shifts in the remaining signals probably also resulted from a combination of electronic factors[101] and steric effects, and also from the new conformation of the O1-C6 tetrahydropyran ring, depicted in Figure 3.5. Here the atoms C3, 4=$CH_2$, C4, C5, C6, C7 and O1 all lie approximately in a plane, giving an envelope shape, with C2 preferentially below this plane so that the C2 methyl group is approximately equatorial. The conformations about the C6-C7 bond were not fixed, but the NOE results above suggested that H7 was close to H5 in a major solution conformation, and this is reasonable, in order to minimise steric interactions.

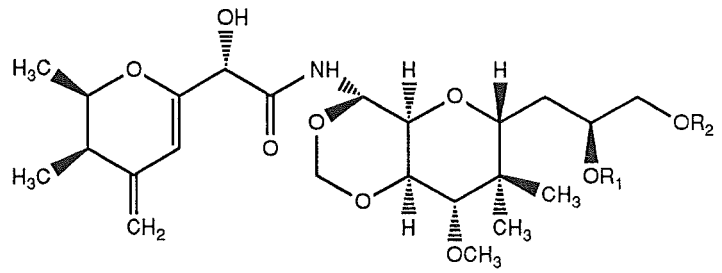


$R_1$=$R_2$=H: 5,6-Dehydromethoxy mycalamide A (**3.11**)
$R_1$=$R_2$=$COCH_3$: 5,6-Dehydromethoxy A 17,18-diacetate (**3.16**)

**Figure 3.5** $^1$H-$^1$H NOE interactions and partial solution conformation of 5,6-dehydromethoxy mycalamide A (**3.11**).

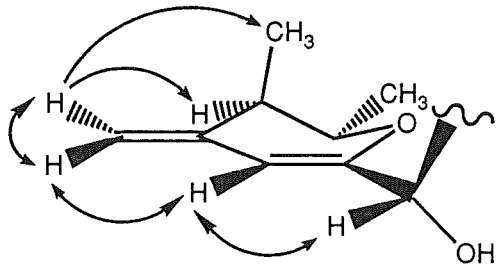


There was insufficient sample of this 5,6-dehydromethoxy mycalamide A derivative (**3.11**) to enable further NMR spectroscopic characterisations, although HRFABMS was achieved, which indicated a molecular formula of $C_{23}H_{37}NO_9$, in accordance with the proposed structure. The reaction above did not seem to be a good method to reprepare this derivative, particularly as

some decomposition had been observed on silica gel and in a stored NMR sample. However, a new route was discovered subsequently from investigations of mycalamide A in mild bases at high temperature. This method will be described briefly here, since it was high yielding and allowed further characterisations on this same derivative. Following this, mechanisms for both acid and base catalysed reactions will be proposed.

### 3.4.5 HIGH TEMPERATURE ELIMINATION REACTION, CATALYSED BY WEAK BASES

The elimination of methanol at C6 in mycalamides A and B occurs readily at high temperatures, as observed under all mass spectroscopy conditions. During high temperature $^1$H NMR studies of mycalamide A in DMSO, it was observed that mycalamide A was stable to temperatures of at least 150°C in solution. However, upon the addition of only a few microliters of pyridine or triethylamine, there occurred a clean reaction, which was almost complete within two hours at 130°C in the sealed sample tube. A $^1$H NMR spectrum of the product showed the presence of the same signals described above for 5,6-dehydromethoxy mycalamide A (**3.11**) and a methanol signal was observed as well. To confirm the identity of this product, the $^1$H NMR spectral data in DMSO were also fully assigned (Table 3.1). Note that in this solvent the signals for the C7-OH and NH protons were observed at quite low fields, suggesting that these protons were involved in strong hydrogen bonding interactions[101]. This reaction was then repeated and the combined product separated from DMSO by elution on a reverse phase pipette column. Full NMR spectroscopic characterisations were then performed in $CDCl_3$, containing a trace of pyridine as usual.

The $^1$H NMR spectrum was conclusively assigned by using the results of COSY and NOE experiments (Tables 3.1 and 3.3). A $^{13}$C NMR spectrum

was recorded and both HMQC and HMBC experiments were performed to assign these signals. The strong HMBC correlations from the C2 and C3 methyl and the 4=CH methylene proton signals (Table 3.4) were used to confirm the assignments of C2 and C3, which had shown only weak correlations in the HMQC spectrum, and to locate C4 (δ142.9 ppm). Note that the C5 resonance, δ103.6 ppm, had been located by the HMQC experiment, and was of typical chemical shift for the structure[117]. The C6 resonance, at δ149.8 ppm, was located by a strong HMBC correlation from H7, and was also similar in chemical shift to those of other enol ethers[117,174,175].

Comparing these $^{13}C$ NMR data with those recorded for mycalamide A (Table 3.2), the largest shifts had occurred in the C5 and C6 resonances due to the presence of the new double bond. However, the chemical shifts of signals assigned to the remaining O1-C6 ring carbons and substituents had also changed significantly, with shifts in the C2 (+6.8), 2-$CH_3$ (-2.0), C3 (-3.6), 3-$CH_3$ (+1.2), C4 (-2.8) and 4=$CH_2$ (-2.5) carbon resonances. These changes were also consistent with the presence of a double bond between C5 and C6[117], and with changes in the ring conformation, as shown in Figure 3.5 above.

### 3.4.6 ELIMINATION MECHANISMS

#### 3.4.6.1 ACID CATALYSED ELIMINATION MECHANISM

The 5,6-dehydromethoxy mycalamide A derivative (**3.11**) was present at a low level in most of the acid catalysed C6 hydrolysis or alkoxy-exchange attempts described above, as indicated. This was not surprising since the intermediate carboxonium ion is in a homoallylic relationship to the terminal alkene and the β (allylic) H5 proton is therefore slightly acidic. Thus the elimination reaction to give 5,6-dehydromethoxy mycalamide A could be expected to compete with substitution reactions under acidic conditions,

especially with poorer nucleophiles and a partially hindered carboxonium ion[170,176]. The mechanism of such an elimination reaction is likely to be E1[176] (Scheme 3.3a), since the reaction conditions were fairly polar, with a good leaving group being present under acidic conditions (eg $CH_3OH$), and the carboxonium ion intermediate was reasonably stable.

**Scheme 3.3** Acid and base catalysed elimination mechanisms for the formation of 5,6-dehydromethoxy mycalamide A (**3.11**).

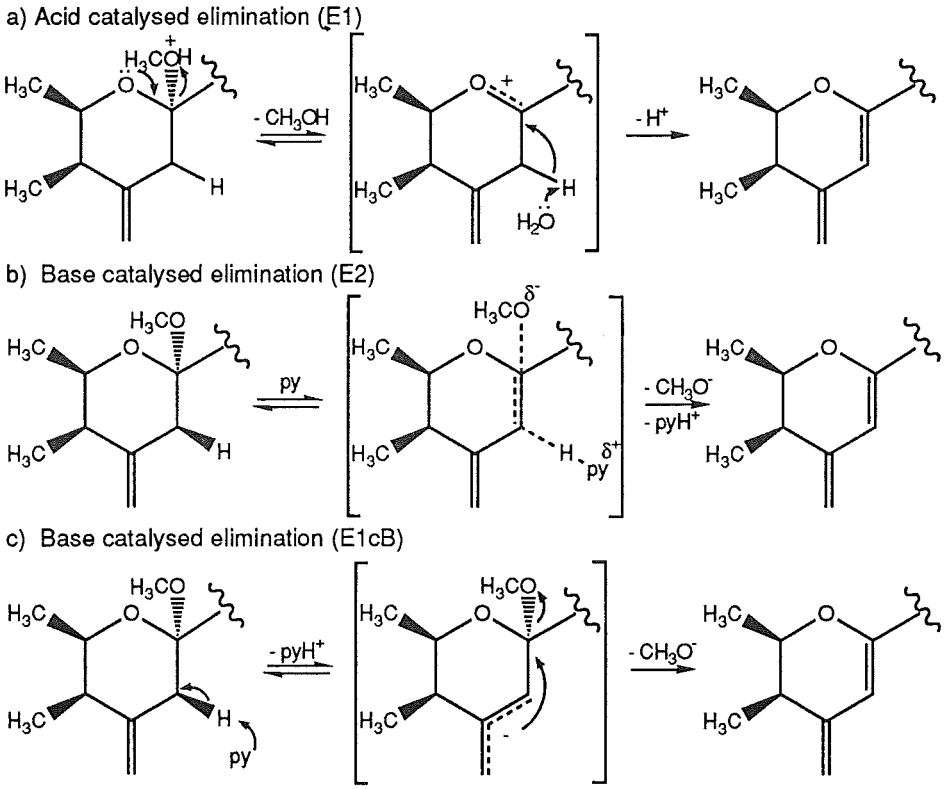


3.4.6.2 BASE CATALYSED ELIMINATION MECHANISM

The mechanism for the base catalysed elimination reaction is likely to lie somewhere in the range E2 to E1cB[176]. The solvent, DMSO, is dipolar and aprotic, but simply applying a high temperature to a solution of mycalamide A in DMSO was insufficient to induce elimination. Pyridine is a relatively poor nucleophile and a weak base[140,177]. In the mycalamide structure, the H5a proton is antiperiplanar to the C6-$OCH_3$ group, which is the preferred

arrangement for an E2 anti elimination reaction[176] (Scheme 3.3b). However, $CH_3O^-$ is a poor leaving group[140] and the H5 protons are slightly acidic so that the transition state may have substantial carbanion character, as in the E1cB mechanism[176] (Scheme 3.3c). The difference between the two extremes is whether $H^+$-Base leaves before (E1cB), or at the same time as (E2) the $CH_3O^-$ group, but this is not essential to the present discussion.

## 3.5 ANALYSIS OF BIOLOGICAL ASSAY RESULTS

The antiviral and P388 assay results for the above derivatives have been listed in Table 3.5. The conversion of mycalamides A and B to pseudomycalamides A and B (**3.7**, **3.8**), having a C6-OH group, has a deactivating effect of 20-40 fold, which is in good agreement with the published results for pederin and pseudopederin[40] (see the introduction to this chapter). Detailed analysis of the solution conformations of pseudomycalamides A and B showed that there were significant differences from those found for mycalamides A and B, particularly in the relative populations of the C6-C7 rotamers. In addition, the higher polarity of pseudomycalamides A and B, due to the extra hydroxyl group, and the potentially different interactions of this group with the unknown active site[15], could be factors involved in the observed drop in the biological activities of these derivatives.

By comparison, the biological activities of 6-ethoxy mycalamide A (**3.10**) were almost the same as those of mycalamide A. The distribution of solution conformations appeared to be the same in both, despite the polarity of the 6-ethoxy compound being slightly less than mycalamide A, as measured by the relative mobilities of these compounds on C18 and silica gel.

The 5,6-dehydromethoxy mycalamide A derivative (**3.11**) was significantly less active than even pseudomycalamide A (**3.7**) and at least 200 times less active than mycalamide A. Again there were probably some changes to the distribution of solution conformations about C6-C7, but also there were different electronic and steric effects caused by the presence of the new C5-C6 double bond and the O1-C6 ring conformation was considerably different. Note that the mobilities of this derivative on both C18 and silica gel lay between those of pseudomycalamide A and mycalamide A, so that the loss in activity would not seem to be associated entirely with different solubility characteristics[1,15].

In summary, it appears that the C6 acetal is very important for the biological activities of mycalamide A. The observation of changes to the solution conformations of this portion of the molecule on derivatisation may be useful in probing the active conformation or site. Such work has not been considered in this study.

## 3.6 ACID CATALYSED DECOMPOSITION STUDIES OF MYCALAMIDE A TRIACETATE

The instability of the mycalamides A and B and pederin to contact with acids has so far been shown to arise mainly from the presence of a homoallylic acetal functionality[132] at C6. Indeed the only products isolated from such reactions have so far involved acid catalysed exhange at C6, elimination across C5-C6, and cleavage of the C6-C7 bond. In an attempt to follow the decomposition further, it was considered desirable to use an acetate protecting group[78] for the hydroxyl groups, since the resulting acetate esters would be stable to mild acid[138], and would increase the mass and reduce the polarity of potential fragments. Furthermore, potential enols at C7 or other

centres would be partially trapped as the vinyl esters. Also, various other 7-*O*-substituted derivatives, including mycalamide B bis-TMS ether (**2.2**) and mycalamide A 7,18-di-p-bromobenzoate (**2.12**), had shown a tendency to undergo a facile elimination-rearrangement reaction in acidic $CDCl_3$ and it was therefore desirable to investigate this reaction further. The results for the above derivatives will be discussed briefly following a presentation of the results obtained in the current study, since this will assist in their interpretation.

### 3.6.1 INITIAL INVESTIGATION, MONITORED BY $^1$H NMR SPECTROSCOPY

A sample of mycalamide A triacetate (**2.18**) was dissolved in $CDCl_3$ containing a trace of trifluoroacetic acid (0.1M) and placed in an NMR sample tube. $^1$H NMR spectroscopy showed a slow reduction in the intensity of signals belonging to mycalamide A triacetate, and the appearance of new signals over several days. After two days at ambient temperature there was about 40% conversion to one major rearranged product, but other minor products were also observed. After five days there were still more components, but there was still residual mycalamide A triacetate present in the mixture. Of particular interest in the $^1$H NMR spectrum of this mixture was a strong singlet at about δ9.16 ppm, suggesting the presence of an aldehyde group[101]. Therefore the reaction products were recovered, washed with water, and then analysed by HPLC. Preparative HPLC initially separated two fractions from a mixture of more polar components, and the latter was then further chromatographed to yield two further fractions, giving four fractions overall, which have been ordered according to increasing polarity.

The $^1$H NMR spectrum of the first fraction showed that it consisted entirely of unreacted mycalamide A triacetate (**2.18**) and the second fraction was similarly found to be a rearranged product ('UNKNOWN 2'). The third fraction was also almost pure by $^1$H NMR spectroscopy, but very small, and

was evidently a cleavage fragment derived from the right-hand portion of mycalamide A triacetate ('UNKNOWN 3'). The final fraction was a complex mixture, with few recognisable signals. The small sample size of the two new compounds required that the reaction be repeated to obtain sufficient sample for accurate NMR spectroscopic characterisation. This was done, but the system was modified by using the milder two-phase technique, developed above for the hydrolysis of mycalamide A, in an attempt to improve the yields, and, possibly, to isolate further degradation products.

### 3.6.2 TWO-PHASE HYDROLYSIS MONITORED BY TLC

A larger sample of mycalamide A triacetate (**2.18**), dissolved in $CH_2Cl_2$, was stirred rapidly with an aqueous p-toluene sulphonic acid solution (0.1M) at 75-80°C in a sealed vial. After one day, silica gel TLC showed that most of the starting material had disappeared, and that there were several products. Following neutralisation and other workup procedures, preparative TLC was performed, which yielded four fractions. These fractions were then examined by $^1H$ NMR spectroscopy, in order of decreasing polarity.

The major fraction (1) was an almost pure sample of UNKNOWN 2 by $^1H$ NMR spectroscopy, so these samples were combined for analysis. The second fraction contained a compound similar to that contained in fraction 1, possibly an isomer ('UNKNOWN 4'), with a small amount of UNKNOWN 2. The third fraction was a mixture and so it was set aside for HPLC separation, while the final fraction was also a mixture, containing the aldehyde fragment, UNKNOWN 3. These 'unknowns' are chacterised below.

### 3.6.3 STRUCTURE OF UNKNOWNS 2 AND 4

Mass spectroscopy showed that the compounds described above as UNKNOWNS 2 and 4 were isomers, of molecular formulae $C_{29}H_{43}NO_{12}$,

which corresponded to a loss of $CH_3OH$ from mycalamide A triacetate (**2.18**). An FTIR spectrum of these isomers showed a small decrease in the frequency of the amide carbonyl stretch (10-14 $cm^{-1}$), compared to similar data for mycalamide A triacetate, which is consistent with further conjugation of this group[96]. There was also evidence for a vinyl (C7) acetate group[96], since there were carbonyl stretching bands at 1765 and 1774 $cm^{-1}$ for the two isomers, in addition to the normal 1740 $cm^{-1}$ acetate band found in mycalamide A triacetate (**2.18**). The $^1H$ NMR spectrum of both compounds also showed a loss of the signals for the 6-$OCH_3$, H7, $H_2$5, and 4=$CH_2$ protons, and the appearance of new signals for an allylic methyl-methine system. These data are consistent with a rearrangement of the exocyclic double bond into the C4-C5 position of the O1-C6 tetrahydropyran ring and an elimination of methanol across C6-C7, to give two isomers about the C6-C7 bond of a fully conjugated, planar dienone from C4 to C8 (**3.12**, **3.13**). These structures were called 'neomycalamides' for ease of reference.

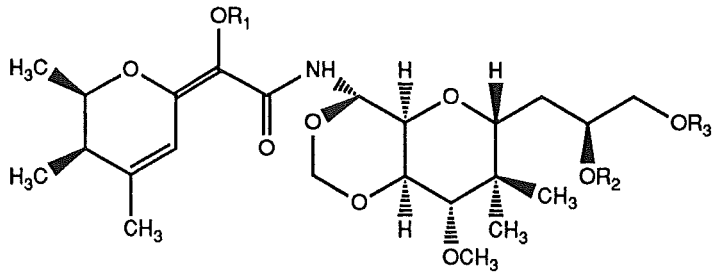


$R_1$=$R_2$=$R_3$=$COCH_3$: *Z* Neomycalamide A triacetate (**3.12**)
$R_1$=$R_3$=$COC_6H_4Br$, $R_2$=H: *Z* Neomyc.A 7,18-di-p-bromobenzoate (**3.18**)

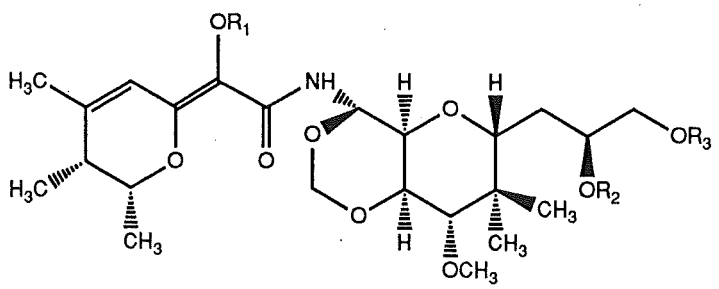


$R_1$=$R_2$=$R_3$=$COCH_3$: *E* Neomycalamide A triacetate (**3.13**)
$R_1$=$R_3$=$COC_6H_4Br$, $R_2$=H: *E* Neomyc.A 7,18-di-p-bromobenzoate (**3.19**)

The complete $^1H$ NMR spectrum of each isomer was assigned with the aid of COSY and proton decoupling experiments (Table 3.6). The two isomers differed most in the chemical shifts of the H2, 2-$CH_3$, H5 and NH resonances, with the shifts for the latter two being very large (>1 ppm). The large downfield shift in the H5 proton resonance of UNKNOWN 4, relative to that of UNKNOWN 2, is consistent with a *Z* geometry at the C6-C7 double bond (**3.12**), since the H5 proton is then close to the C8 carbonyl oxygen, and in the plane of the dienone (Figure 3.6a), thus giving the anomalous chemical shift[123]. Examples of this deshielding by carbonyl groups abound in the literature.

**Figure 3.6** $^1H$-$^1H$ NOE interactions and possible conformations of the neomycalamide A triacetate isomers (**3.12, 3.13**).

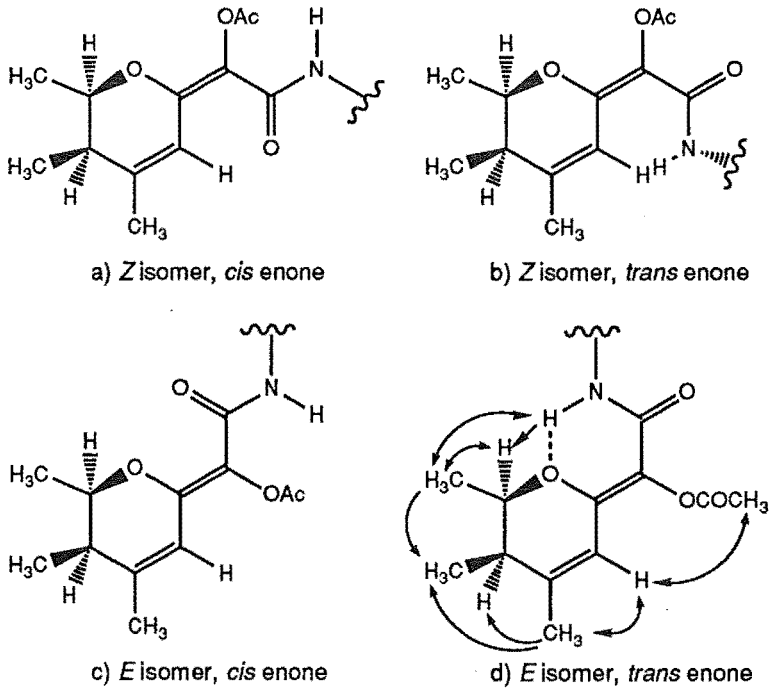


The C6-C8 enone for this *Z* isomer (**3.12**) can only be *cisoid*, otherwise unfavourable steric interactions occur between the ring substituents and the NH9 chain (Figures 3.6a and b). In contrast, the *E* isomer (**3.13**) can be either *cisoid* or *transoid* at the C6-C8 enone (Figures 3.6c and d respectively). If the

enone is *trans*, then the NH proton is close to the ring oxygen, O1, and can form an almost planar 6-membered ring by hydrogen bonding. The chemical shift of this proton resonance (δ8.10 ppm) suggested that it was strongly hydrogen bonded[101], much more so than in the *Z* isomer (**3.12**) or mycalamide A triacetate (**2.18**). This proposal was further supported by the different chemical shifts of the H2 and 2-$CH_3$ proton resonances for the two isomers and by the observation of NOE interactions between these protons and the NH proton (Table 3.3 and Figure 3.6d). Further evidence for the proposed C6-C7 double bond stereochemistry of this *E* isomer was obtained from the observation of NOE interactions between H5 and the C7 acetate methyl protons.

$^{13}C$ NMR spectra were also recorded for the two isomers and, in addition, HMQC and HMBC experiments were performed on the major isomer (*E*, **3.13**) to enable unambiguous $^{13}C$ NMR spectral assignments (Table 3.2). The HMBC correlations obtained have been listed in Table 3.4. The C8 carbon resonance was shifted upfield, compared to its position in mycalamide A triacetate, consistent with α,β-unsaturation[117]. Many of the other O1-C6 ring carbons were also shifted considerably, as expected, due both to electronic factors and to changes in the conformation of this ring.

The chemical shifts of the carbons directly involved in the new dienone system (Table 3.2) were close to those observed in model compounds[174,175,178]. However, either the quaternary C6 or C7 resonance was not observed in the $^{13}C$ NMR spectrum, unless the two were coincident, and only one of the two possible HMBC correlations from H5 were observed. It was assumed that the $^{13}C$ resonance for C7 was less likely to be observed because it could have a longer relaxation time, since the quaternary C7 is itself located between two quaternary carbon atoms. Therefore the signal at δ151.8 ppm, which also showed the HMBC correlation to H5, was tentatively

assigned to C6. Note, however, that this value would be an equally acceptable chemical shift for C7[174,175].

### 3.6.4 STRUCTURE OF 'UNKNOWN 3'

In the introduction to this chapter, it was noted that the hydrolysis of pederin in sulphuric acid/hexane[94] gave an aldehyde fragment, pederenal (**3.1**). This was formed by hydrolysis of the C10 aza acetal of pederin and elimination of $H_2O$ across C12-C13, followed by rearrangement of the new double bond into the C11-C12 position (the C13-OH had originally been incorrectly placed at C12 in the pederin structure because of this result[27,94]). Mycalamide A, which contains many structural features similar to those of pederin, could undergo a similar cleavage reaction.

The EIMS and DCIMS results on UNKNOWN 3 indicated a molecular formula of $C_{16}H_{24}O_7$. An FTIR spectrum showed the presence of a carbonyl stretch at about 1700 $cm^{-1}$, on the shoulder of the carbonyl band for the two acetate groups (1741 $cm^{-1}$), along with a weak C=C stretching band at 1637 $cm^{-1}$, which were indicative of an $\alpha,\beta$-unsaturated aldehyde[96], and were almost identical to the IR bands reported for pederenal[94] (**3.1**). The $^1H$ NMR spectrum contained a singlet at $\delta$9.16 ppm, which was assigned to a C10 aldehyde proton, and a doublet at $\delta$5.84 ppm coupled to a doublet at $\delta$3.61 ppm (2.6 Hz), which were assigned to the H12 and H13 protons, respectively (Table 3.6). There were also resonances for the 13-$OCH_3$, two 14-$CH_3$, H15-H18, and two acetate methyl groups, although there were small shifts in these resonances compared to those recorded for mycalamide A triacetate (**2.18**). These data are all consistent with the structure **3.14**. Note that there was insufficient sample to obtain a $^{13}C$ NMR spectrum.

Difference NOE experiments were performed to analyse the conformation of the C11-C15 ring, and the results listed in Table 3.3 have

been summarised in Figure 3.7. In particular, strong NOE interactions were observed between H10 and H12, and weaker interactions between H13 and H15, and from both H13 and H15 to the equatorial 14-$CH_3$ group, confirming that the relative stereochemistries of the ring carbons had not changed. The conformation of this C11-C15 ring could thus be described as a half-chair[100], with the C16 sidechain substituent in the preferred equatorial position at C15.

**Figure 3.7** Structure and $^1H$-$^1H$ NOE interactions for the 10-aldehyde fragment (**3.14**).

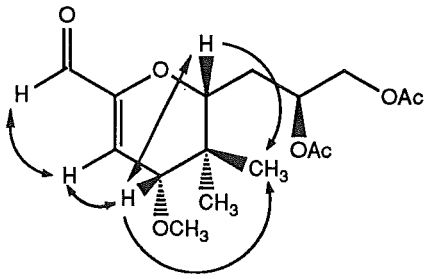


### 3.6.5 OTHER PRODUCTS FROM THE HYDROLYSIS OF MYCALAMIDE A TRIACETATE

#### 3.6.5.1 PRODUCTS FROM TLC FRACTION 3

The $^1H$ NMR spectrum of the third TLC fraction above had indicated a mixture of at least four major components, so this was further analysed by reverse phase HPLC. Three compounds were isolated after preparative chromatography, including a very small amount of unreacted mycalamide A triacetate (**2.18**).

Of the remaining two HPLC fractions, one was assumed to be pseudomycalamide A triacetate (**3.15**), based on certain features of the $^1H$ NMR spectrum. These included the absence of the C6 methoxyl resonance, together with the presence of the two 4=CH, two H5 and H7 resonances, although the latter had shifted considerably from their positions in the $^1H$ NMR

spectrum of mycalamide A triacetate (**2.18**) in the same manner as they had in the spectrum of pseudomycalamide A (**3.7**) compared to that of mycalamide A. However, on comparison of the $^1$H NMR spectrum of the original mixture with the $^1$H NMR spectrum of this fraction, it became apparent that substantial decomposition had occurred during purification, a property which was also characteristic of the pseudomycalamides, as described above.

The remaining HPLC fraction was also a compound related to one observed earlier. The $^1$H NMR spectrum contained signals that were similar to those observed for 5,6-dehydromethoxy mycalamide A (**3.11**), and there were two acetate signals, positioned at C17 and C18, as shown by the downfield chemical shifts of the α proton resonances[101]. The C7-OH proton resonance was also observed, coupled to H7, and being exchanged on addition of $D_2O$. A COSY spectrum was recorded to confirm the $^1$H NMR assignments (Table 3.6), but there was insufficient sample to record a $^{13}$C NMR spectrum. However, HRFABMS confirmed the molecular formula of this 5,6-dehydromethoxy mycalamide A 17,18-diacetate derivative (**3.16**).

### 3.6.5.2 PRODUCTS FROM TLC FRACTION 4

The $^1$H NMR spectrum of the fourth TLC fraction above had indicated a mixture of at least two major components, so this was also further analysed by reverse phase HPLC. Preparative HPLC yielded a small amount of the aldehyde fragment (**3.14**) above, along with another related fragment. The $^1$H NMR spectrum of this compound showed that the signals for the two C14 methyl groups were now superimposed, at δ1.09 ppm, and those for H15 and the C13 methoxyl had also shifted downfield (+0.4, +0.3 ppm, respectively), relative to those in the aldehyde fragment (Table 3.6). There was no aldehyde resonance, and only one other signal apart from those relating to the C16-C18 sidechain, a singlet at δ5.05 ppm. When this was irradiated in an NOE

experiment, the C13 methoxyl resonance was weakly enhanced. Hence this singlet was assigned to an H12 proton, and the presence of a double bond between C12 and C13 was proposed, in order to account for the chemical shift of H12 and the downfield shifts in the C13 methoxyl and C14 methyl signals, compared to data recorded for mycalamide A triacetate (**2.18**). There was evidently no proton at C11 since H12 was a singlet, so that an exocyclic double bond was required at C11. One possibility was that this was a carbonyl group, so that the compound was an α,β-unsaturated lactone (**3.17**). FTIR showed a carbonyl stretching band at about 1720 $cm^{-1}$, on the shoulder of the 1740 $cm^{-1}$ C=O acetate band, and weaker C=C stretching bands at 1665 and 1614 $cm^{-1}$ which would arise from this unsaturated lactone[96]. Further evidence was obtained from HRFABMS, which indicated a compound of molecular formula $C_{15}H_{22}O_7$, consistent with this proposed structure.

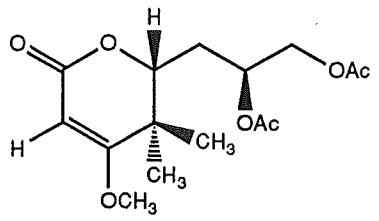


11-Lactone fragment (**3.17**)

## 3.6.6 MECHANISMS OF FORMATION

### 3.6.6.1 NEOMYCALAMIDE A TRIACETATE ISOMERS

The mechanism of formation of the neomycalamide A triacetate isomers (**3.12**, **3.13**) may include two possible pathways (Scheme 3.4). In the first pathway (Scheme 3.4a), an acid catalysed elimination of the C6 methoxyl group and H5 is proposed, in an E1 process[176] as described earlier, to give a 5,6-dehydromethoxy mycalamide A triacetate derivative. This diene could

then undergo an acid catalysed rearrangement, with elimination of H7, to give both isomers of the observed conjugated dienone. The isolation of a small amount of the diene (**3.16**), with no C7 acetate, could arise from a competing acid catalysed hydrolysis of the C7 acetate, which would trap the diene. An alternative pathway (Scheme 3.4b) is the acid catalysed rearrangement of the exocyclic double bond into the ring and then elimination of the C6 methoxyl group and H7 in an E1 process.

**Scheme 3.4** Mechanism of formation of the neomycalamide A triacetate isomers (**3.12, 3.13**) from mycalamide A triacetate (**2.18**).

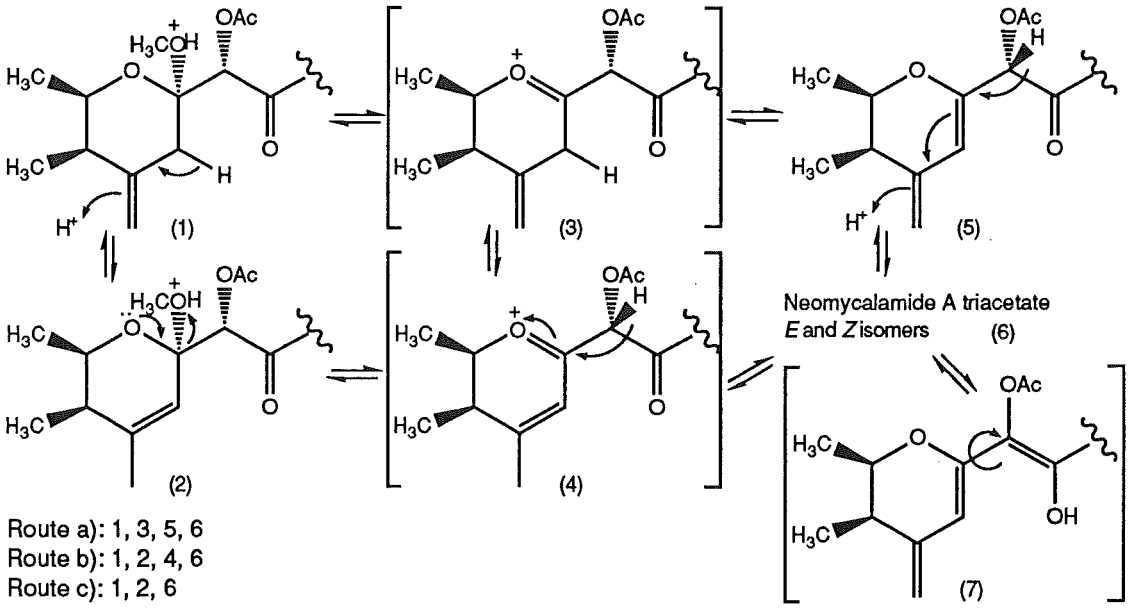


The most stable isomer of neomycalamide A triacetate was the *E* isomer (**3.13**), since there was evidence of some rearrangement of the *Z* isomer to the *E* isomer on silica gel TLC, but not the reverse. Under more forcing acidic conditions, such as in the initial experiment monitored by $^1$H NMR spectroscopy, only the *E* isomer was observed. However, under very mildly acidic conditions, and with a relatively non-polar solvent, there is some evidence that the reactions shown in Scheme 3.4b occur, but with the elimination reaction proceeding by an E2 anti mechanism[176] (Scheme 3.4c).

For example, various 7-*O*-substituted ethers, such as mycalamide B bis-TMS ether (**2.2**), and esters, such as mycalamide A 7,18-di-p-bromobenzoate (**2.12**), underwent this elimination and rearrangement in $CDCl_3$ solution, to give the *Z* isomers of the neomycalamide derivatives almost quantitatively and stereospecifically, as shown by the distinctive downfield allylic H5 resonances. $^1H$ NMR data for *Z* neomycalamide A 7,18-di-p-bromobenzoate (**3.18**) are listed in the Experimental section, with the assignments being verified by the results of a COSY experiment. Note that the *Z* isomer is the expected anti elimination product from elimination of H7 and 6-$OCH_3$ groups. In the latter example, this sample slowly, and quantitatively, rearranged to the *E* isomer (**3.19**) on standing overnight at ambient temperature (data for this isomer are also recorded in the Experimental section only). The intermediate in this rearrangement reaction could be the conjugated dienol, shown in Scheme 3.4. This would be formed by protonation of the carbonyl and rearrangement of the double bonds, and allows for free rotation about C6-C7, as required.

These neomycalamide derivatives can only be formed when the C7 hydroxyl group is substituted, as an ether or ester, since enols are not the most stable tautomer and readily convert to ketones[154]. An attempted deacetylation of the major neomycalamide A triacetate isomer (**3.13**), using potassium carbonate in aqueous methanol, gave a complex mixture of decomposition products. This was not considered further.

### 3.6.6.2 DIACETYL α,β-UNSATURATED ALDEHYDE FRAGMENT

Under acidic conditions both the C10 aza acetal and the C10-O, C12-O methylene acetal can be hydrolysed to give an aldehyde at C10 and an alcohol at C12. The mechanism for this dual hydrolysis is not shown, since there is more than one possible route, depending on which acetal is more acid stable, involving various hemiacetals and carboxonium ion intermediates, and

this standard chemistry has been indicated earlier with the conversion of mycalamide A to pseudomycalamide A (**3.7**). Note, however, that the remaining products of this hydrolysis are formaldehyde and a primary amide. The aldehyde product contains an α-proton and a β-hydroxyl, and is thus an ideal structure for an elimination reaction[176,179], which is assisted by the acidic reaction conditions and elevated temperature, to give the observed α,β-unsaturated aldehyde (**3.14**).

3.6.6.3 OTHER PRODUCTS .

The mechanism of formation of the pseudomycalamide (**3.7**, **3.8**) and 5,6-dehydromethoxy mycalamide (**3.11**) derivatives has been discussed in earlier sections. The remaining product to account for is the diacetyl α,β-unsaturated C11 lactone fragment (**3.17**). It is assumed that this unsaturated lactone is formed by an allylic oxidation on the enol form of the aldehyde (**3.14**) (having double bonds between C12-C13 and C10-C11), or some similarly conjugated derivative, in a fashion similar to the proposed formation of pederolactone (**3.6**). This follows from the known acid catalysed addition reactions of water with enol ethers, such as the one at C11, to give hemiacetals[172]. In the present case, addition of $H_2O$ across C10-C11 would give an allylic hemiacetal, which could then undergo air oxidation to give the observed lactone (**3.17**).

## 3.7 BIOLOGICAL ASSAY RESULTS FOR MYCALAMIDE A TRIACETATE DEGRADATION PRODUCTS AND CONCLUSIONS

The assay results for the compounds discussed above have been listed in Table 3.5. For the products with low sample mass (all except the *E* isomer

of neomycalamide A triacetate (**3.13**) and the starting triacetate (**2.18**)), the biological activity stated may be caused by traces of more active impurities. It is readily apparent that all these compounds were relatively inactive. The neomycalamide derivatives were potentially useful in terms of reducing the number of solution conformations of mycalamide A, but were inactive, probably due mainly to the C7-O substitution, although loss of the C6 acetal may also be a factor. The cleavage fragments isolated from the right hand portion of the molecule (**3.14, 3.17**) were also inactive, as was pederolactone (**3.6**).

The main aim of the study was to investigate the acid decomposition pathway of the mycalamides and, in particular, look at the biological activities of the fragments. From this viewpoint the study was a success, although the isolation of more fragments from the left hand portion would have been useful. It has been shown that the acid instability problems of the mycalamides arise primarily from the presence of the homoallylic C6 acetal functionality, but also from the unusual C10 acetal systems. Acid catalysed hydrolyses, eliminations, rearrangements and, probably, allylic oxidations could therefore account for the rapid decomposition of the mycalamide skeleton on contact with acids.

The earlier work of substitution and elimination reactions at the C6 acetal gave some useful structure-activity correlations which have considerably added to information reported from studies on pederin. It has also given some clear experimental guidelines if any further acid catalysed reactions of mycalamide A or its derivatives are attempted in future studies.

**Table 3.1** $^1$H NMR data[a] for compounds described in Sections **3.2-3.4.**

| | Mycalamide A | Pseudomyc.A (3.7) | Pseudomyc.B (3.8) | 6-Ethoxy myc.A (3.10) | 5,6-Dehydromethoxy myc.A (**3.11**) ($CDCl_3$) | (DMSO) |
|---|---|---|---|---|---|---|
| **H2** | 3.98 (2.7,6.6) | 4.20 (2.6,6.7) | 4.21 (2.5,6.5) | 3.99 (2.7,6.6) | 4.18 (3.1,6.5) | 4.16 (2.5,6.6) |
| **2-$CH_3$** | 1.19 (6.6) | 1.08 (6.6) | 1.09 (6.6) | 1.17 (6.5) | 1.21 (6.5) | 1.19 (6.5) |
| **H3** | 2.23 (2.7,7.0) | 2.22 (2.6,7.0) | 2.22 (2.8,7.0) | 2.23 (2.6,7.1) | 2.45 (2.6,7.0) | 2.49 (2.6,7.0) |
| **3-$CH_3$** | 0.99 (7.0) | 0.99 (7.0) | 1.00 (7.1) | 1.00 (7.1) | 1.01 (7.0) | 1.03 (7.0) |
| **4=CH*Z*** | 4.84 (m) | 4.89 (2.0) | 4.89 (2.0) | 4.83 (m) | 4.67 (m) | 4.70 (m) |
| **4=CH*E*** | 4.72 (m) | 4.77 (1.9) | 4.76 (2.0) | 4.73 (m) | 4.79 (m) | 4.80 (m) |
| **H5a** | 2.36 (m) | 2.81 (1.9,13.8) | 2.81 (2.0,13.8) | 2.38 (m) | | |
| **H5e** | 2.36 (m) | 2.17 (13.8) | 2.16 (14.0) | 2.38 (m) | 5.64 | 5.54 |
| **6-$OCH_3$** | 3.29 | | | | | |
| **H7** | 4.31 | 4.08 | 4.06 | 4.26 | 4.57 | 4.43 (5.3) |
| **7-OH** | | | | | | 6.16 (5.3) |
| **NH9** | 7.51 (9.7) | 7.59 (9.8) | 7.57 (9.1) | 7.50 (9.6) | 7.23 (9.8) | 8.46 (9.3) |
| **H10** | 5.87 (9.7) | 5.82 (9.9) | 5.67 (9.1,9.9) | 5.87 (9.7) | 5.86 (10.0) | 5.80 (9.3) |
| **10-OCH*R*** | 5.13 (6.9) | 5.15 (7.0) | 5.15 (7.0) | 5.13 (7.0) | 5.15 (6.8) | 5.27 (6.9) |
| **10-OCH*S*** | 4.87 (6.9) | 4.89 (6.9) | 4.88 (6.8) | 4.87 (7.0) | 4.88 (6.9) | 4.83 (6.9) |
| **H11** | 3.86 (6.8,9.7) | 3.93 (6.6,10.0) | 3.91 (6.7,10.0) | 3.85 (6.8,9.6) | 3.85 (6.9,10.1) | 4.10 (6.7,9.5) |
| **H12** | 4.22 (6.8,10.3) | 4.24 (6.8,10.5) | 4.23 (6.7,10.5) | 4.22 (6.7,10.2) | 4.24 (6.7,10.6) | 4.15 (6.8,8.9) |
| **H13** | 3.46 (10.3) | 3.47 (10.4) | 3.46 (10.4) | 3.46 (10.3) | 3.48 (10.6) | 3.86 (9.0) |
| **13-$OCH_3$** | 3.55 | 3.56 | 3.56 | 3.56 | 3.56 | 3.56 |
| **14-$CH_3$*R*** | 0.97 | 0.97 | 0.96 | 0.98 | 0.97 | 1.00 |
| **14-$CH_3$*S*** | 0.87 | 0.87 | 0.88 | 0.87 | 0.86 | 0.84 |
| **H15** | 3.62 (5.5,7.1) | 3.58 (m) | 3.30 (m) | 3.62 (5.5,7.0) | 3.56 (m) | ? |
| **H16** | 1.54 (m) | 1.56 (m) | 1.58 (m) | 1.56 (m) | 1.53 (m) | 1.68 (1.4,7.6,14.3) |
| **H16** | 1.54 (m) | 1.56 (m) | 1.58 (m) | 1.56 (m) | 1.53 (m) | 1.34 (m) |
| **H17** | 3.74 (m) | 3.75 (m) | 3.37 (m) | 3.74 (m) | 3.73 (m) | 3.56 (m) |
| **17-$OCH_3$** | | | 3.31 | | | |
| **H18** | 3.57 (3.5,11.3) | 3.56 (m) | 3.53 (3.9,11.4) | 3.57 (m) | 3.56 (3.5,11.3) | ? |
| **H18** | 3.38 (6.2,11.3) | 3.41 (5.6,11.4) | 3.47 (6.0,11.5) | 3.38 (6.7,11.2) | 3.37 (6.1,11.4) | ? |
| **6-OCH** | | | | 3.60 (7.0,9.0) | | |
| **6-OCH** | | | | 3.51 (7.0,9.0) | | |
| **6-$OCH_2CH_3$** | | | | 1.18 (7.0) | | |

[a]All data were recorded in $CDCl_3$ (except **3.11** in DMSO), with chemical shifts in ppm relative to $CHCl_3$, δ7.25 (coupling constants in Hz), or to $CHD_2SOCD_3$, δ2.60 ppm.

**Table 3.2** $^{13}C$ NMR data[a] for compounds described in Chapter 3.

| | Mycalamide A | Pseudomyc.A (3.7) | Pseudomyc.B (3.8) | 6-Ethoxy A (3.10) | 5,6-Dehydro-methoxy A (3.11) | Myc.A triacetate (2.18) | *E* Neomyc.A triacet.(3.13) | *Z* Neomyc.A triacet.(3.12) |
|---|---|---|---|---|---|---|---|---|
| C2 | 69.81 | 68.95 | 68.90 | 69.83 | 76.59 | 69.73 | 76.15 | ? |
| 2-$CH_3$ | 17.88 | 17.87 | 17.87 | 17.92 | 15.88 | 17.87 | 17.40 | 17.21 |
| C3 | 41.37 | 41.43 | 41.46 | 41.41 | 37.72 | 41.24 | 38.13 | 38.14 |
| 3-$CH_3$ | 12.02 | 11.75 | 11.80 | 12.07 | 13.17 | 12.04 | 10.27 | 10.31 |
| C4 | 145.65 | 146.49 | 146.63 | 145.67 | 142.90 | 145.08 | 150.77 | ? |
| 4=$CH_2$ | 110.55 | 110.41 | 110.31 | 110.47 | 108.03 | 110.85 | | |
| 4-$CH_3$ | | | | | | | 22.32 | 22.69 |
| C5 | 33.75 | 35.72 | 35.65 | 33.89 | 103.63 | 34.18 | 112.60 | 114.60 |
| C6 | 99.83 | 97.54 | 97.41 | 99.75 | 149.80 | 99.26 | 151.85 | ? |
| 6-$OCH_3$ | 48.94 | | | | | 48.60 | | |
| C7 | 72.92 | 74.89 | | 73.74 | 72.57 | 71.66 | ? | ? |
| C8 | 171.82 | 174.08 | 174.83 | 171.73 | 171.91 | 167.01 | 162.55 | ? |
| C10 | 73.74 | 73.26 | 73.53 | 73.67 | 73.59 | 73.72 | 74.09 | 73.56 |
| 10-$OCH_2$ | 86.84 | 87.03 | 86.75 | 86.83 | 87.04 | 86.53 | 86.61 | 86.68 |
| C11 | 71.26 | 71.22 | 70.47 | 71.27 | 71.51 | 69.90 | 70.75 | ? |
| C12 | 74.42 | 74.50 | 74.51 | 74.42 | 74.62 | 74.06 | 74.38 | 74.44 |
| C13 | 79.15 | 78.90 | 79.24 | 79.18 | 78.96 | 79.93 | 79.34 | 79.17 |
| 13-$OCH_3$ | 61.81 | 61.93 | 61.89 | 61.82 | 61.91 | 61.55 | 61.81 | 61.86 |
| C14 | 41.66 | 41.91 | 41.72 | 41.65 | 41.84 | 40.90 | 41.54 | ? |
| 14-$CH_3$*R* | 23.11 | 22.93 | 22.99 | 23.13 | 22.92 | 23.69 | 23.08 | 22.94 |
| 14-$CH_3$*S* | 13.49 | 13.22 | 13.18 | 13.52 | 13.17 | 14.40 | 13.58 | 13.24 |
| C15 | 78.99 | 79.45 | 75.15 | 78.97 | 78.64 | 75.53 | 74.64 | 74.53 |
| C16 | 31.99 | 31.55 | 28.76 | 32.02 | 31.79 | 30.08 | 29.60 | 29.36 |
| C17 | 71.64 | 72.21 | 78.79 | 71.52 | 71.72 | 70.01 | 69.89 | 70.28 |
| 17-$OCH_3$ | | | 56.92 | | | | | |
| C18 | 66.49 | 66.47 | 64.01 | 66.51 | 66.42 | 63.57 | 63.58 | 63.80 |
| 6-$OCH_2CH_3$ | | | | 56.71,15.17 | | | | |
| 7-$OCOCH_3$ | | | | | | 169.64,20.65 | 169.52,20.38 | ?,20.44 |
| 17-$OCOCH_3$ | | | | | | 170.60,20.80 | 170.48,20.81 | ?,20.76 |
| 18-$OCOCH_3$ | | | | | | 169.85,21.06 | 170.07,21.06 | ?,21.02 |

[a]All data were recorded in $CDCl_3$, with chemical shifts measured in ppm, relative to $CDCl_3$, δ77.01 ppm.

**Table 3.3** $^{1}H$-$^{1}H$ NOE interactions[a] for compounds in Chapter 3.

| Compound | Signal(s) Irradiated | Signals enhanced (% enhancement) |
|---|---|---|
| Pseudomyc.A | H5a | 3-$CH_3$(1), H5e(14), H7(2) |
| (**3.7**) | H5e (H3) | H2(2)[b], 3-$CH_3$(0.5)[b], 4=CH*Z*(2)[b], 4=CH*E*(4), H5a(16), H7(2) |
| | H7 | H5e(1) |
| Pseudomyc.B | H5a | 3-$CH_3$(1), H5e(21), H7(2) |
| (**3.8**) | H5e | 4=CH*E*(6), H5a(25), H7 (4) |
| | H7 | H5a (1), H5e(2) |
| 6-Ethoxy myc.A | H2 | 2-$CH_3$(1), H3(3), H6u(1)[c] |
| (**3.10**) | H7 (H12) | $H_2$5(0.8), H6d(2)[c], NH(2), H11(2)[b], 14-$CH_3$*S*(0.4)[b] |
| 5,6-Dehydromethoxy | 4=CH*Z* | H3(3), 3-$CH_3$(0.6), 4=CH*E*(14) |
| myc.A (**3.11**) | 4=CH*E* | 4=CH*Z*(14), H5(6) |
| | H5 | 4=CH*E*(4), H7(3) |
| | H7 | H5(4) |
| *E* Neomyc.A triacetate | H2 (H18d[c]) | 2-$CH_3$(2), H3(5), H5(0.8), NH(0.6), H17(1)[b], H18u(8)[b,c] |
| (**3.13**) | 2-$CH_3$ (H16u[c]) | H2(8), H3(3), 3-$CH_3$(2), NH(2), H17(0.7)[b] |
| | 4-$CH_3$ | H3(3), 3-$CH_3$(0.8), H5(10) |
| | H5 | 4-$CH_3$(1), 7-OCO$CH_3$(0.2) |
| | 7-OCO$CH_3$ | H5(2) |
| | NH | H2(1), 2-$CH_3$(0.5), H11(8) |
| 10-Aldehyde fragment | H10 | H12(6) |
| (**3.14**) | H12 | H10(12), H13(3), 13-O$CH_3$(1) |
| | H13 | H12(1), 14-$CH_3$*R*(1), H15(2) |
| | H15 | H13(1), 14-$CH_3$*R*(0.5) |

[a]All data were recorded in $CDCl_3$, except for compound **3.8**, where the solvent was $CD_2Cl_2$
[b]Enhancement interpreted as being due to the irradiation of an overlapping resonance
[c]u and d have been used to designate the upfield and downfield resonances of a geminal pair

**Table 3.4** $^{2}J_{CH}$ and $^{3}J_{CH}$ HMBC correlations[a] for compounds in Chapter 3.

| Compound | Proton | Carbon signal correlated (chemical shift[b]) |
|---|---|---|
| *E* Neomyc.A triacetate | 2-$CH_3$ | C2, C3 |
| (**3.13**) | 3-$CH_3$ | C2, C3, C4 (δ150.75) |
| | 4-$CH_3$ | C3, C4, C5 |
| | H5 | C3, 4-$CH_3$, C6 or C7 (δ151.85) |
| | 7-$OCOCH_3$ | 7-OCO |
| | 10-OCH*R* | C10, C12 |
| | 10-OCH*S* | C10, C12 |
| | H11 | C12, C13 |
| | H12 | C10, 10-$OCH_2$ |
| | H13 | C12, 13-$OCH_3$, C14, 14-$CH_3$*S* |
| | 13-$OCH_3$ | C13 |
| | 14-$CH_3$*R* | C13, C14, 14-$CH_3$*S*, C15 |
| | 14-$CH_3$*S* | C13, C14, 14-$CH_3$*R*, C15 |
| | H15 | C16 |
| 5,6-Dehydromethoxy myc.A | 2-$CH_3$ | C2, C3 |
| (**3.11**) | 3-$CH_3$ | C2, C4 (δ142.9) |
| | 4=$CH_2$ | C3, C5 |
| | H7 | C6 (δ149.8), C8 |
| | 10-OCH*R* | C10, C12 |
| | 10-OCH*S* | C10, C12 |
| | H12 | C10 |
| | 13-$OCH_3$ | C13 |
| | 14-$CH_3$*R* | C13, C14, 14-$CH_3$*S*, C15 |
| | 14-$CH_3$*S* | C13, C14, 14-$CH_3$*R*, C15 |

[a]All data were recorded in $CDCl_3$ (chemical shifts in ppm relative to $CDCl_3$, δ77.01)

**Table 3.5** Biological assay results for compounds in Chapter 3

| Compound | P388 $IC_{50}$[a] | Antiviral Results[b] (ng/disk) | | | | | | | |
|---|---|---|---|---|---|---|---|---|---|
| Mycalamide A | 0.5 | WW | WW | +* | 5 | + | + | +* | 2 |
| Pederolactone (**3.6**) | 120 | WW | +++ | +* | 1000 | ++ | +++ | +* | 500 |
| Pseudomycalamide A (**3.7**) | 9 | WW | WW | +* | 100 | +++ | +++ | +* | 50 |
| Pseudomycalamide B (**3.8**) | 4 | WW | +++ | +* | 50 | + | + | +* | 20 |
| 6-Ethoxy mycalamide A (**3.10**) | 1 | WW | WW | +* | 20 | +++ | +++ | +* | 10 |
| 5,6-Dehydromethoxy A (**3.11**) | 120 | WW | WW | +* | 5000 | - | - | - | 2000 |
| Mycalamide A triacetate (**2.18**) | 45 | WW | WW | +* | 500 | +++ | +++ | +* | 200 |
| *Z* Neo A triacetate (**3.12**) | 220 | WW | WW | +* | 20000 | ++ | ++ | +* | 10000 |
| *E* Neo A triacetate (**3.13**) | 1300 | +++ | ++ | +* | 20000 | - | - | - | 10000 |
| 10-Aldehyde fragment (**3.14**) | 500 | WW | +++ | +* | 10000 | - | - | - | 5000 |
| 5,6-Dehyd.A 17,18-diac.(**3.16**) | 270 | WW | WW | +* | 10000 | - | - | - | 5000 |
| 11-Lactone fragment (**3.17**) | 125 | WW | ++ | +* | 1000 | + | + | +* | 500 |
| *E* Neo A 7,18-di-p-brBz.(**3.19**) | 600 | WW | WW | +* | 2000 | - | - | - | 500 |

[a] In ng/ml. The derivatives are estimated to be better than 95% pure, having been subjected to at least two steps of chromatographic purification in most cases.

[b] -,+,++,+++,WW=antiviral zone size. Results are listed in the order of *Herpes simplex virus*, *Polio virus*, cytotoxicity, loaded sample mass.

Table 3.6 $^1$H NMR data[a] for compounds described in Section 3.6.

| | Mycalamide A triacetate (2,18) | *E* Neomyc.A triacetate (3,13) | *Z* Neomyc.A triacetate (3,12) | 5,6-Dehydro. A 17,18-diacet. (3,16) | 10-Aldehyde fragment (3,14) | 11-Lactone fragment (3,17) |
|---|---|---|---|---|---|---|
| H2 | 3.99 (2.8,6.6) | 4.30 (2.8,6.5) | 4.14 (2.8,6.6) | 4.19 (2.8,6.5) | | |
| 2-$CH_3$ | 1.20 (6.6) | 1.42 (6.5) | 1.23 (6.5) | 1.20 (6.5) | | |
| H3 | 2.25 (2.7,7.0) | 2.07 (2.3,6.8) | 2.01 (m) | 2.44 (2.7,6.9) | | |
| 3-$CH_3$ | 1.03 (7.1) | 1.02 (7.1) | 0.96 (7.1) | 1.00 (7.1) | | |
| 4=CH*Z* | 4.87 (1.8) | | | 4.76 (m) | | |
| 4=CH*E* | 4.76 (1.9) | | | 4.64 (m) | | |
| 4-$CH_3$ | | 1.92 (1.4) | 1.93 (1.4) | | | |
| H5 | | 6.01 (1.5) | 7.35 (1.4) | 5.61 | | |
| H5a | 2.45 (1.8,14.4) | | | | | |
| H5e | 2.38 (14.4) | | | | | |
| 6-$OCH_3$ | 3.18 | | | | | |
| H7/7-OH | 5.47 | | | 4.56/4.29 (4.4) | | |
| NH9 | 7.32 (9.4) | 8.10 (8.6) | 6.54 (9.0) | ? | | |
| H10 | 5.76 (9.0) | 5.84 (8.7,9.8) | 5.82 (9.9,9.9) | 5.76 (9.7) | 9.16 | |
| 10-OCH*R* | 5.06 (6.9) | 5.14 (6.8) | 5.16 (6.8) | 5.13 (7.0) | | |
| 10-OCH*S* | 4.86 (7.0) | 4.85 (6.9) | 4.85 (7.0) | 4.85 (7.0) | | |
| H11 | 3.79 (6.0,8.7) | 3.86 (6.5,9.8) | 3.92 (6.7,9.9) | 3.83 (6.6,9.6) | | |
| H12 | 4.10 (6.0,9.4) | 4.19 (6.6,10.2) | 4.19 (6.7,10.3) | 4.20 (6.7,10.5) | 5.84 (2.6) | 5.05 |
| H13 | 3.36 (9.4) | 3.47 (10.2) | 3.53 (10.4) | 3.46 (10.4) | 3.61 (2.6) | |
| 13-$OCH_3$ | 3.52 | 3.55 | 3.56 | 3.55 | 3.45 | 3.71 |
| 14-$CH_3$*R* | 1.01 | 0.95 | 0.94 | 0.95 | 0.99 | 1.09 |
| 14-$CH_3$*S* | 0.86 | 0.87 | 0.85 | 0.85 | 0.85 | 1.09 |
| H15 | 3.45 (2.4,9.8) | 3.39 (2.0,10.4) | 3.36 (1.9,10.2) | 3.36 (2.2,9.8) | 3.83 (2.5,9.7) | 4.18 (2.5,9.6) |
| H16 | 1.77 (2.5,9.1,14.5) | 1.75 (2.2,9.6,13.9) | 1.77 (2.0,9.0,14.5) | 1.79 (m) | 2.02 (6.6,9.8,14.8) | 2.02 (m) |
| H16 | 1.62 (4.5,9.5,14.5) | 1.64 (3.9,10.3,13.9) | 1.57 (m) | 1.53 (m) | 1.91 (2.5,5.6,14.9) | 1.93 (m) |
| H17 | 4.98 (m) | 5.07 (m) | 5.03 (m) | 5.04 (m) | 5.31 (m) | 5.34 (m) |
| H18 | 4.27 (2.7,12.4) | 4.26 (2.5,12.4) | 4.23 (3.4,12.2) | 4.10 (m) | 4.27 (3.3,12.1) | 4.31 (3.2,12.3) |
| H18 | 4.14 (5.2,12.4) | 4.09 (5.5,12.7) | 4.01 (5.6,12.3) | 4.10 (m) | 4.18 (6.1,12.2) | 4.22 (5.8,12.4) |
| 7-$OCOCH_3$ | 2.20 | 2.24 | 2.21 | | | |
| 17/18-$OCOCH_3$ | 2.05,2.00 | 1.99,1.98 | 2.01,1.99 | 2.05,2.03 | 2.10,2.06 | 2.09,2.06 |

[a]All data were recorded in $CDCl_3$, with chemical shifts in ppm relative to $CHCl_3$, δ7.25 (coupling constants in Hz)

# CHAPTER 4
# HYDROGENATION AND OTHER ADDITIONS TO THE DOUBLE BOND OF MYCALAMIDES A & B AND DERIVATIVES

## 4.1 INTRODUCTION

The hydrogenation of pederin over Adams catalyst and over palladium on charcoal was reported as part of an early study investigating the structure of pederin[27,94]. It was found that crystallisation of the product obtained from the hydrogenation of pederin over Adams catalyst yielded only one isomer of dihydro pederin (**4.1**), as determined by $^1$H NMR spectroscopy, melting point and chromatography[94]. However, a complete analysis of the $^1$H NMR spectral data was not reported, so that the stereochemistry at C4 was undefined. Also no NMR data were given for dihydro pseudopederin (**4.2**), prepared from pseudopederin (**3.5**). The hydrogenation of pederin over palladium on charcoal gave about equal amounts of dihydro pederin (**4.1**) and dihydro deoxy pseudopederin (**4.3**), the latter being obtained by hydrogenolysis of the acetal after a rearrangement of the exocyclic double bond[94]. Again only one isomer was reported, although a complete analysis of the $^1$H NMR spectral data was not performed.

The biological activity data reported for these compounds[40], which measured their *in vitro* activity against HeLa tumour cell cultures, showed that dihydro pederin (**4.1**) and dihydro pseudopederin (**4.2**) were less cytotoxic than the parent compounds. This result was interpreted as being of considerable interest, since the 'high antimitotic activity' appeared to be associated with 'negligible vesicatory effects'[40,180]. However, the dilution series used to establish the relative activities used steps of ten in

concentration, so that this result needed further investigation. Dihydro deoxy pseudopederin (**4.3**) was also reported as showing antimitotic activity[181], although this was not quantified.

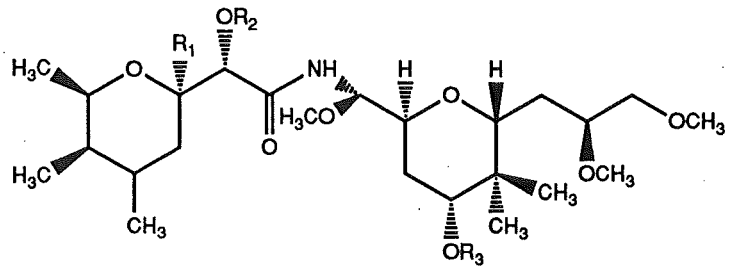


$R_1$=$OCH_3$, $R_2$=$R_3$=H: Dihydro pederin (**4.1**)
$R_1$=OH, $R_2$=$R_3$=H: Dihydro pseudopederin (**4.2**)
$R_1$=H, $R_2$=$R_3$=H: Dihydro deoxy pseudopederin (**4.3**)
$R_1$=$OCH_3$, $R_2$=$R_3$=Ac: Dihydro pederin diacetate (**4.8**)
$R_1$=H, $R_2$=$R_3$=Ac: Dihydro deoxy pseudopederin diacetate (**4.14**)

These results for dihydro pederin (**4.1**) provided a good basis for a similar investigation into the hydrogenation of the mycalamides, which would aim to solve the stereochemistry of the products and determine quantitative structure-activity relationships. It was also hoped that the apparently different cytotoxicity of dihydro pederin would provide a useful lead for synthesising mycalamide derivatives which would be more selective in their action[2]. The work in this chapter describes the results of this study and an extension to other double bond addition reactions, such as epoxidation.

## 4.2 HYDROGENATION OF MYCALAMIDES A AND B OVER ADAMS CATALYST

### 4.2.1 PREPARATION OF DIHYDRO MYCALAMIDE A AND B ISOMERS

Mycalamide A reacted readily with hydrogen, in the presence of Adams catalyst ($PtO_2$), to give a mixture of two dihydro mycalamide A isomers (**4.4**,

**4.5**), in a ratio of about 3:2 by $^1H$ NMR spectroscopy and analytical HPLC (no order intended). This was repeated using mycalamide B as the substrate, to give two isomers of dihydro mycalamide B (**4.6**, **4.7**). Mass spectroscopy of the products confirmed the addition of $H_2$ to mycalamides A and B. The isomers obtained from these reactions were not fully resolved by either reverse phase HPLC or silica gel TLC. However, by collecting three fractions from preparative HPLC, corresponding to cuts on either side of the observed double peak, and recycling the central mixture, it was possible to obtain fractions which were 85-90% rich in one isomer by $^1H$ NMR spectroscopy. These fractions were then subjected to an extensive investigation by NMR spectroscopy, to assign their $^1H$ and $^{13}C$ NMR spectra and to determine their stereochemistries and solution conformations.

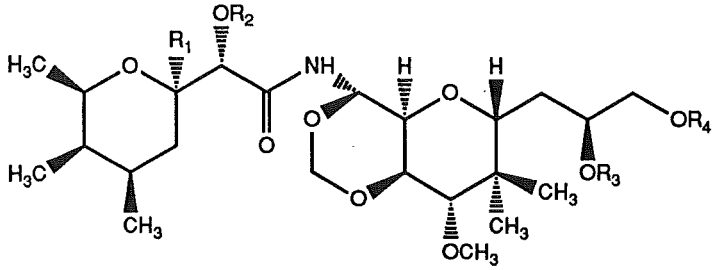


$R_1$=$OCH_3$, $R_2$=$R_3$=$R_4$=H: 4α-Dihydro mycalamide A (**4.4**)
$R_1$=$OCH_3$, $R_2$=$R_4$=H, $R_3$=$CH_3$: 4α-Dihydro mycalamide B (**4.6**)
$R_1$=OH, $R_2$=$R_3$=$R_4$=H: 4α-Dihydro pseudomycalamide A (**4.10**)
$R_1$=H, $R_2$=$R_3$=$R_4$=H: 4α-Dihydro, 6-deoxy pseudomycalamide A (**4.13**)
$R_1$=H, $R_2$=$R_3$=$R_4$=Ac: 4α-Dihydro, 6-deoxy pseudomyc.A triacetate (**4.15**)

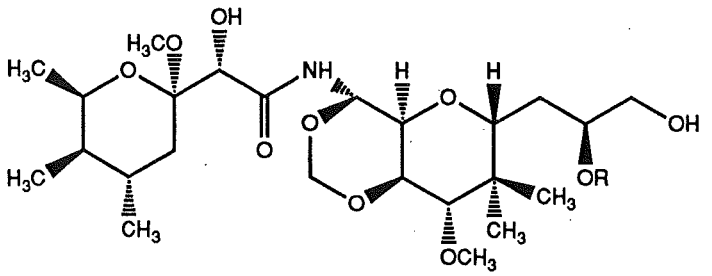


R=H: 4β-Dihydro mycalamide A (**4.5**)
R=$CH_3$: 4β-Dihydro mycalamide B (**4.7**)

### 4.2.2 $^1$H NMR SPECTRAL ASSIGNMENTS, STEREOCHEMISTRY AND SOLUTION CONFORMATION OF THE MAJOR DIHYDRO ISOMER

The $^1$H NMR spectrum of the major dihydro mycalamide A isomer showed the loss of the signals due to the C4 exocyclic methylene protons and the appearance of a third methyl doublet, consistent with hydrogenation at C4. There were large shifts in the O1-C6 ring proton resonances, as expected, and the $^1$H NMR spectrum was assigned with the aid of COSY and NOE experiments, as detailed below, to give the data in Table 4.1.

There were three methyl doublets in the $^1$H NMR spectrum, at δ1.17 (6.6), 1.16 (7.1) and 0.93 (7.1) ppm (coupling constants in Hz). The signal at δ1.17 ppm was almost certainly due to the C2 methyl group since it had the smaller coupling constant, being adjacent to oxygen[102]. The COSY spectrum confirmed this assignment, since this signal showed a correlation to a doublet of quartets at δ4.11 ppm, which was assignable to H2. The methyl doublet at δ1.16 ppm was coupled to a multiplet at δ1.70 ppm, while the remaining doublet, at δ0.93 ppm, was coupled to a multiplet at δ1.33 ppm. There were also two doublet of doublets, at δ1.76 (5.6, 13.8) and δ1.53 (2.9, 14.0) ppm, which could be assigned to the two geminal H5 protons ($D_2O$ was added to exchange out the $H_2O$ signal at δ1.5-1.6 ppm).

These signals were further assigned by an analysis of the results of NOE experiments, performed on both the mycalamide A and B isomers (Table 4.2). These results are summarised as arrows in Figure 4.1a. Irradiation of the H2 resonance gave a strong enhancement of the multiplet at δ1.33 ppm, the methyl doublet at δ1.16 ppm, the C2 methyl resonance and the C6 methoxyl resonance. The observed NOE interaction between H2 and the C6 methoxyl protons suggested that the preferred solution conformation of the O1-C6 tetrahydropyran ring was still a chair conformation, as in mycalamides A and B, with the C6 methoxyl group axial, as favoured by the anomeric

effect[105,106], and the C7 sidechain equatorial as favoured by steric factors. The observed coupling constant between H2 and H3 was almost the same as in mycalamides A and B, so that this assumption appeared to be reasonable, and is further confirmed below. Therefore the H2 and C3 methyl substituents were in an anti relationship, so that the methyl doublet at δ1.16 ppm, which was enhanced by irradiation of H2, was required to be an axial C4 methyl group. Therefore the multiplet at δ1.33 ppm was H3, and the remaining methyl doublet, at δ0.93, must be assigned to the C3 methyl group. Irradiation of the latter enhanced the H3 resonance, the multiplet at δ1.70 ppm (H4) and the signal at δ1.76 ppm, which was therefore assignable to the axial H5 proton, and this could only occur if the O1-C6 ring was in a chair conformation. Other NOE interactions (Table 4.2) supported these assignments, the stereochemistry at C4, and the proposed O1-C6 ring conformation. The complete $^1$H NMR data for both 4β-dihydro mycalamides A and B (**4.5**, **4.7**) have been listed in Table 4.1. (Throughout this chapter, the nomenclature α and β follows the IUPAC recommendations for the naming of substituents in steroids[182], where the hydrogen (or oxygen for epoxides) is the new ring substituent at C4).

**Figure 4.1** $^1$H-$^1$H NOE interactions and solution conformations for the O1-C6 ring of the C4-dihydro mycalamide A and B epimers (**4.4**-**4.7**).

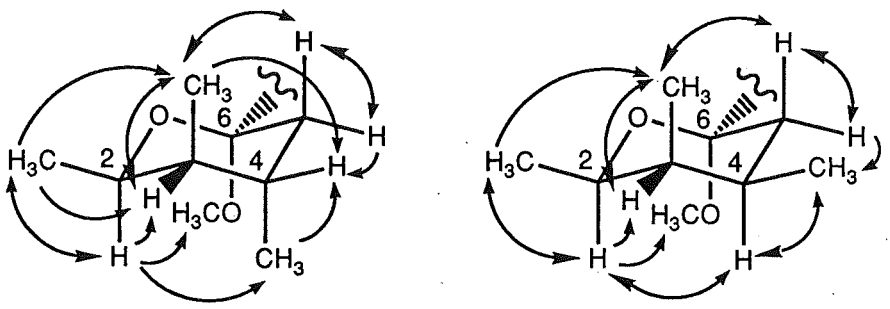


a) Major isomer (4β)

b) Minor isomer (4α)

The C2-C5 vicinal proton-proton coupling constants (Table 4.1) were well within the expected ranges for the stereochemistry and ring conformation stated above. In particular, the magnitudes of the H3-H4, H4-H5e and H4-H5a coupling constants, 2.7, 2.9, and 5.6 Hz, respectively, were in accordance with the equatorial-equatorial relationships for the protons in the first two cases, and the equatorial-axial relationship of the protons for the latter, as predicted by the Karplus equation[98,102].

### 4.2.2 $^1$H NMR SPECTRAL ASSIGNMENTS, STEREOCHEMISTRY AND SOLUTION CONFORMATION OF THE MINOR DIHYDRO ISOMER

The $^1$H NMR spectrum of the minor dihydro mycalamide A isomer (**4.4**) had the same overall features as that of the major isomer, but with substantial chemical shift differences for some resonances. There were three methyl doublets, at δ1.18 (6.6), 0.88 (7.0) and 0.73 (7.1) ppm, which were correlated to signals at δ3.97 (2.3, 6.6), 2.14 and 1.47 ppm, respectively, in a COSY spectrum. Of these methyl doublets, the first could be assigned to the C2 methyl group, but the remaining two could not be distinguished on this evidence. The H5 proton resonances, at δ1.23 and 1.62 ppm were distinctive by their large geminal coupling constant and the resulting strong correlation in the COSY spectrum. The upfield one was coupled to the multiplet at δ2.14 ppm with a coupling constant of around 13 Hz, which could only be satisfied if the protons were in an anti relationship[98]. This geometry required that the upfield H5 resonance be assigned to the axial H5 proton and that the multiplet at δ2.14 be assigned to an axial H4 proton. This, combined with the COSY data above, then enabled direct assignment of the signals for the remaining ring substituents, and hence of the complete $^1$H NMR data for both 4α-dihydro mycalamides A and B (**4.4**, **4.6**) (Table 4.1).

Various NOE experiments were performed to check the $^1H$ NMR assignments, the designated stereochemistry, and the solution conformation of the O1-C6 ring, and the results of these (Table 4.2) have been summarised as arrows in Figure 4.1b. In particular, observed NOE interactions between the 1,3-diaxial substituents, H2 and H4, H2 and 6-$OCH_3$, and 3-$CH_3$ and H5a, confirmed the solution conformation and the stereochemistry at C4. The other vicinal coupling constants, H3-H4 and H4-H5, were both about 3.9 Hz, which is typical for an axial-equatorial relationship of the protons in a 6-membered ring[98].

There were no major differences between the $^1H$ NMR data for the mycalamide A and mycalamide B compounds, except for the C16-C18 sidechain resonances, as expected. However, there were significant chemical shift differences noted on comparing data for the two isomers, particularly for H4, 4-$CH_3$ and H5a, with smaller differences in data for the remaining O1-C6 ring and substituent protons. This is consistent with the difference in stereochemistry at C4, and different shielding and deshielding effects[98,123]. In particular, the signals for axial substituents at C4 were deshielded by the presence of the axial C6 methoxyl group, as was the H2 resonance by an axial methyl group at C4, due to a combination of steric and anisotropic effects. Also the C3 methyl resonance was slightly shielded by an equatorial C4 methyl group, an effect which has been noted in substituted cyclohexane systems[123].

### 4.2.3 $^{13}C$ NMR ASSIGNMENTS FOR THE DIHYDRO MYCALAMIDE A AND B ISOMERS

$^{13}C$ NMR spectra were recorded for all four compounds. An HMQC experiment was performed on both the dihydro mycalamide B isomers (**4.6**, **4.7**), and an HMBC experiment was performed on the major one (**4.7**), to

enable unambiguous assignments of the $^{13}C$ NMR data to be obtained. The HMBC experiment was required to clearly distinguish the C4, C5 and C16 resonances, since the proton signals were overlapping. The strong HMBC correlations observed between the C4 methyl proton resonance and the C4 and C5 carbon signals, and between the C3 methyl resonance and the C2 and C4 signals (Table 4.3) were useful for these assignments. The HMQC correlations to the C3, C4 and C16 signals were also weak for the minor isomer (**4.6**). However, the C5 resonance was clearly located and the C16 resonance could be assigned on the basis of its chemical shift. The only remaining ambiguity was then in the assignment of the C3 and C4 resonances, which were given the values closest to those in the major isomer (**4.7**), since it was reasonably expected that these particular ring carbons would not change in chemical shift by more than 4 ppm with an epimerisation at C4. The $^{13}C$ NMR data for 4α- and 4β-dihydro mycalamide A (**4.4, 4.5**) were then assigned by comparison with the dihydro mycalamide B results (Table 4.4).

On comparing the $^{13}C$ NMR data for the two dihydro isomers, it was apparent that the largest chemical shift differences occurred for C2 and the C3 methyl group. The observed shielding of the C3 methyl carbon resonances in the two 4α isomers (**4.4, 4.6**), due to the presence of the new equatorial C4 methyl group, and the shielding of the C2 (and C6) resonances in the 4β isomers (**4.5, 4.7**), due to the presence of the new axial C4 methyl group, is ascribed to the steric compression of a gauche interaction[117]. This effect is well documented for substituted cyclohexanes[120] and tetrahydropyrans[119].

## 4.2.4 STEREOSELECTIVITY IN THE HYDROGENATION OF MYCALAMIDES A AND B AND PEDERIN

The hydrogenation of mycalamides A and B over Adams catalyst gave an approximately 3:2 ratio of the two isomers, and favoured the 4β isomer, although this may not necessarily be preferred thermodynamically. The mechanism of this heterogeneous catalytic hydrogenation reaction will be discussed in detail later in this chapter. However, it is well known[183] that the addition of hydrogen to double bonds is *cis*, so that the stereochemistry of the major isomer (**4.4, 4.6**) implies that an attack of hydrogen from above the face of the double bond is slightly favoured over an attack from below, as shown in Figure 4.2. Note that both faces would have some steric hindrance, with the top *re* face having the adjacent axial C3 methyl group, and the bottom *si* face having the axial C6 methoxyl group nearby. The chair conformation of the O1-C6 tetrahydropyran ring, which has the exocyclic double bond in a pseudo-equatorial orientation, may allow slightly easier access to the top face, although this may also be influenced by the conformations of the rest of the molecule, especially the C7 sidechain.

**Figure 4.2** The approach of reagents in additions to the exocyclic double bond of mycalamides A and B.

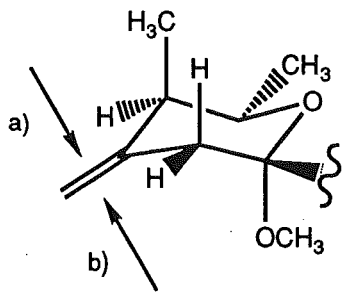


Pederin was hydrogenated under similar experimental conditions, but apparently gave only one isomer[94]. The partial $^1$H NMR data reported for dihydro pederin (**4.1**) were recorded in $d_6$-benzene, which is known to cause

unusual chemical shift effects[98,123]. However, partial $^1$H NMR data were also reported for dihydro pederin diacetate (**4.8**) in $d_6$-acetone[94], which could be directly compared with data for pederin diacetate (**4.9**) in the same solvent. Note that the reported data for pederin in $d_6$-acetone did not differ considerably from the data recorded in $CDCl_3$ (Chapter 1), so that solvent effects could reasonably be ignored. Similarly acetylation had little effect on data for the O1-C6 ring and, in particular, data for the C2 and C3 methyl resonances in pederin diacetate (**4.9**), δ1.15 (6.5) and 0.97 (7.0) ppm, were similar to data for these resonances in mycalamides A and B in $CDCl_3$. Therefore a comparison of such data for compound **4.8** with those recorded for the dihydro mycalamide derivatives could enable the stereochemistry at C4 of dihydro pederin to be determined.

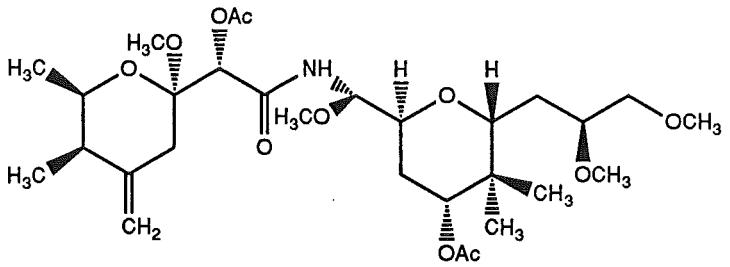


Pederin diacetate (**4.9**)

The three methyl resonances in dihydro pederin diacetate (**4.8**) were observed at δ1.12 (6.5), 0.88 (7.0), and 0.69 (7.0) ppm. The chemical shifts of these methyl groups in dihydro pederin diacetate (**4.8**) were very close to those recorded for 4α-dihydro mycalamides A and B (**4.4**, **4.6**), and could not reasonably arise from a 4β isomer, since this would have substantially less shielded signals for both the the C3 and C4 methyl groups[123], as described above. Therefore the major product from the hydrogenation of pederin with Adams catalyst was probably the 4α isomer, a point which will be referred to in a discussion of the biological assay data in a later section. It is possible that this difference in stereoselectivity occurred because of some longer range

effects associated with the different solution conformations and substituents in pederin compared with the mycalamides, or because of some variation in the exact experimental conditions[183-185].

## 4.3 HYDROLYSIS OF DIHYDRO MYCALAMIDES A AND B

The above NMR spectroscopy experiments on the dihydro mycalamide isomers were performed in $CDCl_3$ with added pyridine and under these conditions the compounds were quite stable. However, in the absence of pyridine, samples of both dihydro mycalamide isomers in $CDCl_3$ solution changed within a few minutes at room temperature, to give new derivatives almost quantitatively. Characteristics of the $^1H$ NMR spectra of the products included the loss of the C6 methoxyl signal, and chemical shift changes in the signals assigned to the H2, 2-$CH_3$, two H5 and H7 protons. There were no new signals, therefore the most likely explanation was that the C6 acetal had been hydrolysed to a hemiacetal under these slightly acidic conditions[139]. HRFABMS confirmed that this was so, and the ready loss of $H_2O$ from the parent ion was also observed in the DCI and DEI mass spectra. Thus the products were isomers of dihydro pseudomycalamide A or B, but only the mycalamide A derivatives (**4.10**, **4.11**) will be described here.

The $^1H$ NMR spectrum of 4α-dihydro pseudomycalamide A (**4.10**) was assigned by comparison with the corresponding data for 4α-dihydro mycalamide A (**4.4**) and by using the results of COSY and selective proton decoupling experiments (Table 4.1). There were shifts observed in the signals assigned to H2 (+0.2), 2-$CH_3$ (-0.1), H4 (+0.1), H5a (+0.4), H5e (-0.2), and H7 (-0.2), which were very similar to those observed on comparison of data for pseudomycalamide A (**3.7**) with data for mycalamide A. The $^{13}C$ NMR spectrum was also directly assignable by noting the shifts in the $^{13}C$ signals

between mycalamide A and pseudomycalamide A (**3.7**) and applying these to the data for 4α-dihydro mycalamide A (**4.4**) (Table 4.4).

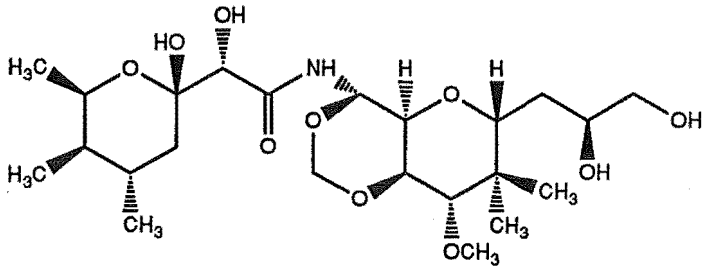


4β-Dihydro 6*S* pseudomycalamide A (**4.11**)

However, the $^{1}H$ NMR spectrum of '4β-dihydro pseudomycalamide A' (**4.11**) was not interpretable in the same way, since the chemical shift differences between these data and those recorded for 4β-dihydro mycalamide A (**4.5**) were quite different from those found above. The spectrum was also less clean, with at least one minor component being evident. The $^{1}H$ NMR spectral data were assigned by using the results of COSY and selective proton decoupling experiments (Table 4.1). These results showed that the H2 and 2-$CH_3$ resonances had hardly shifted with this C6 hydrolysis, whereas other signals, H3 (+0.1), H4 (+0.2), 4-$CH_3$ (-0.1), H7 (+0.2) and NH (-0.2), displayed unusual shifts. Similarly, those signals in the $^{13}C$ NMR spectrum which related to the left hand portion of the molecule (C2-C8) were also of quite different in their chemical shifts to those in the parent compound (**4.5**), so that these data could not be directly assigned.

Two possibilities exist to explain these observations. Firstly, the conformation of the O1-C6 ring could have changed, for example, from a chair to a boat conformation. However, this would probably significantly modify the H2-H3 coupling constant[102], which was not observed, and such alternate conformations would also be expected to be of higher energy[106]. Furthermore, the parent 4β-dihydro mycalamide A derivative (**4.5**) existed in the usual chair conformation, so that reducing the size of the C6 axial

substituent should make this conformation more favourable. Finally, this possibility would not explain the shifts in all the proton and carbon resonances, as listed above. A second possibility is that there had been an *inversion* of configuration at C6 on hydrolysis of the acetal. Note that in the chair conformation of the O1-C6 tetrahydropyran ring of 4β-dihydro mycalamide A (**4.5**) there are three axial substituents. If inversion had occurred at C6, and the hydrolysed product were in the opposite chair conformation, then there would be only two axial substituents to this ring, one being the C6 hydroxyl group, as favoured by the anomeric effect[105]. This would place most substituents in a different environment (compare Figure 3.4) and thus better explain the observed chemical shift differences.

The mechanism for the hydrolysis of the C6 acetal was discussed in Chapter 3. The mechanism for the formation of the hydrolysed C6 epimer may involve either a rearrangement of the hemiacetal[106], as discussed in Section 3.3.5, or the occurrence of some inversion in the hydrolysis mechanism itself, since the reversibility of such reactions cause the more thermodynamically stable product to be formed. Neither compound was stable to long term storage and both contained small amounts of non-hydrolysed dihydro mycalamide A, so that the biological assay results for these derivatives, described in a later section, are unreliable. Therefore a full NMR spectroscopic investigation on these compounds, to complete assignments of the $^{1}H$ and $^{13}C$ NMR spectra and to determine the solution conformations, did not appear to be warranted.

However, it is useful to note that removal of the double bond by hydrogenation does not appear to make mycalamides A and B significantly more acid stable. This is shown by the fact that the hydrolysis of the C6 acetal in the dihydro derivatives appeared to be more facile than in mycalamides A and B, which required the use of p-toluene sulphonic acid in a two-phase

hydrolysis system (Chapter 3). It is possible that this is partly caused by the presence of new steric interactions across the tetrahydropyran ring system between axial C4 sustituents and the C6 oxygen, which are absent in mycalamides A and B. However, the extreme ease of hydrolysis of glycosides[170], and other similar ring acetals, is well known[186], since this property is the basis for the use of tetrahydrofuranyl (THF) and tetrahydropyranyl (THP) ethers as protecting groups for hydroxyl functionalities[78,110,187].

## 4.4 HYDROGENATION OF MYCALAMIDE A OVER PALLADIUM ON CARBON CATALYST

### 4.4.1 PREPARATION AND PURIFICATION OF PRODUCTS

The aim of this study was to prepare and characterise a C6 reduction product analogous to compound **4.3**, derived from pederin, and then to determine its biological activity. Although there were alternative methods for reducing such acetals to catalytic hydrogenation, these generally involved acidic conditions[188-190], and did not seem to be very selective or high-yielding. Thus a reaction similar to that reported for pederin[27,94] was performed on mycalamide A, using 10% palladium on carbon as the catalyst for an hydrogenation reaction. Reverse phase HPLC of the crude reaction product showed that at least five components were present, including the two dihydro mycalamide A isomers (**4.4**, **4.5**), a small amount of unreacted mycalamide A, and two new components. Preparative HPLC thus gave six fractions, including three containing various mixtures of the dihydro mycalamide A isomers and one which was unreacted mycalamide A by $^1$H NMR spectroscopy. Of the remaining fractions, numbers 1 and 3, fraction 1 was quite pure, but fraction 3 was a mixture with one dominant component

and a minor amount of mycalamide A. The major compounds in these two fractions were new derivatives and the structure determinations of these are outlined below.

### 4.4.2 STRUCTURE OF THE COMPOUND IN HPLC FRACTION 1

A HRFABMS measurement on this fraction indicated that the compound had the same molecular formula as mycalamide A. The $^1$H NMR spectrum showed the loss of the signals assigned to both the exocyclic methylene system and also either H2 or H3, since only one of the methyl groups was a clean doublet (the other was a broad singlet). There was also a new, broad methyl singlet at about δ1.6 ppm. A COSY spectrum showed that the methyl doublet was coupled to a multiplet at δ4.19 ppm (6.6 Hz), suggesting that this was due to the methyl group at C2. These results could therefore only be satisfied if there was a double bond between C3 and C4, as in Figure 4.3, so that the compound was $\Delta^3$ mycalamide A (**4.12**). Note that the conformation of the O1-C6 ring in this derivative is restricted, since C2-C5 must be planar. Therefore O1 is drawn above, and C6 below the plane, in a half chair conformation[100], to allow the C7 sidechain to remain equatorial and the C6 methoxyl to remain axial, as preferred.

**Figure 4.3** $^1$H-$^1$H NOE interactions and proposed solution conformation for the O1-C6 ring of $\Delta^3$ mycalamide A (**4.12**).

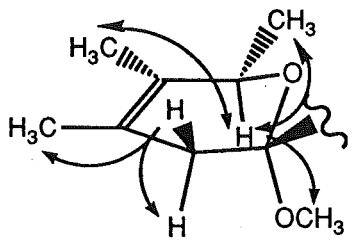

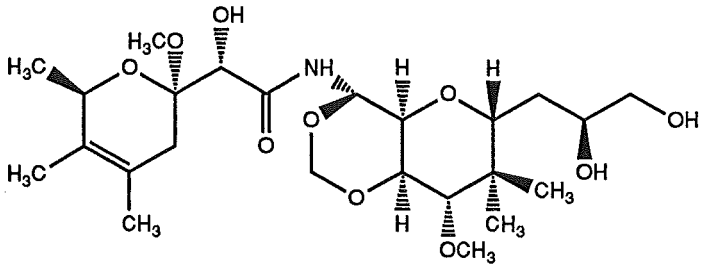

$\Delta^3$ Mycalamide A (**4.12**)

The $^1$H NMR data could therefore be fully assigned (Table 4.5), with the exceptions of the distinction between the C3 and C4 methyl signals and of determining the stereochemistries associated with the geminal H5 resonances. These methyl signals were assigned by analysing the results of various NOE experiments (Table 4.2), which are depicted in Figure 4.3. In particular, NOE interactions were observed between H2 and the protons of the methyl resonance at δ1.58 ppm, and between both H5 protons and the protons of the methyl resonance at δ1.63 ppm. Thus these methyl signals could be assigned to the groups at C3 and C4, respectively.

The H2 and two H5 protons are in a homoallylic relationship, as are the H2 and C4 methyl protons, the C5 methylene and C3 methyl protons, and the C3 and C4 methyl protons. The presence of long range homoallylic coupling[102,104] (typically in the range 1-3 Hz) was indicated by the broadness of all these resonances in the $^1$H NMR spectrum. These couplings were partially resolved by selective proton decoupling experiments. Irradiation of the signal assigned to H2 sharpened the two H5 resonances and the C4 methyl resonance and vice versa. Irradiation of the signal assigned to the C3 methyl group sharpened both H5 resonances, and the upfield one became a sharp doublet of doublets (2.2, 17.3 Hz), whereas the downfield one was a broader doublet of doublets (~2.7, 17.3 Hz). The smaller coupling constants (2.2, 2.7 Hz) were evidently from the two H5 protons to H2 and, of the two values, the larger homoallylic coupling constant is known to be associated with a *transoid* relationship of the protons involved[102,104]. Thus the downfield

H5 resonance was assignable to the 'axial' H5 proton (above the ring as depicted in Figure 4.3). Irradiation of this resonance in an NOE experiment enhanced the H7 signal, whereas irradiation of the other H5 resonance did not, as found for mycalamide B (the H5 resonances were not resolved in mycalamide A). Homoallylic coupling between two vinyl methyl groups in a *cis* relationship is usually of the order of 1 Hz[104] and this is consistent with only the slight broadening of both the C3 and C4 methyl resonances observed here.

The geminal coupling constant for the H5 protons, of 17.3 Hz, was about 3 Hz larger than that observed for mycalamide B. This is because, in this derivative (**4.12**), the two H5 protons are almost symmetrically above and below the plane of the adjacent double bond, which maximises the $\pi$ contribution to the coupling constant[102,160]. The geometry was less favourable for this effect in mycalamide B, where the C5 protons were adjacent to an exocyclic double bond.

There was insufficient sample to obtain a $^{13}C$ NMR spectrum. However, the above evidence leaves little doubt as to the structure of this derivative. The mechanism for its formation will be discussed later in this chapter. Other experiments performed to obtain rearranged double bond isomers will also be described in a subsequent section.

### 4.4.3 STRUCTURE OF THE MAJOR COMPOUND IN HPLC FRACTION 3

The $^1H$ NMR spectrum of fraction 3 had indicated that it contained a mixture of at least three components, including unreacted mycalamide A. However, signals for the new major component were dominant by at least a 3:1 ratio. The major features of the $^1H$ NMR spectrum were the loss of the exocyclic methylene signals, loss of the C6 methoxyl signal and the appearance of a new methyl doublet. There were also shifts in the signals for

the O1-C6 ring protons and H7. The latter resonance appeared as a doublet (4 Hz) and an addition of $D_2O$ to the sample did not alter this, so that this coupling could not arise from the C7 hydroxyl proton. This evidence was consistent with the formation of a 4-dihydro, 6-deoxy pseudomycalamide A derivative (**4.13**), analogous to that obtained from pederin. HRFABMS indicated a molecular formula of $C_{23}H_{41}NO_9$ in support of this structure.

As further evidence, the sample was acetylated, so that the chemical shift and coupling constant of the H7 proton could be clearly distinguished and compared directly with reported data for the pederin equivalent[94] (such data were only reported for the pederin diacetate derivative, **4.14**). The $^1H$ NMR spectrum of the acetylated mycalamide derivative (**4.15**) showed a large downfield shift in the H7 resonance, as expected, and the chemical shift and coupling constant data for this resonance (δ5.28 ppm, 3.0 Hz) were very similar to those reported for the pederin derivative, **4.14** (δ5.23 ppm, 2.5 Hz). The $^1H$ NMR spectrum of 4-dihydro, 6-deoxy pseudomycalamide A triacetate (**4.15**) was then fully assigned using results from a combination of COSY, NOE and proton decoupling experiments (Table 4.5).

The results from various NOE experiments (Table 4.2) have been illustrated in Figure 4.4. In particular, irradiation of the H7 signal gave an enhancement of a multiplet at δ3.86 ppm and this multiplet was also enhanced on irradiation of the signal assigned to H2. Therefore this multiplet was assigned to the new C6 proton, which was then required to be axial to the O1-C6 ring, as expected, in order that the bulky C7 sidechain be equatorial to this ring at C6. Irradiation of the H2 resonance also gave an enhancement of multiplets at δ1.41 and 1.82 ppm, which were assigned to H3 and H4 on the basis of their COSY connectivities. Irradiation of the H6 resonance gave an enhancement of the multiplet at δ1.82 ppm, as well as the H2 and H7 resonances, so that this multiplet had to be assigned to an axial H4 proton.

Thus the conformation of the O1-C6 ring was the usual chair conformation. The two H5 proton resonances were located at about δ1.2 ppm, as shown by a strong correlation in the COSY spectrum from the H6 resonance, and by a selective proton decoupling experiment, irradiating at δ1.2 ppm, which reduced the H6 resonance to a doublet (3 Hz). Thus the stereochemistries at C4 and C6 were clearly defined and the chemical shifts of the C3 and C4 substituents were similar to those in 4α-dihydro mycalamide A (**4.4**).

**Figure 4.4** $^{1}H$-$^{1}H$ NOE interactions and solution conformation for the O1-C6 ring of 4α-dihydro 6-deoxy pseudomycalamide A (**4.13**).

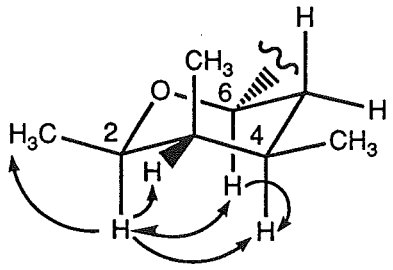


The $^{1}H$ NMR spectrum of the non-acetylated compound (**4.13**) was partially assigned by comparison with the data above. However, there was insufficient sample to enable a complete spectroscopic characterisation, or to allow further purification for analysis of its biological activity. Therefore it was desirable to find an alternative preparation of this derivative which would give a better (purified) yield. The almost quantitative conversion of mycalamide A to 5,6-dehydromethoxy mycalamide A (**3.11**), described in Section 3.4.5, appeared to provide a better starting point, since complete hydrogenation of this diene could give the required derivative directly, although possibly with other isomers. This attempt is described below.

## 4.5 HYDROGENATION OF 5,6-DEHYDROMETHOXY MYCALAMIDE A OVER ADAMS CATALYST

### 4.5.1 PREPARATION AND PURIFICATION OF PRODUCTS

A sample which was about 90% 5,6-dehydromethoxy mycalamide A (**3.11**) was hydrogenated over Adams catalyst to give a mixture of components by $^1$H NMR spectroscopy. Preparative reverse phase HPLC was then performed to give five fractions, which were analysed by $^1$H NMR and mass spectroscopies. Fraction 1 was a small sample of a pure, new derivative, as judged by $^1$H NMR spectroscopy. The structure of this compound will be described later in this section. Fraction 2 was a very small sample of a mixture, which contained a small amount of the compound in fraction 1, together with another compound, by $^1$H NMR spectroscopy. The latter, new compound gave rise to signals in the $^1$H NMR spectrum which suggested the presence of a C4-C5 double bond, but was not considered further due to the poor purity and small size of this sample. Fraction 3 was a pure sample of 4α-dihydro, 6-deoxy pseudomycalamide A (**4.13**) and further NMR spectroscopic characterisations on this sample will be described below. Fractions 4 and 5 were the 4α- and 4β-dihydro mycalamide A isomers (**4.4, 4.5**).

### 4.5.2 FURTHER CHARACTERISATIONS OF 4α-DIHYDRO, 6-DEOXY PSEUDOMYCALAMIDE A

The complete $^1$H NMR spectrum of 4α-dihydro, 6-deoxy pseudomycalamide A (**4.13**) was assigned with the assistance of COSY, selective proton decoupling, and NOE experiments (Table 4.5). Irradiation of a multiplet at δ3.74 ppm in a proton decoupling experiment reduced the multiplicity of the $H_2$5, H7 and H18 resonances, so that this multiplet had to include the H6 and

H17 resonances. Similarly, irradiation of a multiplet at δ1.4 ppm reduced the multiplicity of the H6 resonance (to a doublet, 4 Hz), as well as the multiplicities of the H4 and C3 methyl resonances, so that it contained both the two H5 and H3 resonances. An NOE interaction was observed between H4 and H6 (Table 4.2), so that the O1-C6 ring conformation was the same as determined above for the acetylated derivative (**4.15**). The overlap of resonances and the multiplicity of the signals meant that further analysis of the solution conformations was not practical for this derivative.

A comparison of the chemical shifts of this compound (**4.13**) with those of 4α-dihydro mycalamide A (**4.4**), revealed shifts in the signals assigned to H2 (-0.3), H4 (-0.3), H5a (+0.2), H5e (-0.2) and H7 (-0.2). These shifts could be ascribed to the removal of anisotropic and steric deshielding effects associated with the axial C6 methoxyl group[123], which were observed with several derivatives above. The partial data reported for the pederin derivative[94] (**4.3**) compared well with those found here, suggesting that this pederin equivalent had the same C4 stereochemistry.

Although there was still insufficient sample to obtain a $^{13}C$ NMR spectrum by direct acquisition, the $^{13}C$ resonances were obtained indirectly, by means of HMQC and HMBC experiments performed at higher field strength (500 MHz). The resolution of the $^{13}C$ signals was lower (0.4 ppm), so the results contained an error of ± 0.2 ppm. These $^{13}C$ data are listed in Table 4.4, with the HMBC correlations detailed in Table 4.3. Comparison of these $^{13}C$ NMR chemical shifts with those of 4α-dihydro mycalamide A (**4.4**) showed that there were shifts in the signals assigned to C2 (+7), C4 (+5), C5 (-2), C6 (-22), C7 (+2) and C8 (+2). The direction of these shifts is consistent with standard substituent effects[117] (except the C7 resonance, which is sensitive to the conformations about the C6-C7 and C7-C8 bonds). Note, however, that the removal of shielding effects associated with the C6 methoxyl

group is undoubtedly also important in the large downfield shifts of the C2 and, to a lesser extent, C4 and C7 resonances. Such effects were also noted in other derivatives above, and are well documented[119,120].

4.5.3 STRUCTURE OF THE COMPOUND IN HPLC FRACTION 1

The $^1$H NMR spectrum of fraction 1 showed the loss of the signals for the exocyclic methylene protons and the appearance of a new methyl doublet, consistent with hydrogenation at C4. However, the C5-C6 double bond of the starting diene was still present, as shown by the chemical shifts of the signals for H5 and H7 (the H5 resonance was almost 1 ppm upfield of its chemical shift in the starting compound due to the reduction at C4[101]). Hence this compound was likely to be 4-dihydro, 5,6-dehydromethoxy mycalamide A (**4.16**). The $^1$H NMR spectrum was assigned using results from COSY, proton decoupling and NOE experiments (Table 4.5).

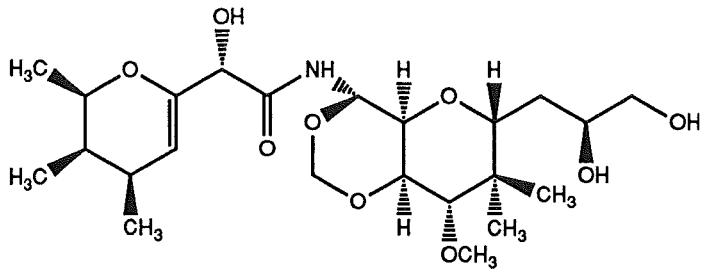


4α-Dihydro, 5,6-dehydromethoxy mycalamide A (**4.16**)

Selective proton decoupling experiments showed that there was an appreciable homoallylic coupling between H4 and H7 (1.5 Hz) and the H5 resonance was also broadened by allylic and long range W couplings[104] to H7 and H3, respectively. The NOE results (Table 4.2) have been illustrated in Figure 4.5. The strong NOE interactions between H2 and H4 required that these protons be in a 1,3 diaxial relationship, so that the C4 stereochemistry was 4α-dihydro. The O1-C6 ring conformation would be slightly distorted from that of 4α-dihydro mycalamide A (**4.4**), since C4-C7 and O1 are all in a plane,

and is best described as a half chair[100] (Figure 4.5). There was insufficient sample to obtain a $^{13}C$ NMR spectrum. However, HRFABMS indicated a compound of molecular formula $C_{23}H_{39}NO_9$, consistent with the proposed structure.

**Figure 4.5** $^1H$-$^1H$ NOE interactions and proposed solution conformation for the O1-C6 ring of 4α-dihydro, 5,6-dehydromethoxy mycalamide A (**4.16**).

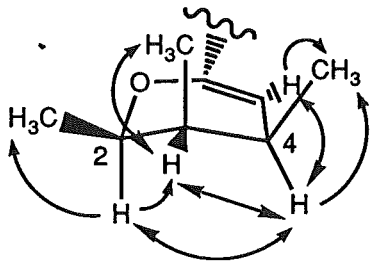


This derivative (**4.16**) represents a partial hydrogenation of the starting diene (**3.11**). Note that the exocyclic double bond has fewer (non-hydrogen) substituents than the C5-C6 double bond and would therefore be preferentially hydrogenated[185]. The method of preparing 4α-dihydro 6-deoxy pseudomycalamide A (**4.13**) from the diene was slightly better in yield than the first reaction, but it was also evident that some decomposition had occurred during the reaction. This was not surprising since the starting material itself was somewhat unstable, having an allylic hydroxyl group, and side reactions could be expected[183,191]. There was no sign of a C4 isomer in either preparation, which does agree with the pederin result, and this observation will be further discussed further, along with the mechanisms of these reactions, in the following section.

## 4.6 MECHANISM OF HETEROGENEOUS CATALYTIC HYDROGENATIONS

The mechanism of the heterogeneous catalytic hydrogenation of double bonds is not thoroughly understood[183] because it is difficult to study. Kinetic data are difficult to interpret because of hydrogen exchange between the substrate and catalyst, even for protons not on a double bond[192], in addition to double bond migrations[185] and isomerisations. The accepted mechanism[183,192] (Scheme 4.1) has the olefin adsorbed onto the surface of the metal, with its less hindered side attached to the catalyst surface. Hydrogen is cleaved into atoms on being adsorbed onto the catalyst surface. In a second step, one hydrogen atom becomes bonded to a carbon atom of the alkene, leaving a catalyst-bound alkyl radical. This radical combines with a second hydrogen atom to give the free alkane in the final step. Hydrogen addition is *syn*, and occurs from the least hindered side of the alkene.

This mechanism explains the possible side reactions of hydrogen exchange, double bond rearrangement and isomerisation, since the catalyst-bound alkyl radical can lose a hydrogen atom from an adjacent carbon to regenerate a catalyst-bound alkene. This is also shown in Scheme 4.1 and will be discussed further below.

Hydrogenation of mycalamides A and B and pederin over Adams catalyst proceeded without rearrangement of the double bond (Scheme 4.1a), and this is consistent with the known properties of this catalyst[185]. However, hydrogenation of mycalamide A over palladium on carbon (10%) gave considerable double bond rearrangement, as observed by the formation of the C3-C4 isomer (**4.12**) and the 4α-dihydro 6-deoxypseudomycalamide A derivative (**4.13**). The rearrangement to the C3-C4 and the C4-C5 positions of the O1-C6 ring appeared to be equally likely, based on the relative masses

of these two products. The favoured position would be expected to be C3-C4, since the double bond is then more substituted, but there are statistical and steric factors to consider also[185]. The mechanism for this rearrangement[183], shown in Scheme 4.1b, is consistent with the observation that the reaction only occurs in the presence of hydrogen[193]. The rearrangement of double bonds on palladium catalysts is well known[185,194].

**Scheme 4.1** Mechanisms of hydrogenation (a), double bond rearrangement (b) and hydrogenolysis (c) in mycalamides A and B. (An asterisk indicates a binding site on the catalyst surface).

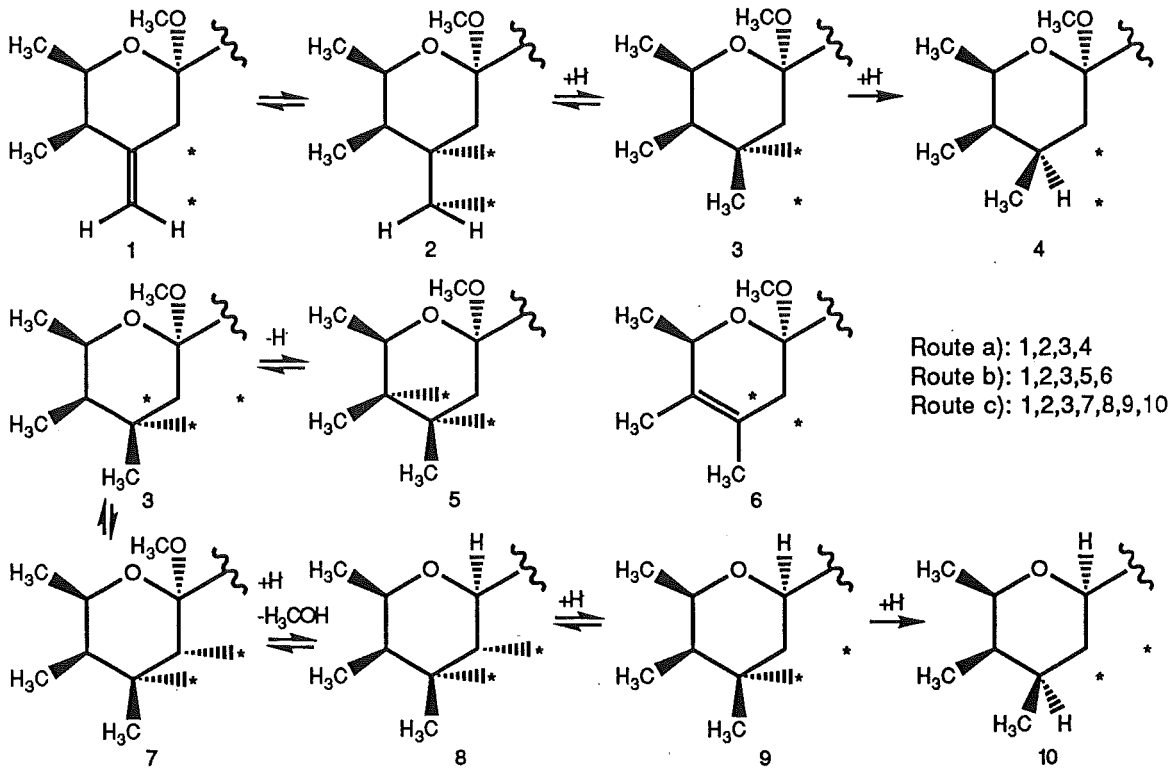


The transposition of the exocyclic double bond into the C4-C5 position of the O1-C6 ring places the C6 acetal in an allylic position, and hydrogenolysis of the methoxyl group is possible, and evidently occurs readily (Scheme 4.1c). Although the exact mechanism is uncertain[191,195], it is evident that the hydrogen atom attacks from the same side as the methoxyl group, since only one C6 isomer was obtained, with the H6 and H2 atoms

both axial. Furthermore, the reduction of the C4-C5 double bond must be more facile than reduction of the C3-C4 double bond, since no $\Delta^{4(5)}$ derivative was obtained, and this is reasonable as it has one less alkyl substituent[185].

The reduction of the C4-C5 double bond appeared to be stereoselective in giving the 4α-dihydro isomer (**4.13**) only. This would require that the addition of hydrogen occur almost exclusively from below the double bond, which is reasonable, since the axial C3 methyl group, and possibly the C7 substituents, could hinder access from above the O1-C6 ring, whereas the bottom face would have much less steric hindrance with the replacement of the axial C6 methoxyl group by a hydrogen atom. The same selectivity occurred in the hydrogenation of the diene (**3.11**) to give the 4α isomer (**4.13**) only, since again there was no axial C6 group, so that attack from below the O1-C6 ring was favoured.

In view of the above, it was a little surprising that no hydrogenolysis at C6 or C7 was detected from hydrogenation of the diene over Adams catalyst[183,191]. It is possible that this required either more forcing conditions or a better leaving group. Thus if a C7-deoxy derivative was desired, it would be better to convert the C7 hydroxyl group to an acetate or sulphonate ester prior to reduction[195]. However this was not investigated.

## 4.7 OTHER ATTEMPTS TO REARRANGE THE EXOCYCLIC DOUBLE BOND OF MYCALAMIDE A

There are several other reagents available for performing double bond rearrangements which do not require the presence of hydrogen, which necessarily reduces the yield of such products. Strong bases cause rearrangement of double bonds[196] and these reactions on mycalamide A will

be described in a later chapter (5). Rearrangements also occur with acids[196], but such reactions would obviously not be useful for the mycalamides.

Another common method is the use of various metal ions (Pd, Pt, Rh, Ru), or metal carbonyl catalysts (eg $Fe_3(CO)_{12}$), which involve the formation of a $\pi$-allyl complex[194,196]. Many of these seem to require the presence of acid as a co-catalyst, or are also potentially oxidising. $RhCl_3$ and $Pd(C_6H_5CN)_2Cl_2$ are two reagents which allow double bond rearrangements under neutral conditions[197], so both were tried in small scale reactions with mycalamide A. The reaction with $RhCl_3$ gave a very large number of products by TLC and the $^1H$ NMR spectrum suggested decomposition. The second reagent was equally unsuccessful, so this work was abandoned.

## 4.8 BIOLOGICAL ASSAY RESULTS FOR MYCALAMIDE HYDROGENATION PRODUCTS

The biological assay results for all the mycalamide derivatives described in this chapter have been listed in Table 4.6. It is apparent that the dihydro mycalamide isomers (**4.4**, **4.5**, **4.6**, **4.7**) have levels of biological activity that are similar to those of mycalamides A and B, as was found for dihydro pederin[40] (**4.1**). However, there appeared to be a consistent difference in biological activity between the dihydro isomers themselves, with the 4β isomer, the major product in the mycalamide reactions, being at least 4-8 times more active than the 4α isomer. The 4β–dihydro mycalamide A isomer (**4.5**) was possibly more active than mycalamide A, but the 4β–dihydro mycalamide B derivative (**4.7**) was of similar activity to mycalamide B. The hydrolysis products, the isomers of dihydro pseudomycalamide A (**4.10**, **4.11**), were 10-20 times less active than the dihydro mycalamide A isomers

(**4.4**, **4.5**), which was consistent with earlier results for C6 acetal hydrolysis (Chapter 3).

There was no apparent difference in the cytotoxicity or selectivity of these dihydro mycalamide isomers. It is likely that the early assay results for the pederin derivatives (**4.1**, **4.2**)[40,180] merely reflected the reduced activities of the 4α-dihydro isomers, compared with those of pederin and pseudopederin (**3.5**), as found above for dihydro mycalamides A and B and also for the corresponding C6 hydrolysis products. The use of 10-fold steps in concentration for this early study could not give a true indication of the $IC_{50}$, or the minimum inhibitory dose[39], which would be better points at which to compare the relative cytotoxicities of pederin and its derivatives. However, the main point of note from these results is that the exocyclic double bond is *not* essential for the biological activities of the mycalamides and pederin.

The other mycalamide hydrogenation reaction products were less active. Surprisingly, the C3-C4 double bond isomer (**4.12**) was about 100 times less active than mycalamide A, although none of the other functional groups had been changed and the polarity was not very different from that of mycalamide A. The conformation of the O1-C6 tetrahydropyran ring was slightly different, the major difference being at C3, where the C3 methyl group was no longer axial. Electronic effects associated with the double bond in the ring could also be significant.

It is also useful to compare the biological activity of 4α-dihydro mycalamide A (**4.4**) with that of 4α-dihydro, 6-deoxy pseudomycalamide A (**4.13**). The latter is at least 300 times less active than the same dihydro isomer with a C6 methoxyl group, and probably substantially less active than the compound with a C6 hydroxyl group. (The latter derivative, **4.10**, was impure so that the comparison was not quantitative. However, compound **4.13** was about 25 times less active than pseudomycalamide A). No data

were reported for the pederin equivalent (**4.3**), although antimitotic activity was claimed[181]. The 4α-dihydro, 5,6-dehydromethoxy mycalamide A derivative (**4.16**) was similarly relatively inactive, as expected, based on results discussed in Chapter 3.

Thus it appears that the C6 acetal is required for the biological activity of the mycalamides, since having a double bond between C5 and C6, or a hydrogen atom to replace the methoxyl group, caused the compounds to become almost inactive. Also the conformation of the O1-C6 tetrahydropyran ring must also be important, although the double bond at C4 is not required for this activity. Therefore other double bond additions were considered in the following studies.

## 4.9 EPOXIDATION OF MYCALAMIDES A AND B

### 4.9.1 PREPARATION AND CHARACTERISATION OF EPOXIDES

Mycalamides A and B were each converted into a mixture of epimeric epoxides using m-chloroperbenzoic acid[198] in $CH_2Cl_2$. These isomers were in a 3:2 ratio, and were separated by preparative silica gel TLC. HRFABMS results indicated the inclusion of one extra oxygen in mycalamides A and B, consistent with this epoxidation. The $^1H$ NMR spectra of both epoxide isomers showed a large upfield shift in the C4' exocyclic methylene resonances and shifts in signals for the remaining O1-C6 ring protons. Results from a COSY experiment were used to assign these spectra for both mycalamide A and B isomers (Table 4.7), with the exception of assigning the stereochemistries associated with the C4' and C5 methylene resonances and determining the C4 stereochemistry. These ambiguities were resolved by considering the results of NOE experiments and from an analysis of the chemical shifts and proton-proton coupling constants. Note that for ease of reference the C4'

methylene resonances will still be given the designations *E* and *Z*, in order to indicate their relationships in space to the other O1-C6 ring substituents, although it is recognised that there is no longer a double bond present.

The observed NOE interactions for both compounds are listed in Table 4.8 and depicted in Figure 4.6. Irradiation of the signal assigned to H2 caused an enhancement of the C6 methoxyl resonance and irradiation of the C3 methyl resonance caused an enhancement of the downfield H5a resonance in both isomers. Therefore the O1-C6 tetrahydropyran ring was in the usual chair conformation, as expected, and the stereochemistry associated with the two H5 signals was assigned. Also, irradiation of the H3 resonance resulted in an enhancement of the more upfield C4' methylene resonance (4-CH*Z*), whereas irradiation of the H5e resonance enhanced the more downfield resonance (4-CH*E*), thus assigning the stereochemistry of these proton resonances. There were no major differences in the NOE data for the isomers, although the major isomer had a 3-$CH_3$ - 4-CH*Z* NOE interaction, suggesting that this was the 4α isomer (**4.17, 4.19**).

**Figure 4.6** $^1$H-$^1$H NOE interactions and solution conformations for the O1-C6 ring of the mycalamide A and B epoxide isomers (**4.17-4.20**).

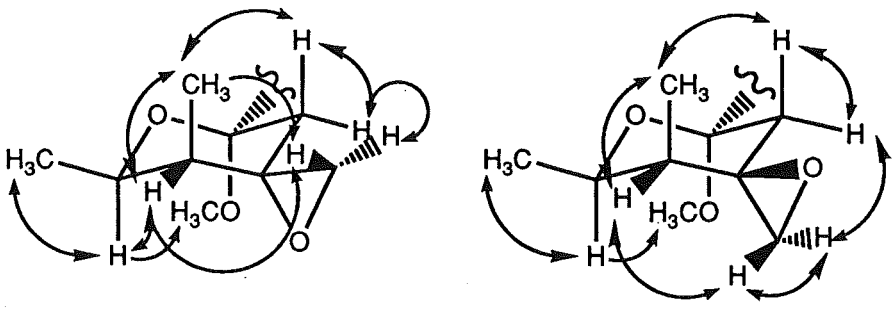


a) Major isomer (4α) b) Minor isomer (4β)

The stereochemistry at C4 was further elucidated from an analysis of the observed long range couplings. As noted in earlier examples, coupling across four bonds in alkanes is maximised for a planar 'W' relationship of the

protons[102,104]. Such a 'W' coupling was observed between the H3 and H5e protons in both isomers, which is consistent with their geometrical relationships (Figure 4.6). However, in the $^1$H NMR spectrum of the minor isomer, predicted to be 4β from the NOE results, there was a long range coupling of 1.5 Hz between the H5a and 4-CH*Z* resonances. In neither isomer do the geometrical relationships between these protons seem to satisfy the requirements for 'W' coupling, although it is best approached in the 4β isomer (**4.18, 4.20**). Long range coupling in exocyclic epoxides has been investigated for various steroidal derivatives and has been found to always involve one of the *pseudo-axial* methylene (4β) protons and an adjacent *axial* methylene proton[199,200]. This common geometrical arrangement has been described as being more like that required for allylic coupling than the 'W' configuration and has been ascribed to favourable σ orbital overlap with a delocalised electron density system above the C-C bond of the epoxide[200]. It is also known that long range couplings across strained ring systems are often unusually large[104]. Thus the stereochemistry of the minor mycalamide epoxide must be 4β, as suggested above.

An analysis of the $^1$H NMR chemical shifts for the O1-C6 ring substituents of the two isomers suggested that similar diaxial deshielding effects[123] were involved as were observed for the dihydro mycalamide derivatives. In particular, the pseudo-axial C4 methylene protons in the 4β isomers (**4.18, 4.20**) were deshielded by the axial C6 methoxyl group and the H2 proton was deshielded in both isomers by the pseudo-axial C4 substituents, but more by oxygen (4α isomers, **4.17, 4.19**).

$^{13}$C NMR spectra were recorded for all four epoxides and an HMQC experiment was performed on the major isomer to confirm the assignments (Table 4.9). Shielding effects were also found here, similar to those observed for the dihydro mycalamide A and B isomers above[117,119,120]. In particular,

C2 was shielded by axial C4 substituents in both epoxide isomers but the C4-oxygen (4α isomer) appeared to have the most influence. Similarly, the C3 methyl group was shielded in both isomers by equatorial substituents at C4, but more by oxygen (4β isomer). The chemical shifts of the C4 and C4' resonances compared well with those found for another exocyclic epoxide[201], with the pseudo-equatorial methylene carbon resonance (4α isomer) appearing more shielded due to a combination of electronic and steric factors[117]. These results were therefore also consistent with the designated stereochemistries of the epoxide isomers, as determined above.

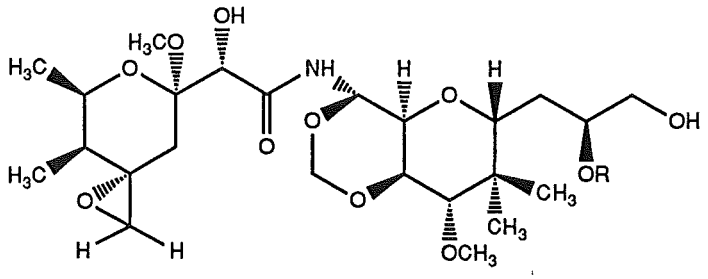


R=H: Mycalamide A 4α-epoxide (**4.17**)
R=$CH_3$: Mycalamide B 4α-epoxide (**4.19**)

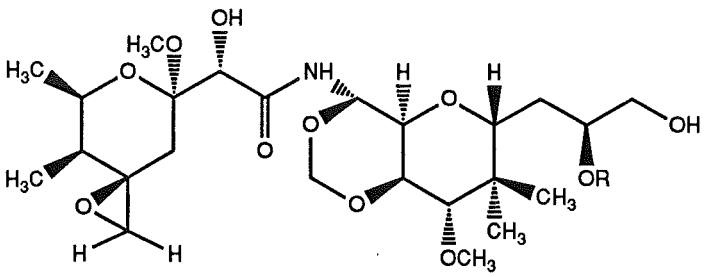


R=H: Mycalamide A 4β-epoxide (**4.18**)
R=$CH_3$: Mycalamide B 4β-epoxide (**4.20**)

### 4.9.2 MECHANISM AND STEREOCHEMISTRY OF THE EPOXIDATION REACTION

According to Bartlett[198], epoxidation occurs by a one step mechanism, involving the addition of one oxygen atom from the peracid to the alkene, as shown in Scheme 4.2. In the epoxidation of mycalamides A and B, the

observed ratio of the two isomers, about 3:2, favoured the 4α isomer. This corresponds to a favoured path of attack (for the peracid) from the bottom face of the exocyclic double bond, the axial side (Figure 4.2b), which is the reverse of that found for hydrogenation. However, it is known that axial attack is generally favoured in epoxidation reactions[202]. Axial substituents on the homoallylic carbon (C6) reverse this preference, whereas an axial methyl group on the allylic carbon (C3) increases it, and both are present in mycalamides A and B. It is also known that hydroxyl groups have a strong *syn*-directing influence by hydrogen bonding to the peracid in the transition state[202]. However, it is unlikely that the latter occurs in the mycalamides, since there are no such groups sufficiently close by. The stereochemical preference in this epoxidation reaction with mycalamides A and B is not strong, although steric effects are known to be more important than in hydrogenation, which could explain this observed difference for the two reactions.

**Scheme 4.2** Mechanism of epoxidation in mycalamides A and B. The reagent can attack from above or below the double bond, giving two isomers.

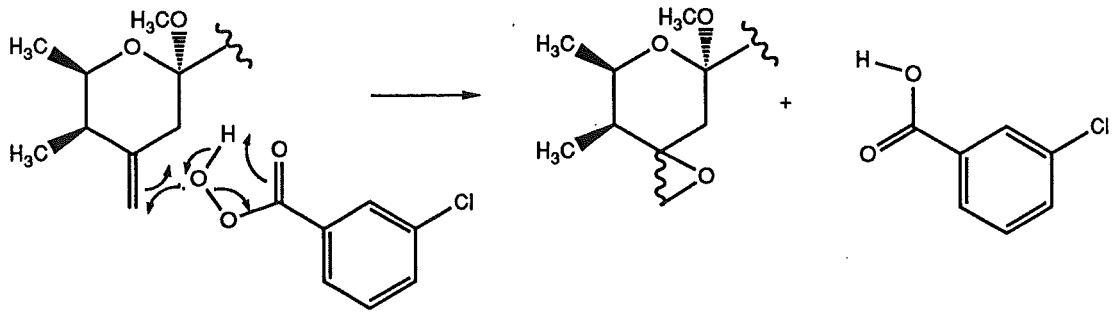


4.9.3 BIOLOGICAL ASSAY RESULTS

The biological assay results for these four epoxide derivatives are recorded in Table 4.6. It is interesting to note that the difference in activity between the two C4 dihydro mycalamide isomers is accentuated for the two

mycalamide epoxide isomers, with the 4α isomer being 7-20 times less active than the 4β isomer. Even the 4β epoxide isomer was 30-40 times less active than the corresponding parent compound (mycalamides A or B). The polarity of these epoxides is slightly higher than the starting compounds. However, the stereoselectivity and the loss of biological activity shown by these products is difficult to explain without a knowledge of the active site. These results therefore follow the pattern of earlier results, where relatively small changes to the structure or conformation of the O1-C6 ring appeared to cause large changes to the observed activity.

## 4.10 OTHER ADDITIONS TO THE EXOCYCLIC DOUBLE BOND

### 4.10.1 ADDITION OF HYDROGEN CHLORIDE WITH ETHYLCHLORO-FORMATE

The reactivity of mycalamides A and B to acids prevented the direct addition of hydrogen halides to the double bond. However, ethyl chloroformate[203] is less reactive than acetyl chloride, which is known to be a good source of 'anhydrous HCl'. Besides being good for acylation, ethyl chloroformate is known to alkylate imides[204] and amides[156]. With the latter in mind, this reagent was reacted with mycalamide B, in the presence of potassium carbonate, to give mostly one product (TLC). However, after workup the product became coloured, and was found to be a mixture by $^1$H NMR spectroscopy and TLC. Preparative TLC gave a pure product by $^1$H NMR spectroscopy, which had two ethyl carbonate esters at C7 and C18, as shown by large downfield shifts in the α-proton signals[101], no change to the amide, and a double bond between C5 and C6 (due to an acid catalysed elimination of the C6 methoxyl group). The latter was shown by the loss of the C6 methoxyl and the usual C5 proton resonances, and the appearance of a

new singlet at δ5.15 ppm, assigned to a single H5 proton, as in previous derivatives (**3.11**, **4.16**), which showed a small long range coupling to the H7 resonance. Also the spectrum showed a loss of the exocyclic methylene signals and contained a new methyl singlet at δ1.58 ppm, which must be assigned to a group at C4. Furthermore, H3 (δ2.53 ppm) was strongly deshielded relative to the dihydro derivatives (+0.9 ppm compared with **4.16**), suggesting the presence of a heteroatom. A COSY spectrum was performed to assign the data for this compound which was given the proposed structure **4.21**.

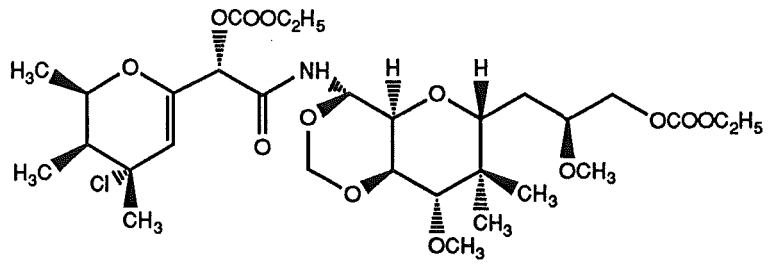


4-Hydrochloro, 5,6-dehydromethoxy mycalamide B bis-ethylcarbonate (**4.21**)

This structure is consistent with an addition of HCl to the exocyclic double bond of the diene (**3.11**) in Markovnikov fashion[205]. The HCl would originate from excess reagent reacting with $H_2O$ in the workup solvents, and would first catalyse an elimination of methanol across C5-C6 in mycalamide B, as observed in earlier work (Chapter 3). To obtain maximum deshielding[123] of the H3 proton, the chlorine atom at C4 must be axial to the ring. This is also consistent with an attack of $Cl^-$ from the less hindered face of the intermediate carbocation, which is from below, because of the adjacent axial C3 methyl group. Note that the allylic tertiary carbocation at C4 could be resonance stabilised using the tetrahydropyran ring oxygen.

Unfortunately this compound was insufficiently stable to enable further spectroscopic characterisations to be performed. However, on the basis of earlier work it would be expected to be inactive. Attempts to cleave the ester

groups with mild base gave mostly decomposition, which was not surprising, since the product would have reactive allylic alcohol (C7) and allylic halide (C4) functionalities. If the C6 acetal could have been easily regenerated, such as by mild acid catalysed addition of methanol to the enol[110], and the hydroxyl groups protected in some way, then this might be a useful reagent for studying addition of HCl at C4, although it is possible that this derivative would still be unstable and formed in low yield. Therefore this work was not pursued further.

### 4.10.2 ATTEMPTED BROMINATION OF MYCALAMIDE A

Mycalamide A is only slightly soluble in $CCl_4$. Addition of a dilute bromine solution in $CCl_4$ to a sample of mycalamide A, stabilised by a trace of pyridine[206], gave, after workup, an approximately 1:1 mixture of unreacted mycalamide A and possibly a major C4 dibromo isomer, with minor components. Attempts to complete the reaction or repeat it, using added $CH_2Cl_2$ and triethylamine, were unsuccessful, since TLC and a $^1H$ NMR spectrum of the products indicated that decomposition had occurred. The mycalamide structure may have been reacting further with bromine in the presence of base, such as in oxidation reactions[207], although care was taken to exclude light. The bromination of mycalamide A could probably have been eventually achieved under optimised conditions. However, the time and material required for the preparation and purification of such a derivative was not considered worthwhile, since some trends in the biological activity of double bond addition products had been determined above.

**Table 4.1** $^1$H NMR data[a] for compounds described in Sections **4.2** and **4.3**.

| | 4α-Dihydro mycalamide A (4.4) | 4β-Dihydro mycalamide A (4.5) | 4α-Dihydro mycalamide B (4.6) | 4β-Dihydro mycalamide B (4.7) | 4α-Dihydro pseudomyc.A (4.10) | 4β-Dihydro, 6*S* pseudomyc.A (4.11) |
|---|---|---|---|---|---|---|
| **H2** | 3.97 (2.3,6.6) | 4.11 (2.7,6.7) | 3.99 (2.4,6.6) | 4.13 (2.7,6.6) | 4.20 (2.4,6.6) | 4.08 (3.0,6.5) |
| **2-CH$_3$** | 1.18 (6.6) | 1.17 (6.6) | 1.19 (6.6) | 1.18 (6.5) | 1.06 (6.6) | 1.19 (6.6) |
| **H3** | 1.47 (2.5,3.9,6.9) | 1.33 (2.7,7.1) | 1.49 (m) | 1.35 (2.4,7.2) | 1.44 (m) | 1.47 (m) |
| **3-CH$_3$** | 0.73 (7.1) | 0.93 (7.1) | 0.75 (7.1) | 0.95 (7.1) | 0.72 (7.0) | 0.88 (7.0) |
| **H4** | 2.14 (3.7,7.0,12.8) | 1.70 (m) | 2.18 (m) | 1.67 (m) | 2.23 (m) | 1.92 (m) |
| **4-CH$_3$** | 0.88 (7.0) | 1.16 (7.1) | 0.86 (7.0) | 1.18 (7.1) | 0.90 (7.0) | 1.04 (7.0) |
| **H5a** | 1.23 (13.0) | 1.76 (5.6,13.8) | 1.17 (13.2) | 1.66 (4.4,14.0) | 1.67 (13.3) | 1.58 (m) |
| **H5e** | 1.62 (3.9,13.9) | 1.53 (2.9,14.0) | 1.63 (3.8,13.9) | 1.50 (2.3,14.2) | 1.42 (4.2,13.3) | 1.52 (m) |
| **6-OCH$_3$** | 3.30 | 3.28 | 3.30 | 3.28 | | |
| **H7** | 4.23 | 4.21 | 4.22 | 4.20 | 3.99 | 4.44 |
| **NH9** | 7.46 (9.6) | 7.45 (9.7) | 7.52 (9.7) | 7.49 (9.5) | 7.49 (9.8) | 7.25 (10.0) |
| **H10** | 5.84 (9.6) | 5.85 (9.7) | 5.76 (9.4) | 5.76 (9.6) | 5.83 (9.9) | 5.84 (10.0) |
| **10-OCH*R*** | 5.13 (6.9) | 5.13 (7.0) | 5.11 (6.9) | 5.12 (7.0) | 5.15 (7.0) | 5.17 (7.0) |
| **10-OCH*S*** | 4.87 (6.9) | 4.87 (7.0) | 4.86 (6.9) | 4.85 (7.0) | 4.89 (7.0) | 4.87 (7.0) |
| **H11** | 3.84 (6.7,9.7) | 3.86 (6.7,9.7) | 3.80 (6.5,9.3) | 3.81 (6.6,9.6) | 3.91 (6.8,10.2) | 3.88 (6.9,10.0) |
| **H12** | 4.22 (6.8,10.1) | 4.22 (6.7,10.1) | 4.19 (6.5,10.0) | 4.20 (6.7,10.3) | 4.24 (6.8,10.5) | 4.22 (6.9,10.5) |
| **H13** | 3.45 (10.2) | 3.46 (10.3) | 3.41 (9.9) | 3.43 (10.3) | 3.48 (10.5) | 3.52 (10.4) |
| **13-OCH$_3$** | 3.56 | 3.56 | 3.55 | 3.55 | 3.56 | 3.56 |
| **14-CH$_3$*R*** | 0.98 | 0.98 | 0.99 | 0.98 | 0.97 | 0.98 |
| **14-CH$_3$*S*** | 0.88 | 0.88 | 0.87 | 0.87 | 0.87 | 0.87 |
| **H15** | 3.63 (6.6) | 3.63 (6.3) | 3.44 (2.3,10.3) | 3.42 (2.5,10.1) | 3.58 (m) | 3.55 (m) |
| **H16** | 1.57 (m) | 1.56 (m) | 1.59 (m) | 1.57 (m) | 1.55 (m) | 1.56 (m) |
| **H16** | 1.57 (m) | 1.56 (m) | 1.55 (m) | 1.57 (m) | 1.55 (m) | 1.50 (m) |
| **H17** | 3.74 (m) | 3.74 (m) | 3.26 (m) | 3.24 (m) | 3.74 (m) | 3.71 (m) |
| **17-OCH$_3$** | | | 3.31 | 3.29 | | |
| **H18** | 3.58 (3.5,11.4) | 3.57 (3.5,11.2) | 3.66 (3.3,12.0) | 3.63 (3.3,11.9) | 3.54 (3.6,11.3) | 3.53 (m) |
| **H18** | 3.37 (6.1,11.2) | 3.38 (5.9,11.3) | 3.48 (5.8,12.0) | 3.47 (5.9,12.0) | 3.40 (5.6,11.3) | 3.35 (6.5,11.3) |

[a]All data were recorded in $CDCl_3$, with chemical shifts in ppm relative to $CHCl_3$, δ7.25 (coupling constants in Hz)

**Table 4.2** $^{1}H$-$^{1}H$ NOE interactions[a] for compounds in Sections **4.2-4.5.**

| Compound | Signal(s) irradiated | Signals enhanced (% enhancement) |
|---|---|---|
| 4β-Dihydro myc.A | H2 | 2-$CH_3$(1), H3(3), 4-$CH_3$(0.8), 6-$OCH_3$(0.3) |
| **(4.5)** | 3-$CH_3$ (2x14-$CH_3$) | H3(5), H4(3), H5a(2), $H_2$16(2)[b] |
| | H5e (H16) | H4(1), H5a(15), H17(4)[b] |
| | H5a | 3-$CH_3$(1), H5e(11), H7(2) |
| | H7 (H12) | 6-$OCH_3$(2), H11(6)[b], 14-$CH_3S$(1) |
| 4β-Dihydro myc.B | H2 | 2-$CH_3$/4-$CH_3$(1), H3(3), 6-$OCH_3$(0.5) |
| **(4.7)** | 2-$CH_3$ (4-$CH_3$) | H2(6), H3(3), 3-$CH_3$(0.6), H4(3)[b] |
| | H3 | H2(4), 3-$CH_3$(1), H4(1) |
| | 3-$CH_3$ | H3(4), H4/H5a(2) |
| | H5e (H16) | H4/H5a(4), 14-$CH_3S$(0.4)[b], 14-$CH_3R$(0.7)[b] |
| | 6-$OCH_3$ | H2(1), H7(4) |
| | H7 (H12) | 6-$OCH_3$(1), H11(4)[b], 14-$CH_3S$(0.4)[b] |
| 4α-Dihydro myc.B | H2 | 2-$CH_3$(2), H3(4), H4(5), 6-$OCH_3$(1) |
| **(4.6)** | 2-$CH_3$ (H5a) | H2(5), 3-$CH_3$(2)[b], H5e(12)[b], H7(2)[b] |
| | H3 ($H_2$16) | H2(3), 3-$CH_3$(2), H4(3), 4-$CH_3$(0.7), 14-$CH_3R$(0.5)[b] |
| | 3-$CH_3$ | H3(5), 2-$CH_3$(0.7), H5a(3) |
| | H4 | H2(4), H3(3), 4-$CH_3$(1), H5e(1) |
| | 4-$CH_3$ (14-$CH_3S$) | H3(3), H4(6), H5e(3), H12(6)[b], 13-$OCH_3$(0.3)[b], $H_2$16(3)[b] |
| | H5e ($H_2$16) | H4(3), 4-$CH_3$(0.5), H5a(18), 14-$CH_3S$(1)[b], 14-$CH_3R$(0.3)[b], H17(3)[b] |
| | H7 (H12) | 6-$OCH_3$(2), H11(4)[b], 14-$CH_3S$(0.9)[b] |
| $\Delta^3$ Mycalamide A | H2 (H12) | 2-$CH_3$(2), 3-$CH_3$(0.8), 6-$OCH_3$(1), H11(7)[b], 14-$CH_3S$(1)[b] |
| **(4.12)** | 2-$CH_3$ | H2(7) |
| | 3-$CH_3$ ($H_2$16) | H2(3), 14-$CH_3S$(2)[b], 14-$CH_3R$(1)[b], H17(7)[b] |
| | H5a | 4-$CH_3$(0.5), H5e(10), H7(2) |
| | H7 | 6-$OCH_3$(1) |
| 4α-Dihydro, 6-deoxy pseudo A triacetate | H2 (13-$OCH_3$) | 2-$CH_3$(2), H3(4), H4(3), H6(3), 10-OCH$R$(1)[b], 14-$CH_3R$(0.6)[b] |
| **(4.15)** | H6 (H11) | H2(4), H4(2), H7(8), NH(5)[b], H12(4)[b] |
| | H7 | H6(3) |
| 4α-Dihydro 6-deoxy mycalamide A | H2 (13-$OCH_3$, H15, H18d[c]) | 2-$CH_3$(2), H4(3), H10(8)[b], H12(7)[b], 14-$CH_3R$(1)[b], H18u(7)[b,c] |
| **(4.13)** | 3-$CH_3$ (14-$CH_3S$) | H3(4), H12(8) |
| | H6 (H17) | H4(6) |
| | H7 (H11) | H12(8)[b] |
| 4α-Dihydro 5,6-dehydromethoxy A | H2 (H12) | 2-$CH_3$(1), H3(5), H4(6), H11(3)[b], 14-$CH_3S$(0.8)[b] |
| **(4.16)** | H3 | H2(6), 3-$CH_3$(2), H4(6) |
| | 3-$CH_3$ (14-$CH_3S$) | H3(5), H12(5)[b] |
| | H4 | H2(5), H3(7), 4-$CH_3$(2), H5(4) |
| | H5 | H4(2), 4-$CH_3$(1) |

[a]All data were recorded in $CDCl_3$

[b]Enhancement interpreted as being due to the irradiation of an overlapping signal

[c]u and d have been used to designate the upfield and downfield resonances of a geminal pair

**Table 4.3** $^{2}J_{CH}$ and $^{3}J_{CH}$ HMBC correlations[a] for compounds in Chapter 4.

| Compound | Proton | Carbon signal correlated |
|---|---|---|
| 4β-Dihydro mycalamide B (**4.7**) | 3-$CH_3$ | C2, C4 |
| | 4-$CH_3$ | C4, C5 |
| | 6-$OCH_3$ | C6 |
| | H7 | C6, C8 |
| | 10-OCH*R* | C10, C12 |
| | 10-OCH*S* | C10, C12 |
| | H11 | C10, C12, C13 |
| | H12 | C10, C13 |
| | H13 | 13-$OCH_3$ |
| | 13-$OCH_3$ | C13 |
| | 14-$CH_3$*R* | C13, C14, C15 |
| | 14-$CH_3$*S* | C13, C14, 14-$CH_3$*R* |
| | 17-$OCH_3$ | C17 |
| 4α-Dihydro 6-deoxy ps.A (**4.13**) | 2-$CH_3$ | C2, C3 |
| | H3/$H_2$5 | C2/C6, C3, C4 |
| | 3-$CH_3$ | C2, C3, C4 |
| | 4-$CH_3$ | C3, C4, C5 |
| | H7 | C5, C8 |
| | 10-OCH*R* | C10 |
| | 10-OCH*S* | C10, C12 |
| | H13 | C12, 13-$OCH_3$, 14-$CH_3$*R*, 14-$CH_3$*S* |
| | 13-$OCH_3$ | C13 |
| | 14-$CH_3$*R* | C13, C14, 14-$CH_3$*S*, C15 |
| | 14-$CH_3$*S* | C13, C14, 14-$CH_3$*R*, C15 |
| | $H_2$16 | C15, C17 |

[a]All data were recorded in $CDCl_3$

Table 4.4 $^{13}C$ NMR data[a] for compounds described in Sections 4.2 and 4.3.

| | 4α-Dihydro mycalamide A (4.4) | 4β-Dihydro mycalamide A (4.5) | 4α-Dihydro mycalamide B (4.6) | 4β-Dihydro mycalamide B (4.7) | 4α-Dihydro pseudomyc.A (4.10) | 4β-Dihydro, 6*S* pseudomyc.A (4.11) | 4α-Dihydro 6-deoxy ps.A (4.13) |
|---|---|---|---|---|---|---|---|
| C2 | 70.88 | 64.92 | 70.80 | 64.79 | 69.83 | 73.02[b] | 77.6 |
| 2-$CH_3$ | 18.46 | 18.28 | 18.49 | 18.40 | 18.48 | 15.41[b] | 18.7 |
| C3 | 37.09 | 37.45 | 37.06 | 37.35 | 37.00 | 37.62 | 37.4 |
| 3-$CH_3$ | 4.36 | 13.04 | 4.49 | 13.07 | 4.04 | 13.20 | 4.8 |
| C4 | 28.94 | 32.11 | 28.83 | 32.19 | 29.00 | ? | 34.0 |
| 4-$CH_3$ | 18.85 | 20.81 | 19.00 | 20.87 | 19.21 | 21.01[b] | 19.2 |
| C5 | 31.10 | 29.51 | 31.09 | 29.22 | 32.68 | 32.03[b] | 29.6 |
| C6 | 99.30 | 100.05 | 99.42 | 100.18 | 97.09 | ? | 77.2 |
| 6-$OCH_3$ | 48.47 | 48.11 | 48.31 | 47.87 | | | |
| C7 | 72.93 | 73.32 | 72.37 | 72.63 | 75.04 | 73.79 | 74.6 |
| C8 | | 171.82 | 171.72 | 171.82 | ? | 167.95 | 173.3 |
| C10 | 73.77 | 73.80 | 74.14 | 74.02 | 73.11 | 73.44 | 73.5 |
| 10-$OCH_2$ | 86.80 | 86.81 | 86.55 | 86.56 | 87.04 | 87.18 | 87.0 |
| C11 | 71.12 | 71.23 | | 70.69 | 71.24 | 71.64 | 71.4 |
| C12 | 74.37 | 74.40 | 74.32 | 74.42 | 74.51 | 74.83[b] | 74.6 |
| C13 | 79.20 | 79.15 | 79.60 | 79.49 | 79.50 | 79.12 | 79.1 |
| 13-$OCH_3$ | 61.81 | 61.82 | 61.72 | 61.77 | 61.94 | 61.84 | 61.8 |
| C14 | 41.59 | 41.63 | | 41.40 | 41.79 | 41.91 | 41.7 |
| 14-$CH_3$*R* | 23.16 | 23.15 | 23.41 | 23.30 | 22.94 | 22.83 | 22.9 |
| 14-$CH_3$*S* | 13.59 | 13.56 | 13.80 | 13.62 | 13.22 | 13.73 | 13.2 |
| C15 | 78.80 | 79.09 | 75.64 | 75.52 | 78.89 | 78.65 | 79.1 |
| C16 | 32.01 | 32.05 | 29.75 | 29.66 | 31.54 | 31.78 | 31.7 |
| C17 | 71.21 | 71.48 | 79.00 | 78.99 | 72.06 | 71.83 | 71.8 |
| 17-$OCH_3$ | | | 56.71 | 56.71 | | | |
| C18 | 66.37 | 66.56 | 63.57 | 63.74 | 66.35 | 66.60 | 66.5 |

[a]All data were recorded in $CDCl_3$, with chemical shifts in ppm relative to $CDCl_3$, δ77.01
[b]Assignments uncertain.

**Table 4.5** $^{1}$H NMR data[a] for compounds described in Sections **4.4-4.10.**

| | $\Delta^3$ Mycalamide A (4.12) | 4α-Dihydro, 6-deoxy ps.A (4.13) | 4α-Dihydro, 6-deoxy ps.A triacet. (4.15) | 4α-Dihydro, 5,6-dehydrometh. myc.A (4.16) | 4-HCl,5,6-dehydrometh. B bis-ethyl carbonate (4.21) |
|---|---|---|---|---|---|
| **H2** | 4.19 (m) | 3.64 (2.2,6.4) | 3.56 (2.4,6.6) | 4.13 (1.7,6.5) | 4.18 (2.8,6.5) |
| **2-CH$_3$** | 1.30 (6.6) | 1.11 (6.4) | 1.10 (6.5) | 1.26 (6.6) | 1.30 (6.5) |
| **H3** | | 1.41 (m) | 1.42 (m) | 1.66 (1.7,5.9,7.1) | 2.53 (2.8,6.9) |
| **3-CH$_3$** | 1.58 (m) | 0.74 (7.0) | 0.74 (7.1) | 0.76 (7.0) | 1.03 (7.0) |
| **H4** | | 1.84 (m) | 1.82 (m) | 2.63 (1.4,5.8,7.3) | |
| **4-CH$_3$** | 1.63 (m) | 0.93 (6.8) | 0.91 (6.8) | 0.95 (7.4) | 1.58 (m) |
| **H5a** | 2.24 (m,17.6) | 1.40 (m) | 1.24 (m) | | |
| **H5e** | 2.08 (m,17.6) | 1.40 (m) | 1.17 (m) | 4.70 (m) | 5.15 (1.1) |
| **H6** | | 3.74 (4.0,5.1,8.8) | 3.86 (3.0,10.7) | | |
| **6-OCH$_3$** | 3.37 | | | | |
| **H7** | 4.30 | 4.00 (4.0) | 5.28 (3.0) | 4.48 (1.5) | 5.35 (1.0) |
| **NH9** | ? | 7.41 (9.9) | 6.95 (9.7) | 7.23 (9.8) | ? |
| **H10** | 5.82 (9.7) | 5.83 (10.0) | 5.74 (9.4) | 5.85 (9.8) | 5.67 (9.5) |
| **10-OCH*R*** | 5.12 (6.9) | 5.15 (7.0) | 5.10 (6.8) | 5.15 (6.7) | 5.14 (7.0) |
| **10-OCH*S*** | 4.86 (6.9) | 4.88 (7.0) | 4.84 (6.9) | 4.89 (6.9) | 4.88 (6.9) |
| **H11** | 3.79 (6.7,9.7) | 3.88 (6.7,10.1) | 3.85 (6.3,9.1) | 3.82 (6.8,10.1) | 3.94 (6.6,9.7) |
| **H12** | 4.21 (6.8,10.3) | 4.24 (6.8,10.4) | 4.16 (6.4,10.1) | 4.23 (6.9,10.5) | 4.22 (6.7,10.5) |
| **H13** | 3.44 (10.3) | 3.48 (10.4) | 3.42 (9.9) | 3.47 (10.6) | 3.44 (10.4) |
| **13-OCH$_3$** | 3.55 | 3.56 | 3.54 | 3.56 | 3.56 |
| **14-CH$_3$*R*** | 0.98 | 0.98 | 0.97 | 0.97 | 0.99 |
| **14-CH$_3$*S*** | 0.87 | 0.87 | 0.85 | 0.87 | 0.87 |
| **H15** | 3.61 (4.3,8.5) | 3.61 (6.4,8.5) | 3.37 (2.1,10.0) | 3.57 (m) | 3.35 (2.4,8.1) |
| **H16** | 1.57 (m) | 1.55 (m) | 1.76 (m) | 1.54 (m) | 1.72 (m) |
| **H16** | 1.57 (m) | 1.55 (m) | 1.62 (m) | 1.54 (m) | 1.62 (m) |
| **H17** | 3.71 (m) | 3.73 (m) | 4.98 (m) | 3.74 (m) | 3.36 (m) |
| **17-OCH$_3$** | | | | | 3.26 |
| **H18** | 3.57 (3.4,11.0) | 3.54 (3.5,11.3) | 4.22 (2.8,12.4) | 3.56 (3.6,11.4) | 4.19 (3.2,11.7) |
| **H18** | 3.38 (5.8,11.1) | 3.39 (5.9,11.3) | 4.05 (5.5,12.4) | 3.36 (6.1,11.3) | 4.04 (5.1,11.7) |
| **-OCH$_2$CH$_3$** | | | | | 4.15,1.27 (7.0) |

[a]All data were recorded in $CDCl_3$, with chemical shifts in ppm relative to $CHCl_3$, δ7.25 (coupling constants in Hz).

**Table 4.6** Biological assay results for compounds in Chapter 4.

| Compound | P388 $IC_{50}$[a] | Antiviral Results[b] (ng/disk) | | | | | | |
|---|---|---|---|---|---|---|---|---|
| Mycalamide A | 0.5 | WW | WW | +* | 5 | + | + | +* | 2 |
| Mycalamide B | 0.1 | WW | WW | +* | 2 | +++ | +++ | +* | 1 |
| 4α-Dihydro mycalamide A (**4.4**) | 0.8 | | WW | +* | 10 | | +++ | +* | 5 |
| 4β-Dihydro mycalamide A (**4.5**) | 0.2 | | WW | +* | 5 | + | + | +* | 2 |
| 4α-Dihydro mycalamide B (**4.6**) | 0.8 | | WW | +* | 10 | | +++ | +* | 5 |
| 4β-Dihydro mycalamide B (**4.7**) | 0.1 | | WW | +* | 5 | ++ | ++ | +* | 2 |
| 4α-Dihydro pseudo A (**4.10**) | 11 | WW | WW | +* | 200 | ++ | + | +* | 50 |
| 4β-Dihydro pseudo A (**4.11**) | 4 | WW | WW | +* | 20 | ++ | ++ | +* | 5 |
| $\Delta^3$ Mycalamide A (**4.12**) | 58 | WW | WW | +* | 1000 | +++ | ++ | +* | 500 |
| 4α-Dihydro, 6-deoxy ps.A (**4.13**) | 250 | WW | WW | +* | 2000 | - | - | - | 1000 |
| 4α-Dihydro, 5,6-dehyd.A (**4.16**) | 650 | +++ | +++ | +* | 2000 | + | ++ | +* | 1000 |
| Myc.A 4α-epoxide (**4.17**) | 115 | | WW | +* | 500 | | - | - | 200 |
| Myc.A 4β-epoxide (**4.18**) | 16 | | WW | +* | 100 | | + | +* | 50 |
| Myc.B 4α-epoxide (**4.19**) | 90 | | WW | +* | 500 | | - | - | 200 |
| Myc.B 4β-epoxide (**4.20**) | .4 | | WW | +* | 40 | | ++ | +* | 20 |

[a]In ng/ml. The derivatives are estimated to be better than 95% pure, having been subjected to at least two steps of chromatographic purification in most cases.
[b] -,+,++,+++,WW=antiviral zone size. Results are listed in the order of *Herpes simplex virus*, *Polio virus*, cytotoxicity, loaded sample mass.

**Table 4.7** $^1$H NMR data[a] for mycalamide A and B epoxides.

| | Mycalamide A 4α-epoxide (4.17) | Mycalamide A 4β-epoxide (4.18) | Mycalamide B 4α-epoxide (4.19) | Mycalamide B 4β-epoxide (4.20) |
|---|---|---|---|---|
| **H2** | 4.34 (2.5,6.6) | 4.15 (2.6,6.6) | 4.35 (2.4,6.6) | 4.18 (2.6,6.5) |
| **2-$CH_3$** | 1.21 (6.6) | 1.23 (6.6) | 1.22 (6.6) | 1.23 (6.6) |
| **H3** | 1.12 (1.3,2.5,7.1) | 1.26 (1.2,2.6,7.0) | 1.11 (1.2,2.5,7.0) | 1.25 (1.2,2.6,7.0) |
| **3-$CH_3$** | 1.00 (7.1) | 1.02 (7.0) | 1.01 (7.0) | 1.04 (7.0) |
| **4-CH*Z*** | 2.55 (4.5) | 2.80 (5.0) | 2.53 (4.5) | 2.79 (4.9) |
| **4-CH*E*** | 2.52 (4.5) | 2.71 (1.5,5.0) | 2.51 (4.6) | 2.69 (1.5,5.0) |
| **H5a** | 2.22 (14.7) | 2.10 (1.5,13.4) | 2.13 (14.6) | 2.03 (1.6,13.4) |
| **H5e** | 1.43 (1.3,14.7) | 1.43 (1.1,13.4) | 1.44 (1.2,14.6) | 1.42 (1.2,13.3) |
| **6-$OCH_3$** | 3.37 | 3.31 | 3.37 | 3.32 |
| **H7** | 4.31 | 4.32 | 4.30 | 4.31 |
| **NH9** | 7.41 (10.0) | 7.33 (9.9) | 7.45 (9.4) | 7.43 (9.6) |
| **H10** | 5.88 (9.9) | 5.88 (9.8) | 5.77 (9.6) | 5.80 (9.6) |
| **10-OCH*R*** | 5.14 (6.9) | 5.14 (6.9) | 5.13 (7.0) | 5.13 (7.0) |
| **10-OCH*S*** | 4.88 (6.9) | 4.88 (6.9) | 4.85 (7.0) | 4.86 (7.0) |
| **H11** | 3.86 (6.8,9.9) | 3.86 (6.7,9.8) | 3.82 (6.7,9.7) | 3.81 (6.8,9.6) |
| **H12** | 4.23 (6.8,10.4) | 4.24 (6.7,10.4) | 4.22 (6.7,10.3) | 4.23 (6.6,10.4) |
| **H13** | 3.47 (10.4) | 3.46 (10.4) | 3.44 (10.3) | 3.45 (10.7) |
| **13-$OCH_3$** | 3.56 | 3.56 | 3.55 | 3.56 |
| **14-$CH_3$*R*** | 0.98 | 0.98 | 0.98 | 0.99 |
| **14-$CH_3$*S*** | 0.88 | 0.88 | 0.87 | 0.88 |
| **H15** | 3.62 (5.3,6.9) | 3.60 (3.2,9.1) | 3.38 (2.4,9.6) | 3.42 (1.9,9.9) |
| **H16** | 1.57 (m) | 1.63 (m) | 1.59 (3.3,9.7,14.2) | 1.65 (4.1,10.0,14.2) |
| **H16** | 1.57 (m) | 1.57 (m) | 1.50 (2.3,9.4,14.1) | 1.52 (2.0,9.6,14.1) |
| **H17** | 3.74 (m) | 3.73 (m) | 3.25 (m) | 3.24 (m) |
| **17-$OCH_3$** | | | 3.30 | 3.32 |
| **H18** | 3.56 (m) | 3.56 (m) | 3.62 (3.1,12.0) | 3.67 (3.3,11.8) |
| **H18** | 3.38 (5.8,11.2) | 3.39 (6.1,11.1) | 3.46 (6.3,12.0) | 3.44 (5.8,11.9) |

[a]All data were recorded in $CDCl_3$, with chemical shifts in ppm relative to $CHCl_3$, δ7.25 (coupling constants in Hz).

**Table 4.8** $^{1}H$-$^{1}H$ NOE interactions[a] for mycalamide A and B epoxides.

| Compound | Signal(s) Irradiated | Signals enhanced (% enhancement) |
|---|---|---|
| Mycalamide A | H2 | 2-$CH_3$(2), H3(2), 6-$OCH_3$(0.7) |
| 4α-epoxide (**4.17**) | H3 (2-$CH_3$) | H2(8), 3-$CH_3$(2), 4-CH*Z*(4) |
| | 3-$CH_3$ | H3(3), H5a(3) |
| | 4-CH*E* | 4-CH*Z*(15), H5e(3) |
| | 4-CH*Z* | H3(2), 4-CH*E*(12) |
| | H5a | 3-$CH_3$(0.8), H5e(16), H7(1) |
| | H5e | 4-CH*E*(4), H5a(21) |
| Mycalamide A | H2 (H7) | 2-$CH_3$(0.9), 6-$OCH_3$(0.8) |
| 4β-epoxide (**4.18**) | 2-$CH_3$ | H2(6) |
| | H3 | H2(6), 4-CH*Z*(2) |
| | 3-$CH_3$ (14-$CH_3$*R*) | 4-CH*Z*(2), H5a(2), H13(3)[b], H15(2)[b], $H_2$16(2)[b] |
| | 4-CH*E* | H5e(5) |
| | 4-CH*Z* | H3(3) |
| | H5a | 3-$CH_3$(0.6), H5e(20), H7(3) |
| | H5e | 4-CH*E*(3), H5a(19), H7(0.6) |
| | H7 (H2) | 6-$OCH_3$(3), H5a(1) |

[a]All data were recorded in $CDCl_3$

[b]Enhancement interpreted as being due to the irradiation of an overlapping signal

**Table 4.9** $^{13}C$ NMR data[a] for mycalamide A and B epoxides.

| | Mycalamide A 4α-epoxide (4.17) | Mycalamide A 4β-epoxide (4.18) | Mycalamide B 4α-epoxide (4.19) | Mycalamide B 4β-epoxide (4.20) |
|---|---|---|---|---|
| **C2** | 67.17 | 68.78 | 67.17 | 68.83 |
| **2-$CH_3$** | 17.55 | 17.72 | 17.57 | 17.78 |
| **C3** | 39.72 | 39.95 | 39.75 | 40.08 |
| **3-$CH_3$** | 9.76 | 7.93 | 9.82 | 8.04 |
| **C4** | 58.42 | 58.59 | 58.32 | 58.42 |
| **4-$CH_2O$** | 50.69 | 56.90 | 50.51 | 56.58 |
| **C5** | 31.40 | 32.23 | 31.39 | 31.99 |
| **C6** | 99.65 | 100.47 | 99.69 | 100.73 |
| **6-$OCH_3$** | 49.03 | 48.60 | 48.88 | 48.36 |
| **C7** | 73.25 | 72.60 | 72.81 | 71.63 |
| **C8** | 171.36 | 171.53 | 171.32 | 171.43 |
| **C10** | 73.61 | 73.76 | 73.78 | 73.96 |
| **10-$OCH_2$** | 86.89 | 86.83 | 86.61 | 86.52 |
| **C11** | 71.40 | 71.27 | 70.83 | 70.88 |
| **C12** | 74.48 | 74.46 | 74.49 | 74.47 |
| **C13** | 79.17 | 79.11 | 79.37 | 79.35 |
| **13-$OCH_3$** | 61.86 | 61.86 | 61.82 | 61.81 |
| **C14** | 41.74 | 41.71 | 41.53 | 41.74 |
| **14-$CH_3$*R*** | 23.05 | 23.07 | 23.17 | 23.18 |
| **14-$CH_3$*S*** | 13.39 | 13.40 | 13.38 | ? |
| **C15** | 79.02 | 78.75 | 75.38 | 75.58 |
| **C16** | 31.94 | 32.23 | 29.48 | 29.73 |
| **C17** | 71.66 | 71.14 | 79.25 | 78.78 |
| **17-$OCH_3$** | | | 56.74 | 56.72 |
| **C18** | 66.56 | 66.44 | 63.95 | 63.36 |

[a]All data were recorded in $CDCl_3$, with chemical shifts in ppm relative to $CDCl_3$, δ77.01.

# CHAPTER 5
# REACTIONS OF MYCALAMIDES A & B AND DERIVATIVES UNDER BASIC CONDITIONS
# PART I

## 5.1 INTRODUCTION

During early chemical degradations on pederin, it was noted that pederin was not affected by heating with a dilute solution of barium methoxide in methanol[27]. This base stability of pederin was utilised in its synthesis. An example of this was the removal of the benzoate ester protecting group with (1M) lithium hydroxide at either room temperature[90,127] or at 50°C[129,132] in a final step. However, pseudopederin (**3.5**) was readily attacked by a barium methoxide solution at room temperature[27,94] and gave pederolactone (**3.6**) and meropederoic acid (**5.1**) as major products, especially when performed in an oxygen atmosphere. (This reaction occurred by cleavage of the C6-C7 bond in a retro-aldol process, followed by oxidation at C7). The same products were also formed when pseudopederin was treated with piperidine[27,94]. Unfortunately, no biological activity data were reported for these cleavage products.

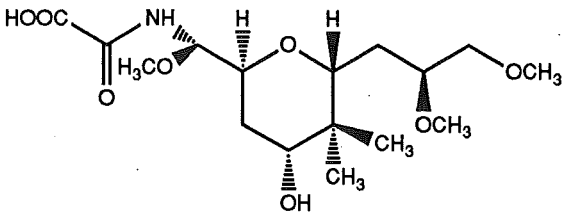


Meropederoic acid (**5.1**)

The treatment of mycalamides A and B with mild bases has been indirectly described in previous chapters. In Chapter 2, both structures were

shown to be stable to pyridine and other amine bases during esterification and silylation reactions, even at 80°C. This stability was extensively utilised for buffering $CDCl_3$ solutions of mycalamide derivatives with pyridine or triethylamine, to prevent acid catalysed decomposition[139], as had been performed for pederin[95] and its derivatives[126]. However, at higher temperatures (130-150°C) in DMSO, it was found that these bases catalysed an elimination of methanol at C5-C6 in mycalamide A, as described in Chapter 3. Mycalamides A and B were also stable to other mild bases at room temperature, as illustrated by the successful removal of acetate ester groups from acetylated derivatives, using solutions of potassium carbonate in aqueous methanol (Chapter 2).

The current investigation of the reactivity of mycalamides A and B to various bases in different solvents and at different temperatures was conducted, initially, for two reasons. Firstly, it was desirable to determine how stable these structures were to base, for use in future synthetic modifications. A second, more direct aim was the base hydrolysis of the amide functionality, which was assumed to be the most base sensitive functional group, apart from the possibility of rearrangement of the exocyclic double bond[196]. In particular, the acetal functionalities, which were most acid sensitive, were expected to be base stable, as in pederin. This chapter describes the first part of this investigation, which yielded some surprising results.

## 5.2 INITIAL INVESTIGATIONS ON MYCALAMIDE A

### 5.2.1 EFFECT OF 0.1M SODIUM HYDROXIDE ON THE P388 ACTIVITY OF MYCALAMIDE A

A small sample of mycalamide A, dissolved in a solution of sodium hydroxide in 90% water/methanol (0.1M), was assayed after two hours and

three days at ambient temperature. Both results were the same as for the control sample, suggesting that mycalamide A was stable to these conditions.

### 5.2.2 SMALL SCALE REACTIONS MONITORED BY TLC AND HPLC

A sample of mycalamide A was treated with a 3mM solution of sodium methoxide in methanol. No reaction was observed by TLC after 5 days at room temperature. Similarly, treatment with a 30mM solution at room temperature and at 40°C for several hours gave no reaction, as monitored by reverse phase HPLC. Finally, mycalamide A was treated with a 1M solution of sodium methoxide at room temperature. There was no evidence of reaction after three hours, but, after 1 day, the starting material had disappeared and there was at least one, more polar product by HPLC. TLC confirmed this in an unusual way, since the observed products were of similar $R_f$ to mycalamide A, but gave a bright blue char following treatment with the usual anisaldehyde reagent (see Experimental) and heating, instead of the usual orange-brown colour. Further preparations and spectroscopic characterisations of these products are therefore described below.

## 5.3 PREPARATION AND CHARACTERISATION OF COMPOUNDS FROM THE REACTION OF MYCALAMIDES A AND B IN THE PRESENCE OF SODIUM METHOXIDE AND OTHER BASES

### 5.3.1 PREPARATION AND SEPARATION OF PRODUCTS

The above reaction was successfully repeated on a larger scale, but this time required gentle heating to achieve complete reaction. TLC of the product clearly showed two distinct spots, not quite resolved, and a $^1H$ NMR spectrum confirmed that there were indeed two similar compounds, in a ratio

of about 4:3. Analysis by reverse phase HPLC showed that there was almost baseline resolution of the two products so preparative HPLC was performed to separate them for spectroscopic analysis.

### 5.3.2 SPECTROSCOPIC CHARACTERISATIONS

HRFABMS spectra of these products showed that they were isomers, with molecular formulae $C_{23}H_{39}NO_9$, which represented a loss of $CH_2O$ from mycalamide A. The $^1H$ NMR spectra of both products showed a loss of the 10-$OCH_2$ doublets of mycalamide A, loss of the coupling between the H10 and amide NH protons and the appearance of a new long range coupling between the H7 and H10 protons. These data could only be satisfied if there was a new 5-membered oxazolidinone ring, arising from a substitution of C7-$O^-$ at C10, with a loss of formaldehyde from the C10-C12 methylene acetal of mycalamide A, to leave an hydroxyl group at C12 (structures **5.2** and **5.3**). In particular, the long range coupling between H7 and H10 could only occur if they were fixed in a ring, and such couplings in 2,5-substituted 1,3-oxazolidin-4-ones are well documented[208,209], as discussed below. Furthermore, the IR spectra of both isomers contained an amide carbonyl stretch at 1715-1720 $cm^{-1}$, which represented a 25-30 $cm^{-1}$ increase in frequency over the value recorded for mycalamide A. This result is consistent with the constrained *cis* geometry of a 5-membered lactam ring[96,210], compared with a normal open chain secondary amide, which would be predominantly *trans* (*Z*) in conformation[107]. Also, preliminary NOE experiments showed that there was an NOE interaction between the H7 and H10 protons in one of the isomers only. This isomer was therefore *cis* (**5.2**), and was the major compound in the initial $^1H$ NMR spectrum of the mixture. Further NOE results are described below in an analysis of the solution conformations of these compounds.

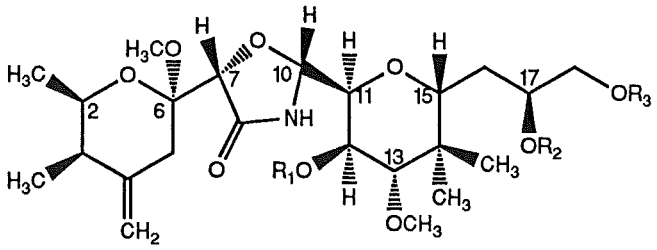

$R_1$=$R_2$=$R_3$=H: Mycalamide A *cis* oxazolidinone (**5.2**)
$R_1$=$R_3$=H, $R_2$=$CH_3$: Mycalamide B *cis* oxazolidinone (**5.9**)

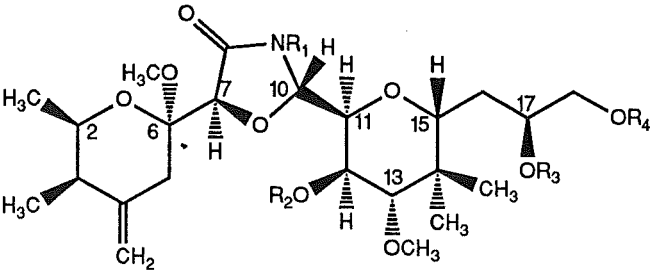

$R_1$=$R_2$=$R_3$=$R_4$=H: Mycalamide A *trans* oxazolidinone (**5.3**)
$R_1$=$R_2$=$R_4$=H, $R_3$=$CH_3$: Mycalamide B *trans* oxazolidinone (**5.10**)
$R_1$=$R_2$=$R_3$=$R_4$=$COCH_3$: *N*-Acetyl myc.A *trans* oxazolidinone triacetate (**5.13**)
$R_1$=$R_2$=$R_3$=$R_4$=$CH_3$: 12,17,18-tri-*O*-Methyl, *N*-methyl myc.A *trans* oxaz.(**5.14**)

The $^1$H NMR spectra of both compounds were therefore assigned using results obtained from COSY experiments, to give the data in Table 5.1. A comparison of the data for the *cis* and *trans* isomers, respectively, with those for mycalamide A, showed that the largest chemical shift differences (in ppm) occurred in the signals assigned to H7 (+0.1), NH (-0.9, +0.4), H10 (-0.3), H12 (-0.2) and H13 (-0.5). These shifts cannot be explained entirely by the usual substituent effects[101]. However, it is likely that the shifts in H10, H12 and H13 partly reflect the release of steric deshielding effects[123], associated with the 10/12-$OCH_2$ group in the *cis*-fused trioxadecalin ring system of mycalamide A. The observed chemical shifts for both isomers were similar, except for those of the NH proton, reflecting its different hydrogen bonding environments in the two compounds[101]. Note that, in general, the C2 and C5 oxazolidinone ring protons in a *cis* relationship are reported to be slightly shielded relative to

those in a *trans* relationship[209], which is also consistent with results found here for the H7 and H10 proton resonances (Table 5.1).

A long range coupling of between 1 and 3 Hz is commonly observed between protons at C2 and C5 in 1,3-oxazolidin-4-ones and is reported to arise from a mechanism through 5 bonds which involves the partially developed $\pi$ system of the amide C-N bond[209]. The magnitude of such couplings in various ring systems[209] appears to depend on the degree of $\pi$ character in this bond between the ring atoms 3 and 4, since a full double bond (such as in a lactone) gives large couplings (5.7 Hz in furanomycin), whereas the absence of a $\pi$ system gives virtually no such coupling. The magnitude of this coupling is also typically larger for the *trans* isomer[209], which was the result found for these mycalamide derivatives. Similar long range couplings between protons in a *trans* relationship have been observed across lactone groups in 1,3-dioxolan-4-ones[211,212] and have been explained by a similar mechanism.

A $^{13}C$ NMR spectrum was recorded for each isomer and the signals assigned by HMQC experiments, to give the data in Table 5.2. An HMBC experiment was also performed on the *trans* isomer, which confirmed the assignments of the quaternary carbon resonances, but did not add any new information (Table 5.3). Compared with the mycalamide A data, there were sizeable shifts in the signals assigned to C7 (+2.9, +4.4), C10 (+7.2, +12.8), C11 (+6.4, +3.0), C12 (-5.4, -5.4) and C13 (+9.0, +7.9) for the *cis* and *trans* isomers, respectively. The direction of these shifts at C11, C12 and C13 were consistent with the usual $\alpha$ and $\beta$ substituent effects associated with converting C12-OR (R=alkyl) into C12-OH[117]. However, the downfield shifts for the C10, C11 and C13 resonances must also have a sizeable contribution from the loss of gauche shielding interactions with the 10/12-$OCH_2$ group[117], as observed for the $^1H$ NMR data above. The differences between the

isomers were largest for the C10 resonance (5.6 ppm), in accordance with a change in stereochemistry at this position, although most of the other C7-C15 resonances also showed significant differences. Also the linewidths of most of the C11-C16 resonances were considerably larger for the *trans* isomer only (Table 5.2), an effect which is discussed further in the following subsection.

### 5.3.3 SOLUTION CONFORMATIONS BY NMR SPECTROSCOPY

The O1-C6 tetrahydropyran rings of both isomers were found to have the same solution conformation as that observed for mycalamides A and B, as expected. (This was shown by the observed NOE interactions between the C3 methyl and H5a protons (Table 5.4) and by the similar proton-proton coupling constants in these compounds). There also appeared to be a similar distribution of solution conformations about C6-C7 in both isomers as discussed for mycalamide B (Chapter 1), as indicated by the strong H7-6-$OCH_3$ and weaker H5a-H7 NOE interactions (Table 5.4).

For the *cis* isomer (**5.2**), there were NOE interactions between the H7 and H10 protons and between the two H5 protons and H11 which clearly demonstrated the stereochemistry of the oxazolidinone ring (Figure 5.1a). For the *trans* isomer (**5.3**), there were NOE interactions between the two H5 protons and H10 and between the H7 and H11 protons, which further confirmed the relative stereochemistries. These NOE results also required that a major solution conformation of both isomers have H7 gauche to 6-O and anti to C5, and that H10 be anti to H11 (Figure 5.1b), as in mycalamide A. The latter is almost certainly the case in the *cis* isomer, since the H10-H11 coupling constant is about 9 Hz, but a considerably smaller value was observed in the *trans* isomer (5.4 Hz). However, there were strong NOE interactions between the H10 and both the H13 and H15 protons in *both* isomers, showing that a major solution conformation does have this anti

relationship between H10 and H11. Note, however, that these NOE interactions appeared to be significantly weaker for the *trans* isomer, and that there was a small NOE interaction between H10 and H11 in both isomers, suggesting the presence of another, minor rotamer, having H10 and H11 gauche.

**Figure 5.1** $^{1}H$-$^{1}H$ NOE interactions and partial solution conformations for mycalamide A *cis* and *trans* oxazolidinones (**5.2** and **5.3**).

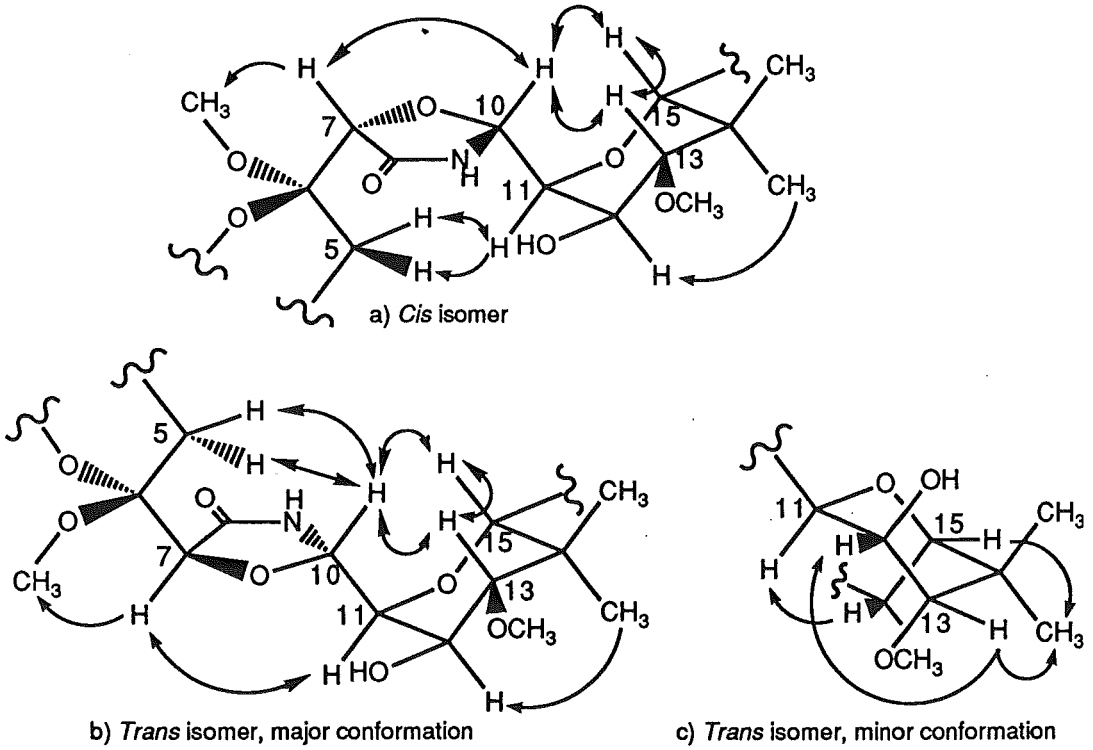


The vicinal proton-proton coupling constants for the C11-C15 tetrahydropyran ring substituents in the *cis* isomer (**5.2**) were similar to those in mycalamides A and B. There were also similar NOE interactions between the axial substituents, such as between H13 and H15, and between H12 and 14-$CH_3S$, suggesting that this C11-C15 ring had the same chair conformation in these compounds. The *trans* isomer (**5.3**) also showed similar NOE interactions to those above, but had additional weaker NOE interactions between the H10 and H12, H12 and H13, H13 and 14-$CH_3S$, and H11 and

H16 protons, suggesting the presence of an alternate chair conformation for this ring (Figure 5.1c). The H10-H11, H11-H12 and H12-H13 coupling constants were also significantly lower for the *trans* isomer than for the *cis* isomer. Conformational averaging between the two chair conformations[102] is proposed to account for all these results on the *trans* isomer. Such exchange was earlier investigated for mycalamide A[19], pederin and pederin dibenzoate[84] (**1.2**) in Chapter 1.

A known method of probing such exchange is to observe the linewidths of affected signals in the $^{13}C$ NMR spectrum as a function of temperature[114,115,121]. Although this was not feasible in the present case due to the small sample size, the spectrum at 23°C did show significant line broadening for several signals assigned to carbon atoms from C10 to C16, particularly those for C11 and 14-$CH_3S$, where the linewidths were 10.2 and 8.4 Hz, respectively, compared with the normal 2 Hz (Table 5.2). Such exchange could also account for changes in chemical shift for many of these resonances, since these would be a weighted average of those in the two conformations.

The effect of the solvent on this exchange was considered by recording the $^1H$ NMR spectra of both isomers in $CD_3OD$ (Table 5.1). Allowing for slight changes in chemical shift with solvent, the data for the *cis* isomer (**5.2**) were almost identical to those recorded in $CDCl_3$. An exception was that some different coupling constants were observed for those resonances corresponding to protons on the C16-C18 sidechain, as expected from earlier studies on mycalamide A (Chapter 1). (An analysis of the coupling constant data for this portion will be presented in a later section). The $^1H$ NMR data in $CD_3OD$ for the *trans* isomer (**5.3**) were also similar to those in $CDCl_3$, except for differences noted above, and importantly, the vicinal proton-proton coupling constants for the H10-H13 portion, which were even smaller than

those observed in $CDCl_3$. This suggested a higher proportion of the alternate chair conformation for the C11-C15 ring of the *trans* isomer in this solvent, and, possibly, the presence of other C10-C11 rotamers. However, the results of some NOE experiments for this isomer in $CD_3OD$ were comparable to those recorded in $CDCl_3$. This was the first mycalamide derivative to have a significant proportion of both chair conformations for this ring in solution. Therefore, in order to investigate this more thoroughly, a molecular mechanics modelling approach was considered.

### 5.3.4 SOLUTION CONFORMATIONS BY MOLECULAR MODELLING

There were three main aims for the investigation of the solution conformations of the mycalamide A oxazolidinone isomers using molecular modelling:-

i) to show that both the C11-C15 tetrahydropyran ring chair conformers were similar in energy, and thus were accessible solution conformations;

ii) to determine the influence of the configuration at C10, and the different hydrogen bonding possibilities on the populations of various conformations;

iii) to calculate averaged coupling constants for the various structures which could be compared with the experimental results.

The computer program used for this work was a modified MODEL program[125], which used MM2 parameters and allowed either grid or statistical conformational searches to be performed, in order to generate a set of lowest energy conformations[122] (conformers having minimised energies within 12.6 kJ $mol^{-1}$ of the lowest energy conformer would be accepted). These were analysed using another computer program[213] to calculate vicinal proton-proton coupling constants, using Haasnoot's generalisation of the Karplus equation[103], and dihedral angles for all the MM2 calculated geometries. These calculated coupling constants could be weighted according to the

minimised energies (and thus the relative populations) of the various conformers.

### 5.3.4.1 GRID SEARCH FOR CONFORMATIONS OF THE C11-C15 RING SUBSTITUENTS

The structures of the mycalamide A oxazolidinone isomers (**5.2**, **5.3**) were too conformationally flexible to perform a complete grid search[124] analysis on the entire molecules[122]. Therefore the structures were simplified to concentrate on interactions between the oxazolidinone and the C11-C15 tetrahydropyran rings, by initially setting a methyl group at C7 in place of the O1-C6 ring and a methyl group at C15 in place of the C16-C18 sidechain. This gave two model structures representing the *cis* and *trans* isomers, differing in the configuration at C10, but having C10 axial to the C11-C15 ring, in the normal chair conformation (structures **5.4A** and **5.5A** - see Figure 5.2). A further two structures for these isomers were also generated, having C10 equatorial to the C11-C15 ring, in the alternate chair conformation (structures **5.4B** and **5.5B** - see Figure 5.2). Grid searches were then performed on all four starting structures, allowing 120° rotations[124,214] about the C10-C11, C12-O and C13-O bonds in the first instance, so that minimised energies could be calculated for all combinations of the three staggered rotamers of these bonds.

The results of this search and a subsequent analysis are summarised in Table 5.6. The conformations obtained have been listed in order of increasing energy for each of the four structures, **5.4A**, **5.4B**, **5.5A** and **5.5B**, respectively, and described by the dihedral angles of the three rotatable bonds. An abbreviated notation for this large set of angles, described in a recent publication[215], has been introduced as a useful method of classifying and comparing the conformers. Here 'A' represents an anti, '-' a (-) gauche,

and '+' a (+) gauche conformation for a particular dihedral angle, in the order C10-C11, C12-O and C13-O, as described in Table 5.5. (The typical bounds for such classifications[214] are (+) gauche 1-119°, (-) gauche -1-(-119°), and anti 121-(-120°)). Vicinal proton-proton coupling constants from C10 to C13 have been calculated for each conformer and the presence of hydrogen bonds has also been noted.

**Figure 5.2** Structures of the model conformers **5.4A**, **5.4B**, **5.5A**, **5.5B**, **5.5C** and **5.5D** used for a grid search, showing the rotatable bonds considered (in bold).

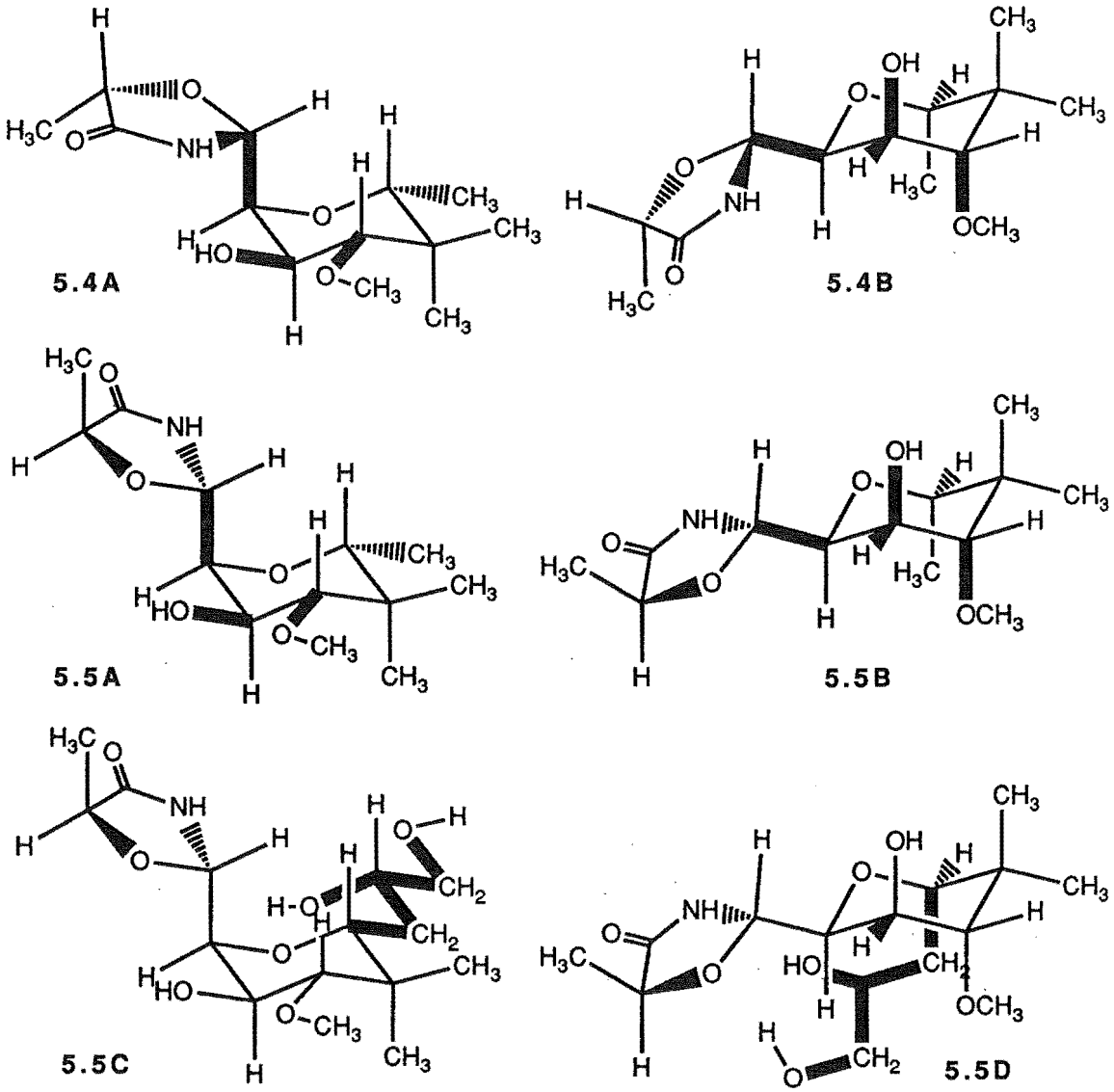

The results show that the lowest energy conformers of the **5.4A**, **5.4B**, **5.5A** and **5.5B** structures were all within 12 kJ $mol^{-1}$, but that the alternate chair conformers (of **5.4B** and **5.5B**) were energetically favoured in each case, contrary to the experimental evidence. The position of the C13 methoxyl group was almost the same in each of the low energy conformers, whereas all rotamers of the C12 hydroxyl group were represented, often with a significant effect on the energy (see conformers 2 and 7 for structure **5.4A**). All rotamers about C10-C11 were also represented and the lowest energy conformers of **5.5A** did not have H10-H11 anti, as required by the observed NOE interactions between H10 and H13 and H15 above. In several cases hydrogen bonds were noted between the amide NH proton and C12-O and between C12-OH and one or more of the C10, C11 and C13 oxygen atoms. The conformers with these hydrogen bonds seemed to fit the NOE results better, since anti H10-H11 conformers were better represented. It has been reported[215] that the MM2 method is not appropriate for the study of hydrogen bonds, as the calculated bonds are not sufficiently strong and are usually too long, and this could account for some discrepancies in the results. (Entropy and solvation effects are also not considered by such calculations[216]). Note that the energy differences between these conformations were not large and some contribution to the error may also have been caused by limitations in the model structures themselves. Whatever the reason, it was clear that the size of the H10-H11 coupling constant could not be studied, nor the absolute energies used to weight the coupling constants between the two chair structures. However, the H11-H12 and H12-H13 coupling constants were similar over the range of conformers within each structure, as expected with the protons being located on a ring, so these represented useful results. A complete discussion and analysis of this work is presented following the second part of this investigation.

### 5.3.4.2 GRID SEARCH FOR CONFORMATIONS OF THE C15-C18 SIDECHAIN

Grid search methods have found only limited use for large molecules, due mainly to the many degrees of freedom of such structures, but this has sometimes been circumvented by the use of 'build-up' procedures[124]. These procedures use the approximation that the conformation of a molecule is largely dependent on short range interactions, so that small segments can be minimised in grid searches, and the lowest energy conformations pieced together. A similar approach was used here to study conformations of the C15-C18 sidechain of mycalamide A *trans* oxazolidinone (**5.3**) for the two possible chair conformations of the C11-C15 ring. The lowest energy conformer of each of the structures **5.5A** and **5.5B** was modified to include the full sidechain of mycalamide A, and then the resulting structures (**5.5C** and **5.5D**) were subjected to a full grid search, allowing 120° rotations about the C15-C16, C16-C17, C17-O, C17-C18 and C18-O bonds.

The results of the two searches are shown in Table 5.7. It is readily apparent that all the lowest energy conformations have the C14-C15-C16-C17 dihedral angle in an anti conformation, and this strong preference is well known for C-glycosides[116]. This result is reflected in the calculated coupling constants between the H15 and the two H16 protons, which were similar for all conformers of both starting structures. (Note that, for the purposes of this analysis, the H16 protons have been designated as pro-*R* (gauche to H15) and pro-*S* (anti to H15). These prochirality assignments are opposite to those stated for pederin and pederin dibenzoate (**1.2**) due to the difference in the C17 substituent[100,112]). Amongst the remaining dihedral angles, there was about equal preference for anti and (+) gauche conformations with few (-) gauche conformations observed for the angles specified. The coupling constants for the rest of the sidechain therefore varied considerably over the

various conformations. However, for structure **5.5C**, there were three low energy conformations which represented about 72% of the total calculated population, while for structure **5.5D**, there were only two low energy conformations which represented about 82% of the total calculated population. The best three sidechain conformers were the same in both searches, and two were found to have hydrogen bonds between C17-OH and C15-O and between C18-OH and C17-O, and a third had a hydrogen bond between C17-OH and C18-O, with four of the five dihedral angles in an anti conformation. These conformations are depicted in Figure 5.3. There were also many other low energy conformations, which have been included in Table 5.6 to give some understanding of the appearance of these higher energy conformations, which vary between the two structures. An analysis of the average coupling constants is presented below.

**Figure 5.3** Major conformations of the C16-C18 sidechain of mycalamide A *trans* oxazolidinone (**5.3**), as calculated by molecular modelling.

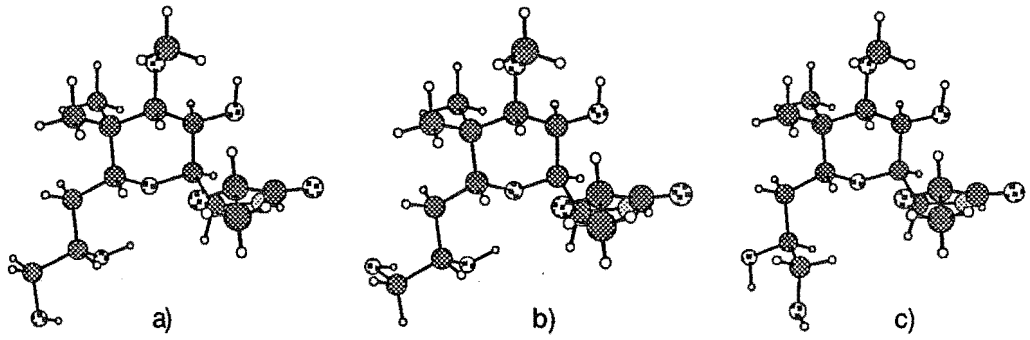


5.3.4.3 COMPARISON OF EXPERIMENTAL AND CALCULATED COUPLING CONSTANTS

The average proton-proton coupling constants for each structure have been calculated by weighting the individual values for each conformer according to its relative population, as estimated by applying a Boltzmann distribution to the individual energies. These results have been presented in a

combined format in Table 5.7 and compared with, primarily, experimental values for the mycalamide A *cis* and *trans* oxazolidinones (**5.2**, **5.3**) measured in $CDCl_3$ solution, rather than those measured in $CD_3OD$. This is because the molecular modelling program considers the molecule in the gas phase, or in a non-polar solvent[215], where intramolecular hydrogen bonds are important, whereas $CD_3OD$ is a solvent which disrupts such bonds, being itself a good hydrogen bond acceptor. There are situations where the presence or absence of hydrogen bonds makes less difference to the conformation, such as within the C11-C15 tetrahydropyran ring, so comparisons of the calculated and experimental data in both solvents are probably justified in this case (H11-H12 and H12-H13 coupling constants).

The first part of Table 5.7 shows the calculated average coupling constants for H10-H11, H11-H12 and H12-H13, derived from grid searches on structures **5.4A**, **5.4B**, **5.5A** and **5.5B**. (These values represent an average of the calculated values for each conformer, weighted by the Boltzmann distribution of their energies). It is clear that there is only reasonable agreement between experimental values for the *cis* isomer (**5.2**) and calculated average values for conformers of the **5.4A** structure, but any contribution to the calculated values from conformers derived from structure **5.4B** would result in poorer agreement. Clearly, only the H11-H12 and H12-H13 coupling constants can be compared, for reasons discussed above involving the contribution of other C10-C11 rotamers. Thus, if only these coupling constants are considered, then this analysis correctly predicts that the C11-C15 ring of mycalamide A *cis* oxazolidinone (**5.2**) must be almost completely in one chair conformation. For the *trans* isomer (**5.3**), the experimental values for these two coupling constants lay between the average values for a single chair conformation (structures **5.5A** and **5.5B**) so that some combination of the two is required. As stated earlier, this could not be

done by applying a Boltzmann distribution over the two sets of conformers for the model structures **5.5A** and **5.5B** because of the much lower energy of the **5.5B** conformers, giving a result close to that shown for a 100% contribution of the latter, in marked contrast to the experimental results. The calculation of intermediate ratios of the two averaged results for conformers of structures **5.5A** and **5.5B** could be justified only because of the small variance of the individual values for each structure (Table 5.5), so that this approximates an interleaving of the two sets of results. Within the limited accuracy of this approach, it appears that an overall contribution of about 80% and 20%, respectively, of conformers from structures **5.5A** and **5.5B** could satisfy both the coupling constants and earlier NOE results for the *trans* isomer (**5.3**) in $CDCl_3$ solution (with the relative contributions in $CD_3OD$ being closer to 70% and 30%, respectively).

The remainder of Table 5.7 shows the calculated average coupling constants between protons on the C15-C18 portion of conformers derived from the modified structures **5.5C** and **5.5D**. There were only small differences between these values for the two structures, representing the two chair conformations of the C11-C15 ring, and comparison with experimental values in $CDCl_3$ solution was surprisingly good, apart from a larger calculated H15-H16*S* coupling constant than observed. This suggests that the three major solution conformations of the sidechain stated above, which have the most influence on the size of the average coupling constant, are also the major solution conformations in $CDCl_3$. These conformations also agree with partial NOE data for this portion (Table 5.3). Since there was little difference between the results for conformers of the two structures **5.5C** and **5.5D**, the relative contributions of conformers from the two structures was not important.

The experimental coupling constants measured in $CD_3OD$ for this portion of the structure were rather different, although the H15-H16 coupling constants were similar, suggesting that the same preference for the C14-C15-C16-C17 dihedral angle to be in an anti conformation still existed. The differences here can be rationalised by the lower preference for conformations having intramolecular hydrogen bonds, such bonds being disrupted in this solvent. No attempt was made to investigate this further.

## 5.4 BASE CATALYSED REACTIONS OF MYCALAMIDES A AND B IN OTHER SOLVENTS

The above sections have described the products obtained from the reaction of mycalamide A with sodium methoxide in dry methanol. If the observed reaction were simply base catalysed, as expected, then it should occur for a range of other base and solvent systems. Indeed, it was found subsequently that the reaction of mycalamide A in DMSO with either barium oxide or potassium hydroxide gave the same oxazolidinone isomers (Table 5.8 and Experimental). However, there was a significant increase in the proportion of the *cis* isomer in the product mixtures from these latter reactions, a point which will be discussed further in a later section.

Under more forcing conditions, the reaction of mycalamide A with potassium hydroxide in DMSO gave a single rearranged oxazolidinone derivative in lower yield. HRFABMS showed that it was an isomer of the earlier compounds. The $^1H$ NMR spectrum of this product was similar to that of mycalamide A *cis* oxazolidinone (**5.2**), but the C4 exocyclic methylene signals and two H5 resonances had been replaced by new signals for an allylic methyl and methine, at $\delta$1.77 and 5.33 ppm, respectively, having a long range coupling[104] of 1.5 Hz. This suggested the formation of a $\Delta^{4(5)}$ isomer

(**5.6**) by a base catalysed rearrangement of the exocyclic double bond into the O1-C6 ring[196]. This compound had the C6 acetal group in an allylic position, so it was not expected to be very stable and was therefore not investigated further.

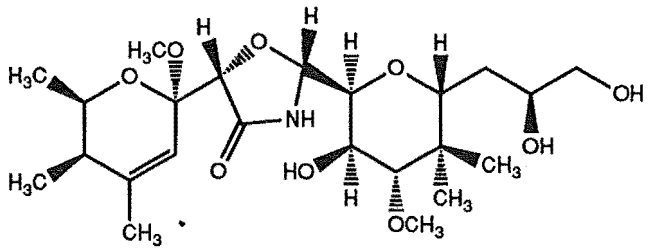

$\Delta^{4(5)}$ Mycalamide A *cis* oxazolidinone (**5.6**)

The reaction of mycalamide A with sodium hydroxide in mixed aqueous solvents was slower and gave two new products in addition to the mycalamide A *cis* and *trans* oxazolidinones by HPLC. These products were separated by HPLC and shown by HRFABMS to be isomers of the original products (**5.2**, **5.3**), although they coeluted with residual mycalamide A, and this represented about a 25% impurity in both samples. The $^1$H NMR spectra of these products were similar to those of the earlier isomers, and were assigned by a combination of NOE and COSY experiments (Table 5.1). However, there were large changes in the chemical shift of the H5 protons (0.2-0.6 ppm), and smaller shifts in the positions of the 6-$OCH_3$, H7 and NH proton resonances. There were long range couplings between H7 and H10 of 1.3 and 2.1 Hz, signifying new *cis* and *trans* oxazolidinone isomers[209], respectively. NOE interactions were observed between the H7 and H10 protons and between *both* H5 protons and H7 for the new *cis* isomer (Table 5.10), and this isomer showed averaged coupling constants for the C10 to C13 portion and chemical shifts from NH9 onwards which were similar to those observed for the original *trans* isomer (**5.3**). The new *trans* isomer had coupling constants and chemical shifts from NH9 onwards which were more similar to those for the

original *cis* isomer (**5.2**). These results could best be explained if these new isomers were C7 epimers of the mycalamide A *cis* and *trans* oxazolidinones, as in structures **5.7** and **5.8**. Such an epimerisation would require the base catalysed removal of the H7 proton, which is α to the amide carbonyl group, to give an enolate ion intermediate[154,155], as discussed for various mycalamide methyl ethers in Chapter 2.

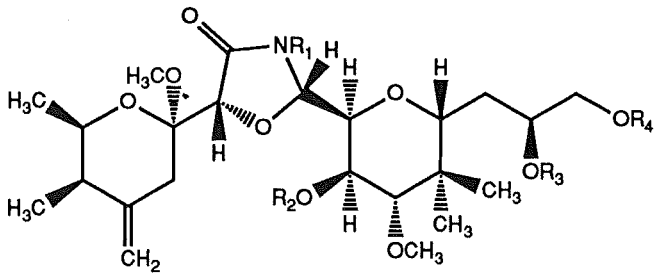

$R_1$=$R_2$=$R_3$=$R_4$=H: 7*S* Mycalamide A *cis* oxazolidinone (**5.7**)
$R_1$=$R_2$=$R_3$=$R_4$=$CH_3$: 12,17,18-tri-*O*-Methyl, *N*-methyl 7*S* A *cis* oxazo.(**5.15**)

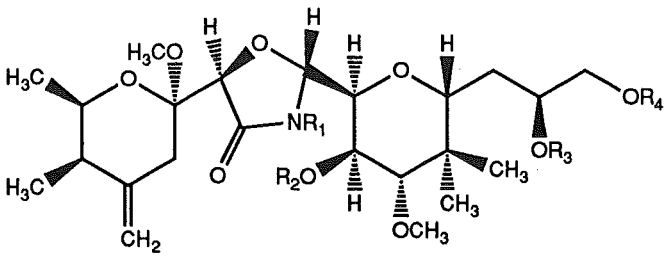

$R_1$=$R_2$=$R_3$=$R_4$=H: 7*S* Mycalamide A *trans* oxazolidinone (**5.8**)
$R_1$=$R_2$=$R_3$=$R_4$=$CH_3$: 12,17,18-tri-*O*-Methyl, *N*-methyl 7*S* A *trans* oxazo.(**5.16**)

The reaction of mycalamide B with potassium hydroxide in DMSO also gave oxazolidinone derivatives (TLC), as expected. The isomers were not separable by reverse phase HPLC but were just resolved by TLC on silica gel. Preparative TLC gave two fractions, which contained isomers of mycalamide B oxazolidinone by HRFABMS, having molecular formulae indicating the same loss of $CH_2O$ from mycalamide B. The $^1H$ NMR spectra were consistent with the formation of *cis* and *trans* oxazolidinone isomers (**5.9, 5.10**), analogous to those obtained from mycalamide A. These were assigned by COSY experiments and by an NOE experiment to give the data in Table 5.9.

The reaction of mycalamide B with sodium methoxide in methanol also gave a mixture of several oxazolidinones (TLC). These were also not resolved by reverse phase HPLC and careful preparative TLC was required to separate two fractions. The $^1$H NMR spectrum of the first fraction showed one major component, mycalamide B *cis* oxazolidinone (**5.9**), and a second, minor component, which was probably a 7*S cis* oxazolidinone derivative. The latter assumption was based on the observations of a small H7-H10 coupling constant[209] (~1 Hz) and widely separated H5 methylene resonances (δ3.1 and 2.1 ppm), which were characteristic in the mycalamide A examples (Table 5.1). The $^1$H NMR spectrum of the second fraction was more complex, as it showed that mycalamide B *trans* oxazolidinone (**5.10**) was the major component of a mixture including two minor components. One was a 7*S trans* oxazolidinone derivative, based on the larger H7-H10 coupling constant[209] (2.5 Hz) and the same spread in the H5 resonances (δ2.9 and 2.1 ppm). The remaining component was not an oxazolidinone derivative since the 10-$OCH_2$ methylene signals were present in the $^1$H NMR spectrum, but nor was it mycalamide B, and was at this point too minor to consider further. Subsequent purification and characterisation of this component will, however, be described in Chapter 6, where the identity of a mycalamide A equivalent from another base catalysed reaction is determined.

## 5.5 MECHANISM OF FORMATION OF THE MYCALAMIDE A AND B OXAZOLIDINONES

The base catalysed formation of an oxazolidinone ring system from mycalamides A and B would require that an intramolecular substitution-elimination reaction occur at the C10 aza acetal site. This must involve both an attack of the C7 hydroxy anion at C10 and the cleavage of the C10-O bond

of the C10-C12 dioxan ring. The latter evidently results in the facile loss of formaldehyde from this C12-O hemiacetal chain to leave a C12 hydroxyl group. This process is summarised in Scheme 5.1.

**Scheme 5.1** Proposed mechanisms to account for the formation of the oxazolidinone derivatives from mycalamides A and B.

a) Reaction via $S_N2$ pathway

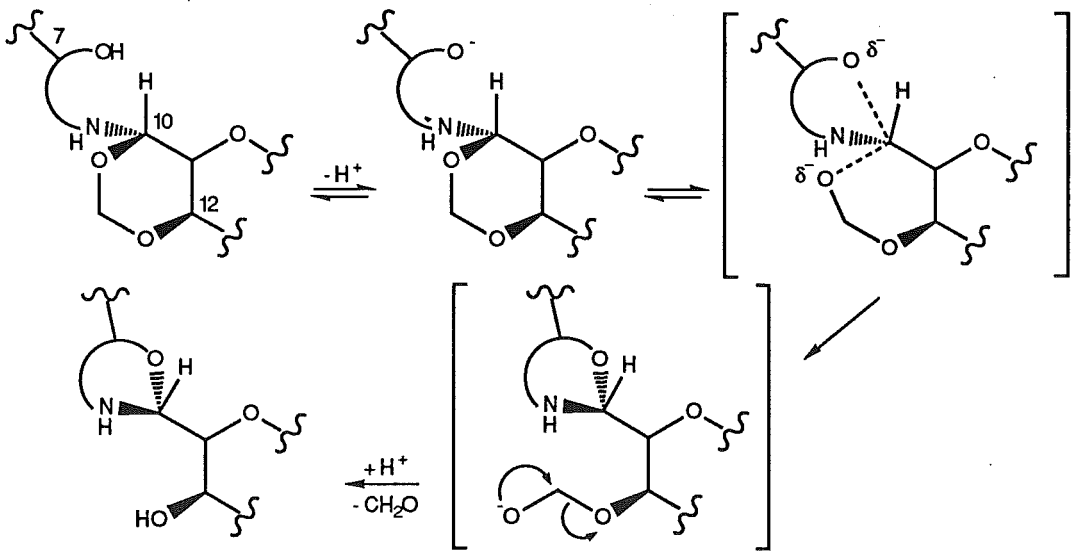


b) Reaction via imine intermediate

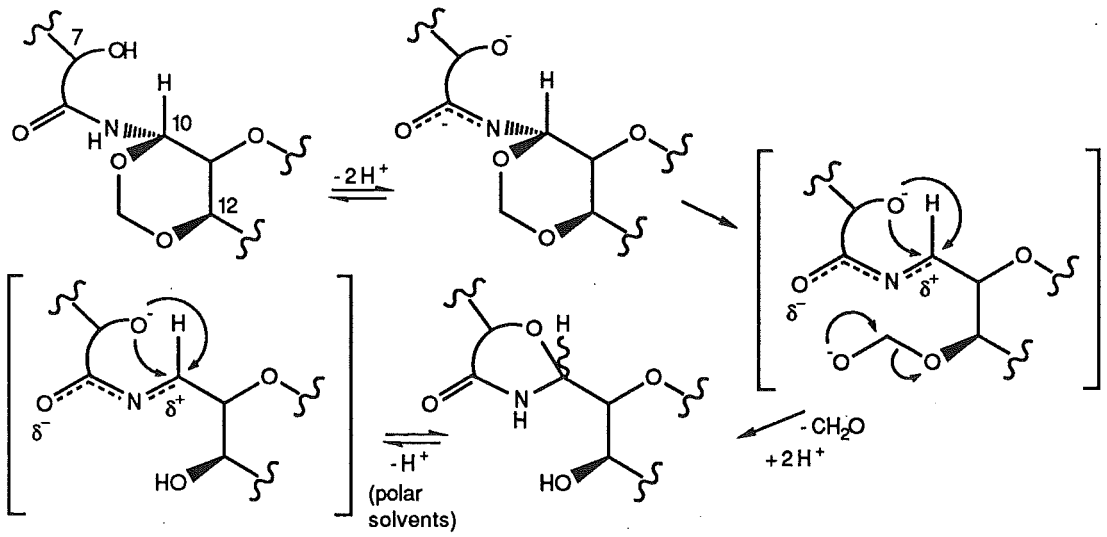


The absolute configurations of mycalamides A and B have recently been verified by synthesis[91]. The NMR spectroscopic evidence described above is consistent with the *cis* and *trans* isomerism of **5.2** and **5.3** being

caused by a difference in stereochemistry at C10. Therefore the *cis* isomer, **5.2**, represents a product with an inversion of configuration at C10, relative to mycalamide A, and the *trans* isomer, **5.3**, represents a retention of the C10 configuration. An $S_N2$-type mechanism[141], as described in Scheme 5.1a, would therefore give the *cis* isomer exclusively (Figure 5.4). Thus, in order to obtain two isomers at C10, there must be some involvement of another reaction intermediate.

**Figure 5.4** Stereochemistry of a proposed intramolecular $S_N2$ reaction in mycalamide A to form oxazolidinone derivatives.

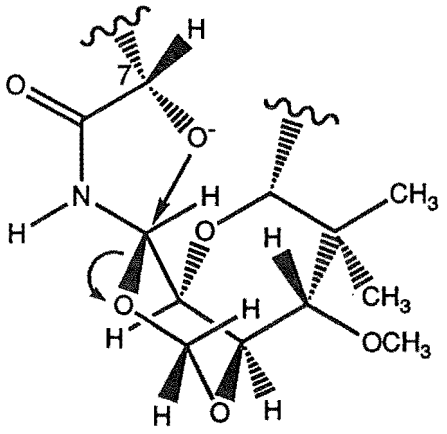


Experimentally, it was found that the *cis* isomer was favoured in most reactions (Table 5.8), and the reactions in DMSO consistently gave a higher proportion of this isomer than those in methanol. Further experiments established that there was no inclusion of deuterium in the products with reactions in $d_4$-methanol and no significant interconversion of the isomers, although prolonged reactions gave poor yields of further new oxazolidinone compounds by TLC and $^1H$ NMR spectroscopy whose identities were not determined. With mixed aqueous solvents there was some C7 isomerisation, and the *trans* isomer (**5.3**) was partially converted into the *cis* isomer (**5.2**), to the extent of about 60% of the reaction mixture. These results suggested that

more than one mechanism could be involved in the reaction and that the extent of involvement of each could depend on the polarity of the solvent.

A common synthesis of 2,5-substituted 4-oxazolidinones involves the condensation of α-hydroxy amides or cyanohydrins with carbonyl compounds in the presence of an acid catalyst[208,210,217,218] and two equilibrium steps involving a hemiacetal intermediate have been proposed to account for yields favouring the more thermodynamically stable *cis* product[209]. In particular, an imine intermediate, described below, was disfavoured due to the "low basicity of the amide nitrogen and because of an unfavourable geometry of the imine intermediate to undergo cyclisation"[209].

In the mycalamide A reaction, if intermediates involving direct participation of the base or solvent are excluded, then the only alternative is to propose the involvement of some ionic intermediate at C10, probably involving stabilisation from the amide nitrogen. It has been established from earlier work on the methylation of mycalamide A (Chapter 2) that there is some formation of the amide anion[156] under these strongly basic conditions, since *N*-methylation was achieved readily in the presence of methyl iodide. Such an anion could stabilise the cleavage of the C10-O bond by the donation of electron density to C10, to form a (delocalised) imine intermediate (Scheme 5.1b). Note that this appears more likely under these basic conditions than an iminium ion formed directly from the amide, since amides are very weak bases[219]. Such an intermediate would allow an attack of the C7 hydroxy anion on either face of the double bond at C10 to give the two isomers. Note that there is some precedence for the involvement of such intermediates in various reactions of amides[155,220].

For the reactions in DMSO, it would appear that there is a strong contribution from an $S_N2$-like mechanism, in order to account for the high proportion of inversion[141] at C10. (Alternatively an imine intermediate with

tight ion-pairing[158] could explain this result). In solvents which favour ionisation to a greater extent[140], such as methanol and particularly aqueous solvents, there was a much lower preference for inversion. This is interpreted as suggesting that a mechanism which involves an ionic intermediate, such as the imine intermediate discussed above, would be the favoured mechanism under more polar conditions. This is supported by the observed formation of C7 epimers only under the more polar conditions, which certainly requires the involvement of an ionic intermediate[154,155]. Also, the step involving attack of the C7 hydroxy anion on the imine intermediate to form the oxazolidinone ring must be reversible under aqueous conditions since the racemisation of the *trans* isomer at C10 was observed. However, this barely occured in DMSO, and this is taken as further evidence for the proposals above.

## 5.6 ACID CATALYSED DECOMPOSITION OF MYCALAMIDE A OXAZOLIDINONES

The synthesis of oxazolidinones by condensing α-hydroxy amides with carbonyl compounds in the presence of an acid catalyst relies on the removal of water from the reaction[208,209], which is often done azeotropically[218]. Consequently, it is known that the products can be hydrolysed by dilute acids to give the starting compounds[217]. In the present case, mycalamide A *trans* oxazolidinone (**5.3**) was dissolved in $CDCl_3$ with no pyridine added and monitored with time. After one day the compound had undergone elimination of methanol across C6-C7 and the exocyclic double bond had rearranged into the C4-C5 positions of the O1-C6 ring to give a *Z* neomycalamide A oxazolidinone derivative (**5.11**). This was shown by the presence of a new allylic system at δ1.9 and 6.9 ppm, as discussed in Chapter 3. The same occurred for the *cis* isomer (**5.2**), to give structure **5.12**, and the $^1H$ NMR data

for these products are recorded in the Experimental section. This facile reaction in $CDCl_3$ could not be reproduced, and the starting compound degraded slowly to a mixture in which the major fragment was pederolactone (**3.6**). The mycalamide structure was clearly too acid sensitive to isolate other products, as expected.

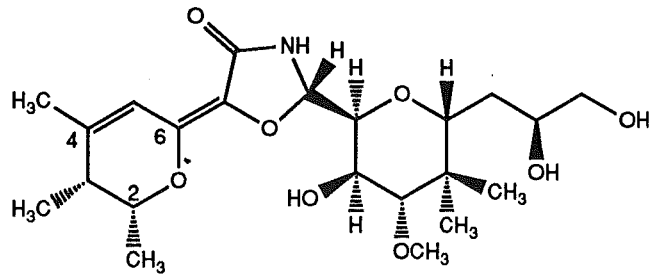

10*S* Neomycalamide A oxazolidinone (**5.11**)

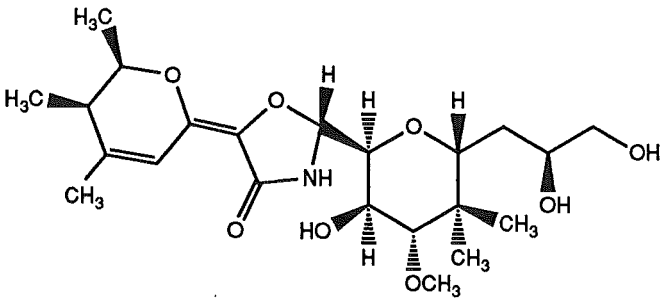

10*R* Neomycalamide A oxazolidinone (**5.12**)

One recent review[221] stated that little was known about the chemistry of 4-oxazolidinones, apart from this acid catalysed hydrolysis and their methylation[218]. An earlier review[217] was more extensive, reporting these reactions, together with their acetylation and hydrogenation. More recently there has been a systematic investigation of the formation and behaviour of these compounds by some Romanian investigators[222-226]. The following section describes the preparation of some simple derivatives of the mycalamide oxazolidinones, which provided some interesting results.

## 5.7 DERIVATIVES OF MYCALAMIDE A OXAZOLIDINONES

### 5.7.1 PREPARATION AND CHARACTERISATION OF A TETRAACETYL DERIVATIVE

Mycalamide A *trans* oxazolidinone (**5.3**) was acetylated with pyridine and acetic anhydride in the usual manner until there was a single product (TLC). HRFABMS showed that the product had a molecular formula of $C_{31}H_{47}NO_{13}$, which required the replacement of the four exchangeable protons in **5.3** by acetyl groups. A $^1H$ NMR spectrum showed the presence of at least three *O*-acetyl methyl resonances, corresponding to the esters at C12, C17 and C18, as demonstrated by the large downfield shifts in the α-proton signals (0.5-1.3 ppm, Table 5.9), which were assigned by a COSY experiment. It also showed an acetyl methyl resonance at δ2.46 ppm, which would arise from an acetyl group on the oxazolidinone ring.

The acetylation of oxazolidinones is known to occur, but there was some doubt as to the structure of the product in at least one report[217]. The most likely position for acetylation would appear to be at the nitrogen atom, to give an imide (structure **5.13**), since this nitrogen in **5.3** may be more reactive than its counterpart in the predominantly *trans* open chain amide of mycalamide A, due to its greater accessibility. The alternative reaction site is the carbonyl oxygen, to give a derivative having a double bond between C8 and the nitrogen, with an *O*-acetyl group at C8. This would represent a vinyl acetate, the structure being an *O*-acyl imidate, which would have a characteristic band in the IR spectrum[96] (compare results for the neomycalamide A triacetate isomers, **3.12** and **3.13**, in Chapter 3). No evidence seemed to be observed for this in the FTIR spectrum, suggesting that the former structure was correct. Furthermore, the H7-H10 coupling constant was smaller in this derivative, whereas a double bond between C8 and the

amide N would be predicted to increase the size of this coupling[209]. The deshielding of these acetyl methyl protons would be consistent with their being close to another carbonyl group[123] and the C8 carbonyl is probably almost in the plane of the *N*-acetyl group due to the delocalisation of electron density over the complete imide system (Figure 5.5). The carbonyl group of amides is also usually only reactive in the presence of silver salts or with strong alkylating reagents under almost neutral conditions[156].

**Figure 5.5** $^{1}H$-$^{1}H$ NOE interactions and partial solution conformation for *N*-acetyl mycalamide A *trans* oxazolidinone triacetate (**5.13**).

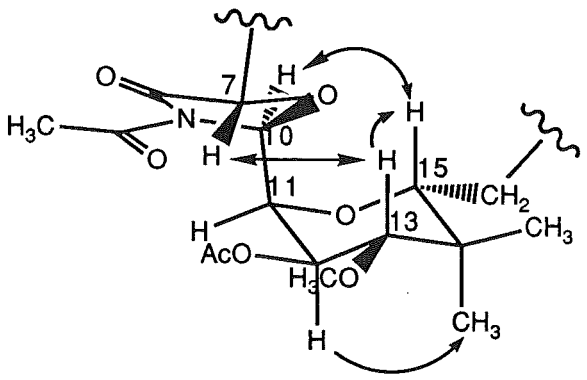


Further evidence for an *N*-acetyl group was obtained from an analysis of chemical shifts observed in a $^{13}C$ NMR spectrum of this compound, as assigned by an HMQC experiment (Table 5.2). There were significant downfield shifts in the C10 and C12 resonances (+6.1, +1.6 ppm respectively), and upfield shifts in the β carbon resonances, C8 (-1.0), C11 (-2.2) and C13 (-2.9), which were consistent with expected substituent effects[117] for acetylation at C10-N and C12-O. (The C7 and C8 resonances could be expected to show different shifts for acetylation of the C8 oxygen). There were also other minor shifts in the C11-C15 tetrahydropyran ring carbon resonances which were indicative of a change to the average solution conformation of this ring, as discussed below.

## 5.7.2 SOLUTION CONFORMATIONS OF *N*-ACETYL MYCALAMIDE A *TRANS* OXAZOLIDINONE 12,17,18-TRIACETATE

The C11-C15 ring proton-proton coupling constants for **5.13** did not show the same averaged behaviour as those for the non-acetylated compound (**5.3**), and were more consistent with the presence of predominantly one chair conformation, as found in mycalamide A and the *cis* oxazolidinone isomer (**5.2**). Similarly, the carbon resonances for this ring were less broad and the chemical shift of the C14, 14-$CH_3R$ and 14-$CH_3S$ resonances were also closer to those observed for mycalamide A. The results of difference NOE experiments, detailed in Table 5.10, required that there still be a small proportion of the alternate chair as well as the normal chair conformation, but such interactions, such as between $H_2$16 and H11 and H12 and H13, were weaker than those in the non-acetylated *trans* isomer (**5.3**).

The H10-H11 coupling constant was only 1.4 Hz in this derivative (**5.13**), suggesting a predominantly gauche relationship between these protons[98] in solution. There were strong NOE interactions between the H7 and H13, H10 and H11, and H10 and H15 protons, but not between H10 and H13. These data required that the oxazolidinone and C11-C15 rings have the major solution conformation shown in Figure 5.5. The large downfield shift in the H11 resonance (+0.6 ppm) is consistent with deshielding by the *N*-acetyl carbonyl group[98,123] in this conformation. Also, the downfield shifts in the H7, H13 and H15 resonances are explained by a combination of steric interactions and dipolar anisotropic effects associated with the C10 oxygen[123]. Similar interactions may also contribute to the shielding[117] of the C13 and C15 carbon resonances, and to the deshielding of the C10 resonance in this conformation.

A molecular mechanics minimisation of this conformation showed that it was a local minimum but that other C10-C11 rotamers were also energetically

favourable. However, the absence of NOE evidence for these other conformations would suggest that the conformation shown in Figure 5.5 is predominant in $CDCl_3$ solution. This illustrates the point that hydrogen bonding involving the C12 hydroxyl group may be an important factor in the favouring of an anti relationship between H10 and H11 in the original *trans* isomer (**5.3**), despite such a conformation being poorly represented in the earlier molecular mechanics calculations. Note that acetylation at the C12-O and N positions would not appear to introduce unfavourable steric interactions to destabilise a conformation having H10 and H11 anti (see Figure 5.1b). However, it does appear to have favoured the normal chair conformation of the C11-C15 ring, possibly because the addition of a more bulky substituent at C12 could introduce more unfavourable steric interactions in the minor alternate chair conformation where this substituent is axial (see Figure 5.1c).

### 5.7.3 PREPARATION, CHARACTERISATION AND PARTIAL SOLUTION CONFORMATIONS OF A SERIES OF METHYLATED DERIVATIVES

Methylation of mycalamide A *trans* oxazolidinone (**5.3**), using potassium hydroxide and methyl iodide in DMSO[151], as in Chapter 2, gave one less polar product, initially, by TLC. On standing overnight, this reaction mixture became about a 1:1 mixture of two major products, and subsequent workup and preparative TLC separated these, together with a third minor fraction. HRFABMS showed that all the products were isomers, of molecular formulae $C_{31}H_{47}NO_{13}$, which required the replacement of the four exchangeable protons in the starting compound by methyl groups. An NMR spectroscopic characterisation and an analysis of the major solution conformation is described for each product below.

### 5.7.3.1 12,17,18-TRI-*O*-METHYL, *N*-METHYL MYCALAMIDE A *TRANS* OXAZOLIDINONE

The $^1$H NMR spectrum of the product which was of lowest $R_f$ on silica gel TLC and was initially major showed that this was 12,17,18-tri-*O*-methyl, *N*-methyl mycalamide A *trans* oxazolidinone (**5.14**), having one *N*-methyl and five methoxyl resonances. There were upfield shifts in the signals corresponding to the α-protons, H10, H12, H17 and both H18's, consistent with this methylation[101], as assigned by a COSY experiment (Table 5.9). A partial assignment of the methoxyl resonances was achieved using results from various NOE experiments (Table 5.10). A $^{13}$C NMR spectrum was also recorded for this isomer, and this was partially assigned to give the data in Table 5.2.

NOE experiments were performed to examine the solution conformations of this derivative (Table 5.10). The strong NOE interactions observed between the H7 and H13, H10 and H11, and H10 and H15, but not the H10 and H13 protons, indicated that this derivative has the same major solution conformation as the acetylated derivative (**5.13**) above (see Figure 5.5). The H10-H11 coupling constant was also small, as above, and the H11 resonance was slightly deshielded in this conformation. The observed NOE interactions between the H16 and H11 and the H13 and 14-$CH_3S$ protons suggested the presence of a small population of the alternate chair conformation, which was further supported by the observation of slightly averaged H11-H12 and H12-H13 coupling constants and the broadening of some resonances in the $^{13}$C NMR spectrum.

### 5.7.3.2 12,17,18-TRI-*O*-METHYL, *N*-METHYL 7*S* MYCALAMIDE A *CIS* OXAZOLIDINONE

The $^1$H NMR spectrum of the other major product, of highest $R_f$ on TLC, which appeared to have been formed from the methylated derivative above, showed that it was probably a *cis* isomer, based on the less than 1 Hz coupling between the H7 and H10 protons[209]. Furthermore, it was likely to be a C7 epimer (structure **5.15**), since the two H5 resonances were well separated in chemical shift. This would account for its formation from the methylated *trans* oxazolidinone derivative (**5.14**) above, since this represents an epimerisation at C7, via the enolate, under the basic reaction conditions[155]. The five methoxyl resonances were all clustered within 0.1 ppm in the $^1$H NMR spectrum, and there were substantial differences in the chemical shifts and coupling constants for the central tetrahydropyran ring protons and its substituents, as assigned by COSY and NOE experiments (Tables 5.9 and 5.10). In particular, the chemical shifts of signals assigned to the H13, 13-$OCH_3$, 14-$CH_3R$, 14-$CH_3S$, H15 and H16*S* protons, and the coupling constants between H11 and H12 and H12 and H13, were consistent with the C11-C15 tetrahydropyran ring being mostly in the alternate chair conformation, as found for a tribenzyl derivative (**2.47**) in Chapter 2. This was also reflected in the chemical shifts of signals in a $^{13}$C NMR spectrum, as assigned by an HMQC experiment (Table 5.2), particularly the 13-$OCH_3$, C14, 14-$CH_3R$, and 14-$CH_3S$ resonances.

NOE experiments were performed to further examine the solution conformations (Table 5.10). NOE interactions were observed between the H10 and H12, H11 and H16*S*, H12 and H13 protons, and between both C14 methyl groups and the H13 and H15 protons, consistent with this alternate chair conformation. The NOE interactions between the H7 and H10 and between the two H5 and both the H11 and H12 protons were indicative of a

*cis* substitution of the oxazolidinone ring and a mostly anti relationship between the H10 and H11 protons (see Figure 5.1a). The latter was also consistent with the observed H10-H11 coupling constant[98] (7.5 Hz). The NOE interactions between both H5 protons and H7 were also indicative of the epimerisation at C7, as above.

The two major products from the methylation of mycalamide A *trans* oxazolidinone (**5.14** and **5.15**) therefore have quite different major solution conformations, but differ only in the stereochemistry at C7. However, this epimerisation could introduce unfavourable steric interactions between the two tetrahydropyran ring systems in the new *cis* isomer. These would be reduced by having the alternate chair conformation for the C11-C15 ring, since C10 would then be an equatorial rather than an axial substituent of this ring (see Figure 5.1c). It is interesting that mycalamide A *cis* oxazolidinone (**5.2**) does not show a significant proportion of this alternate chair conformation. However, this structure does not have the extra *O*-methyl and *N*-methyl groups and has an opposite configuration at two centers (C7 and C10).

### 5.7.3.3 12,17,18-TRI-*O*-METHYL, *N*-METHYL 7*S* MYCALAMIDE A *TRANS* OXAZOLIDINONE

The $^1$H NMR spectrum of the remaining minor product, of intermediate $R_f$ on TLC, showed that it was a *trans* isomer, based on the size of the H7-H10 coupling constant[209] (2.3 Hz), and that it was probably a C7 epimer, based on the large spread in chemical shift of the two H5 resonances. The spectrum was comparable to that of 7*S* mycalamide A *trans* oxazolidinone (**5.8**), but showed an *N*-methyl and five methoxyl resonances, along with shifts in the signals for the α-protons, consistent with methylation[101]. This derivative (**5.16**) must therefore arise from an epimerisation at both C7 and C10, which

would require an opening of the oxazolidinone ring, presumably to give an imine intermediate[155].

**Figure 5.6** $^1$H-$^1$H NOE interactions and partial solution conformation for 12,17,18-tri-*O*-methyl, *N*-methyl 7*S* mycalamide A *trans* oxazolidinone (**5.16**).

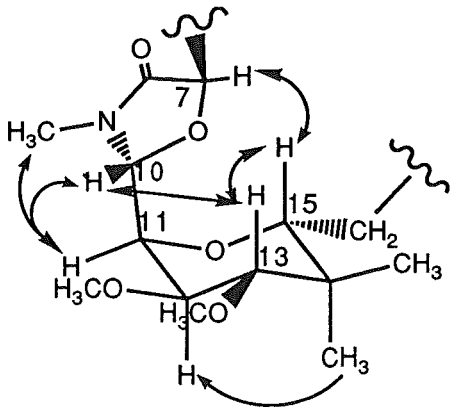


There was insufficient sample to perform a full NMR characterisation so the reaction was repeated on mixed mycalamide B *cis* and *trans* oxazolidinone isomers (**5.9**, **5.10**). The four products were separated by a combination of preparative TLC and HPLC, as described for the new product below. This allowed the $^1$H NMR spectrum of the present derivative to be fully assigned (Table 5.9) by using a combination of results from COSY and NOE experiments (Table 5.10), which also gave an indication of the major solution conformations of this derivative. In particular, strong NOE interactions between the H7 and H15, N-$CH_3$ and H11, H10 and H11, H10 and H13, but not the H10 and H15 protons, showed that this compound must have the major partial solution conformation shown in Figure 5.6 (above). The H10 and H11 protons are in a gauche relationship in this conformation, which is consistent with the small H10-H11 coupling constant[98], but this was a different C10-C11 rotamer from that observed for the acetylated and methylated mycalamide A *trans* oxazolidinone derivatives (**5.13**, **5.14**) above. The conformation of the C11-C15 ring was predominantly the usual chair

conformation as shown by NOE interactions between H13 and H15, and H12 and 14-$CH_3S$, and by the size of the H11-H12 and H12-H13 coupling constants. There was insufficient sample to record a $^{13}C$ NMR spectrum.

### 5.7.3.4 8,12,17,18-TETRA-*O*-METHYL MYCALAMIDE A *CIS* OXAZOLIDINONE

There was a fourth product from the repeated methylation reaction, which was formed in low yield and was coincident on silica gel TLC with the methylated 7*S* mycalamide A *cis* oxazolidinone derivative (**5.15**). Separation of these two derivatives was achieved by reverse phase HPLC to give a fourth isomer by HRFABMS. The $^1H$ NMR spectrum of this new product suggested that it was not *N*-methylated but *O*-methylated at the amide functionality. This was inferred from the presence of a new methoxyl resonance at δ3.94 ppm, which was more consistent with an *O*-methyl imidate functionality[101] (structure **5.17**). The presence of a full double bond between C8 and the amide nitrogen was also suggested by the larger long range coupling constant between H7 and H10 of 3.0 Hz[209]. Unfortunately there was insufficient sample to observe longer range NOE interactions to verify the proposed *cis* stereochemistry of the oxazolidinone ring, or to record a $^{13}C$ NMR spectrum. However, this was the only C7-C10 configuration not represented above and so this would seem to be a likely product.

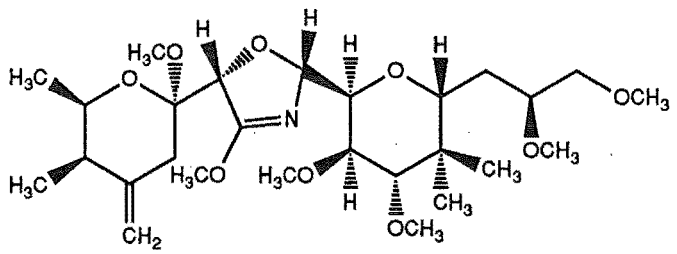


8,12,17,18-tetra-*O*-Methyl, mycalamide A *cis* oxazolidinone (**5.17**)

The $^1H$ NMR spectrum was assigned by using the results obtained from a COSY experiment. NOE interactions were observed between H10 and both H13 and H15, suggesting that H10 and H11 were predominantly in an anti relationship, which agreed with the observed H10-H11 coupling constant[98] (8.3 Hz). This result also implied that the C11-C15 ring was mainly in the usual chair conformation, which was required by the size of the H11-H12 and H12-H13 coupling constants, which were close to those recorded for mycalamide A *trans* oxazolidinone (**5.3**).

The fact that alkylation of the amide oxygen was preferred to alkylation of the amide nitrogen under reaction conditions which did not favour the former[156,157], suggested that the amide nitrogen in the *cis* isomer was too hindered to undergo competitive reaction, or that an *N*-alkylated product was less stable. These proposals would seem reasonable on steric grounds, since methylation of the C12 hydroxyl group could hinder a reaction of the nearby amide nitrogen (Figure 5.1). Alternatively, there is some precedent for compounds having strong intramolecular hydrogen bonds to be difficult to methylate[227].

### 5.7.4 CONCLUSIONS

This methylation study has given derivatives with different C10-C11 rotamers as major solution conformations, which also had different relative populations of the two possible chair conformations of the C11-C15 tetrahydropyran ring. The coupling constant data for these derivatives could be compared with those calculated by molecular modelling. The observed products from methylation and acetylation of the mycalamide oxazolidinones have illustrated the reactivity of this new ring system and further confirmed the structure and stereochemistry of the original isomers and the reaction mechanisms. Some attempt has been made to show the influence of

hydrogen bonding and steric factors in the observed solution conformations of the various oxazolidinones. It was apparent that molecular modelling could not accurately predict which were the favoured solution conformations, possibly due to inadequacies in both the program and the model structures, but was still a useful tool for conformational analysis.

## 5.8 BIOLOGICAL ASSAY RESULTS

The assay results for all the compounds in this chapter are shown in Table 5.11. As expected on the basis of earlier results (Chapter 2) these derivatives were not active, having a derivatised C7 hydroxyl group, and any activity indicated by the results could be due to the presence of residual amounts of unresolved mycalamide A or B. This confirms earlier findings that the central portion of mycalamide A is very important for the expression of its activity. This work did not achieve the desired amide hydrolysis or yield biologically active compounds, but the unusual base reactivity of the C10 aza acetal was a useful result, which suggested further possibilities for the study of this important region of the molecule.

**Table 5.1** $^1$H NMR data[a] for mycalamide A oxazolidinones

| | Myc.A *cis* oxazolidinone (5.2) | Myc.A *trans* oxazolidinone (5.3) | Myc.A *cis* oxazolidinone ($CD_3OD$) | Myc.A *trans* oxazolidinone ($CD_3OD$) | 7*S* Myc.A *cis* oxazolidinone (5.7) | 7*S* Myc.A *trans* oxazolidinone (5.8) |
|---|---|---|---|---|---|---|
| **H2** | 3.95 (2.5,6.6) | 3.95 (2.6,6.5) | 3.91 (2.7,6.5) | 3.91 (2.6,6.5) | 3.95 (2.6,6.6) | 3.94 (2.4,6.6) |
| **2-$CH_3$** | 1.20 (6.6) | 1.19 (6.6) | 1.17 (6.6) | 1.17 (6.6) | 1.15 (6.5) | 1.17 (6.5) |
| **H3** | 2.21 (2.2,7.0) | 2.22 (2.8,7.0) | 2.19 (2.7,7.1) | 2.21 (2.6,7.0) | 2.19 (2.3,6.7) | 2.20 (2.4,6.7) |
| **3-$CH_3$** | 1.05 (6.9) | 1.04 (6.9) | 1.02 (7.0) | 1.01 (7.0) | 0.99 (6.7) | 1.02 (7.0) |
| **4=CH*Z*** | 4.83 (1.9) | 4.85 (2.0) | 4.80 (2.0) | 4.82 (1.9) | 4.82 (2.1) | 4.83 (2.0) |
| **4=CH*E*** | 4.73 (1.9) | 4.74 (1.9) | 4.66 (2.1) | 4.67 (2.0) | 4.70 (2.0) | 4.71 (2.1) |
| **H5a** | 2.40 (2.0,13.8) | 2.48 (1.9,13.7) | 2.37 (2.0,13.8) | 2.41 (2.0,13.9) | 3.05 (2.1,14.3) | 2.92 (2.0,14.4) |
| **H5e** | 2.28 (13.9) | 2.32 (13.7) | 2.32 (14.0) | 2.28 (13.8) | 2.11 (14.2) | 2.13 (14.3) |
| **6-$OCH_3$** | 3.30 | 3.31 | 3.27 | 3.28 | 3.36 | 3.43 |
| **H7** | 4.39 (1.5) | 4.45 (2.4) | 4.39 (1.7) | 4.45 (2.6) | 4.33 (1.3) | 4.28 (2.1) |
| **NH9** | 6.58 | 7.87 | | | 8.04 | 6.67 |
| **H10** | 5.59 (1.6,8.9) | 5.62 (2.3,5.3) | 5.65 (1.8,8.5) | 5.51 (2.6,3.4) | 5.6 (1.4,6.9) | 5.67 (2.2,8.6) |
| **H11** | 3.88 (6.8,8.9) | 3.93 (5.4,5.4) | 3.73 (6.6,8.6) | 3.85 (3.6,5.0) | 4.06 (6.0,6.7) | 3.84 (6.9,8.7) |
| **H12** | 3.97 (6.7,9.8) | 4.00 (5.6,7.4) | 3.89 (6.6,9.6) | 3.92 (5.1,6.5) | 4.01 (6.1,8.3) | 3.97 (6.9,9.7) |
| **H13** | 2.96 (9.6) | 2.98 (7.5) | 3.04 (9.5) | 3.10 (6.6) | 3.04 (8.1) | 2.95 (9.7) |
| **13-$OCH_3$** | 3.61 | 3.56 | 3.58 | 3.51 | 3.59 | 3.60 |
| **14-$CH_3$*R*** | 0.98 | 1.03 | 0.97 | 1.06 | 0.98 | 0.97 |
| **14-$CH_3$*S*** | 0.89 | 0.88 | 0.86 | 0.87 | 0.86 | 0.88 |
| **H15** | 3.60 (2.5,9.8) | 3.54 (2.2,8.4) | 3.60 (1.7,10.0) | 3.62 (2.9,10.2) | 3.47 (3.1,9.5) | 3.61 (m) |
| **H16** | 1.60 (2.5,4.2,14.6) | 1.71 (1.2,8.4,15.2) | 1.74 (1.7,5.3,14.6) | 1.81 (5.7,9.9,14.5) | 1.62 (m) | 1.55 (m) |
| **H16** | 1.51 (6.9,9.7,14.6) | 1.58 (2.3,4.1,15.2) | 1.48 (6.9,10.1,14.7) | 1.68 (2.9,6.6,14.7) | 1.55 (m) | 1.55 (m) |
| **H17** | 3.91 (m) | 3.89 (m) | 3.89 (m) | 3.78 (m) | 3.88 (m) | 3.86 (m) |
| **H18** | 3.62 (6.5,11.1) | 3.59 (3.8,11.2) | 3.59 (3.8,11.2) | 3.54 (4.3,11.2) | 3.59 (m) | 3.57 (m) |
| **H18** | 3.56 (4.1,11.2) | 3.54 (6.7,11.2) | 3.51 (4.8,11.3) | 3.49 (4.8,11.3) | 3.59 (m) | 3.50 (6.3,11.2) |

[a]All data were recorded in $CDCl_3$, unless otherwise specified, with chemical shifts in ppm relative to $CHCl_3$, δ7.25 or $CHD_2OD$, δ3.30 (coupling constants in Hz).

**Table 5.2** $^{13}C$ NMR data[a] for mycalamide A and B oxazolidinones and derivatives and selected linewidths[a].

| | Myc.A *cis* oxazolidinone (5.2) | Myc.A *trans* oxazolidinone (5.3) | *N*-Acetyl A *trans* oxazolidinone triacetate (5.13) | Myc.B *cis* oxazolidinone (5.9) | 12,17,18-tri-*O*-Me, *N*-methyl A *trans* oxazo.(5.14) | 12,17,18-tri-*O*-Me, *N*-methyl 7*S* A *cis* oxazo.(5.15) |
|---|---|---|---|---|---|---|
| C2 | 69.31 (2.3) | 69.29 (2.5) | 69.51 | 69.18 | 69.08 | 69.39 |
| 2-$CH_3$ | 17.87 (2.3) | 17.86 (2.3) | 17.82 | 17.89 | 17.96 | 17.46 |
| C3 | 41.72 (2.2) | 41.61 (2.3) | 41.41 | 41.77 | 41.76 | 41.60 |
| 3-$CH_3$ | 11.70 (2.3) | 11.80 (2.2) | 11.67 | 11.77 | 11.84 | 11.80 |
| C4 | 146.07 (2.2) | 146.37 (2.2) | 145.60 | ? | 146.94 | 146.93 |
| 4=$CH_2$ | 110.03 (2.7) | 109.75 (2.9) | 110.39 | 109.64 | 109.30 | 109.26 |
| C5 | 33.76 (2.4) | 33.65 (2.7) | 33.53 | 33.81 | 33.64 | 32.80 |
| C6 | 98.82 (1.9) | 99.28 (1.8) | 99.44 | 98.32 | 99.30 | 98.61 |
| 6-$OCH_3$ | 48.54 (1.9) | 48.81 (2.7) | 48.68 | 48.62 | 48.41 | 50.87 |
| C7 | 75.68 (2.4) | 77.12 (3.0) | 78.09 | 74.96 | 78.21 | 80.87 |
| C8 | 170.02 (2.1) | 171.63 (2.2) | 170.61 | ? | 168.46 | 168.89 |
| N-$CH_3$ | | | | | 27.53 | 28.96 |
| C10 | 80.83 (2.6) | 86.41 (2.8) | 92.49 | 80.84 | 94.70 | 89.67 |
| C11 | 77.58 (2.8) | 74.12 (10.2) | 71.90 | ? | 70.50 | 71.75 |
| C12 | 68.89 (2.1) | 68.89 (3.6) | 70.49 | 69.04 | 79.53 | 74.89 |
| 12-$OCH_3$ | | | | | 59.20 | 57.28 |
| C13 | 88.02 (2.1) | 86.88 (2.6) | 83.97 | 88.02 | 85.06 | 81.21 |
| 13-$OCH_3$ | 63.09 (2.0) | 61.73 (2.9) | 61.88 | 63.00 | 61.31 | 59.34 |
| C14 | 41.50 (2.4) | 39.81 (4.3) | 41.50 | ? | ? | 36.35 |
| 14-$CH_3$*R* | 23.42 (2.2) | 24.43 (4.0) | 23.53 | 23.41 | 24.01 | 27.27 |
| 14-$CH_3$*S* | 13.78 (2.7) | 16.28 (8.4) | 14.06 | 13.67 | 15.40 | 22.69 |
| C15 | 78.58 (2.3) | 79.56 (5.0) | 77.22 | 75.63 | 76.69 | 78.18 |
| C16 | 31.44 (2.5) | 31.01 (3.4) | 29.95 | 29.45 | 29.88 | 29.45 |
| C17 | 72.04 (2.1) | 72.48 (2.4) | 70.14 | 78.92 | 76.89 | 78.18 |
| 17-$OCH_3$ | | | | 56.94 | 57.11 | 57.62 |
| C18 | 66.74 (2.2) | 66.76 | 64.93 | 62.94 | 70.72 | 72.61 |
| 18-$OCH_3$ | | | | | 59.23 | 58.80 |
| $NCOCH_3$ | | | 24.52 | | | |
| 3x-$OCOCH_3$ | | | 21.12,20.99 | | | |
| | | | 20.76 | | | |

[a]All data were recorded in $CDCl_3$, with chemical shifts in ppm relative to $CDCl_3$, δ77.01 (linewidths in Hz).

**Table 5.3** $^{2}J_{CH}$ and $^{3}J_{CH}$ HMBC correlations[a] for mycalamide A *trans* oxazolidinone (**5.3**).

| Proton | Carbon signal correlated |
|---|---|
| 2-$CH_3$ | C2, C3 |
| 3-$CH_3$ | C2, C3, C4 |
| 2x4=CH | C3,C5 |
| 2xH5 | C4, 4=$CH_2$, C6 |
| 6-$OCH_3$ | C6 |
| H7 | C6 |
| H13 | C12, 13-$OCH_3$, C14 |
| 13-$OCH_3$ | C13 |
| 14-$CH_3$*R* | C13, C14, 14-$CH_3$*S*, C15 |
| 14-$CH_3$*S* | C13, C14, 14-$CH_3$*R*, C15 |

[a]All data were recorded in $CDCl_3$

**Table 5.4** $^{1}H$-$^{1}H$ NOE interactions[a] for compounds in Sections **5.2-5.6.**

| Compound | Signal(s) irradiated | Signals enhanced (% enhancement) |
|---|---|---|
| Myc.A *cis* oxazol. (**5.2**) | H5a | 3-$CH_3$(0.6), H5e(10), H7(1) |
| | H5e | 4=CH*E*(3), H5a(12), H11(1), H7(0.4) |
| | H7 | 6-$OCH_3$(2), H10(1) |
| | H10 | H7(2), H11(2), H13(7), H15(6) |
| | H11 (H17) | H5a(1), H5e(1), H10(2), H16d(1)[b,c] |
| | H13 | H10(8), 13-$OCH_3$(2), 14-$CH_3R$(1), H15(2) |
| | 14-$CH_3R$ | H13(4), 13-$OCH_3$(1), 14-$CH_3S$(1), H15(3), H16d(2)[c] |
| | 14-$CH_3S$ | H12(5), H16d(2)[c], H16u(3)[c] |
| | H15 (13-$OCH_3$, $H_2$18) | H10(7), H13(10)[b], 14-$CH_3R$(2), 14-$CH_3S$(0.4)[b], 2xH16(2)[b], H17(4)[b] |
| | $H_2$16 | 14-$CH_3R$(1), 14-$CH_3S$(1), H15/$H_2$18(2), H17(4) |
| Myc.A *trans* oxazol. (**5.3**) | H5a | 3-$CH_3$(0.5), H5e(8), H7(1), H10(0.4) |
| | H5e | 4=CH*E*(2), H5a(9), H7(0.4), H10(1) |
| | H7 | H5a(1), 6-$OCH_3$(2), H11(0.5), H13(0.9) |
| | H10 | H5a(0.4), H5e(0.8), H11(2), H12(1), H13(3), H15(2) |
| | H11 (H2, H17) | 2-$CH_3$(1)[b], H3(2)[b], H5a(0.4)[b], 6-$OCH_3$(0.6)[b], H7(0.8), H10(3), H16d(1)[b,c] |
| | H13 | H10(4), H12(2), 13-$OCH_3$(2), 14-$CH_3S$(0.4), 14-$CH_3R$(1), H15(2) |
| | 14-$CH_3R$ (3-$CH_3$) | H3(4)[b], H13(4), 13-$OCH_3$(1), 14-$CH_3S$(1), H15(3), H16u(3)[c] |
| | 14-$CH_3S$ | H12(4), H13(1), H16d(2)[c], H16u(1)[c] |
| | H15 (13-$OCH_3$, $H_2$18) | H10(4), H13(7), 14-$CH_3R$(1), 14-$CH_3S$(0.4), 2xH16(2)[b], H17(5)[b] |
| | $H_2$16 | H11(2), 13-$OCH_3$(1), 14-$CH_3R$(1), 14-$CH_3S$(1), H15/H18u(2)[c], H17(3) |
| Myc.A *trans* oxazol. (**5.3**) in $CD_3OD$ | H10 | H5e(1), H11(4), H12(1), H13(2), H15(2) |
| | H13 | H10(2), H12(2), 13-$OCH_3$(2), 14-$CH_3R$(1), H15(3) |
| | 14-$CH_3S$ | H12(4), H13 (1), 14-$CH_3R$(1) |
| | H15 (13-$OCH_3$) | H10(3), H13(3), 14-$CH_3S$(0.3), 14-$CH_3R$(1) |
| 7*S* Myc.A *cis* oxazolidinone (**5.7**) | H5a (H13) | 3-$CH_3$(0.8), H5e(16), H7(2), H10(4)[b], 13-$OCH_3$(1)[b], 14-$CH_3R$(1)[b], H15(2)[b] |
| | H5e | 4=CH*E*(4), H5a(16), H7(2) |
| | H7 | H5e(1), 6-$OCH_3$(1) |
| | H10 | H7(1), H13(3), H15(3) |
| Myc.B *cis* oxazol. (**5.9**) | H7 | 6-$OCH_3$(2) |
| | H10 | H13(5), H15(5) |

[a]All data were recorded in $CDCl_3$, unless otherwise specified.

[b]Enhancement interpreted as being due to the irradiation of an overlapping signal

[c]u and d have been used to designate the upfield and downfield resonances of a geminal pair

**Table 5.5** Molecular modelling results for structures **5.4A**, **5.4B**, **5.5A** and **5.5B**.

| %[a] | MM2[b] energy | Conf.[c] Code | Dihedral angles[d] a) | b) | c) | Vicinal coupling constants[e](dihed.angle) J10-11 | J11-12 | J12-13 | H-Bonds (NH/OH-O) |
|---|---|---|---|---|---|---|---|---|---|
| **5.4A** | | | | | | | | | |
| 57.7 | 139.4 | +A- | 51 | 165 | -112 | 8.8(176) | 5.6(47) | 9.1(-175) | 9-12 |
| 24.3 | 141.5 | -A- | -80 | 164 | -111 | 1.9(49) | 6.2(42) | 8.9(-173) | |
| 5.9 | 145.1 | ++- | 47 | 59 | -99 | 8.9(172) | 5.6(47) | 9.0(-174) | 9-12 |
| 4.0 | 146.1 | A+- | 153 | 54 | -97 | 2.0(-75) | 6.5(40) | 8.6(-170) | 12-10 |
| 3.7 | 146.3 | -+- | -82 | 69 | -99 | 2.1(47) | 6.2(43) | 8.7(-171) | |
| 2.8 | 146.9 | AA- | 152 | 166 | -113 | 1.9(-76) | 6.4(41) | 8.8(-172) | |
| 1.1 | 149.4 | --- | -88 | -71 | -99 | 2.7(42) | 6.6(39) | 8.4(-168) | 12-10 |
| 0.5 | 151.1 | +AA | 48 | 171 | -155 | 8.9(172) | 5.7(47) | 8.7(-171) | 9-12,12-13 |
| **5.4B** | | | | | | | | | |
| 49.0 | 130.3 | A+- | -177 | 89 | -88 | 4.4(-52) | 1.2(-54) | 2.3(-73) | |
| 19.1 | 132.7 | A+- | -179 | 119 | -88 | 4.2(-54) | 1.1(-54) | 2.3(-72) | |
| 12.4 | 133.8 | AA- | -177 | 144 | -88 | 4.4(-52) | 1.2(-54) | 2.2(-74) | |
| 9.4 | 134.4 | --- | -60 | -14 | -88 | 0.8(64) | 1.0(-57) | 2.3(-73) | 12-10 |
| 6.8 | 135.3 | -+- | -67 | 56 | -87 | 1.2(58) | 0.8(-59) | 2.4(-72) | 12-10 |
| 2.1 | 138.2 | +-- | 66 | -36 | -88 | 8.0(-171) | 1.0(-56) | 2.3(-73) | |
| 0.7 | 140.9 | A-- | -175 | -36 | -87 | 4.5(-51) | 0.9(-58) | 2.4(-72) | |
| 0.5 | 142.0 | +A- | 66 | 179 | -89 | 8.0(-170) | 1.4(-52) | 2.1(-75) | |
| **5.5A** | | | | | | | | | |
| 48.9 | 142.6 | -A- | -83 | 163 | -113 | 1.4(-75) | 6.5(40) | 8.7(-171) | |
| 17.0 | 145.2 | -+- | -83 | 66 | -99 | 1.4(-76) | 6.6(40) | 8.4(-169) | |
| 12.0 | 146.1 | +A- | 54 | 165 | -116 | 2.2(57) | 6.7(39) | 8.8(-172) | |
| 10.3 | 146.5 | AA- | 163 | 164 | -111 | 8.5(169) | 5.7(47) | 9.0(-174) | |
| 9.6 | 146.7 | A+- | 161 | 43 | -97 | 8.5(167) | 6.0(44) | 8.7(-171) | 12-10 |
| 1.6 | 151.1 | ++- | 51 | 64 | -100 | 2.5(54) | 6.6(39) | 8.6(-170) | |
| 0.6 | 153.7 | A-- | 166 | -49 | -102 | 8.6(171) | 5.5(49) | 9.0(-174) | 12-10 |
| **5.5B** | | | | | | | | | |
| 40.6 | 138.2 | A+- | 174 | 87 | -58 | 8.7(177) | 0.7(-59) | 2.8(-69) | |
| 29.1 | 139.0 | +A- | 68 | -180 | -64 | 1.3(69) | 1.0(-57) | 2.4(-72) | 9-12 |
| 12.2 | 141.2 | AA- | 172 | 152 | -57 | 8.7(176) | 0.7(-60) | 2.7(-70) | |
| 8.9 | 142.0 | A-- | 172 | -29 | -55 | 8.7(175) | 0.5(-63) | 3.0(-67) | 12-11 |
| 5.4 | 143.2 | --- | -62 | -18 | -55 | 2.7(-59) | 0.5(-63) | 2.8(-68) | 12-10,12-11 |
| 2.8 | 144.9 | +-- | 62 | -38 | -55 | 1.9(61) | 0.3(-65) | 3.0(-67) | 9-12,12-11 |
| 1.1 | 147.1 | -+- | -70 | 70 | -60 | 2.1(-65) | 0.4(-64) | 2.9(-68) | 12-10 |

[a]Relative population (Boltzmann distribution) [b]In kJ $mol^{-1}$ [c]Code for dihedral angles a)-e) where 'A'=anti, '+'= (+) gauche, '-'= (-) gauche conformations [d]Dihedral angles:- a) O-C10-C11-O b) C11-C12-O-H c) C12-C13-O-$CH_3$ [e]Calculated coupling constants in Hz.

**Table 5.6** Molecular modelling results for structures **5.5C** and **5.5D**.

| | MM2[b] | Conf.[c] | Dihedral angles[d] | | | | | Vicinal coupling constants (dihedral angle)[e] | | | | | | H-Bonds |
|---|---|---|---|---|---|---|---|---|---|---|---|---|---|---|
| %[a] | energy | code | a) | b) | c) | d) | e) | J15-16*R* | J15-16*S* | J16*R*-17 | J16*S*-17 | J17-18*R* | J17-18*S* | (OH-O) |
| 35.3 | 146.9 | AAA+- | 179 | 164 | 179 | 63 | -55 | 2.2(60) | 11.6(177) | 1.0(-78) | 10.4(167) | 10.5(-178) | 3.1(60) | 17-15;18-17 |
| 23.8 | 147.8 | AA+++ | 179 | 164 | 62 | 59 | 53 | 2.2(59) | 11.6(177) | 1.0(-79) | 10.3(166) | 0.6(65) | 3.2(-57) | 17-15;18-17 |
| 12.7 | 149.4 | A+AAA | -179 | 61 | 174 | -178 | -180 | 2.0(62) | 11.6(179) | 11.3(175) | 4.2(59) | 10.8(179) | 3.5(56) | 17-18 |
| 5.7 | 151.4 | A+A+- | -177 | 64 | 175 | 69 | -55 | 1.8(64) | 11.4(-179) | 11.4(178) | 3.8(62) | 10.7(180) | 3.3(58) | 18-17 |
| 5.1 | 151.7 | A++++ | -179 | 60 | 58 | 64 | 55 | 1.9(63) | 11.5(180) | 11.1(173) | 4.4(58) | 0.8(61) | 2.9(-60) | 18-17 |
| 3.9 | 152.4 | A++-A | -180 | 59 | 57 | -70 | 175 | 2.0(62) | 11.6(179) | 11.1(173) | 4.5(58) | 0.9(60) | 2.8(-61) | 17-18 |
| 3.2 | 152.8 | AA-+A | -179 | 165 | -66 | 62 | -176 | 2.0(61) | 11.6(178) | 1.0(-78) | 10.4(167) | 4.7(-62) | 10.6(177) | 17-15 |
| 2.5 | 153.5 | A+AA+ | -180 | 62 | 178 | -175 | 83 | 2.1(61) | 11.6(179) | 11.3(176) | 4.1(60) | 10.4(-177) | 3.0(61) | 17-18 |
| 2.2 | 153.8 | A-AAA | -168 | -70 | -171 | 177 | -177 | 1.2(72) | 10.9(-171) | 5.6(49) | 1.4(-66) | 9.4(-169) | 2.3(68) | 17-18 |
| 0.9 | 156.0 | AA++A | 179 | 162 | 53 | 59 | 175 | 2.2(60) | 11.6(177) | 1.0(-79) | 10.2(165) | 1.3(56) | 2.3(-65) | 17-15 |
| 0.9 | 156.0 | AAA+A | -180 | 164 | -172 | 65 | -176 | 2.1(61) | 11.6(178) | 1.0(-78) | 10.4(167) | 9.6(-170) | 2.2(68) | 17-15 |
| 0.8 | 156.4 | AAAAA | -169 | 171 | 179 | -172 | -178 | 1.3(71) | 11.0(-172) | 1.2(-71) | 11.1(174) | 10.6(-179) | 3.2(59) | 17-18 |
| 0.7 | 156.7 | AA+-A | -161 | -178 | 60 | -42 | 170 | 1.0(80) | 10.0(-163) | 2.2(-60) | 11.7(-175) | 0.8(61) | 2.8(-60) | |
| 0.6 | 157.0 | AA-+- | 180 | 164 | -69 | 58 | -77 | 2.1(61) | 11.6(178) | 1.0(-79) | 10.3(166) | 4.1(-66) | 10.5(173) | 17-15 |
| 0.6 | 157.2 | A+++A | -178 | 59 | 49 | 65 | 175 | 1.8(64) | 11.5(-179) | 11.2(174) | 4.4(58) | 1.6(52) | 2.1(-68) | |
| 49.4 | 136.6 | AAA+- | -176 | 168 | 180 | 73 | -55 | 2.2(60) | 11.6(176) | 1.1(-73) | 11.1(173) | 10.4(-177) | 3.0(61) | 17-10,15;18-17 |
| 32.8 | 137.6 | AA+++ | -176 | 165 | 64 | 72 | 52 | 2.2(59) | 11.7(175) | 1.0(-76) | 10.8(171) | 0.6(66) | 3.4(-55) | 17-10,15;18-17 |
| 4.1 | 142.8 | A+AAA | 175 | 59 | 175 | -177 | 179 | 3.0(53) | 11.6(169) | 11.2(175) | 4.0(61) | 10.7(179) | 3.5(57) | 17-18 |
| 3.5 | 143.1 | AA-+A | -176 | 165 | -66 | 73 | -176 | 2.2(60) | 11.7(176) | 1.0(-75) | 10.9(171) | 4.6(-63) | 10.6(176) | 17-10,15 |
| 2.2 | 144.3 | A+AA- | 175 | 58 | 170 | 156 | -82 | 3.0(53) | 11.6(169) | 11.2(174) | 4.1(60) | 11.1(173) | 4.2(51) | |
| 1.3 | 145.6 | A+AA+ | 175 | 60 | 180 | -175 | 82 | 3.1(52) | 11.6(168) | 11.3(175) | 3.9(61) | 10.3(-176) | 2.8(62) | 17-18 |
| 1.1 | 146.0 | AA++A | -176 | 163 | 55 | 72 | 175 | 2.3(59) | 11.7(175) | 1.0(-76) | 10.8(170) | 1.2(56) | 2.4(-64) | 17-10,15 |
| 1.0 | 146.2 | AAA+A | -176 | 166 | -171 | 75 | -178 | 2.2(60) | 11.7(176) | 1.1(-75) | 10.9(172) | 9.6(-170) | 2.2(69) | 17-10,15 |
| 1.0 | 146.4 | A++-A | 177 | 60 | 58 | -70 | 175 | 2.7(55) | 11.7(171) | 11.3(175) | 3.9(61) | 0.8(61) | 2.9(-59) | 17-18 |
| 0.8 | 146.7 | A+A+- | 178 | 62 | 176 | 70 | -55 | 2.8(55) | 11.7(171) | 11.4(177) | 3.7(63) | 10.6(180) | 3.3(58) | 18-17 |
| 0.8 | 146.8 | A++++ | 179 | 61 | 59 | 65 | 55 | 2.5(57) | 11.7(173) | 11.3(176) | 3.8(62) | 0.8(62) | 3.0(-58) | 18-17 |
| 0.7 | 147.3 | AA-+- | -175 | 166 | -70 | 71 | -76 | 2.1(60) | 11.6(176) | 1.0(-75) | 10.9(171) | 4.1(-66) | 10.5(173) | 17-10,15 |
| 0.6 | 147.5 | A-AAA | -162 | -61 | -172 | 178 | -176 | 1.1(73) | 10.9(-172) | 4.3(57) | 2.6(-55) | 9.5(-169) | 2.3(68) | 17-18 |

[a]Relative population (Boltzmann distribution) [b]In kJ $mol^{-1}$ [c]Code for dihedral angles a)-e) where 'A'=anti, '+'= (+) gauche, '-'= (-) gauche conformations
[d]Dihedral angles:- a) C14-C15-C16-C17 b) C15-C16-C17-C18 c) C16-C17-C18-O d) C16-C17-O-H e) C17-C18-O-H [e]Calculated couplings in Hz.

**Table 5.7** Comparison of experimental coupling constants for compounds **5.2** and **5.3** with calculated average values for conformers of structures **5.4A**, **5.4B**, **5.5A**, **5.5B**, **5.5C** and **5.5D**.

| Structures | Coup. const. | Vicinal coupling constants[a] Experimental $CDCl_3$ | Experimental $CD_3OD$ | Calculated average values[b] A(C) str | B(D) str | Ratios[c] (5.5A/5.5B) 90% | 85% | 80% | 75% | 70% |
|---|---|---|---|---|---|---|---|---|---|---|
| **5.2, 5.4A/B** | J10-11 | 8.9 | 8.5 | 6.4 | 3.9 | | | | | |
| | J11-12 | 6.8 | 6.6 | 5.8 | 1.1 | | | | | |
| | J12-13 | 9.7 | 9.6 | 9.0 | 2.3 | | | | | |
| **5.3, 5.5A/B** | J10-11 | 5.3 | 3.5 | 3.0 | 6.0 | 3.3 | 3.5 | 3.6 | 3.8 | 3.9 |
| | J11-12 | 5.6 | 5.1 | 6.4 | 0.7 | 5.8 | 5.5 | 5.3 | 5.0 | 4.7 |
| | J12-13 | 7.5 | 6.6 | 8.7 | 2.7 | 8.1 | 7.8 | 7.5 | 7.2 | 6.9 |
| **5.3, 5.5C/D** | J15-16*R* | 2.2 | 2.9 | 2.1 | 2.2 | | | | | |
| | J15-16*S* | 9.6 | 10.1 | 11.6 | 11.6 | | | | | |
| | J16*R*-17 | 4.1 | 6.6 | 4.2 | 1.8 | | | | | |
| | J16*S*-17 | 8.4 | 5.7 | 8.3 | 10.4 | | | | | |
| | J17-18*R* | 6.7 | 4.8 | 6.8 | 7.8 | | | | | |
| | J17-18*S* | 3.8 | 4.3 | 3.5 | 3.3 | | | | | |

[a]Coupling constants in Hz [b]Calculated constants were averaged over all conformers using a Boltzmann distribution on the energies [c]Ratios of the calculated average values for structure **5.5A** over those for structure **5.5B**.

**Table 5.8** Summary of syntheses and reactions of mycalamide oxazolidinones for various bases and solvents[a].

| Compound | Base | Solvent | Temp. | Time | Products (% of total) |
|---|---|---|---|---|---|
| Mycalamide A | NaOH (2M) 50% | $H_2O$/MeOH | 55 | 10 | **5.2**(35),**5.3**(35),**5.7**(15),**5.8**(15) |
| | NaOMe (1M) | MeOH | 20 | 24 | **5.2**(55),**5.3**(45) |
| | $NaOCD_3$ (3M) | $CD_3OD$ | 20+50 | 24+2 | **5.2**(40),**5.3**(30), (mixed prods) |
| | BaO | DMSO | 50 | 16 | **5.2**(70),**5.3**(30) |
| | KOH | DMSO | 20 | 96 | **5.2**(>90) |
| | KOH | DMSO | 80+105 | 24+24 | **5.6**(>90) |
| Mycalamide B | NaOMe (1M) | MeOH | 20+40 | 24+24 | **5.9**(35),**5.10**(35), (C7-epimers + ?) |
| | KOH | DMSO | 40 | 24 | **5.9**(65),**5.10**(35) |
| A *cis* ox. (**5.2**) | $NaOCD_3$ (4M) | $CD_3OD$ | 70 | 2 | **5.2**(50), (mixed prods - no **5.3**) |
| A *trans* (**5.3**) | NaOH (1M) 40% | $H_2O$/MeOH | 60 | 24 | **5.2**(60), (**5.3** + decomp.) |
| | KOH | DMSO | 20 | 96 | **5.3**(>90, no reaction) |

[a]Temperature in °C, reaction time in hours.

**Table 5.9** $^1$H NMR data[a] for mycalamide A and B oxazolidinone derivatives

| | Myc.B *cis* oxazolidinone (5.9) | Myc.B *trans* oxazolidinone (5.10) | *N*-Acetyl A *trans* oxazo. triacet.(5.13) | 12,17,18-tri-*O*-Me, *N*-Me 7*S* A *cis* oxazo.(5.15) | 12,17,18-tri-*O*-Me, *N*-Me A *trans* oxazo.(5.14) | 12,17,18-tri-*O*-Me, *N*-Me 7*S* A *trans* oxazo.(5.16) | 8,12,17,18-tetra-*O*-Me, myc.A *cis* oxazo.(5.17) |
|---|---|---|---|---|---|---|---|
| H2 | 3.93 (2.3,6.6) | 3.94 (2.6,6.6) | 3.95 (2.6,6.5) | 3.86 (2.5,6.7) | 3.93 (2.5,6.6) | 3.80 (2.7,6.5) | 3.94 (2.6,6.6) |
| 2-$CH_3$ | 1.19 (6.6) | 1.18 (6.2) | 1.19 (6.6) | 1.15 (6.7) | 1.19 (6.6) | 1.08 (6.5) | 1.17 (6.6) |
| H3 | 2.19 (2.4,7.0) | 2.21 (2.6,6.6) | 2.20 (2.5,7.0) | 2.17 (2.7,7.0) | 2.20 (2.6,7.1) | 2.16 (2.5,6.9) | 2.19 (2.5,7.1) |
| 3-$CH_3$ | 1.04 (7.0) | 1.04 (6.8) | 1.00 (7.0) | 0.96 (7.0) | 1.05 (7.0) | 0.96 (7.0) | 1.00 (7.0) |
| 4=CH*Z* | 4.82 (1.8) | 4.84 (2.0) | 4.86 (1.8) | 4.80 (2.0) | 4.82 (1.9) | 4.80 (2.1) | 4.81 (2.0) |
| 4=CH*E* | 4.70 (1.9) | 4.72 (1.8) | 4.75 (1.8) | 4.68 (2.0) | 4.68 (1.9) | 4.69 (2.0) | 4.65 (2.0) |
| H5a | 2.39 (1.8,13.7) | 2.47 (2.0,13.7) | 2.21 (1.8,13.8) | 3.20 (2.0,14.2) | 2.29 (1.9,13.8) | 3.19 (2.1,14.0) | 2.07 (2.0,14.0) |
| H5e | 2.33 (13.8) | 2.32 (13.8) | 2.37 (13.8) | 2.00 (14.1) | 2.20 (13.6) | 1.99 (13.9) | 2.30 (14.0) |
| 6-$OCH_3$ | 3.30 | 3.30 | 3.32 | 3.40 | 3.31 | 3.33 | 3.25 |
| H7 | 4.34 (1.9) | 4.38 (2.2) | 4.63 (1.5) | 4.26 | 4.51 (2.5) | 4.20 (2.3) | 4.63 (3.2) |
| 8-$OCH_3$ | | | | | | | 3.94 |
| NH9 | 6.65 | | | | | | |
| N-$CH_3$ | | | | 3.00 | 2.95 | 2.87 | |
| H10 | 5.52 (1.6,8.8) | 5.57 (2.2,6.1) | 6.00 (1.4,1.4) | 5.16 (7.5) | 5.28 (2.4) | 5.44 (2.1) | 5.69 (3.0,8.3) |
| H11 | 3.84 (6.6,8.7) | 3.80 (5.1,6.1) | 4.50 (1.4,6.8) | 4.01 (2.3,7.6) | 4.07 (2.0,6.1) | 4.15 (1.9,7.4) | 3.76 (5.8,8.3) |
| H12 | 3.94 (6.7,9.6) | 3.97 (5.1,7.4) | 5.02 (6.7,9.5) | 3.52 (2.3,2.7) | 3.51 (5.8,7.8) | 3.63 (7.5,9.7) | 3.51 (5.8,8.0) |
| 12-$OCH_3$ | | | | 3.41 | 3.37 | 3.49 | 3.46 |
| H13 | 2.95 (9.8) | 2.93 (7.3) | 3.39 (9.4) | 2.97 (2.7) | 3.27 (8.0) | 3.47 (9.7) | 3.04 (8.0) |
| 13-$OCH_3$ | 3.59 | 3.54 | 3.48 | 3.35 | 3.48 | 3.52 | 3.53 |
| 14-$CH_3$*R* | 0.97 | 1.03 | 0.94 | 1.16 | 0.96 | 0.89 | 0.99 |
| 14-$CH_3$*S* | 0.89 | 0.88 | 0.88 | 0.91 | 0.86 | 0.84 | 0.89 |
| H15 | 3.46 (3.9,8.3) | 3.40 (2.6,10.5) | 3.77 (5.0,7.5) | 3.45 (3.6,12.0) | 3.62 (2.4,9.6) | 3.72 (1.5,10.4) | 3.27 (m) |
| H16 | 1.67 (m) | 1.85 (m) | 1.73 (m) | 2.29 (7.4,11.6,14.3) | 1.74 (4.4,9.6,14.2) | 1.68 (1.4,8.2,14.7) | 1.75 (m) |
| H16 | 1.67 (m) | 1.70 (m) | 1.73 (m) | 1.64 (3.4,9.9,14.7) | 1.63 (2.4,8.0,14.2) | 1.44 (2.6,10.3,14.5) | 1.75 (m) |
| H17 | 3.64 (m) | 3.50 (m) | 5.23 (m) | 3.26 (m) | 3.43 (m) | 3.30 (m) | 3.71 (m) |
| 17-$OCH_3$ | 3.38 | 3.43 | | 3.34 | 3.38 | 3.32 | 3.36 |
| H18 | 3.79 (4.6,11.7) | 3.78 (4.5,11.2) | 4.26 (3.3,12.1) | 3.51 (2.7,9.1) | 3.48 (m) | 3.37 (m) | 3.53 (m) |
| H18 | 3.69 (5.1,11.7) | 3.62 (6.5,11.2) | 4.12 (6.7,12.1) | 3.40 (m) | 3.43 (m) | 3.31 (m) | 3.45 (m) |
| 18-$OCH_3$ | | | | 3.35 | 3.38 | 3.49 | 3.38 |

[a]All data were recorded in $CDCl_3$, with chemical shifts in ppm relative to $CHCl_3$, δ7.25 (coupling constants in Hz).

**Table 5.10** $^{1}H$-$^{1}H$ NOE interactions[a] for compounds in Section **5.7.**

| Compound | Signal(s) irradiated | Signals enhanced (% enhancement) |
|---|---|---|
| *N*-Acetyl myc.A *trans* oxazo.triacet. (**5.13**) | H5a (H3) | H2(9)[b], 2-$CH_3$(0.5)[b], 3-$CH_3$(3), 4=CH*Z*(5)[b], H5e(21), H7(2), H10(1) |
| | H5e | 4=CH*E*(6), H5a(14), H7(0.7), H10(2) |
| | H7 | 6-$OCH_3$(2), H13(4), 13-$OCH_3$(0.3) |
| | $NCOCH_3$ | H10(0.8) |
| | H10 | H5e(1), $NCOCH_3$(0.4), H11(6), H15(3) |
| | H11 | H10(8), H12(11) |
| | H12 | H11(10), H13(1), 13-$OCH_3$(0.3), 14-$CH_3S$(2) |
| | H13 | H7(7), H12(1), 13-$OCH_3$(2), 14-$CH_3R$(1), H15(7) |
| | H15 | H10(5), H13(5), 14-$CH_3R$(1), H17(4), H18d(2)[c] |
| | $H_2$16 (OAc) | H11(3)[b], 14-$CH_3S$(2), 14-$CH_3R$(1), H15(6), H17(9), 2xH18(2) |
| | H17 | H10(0.9), H15(3), $H_2$16(2), H18d(3)[c], H18u(2)[c] |
| | H18d[c] | H10(0.5), H15(0.8), H17(5), H18u(11)[c] |
| | H18u[c] | H10(2), H17(2), H18d(17)[c] |
| 12,17,18-tri-*O*-Me, *N*-Me myc.A *trans* oxazo. (**5.14**) | H5a | 3-$CH_3$(1), H5e(7), H7(1), H10(0.7) |
| | H5e (H3) | H2(5)[b], 2-$CH_3$(0.7)[b], 3-$CH_3$(2)[b], 4=CH*E*(3), 4=CH*Z*(4)[b], N-$CH_3$(0.2), H10 (1) |
| | H7 | 6-$OCH_3$(2), H13(2) |
| | N-$CH_3$ | H10(4), H11(5), 12-$OCH_3$(0.9) |
| | H10 | H5e(0.7), N-$CH_3$(1), H11(4), H15(2), H17/H18(1) |
| | H11 | H7(0.9), N-$CH_3$(2), H10(6), H12(6), 12-$OCH_3$(0.5) |
| | H12 (13-$OCH_3$) | H11(8), 12/18-$OCH_3$(1), H13(4), 14-$CH_3S$(1) |
| | H13 (6-$OCH_3$) | H7(6)[b], 13-$OCH_3$(2), 14-$CH_3R$(1), H15(4) |
| | 14-$CH_3R$ | H13(5), 13-$OCH_3$(0.8), H15(4) |
| | 14-$CH_3S$ | H12(4), 14-$CH_3R$(0.7), H16(3) |
| | H15 | H10(4), H13(4), 14-$CH_3R$(0.9), H17/H18(1) |
| | $H_2$16 | H11(2), 14-$CH_3S$(1), 14-$CH_3R$(0.8), H15(4), H17/H18(6), 17/18-$OCH_3$(0.4) |
| 12,17,18-tri-*O*-Me, *N*-Me 7*S* myc.A *cis* oxazo. (**5.15**) | H2 | H3(5), 2-$CH_3$(1), 6-$OCH_3$(0.8) |
| | H5a | 3-$CH_3$(0.8), H5e(22), H7(2), H11(1), H12(0.8) |
| | H5e | 4=CH*E*(5), H5a(20), H7(5), H12 (1) |
| | H7 | H5a(0.6), H5e(1), 6-$OCH_3$(0.5), H10(1) |
| | N-$CH_3$ (H13) | H10(7), H12(1), 12-$OCH_3$(0.6), H17(1) |
| | H10 | H7(1), N-$CH_3$(1), H11(1), H12(0.8) |
| | H11 | H5a(0.9), N-$CH_3$(0.3), H10(2), H12(5), H16*S*(5), H17(2) |
| | H12 (H18) | H5a(0.9), H5e(0.8), H10(2), H11(6), 12-$OCH_3$(2), H13(3), 13/17/18-$OCH_3$(1), H17(2)[b] |
| | H13 | H12(3), 12-$OCH_3$(1), 13-$OCH_3$(2), 14-$CH_3S$(0.4), 14-$CH_3R$(0.7) |
| | 14-$CH_3R$ (2-$CH_3$) | H2(5)[b], H3(3)[b], 3-$CH_3$(0.7), H10(1), 12-$OCH_3$(0.9), H13(6), 13/17/18-$OCH_3$(0.5), 14-$CH_3S$(1), H15(4) |
| | 14-$CH_3S$ | H12(1), H13(4), 14-$CH_3R$(1), H15(4), H16*R*(2) |
| | H16*S* | H11(4), H16*R*(3) |

[a]All data were recorded in $CDCl_3$

[b]Enhancement interpreted as being due to the irradiation of an overlapping signal

[c]u and d have been used to designate the upfield and downfield resonances of a geminal pair

**Table 5.10 cont'd** $^1H$-$^1H$ NOE interactions[a] for compounds in Section **5.7.**

| Compound | Signal(s) Irradiated | Signals enhanced (% enhancement) |
|---|---|---|
| 12,17,18-tri-*O*-Me, *N*-Me 7*S* myc.A *trans* oxazo. (**5.16**) | H2 | H3(3), 2-$CH_3$(0.7), 6-$OCH_3$(0.4) |
| | H5a | 3-$CH_3$(1), H5e(18), H7(2) |
| | H5e | 4=CH*E*(4), H5a(21), H7(4) |
| | H7 (H11) | H5e(2), 6-$OCH_3$(0.4), H15(4), H17(2) |
| | N-$CH_3$ | H10(2), H11(4) |
| | H10 | N-$CH_3$(0.9), H11(8), 12-$OCH_3$(0.9), H13 (2) |
| | H11 | N-$CH_3$(2), H10(10), H12(5), 12-$OCH_3$(0.6) |
| | 14-$CH_3$*R* | H13(5), 13-$OCH_3$(1), H15(5) |
| | 14-$CH_3$*S* | H12(5) |
| | H15 | H7(5), H13(5), 14-$CH_3$*R*(1), H17(3) |
| 8,12,17,18-tetra-*O*-Me myc.A *cis* oxazo. (**5.17**) | H7 (4=CH*E*) | 4=CH*Z*(11)[b], 6-$OCH_3$(2) |
| | H10 | H13(7), H15(4) |

[a]All data were recorded in $CDCl_3$

[b]Enhancement interpreted as being due to the irradiation of an overlapping signal

[c]u and d have been used to designate the upfield and downfield resonances of a geminal pair

**Table 5.11** Biological assay results for compounds in Chapter 5.

| Compound | P388 $IC_{50}$[a] | Antiviral Results[b] (ng/disk) | | | | | | | |
|---|---|---|---|---|---|---|---|---|---|
| Mycalamide A | 0.5 | WW | WW | +* | 5 | + | + | +* | 2 |
| Mycalamide B | 0.1 | WW | WW | +* | 2 | +++ | +++ | +* | 1 |
| Myc.A *cis* oxazolidinone (**5.2**) | 300 | WW | WW | +* | 5000 | +++ | ++ | +* | 2000 |
| Myc.A *trans* oxazolidinone (**5.3**) | 400 | WW | WW | +* | 5000 | + | ++ | +* | 2000 |
| Myc.B *cis* oxazolidinone (**5.8**) | 21 | WW | WW | +* | 500 | +++ | ++ | +* | 200 |
| Myc.B *trans* oxazolidinone (**5.9**) | 95 | WW | WW | +* | 4000 | +++ | +++ | +* | 2000 |
| 10*S* Neomyc.A oxazo. (**5.11**) | 600 | WW | WW | +* | 10000 | ++ | +++ | +* | 2500 |
| 10*R* Neomyc.A oxazo. (**5.12**) | 800 | WW | WW | +* | 10000 | - | - | - | 2500 |
| *N*-acet.A *trans* oxazo.triacet. (**5.13**) | 5000 | | | | | - | - | - | 40000 |
| 12,17,18-tri-*O*-Me, *N*-Me myc.A *trans* oxazolidinone (**5.14**) | >12500 | | | | | - | - | - | 40000 |
| 12,17,18-tri-*O*-Me, *N*-Me 7*S* myc.A *cis* oxazo. (**5.15**) | >12500 | | | | | - | - | - | 40000 |
| 12,17,18-tri-*O*-Me, *N*-Me 7*S* myc.A *trans* oxazo. (**5.16**) | >12500 | | | | | - | - | - | 40000 |

[a] In ng/ml. The derivatives are estimated to be better than 95% pure, having been subjected to at least two steps of chromatographic purification in most cases.

[b] -,+,++,+++,WW=antiviral zone size. Results are listed in the order of *Herpes simplex virus*, *Polio virus*, cytotoxicity, loaded sample mass.

# CHAPTER 6
# REACTIONS OF MYCALAMIDES A & B AND DERIVATIVES UNDER BASIC CONDITIONS
# PART 2

## 6.1 INTRODUCTION

The C10-C12 dioxan ring, having an α-*N*-amido group at C10, is a substructure unique to mycalamides A and B and onnamide A[228]. The possible biological importance of this substructure was postulated in a recent paper reporting the synthesis of mycalamides A and B, with the possibility of eliminative cleavage of the C10-O bond causing activation of this system[91]. Exchange reactions were performed at the C10 aza acetal site in pederin, but only acid catalysed conditions were studied, for which protection of the exocyclic double bond was required[127,130]. Pederin was apparently stable to refluxing with dilute sodium methoxide in methanol[27], but it is still likely that base catalysed reactions could occur under more forcing conditions.

The observed base catalysed reactions of mycalamides A and B in the preceding chapter (5) suggested that the C10 position could be a general site for nucleophilic substitution under basic conditions. In order to study this further, and to consider the possibility of base catalysed amide hydrolysis, it was clearly necessary to use a base stable protecting group for the C7 hydroxyl group to prevent formation of the oxazolidinones. Esters and silyl ethers were not sufficiently base stable[131,138] but the mycalamide methyl and benzyl ethers, whose preparations were described in Chapter 2, were expected to be quite stable to such conditions[138]. The mycalamide methyl ether derivatives suffered from the disadvantages of being poorly resolved on

various chromatographic systems and that the protecting groups were not selectively removable, whereas the benzyl ethers were better suited in both respects. Furthermore, the C7 hydroxyl group was the first site to undergo alkylation under normal conditions, so that various suitably protected derivatives had been synthesised, and these provided a useful starting point for further base reactivity studies.

## 6.2 PREPARATION AND CHARACTERISATION OF PRODUCTS FROM THE REACTION OF 7-*O*-ALKYL, *N*-ALKYLATED MYCALAMIDE B WITH POTASSIUM HYDROXIDE IN DMSO

### 6.2.1 PREPARATION AND PURIFICATION OF PRODUCTS FROM A TRI-BENZYLATED MYCALAMIDE B DERIVATIVE

The mycalamide benzyl ether which had been prepared in the largest quantity was the fully substituted compound, 7,18-di-*O*-benzyl, *N*-benzyl mycalamide B (**2.46**), which was also readily formed from mycalamide B in high yield and represented a well protected derivative. This derivative was treated with potassium hydroxide in DMSO at 60°C until most of the starting material had disappeared, as monitored by silica gel TLC. Workup and preparative TLC gave a number of fractions, including one of unreacted starting material, but, of the remainder, only one, more polar fraction was pure, as shown by $^1$H NMR spectroscopy, and this fraction represented about half of the product mass by weight. The remaining fractions were complex mixtures, with no identifiable components apparent, and no attempt was made to purify these fractions further.

## 6.2.2 SPECTROSCOPIC CHARACTERISATION OF THE MAJOR PRODUCT

The starting compound, 7,18-di-*O*-benzyl, *N*-benzyl mycalamide B (**2.46**), had a molecular formula of $C_{46}H_{61}NO_{10}$. HRCIMS of the major product indicated a compound of molecular formula $C_{29}H_{61}NO_7$, so that this was clearly a cleavage product. The molecular ion ($MH^+$) also appeared to lose CO readily. An FTIR spectrum showed a strong carbonyl stretching band at 1689 $cm^{-1}$, so that the amide functionality was still present. The $^1H$ NMR spectrum contained resonances from only the right hand portion of the starting structure, from H10 onwards, and two singlets at δ8.05 and 8.21 ppm, suggestive of a formamide derivative[101]. In fact all the signals in the $^1H$ NMR spectrum were duplicated in a ratio of about 1:1. This was consistent with the classical behaviour of *N,N*-di-substituted formamides, which display slow conformational exchange between the two possible geometric forms of the amide C-N bond, due to the restricted rotation caused by its partial double bond character[107,229]. (Note that these forms are called conformations[100,107] and the resulting conformational isomers are given the designations *E* and *Z*. In the following text however, these will be referred to as isomers, for sake of brevity, where this refers strictly to conformational isomerism). A common example is *N,N*-dimethylformamide (DMF) in which the two methyl peaks do not reach coalescence in the $^1H$ NMR spectrum until about 123°C[98]. The structure **6.1**, including all the atoms from C8 onwards, would therefore satisfy all the spectroscopic evidence above for this cleavage product.

The $^1H$ NMR spectrum of **6.1**, containing the two isomers discussed above, was assigned by using the results of COSY and NOE experiments, to give the data in Table 6.1. The largest difference in chemical shift between proton resonances in the two isomers occurred for the H10 protons (1.3 ppm). This reflects the large dipolar anisotropic shielding effects associated with the

amide carbonyl group[123]. In particular, the downfield H10 resonance must be associated with the *Z* isomer of the amide (Figure 6.1) since this would allow maximum deshielding. This was confirmed by the results of NOE experiments (Table 6.2), since irradiation of the signal at δ8.05 ppm gave an enhancement of the upfield H10 resonance, whereas irradiation of the other H8 resonance gave an enhancement of a signal assigned to the amide *N*-benzyl methylene protons. The latter assignment was based on an observed NOE interaction between the H11 and *N*-benzyl protons for both isomers. The H13 and H15 proton resonances for each isomer were located by the observation of similar enhancements on irradiation of the two H10 resonances. Note that this required that the solution conformation of the trioxadecalin ring system be the same in both isomers as for the starting compound, which was consistent with the observed chemical shifts and vicinal proton-proton coupling constants. These results have been summarised in Figure 6.1. A similar conformational equilibration was observed for the parent compound, **2.46**, as described in Chapter 2, but the more complex structure of the latter compound gave both a different ratio of the two amide isomers and probably a different rate of interconversion, resulting in an increased line broadening of the proton resonances at room temperature[107].

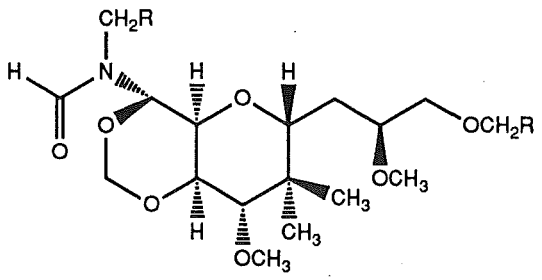


R=Ph: *N*-Benzyl, *N*-formyl fragment (**6.1**)
R=H: *N*-Methyl, *N*-formyl fragment (**6.2**)

A $^{13}C$ NMR spectrum was also recorded, which showed the same doubling of resonances. An HMQC experiment was used to assign most of

the resonances to give the data in Table 6.3. The new C8 formyl resonances were observed at δ164.9 and 164.2 ppm, upfield of their position in the starting compound, as expected[117], and there were shifts in many other resonances also. The C10 resonance associated with the *Z* isomer was more shielded than that for the *E* isomer, by 7.2 ppm, which was due to an interaction with the amide carbonyl group[117,118]. Similarly, the *N*-$CH_2$ resonance associated with the *E* isomer was the more shielded from a similar effect. The remaining resonances could not be assigned to a particular isomer, but the chemical shift differences between resonances for the two isomers were generally small, with the largest for the C17 resonance (1.1 ppm), suggesting a long range interaction of the amide with the sidechain.

**Figure 6.1** Selected $^1H$-$^1H$ NOE interactions and partial solution conformations for *N*-alkyl, *N*-formyl mycalamide derivatives (R=Ph: **6.1**, R=H: **6.2**).

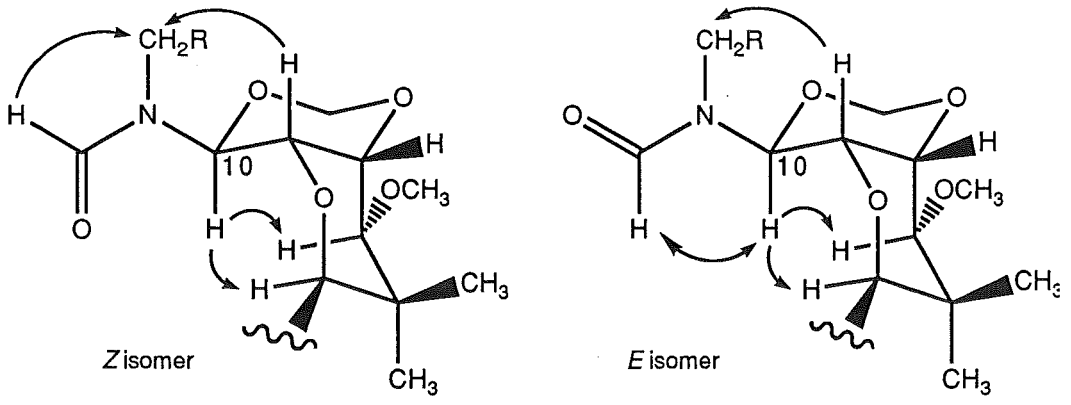


6.2.3 REACTION OF METHYLATED DERIVATIVES

Initially, it seemed surprising that a cleavage in the protected mycalamide structure had occurred between C7 and C8, rather than at the tertiary amide C-N bond. To confirm that this was not an anomalous reaction related to the size of the benzyl protecting groups, the reaction of the fully methylated compound was also considered. Thus 7,17,18-tri-*O*-methyl, *N*-

methyl mycalamide A (**2.26**) was reacted with potassium hydroxide in DMSO at 70°C, until TLC showed a complete loss of starting material. After workup, $^1$H NMR spectroscopy showed the presence of a single product, probably an *N,N*-disubstituted formamide derivative, obtained in excellent yield. HRCIMS showed the formation of a compound of molecular formula $C_{17}H_{31}NO_7$, which was correct for a formamide derivative of structure **6.2**, representing cleavage between C7 and C8 in compound **2.26**. An IR spectrum also confirmed the presence of the amide functionality in this product.

The $^1$H NMR spectrum showed two formyl proton resonances, at δ8.25 and 8.16 ppm, two *N*-methyl resonances, at δ3.00 and 2.94 ppm, and two H10 resonances, at δ6.09 and 5.15 ppm, while most other resonances were also doubled (Table 6.1). The complete spectrum was assigned using results from COSY and NOE experiments. In particular, NOE interactions were observed between one H8 and one *N*-methyl group and between the second H8 and one of the H10 protons (Table 6.2), confirming the presence of the same two amide isomers. The $^{13}$C NMR spectrum showed similarly large differences in the chemical shifts of the two C10 and the two *N*-methyl resonances (Table 6.3), as assigned by an HMQC experiment, which were also consistent with previous results.

The observed cleavage reaction betwen C7 and C8 in *N*-alkylated derivatives appeared to be more facile for methyl than for benzyl derivatives. However, no fragments from the left hand portion of the molecule had been isolated from either reaction. A $^1$H NMR spectrum of the evaporated aqueous-DMSO fraction from the above reaction showed no significant resonances apart from residual DMSO. It is possible that such a fragment was unstable under the reaction conditions, decomposing to a mixture of components.

This reaction therefore illustrated the comparative base stability of the amide functionality under these relatively anhydrous conditions, compared

with that of neighbouring functional group systems associated with it. It was noteworthy that no reaction occurred at C10 for these substrates, a point which will be discussed in a later section. Further attempts at base catalysed cleavage on the same *N*-methyl substrate, **2.26**, using sodium methoxide in methanol, or sodium hydroxide in aqueous methanol at high temperatures, gave only slow decomposition, with no single major product being observed by $^1$H NMR spectroscopy. Therefore the desired base hydrolysis of the amide, which could occur under these aqueous alkaline conditions, did not yield useful results, whereas the above reaction was both interesting and potentially useful. The benzyl protecting groups of the *N*-formyl fragment in the previous subsection could potentially be removed by catalytic hydrogenolysis[78,131] to ascertain the biological activity of the equivalent mycalamide B cleavage product. However there was insufficient time to investigate this possibility.

### 6.2.4 DISCUSSION OF A POSSIBLE MECHANISM OF CLEAVAGE

The C6-C8 substructure of mycalamides A and B has certain similarities to an α-hydroxy, β-dicarbonyl system, a system which is often encountered in carbohydrate chemistry[230], since the C6 acetal is a masked carbonyl group. It has been established that enolisation at C7-C8 occurs readily under the basic reaction conditions used above, since C7 epimers were isolated from longer methylation reactions (Chapter 2). However, the presence of the alkyl ether group, protecting the C7 hydroxyl in the substrates above, makes it difficult to envisage further reaction.

It is proposed that the observed cleavage occurs via an intermediate formed by a base catalysed 1,2-hydride shift[231] from C7 to C8, as in Scheme 6.1. This is the equivalent of an α-hydroxy carbonyl isomerisation, via the enol, but would require the substitution of hydroxide ion at C7. Note that traces of water would be present in the reaction mixture from incomplete

drying of the solvent, DMSO. This intermediate could then undergo a reverse Claisen or aldol-type reaction[79,232,233], involving cleavage of the C7-C8 bond, to give the observed product and some smaller fragment, where the latter could undergo further rearrangement and decomposition[233] (Scheme 6.1).

**Scheme 6.1** Proposed mechanism for the base catalysed cleavage of 7-*O*-alkyl, *N*-alkyl mycalamide derivatives (R=$CH_3$: **2.26**, R=$CH_2Ph$: **2.46**).

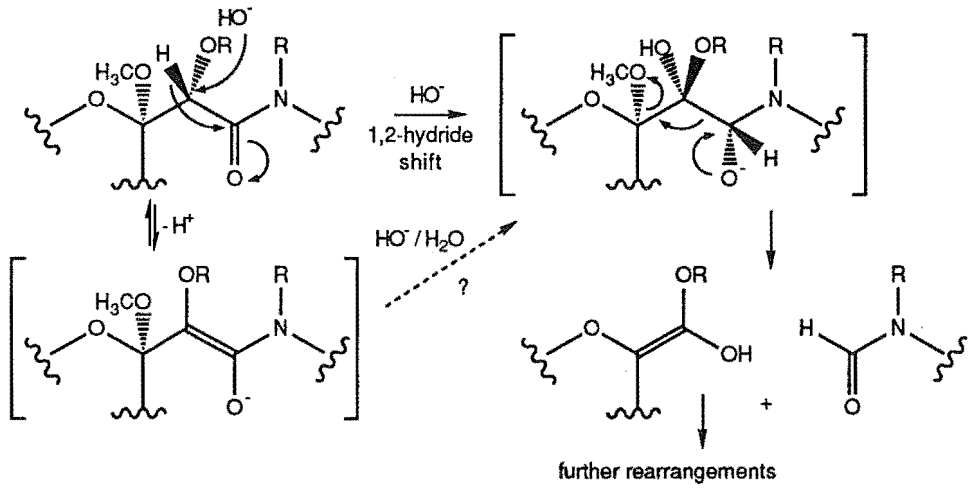


Reverse aldol reactions are common degradative reactions of β-dicarbonyl derivatives[230,233]. However it is possible that some alternative mechanism is involved. It would be difficult to prove a particular mechanism with only one product being stable, and deuterium labelling methods would not be useful due to the easy exchange of protons at C7 (and C8) via enolisation reactions.

## 6.3 BASE CATALYSED REACTIONS OF 7-*O*-BENZYL MYCALAMIDE DERIVATIVES

It was noted above that the use of *N*-alkylated mycalamide derivatives for reactions in base appeared to protect the C10 aza acetal functionality from reaction. Although it was possible that steric factors were involved, it appeared more likely that the different base reactivities of the secondary and tertiary *N*-amido acetals were related to the presence or absence of an exchangeable proton, just as for the case of hemiacetals compared with acetals[106,170]. In particular, the removal of the NH proton to facilitate the formation of an imine intermediate[220], and thus the cleavage of the aza acetal, was postulated in the formation of the mycalamide oxazolidinones in the previous chapter. The reactions of mycalamide A 7-benzyl ethers were therefore considered to investigate this in more detail.

### 6.3.1 THE REACTION OF 7-*O*-BENZYL MYCALAMIDE A WITH BARIUM OXIDE IN DMSO

7-*O*-Benzyl mycalamide A (**2.39**) was treated with barium oxide in DMSO at 70°C for 8 hours to give a mixture of starting material and another compound of higher $R_f$ on silica gel TLC. Separation by preparative TLC gave a new derivative, which was isomeric with 7-*O*-benzyl mycalamide A by DCIMS.

The $^1$H NMR spectrum of this new isomer showed large changes in the chemical shifts and coupling constants for substituents of the trioxadecalin ring system, compared with data for 7-*O*-benzyl mycalamide A, and these data were assigned by using the results of COSY and NOE experiments (Table 6.4). In particular, the observed vicinal proton-proton coupling constants (in Hz) for H10-H11 (2.0), H11-H12 (1.8) and H12-H13 (2.4), were indicative of

the opposite chair-chair conformation being the major solution conformation for the trioxadecalin ring system of this derivative, just as for 7,8,18-tri-*O*-benzyl mycalamide B (**2.47**) (see also Figure 2.2). There were also significant changes in the chemical shifts of the NH (+0.5), H10 (-0.5), H12 (-0.5), H13 (-0.6), 13-$OCH_3$ (-0.2), 14-$CH_3S$ (+0.3), H16d (+0.7) and H17 (-0.2) proton resonances (Table 6.4), compared with data for **2.39**, consistent with this conformational change. Irradiation of H10 in an NOE experiment gave enhancements of the upfield 10-OCH, H11 and H12 resonances, irradiation of the upfield 10-OCH resonance gave enhancements of H10 and H12, and irradiation of H12 caused enhancement of the H10 and upfield 10-OCH resonances (Table 6.2). These data required that the C10-C12 dioxan ring be in the opposite chair conformation, where the H10, 10-OCH*S* and H12 protons could all be axial, and that the configuration at C10 be opposite to that in 7-*O*-benzyl mycalamide A (**2.39**). Other NOE interactions, such as between H12 and H13, and between H13 and both of the 14-$CH_3$ groups, required that the C11-C15 ring also be in the opposite chair conformation to that normally observed, as deduced from the results above. These results are summarised in Figure 6.2, for structure **6.3**.

**Figure 6.2** Selected $^1H$-$^1H$ NOE interactions and partial solution conformation for 7-*O*-benzyl 10*R* mycalamide A derivatives (**6.3** and **6.4**).

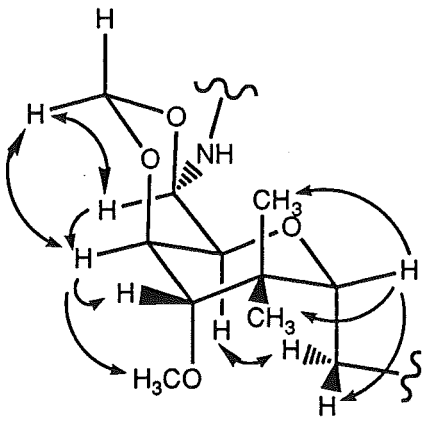

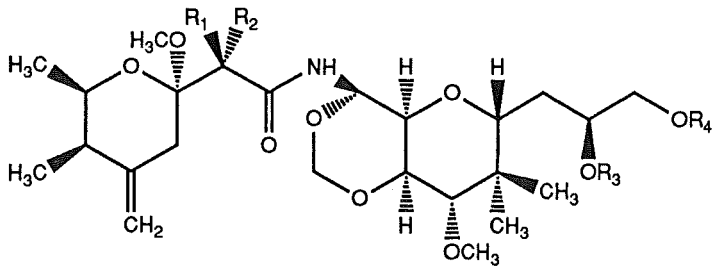

$R_1$=$R_3$=$R_4$=H, $R_2$=$OCH_2Ph$: 7-*O*-Benzyl 10*R* mycalamide A (**6.3**)
$R_1$=$R_3$=H, $R_2$=$OCH_2Ph$, $R_4$=$CH_2Ph$: 7,18-di-*O*-Benzyl 10*R* myc.A (**6.4**)
$R_1$=D, $R_2$=$OCH_2Ph$, $R_3$=$R_4$=H: 7-Deutero, 7-*O*-benzyl 10*R* myc.A (**6.10**)
$R_1$=$OCH_2Ph$, $R_2$=D, $R_3$=$R_4$=H: 7-Deutero, 7*S*-*O*-benzyl 10*R* myc.A (**6.13**)
$R_1$=$R_3$=$R_4$=H, $R_2$=OH: 10*R* Mycalamide A (**6.17**)
$R_1$=$R_4$=H, $R_2$=OH, $R_3$=$CH_3$: 10*R* Mycalamide B (**6.18**)

A $^{13}C$ NMR spectrum was also obtained on a combined sample and the data assigned by an HMQC experiment (Table 6.5). The significant shifts were in the C10 (+3.0), 10-$OCH_2$ (+4.8), C11 (-9.9) and C12 (-1.9) resonances, since the shifts in the other resonances were similar to those observed for 7,8,18-tri-*O*-benzyl mycalamide B (**2.47**) (Section 2.5.2), and were related to changes in the populations of the chair-chair conformations of this ring system. It is proposed that the main reason for this observed conformational change on epimerisation at C10 is to minimise steric interactions, since the alternate chair-chair conformation allows the bulky amide sidechain to remain equatorial to the dioxan ring at C10, as in mycalamides A and B (compare Figure 1.6).

This epimerisation at C10 under basic conditions was also observed for some C7-dimethoxybenzyl ethers of mycalamides A and B during the total synthesis of these compounds[91]. A discussion of the mechanism of this unusual reaction is presented in a following subsection.

### 6.3.2 FACILE SYNTHESIS OF 7-*O*-BENZYL 10*R* MYCALAMIDE A AND DERIVATIVES

In order to prepare a larger quantity of 7-*O*-benzyl 10*R* mycalamide A (**6.3**) to complete the above characterisations, a more direct synthetic method was required. Adaptation of the Kuhn methylation procedure[150], using barium oxide as the base in DMSO[77], was an obvious alternative to the Johnstone method[151] (Chapter 2), since it was expected that the milder base would give greater selectivity, yet permit the epimerisation observed above.

The reaction of mycalamide A with benzyl bromide and barium oxide in DMSO at 60°C for 2 hours gave a mixture of four compounds by silica gel TLC. Preparative TLC separated these products and $^1$H NMR spectroscopy showed that these were 7-*O*-benzyl mycalamide A (**2.39**), 7,18-di-*O*-benzyl mycalamide A (**2.40**) and their C10 epimers (**6.3**, **6.4**), in about equal quantities. The new derivative from this synthesis, 7,18-di-*O*-benzyl 10*R* mycalamide A (**6.4**) was also fully characterised by NMR and mass spectroscopies. In particular, a more complete set of NOE data were recorded (Table 6.2) to conclusively assign the stereochemistry associated with the C14 methyl and C16 methylene resonances. Of significance was the enhancement of the downfield H16 resonance on irradiation of H11, and vice versa, so that this could be assigned to be pro-*S* on the basis of the molecular modelling work described in Chapter 5. Also, irradiation of the upfield 14-$CH_3$ resonance gave weak enhancements of the axial 13-$OCH_3$ and H16*R* proton resonances, so that this was assignable to the equatorial pro-*S* C14 methyl group. The $^1$H NMR spectral data were fully assigned by comparison with data for 7-*O*-benzyl 10*R* mycalamide A (Table 6.4) and these assignments were confirmed by a COSY experiment. A $^{13}$C NMR spectrum was also recorded and assigned using an HMQC experiment (Table 6.5).

It was significant that no amide benzylation was observed under these reaction conditions, whereas methylation occurred readily. This may indicate that the amide anion was being formed[156], but in low concentration, so that benzylation of the amide nitrogen was not sufficiently competitive, being also hindered by the benzyl ether at C7 and the size of the reagent. However, a C7 methoxyl group would give less steric hindrance to reactions of the amide anion, while the reagent for methylation, methyl iodide, is also smaller, so that methylation of both groups is reasonable. For the benzylation reaction, the more forcing conditions of potassium hydroxide in DMSO[151] probably increases the concentration of the amide anion sufficiently to overcome such steric factors.

### 6.3.3 DISCUSSION OF THE MECHANISM OF EPIMERISATION AT C10

The formation of an epimer at C10 requires the cleavage and readdition of one of its substituents. The best leaving group under basic conditions is the alkoxy oxygen of the C10-C12 dioxan ring, as shown by the formation of the oxazolidinone derivatives in the previous chapter (5). It is likely that these reactions both involve a similar imine intermediate, since they occur under essentially the same experimental conditions. Therefore a proposed mechanism for this epimerisation would begin with deprotonation of the amide to give the amide anion (a known intermediate from alkylation reactions) and, subsequently, the formation of an imine intermediate, by cleavage of the C10-O bond and formation of a second C10-N bond (Scheme 6.2a).

Note that C10 would have some electrophilic character, due to the combined electron withdrawing inductive effects of the amide nitrogen and alkoxy groups[170], so that the donation of some electron density from the amide anion in this reaction is not unreasonable. This is also consistent with the known nucleophilicity of the amide nitrogen under basic conditions[147,155].

Also, despite alkoxide ions being relatively poor leaving groups[140], it is known that α-amino ethers react with Grignard reagents[234,235], and other basic nucleophiles such as hydride ions[236], in substitution reactions which involve a preferential cleavage of the C-O bond. Furthermore, the partial breakdown of the *cis*-fused trioxadecalin ring system by C10-O bond cleavage may be compensated for by the relief of gauche interactions between C13 and the 12-$OCH_2$ carbon and between C10 and the opposite dioxan ring atoms.

**Scheme 6.2** Possible mechanisms for the base catalysed epimerisation of 7-*O*-benzyl mycalamide derivatives (**2.39**, **2.40**) at C10.

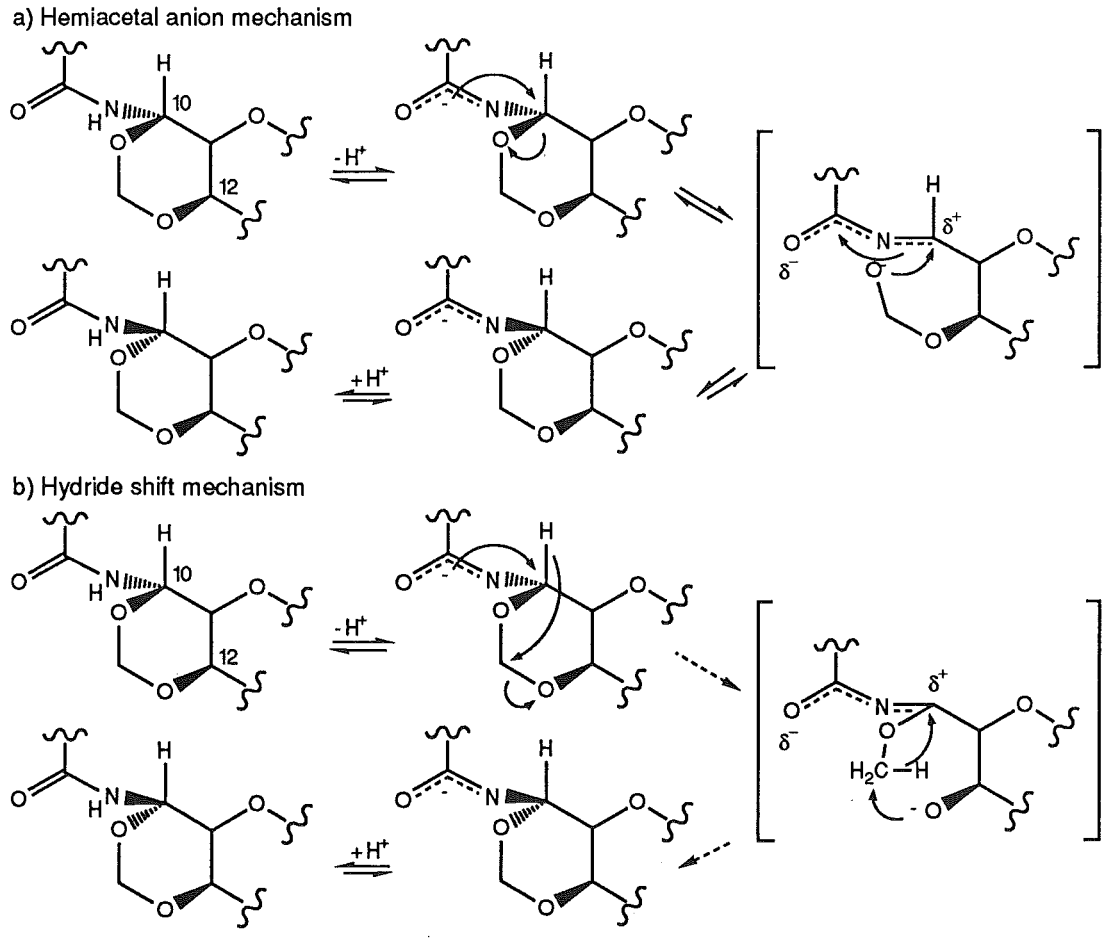


However, the cleavage of the C10-O bond would give a hemiacetal anion from the methylene acetal, C12-$OCH_2$-$O^-$, which must be unstable[237,238]. Such an anion would also be an effective intramolecular

nucleophile[140], so that an immediate reattack of the electrophilic imine carbon, C10, is likely, resulting in either reformation of the starting compound or its C10 epimer (Scheme 6.2a). If this is not possible because C10 has already undergone substitution, such as by C7-$O^-$ to give an oxazolidinone ring, then this hemiacetal would be likely to lose formaldehyde to give C12-O(H), as discussed in the previous chapter. The possibility of the involvement of such an unstable hemiacetal anion is best summarised by the following statement by C. D. Hurd[237]:- "Since compounds of these structures (hemiacetals) generally are not isolable as such from the simple aldehydes, they are sometimes disregarded in chemical reactions, whereas in many instances they are the vital intermediates".

The mechanism of the base catalysed racemisation of α-methyl-α-acetamidonitriles was elucidated by extensive kinetic studies, and was reported to proceed by elimination and readdition of the elements of HCN, i.e. via an imine intermediate[220]. A requirement for this reaction was that the amide nitrogen have a hydrogen atom attached. The rate determining step was expulsion of the leaving group, cyanide ion, from the amide anion, to yield an imine intermediate. Other analogous reaction mechanisms include the isomerisation of glycosylamines via an open chain imine[170] (anil), and the isomerisation of cyclic hemiacetals via an open chain aldehyde[106].

Additional experimental evidence is presented here in support of the above mechanism for epimerisations at C10 in 7-*O*-benzyl mycalamide A (**2.39**):-

i) no reaction was observed in the absence of base, or with amine bases

ii) other strong bases such as sodium methoxide in methanol effected the same transformation,

iii) *N*-methylation could be achieved readily under similar reaction conditions,

iv) no epimerisation was observed when the amide nitrogen was alkylated,

v) there was no incorporation of deuterium at C10 when the reaction was performed in deuterated methanol, despite more than 80% inclusion at C7,
vi) the epimerisation reaction was reversible.
The evidence presented in points ii), v) and vi) will be described in the following subsection.

Two alternatives to the above mechanism include the loss of the H10 substituent as either proton or hydride ion. The former would give an amidomethyl carbanion. Such species have been reported[155], but only where there was an α-carbonyl or α-cyano substituent adjacent for resonance stabilisation, and would therefore require a very strong base to obtain from the mycalamide structure. This unlikely possibility is refuted experimentally since there was no inclusion of deuterium at C10 for a reaction in deuterated methanol. A second alternative is the loss of H10 as hydride ion. Direct exchange with the solvent would seem to be unlikely. However, a hydride shift mechanism, similar to that which occurs in the Cannizzaro reaction[237,239], has been outlined in Scheme 6.2b. This involves a shift of hydride ion from C10 to 10-$OCH_2$, with cleavage of the $CH_2$-O(-C12) bond and formation of a new C10-N double bond from the amide anion. However, it is difficult to envisage a reverse reaction to reform the dioxan ring, making this an unlikely alternative. Furthermore, the intermediate imidate formed would probably be unstable, whereas no decomposition products were observed in the reaction above. A third possibility is a cleavage of the C-N bond and readdition, but the latter would also seem to be rather unlikely. Therefore the best mechanism to account for this epimerisation at C10 under basic conditions appears to be the original proposal.

### 6.3.4 CHARACTERISATION OF PRODUCTS FROM THE REACTION OF 7-*O*-BENZYL 10*R* MYCALAMIDE A WITH SODIUM METHOXIDE IN DEUTEROMETHANOL

The title reaction was performed in $d_1$-methanol, with the aims of checking for deuterium exchange at C10 during epimerisation, determining the reversibility of this epimerisation, and of examining the influence of a nucleophilic base on the reaction products obtained. Thus 7-*O*-benzyl 10*R* mycalamide A (**6.3**) was reacted with a solution of 1.5M sodium methoxide in deuteromethanol at 60°C for 2.5 hours, when TLC showed that most of the starting material had been consumed. Analysis by $^1$H NMR spectroscopy showed that a complex mixture of several compounds had been formed, but reverse phase HPLC indicated that most of these components were resolved. Preparative HPLC gave eight fractions, of which the first five were most significant, although all were less than 0.5 mg in mass. These fractions were analysed by $^1$H NMR and mass spectroscopies, and are described in order of their increasing HPLC retention times.

#### 6.3.4.1 HPLC FRACTION 1

The $^1$H NMR spectrum of the first, most polar fraction was very weak, and the multiplicity and identity of some resonances were difficult to determine. However there was also a notable absence of the two 10-OCH and H7 resonances. Partial data were obtained (Table 6.6), which included an H10 resonance shifted strongly downfield, at δ6.78 ppm (2.0,10.6 Hz), coupled to a multiplet at δ4.19 ppm. The latter was further coupled to a doublet at δ2.74 (9.1 Hz), as shown by a selective proton decoupling experiment. The chemical shifts, multiplicities and coupling constants[101] suggested that there was a double bond between C10 and C11 since the resonances at δ4.19 and δ2.74 ppm must be assigned to the H12 and H13

protons. This was supported by small shifts in the resonances of other ring substituents, particularly H15 (-0.3), compared to data for 7-*O*-benzyl mycalamide A (**2.39**). Note that the upfield shift in the H13 resonance (-0.7) would be associated with the loss of the C10-C12 methylene acetal to leave an hydroxyl group at C12[101,123], as shown for the mycalamide oxazolidinone derivatives in the previous chapter. The absence of the H7 resonance indicated the incorporation of deuterium at C7 by enolisation.

The sample was too small to perform further NMR spectroscopic analyses. However, a HRFABMS result was obtained, which indicated a compound of molecular formula $C_{30}H_{44}DNO_9$, in agreement with the proposed structure, **6.5**. Further characterisations will be described for a similar derivative, obtained from mycalamide A, later in this chapter. However, it is useful to note that this enamide structure is the tautomer of the proposed imine intermediate and that an analogous minor product was isolated from the racemisation of α-methyl-α-acetamidonitriles[220].

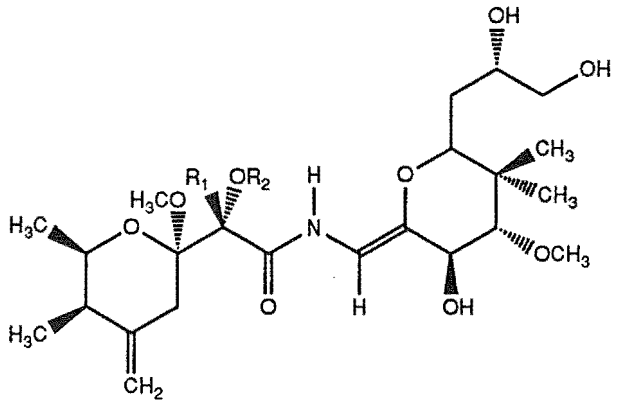


$R_1$=D, $R_2$=$CH_2$Ph: 7-Deutero, 7-*O*-benzyl, *Z*Δ[10] 10-deformyl myc.A (**6.5**)
$R_1$=$R_2$=H: *Z*Δ[10] 10-Deformyl mycalamide A (**6.16**)

6.3.4.2 HPLC FRACTION 2

The $^1$H NMR spectrum of the second HPLC fraction (major) was much more informative. It showed a new methoxyl resonance, loss of the two 10-

OCH and H7 resonances (implying a high incorporation of deuterium at C7), but an H10 resonance of normal multiplicity and intensity. Irradiation of H10 in an NOE experiment gave an enhancement of the methoxyl resonance at δ3.45 ppm, whereas irradiation of H13 enhanced a methoxyl resonance at δ3.44 ppm (Table 6.2), so that these methoxyl resonances could be assigned to groups at C10 and C13, respectively. Thus this derivative was probably a C10-*O*-methyl substitution product, having an hydroxyl group at C12. The remainder of the $^1$H NMR spectrum was assigned with the assistance of a COSY experiment (Table 6.6). There were shifts in the H10 (-0.5), H12 (-0.4), H13 (-0.4), 13-$OCH_3$ (-0.1), 14-$CH_3R$ (+0.1) and H16 (+0.3) proton resonances, compared to data for 7-*O*-benzyl mycalamide A (**2.39**), and a smaller observed H12-H13 coupling constant (5.6 Hz), suggestive of a mixture of the two possible chair conformations of the C11-C15 tetrahydropyran ring, as described in the previous chapter (5). Irradiation of the H11/H12 multiplet in an NOE experiment gave enhancements in the H10, H13, 14-$CH_3S$ and the more downfield H16 resonances (Table 6.2), confirming the presence of both these conformations.

These data were therefore consistent with the structure **6.6**, which was further supported by a HRFABMS result, indicating a compound of molecular formula $C_{31}H_{48}DNO_{10}$. Note that the stereochemistry at C10 was not conclusive from these data. However, the conformational behaviour of this compound was rather different from that observed for pederin (Chapter 1), which has a similar structure, so that it is proposed that the stereochemistry at C10 in this derivative is also different (i.e. 10*R*). This assignment was consistent both with the conformational behaviour of 7-*O*-benzyl 10*R* mycalamide A (**6.3**) and with the reportedly higher thermodynamic stability of the 10*R* over the 10*S* pederin derivatives, which caused the former (C10 epimers) to predominate in acid catalysed exchange equilibria[130].

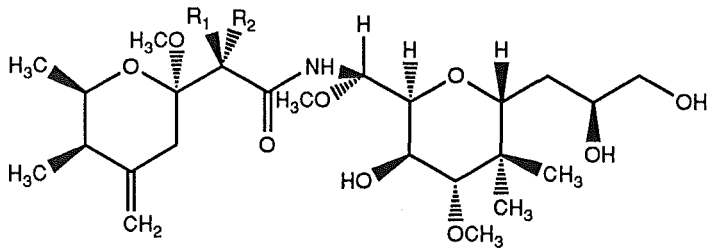

$R_1$=D, $R_2$=$OCH_2Ph$: 7-Deutero, 7-*O*-benzyl, 10*R*-*O*-methyl myc.A (**6.6**)
$R_1$=$OCH_2Ph$, $R_2$=D: 7-Deutero, 7*S*-*O*-benzyl, 10*R*-*O*-methyl myc.A (**6.9**)

6.3.4.3 HPLC FRACTION 3

The $^1H$ NMR spectrum of the third HPLC fraction was again very weak and showed a mixture of three main components, in a ratio of about 4:2:1. The most minor component of the three was the 7-deutero, 7-*O*-benzyl, 10*R*-*O*-methyl mycalamide A derivative (**6.6**) above, and the next smallest component was 7-deutero, 7-*O*-benzyl mycalamide A (**6.7**), representing an epimerisation at C10 without incorporation of deuterium at this position. The major component was a new derivative, but only partial data (Table 6.6) could be obtained due to the presence of the other compounds and the small sample size. There was a new methoxyl resonance at δ3.43 ppm, in addition to similar resonances at δ3.57 and 3.23 ppm, which were assigned to the groups at C10, C13 and C6, respectively. Therefore this derivative was probably 7-deutero, 7-*O*-benzyl, 10-*O*-methyl mycalamide A (**6.8**). The chemical shifts of the H10, 13-$OCH_3$, 14-$CH_3R$ and 14-$CH_3S$ resonances suggested that the major conformation of the C11-C15 ring of this derivative was the same as that for 7-*O*-benzyl mycalamide A (**2.39**). Therefore the stereochemistry at C10 was probably the same as for pederin and 7-*O*-benzyl mycalamide A.

The HRFABMS spectrum of this fraction showed two dominant $MK^+$ ions (*m/z* 635 and 633), in a ratio of about 4:1, respectively. This suggested that the major component of this fraction had a molecular formula of $C_{31}H_{48}DNO_{10}$, consistent with this being an isomer of compound **6.6** above,

whereas the minor ion implied a molecular formula of $C_{31}H_{46}DNO_{10}$, consistent with structure **6.7**. However there was insufficient material to perform further work on this compound.

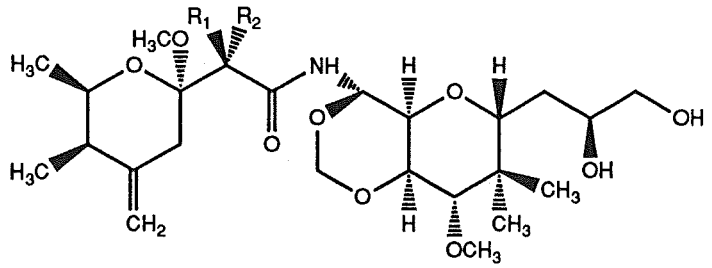

$R_1$=D, $R_2$=$OCH_2Ph$: 7-Deutero, 7-*O*-benzyl mycalamide A (**6.7**)
$R_1$=$OCH_2Ph$, $R_2$=D: 7-Deutero, 7*S*-*O*-benzyl mycalamide A (**6.11**)
$R_1$=OH, $R_2$=H: 7*S* Mycalamide A (**6.24**)

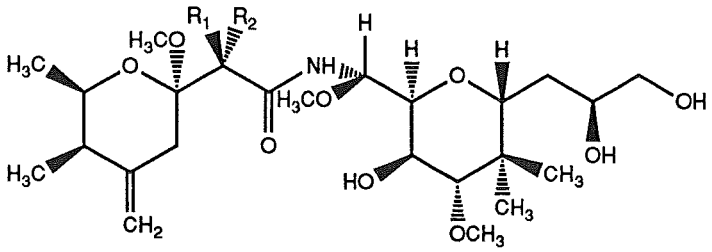

$R_1$=D, $R_2$=$OCH_2Ph$: 7-Deutero, 7-*O*-benzyl, 10*S*-*O*-methyl myc.A (**6.8**)
$R_1$=$OCH_2Ph$, $R_2$=D: 7-Deutero, 7*S*-*O*-benzyl, 10*S*-*O*-methyl myc.A (**6.12**)

6.3.4.4 HPLC FRACTION 4

The $^1H$ NMR spectrum of the fourth HPLC fraction showed that this consisted of another pure compound, which was also a 10-*O*-methyl derivative, as indicated by the presence of three methoxyl resonances, at δ3.45, 3.44 and 3.35 ppm. The chemical shifts of most resonances in this spectrum were very similar to those of 7-deutero, 7-*O*-benzyl 10*R*-*O*-methyl mycalamide A (**6.6**), but there was a significant difference in the chemical shifts of the H5a (+0.2), H5e (-0.3) and 6-$OCH_3$ (+0.2) proton resonances. This separation in the chemical shifts of the H5 resonances was earlier shown to be indicative of an epimerisation at C7 (Chapters 2 and 5), so that the structure was probably 7-deutero, 7*S*-*O*-benzyl, 10*R*-*O*-methyl mycalamide A

(**6.9**). The $^1$H NMR data were readily assigned by comparison with the data for compound **6.6** and by selective proton decoupling experiments, including the irradiation of H10 and H13, which elucidated the chemical shifts and coupling constants for the H11 and H12 proton resonances (Table 6.6). The vicinal proton-proton coupling constants and chemical shifts for substituents of the C11-C15 ring indicated that the same mixture of conformations for this ring were present in this derivative as for 7-deutero, 7-*O*-benzyl 10*R*-*O*-methyl mycalamide A (**6.6**), as expected. Good HRFABMS data were also obtained for this compound, supporting the proposed structure.

6.3.4.5 HPLC FRACTIONS 5 AND 6

The $^1$H NMR spectrum of the fifth HPLC fraction showed that this consisted almost entirely of starting material, 7-*O*-benzyl 10*R* mycalamide A, but with at least 80% incorporation of deuterium at C7 by integration (structure **6.10**). This fraction also contained a minor amount of the compound in fraction 4 above.

The $^1$H NMR spectrum of the sixth HPLC fraction was rather weak, but showed the presence of one reasonably pure component, which had data very similar to those of 7-*O*-benzyl mycalamide A (**2.39**). However, the two H5 resonances were well spread in chemical shift and the C6 methoxyl resonance was shifted downfield (Table 6.6). Therefore this was likely to be 7-deutero, 7*S*-*O*-benzyl mycalamide A (**6.11**) and the molecular formula for this structure was confirmed by HRFABMS. Unfortunately there was insufficient sample to perform further studies on this derivative or even to obtain complete $^1$H NMR spectral data.

### 6.3.4.6 HPLC FRACTIONS 7 AND 8

The $^1$H NMR spectrum of the seventh HPLC fraction was also weak, but showed that it consisted of a mixture of two major components, of which the slightly dominant component was new, but the other was the compound in fraction 6 above, arising from incomplete resolution of these peaks during separation by HPLC. The resonances for the new component could still be distinguished in the mixture, enabling a partial assignment of the data (Table 6.6). In particular, this compound was clearly a fourth 10-*O*-methyl derivative, and probably the C7 epimer of the isomer in fraction 3, based on the chemical shifts of the two H5 and C6 methoxyl resonances and the similarity of data relating to H10 and substituents of the C11-C15 ring. These data suggested that the major solution conformation of this portion of the structure was similar to that of 7-*O*-benzyl mycalamide A and pederin. Therefore this compound was assigned the structure **6.12**, but the sample was too small to purify or to perform further characterisations on it.

The $^1$H NMR spectrum of the eighth HPLC fraction was very weak, but revealed the presence of one major compound retaining the C10-C12 methylene acetal. The spectrum was similar to that obtained for 7-deutero, 7-*O*-benzyl 10*R* mycalamide A, **6.10** (fraction 5), where the chemical shifts and coupling constants indicated that the major solution conformation of the trioxadecalin ring system was an opposite chair-chair conformation to that found in mycalamide A. However, there were additional shifts in the two H5 and C6 methoxyl resonances, which suggested that this was a C7 epimer, 7-deutero, 7*S*-*O*-benzyl 10*R* mycalamide A (**6.13**), and partial $^1$H NMR spectral data are listed in Table 6.6. Again this sample was too small to perform further characterisations of this derivative.

### 6.3.4.7 COMPARISONS WITH PRODUCTS FROM A REACTION ON 7-*O*-BENZYL MYCALAMIDE A

An additional experiment was performed, involving similar reaction conditions to those above, but beginning with 7-*O*-benzyl mycalamide A (**2.39**), to investigate the possible influence of the C10 stereochemistry of the substrate on the ratio of products obtained. Thus, after reaction in a 1M solution of sodium methoxide in methanol for two hours at 70°C, the reaction was worked up and the crude mixture examined by $^1$H NMR spectroscopy.

The $^1$H NMR spectrum of the mixture was complex, as expected, but the methoxyl resonances, in particular, were distinctive for all of the derivatives above, enabling them to be easily recognised. All of the above products were present so this spectrum was compared directly with that obtained for the crude reaction mixture (from 7-*O*-benzyl 10*R* mycalamide A) above. Ignoring deuterium uptake at C7, it was found that the major isomer from the first reaction, 7-*O*-benzyl 10*R*-*O*-methyl mycalamide A (**6.6**), was also the major product of this reaction, but there was more 7-*O*-benzyl 10*R* mycalamide A (**6.3**), less of the C7 epimers, and less of the elimination product, **6.5**. The latter results were probably due to the slightly less basic conditions used in this second reaction. The epimerisations at C10 and the similarity in the ratios of the 10-*O*-methyl substitution products were indicative of the involvement of a common imine intermediate in this reaction. However it was not established whether epimerisation at C10 could occur for the 10-*O*-methyl derivatives via the same intermediate. From the work above and the observed reactions of the mycalamide oxazolidinones (Chapter 5) this was probable, despite the fact that methoxide ion was also a poor leaving group[140]. Note that pederin was not subjected to such strongly basic reaction conditions[27,94,129,132]

### 6.3.4.8 CONCLUSIONS

It has been shown that, overall, nine compounds were formed from the reaction of 7-*O*-benzyl 10*R* mycalamide A (**6.3**) with sodium methoxide in $d_1$-methanol. These consisted of four isomers of 7-deutero, 7-*O*-benzyl mycalamide A (**6.7**), involving epimerisations at either or both of the C7 and C10 positions (fractions 3, 5, 6, 8), four isomers of 7-deutero, 7-*O*-benzyl, 10-*O*-methyl mycalamide A (**6.8**), arising from a reaction involving substitution of methoxide ion at C10, loss of the C10-C12 methylene acetal, and similar epimerisations at C7 (fractions 2, 3, 4, 7), and an elimination product, 7-deutero, 7-*O*-benzyl, $\Delta^{10}$ 10-deformyl mycalamide A (**6.5**) (fraction 1). Significantly, deuterium was incorporated only at C7, not C10, during the epimerisations observed, as stated above.

These reactions would be very useful for preparing C10-*O*-alkyl mycalamide derivatives, analogous to pederin, provided that the benzyl protecting group could be removed quantitatively. In particular, such derivatives would be increasingly dominant with longer reaction times, since the complete loss of the C10-C12 methylene acetal to yield C12-$O^-$ and formaldehyde would almost certainly be irreversible. From shorter reactions, isomers at both C7 and C10 of mycalamide A could be obtained. Unfortunately time did not permit further investigations of these possibilities.

## 6.3.5 FURTHER PRODUCTS FROM THE REACTIONS OF 7-MONO- AND 7,18-DI-*O*-BENZYL MYCALAMIDE A WITH BARIUM OXIDE IN DMSO

Having demonstrated the potential for epimerisation and substitution at C10 in 7-*O*-benzyl mycalamide A (**2.39**), there was still the question of its reactivity under more forcing, non-nucleophilic basic conditions. In particular, it was of interest to ascertain whether the same cleavage reaction occurred for

this derivative as for the *N*-benzylated compound, 7,18-di-*O*-benzyl, *N*-benzyl mycalamide B (**2.46**), described at the beginning of this chapter.

Therefore a mixture of 7-*O*-benzyl mycalamide A (**2.39**), 7,18-di-*O*-benzyl mycalamide A (**2.40**) and their C10 epimers (**6.3**, **6.4**) was prepared according to the method described in Section 6.3.2, and this was then heated further with barium oxide in DMSO for 16 hours at 80°C. The reaction was monitored by TLC and this showed the gradual disappearance of all four compounds to yield what appeared to be a single product. However, reverse phase HPLC showed the presence of two well-resolved components, which were therefore separated prior to analysis. DCIMS showed that the two products were isomers, of molecular formulae $C_{18}H_{25}NO_4$, so that these were new cleavage products. The FTIR spectra of these isomers both contained a strong carbonyl stretch at 1685 $cm^{-1}$, indicating the presence of the amide functionality.

A $^1H$ NMR spectrum of the first fraction revealed resonances derived from the left hand portion of 7-*O*-benzyl mycalamide A (**2.39**) to the amide, but there were no resonances from C10 onwards. There were two very broad singlets at δ6.35 and 5.43 ppm, indicative of protons on the nitrogen of a primary amide, which were non-equivalent due to the restricted rotation about the C-N bond and the shielding effects associated with the amide carbonyl group[107], as discussed in earlier sections. There were also small shifts in the H7 (-0.1) and upfield 7-OCH (-0.1) proton resonances (Table 6.4). A $^{13}C$ NMR spectrum was also recorded, which showed similar chemical shifts to those recorded for the left hand portion of 7-*O*-benzyl mycalamide A (**2.39**), except for minor shifts in the C7 (-1.7) and C8 (+1.5) resonances (Table 6.5). These data were therefore consistent with cleavage of the C10-N bond in the starting compounds to give a primary amide fragment. In fact the underivatised primary amide, pederamide (**3.4**), has been reported as a cleavage fragment

from pederin under mildly acidic conditions[126] and has been synthesised[133,240]. A comparison of the $^1$H NMR data above with those reported for pederamide[133] showed good agreement, allowing for some differences around C7 due to the presence of the benzyl ether functionality, confirming that this was 7-*O*-benzyl pederamide (**6.14**).

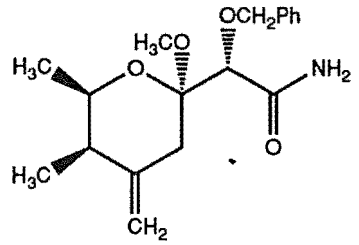


7-*O*-Benzyl pederamide (**6.14**)

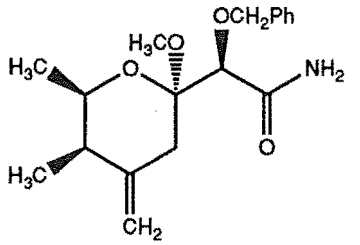


7*S*-*O*-Benzyl pederamide (**6.15**)

The $^1$H NMR spectrum of the second fraction was very similar to that of the first fraction above but there were shifts in the H5a (+0.3), H5e(-0.3), 6-$OCH_3$ (+0.3), H7 (+0.1), upfield 7-OCH (+0.1) and downfield NH (+0.2) proton resonances (Table 6.4), which were indicative of an epimerisation at C7. A $^{13}$C NMR spectrum also showed a shift in the C7 (+1.9) and 7-$OCH_2$ (+1.3) resonances, compared to data for 7-*O*-benzyl pederamide (Table 6.5). Therefore this was 7*S*-*O*-benzyl pederamide (**6.15**), obtained from the compound above by an enolisation reaction under the basic reaction conditions.

NOE experiments were performed to examine the solution conformations of these two derivatives. However, almost identical results were obtained for both C7 isomers (Table 6.2), indicating that the C7-N9 chain portions were quite flexible. Note that selective irradiation of one NH resonance was not possible due to conformational and chemical exchange.

The observed cleavage of the C10-N bond of 7-*O*-benzyl mycalamide A (**2.39**) and derivatives under these basic conditions represents an hydrolysis of the proposed imine intermediate. In this reaction it is proposed that an

unstable hemiaminal[241,242] is formed by substitution of hydroxide ion at C10, as shown in Scheme 6.3, which then breaks down to give the corresponding primary amide and an aldehyde. This reaction is exactly the reverse of the known base catalysed condensation of primary amides with aldehydes to give acylated amino alcohols[241], which often react further to give alkylidene bisamides. That this cleavage did not occur for *N*-alkylated substrates is further evidence for the involvement of an imine intermediate in these base catalysed reactions. Evidently the aldehyde formed is unstable under the reaction conditions, since no other products could be isolated. This is consistent with the reactivity of aldehydes under alkaline conditions, permitting further rearrangements and degradations[233].

**Scheme 6.3** Proposed mechanism for the base catalysed cleavage of 7-*O*-benzyl mycalamide A derivatives (**2.39**, **2.40**, **6.3**, **6.4**).

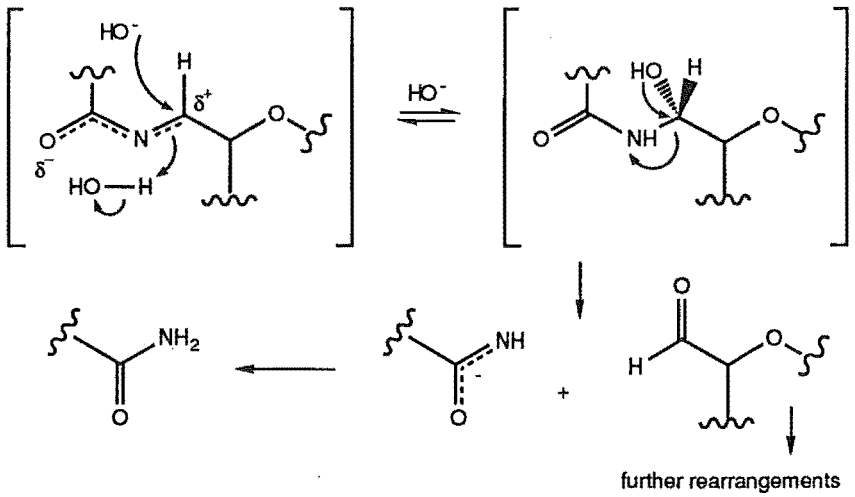


Thus two different cleavages of the mycalamide structure had been achieved, using a benzyl protecting group for the C7 hydroxyl, which have been shown to depend on the substitution state of the amide nitrogen. However, the presence of an ether group at C7 was not favourable for determining structure-activity relationships, since such derivatives were relatively inactive (Chapter 2). Therefore attention was focused again on

mycalamide A as a substrate, since it was possible that substitution reactions could be performed at C10 under mildly basic conditions at high temperature. Note, however, that the nucleophile could not itself be a strong base since this would favour the formation of mycalamide A oxazolidinone derivatives. These investigations on mycalamide A are described below.

## 6.4 REACTIONS OF MYCALAMIDE A IN THE PRESENCE OF SODIUM AZIDE IN DMSO

Azide ion is a good nucleophile in both protic and dipolar aprotic solvents[153,243]. Substitution reactions involving this nucleophile have been studied for various substrates, ranging from simple alkyl halides and tosylates to more complex sugar derivatives[147]. Commonly dipolar aprotic solvents, such as DMF or DMSO, have been used in these reactions, since the anions are much less solvated than in protic solvents but the polarisable charged transition states are more solvated, so that bimolecular reactions of anions are much faster in these solvents[243]. Despite these advantages, the reactions of various partially protected sugar derivatives, containing tosylate leaving groups, with sodium azide in DMF required temperatures of 140°C for several hours to effect substitution[147].

### 6.4.1 PREPARATION AND PURIFICATION OF PRODUCTS FROM MYCALAMIDE A

The reaction of mycalamide A with sodium azide in DMSO at 130-140°C was slow, but after four days a number of products were observed by silica gel TLC. Preparative TLC gave six fractions (ordered according to increasing $R_f$), which were examined initially by $^1H$ NMR spectroscopy. This showed that three fractions (1, 2 and 6) were pure compounds but fractions 3,

4 and 5 were still mixtures. Fraction 3 was a mixture of unreacted mycalamide A and mycalamide A *cis* and *trans* oxazolidinones (**5.2**, **5.3**) so this was not considered further. However, fractions 4 and 5 contained at least three different components, including mycalamide A *trans* oxazolidinone (**5.3**), so these fractions were further examined by reverse phase HPLC. Separation of the components by HPLC gave three further fractions containing unknown compounds, so that overall six new products had been isolated from this reaction, excluding unreacted mycalamide A and mycalamide A *cis* and *trans* oxazolidinones. These products were then examined by NMR and mass spectroscopies.

### 6.4.2 CHARACTERISATION OF THE MAJOR PRODUCT

The major product from the reaction (from fraction 2) represented about half of the purified products by mass. HRFABMS showed that it had a molecular formula of $C_{23}H_{39}NO_9$, corresponding to a loss of $CH_2O$ from mycalamide A. The $^1H$ NMR spectrum showed an absence of the two 10-OCH and H11 resonances, and shifts in the NH (+1.1), H10 (+0.8), H13 (-0.7), H15 (-0.2), $H_2$16 (+0.2), H17 (+0.2) and two H18 (+0.1) proton resonances, as assigned by a COSY experiment (Table 6.7). The observed shifts in the NH-H15 resonances and the 2 Hz coupling constant between H10 and H12 were consistent with the presence of a double bond between C10 and C11 and an hydroxyl group at C12[101,104], as proposed for a 7-*O*-benzyl derivative (**6.5**) earlier in this chapter. The shifts in the C16-C18 sidechain proton resonances suggested that the solution conformations of this substructure were significantly affected by the elimination, and NOE experiments were performed to investigate this and to solve the stereochemistry of the double bond substituents at C10.

**Figure 6.3** Selected $^1H$-$^1H$ NOE interactions and partial solution conformations for $\Delta^{10}$ 10-deformyl mycalamide A isomers (**6.16** and **6.19**).

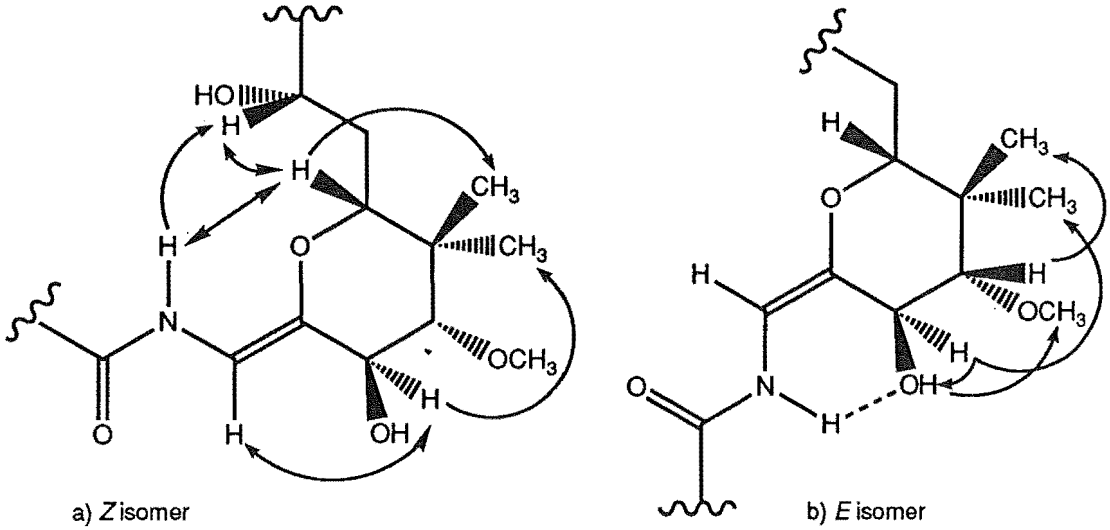


There were NOE interactions between the H10 and H12 protons, as well as between the NH and H15 and H17 protons (Table 6.8), which required that the double bond stereochemistry be *cis*, i.e. a *Z* isomer, as shown in Figure 6.3a, so that the structure was *Z* $\Delta^{10}$ 10-deformyl mycalamide A (**6.16**). There was also a weak interaction between H7 and H10 which suggested the presence of a small amount of the *E* geometry about the C8-N amide bond in solution. Other NOE interactions, including H12-14-$CH_3$*S* and H13-H15, were indicative of the normal chair conformation for the C11-C15 ring, albeit slightly distorted by the new exocyclic double bond. This was in agreement with the chemical shifts for the ring substituents and the 9 Hz coupling constant between the H12 and H13 protons, requiring that these protons be in an anti relationship[98]. Also, the geometric relationship between an axial H12 proton and the exocyclic H10 proton was analogous to that observed between the axial H5 proton and the exocyclic 4=CH*E* proton, in agreement with the observed long range proton coupling constants of 2 Hz in each case[104]. The coupling constants between H15 and the two H16 protons were also

indicative of a major conformation about C16-C17 having C17 anti to C14, which was consistent with the observed long range NOE interaction between NH and H17 (Figure 6.3a).

A $^{13}C$ NMR spectrum of this derivative was assigned using HMQC and HMBC experiments (Tables 6.9 and 6.10). The C10 and C11 resonances were located at δ104.9 and 141.7 ppm, consistent with the presence of a new double bond[117]. There were also large shifts in the C8 (-4.5), C12 (-4.8), C13 (+11.6) and C15 (+6.0) resonances associated with this unsaturated enamide structure, and with the cleavage of the methylene acetal at C12 to an hydroxyl group, as discussed above.

The formation of this enamide derivative (**6.14**) provided some support for the proposed involvement of its tautomer, the imine intermediate, in this reaction also, as implied by the presence of both mycalamide oxazolidinone isomers in the product mixture. In particular, it appeared that the azide ion in DMSO was behaving as a significantly strong base, to facilitate formation of the amide anion and removal of the C11 proton, although this required high reaction temperatures where elimination reactions might be expected to be more competitive with substitution reactions[176]. This basicity is consistent with the the reported properties of azide ion and even halide ions in dipolar aprotic solvents, being much more reactive towards hydrogen than in protic solvents, so that they behave as both strong bases and powerful nucleophiles[243].

There is some conjugation possible between the C10-C11 double bond and the amide π system which may stabilise this compound. Physical evidence for this conjugation is the observed UV absorbance of this compound at λ=254 nm on silica gel TLC plates. Some antibiotics[244,245] have also been isolated containing a similar alkoxy enamide structural fragment[228], and this enabled some comparison of the $^{13}C$ NMR data.

However this substructure was clearly uncommon. The biological activity of this derivative will be discussed with other results at the end of this chapter.

### 6.4.3 CHARACTERISATION OF THE MINOR PRODUCTS

#### 6.4.3.1 10*R* MYCALAMIDE A (AND B)

The product obtained in the next highest yield (~12%, from HPLC on TLC fractions 4 and 5) was much smaller in mass (less than 1 mg). A $^{1}$H NMR spectrum was very similar to that obtained for 7-*O*-benzyl 10*R* mycalamide A (**6.3**), but without the benzyl resonances and related substituent effects[101]. The data were readily assigned using results from a COSY experiment and selective decoupling experiments (Table 6.7). The chemical shifts and vicinal proton-proton coupling constants for substituents of the trioxadecalin ring system were indicative of the presence of the opposite chair-chair conformation to that found for mycalamide A as the major solution conformation for this system in this derivative. NOE experiments (Table 6.8) gave almost identical results to those for the 7-*O*-benzyl 10*R* mycalamide A derivatives (**6.3**, **6.4**), requiring that there be an inversion of configuration at C10 in mycalamide A, accounting for the conformational changes above. Partial $^{13}$C NMR data were obtained by direct acquisition, and the remaining data were obtained indirectly from HMQC and HMBC experiments performed at 500 MHz (Tables 6.9 and 6.10). These data were similar to those obtained for the 7-*O*-benzyl derivatives, except in the vicinity of C7. HRFABMS confirmed that this compound was an isomer of mycalamide A. Therefore all the evidence above was consistent with the proposed structure, 10*R* mycalamide A (**6.17**).

Interestingly, 10*R* mycalamide A (**6.17**) had a significantly longer retention time on reverse phase HPLC than mycalamide A, just as observed for the 7-*O*-benzyl derivatives, but these compounds were not resolved on

silica gel TLC. The isolation and characterisation of this derivative prompted a review of earlier results from the reactions of mycalamides A and B with various bases, described in the previous chapter (5). One fraction from a reaction of mycalamide B with sodium methoxide in methanol had given a mixture of mycalamide B *trans* oxazolidinone and an unknown mycalamide B derivative containing the C10-C12 methylene acetal by $^1$H NMR spectroscopy. Reexamination of this spectrum showed that there were resonances consistent with a 10*R* mycalamide B compound (**6.18**) and, by using the retention time characteristics of such compounds on reverse phase HPLC, this was readily purified. The $^1$H NMR spectrum of this sample was very similar to that of 10*R* mycalamide A, and was readily assigned with the assistance of a COSY experiment (Table 6.7) and NOE experiments to assign the methoxyl resonances (Table 6.8). Although the sample was too small to obtain $^{13}$C NMR data, the molecular formula was readily confirmed by HRFABMS. Therefore the isolation of these compounds was further indication of the possible involvement of a common imine intermediate in these reactions.

6.4.3.2 *E* ISOMER OF THE ENAMIDE, $\Delta^{10}$ 10-DEFORMYL MYCALAMIDE A

The yields of the remaining four products were less than 10%, corresponding to sample masses of less than 0.5 mg. The $^1$H NMR spectrum of one sample (from HPLC on TLC fraction 5) was very similar to that of the major product, *Z* $\Delta^{10}$ 10-deformyl mycalamide A (**6.16**), suggesting that it was the *E* isomer of the C10-C11 double bond (**6.19**). There was an absence of the two 10-OCH and H11 resonances and a long range coupling (1.7 Hz) was observed between H10 and H12[104]. However, the H12 resonance was further split by coupling to a sharp doublet at δ2.65 ppm (2.7 Hz), as shown by a selective proton decoupling experiment. This new resonance was assigned to the C12 hydroxyl proton since it was removed on addition of $D_2O$. A COSY

experiment was recorded to confirm further assignments of the $^1$H NMR data (Table 6.7). There were shifts in the H5a (-0.3), H5e (-0.1), NH (+0.9), H10 (+0.3), H12 (+0.2) and H13 (+0.2) proton resonances, compared with data for the *Z* isomer, consistent with a different geometry of the C10-C11 double bond, causing different electronic[101] and shielding effects[123] between the substituents. Of particular note was the observation of the NH resonance at δ9.43 ppm, suggesting that this proton was involved in a strong hydrogen bonding interaction[101]. The observation of the C12 hydroxyl resonance, not normally observed, suggested that the C12 oxygen could be involved in this hydrogen bond. In fact the *E* geometry of the C10-C11 double bond allows the NH proton to be close to the C12 oxygen, and a 6-membered ring would be formed by a hydrogen bond between these atoms (Figure 6.3b). The conformation of this new ring could be described as an envelope, since the partial conjugation of the enamide would cause the NH proton to be approximately in the plane of this π system[107], with the N, C10, C11 and C12 atoms. The solution conformation of the C11-C15 ring was the same in both isomers, as shown by the chemical shifts, the similarity in the magnitude of the H12-H13 coupling constant, and by the observation of similar NOE interactions (Table 6.8).

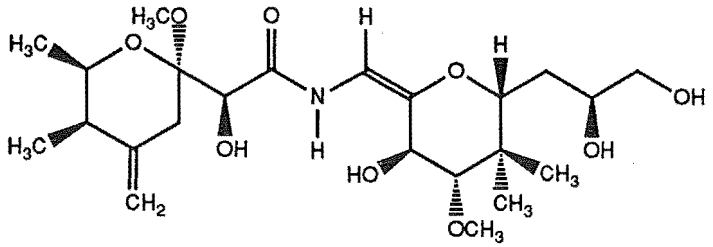


*E* $\Delta^{10}$ 10-Deformyl mycalamide A (**6.19**)

It was interesting that, despite the observed hydrogen bonding interaction in this isomer and the *trans* stereochemistry, it was the minor product of the two isomers. It is possible that unfavourable steric interactions

between the amide nitrogen and the C12 and C12 oxygen atoms, being on the same side of the double bond, are a factor in this. The polarity of this compound was close to that of mycalamide A on both silica gel and reverse phase HPLC and, during an attempt to purify this sample for further biological assays, the sample was unfortunately lost. Hence no mass spectroscopy measurement was obtained, but the $^1$H NMR data discussed above permitted little ambiguity about the structure of this product.

6.4.3.3 PEDERAMIDE

Another minor product (from TLC fraction 6) was found to be pederamide (**3.4**) by $^1$H NMR spectroscopy (Table 6.4), FTIR, CIMS and HREIMS, there being good agreement with the reported data for this derivative[126,133]. In a further experiment, the major product of this reaction, *Z* $\Delta^{10}$ 10-deformyl mycalamide A (**6.16**), was treated with sodium azide in DMSO for six days at 90°C. The major product after workup and preparative TLC was found to be pederamide (**3.4**), although there was also some unreacted starting material and a trace amount of some unknown mycalamide A oxazolidinone derivatives. Therefore pederamide would be a major hydrolysis product from longer reactions of mycalamide A with azide ion. This larger sample of pederamide enabled a $^{13}$C NMR spectrum to be recorded and assigned (Table 6.9), thus adding to the existing data for this derivative, and also allowed more reliable biological assay results to be obtained.

6.4.3.4 11*R* MYCALAMIDE A *TRANS* OXAZOLIDINONE

The remaining two products were mycalamide A oxazolidinone derivatives by their characteristic blue chars on silica gel TLC plates following visualisation with anisaldehyde. The major one was the lowest $R_f$ on silica gel of all the products (TLC fraction 1). A $^1$H NMR spectrum showed a coupling

constant of 2 Hz between the H7 and H10 protons, suggesting the formation of a mycalamide A *trans* oxazolidinone derivative[209]. However, there were shifts in the H10 and H13 proton resonances, and the overlap of signals hindered further assignments. The sample was therefore reanalysed in $CD_3OD$ in an attempt to simplify the spectrum.

Irradiation of H10 in a selective proton decoupling experiment located the H11 resonance in the new $^1H$ NMR spectrum, at δ3.12 ppm, which had the unusual coupling constants of 1.1 and 9.9 Hz to H10 and H12 respectively, indicative of gauche and anti relationships between these protons[102]. Irradiation of H11 in an NOE experiment gave enhancements of the H10 and H13 resonances (Table 6.8). These results, and the large coupling constant between H12 and H13, required that the C11-C15 ring be almost entirely in the normal chair conformation (which was different from that observed for mycalamide A *trans* oxazolidinone, **5.3**), but that the configuration at C11 be inverted, as shown in Figure 6.4 and in structure **6.20**. A COSY experiment was performed which assigned the remainder of the $^1H$ NMR data (Table 6.11). The observed shifts in the H10 (0.1), H11 (-0.7), H12 (-0.2), H13 (-0.3), 14-$CH_3$*R* (-0.1) and H15 (-0.4) proton resonances, compared with data for mycalamide A *trans* oxazolidinone (**5.3**), were also consistent with this epimerisation at C11 and the proposed solution conformation. The molecular formula for this 11*R* mycalamide A *trans* oxazolidinone derivative (**6.20**) was verified by HRFABMS.

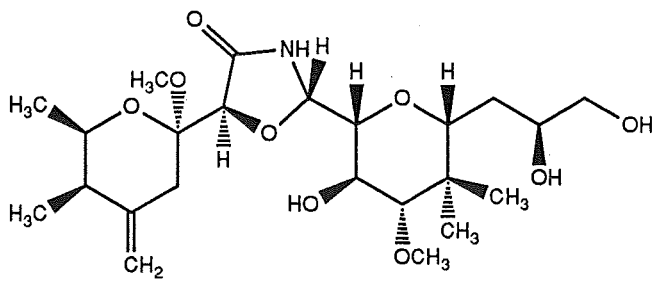


11*R* Mycalamide A *trans* oxazolidinone (**6.20**)

**Figure 6.4** $^{1}H$-$^{1}H$ NOE interactions and partial solution conformation for 11*R* mycalamide A *trans* oxazolidinone (**6.20**)

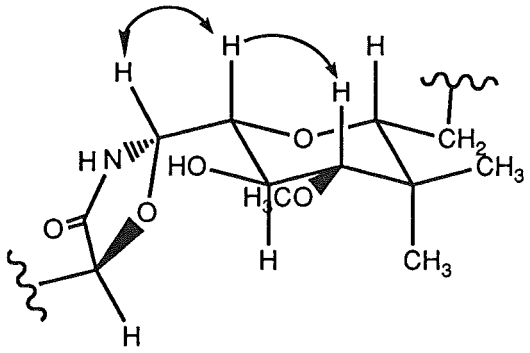


The $^{1}H$ NMR spectrum in $CDCl_3$ was able to be assigned by comparison with the data above, and this is included (Table 6.11) to enable further comparisons of this data with those of mycalamide A *trans* oxazolidinone (**5.3**). The only major difference from the data above was in the size of the H10-H11 coupling constant, 5.0 Hz, compared with 1.2 Hz above. This reflected only a small difference in the relative populations of the various rotamers about the C10-C11 bond, indicative of the greater importance of intramolecular hydrogen bonding interactions in this solvent. In particular, hydrogen bonding interactions are possible between C12-OH and C10-N or C10-O, or NH and C12-O or C11-O, which result in dihedral angles between H10 and H11 closer to 0 or 180°, thus increasing the size of the coupling constant according to the Karplus equation[98]. However, the exact conformations were not investigated further.

This product represents an addition of the C7-O-H group across the top face of the (*Z*) C10-C11 enamide double bond. The addition of alcohols to activated double bonds is well known[110,246], and here C10 is electrophilic, and therefore more susceptible to nucleophilic attack by the C7 oxygen.

### 6.4.3.5 $\Delta^{11(12)}$ MYCALAMIDE A *TRANS* OXAZOLIDINONE

The final fraction (from HPLC on TLC fraction 4) was a very small sample, of similar polarity to mycalamide A. The $^1$H NMR spectrum was weak and showed an absence of the two 10-OCH doublets, and the presence of coupled H10 and H7 proton resonances, at δ5.41 and 4.42 ppm (2.0 Hz), indicative of a mycalamide A *trans* oxazolidinone derivative, as above. However, the H10 resonance appeared only as a doublet, being completely decoupled on irradiation of H7, and was shifted slightly upfield, compared to that for mycalamide A *trans* oxazolidinone (**5.3**). There was a small downfield shift (+0.2 ppm) in the H15 resonance, which was partially decoupled by selective irradiation at δ1.55 ppm, performed to reduce the intensity of the $H_2O$ resonance, implying the location of one of the H16 resonances at this chemical shift. There was also a significant upfield shift (-0.2) in the C13 methoxyl resonance, whereas the C14 methyl proton resonances were not greatly affected. There was a doublet at δ5.18 ppm coupled to a second doublet at δ3.33 ppm (2.6 Hz), as shown by a proton decoupling experiment, which were assigned to the H12 and H13 protons, respectively. Note that there was no H11 proton, as shown by the multiplicity of the H10 resonance, so that there must be a double bond between C11 and C12, which would also account for the observed chemical shifts[101]. Therefore the structure was **6.21**, and the remaining $^1$H NMR data were readily assigned (Table 6.11). HRFABMS showed a compound of molecular formula $C_{23}H_{37}NO_8$, representing a loss of $H_2O$ from mycalamide A *trans* oxazolidinone, in agreement with the proposed structure. This derivative could arise from a substitution of the C7 oxygen at the C10 position of the enamide derivative (**6.16**), and migration of the C10-C11 double bond to C11-C12, with elimination of the allylic C12 hydroxyl group.

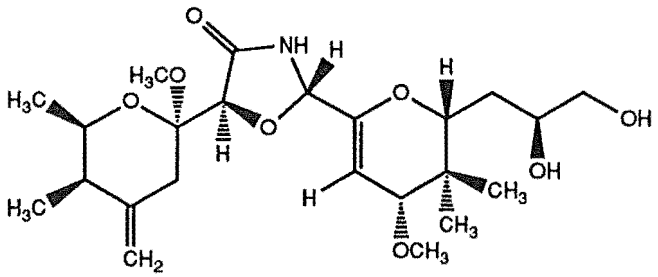

$\Delta^{11}$ Mycalamide A *trans* oxazolidinone (**6.21**)

Therefore the products from the reaction of mycalamide A with sodium azide had been identified and characterised as much as sample size would permit. Some unexpected products were obtained, exemplifying the base chemistry of this aza acetal substructure, which could give important structure-activity correlations. Before describing these results, it is useful to consider the results of two further reactions involving basic conditions, also performed on mycalamide A.

## 6.5 OTHER REACTIONS - REDUCTION AND OXIDATIVE CLEAVAGE OF MYCALAMIDE A

### 6.5.1 REACTIONS OF MYCALAMIDE A WITH SODIUM BOROHYDRIDE IN DMSO

It was proposed that the reactivity of the C10 aza acetal under basic conditions could permit the reduction of this system. Sodium borohydride in dipolar aprotic solvents is reported to be an effective source of nucleophilic hydride ion[247], which can be utilised for the reductive displacement of primary and secondary alkyl halides and sulphonate esters. In particular, the use of dipolar aprotic solvents accelerates the rate of nucleophilic substitution reactions ($S_N2$), without greatly enhancing other forms of attack, such as carbonyl additions[247]. The mildness of the borohydride reagent also allows more selective reactions to be performed, since carboxylic acids, esters and

amides are not affected, whereas lithium aluminium hydride, for example, is much less selective.

Mycalamide A was reacted with a very large excess of sodium borohydride in DMSO at 130°C for two days. After workup, TLC indicated that there was a mixture of at least three products, dominated by mycalamide oxazolidinone compounds. A $^1$H NMR spectrum of this mixture showed that the major product was mycalamide A *trans* oxazolidinone (**5.3**), with a minor amount of the *cis* isomer (**5.2**). However, there was also a minor amount of some mycalamide derivative not containing an oxazolidinone ring and having no C10 methylene acetal system. Preparative TLC gave five fractions, of which three were mixtures of unreacted mycalamide A and mycalamide A *cis* and *trans* oxazolidinones by $^1$H NMR spectroscopy. The remaining two fractions (1 and 2) contained new derivatives, which were then analysed by NMR and mass spectroscopies.

6.5.1.1 CHARACTERISATION OF THE COMPOUND IN FRACTION 1

The first compound (from TLC fraction 1) was more polar than mycalamide A and represented almost one quarter of the purified products by mass, discounting unreacted mycalamide A. HRFABMS indicated a compound of molecular formula $C_{24}H_{41}NO_9$, corresponding to a loss of CO from mycalamide A. An FTIR spectrum included a carbonyl stretching band at 1660 cm$^{-1}$, representing a 20 cm$^{-1}$ shift to lower frequency of the secondary amide band. This was consistent with the removal of the electron withdrawing acetal oxygen substituent at C10, allowing more electron density to be donated by the amide nitrogen to the carbonyl group[96].

The $^1$H NMR spectrum showed a loss of the two 10-OCH doublets of the mycalamide A spectrum, and shifts in the NH (-0.4), H10 (-2.1), H11 (+0.3), H12 (-0.3), H13 (-0.6) proton resonances, as assigned by a COSY experiment

(Table 6.7). The NH resonance appeared as a triplet (6.7 Hz), coupled to a two proton triplet at δ3.75 ppm (6.7 Hz), which was further coupled to a quartet at δ4.15 ppm (6.7 Hz). The latter was coupled to a doublet of doublets at δ3.91 (6.7, 9.6), which was in turn coupled to a doublet at δ2.91 ppm, which were the H12 and H13 resonances, respectively. Therefore these data required that there be two protons at C10, but these happened to be coincident in the $^1H$ NMR spectrum[98], accounting for the multiplicities and chemical shifts of the resonances above. Thus hydrogenolysis of the C10 aza acetal had been achieved to give the structure **6.22**, including an hydroxyl group at C12. Note that the loss of the acetal group at C12 would explain the observed large upfield shift in the H13 proton resonance, as described for earlier derivatives.

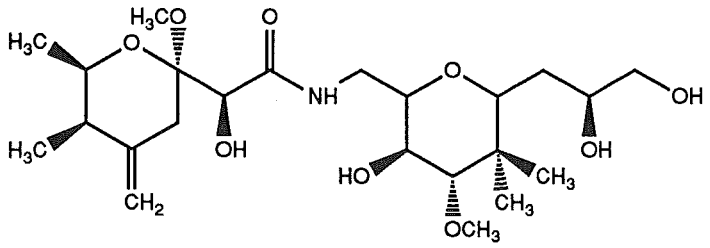


10,12-*O*-Dihydro mycalamide A (**6.22**)

NOE experiments were performed to examine the solution conformations of this central amide chain and C11-C15 ring portion, but these investigations were partly restricted by the coincidence of the two H10 proton resonances. The observed NOE interactions, H12-14-$CH_3$*S*, H13-H15, and $H_2$10-H13 were indicative of the normal chair conformation being the major solution conformation for the C11-C15 ring. There were also enhancements of the NH and $H_2$10 resonances on irradiation of H11, and enhancements of $H_2$10 and H11 on irradiation of the NH resonance. The observed vicinal coupling constants between both H10 protons and the NH and H11 protons were of similar magnitude, 6.7 Hz. This suggested that there were several conformations about the C10-N and C10-C11 bonds, since this value is close

to that for a freely rotating fragment[248], in which the main factor governing the magnitude of the coupling constant is electronegativity[102]. Interestingly, this was in contrast with the analogous system H15-$H_2$16-H17 on the other side of the ring, where there were two resolved coupling constants from H15 to the two H16 protons, although these were also probably averaged values.

A $^{13}C$ NMR spectrum was recorded and the data assigned by an HMQC experiment (Table 6.9). The C10 resonance was substantially upfield, at δ36.3 ppm, typical of a methylene carbon attached to a heteroatom, and there were related shifts in the C11 (+3.3), C12 (-5.0), C13 (+7.6) and C15 (-1.2) carbon resonances, consistent with the proposed structure[117].

### 6.5.1.2 CHARACTERISATION OF THE COMPOUND IN FRACTION 2

The second compound (from TLC fraction 2) was also more polar than mycalamide A, but there was less than 0.5 mg in this fraction. The $^1H$ NMR spectrum showed that this was a $\Delta^{4(5)}$ mycalamide A *trans* oxazolidinone derivative (**6.23**), analogous to the *cis* isomer (**5.6**) described in the previous chapter (5). The distinctive features, compared to data for mycalamide A *trans* oxazolidinone (**5.3**), were loss of the two 4=CH methylene resonances and appearance of a new allylic methyl-methine system, involving a long range coupling constant of 1.5 Hz[104]. The $^1H$ NMR spectrum was partially assigned (Table 6.11), but the small sample size and the presence of impurities in the sample prevented a more complete analysis. This derivative also proved to be unstable in $CDCl_3$ solution containing a trace of pyridine. However, a HRFABMS result was obtained, confirming the molecular formula of this product.

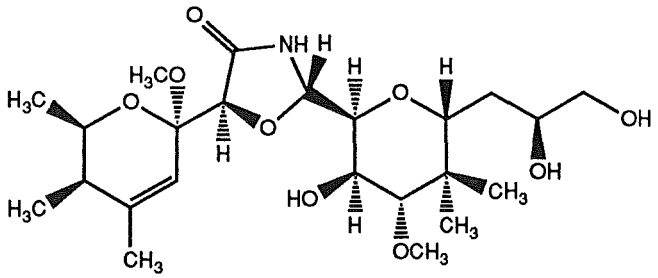

$\Delta^{4(5)}$ Mycalamide A *trans* oxazolidinone (**6.23**)

### 6.5.1.3 ANALYSIS AND COMPARISONS WITH OTHER REDUCTION ATTEMPTS

The predominance of the mycalamide A oxazolidinone derivatives in the product mixture from the above reaction indicated that the reagent was behaving as a base as well as a nucleophile, but this associated basicity was to be expected with anions in DMSO[243], as discussed earlier. Despite this, a significant degree of hydrogenolysis of the aza acetal was achieved, although it was uncertain whether this represented a direct $S_N2$ displacement at C10, or the reduction of an imine intermediate. Finally, in other attempts at reduction, no reaction was observed between mycalamide A and sodium borohydride in ethanol, or between mycalamide A and lithium aluminium hydride in refluxing THF, although in the latter case prolonged reaction appeared to give decomposition, so these reactions were abandoned.

## 6.5.2 REACTIONS OF MYCALAMIDE A WITH BARIUM OXIDE IN BENZENE

The work described in the previous chapter and the work above has concentrated on exploring the base catalysed reactions of mycalamide A in protic or dipolar aprotic solvents. However, the results of successful methylation reactions in benzene, described in Chapter 2, suggested that the base catalysed reactions of mycalamide A in non-polar solvents should also be investigated. In particular, it was proposed that a different reactivity would be observed because substitution reactions, such as involved in the formation

of the mycalamide A oxazolidinones, would be strongly disfavoured[140]. However, the existence of ion pairs was likely[158,140,176], which could permit some reactions to occur.

### 6.5.2.1 ISOLATION AND CHARACTERISATION OF PRODUCTS FROM A REACTION AT 100°C

Mycalamide A was reacted with barium oxide in benzene for 20 hours at 100°C in a sealed vial. Solvent partition of the residue gave two fractions containing chloroform and water soluble material respectively. In this case most of the product mass was water soluble.

A $^1$H NMR spectrum of the organic fraction showed the presence of mycalamide A, 10*R* mycalamide A (**6.17**), and one other unknown mycalamide A derivative which also retained the C10-C12 methylene acetal. Analysis by reverse phase HPLC further confirmed the presence of 10*R* mycalamide A, but the new component was not separable from mycalamide A. However, the new component was of higher $R_f$ than mycalamide A and 10*R* mycalamide A (**6.17**) on silica gel TLC, so it was easily purified. The overall yield of this new compound was less than 10%.

The $^1$H NMR spectrum of this fraction was weak, but very similar to that of mycalamide A, and was readily assigned with the assistance of further results from proton decoupling experiments and a COSY experiment. There were shifts in the H5a (+0.3), H5e (-0.1) and NH (-0.1) proton resonances (Table 6.7), which suggested that a C7 epimer of mycalamide A had been formed (**6.24**), based on earlier results. This was also consistent with the known base catalysed reactions of mycalamide A and derivatives, given the presence of 10*R* mycalamide A (**6.17**) in the reaction mixture. An NOE experiment showed the typical enhancement of the C6 methoxyl resonance on irradiation of H7. However, the small sample size prevented further NMR

spectroscopic examination of this important derivative. A low resolution FABMS spectrum showed an ion peak at *m/z* 472, consistent with the expected $MH^+$-$CH_3OH$ ion, but this was weak and it was possible that some decomposition of the sample had occurred, so that no high resolution result could be obtained.

A $^1H$ NMR spectrum of the water soluble material from the reaction contained resonances relating to the left hand portion of the mycalamide A structure to C7. It was evident that the O1-C6 tetrahydropyran ring was intact since the observed coupling constants and chemical shifts of the substituents were similar to those for mycalamide A. Furthermore, NOE interactions were observed between the the H2 and 6-$OCH_3$ protons and the H5a and 3-$CH_3$ protons, consistent with the usual chair conformation for this ring. There were small shifts in the H2 (-0.2), two H5 (<0.1) and 6-$OCH_3$ (-0.2) resonances (Table 6.7), compared with data for mycalamide A, but there were no H7 or other proton resonances related to the structure.

A $^{13}C$ NMR spectrum was also recorded which showed shifts in the C4 (+2.4), C5 (+3.3), C6 (+1.2) and 6-$OCH_3$ (+2.1) carbon resonances (Table 6.9), but there were no other related signals to suggest a C7 substituent. However, the $^{13}C$ NMR chemical shifts[117], the evidence from the $^1H$ NMR spectrum, and the physical evidence that this was a water- and methanol-soluble salt, were consistent with possibility that the remaining substituent at C6 was a carboxylate anion (**6.25**). This proposal was later verified by negative ion HRFABMS, which showed a very intense $M^-$ ion peak at *m/z* 199, indicative of a molecular formula of $C_{10}H_{15}O_4$, and a weaker $M^-$-$CH_3OH$ ion at *m/z* 167, as expected for the C6 acetal system. This structure could possibly arise from air oxidation at C7 and cleavage between C7 and C8 under basic conditions, although not necessarily in that order. In an attempt to provide further evidence for the presence of a carboxylate salt, a methylation reaction

was attempted, using barium oxide and methyl iodide in DMSO[249]. This was unsuccessful in that decomposition occurred, as observed by TLC and $^1$H NMR spectroscopy. Note that diazomethane methylations required the presence of an acidic hydrogen to activate the reagent, whereas acidic conditions, required to convert the salt into a carboxylic acid, were undesirable due to the acid lability of the C6 acetal. Therefore this methylation attempt was abandoned.

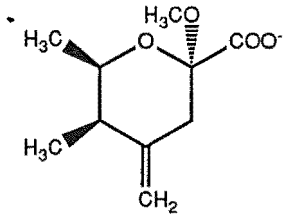


7-Carboxylate fragment (**6.25**)

No products from the right hand portion of the mycalamide A structure were isolated in this reaction. However, there were a number of low intensity resonances present in the $^1$H NMR spectrum of the water soluble fraction which could have resulted from the decomposition of such a fragment. Therefore the initial reaction was repeated at lower temperature in an attempt to trace this missing fragment.

### 6.5.2.2 ISOLATION AND CHARACTERISATION OF PRODUCTS FROM A REACTION AT 80°C

Mycalamide A was reacted with barium oxide in benzene for two hours at 80°C, monitoring by TLC. After workup, the evaporated residue was solvent partitioned, as above, to give organic and water soluble fractions.

The $^1$H NMR spectrum of the organic soluble fraction showed that the major component was unreacted mycalamide A. There were apparently no C7 or C10 epimers of mycalamide A present in this mixture, but there were

some minor resonances corresponding to at least two unknown mycalamide components. Preparative silica gel TLC separated out a fraction containing material which was of significantly higher $R_f$ than both mycalamide A and the trace amounts of the C7 epimer. A $^1H$ NMR spectrum of this fraction showed that it was a mixture of the two new components, but did not permit conclusive identification of their structure, and the sample was too small to attempt further purification and characterisations. Note, however, that both components appeared to contain the full mycalamide structure, including the normal chair-chair conformation of the trioxadecalin ring system, except that the H7 resonances appeared to be absent. The two pairs of H5 resonances were well dispersed and shifted downfield from their positions in the mycalamide A spectrum, as follows, H5a (+0.6, +0.5) and H5e (+0.2, +0.2). The two derivatives differed most in the chemical shifts of the H5a and 6-$OCH_3$ resonances, and in those of other nearby substituents. From this limited evidence it is possible to suggest that these compounds contained a C7 ketone functionality, arising from air oxidation under basic conditions, and that they could be epimeric at C6. The biological activity of such derivatives would be most interesting, in view of the proposed importance of the C7 hydroxyl group and neighbouring entities. However, there was insufficient time to obtain more of these derivatives, which were formed in low yields and could be difficult to separate.

The $^1H$ NMR spectrum of the water soluble fraction contained resonances for the C7 carboxylate fragment (**6.25**), but also resonances from some fragment arising from the right hand portion of mycalamide A. In particular, there were two sets of signals, indicative of one or more compounds containing the C10-C15 trioxadecalin ring system and the C16-C18 sidechain, but the substituent at C10 was uncertain. The chemical shifts of the two H10 resonances were $\delta$5.83 and 5.95 ppm, so that the amide nitrogen and

probably C8 were likely to be present. There were some rather weak singlets between δ8.2 and 8.4 ppm which could suggest that this was the salt of a formamide derivative, such as isolated from the base catalysed cleavage of *N*-alkylated mycalamides, described earlier in this chapter. However, irradiation of these signals in an NOE experiment gave no obvious enhancements, whereas irradiation of both H10 resonances enhanced the 10-OCH*R* and H15 resonances. An alternative possibility for the structure is an isonitrile[250], formed by dehydration of the formamide derivative (such a compound could in turn be oxidised to an isocyanate or undergo elimination[176,251]). However no conclusive mass spectroscopy measurements were obtained on this latter fragment to better establish its structure and it would not be easily purified, so work on it was not pursued.

Thus the main features of the base chemistry of mycalamide A in non-polar solvents appeared to be oxidative cleavage at C7-C8, with minor amounts of epimerisation at C7 and C10 at temperatures of 100°C, and, apparently, the formation of some intact C7 oxidation products at slightly lower temperatures. Further oxidation reactions of mycalamides A and B will be discussed in the next chapter (7).

## 6.6 BIOLOGICAL ACTIVITY RESULTS

The biological assay results for derivatives in this chapter are listed in Table 6.12. None of the 7-*O*-benzyl mycalamide derivatives (**6.3-6.15**) had significant activity, as expected, based on results for 7-*O*-alkyl mycalamide derivatives in Chapter 2. The *N*-formyl fragments (**6.1** and **6.2**) were also inactive. However, the most significant results were for those derivatives which had lost the C10-C12 methylene acetal. The enamide products (**6.16** and **6.19**), containing a double bond between C10 and C11 and an hydroxyl

group at C12, were both at least 100 times less active than mycalamide A, and the major, *Z* isomer was certainly inactive. Hydrogenolysis of the acetal gave a product (**6.22**) which was about 40 times less active than mycalamide A. These results suggested that the conformation of this central portion of the mycalamide structure could not be significantly altered without a dramatic loss of activity. The C10 aza acetal system itself appeared to be less essential than the C6 acetal system (Chapter 4) but the presence of some alkoxy group at C10, such as in pederin, still appeared to be advantageous for the biological activity.

A further interesting feature was the extremely low activity of the C7 and C10 epimers. The biological activity of 10*R* mycalamide A (**6.17**) was at least 500 times less than for mycalamide A, and 10*R* mycalamide B (**6.18**) was at least 100 times less active than mycalamide B. Note that the stated activity of 10*R* mycalamide B was probably not a true indication, since the sample was very small and a 1% impurity of mycalamide B could account for this assay result. Similarly, 7*S* mycalamide A (**6.24**) was at least 400 times less active than mycalamide A. Therefore this proved that the chirality of the central portion of mycalamides A and B was vitally important. Similarly specific results were noted for cycloheximide (**0.14**), emetine (**0.13**) and related compounds, where only structures having the natural configuration at the central secondary hydroxyl or amine carbon atom were active[49,53], and such results are common[16].

The remaining cleavage products were inactive within the limits of purity. In particular, pederamide (**3.4**) was at least 15000 times less active than mycalamide A, and the water soluble salts, obtained from a proposed cleavage of mycalamide A at C7-C8, were also relatively inactive. Therefore it was evident that both halves of the mycalamide structure were required for the biological activity. Importantly, the pederamide portion was not an active

substructure, and nor was it an ideal derivative for preparing *N*-alkyl analogues, as first considered, since the reactions possible were limited and adequate protection for the C7 hydroxyl group would be required.

These results have demonstrated some important structure-activity relationships for mycalamides A and B. Therefore this detailed study of the base catalysed reactions of mycalamide A and its derivatives in various solvents was worthwhile, having also elucidated some interesting chemistry of the central portion of mycalamide A.

**Table 6.1** $^{1}H$ NMR data[a,b] for compounds in Section **6.2.**

| | *N*-Benzyl, *N*-formyl fragment (**6.1**) | | *N*-Methyl, *N*-formyl fragment (**6.2**) | |
|---|---|---|---|---|
| | *E* isomer | *Z* isomer | *E* isomer | *Z* isomer |
| **H8** | 8.05 | 8.21 | 8.25 | 8.16 |
| **N-$CH_2$Ph** | 4.53,4.44 (12.0) | 4.51 | | |
| **N-$CH_3$** | | | 2.94 | 3.00 |
| **H10** | 4.87 (9.3) | 6.18 (10.4) | 5.15 (9.6) | 6.09 (10.4) |
| **10-OCH*R*** | 4.95 (6.9) | 5.14 (6.7) | 5.13 (6.8) | 5.16 (6.8) |
| **10-OCH*S*** | 4.82 (6.8) | 4.86 (6.7) | 4.90 (6.8) | 4.88 (6.7) |
| **H11** | 4.13 (7.1,9.4) | 4.05 (6.8,10.5) | 4.26 (7.0,9.6) | 4.19 (7.0,10.6) |
| **H12** | 4.19 (7.0,10.1) | 4.21 (6.9,10.8) | 4.30 (7.2,10.2) | 4.27 (10.5) |
| **H13** | 3.26 (10.0) | 3.50 (10.7) | 3.43 (10.4) | 3.53 (10.5) |
| **13-$OCH_3$** | 3.55 | 3.55 | 3.57 | 3.58 |
| **14-$CH_3$*R*** | 0.97 | 0.93 | 0.99 | 0.97 |
| **14-$CH_3$*S*** | 0.82 | 0.84 | 0.88 | 0.87 |
| **H15** | 3.26 (10.0) | 3.32 (9.8) | 3.37 (8.9) | 3.25 (9.7) |
| | (no geometry assigned below) | | (no geometry assigned below) | |
| **H16** | 1.72 (m) | 1.72 (m) | 1.76 (m) | 1.76 (m) |
| **H16** | 1.54 (m) | 1.54 (m) | 1.50 (m) | 1.50 (m) |
| **H17** | 3.35 (m) | 3.20 (m) | 3.28 (m) | 3.28 (m) |
| **17-$OCH_3$** | 3.35 | 3.30 | 3.31 | 3.31 |
| **H18** | 3.57 (2.3,7.7) | 3.44 (4.3,10.0) | 3.4 (m) | 3.4 (m) |
| **H18** | 3.45 (m) | 3.37(3.8,9.9) | 3.3 (m) | 3.3 (m) |
| **18-$OCH_2$Ph** | 4.59,4.52 (12.0) | 4.59,4.44 (12.0) | | |
| **18-$OCH_3$** | | | 3.36 | 3.32 |

[a]All data were recorded in $CDCl_3$, with chemical shifts in ppm relative to $CHCl_3$, δ7.25 (coupling constants in Hz). [b]Aromatic proton resonances (not listed) appeared as unresolved multiplets between δ7.5-7.2 ppm.

**Table 6.2** $^{1}H$-$^{1}H$ NOE interactions[a] for compounds in Sections **6.2-6.3**.

| Compound | Signal(s) irradiated | Signals enhanced (% enhancement) |
|---|---|---|
| *N*-Benzyl, *N*-formyl fragment (**6.1**) | H8*E*[d] | H10*E*(12), H18*E*(1)[d] |
| | H8*Z*[d] | N-$CH_2$*Z*(2) |
| | H10*E* (2x10-OCH*S*) | H8*E*(19), 2x10-OCH*R*(18)[b], H13*E*/H15*E*(10), 13-$OCH_3$*Z*(0.5) |
| | H10*Z*[d] | 10-OCH*R*(5), H13*Z*(4), H15*Z*(7) |
| | H12*E* (H11*E*)[d] | N-$CH_2$*E*(0.7)[b], 14-$CH_3$*S*(1) |
| | H11*Z*[d] | N-$CH_2$*Z*(2), H12*Z*(4) |
| *N*-Methyl, *N*-formyl fragment (**6.2**) | H8*E*[d] | H10*E*(7)[d] |
| | H8*Z*[d] | N-$CH_3$*Z*(1) |
| | N-$CH_3$*E*[d] | H11*E*(4) |
| | N-$CH_3$*Z*[d] | H8*Z*(8), H11*Z*(4) |
| | H10*E* (2x10-OCH*R*) | H8*E*(12), H10*Z*(5), 2x10-OCH*S*(15)[b], H13*E*(5), H13*Z*(4), 2x13-$OCH_3$(0.5), H15*E*(4) |
| | H10*Z*[d] | 10-OCH*R*(5), H13*Z*(3), 13-$OCH_3$*Z*(0.5), H15*Z*(3) |
| 7-*O*-Benzyl, 10*R* myc.A (**6.3**) | 6-$OCH_3$ | H2(5), H7(4) |
| | H7 | 6-$OCH_3$(2), 7-OCHu(4)[c], NH(3) |
| | H10 | 10-OCH*S*(5), H11(5), H12(2) |
| | 10-OCH*S* (4=CH*Z*, 7-OCHd[c]) | H3(3)[b], 4=CH*E*(14)[b], 7-OCHu(5)[b,c], H10(7), 10-OCH*R*(21), H12(5) |
| | H12 | H10(3), 10-OCH*S*(4), H13(3), 13-$OCH_3$(1) |
| | H13 | H12(4), 13-$OCH_3$(2), 14-$CH_3$*R*(1), 14-$CH_3$*S*(0.4) |
| 7,18-di-*O*-Benzyl, 10*R* myc.A (**6.4**) | H7 | 6-$OCH_3$(2), 7-OCHd(1)[c], 7-OCHu(4)[c], NH(3) |
| | NH | 6-$OCH_3$(0.4), H7(5), H11(2) |
| | H10 | 10-OCH*S*(5), H11(6), H12(3) |
| | 10-OCH*R* | 10-OCH*S*(17) |
| | 10-OCH*S* (4=CH*Z*, 7-OCHd[c]) | H3(3)[b], H7(1)[b], 7-OCHu(8)[b,c], H10(8), 10-OCH*R*(25), H12(4) |
| | H11 | H10(4), H16*S*(4) |
| | H12 | H10(2), 10-OCH*S*(2), H11(2), H13(2), 13-$OCH_3$(0.8) |
| | H13 | H12(4), 13-$OCH_3$(2), 14-$CH_3$*R*(1), 14-$CH_3$*S*(0.4) |
| | 14-$CH_3$*R* | H13(7), 14-$CH_3$*S*(0.9), H15(7) |
| | 14-$CH_3$*S* | H13(5), 13-$OCH_3$(0.6), 14-$CH_3$*R*(1), H15(4), H16*R*(5), H16*S*(2) |
| | H15 | 14-$CH_3$*R*(1), 14-$CH_3$*S*(0.5), H16*R*(3) |
| | H16*R* | 14-$CH_3$*S*(0.7), H15(4), H16*S*(10), H17(4) |
| | H16*S* (H3) | H2(7)[b], 3-$CH_3$(1)[b], 4=CH*Z*(3)[b], H11(10), H16*R*(10), H17(5) |
| | $H_2$18 (13-$OCH_3$) | H12(2)[b], H13(5)[b], 18-$OCH_2$(2) |
| 7-D, 7-*O*-benzyl, 10-*R*-*O*-methyl myc.A (**6.6**) | H10 | 10-$OCH_3$(2) |
| | H11/H12 | H10(2), H13(2), 14-$CH_3$*S*(0.5), H16*S*(2) |
| | H13 | 13-$OCH_3$(2), 14-$CH_3$*R*(1) |
| 7-*O*-Benzyl pederamide (**6.14**) | H2 | 2-$CH_3$(1), H3(3), 6-$OCH_3$(0.7) |
| | H5a | 3-$CH_3$(0.6), H5e(7), H7(1) |
| | H5e | 4=CH*E*(2), H5a(8), H7(0.4) |
| | 6-$OCH_3$ | H2(2), H7(4) |
| | H7 | 6-$OCH_3$(1), 7-OCHd(0.5)[c], 7-OCHu(2)[c] |
| | 2xNH | H7(2) |

[a]All data were recorded in $CDCl_3$

[b]Enhancement interpreted as being due to the irradiation of an overlapping resonance

[c]u and d have been used to designate the upfield and downfield resonances of a geminal pair

[d]*E* and *Z* have been used to designate signals for the two conformational isomers of the amide.

**Table 6.2 cont'd** $^{1}H$-$^{1}H$ NOE interactions[a] for compounds in Section **6.3**.

| Compound | Signal(s) irradiated | Signals enhanced (% enhancement) |
|---|---|---|
| 7*S*-*O*-Benzyl pederamide (**6.15**) | H2 | 2-$CH_3$(1), H3(4), 6-$OCH_3$(1) |
| | H5a | 3-$CH_3$(0.5), H5e(12), H7(0.6) |
| | H5e | 4=CH*E*(2), H5a(14), H7(0.4) |
| | 6-$OCH_3$ | H2(2), H7(4) |
| | H7 | 6-$OCH_3$(1), 7-OCHd(2)[c], 7-OCHu(1)[c] |
| | 7-OCHd[c] (4=CH*Z*) | H3(3)[b], 4=CH*E*(15)[b], H7(2) |
| | 2xNH | H7(0.7), H5a(0.9) |

[a]All data were recorded in $CDCl_3$
[b]Enhancement interpreted as being due to the irradiation of an overlapping resonance
[c]u and d have been used to designate the upfield and downfield resonances of a geminal pair

**Table 6.3** $^{13}C$ NMR data[a,b] for compounds in Section **6.2** (no assignment has been made to particular conformational isomers, except where stated).

| | *N*-Benzyl, *N*-formyl fragment (**6.1**) | | *N*-Methyl, *N*-formyl fragment (**6.2**) | |
|---|---|---|---|---|
| **C8** | 164.92 | 164.15 | 164.10 | 163.64 |
| **N-$CH_2$Ph** | 43.68 (*E*) | 46.43 (*Z*) | | |
| **N-$CH_3$** | | | 25.17 (*E*) | 29.16 (*Z*) |
| **C10** | 82.21 (*E*) | 75.04 (*Z*) | 81.84 (*E*) | 74.42 (*Z*) |
| **10-$OCH_2$** | 86.96 | 86.34 | 87.12 | 86.56 |
| **C11** | 67.37 | 67.11 | 66.71 | 66.71 |
| **C12** | 74.63 | 74.37 | 74.67 | 74.51 |
| **C13** | 79.25 | 78.94 | 79.18 | 79.04 |
| **13-$OCH_3$** | 61.86 | 61.86 | 61.86 | 61.86 |
| **C14** | 41.86 | 41.66 | 41.93 | 41.81 |
| **14-$CH_3$*R*** | 23.11 | 22.98 | 23.12 | 22.90 |
| **14-$CH_3$*S*** | 13.09 | 13.09 | 13.00 | 13.00 |
| **C15** | 75.96 | 75.22 | 75.93 | 75.26 |
| **C16** | 30.73 | 30.23 | 30.70 | 29.88 |
| **C17** | 77.97 | 76.86 | 77.90 | 77.58 |
| **17-$OCH_3$** | 57.05 | 57.05 | 57.13 | 56.76 |
| **C18** | 70.58 | 70.58 | 74.17 | 73.22 |
| **18-$OCH_2$Ph** | 73.37 | 73.19 | | |
| **18-$OCH_3$** | | | 59.20 | 59.12 |

[a]All data were recorded in $CDCl_3$, with chemical shifts in ppm relative to $CHCl_3$, δ77.01.
[b]Aromatic carbon resonances are listed in the Experimental section.

Table 6.4 $^1$H NMR data[a] for compounds in Section 6.3.

| | 7-*O*-Benzyl myc.A (2.39) | 7-*O*-Benzyl 10*R* myc.A (6.3) | 7,18-di-*O*-Benzyl 10*R* myc.A (6.4) | Pederamide (3.4) | 7-*O*-Benzyl ped. (6.14) | 7*S*-*O*-Benzyl ped. (6.15) |
|---|---|---|---|---|---|---|
| **H2** | 3.88 (2.7,6.6) | 3.89 (2.7,6.5) | 3.87 (2.8,6.6) | 4.03 (2.8,6.6) | 3.90 (2.8,6.6) | 3.93 (2.7,6.6) |
| **2-CH$_3$** | 1.17 (6.6) | 1.17 (6.6) | 1.13 (6.6) | 1.18 (6.6) | 1.13 (6.7) | 1.17 (6.6) |
| **H3** | 2.19 (2.5,7.0) | 2.19 (2.9,7.0) | 2.16 (3.0,7.3) | 2.25 (2.6,7.3) | 2.20 (2.5,7.0) | 2.20 (2.5,7.1) |
| **3-CH$_3$** | 0.97 (7.0) | 0.99 (7.1) | 0.99 (7.1) | 0.98 (7.1) | 0.97 (7.1) | 1.03 (7.0) |
| **4=CH*Z*** | 4.82 (1.8) | 4.81 (1.9) | 4.78 (1.9) | 4.86 (2.0) | 4.82 (2.0) | 4.81 (2.1) |
| **4=CH*E*** | 4.72 (1.9) | 4.71 (1.9) | 4.67 (1.9) | 4.75 (2.0) | 4.72 (2.1) | 4.67 (2.1) |
| **H5a** | 2.48 (1.9,14.4) | 2.45 (1.9,14.4) | 2.44 (1.9,14.6) | 2.14 (2.1,14.3) | 2.52 (2.1,14.4) | 2.78 (2.2,14.1) |
| **H5e** | 2.41 (14.3) | 2.32 (14.6) | 2.35 (14.1) | 2.33 (14.0) | 2.38 (14.5) | 2.08 (14.0) |
| **6-OCH$_3$** | 3.14 | 3.19 | 3.07 | 3.32 | 3.07 | 3.35 |
| **H7/7-OH** | 4.10 | 4.02 | 3.99 | 4.25/3.88 | 3.97 | 4.06 |
| **7-OCH$_2$Ph** | 4.77,4.68 (11.2) | 4.80,4.53 (11.3) | 4.81,4.48 (11.5) | | 4.82,4.55 (11.8) | 4.78,4.68 (11.5) |
| **NH9** | 7.24 (10.0) | 7.77 (9.3) | 7.91 (9.5) | 6.78 | 6.35 | 6.50 |
| **NH9** | | | | 5.60 | 5.43 | 5.38 |
| **H10** | 5.93 (10.1) | 5.46 (2.1,9.3) | 5.43 (2.1,9.1) | | | |
| **10-OCH*R*** | 5.13 (7.0) | 5.07 (6.6) | 5.05 (6.6) | | | |
| **10-OCH*S*** | 4.84 (7.0) | 4.83 (6.9) | 4.82 (6.6) | | | |
| **H11** | 3.80 (6.8,10.0) | 3.81 (1.9,1.9) | 3.78 (2.0,2.0) | | | |
| **H12** | 4.23 (6.8,10.5) | 3.75 (1.7,2.4) | 3.74 (1.9,2.4) | | | |
| **H13** | 3.49 (10.5) | 2.92 (2.4) | 2.91 (2.3) | | | |
| **13-OCH$_3$** | 3.56 | 3.38 | 3.37 | | | |
| **14-CH$_3$*R*** | 0.98 | 1.21 | 1.20 | | | |
| **14-CH$_3$*S*** | 0.88 | 0.91 | 0.91 | | | |
| **H15** | 3.68 (5.8,6.9) | 3.64 (3.0,12.1) | 3.58 (3.2,11.8) | | | |
| **H16** | 1.55 (m) | 2.25 (7.1,12.1,15.1) | 2.22 (6.7,11.9,15.0) | | | |
| **H16** | 1.50 (m) | 1.44 (3.1,5.0,15.4) | 1.54 (3.3,5.9,15.2) | | | |
| **H17** | 3.82 (m) | 3.65 (m) | 3.82 (m) | | | |
| **H18** | 3.62 (3.5,11.3) | 3.51 (3.4,11.0) | 3.40 (3.6,9.5) | | | |
| **H18** | 3.39 (6.0,11.2) | 3.33 (7.5,11.0) | 3.30 (7.1,9.4) | | | |
| **18-OCH$_2$Ph** | | | 4.50,4.43 (12.0) | | | |

[a]All data were recorded in $CDCl_3$, with chemical shifts in ppm relative to $CHCl_3$, δ7.25 (coupling constants in Hz). [b]Aromatic proton resonances (not listed) appeared as unresolved multiplets between δ7.5-7.2 ppm.

**Table 6.5** $^{13}C$ NMR data[a,b] for compounds in Section **6.3**.

| | 7-*O*-Benzyl myc.A (2.39) | 7-*O*-Benzyl 10*R*A (6.2) | 7,18-di-*O*-Ben. 10*R*A (6.4) | 7-*O*-Benzyl ped. (6.14) | 7*S*-*O*-Benzyl ped. (6.15) |
|---|---|---|---|---|---|
| **C2** | 69.38 | 69.66 | 69.46 | 69.36 | 68.99 |
| **2-$CH_3$** | 17.80 | 17.74 | 17.77 | 17.83 | 17.96 |
| **C3** | 41.38 | 41.37 | 41.50 | 41.46 | 41.34 |
| **3-$CH_3$** | 11.76 | 11.82 | 11.81 | 11.90 | 11.79 |
| **C4** | 146.48 | 146.46 | 146.57 | 146.25 | 146.79 |
| **4=$CH_2$** | 109.91 | 110.08 | 109.87 | 109.99 | 109.66 |
| **C5** | 34.61 | 34.39 | 34.18 | 33.81 | 32.90 |
| **C6** | 100.09 | 99.65 | 99.72 | 99.74 | 100.54 |
| **6-$OCH_3$** | 49.22 | 49.59 | 48.83 | 48.64 | 49.43 |
| **C7** | 80.81 | 81.28 | 79.95 | 79.14 | 81.03 |
| **7-$OCH_2Ph$** | 73.24 | 73.43 | 73.31 | 72.98 | 74.30 |
| **C8** | 170.59 | 169.81 | 170.03 | 172.05 | 171.44 |
| **C10** | 74.19 | 77.20 | 77.26 | | |
| **10-$OCH_2$** | 86.86 | 91.59 | 91.42 | | |
| **C11** | 71.66 | 61.81 | 61.54 | | |
| **C12** | 74.56 | 72.69 | 72.71 | | |
| **C13** | 79.24 | 83.74 | 83.84 | | |
| **13-$OCH_3$** | 61.88 | 59.25 | 59.26 | | |
| **C14** | 41.82 | 36.65 | 36.64 | | |
| **14-$CH_3$*R*** | 22.98 | 27.35 | 27.41 | | |
| **14-$CH_3$*S*** | 13.26 | 22.47 | 22.50 | | |
| **C15** | 78.98 | 80.92 | 80.48 | | |
| **C16** | 32.02 | 30.41 | 30.71 | | |
| **C17** | 71.70 | 71.50 | 69.69 | | |
| **C18** | 66.74 | 66.31 | 73.85 | | |
| **18-$OCH_2Ph$** | | | 73.25 | | |

[a]All data were recorded in $CDCl_3$, with chemical shifts in ppm relative to $CDCl_3$, δ77.01.
[b]Aromatic carbon resonances are listed in the Experimental section.

**Table 6.6** $^{1}H$ NMR data[a,b] for compounds in Section **6.3.**

| | 7-D, 7-*O*-benzyl $\Delta^{10}$ 10-deformyl myc.A (6.5) | 7-D, 7-*O*-benzyl 10*R*-*O*-methyl A (6.6) | 7-D, 7-*O*-benzyl 10*S*-*O*-methyl A (6.8) | 7-D, 7*S*-*O*-benzyl 10*R*-*O*-methyl A (6.9) | 7-D, 7*S*-*O*-benzyl myc.A (6.11) | 7-D, 7*S*-*O*-benzyl 10*S*-*O*-methyl A (6.12) | 7-D, 7*S*-*O*-benzyl 10*R* myc.A (6.13) |
|---|---|---|---|---|---|---|---|
| **H2** | 3.88 (2.5,6.6) | 3.91 (2.6,6.7) | ? | 3.94 (2.6,6.6) | 3.89 (2.7,6.5) | 3.94 (m) | 3.91 (2.5,6.5) |
| **2-$CH_3$** | 1.13 (6.6) | 1.14 (6.7) | 1.16 (6.6) | 1.17 (6.5) | 1.17 (6.5) | 1.17 (6.4) | 1.17 (6.6) |
| **H3** | 2.19 (2.5,7.0) | 2.19 (2.5,7.1) | 2.21 (m) | 2.20 (2.6,7.0) | 2.19 (2.6,7.0) | 2.19 (m) | 2.18 (m) |
| **3-$CH_3$** | 0.93 (7.1) | 0.98 (7.1) | 0.99 (7.2) | 1.03 (7.0) | 1.03 (7.0) | 1.01 (6.9) | 1.01 (7.0) |
| **4=CH*Z*** | 4.80 (2.0) | 4.81 (1.9) | 4.82 (m) | 4.83 (1.9) | 4.84 (m) | 4.82 (m) | 4.82 (m) |
| **4=CH*E*** | 4.70 (2.0) | 4.71 (1.9) | 4.72 (m) | 4.67 (2.0) | 4.71 (m) | 4.68 (m) | 4.68 (m) |
| **H5a** | 2.66 (2.0,14.2) | 2.64 (1.9,14.5) | 2.54 (1.9,14.0) | 2.85 (2.0,13.7) | 2.83 (m,13.9) | 2.75 (m,14.0) | 2.74 (m,14.5) |
| **H5e** | 2.32 (14.2) | 2.37 (14.5) | 2.47 (13.9) | 2.08 (13.7) | 2.07 (13.9) | 2.07 (14.2) | 2.07 (14.6) |
| **6-$OCH_3$** | 3.14 | 3.18 | 3.23 | 3.35 | 3.37 | 3.35 | 3.35 |
| **7-$OCH_2Ph$** | 4.72 (11.7) | 4.72 (11.7) | 4.75 (11.2) | 4.74 (11.4) | 4.75 (11.7) | 4.77 (m) | 4.79 (m) |
| **7-$OCH_2Ph$** | 4.51 (11.8) | 4.59 (11.7) | 4.70 (11.3) | 4.68 (11.6) | 4.70 (11.6) | 4.72 (m) | 4.75 (m) |
| **NH9** | ? | 7.16 (9.0) | ? | ? | ? | ? | ? |
| **H10** | 6.78 (2.0,10.6) | 5.41 (6.3,9.1) | 5.63 (4.4,10.2) | 5.38 (6.9,9.0) | 5.80 (10.1) | 5.55 (3.4,10.5) | 5.45 (2.3,8.9) |
| **10-OCH*R*** | | | | | 5.12 (6.9) | | 5.07 (6.6) |
| **10-OCH*S*** | | | | | 4.85 (6.9) | | 4.81 (6.6) |
| **10-$OCH_3$** | | 3.45 | 3.43 | 3.45 | | 3.38 | |
| **H11** | | 3.85 | ? | 3.82 (4.4,6.9) | 3.82 (7.3,10.3) | ? | 3.81 (m) |
| **H12** | 4.19 (2.1,9.2) | 3.85 | ? | 3.77 (4.6,6.1) | 4.23 (7.1,10.4) | ? | 3.75 (m) |
| **H13** | 2.74 (9.1) | 3.09 (5.6) | ? | 3.07 (6.1) | 3.44 (10.6) | 3.15 (8.3) | 2.91 (2.2) |
| **13-$OCH_3$** | 3.63 | 3.44 | 3.57 | 3.44 | 3.56 | 3.55 | 3.37 |
| **14-$CH_3$*R*** | 0.93 | 1.10 | 0.95 | 1.08 | 0.96 | 0.98 | 1.19 |
| **14-$CH_3$*S*** | 0.91 | 0.87 | 0.85 | 0.87 | 0.87 | 0.85 | 0.90 |
| **H15** | 3.31 (3.1,8.8) | 3.77 (1.9,11.2) | ? | 3.73 (2.0,9.2) | 3.69 (m) | ? | 3.59 (m) |
| **H16** | ? | 1.84 (4.0,11.4,15.5) | ? | 1.78 (m) | ? | ? | ? |
| **H16** | ? | 1.43 (1.9,2.7,15.5) | ? | 1.43 (m,15.5) | ? | ? | ? |
| **H17** | ? | 3.77 (m) | ? | 3.76 (m) | ? | ? | ? |
| **H18** | ? | 3.50 (3.8,11.2) | ? | 3.48 (4.0,11.8) | ? | ? | ? |
| **H18** | ? | 3.41 (7.2,11.2) | ? | 3.38 (7.0,11.9) | ? | ? | ? |

[a]All data were recorded in $CDCl_3$, with chemical shifts in ppm relative to $CHCl_3$, δ7.25 (coupling constants in Hz). [b]Aromatic proton resonances (not listed) appeared as unresolved multiplets between δ7.5-7.2 ppm.

**Table 6.7** $^1$H NMR data[a] for compounds described in Sections **6.4** and **6.5**.

| | *E*$\Delta^{10}$ 10-Deform. myc.A (6.19) | *Z*$\Delta^{10}$ 10-Deform. myc.A (6.16) | 10*R* Myc.A (6.17) | 10*R* Myc.B (6.18) | 10,12-*O*-Dihydro myc.A (6.22) | 7*S* Myc.A (6.24) | 7-Carboxylate fragment (6.25) |
|---|---|---|---|---|---|---|---|
| **H2** | 4.01 (2.6,6.5) | 3.96 (2.7,6.6) | 4.05 (2.7,6.4) | 4.04 (2.7,6.6) | 4.00 (2.7,6.5) | 3.97 (2.6,6.6) | 3.79 (2.7,6.6) |
| **2-CH$_3$** | 1.19 (6.6) | 1.19 (6.6) | 1.22 (6.5) | 1.21 (6.5) | 1.18 (6.6) | 1.18 (6.5) | 1.14 (6.6) |
| **H3** | 2.20 (2.2,7.0) | 2.21 (2.5,7.1) | 2.23 (2.5,7.0) | 2.22 (2.3,7.0) | 2.23 (2.5,7.0) | 2.23 (2.5,7.0) | 2.25 (2.2,7.1) |
| **3-CH$_3$** | 0.94 (7.1) | 0.95 (7.0) | 1.06 (7.2) | 1.05 (7.3) | 0.98 (7.0) | 1.02 (7.0) | 0.98 (7.1) |
| **4=CH*Z*** | 4.82 (1.8) | 4.82 (1.8) | 4.84 (1.8) | 4.83 (1.9) | 4.84 (1.9) | 4.86 (1.9) | 4.86 (2.1) |
| **4=CH*E*** | 4.71 (1.9) | 4.72 (1.8) | 4.72 (1.9) | 4.71 (2.0) | 4.73 (2.0) | 4.76 (1.9) | 4.70 (2.1) |
| **H5a** | 2.05 (1.9,14.4) | 2.31 (1.9,14.4) | 2.14 (2.0,14.2) | 2.12 (1.9,14.0) | 2.22 (2.0,14.4) | 2.62 (2.0,14.4) | 2.44 (2.1,14.4) |
| **H5e** | 2.28 (14.1) | 2.39 (14.3) | 2.28 (14.2) | 2.27 (14.0) | 2.35 (14.2) | 2.28 (14.4) | 2.28 (14.2) |
| **6-OCH$_3$** | 3.31 | 3.29 | 3.32 | 3.32 | 3.30 | 3.32 | 3.06 |
| **H7** | 4.21 (4.1) | 4.23 | 4.22 (2.7) | 4.22 (3.9) | 4.23 | 4.26 | |
| **7-OH** | 3.96 (4.1) | | 3.86 (2.9) | 3.90 (3.9) | | | |
| **NH9** | 9.43 (10.8) | 8.56 (10.4) | 8.30 (9.4) | 8.28 (9.3) | 7.13 (6.7) | 7.38 (9.8) | |
| **H10/H$_2$10** | 6.94 (1.7,10.8) | 6.69 (2.0,10.4) | 5.41 (2.2,9.3) | 5.42 (2.3,9.6) | /3.75 (6.7) | 5.85 (9.9) | |
| **10-OCH*R*** | | | 5.02 (6.7) | 5.01 (6.6) | | 5.13 (7.0) | |
| **10-OCH*S*** | | | 4.79 (6.6) | 4.78 (6.7) | | 4.87 (7.0) | |
| **H11** | | | 3.78 (1.5,2.0) | 3.72 (1.6,2.3) | 4.15 (6.7) | 3.85 (6.8,10.0) | |
| **H12** | 4.36 (2.2,9.5) | 4.20 (2.1,9.0) | 3.73 (1.5,2.3) | 3.69 (1.6,2.3) | 3.91 (6.7,9.6) | 4.24 (6.9,10.6) | |
| **12-OH** | 2.65 (2.7) | | | | | | |
| **H13** | 2.91 (9.5) | 2.76 (9.0) | 2.92 (2.3) | 2.92 (2.3) | 2.91 (9.6) | 3.45 (10.5) | |
| **13-OCH$_3$** | 3.66 | 3.62 | 3.38 | 3.38 | 3.58 | 3.56 | |
| **14-CH$_3$*R*** | 0.97 | 0.96 | 1.21 | 1.20 | 0.97 | 0.98 | |
| **14-CH$_3$*S*** | 0.94 | 0.93 | 0.94 | 0.94 | 0.87 | 0.88 | |
| **H15** | 3.42 (4.1,8.6) | 3.41 (2.8,9.3) | 3.66 (2.9,11.7) | 3.53 (3.0,11.9) | 3.63 (5.7,7.3) | 3.54 (3.8,8.6) | |
| **H16** | 1.68 (m) | 1.72 (m) | 2.26 (7.8,11.7,15.6) | 2.38 (4.0,12.3,15.1) | 1.60 (m) | 1.56 (m) | |
| **H16** | 1.68 (m) | 1.72 (m) | 1.53 (2.9,4.7,15.4) | 1.59 (3.1,8.3,15.3) | 1.60 (m) | 1.56 (m) | |
| **H17** | 3.93 (m) | 3.98 (m) | 3.65 (m) | 3.30 (m) | 3.85 (m) | 3.73 (m) | |
| **17-OCH$_3$** | | | | 3.35 | | | |
| **H18** | 3.65 (3.8,11.0) | 3.70 (3.4,11.0) | 3.65 (3.2,11.0) | 3.75 (3.3,11.9) | 3.58 (3.8,11.0) | 3.62 (3.5,11.0) | |
| **H18** | 3.51 (6.0,11.1) | 3.52 (7.3,11.0) | 3.48 (7.0,11.0) | 3.54 (5.5,11.6) | 3.47 (6.1,11.2) | 3.32 (6.6,11.2) | |

[a]Data for compound **6.25** were recorded in $D_2O$, with chemical shifts in ppm relative to dioxan, δ3.70 ppm. All other data were recorded in $CDCl_3$, with chemical shifts relative to $CHCl_3$, δ7.25 ppm, (coupling constants in Hz).

**Table 6.8** $^{1}H$-$^{1}H$ NOE interactions[a] for compounds in Sections **6.4**-**6.5**.

| Compound | Signal(s) Irradiated | Signals enhanced (% enhancement) |
|---|---|---|
| *Z* $\Delta^{10}$ 10-Deformyl myc.A (**6.16**) | H5a | 3-$CH_3$(0.9) |
| | H5e | 4=CH*E*(2), H7(0.8) |
| | H7 (H12) | H5a(0.9), H5e(0.6), 6-$OCH_3$(2), NH(2), H10(0.8) 14-$CH_3S$(0.6)[b] |
| | NH | H7(4), H10(2), H15(1), H17(2) |
| | H10 | H7(2), H12(2), H13(0.5) |
| | H12 (H7) | 6-$OCH_3$(0.9)[b], H10(1), H13(1), 14-$CH_3S$(1) |
| | H13 | 13-$OCH_3$(3), 14-$CH_3R$(0.8), H15(6) |
| | 2x14-$CH_3$ (3-$CH_3$) | H3(6)[b], H5a(2)[b], H12(5), H13(6), 13-$OCH_3$(1), H15(6), $H_2$16(3) |
| | H15 (6-$OCH_3$, H18u[c]) | H7(2)[b], NH(2), H10(1), H12(2), H13(7), 14-$CH_3R$(1) H17(2) |
| | $H_2$16 | 14-$CH_3R$(1), 14-$CH_3S$(2), H15(3), H17(6), 2xH18(1) |
| | H17 (H2) | 2-$CH_3$(2)[b], H3(5)[b], 6-$OCH_3$(1)[b], H15(3), $H_2$16(1) |
| | H18d[c] (13-$OCH_3$) | H7(2), H10(0.8)[b], H12(2)[b], H13(1)[b], H17(1), H18u(8) |
| | H18u[c] (13-$OCH_3$) | H7(1), H10(0.7)[b], H12(1)[b], H13(1)[b], H17(1), H18d(8) |
| *E* $\Delta^{10}$ 10-Deformyl myc.A (**6.19**) | NH | H7(5) |
| | H12 | 12-OH(8), 14-$CH_3S$(2) |
| | 12-OH | H12(6), 13-$OCH_3$(0.6) |
| | H13 | 13-$OCH_3$(2), 14-$CH_3R$(1), H15(4) |
| 10*R* Myc.A (**6.17**) | H5a | 3-$CH_3$(1), H5e(21) |
| | H7 | 6-$OCH_3$(3) |
| | NH | H7(5) |
| | H10 | 10-OCH*S*(7), H11(4), H12(3) |
| | 10-OCH*S* | H10(9), 10-OCH*R*(30), H12(7) |
| | H13 | H12(4), 13-$OCH_3$(2), 14-$CH_3S$(1) |
| | 14-$CH_3S$ | H13(5), 13-$OCH_3$(0.5), 14-$CH_3R$(1), H15(4) H16*R*(6) |
| | H15 (H18d[c]) | 14-$CH_3R$(2), 14-$CH_3S$(0.5), H16*R*(4), H18u(5)[b,c] |
| | H16*R* | 14-$CH_3S$(1), H15(4), H16*S*(8) |
| | H16*S* (H3, H5e) | H2(6)[b], 3-$CH_3$(1)[b], 4=CH*E*(4)[b], 4=CH*Z*(6)[b], H11(6) |
| 10*R* Myc.B (**6.18**) | H7 | 6-$OCH_3$(2) |
| | H13 | H12(5), 13-$OCH_3$(2), 14-$CH_3R$(2) |
| Pederamide (**3.4**) | H2 | 2-$CH_3$(0.9), H3(3), 6-$OCH_3$(0.4) |
| | H5a | 3-$CH_3$(0.7), H5e(11), H7(0.8) |
| | H5e | 4=CH*E*(3), H5a(6) |
| | H7 | 6-$OCH_3$(1) |
| | 7-OH | H7(0.8) |
| | 2xNH | H7(4) |
| 11*R* A *trans* oxazol. (**6.20**) | H10 | H11(8) |
| | H11 | H10(12), H13(5) |
| 10,12-*O*-Dihydro (**6.22**) | H7 | 6-$OCH_3$(2), NH(3) |
| | NH | H7(3), $H_2$10(2), H11(2) |
| | $H_2$10 | NH(2), H11(2), H13(4) |
| | H11 | NH(1), $H_2$10(1), H12(5) |
| | H12 | H11(4), 14-$CH_3S$(0.7) |
| | H13 | $H_2$10(2), 13-$OCH_3$(2), 14-$CH_3R$(0.8), H15(2) |

[a]Data for compound **6.25** were recorded in $D_2O$. All other data were recorded in $CDCl_3$
[b]Enhancement interpreted as being due to the irradiation of an overlapping signal
[c]u and d have been used to designate the upfield and downfield resonances of a geminal pair

**Table 6.8 cont'd** $^{1}H$-$^{1}H$ NOE interactions[a] for compounds in Section **6.5.**

| Compound | Signal(s) irradiated | Signals enhanced (% enhancement) |
|---|---|---|
| 7*S* Myc.A (**6.24**) | H7 | 6-$OCH_3$(2) |
| 7-Carboxylate | H2 | 2-$CH_3$(2), H3(5), 6-$OCH_3$(2) |
| fragment (**6.25**) | H5a | 3-$CH_3$(1), H5e(19) |
| | H5e (H3) | H2(3)[b], 2-$CH_3$(0.5)[b], 3-$CH_3$(0.5)[b], 4=CH*Z*(2)[b], H5a(14) |
| | 6-$OCH_3$ | H2(4) |

[a]Data for compound **6.25** were recorded in $D_2O$. All other data were recorded in $CDCl_3$
[b]Enhancement interpreted as being due to the irradiation of an overlapping signal
[c]u and d have been used to designate the upfield and downfield resonances of a geminal pair

**Table 6.9** $^{13}C$ NMR data[a] for compounds described in Sections **6.4** and **6.5**

| | *Z*$\Delta^{10}$ 10-Deform. myc.A (**6.16**) | 10*R* Myc.A (**6.17**) | 10,12-*O*-Dihydro myc.A (**6.22**) | Pederamide (**3.4**) | 7-Carboxylate fragment (**6.25**) |
|---|---|---|---|---|---|
| **C2** | 69.81 | 69.70 | 69.45 | 69.41 | 70.69 |
| **2-$CH_3$** | 18.15 | 17.96 | 17.99 | 17.97 | 17.85 |
| **C3** | 41.42 | 41.55 | 41.41 | 41.46 | 41.69 |
| **3-$CH_3$** | 11.82 | 11.84 | 12.08 | 12.13 | 12.20 |
| **C4** | 145.90 | 145.80 | 145.64 | 145.22 | 148.03 |
| **4=$CH_2$** | 110.17 | 110.64 | 110.52 | 110.88 | 110.90 |
| **C5** | 33.61 | 32.88 | 33.25 | 32.76 | 37.48 |
| **C6** | 99.91 | 99.80 | 99.93 | ? | 101.06 |
| **6-$OCH_3$** | 48.98 | 48.47 | 48.67 | 48.34 | 50.99 |
| **C7** | 73.14 | 70.45 | 72.05 | 70.39 | |
| **C8** | 167.32 | 172.30 | 171.66 | 171.75 | |
| **C10** | 104.92 | 77.30 | 36.25 | | |
| **10-$OCH_2$** | | 91.25 | | | |
| **C11** | 141.65 | 61.05 | 74.51 | | |
| **C12** | 69.60 | 72.35 | 69.45 | | |
| **C13** | 90.72 | 83.51 | 86.78 | | |
| **13-$OCH_3$** | 62.59 | 59.31 | 62.67 | | |
| **C14** | 41.46 | 36.62 | 41.15 | | |
| **14-$CH_3$*R*** | 22.89 | 27.08 | 23.70 | | |
| **14-$CH_3$*S*** | 13.74 | 22.89 | 14.42 | | |
| **C15** | 85.01 | 81.54 | 77.75 | | |
| **C16** | 31.79 | 30.00 | 31.41 | | |
| **C17** | 71.63 | 70.45 | 71.86 | | |
| **C18** | 66.61 | 66.24 | 66.75 | | |

[a]Data for compound **6.25** were recorded in $D_2O$, with chemical shifts in ppm relative to dioxan, δ67.4. All other data were recorded in $CDCl_3$, with chemical shifts relative to **C**$DCl_3$, δ77.01.

**Table 6.10** $^{2}J_{CH}$ and $^{3}J_{CH}$ HMBC correlations[a] for compounds in Chapter 6.

| Compound | Proton | Carbon signal correlated |
|---|---|---|
| *Z*$\Delta^{10}$ 10-Deformyl myc.A (**6.16**) | H2 | 3-$CH_3$ |
| | 2-$CH_3$ | C2, C3 |
| | H3 | 3-$CH_3$,C4, 4=$CH_2$, C5 |
| | 3-$CH_3$ | C2, C3, C4 |
| | 4=CH*E/Z* | C3, C5 |
| | H5a/e | C3, C4, 4=$CH_2$, C6 |
| | 6-$OCH_3$ | C6 |
| | H7 | C6, C8 |
| | H10 | C11 |
| | H12 | C11, C13 |
| | H13 | C12, 13-$OCH_3$, C14, 14-$CH_3$*R*, 14-$CH_3$*S* |
| | 13-$OCH_3$ | C13 |
| | 14-$CH_3$*R* | C13, C14, 14-$CH_3$*S*, C15 |
| | 14-$CH_3$*S* | C13, C14, 14-$CH_3$*R*, C15 |
| | $H_2$16 | C15, C17, C18 |
| 10*R* Myc.A (**6.17**) | 2-$CH_3$ | C2, C3 |
| | 3-$CH_3$ | C2, C3, C4 |
| | 4=CH*E/Z* | C3, C5 |
| | H5e | C3 |
| | 6-$OCH_3$ | C6 |
| | H7 | C6, C8 |
| | 10-OCH*R/S* | C10,C12 |
| | H13 | 13-$OCH_3$ |
| | 13-$OCH_3$ | C13 |
| | 14-$CH_3$*R* | C13, C14, 14-$CH_3$*S*, C15 |
| | 14-$CH_3$*S* | C13, C14, 14-$CH_3$*R*, C15 |

[a]All data were recorded in $CDCl_3$

**Table 6.11** $^{1}$H NMR data[a] for mycalamide A *trans* oxazolidinone derivatives, described in Sections **6.4** and **6.5**.

| | 11*R* Myc.A *trans* oxazo.($CD_3OD$) (6.20) | 11*R* Myc.A *trans* oxazolidinone (6.20) | $\Delta^{11}$ Myc.A *trans* oxazolidinone (6.21) | $\Delta^{4(5)}$ Myc.A *trans* oxazolidinone (6.23) |
|---|---|---|---|---|
| **H2** | 3.90 (2.5,6.6) | 3.94 (2.4,6.4) | 3.94 (2.6,6.4) | 4.18 (2.7,6.5) |
| **2-$CH_3$** | 1.16 (6.6) | 1.17 (6.5) | 1.18 (6.6) | 1.16 (6.6) |
| **H3** | 2.20 (2.3,7.1) | 2.18 (2.7,7.0) | 2.20 (2.8,6.9) | 2.10 (m) |
| **3-$CH_3$** | 1.02 (7.1) | 1.01 (7.1) | 1.03 (6.9) | 0.95 (7.0) |
| **4=CH*Z*** | 4.80 (1.8) | 4.82 (2.0) | 4.83 (2.0) | |
| **4=CH*E*** | 4.64 (1.9) | 4.68 (2.0) | 4.71 (2.0) | |
| **4-$CH_3$** | | | | 1.78 (1.5) |
| **H5a** | 2.35 (1.9,13.8) | 2.43 (2.0,13.8) | 2.44 (2.0,14.2) | |
| **H5e** | 2.22 (13.7) | 2.25 (14.0) | 2.30 (14.0) | |
| **H5** | | | | 5.32 (1.5) |
| **6-$OCH_3$** | 3.23 | 3.27 | 3.30 | 3.36 |
| **H7** | 4.37 (2.1) | 4.36 (2.1) | 4.42 (2.0) | 4.17 (2.5) |
| **NH9** | ? | ? | ? | ? |
| **H10** | 5.40 (1.2,2.2) | 5.31 (2.2,4.9) | 5.41 (2.0) | 5.63 (2.6,5.9) |
| **H11** | 3.12 (1.1,9.9) | 3.22 (5.0,9.4) | | 3.91 (5.9) |
| **H12** | 3.72 (9.6) | 3.66 (9.3) | 5.18 (2.6) | 3.97 (5.7,7.5) |
| **H13** | 2.75 (9.3) | 2.78 (9.1) | 3.33 (2.6) | 2.89 (7.5) |
| **13-$OCH_3$** | 3.60 | 3.61 | 3.34 | 3.52 |
| **14-$CH_3$*R*** | 0.92 | 0.94 | 0.95 | 1.02 |
| **14-$CH_3$*S*** | 0.82 | 0.84 | 0.90 | 0.89 |
| **H15** | 3.25 (m) | 3.35 (5.0,7.6) | 3.84 (2.5,9.4) | ? |
| **H16** | 1.75 (2.1,7.5,14.3) | 1.65 (m) | 1.70 (m) | ? |
| **H16** | 1.53 (5.0,10.4,14.3) | 1.60 (m) | 1.55 (m) | ? |
| **H17** | 3.79 (m) | 3.87 (m) | 3.90 (m) | ? |
| **H18** | 3.55 (3.5,11.3) | 3.59 (m) | 3.63 (3.3,11.5) | ? |
| **H18** | 3.46 (5.9,11.5) | 3.45 (5.8,11.1) | 3.48 (6.2,11.6) | ? |

[a]All data were recorded in $CDCl_3$, unless otherwise specified, with chemical shifts in ppm relative to $CHCl_3$, δ7.25, or $CHD_2OD$, δ3.30 (coupling constants in Hz).

**Table 6.12** Biological assay results for compounds in Chapter 6.

| Compound | P388 $IC_{50}$[a] | Antiviral Results[b] (ng/disk) | | | | | | | |
|---|---|---|---|---|---|---|---|---|---|
| Mycalamide A | 0.5 | WW | WW | +* | 5 | + | + | +* | 2 |
| Mycalamide B | 0.1 | WW | WW | +* | 2 | +++ | +++ | +* | 1 |
| *N*-Benzyl, *N*-formyl frag.(**6.1**) | >12500 | - | - | - | 40000 | | | | |
| *N*-Methyl, *N*-formyl frag.(**6.2**) | 800 | | +++ | +* | 20000 | + | ++ | +* | 10000 |
| 7-*O*-Benzyl myc.A (**2.39**) | 90 | WW | WW | +* | 1000 | - | - | - | 500 |
| 7-*O*-Benzyl 10*R* A (**6.3**) | 600 | WW | WW | +* | 20000 | ++ | +++ | +* | 10000 |
| 7,18-Di-*O*-Benzyl 10-*R* A (**6.4**) | 1300 | WW | WW | +* | 20000 | ++ | ++ | +* | 10000 |
| 7-D, 7-*O*-Bn. $\Delta^{10}$ 10-de.(**6.5**) | 600 | - | - | - | 2000 | | | | |
| 7-D, 7-*O*-Bn. 10*R*-*O*-Me.(**6.6**) | >1250 | - | - | - | 2000 | | | | |
| 7-D, 7-*O*-Bn. 10*S*-*O*-Me.(**6.8**) | >1250 | - | - | - | 2000 | | | | |
| 7-D, 7*S*-*O*-Bn. 10*R*-*O*-..(**6.9**) | >1250 | - | - | - | 2000 | | | | |
| 7-D, 7*S*-*O*-Benzyl A (**6.11**) | >1250 | | | | | | | | |
| 7-*O*-Benzyl ped. (**6.14**) | 800 | WW | WW | +* | 5000 | - | - | - | 2000 |
| 7*S*-*O*-Benzyl ped. (**6.15**) | 800 | WW | WW | +* | 5000 | - | - | - | 2000 |
| *E* $\Delta^{10}$ 10-Deformyl A (**6.19**) | >50 | | | | | | | | |
| *Z* $\Delta^{10}$ 10-Deformyl A (**6.16**) | 1500 | WW | +++ | +* | 20000 | - | + | +* | 10000 |
| 10*R* Myc.A (**6.17**) | 300 | WW | WW | +* | 5000 | - | - | - | 2000 |
| 10*R* Myc.B (**6.18**) | 7 | WW | WW | +* | 200 | +++ | +++ | +* | 100 |
| Pederamide (**3.4**) | 7500 | - | - | - | 40000 | | | | |
| 11*R* A *trans* oxazo (**6.20**) | 120 | WW | WW | +* | 4000 | + | ++ | +* | 2000 |
| 10,12-*O*-Dihydro myc.A (**6.22**) | 20 | WW | WW | +* | 500 | +++ | +++ | +* | 200 |
| 7*S* Myc.A (**6.24**) | 180 | | | | | | | | |
| 7-Carboxylate fragment (**6.25**) | 110 | WW | +++ | +* | 500 | | | | |

[a] In ng/ml. The derivatives are estimated to be better than 95% pure, having been subjected to at least two steps of chromatographic purification in most cases.

[b] -,+,++,+++,WW=antiviral zone size. Results are listed in the order of *Herpes simplex virus*, *Polio virus*, cytotoxicity, loaded sample mass.

# CHAPTER 7
# OXIDATION OF MYCALAMIDES A AND B

## 7.1 INTRODUCTION

In view of the proposed importance of the C7 hydroxyl group and, to a lesser extent, the substituents of the C16-C18 sidechain for the biological activity of mycalamides A and B (Chapters 2 and 6), it was of interest to consider the oxidation of the hydroxyl groups present in these structures. Selective oxidation of the primary hydroxyl group would also generate a reactive centre which could then permit further modifications of this portion of the structure. Furthermore, reduction of an aldehyde group would represent a facile method for the introduction of an isotopic label, such as deuterium, into the mycalamide structure, for potential use in mode of action or pharmacokinetic studies[73].

Pederone (**7.1**), a natural product isolated in low yield together with pederin and being a C13 ketone pederin derivative, was reported to show strong biological activity[28], although this was not quantified. Preliminary degradative work on pederin and pseudopederin (**3.5**) included oxidation with potassium permanganate, but this gave unsatisfactory results, with a large number of products being formed that were difficult to separate[27]. Pederin was reported to be stable to oxidation using lead tetraacetate in benzene solution[94]. However, pseudopederin reacted readily under these conditions to give isopederolactone (**7.2**), an isomer of pederolactone (**3.6**), and an aqueous carboxylic acid fraction which yielded pederenal (**3.1**) on acid hydrolysis[27,94]. Various other oxidations were also performed on pederin fragments, during its synthesis, including a Collins oxidation[240] (see

below), and an oxalyl chloride-DMSO-triethylamine reagent[129,252,253] at low temperature to successfully oxidise the C7 hydroxyl group.

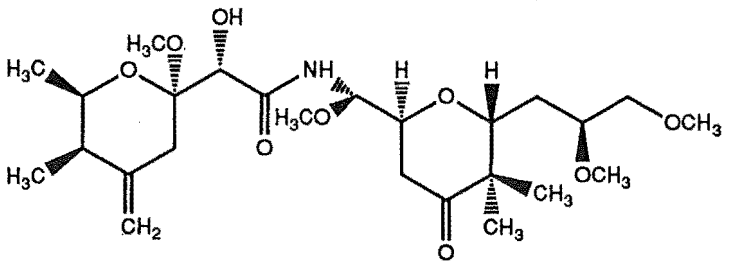


Pederone (**7.1**)

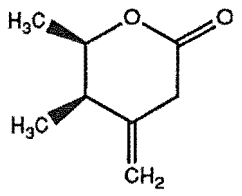


Isopederolactone (**7.2**)

There are a vast number of oxidising agents available for the oxidation of alcohols and a cursory survey is presented here[254]. Strong oxidising agents include reagents such as potassium permanganate, acid dichromate, magnesium dioxide and ruthenium tetroxide. Several chromium VI reagents are commonly used, including the Jones reagent (chromic acid and sulphuric acid in water), the Collins reagent (pyridine-chromium trioxide), the Corey reagent (pyridinium chlorochromate) and pyridinium dichromate[255]. Other reagents include morpholine-*N*-oxide and a ruthenium complex[256], lead tetraacetate-pyridine[257] and DMSO based reagents[253,258,259]. The latter include the Moffat reaction (dicyclohexylcarbodiimide (DCC), DMSO and anhydrous phosphoric or trifluoroacetic acids), and variations using acetic anhydride, sulphur trioxide-triethylamine-pyridine, oxalyl chloride (Swern oxidation) and tosyl chloride amongst many. Of these, oxalyl chloride has been reported to be the best activator of DMSO, giving good yields, with few side reactions[253]. Most reagents convert primary alcohols to aldehydes and secondary alcohols to ketones, but some of the strong oxidants oxidise aldehydes further to carboxylic acids. There are also reagents available for the selective oxidation of both primary and secondary alcohols, which will be discussed in later sections. However, clearly acidic conditions were not appropriate for studies on the mycalamides. An alternative to the above

reagents is the Oppenauer oxidation[254], involving the use of ketones in the presence of strong base, but this was also not appropriate for the mycalamides. This chapter describes the results of some initial investigations on the oxidation of mycalamides A and B, but there is certainly scope for further work in this area.

## 7.2 OXIDATIONS OF MYCALAMIDE B

### 7.2.1 TRIAL OXIDATION USING PYRIDINIUM DICHROMATE

Pyridinium dichromate has been reported to be a nearly neutral oxidising reagent for selectively converting alcohols to aldehydes or ketones and is more convenient to prepare and store than the Collins reagent[255]. It was also reported to be very efficient at oxidation and tolerant of acid and base sensitive functionalities, including unsaturated alcohols and substrates containing acetal groups. Therefore this reagent seemed to be a good choice to begin an oxidation study of mycalamides A and B. Mycalamide B was chosen for initial investigations since it contained one less hydroxyl group than mycalamide A, thus reducing the possibilities for oxidation. The reagent was readily prepared according to the literature method[255] to give a good yield of orange crystals.

Mycalamide B was reacted with a slight excess of pyridinium dichromate in dichloromethane at room temperature and monitored by TLC. After three days TLC showed a mixture of starting material and products, so the reaction was stopped. A $^1$H NMR spectrum of the crude mixture obtained after workup indicated a large mixture of components, including four aldehyde signals between δ9.5-9.8 ppm and resonances that were characteristic of pederolactone (**3.6**). There was very little mycalamide B present, but there were resonances requiring the presence of the C10-C12 methylene acetal

and the H7 proton in some components. Analysis by HPLC showed some unresolved components near to the retention time of mycalamide B, and at least three minor, more retained components. Therefore this did not appear to be a useful oxidation method, since there had been some acid catalysed rearrangement and oxidative cleavage, involving the sensitive homoallylic acetal, and the resulting components were not able to be separated.

### 7.2.2 SELECTIVE OXIDATION OF PRIMARY OR SECONDARY ALCOHOLS

In considering alternative methods of oxidation it was decided to focus on the use of more selective oxidising agents. There are some reagents available for the preferential oxidation of secondary over primary hydroxyl groups. The combination of chlorine and pyridine, for example, oxidises both groups, but the oxidation of secondary hydroxyl groups is substantially faster[207]. Bromine, in the presence of stannoxane or distannoxane, was similarly effective[260]. However neither method would be useful for use on the mycalamides due to the presence of the exocyclic double bond. Another method, involving sodium bromate and cerium IV ammonium nitrate[261], was also not effective in the presence of a double bond. Finally, the use of trityl tetrafluoroborate as oxidant involved acidic conditions and so was also not useful in the present context[262]. Therefore the selective oxidation of secondary hydroxyl groups in mycalamides A or B did not appear to be feasible, since each of the methods available involved either the use of halogens, or generated acidic conditions. An alternative approach was the use of protecting groups, but there was insufficient time to investigate this possibility.

There are few reagents which preferentially oxidise primary over secondary hydroxyl groups. Platinum dioxide in the presence of oxygen[263] has a reportedly high selectivity, although it is claimed by some that these

results are not easily reproducible[264]. However, tris-triphenylphosphine ruthenium II chloride, a reagent which is useful for hydrogen-deuterium exchange of primary alcohols at very high temperature[265], for homogeneous transfer hydrogenolysis of $CCl_4$[266] and for catalytic hydrogenation in the presence of alcohols or base[267], has been reported to show selectivities of up to 50:1 for the preferential oxidation of primary hydroxyl groups at room temperature[264]. This reagent could be used in the presence of anhydrous base for acid sensitive compounds, so this method was selected for a trial study on mycalamide B.

### 7.2.2.1 PREPARATION AND SEPARATION OF PRODUCTS FROM THE REACTION OF MYCALAMIDE B WITH A RUTHENIUM II COMPLEX

Mycalamide B was reacted with tris-triphenylphosphine ruthenium II chloride, in the presence of potassium carbonate, in benzene for seven hours at 60°C, to give a mixture of starting material and several products by silica gel TLC. A $^1H$ NMR spectrum of the crude mixture obtained after workup indicated a mixture of at least four major components, including unreacted mycalamide B, and there were some weak resonances at δ8.9-9.0 ppm. Preparative TLC gave five fractions, of which two contained only reagent-derived material, one fraction was almost pure mycalamide B, one fraction was a fairly clean mixture of two major components, and the final fraction was smaller and contained one major component with many other minor ones, by $^1H$ NMR spectroscopy. These latter two fractions were further purified by reverse phase HPLC, in an attempt to isolate the three major components identified in these fractions. This yielded eight further fractions, but only two fractions were of sufficient mass and purity to characterise. Of the remaining fractions, which were all of very low mass, three were unresolved mixtures, one contained only reagent-derived material, and two were of good purity, but

were still too small to enable a conclusive solution of their structures, by $^1H$ NMR spectroscopy. (Subsequently, one of these latter compounds was identified as 18-normycalamide A 17-aldehyde (**7.5**)).

7.2.2.2 CHARACTERISATION OF THE MAJOR PRODUCTS

The $^1H$ NMR spectrum of the first major fraction indicated the presence of the C7 hydroxyl and both the C6 and C10 acetal systems, but the C16-C18 sidechain had certainly been affected. However, surprisingly, there was no aldehyde resonance present to indicate oxidation of the primary hydroxyl group. There was a doublet at δ6.39 ppm (12.8 Hz), coupled to a doublet of doublets, at δ4.57 ppm, which was further coupled to a doublet at δ3.76 ppm (8.8 Hz), as shown by selective proton decoupling experiments. These resonances were assigned to protons at positions from C15 to the end of the sidechain, since the remainder of the $^1H$ NMR data were relatively unchanged from those of mycalamide B and could be readily assigned (Table 6.1). Significantly there was a downfield shift in the C17 methoxyl resonance (+0.2 ppm). The observed chemical shifts, multiplicities and coupling constants for the unassigned resonances above were indicative of the presence of a double bond between C16 and C17, as in structure **7.3**.

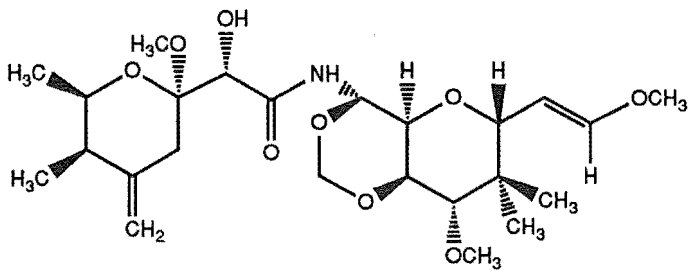


*E* $\Delta^{16}$ 18-Normycalamide B (**7.3**)

A series of NOE experiments were performed to enable conclusive assignments of these data, to determine the stereochemistry of the double bond, and to investigate the solution conformations of this portion of the

structure. The results of these experiments are summarised in Figure 7.1a and listed in Table 7.2. Irradiation of H10 enhanced the resonance at δ3.76 ppm, along with the H13 and 10-OCH*R* resonances, so that this new resonance could be assigned to the H15 proton. Irradiation of H15 enhanced the H10 resonance, and the resonance at δ6.39 ppm, to which it was not coupled, so that this was assigned to the vinyllic H17 proton. Similarly, irradiation of the H16 resonance (δ4.57 ppm) caused an enhancement of the C17 methoxyl resonance, requiring that the geometry of the double bond be *E*, with the H16 and H17 protons in a *trans* relationship, in agreement with the 12.6 Hz vicinal coupling constant observed[102]. Also the H15 and H16 protons were evidently mostly in an anti relationship, based on the magnitude of the observed vicinal coupling constant[102] (8.8 Hz), in agreement with the observed NOE interaction between the H15 and H17 protons.

**Figure 7.1** Selected $^1$H-$^1$H NOE interactions and partial solution conformations of isomers of $\Delta^{16}$ 18-normycalamide B (**7.3**, **7.4**).

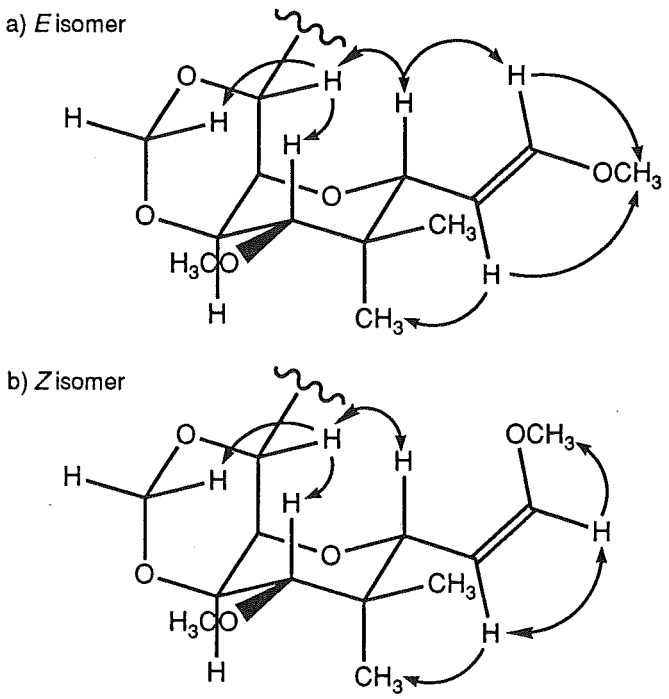

The sample was too small to record a $^{13}C$ NMR spectrum directly. However, partial $^{13}C$ NMR data were obtained indirectly from an HMQC experiment, recorded at 500 MHz (Table 7.3). The C15 resonance was shifted downfield (+3 ppm), compared with data for mycalamide B, consistent with the presence of a double bond between C16 and C17. Also the chemical shift of the C17 resonance, δ147 ppm, was similar to that observed for methyl vinyl ether[117], δ153.2 ppm, consistent with this proposed structure. Further evidence was obtained from HRFABMS, which indicated a molecular formula of $C_{24}H_{39}NO_9$, and from an FTIR spectrum, which showed a band at 1656 $cm^{-1}$, assignable to the more intense C=C stretching band of the vinyl ether[96].

The $^1H$ NMR spectrum of the second fraction was similar to that of the first fraction, but there were large changes in the chemical shifts and coupling constants of resonances from C15 to C17, suggestive of an alternate geometry of the C16-C17 double bond (structure **7.4**). In particular, there were shifts in the H15 (+0.6), H16 (-0.3), H17 (-0.5) and 17-$OCH_3$ (+0.1) proton resonances (Table 7.1), compared with the above data, and a smaller H16-H17 vicinal coupling constant (6.6 Hz), indicative of a *Z* isomer[102]. NOE interactions were observed betwen the H16 and H17 protons (Table 7.2), consistent with this assignment. The 9 Hz coupling constant between the H15 and H16 protons was indicative of a mostly anti relationship between these protons, as above, so that the only major difference between the solution conformations of the two isomers was in the positions of the H17 and 17-$OCH_3$ substituents. The different chemical shifts of the H16 resonances in the two isomers were consistent with standard substituent effects[101]. The shifts in the H15 and H17 resonances were not predicted, but probably represented the results of long range anisotropic deshielding effects[123] associated with adjacent ether oxygen groups at C17 and C15, respectively, for the two

isomers (Figure 7.1). These effects were further confirmation of the stereochemistry of the C16-C17 double bond in each compound.

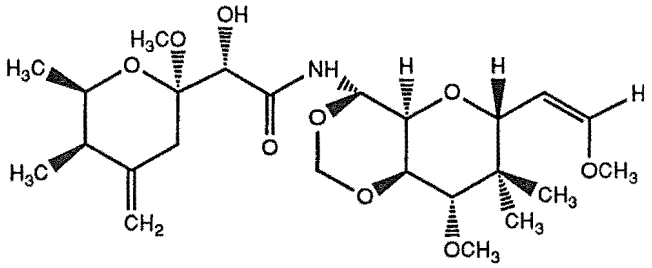


*Z*$\Delta^{16}$ 18-Normycalamide B (**7.4**)

No $^{13}C$ NMR data were obtained for this compound, but the molecular formula was readily confirmed by HRFABMS. The biological activity of both derivatives will be described in a following section.

7.2.2.3 REACTION MECHANISMS

The oxidation of alcohols by ruthenium complexes is reported to involve the formation of a ruthenium alkoxide (Scheme 7.1a), which normally undergoes β-elimination, with removal of hydride ion from the α-carbon and cleavage of the metal-oxygen bond, to produce the carbonyl compound and an hydrido-ruthenium complex[256,264]. This complex was hydrido-chloro-tris-triphenylphosphine ruthenium in the present case, and was capable of oxidising another mole equivalent of an alcohol[264]. In an alternative oxidation procedure, this method could be made catalytic by the presence of an amine-*N*-oxide, which could reoxidise the ruthenium complex, but this reportedly resulted in a significant reduction in selectivity[256].

No C18 aldehyde products were isolated from the reaction with mycalamide B, although it is possible that such compounds were formed but decomposed, or underwent rearrangement, under the basic reaction conditions. It was initially more difficult to account for the formation of the observed major products of the reaction, the isomers of $\Delta^{16}$ 18-

normycalamide B (**7.3**, **7.4**). However, it is known that tertiary phosphine complexes of ruthenium chloride react with alcohols in the presence of base to give very stable hydrido-carbonyl ruthenium complexes[268]. In such reactions the alcohol is degraded by oxidation then decarbonylation, so that ethanol gives methane. The process is called hydridocarbonylation and is known to be the predominant reaction under basic conditions. The mechanism[268] (Scheme 7.1b) is believed to involve the initial formation of the ruthenium alkoxide, followed by a base-promoted hydride transfer to the ruthenium to give a metal-aldehyde complex, which in turn breaks down to give a ruthenium carbonyl complex, via an isocarbonyl complex, instead of eliminating the aldehyde. This decarbonylation of the original alcohol is reportedly favoured by the stability of the ruthenium carbonyl complex product and the availability of a metal ligand position following the splitting of the original halogen bridge. In the present case (Scheme 7.1b), it is proposed that the decarbonylation occurs by a base-promoted β-elimination, including loss of one H16 proton, cleavage of the C17-C18 bond, and loss of hydride ion from C18, in the usual manner. A similar decarbonylation of aldehydes also occurs with Wilkinsons catalyst, tris-triphenylphosphine rhodium chloride, under the influence of heat and light, to give alkanes and a rhodium carbonyl complex[269].

The formation of a C17-aldehyde derivative (**7.5**) as a minor product from the oxidation of mycalamide B (as indicated at the end of Section 7.2.2.1 and characterised in a later section) would probably arise from the breakdown of the $\Delta^{16}$ 18-normycalamide B isomers (**7.3**, **7.4**) in the presence of traces of acid. In particular, acid catalysed addition of $H_2O$ to an enol ether[172] would give a hemiacetal at C17, which would readily lose methanol to yield the required aldehyde (Scheme 7.2).

**Scheme 7.1** Proposed mechanisms for the oxidation and decarbonylation reactions of mycalamide B with a ruthenium II complex.

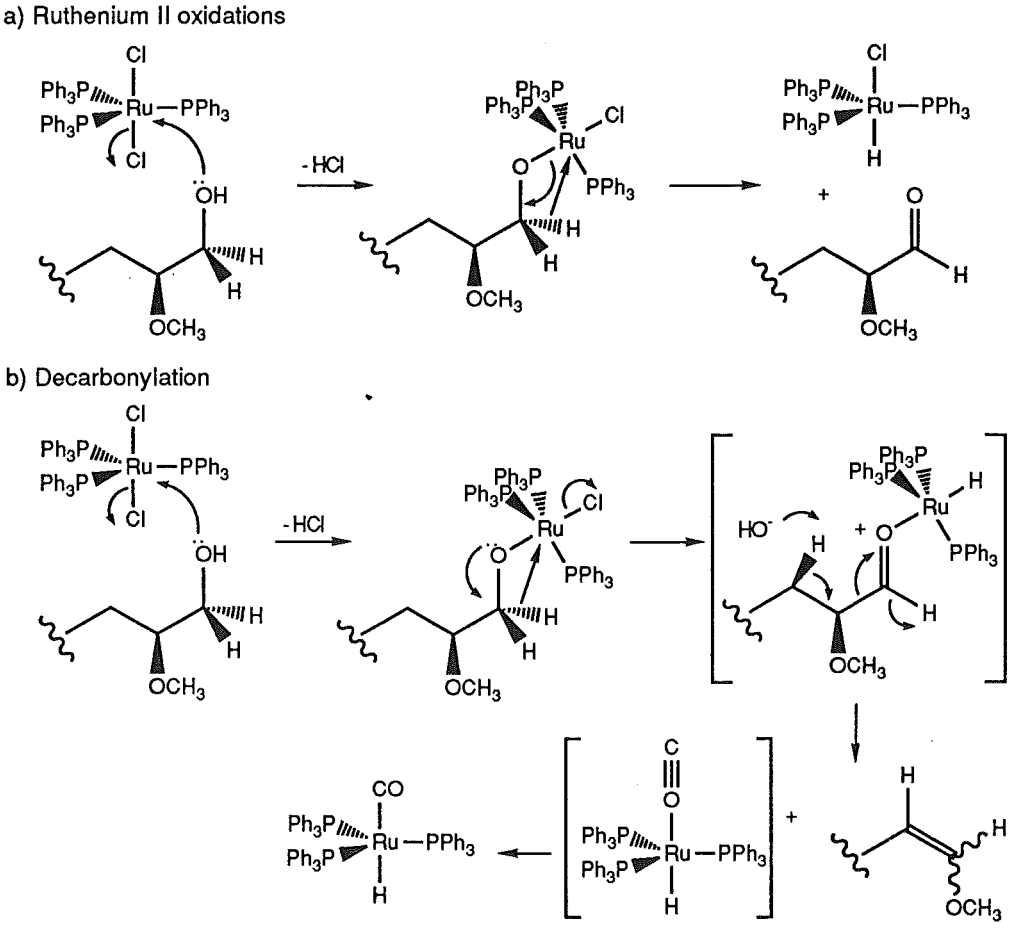


**Scheme 7.2** Mechanism of formation of 18-normycalamide A 17-aldehyde (**7.5**) from the hydrolysis of $\Delta^{16}$ 18-normycalamide B (**7.3**, **7.4**)

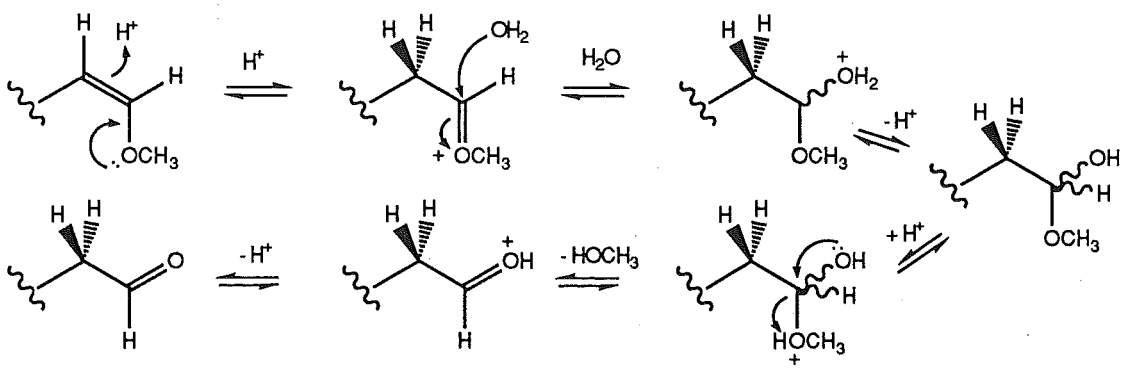

## 7.3 OXIDATIONS OF MYCALAMIDE A

### 7.3.1 REACTIONS OF MYCALAMIDE A WITH TRIS-TRIPHENYLPHOSPHINE RUTHENIUM II CHLORIDE

In view of the partial success obtained with using this ruthenium complex for the selective oxidation of the sidechain of mycalamide B, it was then of interest to consider reactions on mycalamide A. In particular, it was expected that an aldehyde product could be obtained in this way, which could permit further modifications to this portion of the molecule.

A trial reaction of mycalamide A with tris-triphenylphosphine ruthenium II chloride in benzene, in the absence of base, was very slow at room temperature, as monitored by TLC. After two days the reaction was stopped and crude separation was performed by silica gel column chromatography to remove reagents and unreacted mycalamide A. A $^1$H NMR spectrum of the product fraction showed the presence of one mycalamide A derivative, having an aldehyde triplet at δ9.55 ppm, although there was also unresolved reagent-derived material and traces of decomposition, and the sample was not stable, due probably to the presence of trace amounts of acid. (Note that the multiplicity of this aldehyde resonance suggested that this product was possibly an 18-normycalamide A 17-aldehyde derivative, **7.5**). This reaction had only proceeded to the extent of about 50% so it was repeated, this time in the presence of potassium carbonate, for two hours at 50°C. Preliminary column chromatography, then preparative TLC gave two fractions, one containing only traces of mycalamide A and reagent-derived material, and the other consisting of products. However, a $^1$H NMR spectrum of this product fraction was dominated by reagent-derived material, and the resonances relating to the mycalamide products were weak and indicated a complex mixture. This decomposition could have been due to heating the products in

the presence of base, causing further reactions and rearrangements. This method was therefore abandoned in favour of some alternative method which would give clean oxidation under mild reaction conditions and would allow good separation of the reagents from the products.

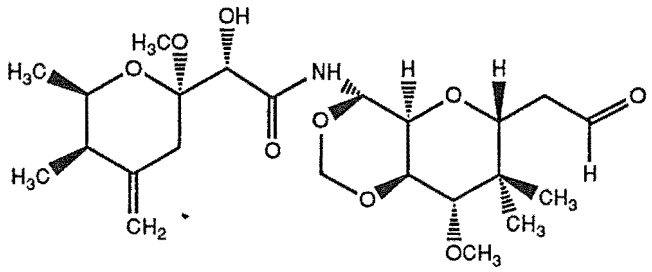

18-Normycalamide A 17-aldehyde (**7.5**)

## 7.3.2 REACTIONS OF MYCALAMIDES A AND B WITH LEAD TETRAACETATE IN BENZENE-PYRIDINE

The proposed initial product from the above reaction of mycalamide A with the ruthenium II complex, 18-normycalamide A 17-aldehyde (**7.5**), should be more easily obtainable by oxidative cleavage of the C17-C18 diol of mycalamide A with sodium periodate or lead tetraacetate[270]. In fact, the combination of lead tetraacetate with pyridine has been reported to be effective for the oxidation of both primary and secondary alcohols[257], and the advantage of incorporating an amine base for neutralisation suggested that this could be useful for reactions on mycalamides A and B. However, a trial reaction of mycalamide B with these reagents for one day at 30°C gave no reaction by TLC and $^1$H NMR spectroscopy.

Mycalamide A was reacted with lead tetraacetate in a 1:1 mixture of benzene and pyridine for 1.5 hours at room temperature to give one product of higher $R_f$, cleanly, by silica gel TLC. A $^1$H NMR spectrum of the product obtained after workup showed the presence of a single pure mycalamide A derivative, obtained in quantitative yield. This product was found to be the

same as that obtained earlier, from the reaction of mycalamide A with the ruthenium II complex, and in lower yield from a similar reaction on mycalamide B, described above. Some features of this $^1$H NMR spectrum included the aldehyde triplet at δ9.55 ppm, which was coupled to a multiplet at δ2.36 ppm, which in turn was coupled to a doublet of doublets at δ4.09 ppm. These resonances could be assigned to the H17, $H_2$16, and H15 protons, respectively, since the assignments of the remaining $^1$H NMR data (Table 7.1) were obvious from comparisons with data for mycalamide A and were confirmed by COSY and NOE experiments. Note that the shifts in the H15 (+0.5) and $H_2$16 (+0.8) proton resonances were entirely consistent with the presence of an aldehyde group at C17, involving electronic[101] and anisotropic deshielding effects[123]. Also the size of the vicinal coupling constants between H17 and the two H16 protons, of 2.0 and 2.6 Hz, was typical of the coupling between aldehyde protons and adjacent α-protons[102], since this is reduced in magnitude by the two bonds to the electronegative oxygen atom. There were also shifts in the H5a (-0.3) and H11 (-0.1) proton resonances, suggestive of the involvement of some longer range effects. Therefore the $^1$H NMR data for this derivative were consistent with the proposed structure, 18-normycalamide A 17-aldehyde (**7.5**).

NOE experiments were performed to examine the solution conformations of this derivative. There were similar interactions across the trioxadecalin ring system to those observed for mycalamide A, including H15-H10, H15-H13, 14-$CH_3$*S*-H12, indicating that the solution conformation of this system was the same, in agreement with the observed chemical shifts and coupling constants. There were other NOE interactions, including H15-H17, H15-$H_2$16, and $H_2$16-H17, which suggested that this portion of the structure was a mixture of several conformations, in agreement with the averaged vicinal coupling constants observed. However, there was also a very

significant NOE interaction between the H17 and H5a protons, as found earlier for mycalamide B, and possibly for mycalamide A (Chapter 1). Such evidence could account for the anomalous chemical shift of the H5a proton resonance, compared to data for mycalamide A, since some anisotropic shielding interaction with the C17 carbonyl group[123] could occur. These effects are further considered in a molecular modelling study of the conformations of this structure, described below.

A $^{13}C$ NMR spectrum was recorded for this derivative and the data obtained were readily assigned by comparison with data for mycalamide A (Table 7.3). There was a resonance at δ200.5 ppm, assignable to the aldehyde carbon, and there were shifts in some other resonances, including C7 (-1.6), C15 (-4.9) and C16 (+11.4), consistent with this structure[117]. In addition to this NMR evidence, an FTIR spectrum displayed a new carbonyl stretching band at 1725 $cm^{-1}$, indicative of the aldehyde group[96], and HRFABMS indicated a molecular formula of $C_{23}H_{37}NO_9$, corresponding to a loss of $CH_4O$ from mycalamide A.

**Scheme 7.3** Mechanism of oxidative cleavage of mycalamide A with lead tetraacetate

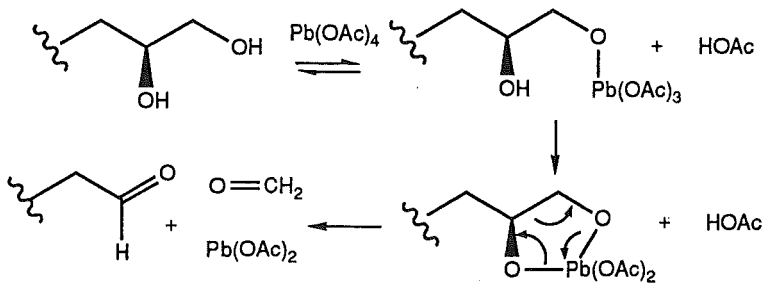


The mechanism for this oxidation, as proposed by Criegee[270], involves firstly a slow coordination of both oxygens of the diol onto the lead centre, with displacement of two molecules of acetic acid, to give a cyclic coordination complex (Scheme 7.3 above). This is followed by a series of shifts in the

electron pairs, with cleavage of the two metal oxygen bonds and the central carbon-carbon bond, to yield two carbonyl compounds and a reduced lead II species (lead diacetate). In the present case the two carbonyl compounds are 18-normycalamide A 17-aldehyde (**7.5**) and formaldehyde.

### 7.3.3 MOLECULAR MODELLING OF 18-NORMYCALAMIDE A 17-ALDEHYDE

A molecular modelling study was performed with the aim of determining the lowest energy conformations for this structure, to compare with evidence obtained from the NMR studies above. This was a better structure to analyse than mycalamides A and B, having $3^3$ less degrees of freedom[214] (17-O, 17-18, 18-O fixed or removed), but was still too challenging to consider a full grid search involving rotations of all freely rotatable bonds. In order to simplify the task, some constraints were imposed, based on existing knowledge from previous modelling studies (Chapter 5) and evidence from the NMR studies above and in Chapter 1. In particular, it was known that the two methoxyl groups, at C6 and C13, both had preferred orientations, and that the C8-N and N-C10 bonds could be fixed, since the amide conformation was mostly *trans* (Chapters 1 and 2), while the NH and H10 protons were mostly in an anti relationship, based on the observed 9.5 Hz coupling constant[102]. Furthermore, the conformations of the three rings were evidently the same as for mycalamide A, so that these could also be fixed. Thus the only remaining rotatable bonds were C6-C7, C7-O, C7-C8, C15-C16 and C16-C17.

The starting structure (**7.5**) was obtained from the crystal structure coordinates for pederin di-p-bromobenzoate[93] (**1.1**), by adjusting the substituents at C7, C10, C12, C13 and C17, setting both H-C10-C11-H and N-C10-O-$CH_2$ anti, and introducing the third ring, as for mycalamide A (Chapter 1). In order to accurately determine the conformations about bonds between one $sp^2$ centre and an $sp^3$ centre, 30° rotations were recommended, in

contrast to the normal 120° rotations for bonds between two $sp^3$ centres[124,214]. Two of the five rotatable bonds in the present structure were affected, so that a full grid search was not feasible with the computing resources available. An alternative method was a Monte Carlo statistical conformational search[124,214,216]. This method performed random, rather than systematic, dihedral angle rotations to the starting conformer, to generate further conformers. These conformers were accepted if their minimised energies were lower, or within 14.6 kJ $mol^{-1}$ of the existing lowest energy conformation. A maximum of 200 conformations was set as the criterion for stopping the search. Further energy minimisations were performed on this set of conformers and equivalent conformers discarded in the usual way.

This search was thus performed, using the parameters described above and the same modified MODEL program[125] described in earlier chapters, to generate a set of lowest energy conformations. These MM2-calculated geometries were analysed[213] to give the results in Table 7.4, and were weighted according to their minimised energies by applying a Boltzmann distribution, to obtain approximate relative populations. Note that only conformers within 12 kJ $mol^{-1}$ of the lowest energy conformer have been shown. Also it was necessary to edit the output file since a few structures were non-unique, differing in their dihedral angles by less than 5° (such problems are known to occur with MM2 minimisations[214]).

An examination of the dihedral angles shows that the C5-C6-C7-C8 angle was most often in a (-) gauche conformation, and that the C14-C15-C16-C17 angle was anti in all cases except conformer number 4. Distances between the H7 proton and the H5a, H5e, 6-O**C**, and N**H** atoms have been shown, along with the H5a-NH and H5a-H17 distances, for each conformer. These results show that in most of the calculated conformers H7 was within 3 Å of the C6 methoxyl carbon, in agreement with the NOE results. Other

conformers, with H7 close to H5a and H5e (within 3 Å) were also represented, but while there was experimental evidence for the former, there was no significant NOE interaction between H7 and H5e. Several conformers also showed small H5a-NH, H5a-H17 and H7-NH distances, consistent with the observed NOE results. All of the conformers contained intramolecular hydrogen bonding interactions, in particular between the C7 hydroxyl proton and one or more of the C6 acetal, C8 carbonyl, or C17 carbonyl oxygens, and between the amide NH proton and one or more of the C6 acetal, C7 hydroxyl, or C17 carbonyl oxygens.

The first four lowest energy conformers together represented about 79% of the total population of conformations for this structure, and these have been examined in more detail. However, the first lowest energy conformer (Figure 7.2a) was anomalous in containing H7 close to H5e, suggesting that the ordering of these conformers was unreliable (see below). By comparison, conformer 2 (Figure 7.2b) satisfied all the major NOE results, having H17 close to both H5a (2.7 Å) and H15, and H7 close to both the C6 methoxyl group (2.6 Å) and the NH proton (2.5 Å). Conformer 3 (Figure 7.2c) represented the experimentally second major C6-C7 rotamer, having H7 close to H5a (2.3 Å), while conformer 4 (Figure 7.2d) was a C15-C16 rotamer of conformer 2. Note that a combination of conformers 2, 4 and a third C15-C16 rotamer was required, in order to satisfy the observed vicinal coupling constants between H15 and the two H16 protons (5.2, 7.3 Hz), since the calculated values (in Hz) for conformers 2 and 4 were (2.0,11.5) and (5.5, 1.3), respectively. Therefore conformers 2,3 and 4, with probably a third C15-C16 rotamer, would satisfy all the observed NOE and coupling constant data obtained on this derivative.

**Figure 7.2** Major conformations of 18-normycalamide A 17-aldehyde (**7.5**), as calculated by molecular modelling.

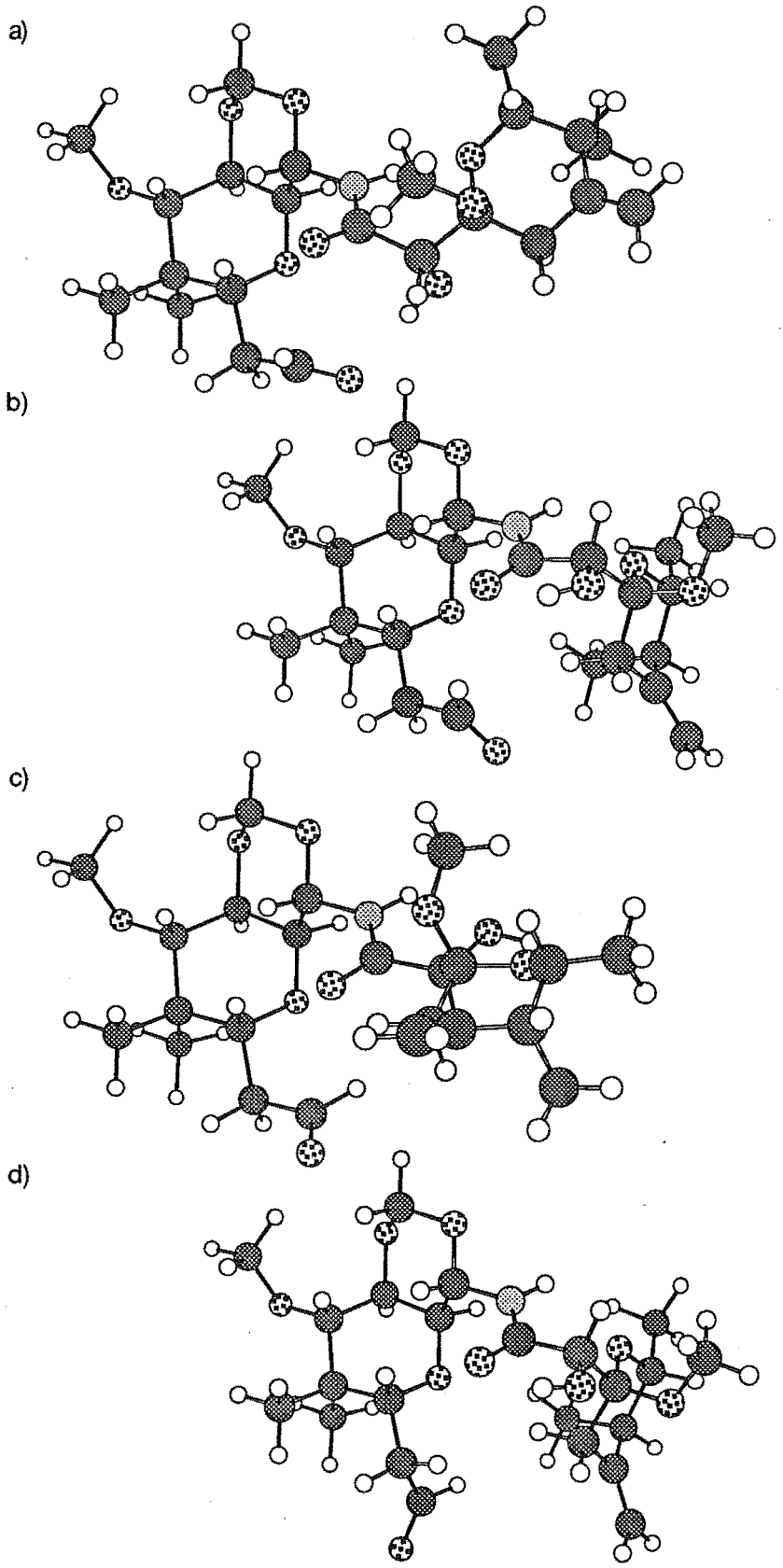

Significantly then, this work has linked the major C6-C7 rotamer with a low energy C16-C17 sidechain conformation, such that H5a and H17 are close in space. A consideration of other distances further showed that H17 was reasonably close to H7 in conformer 3 (2.9 Å), to C7-OH in conformer 1 (3.2 Å), but not close to the NH proton in any of the conformers. Therefore a long range effect from the different C17 substituents in mycalamide A and 18-normycalamide A 17-aldehyde (**7.5**) to C7 could account for the observed shift in the C7 carbon resonance for the two compounds. Hence this modelling work was quite successful, but earlier remarks (Chapter 5), regarding the limitations of such programs to order various conformations that are close in energy when hydrogen bonding effects were involved[215], are also applicable here. Furthermore, it has also been noted that global energy minima found by such methods are unlikely to remain so when entropy and solvation effects are included[122,216]. Thus it is the set of low energy conformations that is important.

### 7.3.4 SOLUTION CONFORMATIONS OF THE HEMIACETALS OF 18-NOR-MYCALAMIDE A 17-ALDEHYDE IN $D_4$-METHANOL

Further to the molecular modelling work above, it was considered of interest to examine the solution conformations of this aldehyde derivative in $CD_3OD$. However, the $^1H$ NMR spectrum indicated that the aldehyde functionality had reacted with the solvent (containing about 0.1% pyridine) to give an approximately 1:1 mixture of two isomeric hemiacetals. This was of interest because of the varying effects of this modification on resonances throughout the molecule. The $^1H$ NMR data were assigned (Table 7.1) using COSY and NOE experiments. Of particular interest was the unusually large effect on the chemical shift of the H7 resonance for the two isomers (0.08 ppm), and many of the other O1-C6 ring substituents were also significantly

affected. The two H15 resonances were most affected, being spread by 0.1 ppm.

A $^{13}C$ NMR spectrum was recorded to further examine these effects, and this was assigned by an HMQC experiment (Table 7.3). The chemical shifts of the C17 carbon resonances, δ97.9 and 98.0 ppm, were consistent with the formation of a hemiacetal at this position[117]. There were also related shifts in the C15 (+3.2, 3.0) and C16 (-5.2, -5.8 ppm) carbon resonances, compared to data for 18-normycalamide A 17-aldehyde (**7.5**). Interestingly the 14-$CH_3S$ and C11 resonances, and to a lesser extent the resonances of other carbons belonging to the trioxadecalin ring system, were rather broad, indicative of some exchange with an increased population of the alternate chair-chair conformation, whereas this was not significant in data for 18-normycalamide A 17-aldehyde. (This effect was also a factor in the chemical shifts of these resonances and the vicinal proton-proton coupling constants, as discussed for derivatives in previous chapters).

Comparing the $^{13}C$ NMR data for the two isomers, the largest differences occurred in the chemical shifts of the C7 (0.5) and C16 (0.6) carbon resonances. However, the C7 hydroxyl group was evidently not directly involved in these hemiacetals, as initially postulated, since the chemical shift of C7 was almost identical to that of mycalamide A in this solvent, whereas an ether linkage would cause a large downfield shift in this resonance (Chapter 2). Therefore it was likely that the structure of these isomers was simply **7.6**, representing the base catalysed addition of $CD_3OD$ across the aldehyde carbonyl bond[238]. Note that when the solvent was removed from this sample and it was redissolved in $CDCl_3$ the $^1H$ NMR spectrum indicated that only the aldehyde derivative (**7.5**) was present. This was consistent with the properties of open chain hemiacetals[237], which are stable only in alcohol solution because they are in rapid kinetic equilibrium

with their parent alcohol and aldehydes[238], with which they are similar in energy.

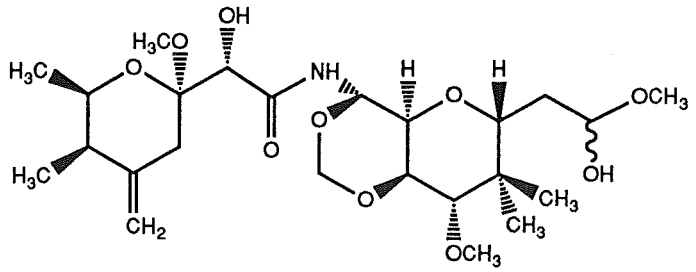


18-Normycalamide A 17-aldehyde hemiacetals (**7.6**)

The solution conformations of the hemiacetals (**7.6**) were further investigated by NOE experiments (Table 7.2). These results confirmed the presence of the major conformation of the trioxadecalin ring system and the usual C6-C7 rotamers. There was no NOE interaction between H7 and H17, but the H5a-H17 interaction was present for one of the hemiacetal isomers. Hence from these results the stereochemistry at C17 did appear to have a significant effect on the environment of C5 and C7, a result which was interesting, given the proposed importance of the C6-C10 substructure for the biological activity of mycalamides A and B (Chapters 2-6 and 8).

## 7.4 REACTIONS OF 18-NORMYCALAMIDE A 17-ALDEHYDE

The quantitative oxidative cleavage of mycalamide A to 18-normycalamide A 17-aldehyde (**7.5**), using lead tetraacetate in benzene-pyridine[257], provided a good source of a derivative with a reasonably reactive functional group, which could allow further selective modifications of this shortened C16-C17 sidechain of mycalamide A. In particular, reactions such as reduction, reductive amination, the formation of imines, hydrazones, cyanohydrin and bisulphite adducts, were potentially possible[238,271,272], although reaction conditions would be required which would not affect other

functional groups in the molecule. Such derivatives were likely to show good biological activity, based on results in Chapter 2, so that effects such as substituent size and polarity, and the stereochemistry at C17, could potentially be studied.

### 7.4.1 REDUCTION WITH SODIUM BOROHYDRIDE

18-Normycalamide A 17-aldehyde (**7.5**) reacted readily with sodium borohydride in methanol at room temperature to give a single product of lower $R_f$ on silica gel TLC. HRFABMS of the fraction obtained from workup indicated the presence of a compound of molecular formula $C_{23}H_{39}NO_9$, suggesting that this was the corresponding alcohol, **7.7**, from reduction. An FTIR spectrum confirmed the loss of the carbonyl stretching band at 1725 $cm^{-1}$, assigned to the aldehyde group in the starting material.

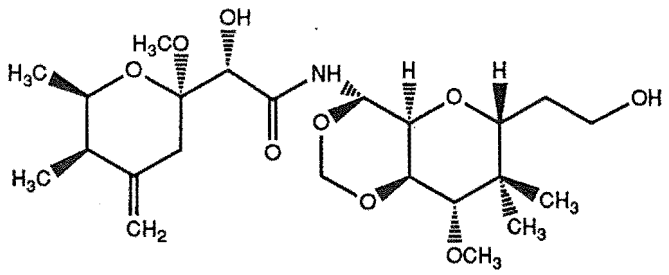


18-Normycalamide A (**7.7**)

The $^1H$ NMR spectrum showed no trace of the aldehyde but there was a new two-proton multiplet at δ3.50 ppm, along with a single-proton triplet (6.5 Hz) at δ2.96 ppm. The latter was assigned to the new C17 hydroxyl proton, being coupled to the resonance at δ3.50 in a COSY spectrum, and since it was removed on addition of $D_2O$. The H15 (-0.5), and two H16 (-0.7, -1.0) proton resonances were also shifted substantially upfield, compared to data for 18-normycalamide A 17-aldehyde (Table 7.1), indicative of this reduction[101]. Also H5a was less shielded in this derivative (+0.2).

Interestingly, the observed vicinal coupling constants between H15 and the two H16 protons (1.3, 10.5) were rather different in this derivative than for 18-normycalamide A 17-aldehyde, suggesting a different average solution conformation for this portion of the structure. These values were in fact indicative of an almost fixed anti geometry for the C14-C15-C16-C17 dihedral angle (see Chapter 5), so that the downfield H16 proton, having the smaller H15-H16 coupling constant, was probably pro-*R* and the upfield H16-proton pro-*S* in stereochemistry, based on earlier results. The coupling constants from these two H16 protons to the two H17 protons were also extracted from the $^1$H NMR spectrum. The size of these constants, 3.5, 3.5 and 5.7, 8.9 Hz from the H16*S* and H16*R* protons respectively, suggested that there was some preferred conformation about this C16-C17 bond, possibly with H16*S* anti to C17-O, to give the required gauche and anti relationships (Figure 7.3). Unfortunately, the overlap of the two H17 and the H13 proton resonances restricted a complete analysis of this portion of the structure using NOE experiments.

**Figure 7.3** Selected $^1$H-$^1$H NOE interactions and partial solution conformation of 18-normycalamide A (**7.7**).

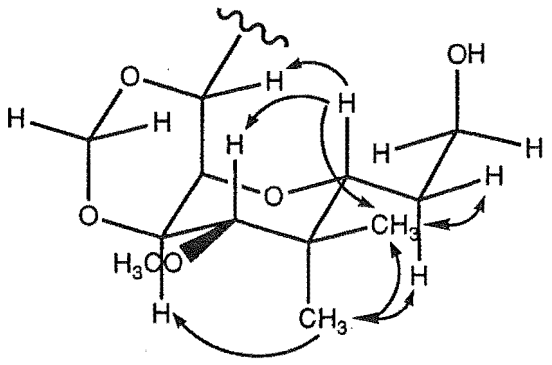


Some NOE experiments were performed to examine the solution conformations of the remainder of the structure (Table 7.2). NOE effects from irradiations of 14-$CH_3$*R* and 14-$CH_3$*S* confirmed the stereochemical

assignment of the H16*R* and H16*S* protons, along with the conformation of the trioxadecalin ring system, which could be inferred from the observed chemical shifts and coupling constants. Also the same NOE interaction between the H5a and H17 protons was observed. The remaining results were similar to those obtained for other derivatives above and for mycalamide A.

A $^{13}C$ NMR spectrum was also recorded and this contained a new resonance at δ58.5 ppm, which was assigned to the C17 methylene carbon. There were also shifts in the C15 (+1.4) and C16 (-11.5) resonances (Table 7.3), consistent with the presence of a primary hydroxyl group at C17, rather than an aldehyde[117]. The remaining data were readily assigned by comparison with those of mycalamide A. This structure (**7.7**) was equivalent to the replacement of the C18 group in mycalamide A by hydrogen, hence the name 18-normycalamide A. Biological assay data for this derivative are described in a following section.

### 7.4.2 ATTEMPTED REACTION OF 18-NORMYCALAMIDE A 17-ALDEHYDE WITH SODIUM BISULPHITE AND OTHER REACTIONS

Most carbonyl addition reactions are reversible[238], apart from reductions or reactions with Grignard reagents, and the latter would not be possible on mycalamides A and B without protection of the C7 hydroxyl and amide nitrogen groups (Chapters 5 and 6). Simple aldehydes react quantitatively only with sodium bisulphite or hydrogen cyanide, and the addition products are sufficiently stable to be isolable. Bisulphite ion ($HSO_3^-$) is a weak acid[238] ($pk_a$=7.2) but an excellent sulphur nucleophile. The products are ionic salts, which are water soluble and potentially crystalline. In a trial reaction, 18-normycalamide A 17-aldehyde (**7.5**) was reacted with a solution of sodium bisulphite in aqueous methanol for 16 hours at room temperature, followed by 1.5 hours at 50°C, monitoring by TLC. The more

polar product material streaked on both silica gel and reverse phase TLC, so the reaction was worked up and examined by $^1H$ NMR spectroscopy in deuterated methanol. However, the spectrum obtained was of very poor signal to noise ratio and indicated decomposition, with few resolved resonances relating to the mycalamide skeleton apparent. It was probable that the slight acidity of this reagent could have caused breakdown of the acetal moeities in mycalamide A, leading to this result.

A similar problem was likely to be encountered with other acid catalysed additions, including the formation of acetals and imines from reactions with alcohols and amines respectively[272], since the C6 acetal was very reactive under such conditions. The formation of a cyanohydrin was not explored, but this reaction was base catalysed[238], and such reaction conditions were probably more favourable with the mycalamides. Reductive amination[271,273] was also a possibility that was not investigated. Another alternative was selective oxidation of the aldehyde group, but the reagents which effect this transformation, including aqueous bromine solutions[258], or alkaline silver oxide[274], were not favourable for reactions on the mycalamides. In fact the most common synthetic methods for the oxidation of aldehydes were reported to be the strong oxidising agents, permanganate or chromic acid[274].

## 7.5 BIOLOGICAL ASSAY RESULTS AND CONCLUSIONS

The biological assay results for the four compounds described in this chapter have been listed in Table 7.5, together with results for mycalamides A and B, included for reference. The two major compounds derived from the oxidation of mycalamide B, which contained a double bond between C16 and C17 and no C18 (**7.3** and **7.4**), were both significantly less active than

mycalamide B. The *Z* isomer was the most active, but was still almost 100 times less active than mycalamide B, while the *E* isomer was between 3 to 4 times less active again. This was an unexpected result, since it was thought that this portion of the mycalamide B structure would be less biologically sensitive to structural changes. However, the compounds did appear to show some genuine biological activity, having been carefully purified through two stages of chromatographic separation.

Of more interest was the potent biological activity of 18-normycalamide A 17-aldehyde (**7.5**) and 18-normycalamide A (**7.7**), which both appeared to be more active than mycalamide A itself, but slightly less active than mycalamide B. The biological activity of these derivatives should perhaps be further evaluated, as these were potentially useful mycalamide analogues.

There is potential for further studies from this work. Further reactions of the aldehyde could be explored, along with the oxidation of the C7 hydroxyl group, which could probably best be achieved under conditions involving amine bases to avoid acid instability problems. Unfortunately there was not time to investigate all these possibilities in the current research.

**Table 7.1** $^1$H NMR data[a] for compounds in Chapter 7.

| | *E*$\Delta^{16}$ 18-Nor-myc.B (7.3) | *Z*$\Delta^{16}$ 18-Nor-myc.B (7.4) | 18-Normyc.A 17-ald.(7.5) | 18-Normyc.A 17-ald. hemiacetals (isomeric forms) | (7.6) | 18-Normyc.A (7.7) |
|---|---|---|---|---|---|---|
| **H2** | 4.04 (3.0,6.6) | 4.04 (2.9,6.5) | 4.02 (2.8,6.6) | 3.87 (2.7,6.6) | 3.91 (2.7,6.6) | 4.03 (2.8,6.5) |
| **2-CH$_3$** | 1.17 (6.6) | 1.17 (6.7) | 1.18 (6.6) | 1.18 (6.6) | 1.16 (6.6) | 1.20 (6.6) |
| **H3** | 2.22 (3.2,7.4) | 2.22 (2.9,7.3) | 2.23 (2.8,7.1) | 2.21 (2.7,7.0) | 2.19 (2.7,7.0) | 2.26 (2.8,7.0) |
| **3-CH$_3$** | 0.98 (7.3) | 0.98 (7.3) | 0.93 (7.1) | 0.96 (7.0) | 0.97 (7.0) | 1.00 (7.1) |
| **4=CH*Z*** | 4.82 (1.8) | 4.82 (1.9) | 4.85 (1.9) | 4.81 (2.0) | 4.79 (2.0) | 4.86 (1.8) |
| **4=CH*E*** | 4.69 (1.8) | 4.70 (1.8) | 4.77 (1.9) | 4.64 (2.0) | 4.64 (2.0) | 4.76 (1.8) |
| **H5a** | 2.14 (1.9,13.9) | 2.16 (1.9,14.0) | 2.06 (1.9,14.2) | 2.42 (2.1,14.1) | 2.39 (2.0,14.2) | 2.22 (2.0,14.2) |
| **H5e** | 2.24 (14.0) | 2.25 (13.9) | 2.36 (14.1) | 2.30 (14.3) | 2.29 (14.3) | 2.41 (14.0) |
| **6-OCH$_3$** | 3.30 | 3.31 | 3.30 | 3.26 | 3.24 | 3.31 |
| **H7** | 4.26 (3.2) | 4.25 (2.8) | 4.27 | 4.31 | 4.23 | 4.31 |
| **7-OH** | 3.87 (3.3) | 3.96 (2.8) | | | | 3.71 |
| **NH9** | 7.33 (9.7) | 7.41 (9.3) | 7.47 (9.5) | | | 7.51 (9.6) |
| **H10** | 5.93 (9.7) | 5.95 (9.3) | 5.88 (9.5) | 5.75 (8.4) | 5.72 (8.4) | 5.83 (9.6) |
| **10-OCH*R*** | 5.15 (6.8) | 5.15 (6.9) | 5.14 (7.0) | 5.16 (6.9) | 5.16 (6.9) | 5.14 (6.9) |
| **10-OCH*S*** | 4.90 (6.8) | 4.87 (7.0) | 4.88 (7.0) | 4.82 (7.0) | 4.78 (7.0) | 4.88 (6.9) |
| **H11** | 3.74 (6.3,9.8) | 3.77 (6.4,9.3) | 3.77 (6.6,9.5) | 3.93 (6.5,8.4) | 3.85 (6.5,8.4) | 3.77 (7.1,9.7) |
| **H12** | 4.21 (6.3,10.2) | 4.18 (6.2,9.6) | 4.21 (6.6,10.1) | 4.14 (6.6,9.3) | 4.14 (6.6,9.3) | 4.24 (7.1,10.5) |
| **H13** | 3.49 (10.2) | 3.51 (9.6) | 3.50 (10.1) | 3.57 (9.3) | 3.57 (9.3) | 3.47 (10.4) |
| **13-OCH$_3$** | 3.56 | 3.55 | 3.57 | 3.54 | 3.54 | 3.57 |
| **14-CH$_3$*R*** | 0.94 | 0.95 | 0.93 | 1.02 | 1.00 | 1.00 |
| **14-CH$_3$*S*** | 0.87 | 0.85 | 0.87 | 0.83 | 0.83 | 0.85 |
| **H15** | 3.76 (8.9) | 4.39 (9.0) | 4.09 (5.2,7.3) | 3.61 (2.4,9.4) | 3.51 (4.7,8.3) | 3.64 (1.3,10.5) |
| **H16** | 4.57 (8.7,12.5) | 4.25 (6.6,8.9) | 2.36 (2.6,7.3) | 1.61 (m) | 1.58 (m) | 1.67 (1.4,5.7,8.9,14.5) |
| **H16** | | | 2.36 (2.0,5.2) | 1.61 (m) | 1.58 (m) | 1.37 (3.5,3.5,10.6,14.4) |
| **H17/H$_2$17** | 6.39 (12.6) | 5.89 (6.6) | 9.55 (2.0,2.6) | 4.52 (m) | 4.51 (m) | /3.50 (m) |
| **17-OCH$_3$** | 3.44 | 3.52 | | | | |
| **17-OH** | | | | | | 2.96 (6.5) |

[a]Data for structure **7.6** were recorded in $CD_3OD$, with chemical shifts in ppm relative to $CHD_2OD$, δ3.30 ppm. All other data were recorded in $CDCl_3$ with chemical shifts relative to $CHCl_3$, δ7.25 ppm (coupling constants in Hz).

**Table 7.2** $^{1}H$-$^{1}H$ NOE interactions[a] for compounds in Chapter 7.

| Compound | Signal(s) irradiated | Signals enhanced (% enhancement) |
|---|---|---|
| *E* Δ16, 18-Nor-myc.B (**7.3**) | H10 | 10-OCH*R*(4), H13(3), H15(8) |
| | H15 (H11) | H10(13), H12(7)[b], 14-$CH_3$*R*(1), H17(15) |
| | H16 | 14-$CH_3$*S*(1), 17-$OCH_3$(2) |
| | H17 | H15(5), 17-$OCH_3$(0.5) |
| *Z* Δ16, 18-Nor-myc.B (**7.4**) | H10 (H17) | 10-OCH*R*(4), H13(5), H15(10)[b], H16(10)[b], 17-$OCH_3$(2)[b] |
| | H15 | H10(5), H13(3), H17(2) |
| | H16 (H7) | 6-$OCH_3$(3)[b], 14-$CH_3$*S*(2), H17(7) |
| | H17 (H10) | 10-OCH*R*(3)[b], H13(4)[b], H15(8), H16(9), 17-$OCH_3$(2) |
| 18-Normyc.A 17-ald. (**7.5**) | H5a | 3-$CH_3$(0.6), H5e(12), H7(0.4), NH(1), H17(1) |
| | H7 | 6-$OCH_3$(3), NH(3) |
| | 14-$CH_3$*R* | H13(4), 13-$OCH_3$(0.7), 14-$CH_3$*S*(1), H15(5), $H_2$16(2) |
| | 14-$CH_3$*S* | H12(7), 13-$OCH_3$(0.3), 14-$CH_3$*R*(1), $H_2$16(2), H17(0.8) |
| | H15 | H10(7), H13(3), 14-$CH_3$*R*(0.9), $H_2$16(2), H17(4) |
| | $H_2$16 (H5e) | 4=CH*E*(2)[b], H5a(6)[b], 14-$CH_3$*R*(1), 14-$CH_3$*S*(1), H15(2), H17(4) |
| | H17 | H5a(0.7), H15(2), $H_2$16(0.9) |
| 18-Normyc.A 17-ald. hemiacetals (**7.6**) | H5a | 3-$CH_3$(0.8), H5e(9), H7d(1)[c], H7u(3)[c], H17(2) |
| | H5e | 4=CH*E*(5), H5a(15), H5a(9), H7d(0.4)[c], H7u(0.4)[c] |
| | 6-$OCH_3$d[c] | H2(3), H7d(13)[c], H7u(2)[c] |
| | H7d[c] | 6-$OCH_3$d(3)[c] |
| | H7u[c] | 6-$OCH_3$u(2)[c] |
| | H10 | 10-OCH*R*(5), H13(4), H15d(7)[c], H15u(7)[c] |
| | 14-$CH_3$*R* (3-$CH_3$) | H3(1), H13(5), 13-$OCH_3$(0.6), 14-$CH_3$*S*(0.7), H15d(6)[c], H15u(4)[c], $H_2$16(2) |
| | 14-$CH_3$*S* (3-$CH_3$, 14-$CH_3$*R*) | H3(1), H12(9), H13(2), 13-$OCH_3$(0.5), H15d(2)[c] H15u(3)[c], $H_2$16(2) |
| | H15d[c] (H13, 13-$OCH_3$) | H10d(12)[c], 10-OCH*R*(3), 14-$CH_3$*S*(0.3), 14-$CH_3$*R*d(1.5)[c], 14-$CH_3$*R*u(0.7)[c], $H_2$16(0.7), H17(2) |
| | H15u[c] (13-$OCH_3$) | H10d(10)[c], 10-OCH*R*(1), 14-$CH_3$*S*(0.2), 14-$CH_3$*R*d(1.5)[c], 14-$CH_3$*R*u(0.7)[c], $H_2$16(0.7), H17(2) |
| | $H_2$16 | 2xH11(2), 14-$CH_3$*S*(2), 2x14-$CH_3$*R*(1), 2xH15(4), H17(13) |
| | H17 | H5a(0.8), 2xH15(2), $H_2$16(1) |
| 18-Normyc.A (**7.7**) | H5a (H3) | H2(5)[c], 3-$CH_3$(2), 4=CH*Z*(3)[b], H5e(23), H7(2), $H_2$17(0.9) |
| | H5e | 4=CH*E*(5), H5a(21), 6-$OCH_3$(0.2) |
| | H7 | H5a(0.8), 6-$OCH_3$(3), NH(3) |
| | 14-$CH_3$*R* (3-$CH_3$) | 2-$CH_3$(0.7)[b], H3/H5a(3)[b], H13(4), 13-$OCH_3$(1), 14-$CH_3$*S*(2), H15(4), H16*R*(5) |
| | 14-$CH_3$*S* | H12(8), 14-$CH_3$*R*(1), H16*S*(6) |
| | H15 (13-$OCH_3$) | H10(10), H13(5), 14-$CH_3$*R*(1) |
| | H16*R* | 14-$CH_3$*R*(2), H15(4), H16*S*(11), $H_2$17(2) |
| | H16*S* | 14-$CH_3$*S*(1), H16*R*(10), $H_2$17(2) |
| | $H_2$17 (H13, 13-$OCH_3$) | H5a(2), H10(0.6)[b], 10-OCH*R*(0.7)[b], 14-$CH_3$*R*(0.3)[b], H15(1), H16*R*(5), H16*S*(5) |

[a]Data for compound **7.6** were recorded in $CD_3OD$. All other data were recorded in $CDCl_3$

[b]Enhancement interpreted as being due to the irradiation of an overlapping signal

[c]u and d have been used to designate the more upfield or more downfield resonance, associated with one of the two isomeric hemiacetals (not assigned)

**Table 7.3** $^{13}C$ NMR data[a] for compounds in Chapter 7.

| | 18-Normyc.A 17-ald.(7.5) | 18-Normyc.A 17-ald hemiacet. (isomeric forms) (7.6) | | 18-Normyc.A (7.7) | $E\Delta^{16}$, 18-Normyc.B (7.3) |
|---|---|---|---|---|---|
| **C2** | 69.61 | 71.23 | 71.20 | 69.79 | 69.6 |
| **2-$CH_3$** | 17.99 | 18.45 | 18.41 | 17.97 | 17.7 |
| **C3** | 41.28 | 43.34 | 43.25 | 41.31 | 41.0 |
| **3-$CH_3$** | 12.17 | 12.80 | 12.62 | 12.04 | 12.2 |
| **C4** | 145.07 | 148.48 | 148.23 | 145.13 | ? |
| **4=$CH_2$** | 111.01 | 110.65 | 110.34 | 111.04 | 111.0 |
| **C5** | 33.23 | 34.79 | 34.79 | 33.41 | 33.0 |
| **C6** | 100.05 | 101.66 | 101.66 | 99.90 | ? |
| **6-$OCH_3$** | 48.54 | ? | ? | 48.76 | 48.2 |
| **C7** | 71.31 | 74.00 | 73.52 | 71.76 | 70.7 |
| **C8** | 171.91 | 174.52 | 174.45 | 172.35 | ? |
| **C10** | 74.16 | 75.42 | 75.42 | 74.35 | 73.7 |
| **10-$OCH_2$** | 86.60 | 87.81 | 87.68 | 86.59 | 87.0 |
| **C11** | 70.78 | 70.54 | 70.54 | 71.66 | ? |
| **C12** | 74.25 | 75.75 | 75.75 | 74.78 | ? |
| **C13** | 79.20 | 81.37 | 81.37 | 79.40 | ? |
| **13-$OCH_3$** | 61.79 | 62.09 | 62.02 | 61.87 | 61.7 |
| **C14** | 40.97 | ? | ? | 41.37 | ? |
| **14-$CH_3R$** | 23.38 | 24.33 | 24.18 | 23.14 | 23.8 |
| **14-$CH_3S$** | 14.04 | 15.40 | 15.40 | 13.38 | 13.9 |
| **C15** | 74.06 | 77.29 | 77.10 | 75.41 | 78.5 |
| **C16** | 43.35 | 38.11 | 37.54 | 31.86 | ? |
| **C17** | 200.52 | 97.98 | 97.92 | 58.50 | 147.0 |
| **17-$OCH_3$** | | | | | 55.9 |

[a]Data for structure **7.6** were recorded in $CD_3OD$, with chemical shifts in ppm relative to $CD_3OD$, δ49.30 ppm. All other data were recorded in $CDCl_3$, with chemical shifts relative to $CHCl_3$, δ77.01 ppm.

**Table 7.4** Molecular modelling results for 18-normycalamide A 17-aldehyde (**7.5**)

| | MM2[b] | Dihedral angles[c] | | | | | Distances[d] | | | | | | H-Bonds |
|---|---|---|---|---|---|---|---|---|---|---|---|---|---|
| %[a] | Energy | a) | b) | c) | d) | e) | f) | g) | h) | i) | j) | k) | (OH/NH-O) |
| 33.2 | 224.5 | -162 | -61 | 69 | -172 | -103 | 3.3 | 2.8 | 3.0 | 3.8 | 6.1 | 3.6 | 7OH-17O, NH-O1 |
| 24.1 | 225.3 | -62 | 0 | -69 | -179 | -134 | 3.7 | 3.9 | 2.6 | 3.6 | 2.7 | 2.5 | 7OH-8O, NH-O1 |
| 12.8 | 226.9 | 76 | -178 | 129 | -176 | 134 | 2.3 | 3.0 | 4.0 | 5.2 | 4.0 | 3.2 | 7OH-O1, NH-7O |
| 8.5 | 227.8 | -55 | -7 | -67 | 74 | -132 | 3.8 | 3.9 | 2.7 | 3.4 | 2.9 | 2.5 | 7OH-8O, NH-O1 |
| 4.7 | 229.3 | -57 | -64 | 99 | -180 | -2 | 3.7 | 3.9 | 2.7 | 2.6 | 7.3 | 3.5 | 7OH-17O, NH-7O |
| 2.8 | 230.6 | -58 | 12 | -76 | -177 | 4 | 3.8 | 3.9 | 2.6 | 3.7 | 7.2 | 2.4 | 7OH-8O, NH-O1,17O |
| 2.7 | 230.7 | 49 | -63 | 62 | -169 | -102 | 2.5 | 3.3 | 4.0 | 4.2 | 5.4 | 3.6 | 7OH-17O, NH-6O |
| 2.1 | 231.3 | -63 | -58 | 95 | -174 | 7 | 3.8 | 3.9 | 2.6 | 2.4 | 6.9 | 3.5 | 7OH-17O, NH-7O |
| 2.0 | 231.4 | -55 | -10 | -49 | -163 | 20 | 3.7 | 3.9 | 2.7 | 3.0 | 3.2 | 2.8 | 7OH-8O, NH-O1 |
| 1.6 | 232.1 | -63 | -173 | 108 | -177 | -129 | 3.8 | 3.9 | 2.7 | 2.8 | 5.7 | 3.4 | 7OH-6O,NH-7O |
| 1.4 | 232.4 | -59 | 8 | -18 | -173 | 10 | 3.8 | 3.9 | 2.6 | 2.3 | 4.2 | 3.2 | 7OH-8O,17O, NH-O1 |
| 1.2 | 232.6 | -55 | 178 | 121 | -175 | 137 | 3.7 | 3.9 | 2.7 | 3.4 | 5.5 | 3.3 | 7OH-6O, NH-7O |
| 0.7 | 233.9 | -58 | -2 | -71 | -84 | -7 | 3.8 | 3.9 | 2.7 | 3.6 | 4.7 | 2.5 | 7OH-8O, NH-O1 |
| 0.7 | 233.9 | 73 | -176 | 126 | 73 | -134 | 2.3 | 3.1 | 4.0 | 5.2 | 6.4 | 3.2 | 7OH-O1, NH-7O |
| 0.6 | 234.3 | -60 | 176 | -62 | -178 | -131 | 3.7 | 3.9 | 2.7 | 3.4 | 2.7 | 2.6 | 7OH-6O, NH-O1 |
| 0.5 | 234.7 | -61 | -177 | 100 | -174 | 135 | 3.8 | 3.9 | 2.7 | 2.6 | 5.7 | 3.4 | 7OH-6O, NH-7O |
| 0.3 | 236.4 | -59 | 21 | -84 | -83 | -8 | 3.8 | 3.9 | 2.6 | 3.9 | 4.4 | 2.4 | 7OH-8O |

[a]Relative population (Boltzmann distribution) [b]In kJ mol$^{-1}$ [c]Dihedral angles:- a) C5-C6-C7-C8 b) H-O-C7-C8 c) C6-C7-C8-N d) C14-C15-C16-C17 e) C15-C16-C17-O [d]Distances (in Å):- f) H5a-H7 g) H5e-H7 h) 6OC-H7 i) H5a-NH j) H5a-H17 k) H7-NH

**Table 7.5** Biological assay results for compounds in Chapter 7.

| Compound | P388 $IC_{50}$[a] | Antiviral Results[b] (ng/disk) | | | | | | | |
|---|---|---|---|---|---|---|---|---|---|
| Mycalamide A | 0.5 | WW | WW | +* | 5 | + | + | +* | 2 |
| Mycalamide B | 0.1 | WW | WW | +* | 2 | +++ | +++ | +* | 1 |
| *E* $\Delta^{16}$ 18-Normyc.B (**7.3**) | 34 | WW | WW | +* | 2000 | ++ | +++ | +* | 1000 |
| *Z* $\Delta^{16}$ 18-Normyc.B (**7.4**) | 10 | WW | +++ | +* | 200 | - | - | - | 100 |
| 18-Normyc.A 17-ald. (**7.5**) | 0.2 | WW | WW | +* | 5 | +++ | +++ | +* | 2 |
| 18-Normyc.A (**7.7**) | 0.2 | WW | WW | +* | 5 | +++ | +++ | +* | 2 |

[a] In ng/ml. The derivatives are estimated to be better than 95% pure, having been subjected to at least two steps of chromatographic purification in most cases.

[b] -,+,++,+++,WW=antiviral zone size. Results are listed in the order of *Herpes simplex virus*, *Polio virus*, cytotoxicity, loaded sample mass.

# CHAPTER 8
# STRUCTURE-ACTIVITY RELATIONSHIPS IN MYCALAMIDES A AND B AND THE SYNTHESIS OF A MODEL COMPOUND

## 8.1 INTRODUCTION

The biological assay results for more than one hundred and ten derivatives of mycalamides A and B have enabled the elucidation of some important structure-activity relationships. These results are reviewed in this chapter and the most promising analogues highlighted. Some of these analogues have been specified in exemplification of a patent on mycalamides A and B (and their derivatives) as potential antitumour agents[68,69]. The possible correlation between the *in vitro* antiviral and antileukemic (P388) assay results for these mycalamide derivatives is also investigated.

With such complex molecules as the mycalamides, it was difficult to examine thoroughly the importance of all structural features. Most work has centred on the modification of particular functional groups, but even this has not been exhaustive, as noted in earlier chapters. However, within the limitations of the work performed, it has been established that some structural features were certainly important for the biological activity, particularly the central amide portion of the molecule.

Aspects of the syntheses of pederin and the mycalamides A and B will be reviewed as a background to the design of compounds containing some of these important structural features. There is much current interest, for example, in the development of peptide mimics as new clinical agents[65,66,275]. As increasingly more efficient syntheses of the natural products are developed, there is clearly some potential for the further

development of simple analogues. The design of active, conformationally restricted molecules[70,71,92] may also enable more information to be obtained about the exact nature of the active site with which these compounds interact. The work described in this chapter may thus assist in the further development of the mycalamides A and B and related compounds as potential antitumour agents.

## 8.2 STRUCTURE-ACTIVITY RELATIONSHIPS IN MYCALAMIDES A AND B

### 8.2.1 SUMMARY OF BIOLOGICAL ACTIVITY DATA

The complete set of biological assay results for all the mycalamide derivatives presented in previous chapters has been summarised graphically in Figure 8.1. This graph illustrates the relationship between the *in vitro* antiviral and P388 antileukemic assay results by expressing the logarithm of the P388 $IC_{50}$ value (in ng/ml) versus the logarithm of the minimum antiviral loading (in ng/disk) required for a whole-well antiviral response. Note that the data set has been edited to exclude those compounds with a P388 $IC_{50}$ value in excess of 500 ng/ml for clarity of presentation (such derivatives can safely be considered to be inactive within the limits of purity, as discussed below). It is apparent that there is a strong correlation between the two sets of biological assay results within experimental error (see below). This correlation is probably indicative of a common mode of action for all the derivatives as for the parent compounds, that is, an inhibition of protein synthesis[53,57], as expected. In particular, there are no derivatives with significantly more selective antiviral or P388 antileukemic activity.

**Figure 8.1** Graph of the logarithm of the P388 $IC_{50}$ (in ng/ml) versus the logarithm of the minimum loading (in ng/disk) for a whole-well antiviral response for compounds in this thesis.

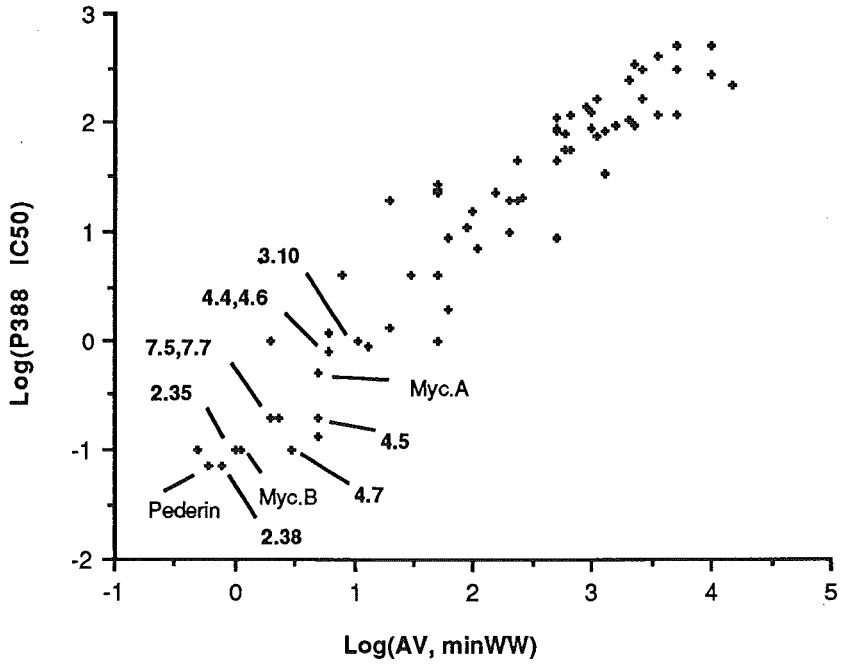


The derivatives displaying the most potent biological activity were found to be (no order intended): 18-*O*-methyl mycalamide A (**2.35**), 17,18-di-*O*-methyl mycalamide A (**2.38**), 4α-dihydro mycalamides A and B (**4.4**, **4.6**), 4β-dihydro mycalamides A and B (**4.5**, **4.7**), 18-normycalamide A (**7.7**), 18-normycalamide A 17-aldehyde (**7.5**), and, to a lesser extent, the following esters: mycalamide A 18-p-bromobenzoate (**2.10**), mycalamide B 18-monoacetate (**2.20**), mycalamide B 7-monoacetate (**2.21**), mycalamide B 18-mesylate (**2.23**) and 17,18-di-*O*-methyl mycalamide A 7-monoacetate (**2.36**). Of these derivatives, the compounds 18-*O*-methyl mycalamide A (**2.35**), 17,18-di-*O*-methyl mycalamide A (**2.38**) and 18-normycalamide A (**7.7**) were perhaps the most promising analogues. Note that the 4β-dihydro mycalamides A and B (**4.5**, **4.7**) were also of some interest, but appeared to

be more susceptible to acid catalysed hydrolysis. Really, to determine the best analogues, the derivatives would need to be tested over a much wider range of assay systems[1,2,13].

There are several possible sources of error in these biological assay results. The most crucial and difficult to determine source of error was the possible contamination of less active derivatives from trace amounts of more active derivatives, such as unresolved mycalamides A and B. There were significant uncertainties in the sample masses for fractions of less than 1 mg in size, which necessarily caused potential errors in the concentrations of samples submitted for assay. There were also physical errors involved in the preparation of dilution series and minor statistical variations between individual assay runs. In particular, part of the error in the P388 assay result arose from the calculation of the $IC_{50}$ value from a relatively small number of data points (performed by assuming straight line connections between points and interpolating a result between these). To counter this, at least two $IC_{50}$ values were calculated for each derivative and the results averaged. There were generally insufficient measurements performed to present a better statistical view of the overall errors in the stated assay results. However, it has been found by experience that the uncertainty is up to a factor of two either side of the result, which may be considerably higher for compounds having stated activities less than one percent of those of mycalamides A and B (P388 $IC_{50}$'s of greater than 50 and 10, respectively), since chromatographic purity may then be in question, as indicated above.

### 8.2.2 REVIEW OF RESULTS BY STRUCTURAL CLASS

The mycalamide TMS ethers had activities similar to the parent compounds, but this result was questionable since these TMS ethers are readily hydrolysed[138]. The mycalamide TBDMS ethers displayed less activity

with increasing substitution of the hydroxyl groups of the mycalamides, so that the di- or tri-substituted ethers were inactive and even the mono-substituted ethers had little activity. Similarly, of the mycalamide p-bromobenzoate esters, only mycalamide A 18-p-bromobenzoate (**2.10**) had significant activity and the more substituted esters were much less active. Monoacetylation of mycalamide B was mildly deactivating (~10-fold), whereas complete acetylation of mycalamides A or B gave derivatives at least 100 times less active. However, mycalamide B 18-mesylate (**2.23**) seemed to be as active as mycalamide B. Analysis of the biological activity of the mycalamide methyl ethers showed that methylation of the C7 hydroxyl group was the most deactivating, whereas methylation of the C17 or C18 groups was slightly activating. Methylation of the amide was also deactivating. Similar results were found for benzylation of these groups.

The C6 acetal seemed to be important since the pseudomycalamides A and B (**3.7**, **3.8**) were significantly less active and the 4α-dihydro, 6-deoxy pseudomycalamide A (**4.13**) and 5,6-dehydromethoxy mycalamide A (**3.11**) derivatives were relatively inactive, whereas 6-ethoxy mycalamide A (**3.10**) was of similar activity to mycalamide A. All rearrangement and cleavage fragments arising from the acid catalysed hydrolysis of mycalamide A triacetate were inactive. Hydrogenation of the double bond of mycalamides A and B gave two isomers, where the 4β isomers were of about equal activity to the parent compounds, but the 4α isomers were slightly less active. Similarly, comparing the two epoxide isomers of mycalamides A and B, the 4α isomers were much less active than the 4β isomers and even the latter compounds were not very active. Rearrangement of the double bond to the C3-C4 position also resulted in a loss of activity.

All the derivatives containing an oxazolidinone ring were inactive, since the C7 hydroxyl group was substituted. Importantly, all other compounds

derived from base catalysed epimerisations or cleavages at C7 and C10 were inactive. Removal of the C10-C12 methylene acetal system to leave a double bond between C10 and C11 was completely deactivating and hydrogenolysis of this system also gave significant loss of activity. By comparison, the removal of C18 by oxidative decarbonylation was slightly activating, provided that a double bond was not introduced between C16 and C17.

### 8.2.3 STRUCTURE-ACTIVITY THEORIES AND ANALYSIS OF RESULTS

Fundamental to the study of correlations between structure and activity is the knowledge that messengers and enzymes of each organism depend strongly on small details of their chemical structure, without which their characteristic biological activity is lost. Small changes to these details can result in large changes to their degree of action. Potential natural and synthetic drugs show a similar dependence on minute detail. Current insight into structure-activity relationships has come from studies of physical properties and the receptor theory[15]. For example, three characteristics of the action of drugs indicate that these are concentrated by cells on specific areas known as receptors: the high dilution ($10^{-9}$M) at which solutions of drugs are potent, the specific recognition of a particular chirality (illustrating the importance of shape) and the high biological specificity of some drugs.

Historically, it was believed that structure-activity relationships depended on the presence of particular chemical substituents or nuclei[15]. The importance of physical properties in these correlations is now well accepted and can be summarised by three factors[15,75]: partition coefficients (a measure of relative solubility and thus comparative distribution), ionisation (and other measurements of electronic distribution) and shape (steric fit for interaction with an active receptor site). In this work, considerable emphasis has been placed on the study of shape, with the solution conformations of

derivatives being extensively investigated by $^{1}H$ NMR spectroscopy and, on occasions, molecular modelling. Here it was found that the derivatives with solution conformations most like those of mycalamides A and B displayed the most potent biological activity. Attempts to introduce further unsaturation into the molecule to reduce the possible solution conformations always gave rise to derivatives with little biological activity. However, despite understanding the major solution conformations of mycalamides A and B, it is still not known what is the 'active' conformation[70,71] (at the receptor[15]), as stated in earlier chapters.

No other direct assessment was made of electronic distribution, although it was observed that the C7 hydroxyl and amide NH groups were sites for potential ionisation under basic conditions, being readily alkylated with concurrent loss of biological activity. Thus it is probable that these groups would be directly involved in interactions with the active site and, possibly, receptor binding (pederin binds to a site on the ribosome[47,49] to inhibit translation in protein synthesis[46] and mycalamides A and B have a similar mechanism of action[57]). Note, however, that some local regions of electronic distribution in these compounds could also be estimated by analysing $^{1}H$ and $^{13}C$ NMR chemical shift data.

The small scale preparations and lack of a strong UV chromophore in mycalamides A and B and derivatives meant that these were not amenable to the measurement of partition coefficients[15], which are usually measured for octanol and water solutions[1,75]. Some crude assessment of the relative polarities could possibly be obtained from a study of the retention characteristics[75] of the various derivatives on C18 reverse phase material or silica gel. It was noted, however, that many derivatives which had similar retention times to mycalamides A and B displayed vastly differing levels of biological activity. Therefore it is proposed that solubility is not a major factor

in the above results and a more detailed analysis was not attempted due to time constraints.

The structure-activity correlations discussed above for the mycalamides are complex, since it appeared that few changes could be made to the structure without substantial loss of biological activity. However, it was clear that the region from C6 to C10 was most important, since cleavages, epimerisations and functional group modifications to elements of this portion always resulted in almost completely inactive derivatives. One of the original aims of this research was to synthesise a model compound, including some biologically important structural features. This proposal stems from an established concept that the molecular structure of natural products can often be simplified by removing non-essential structural portions, while still retaining the desired therapeutic action[4]. Historically, the simplification of the structure of cocaine to give the local anaesthetic procaine was the first of many notable successes in this area[4]. The following section reviews some aspects of the syntheses of pederin and mycalamides A and B as a background to this synthetic attempt.

## 8.3 SYNTHESIS OF A MODEL COMPOUND

### 8.3.1 APPROACHES TO THE SYNTHESES OF PEDERIN AND MYCALAMIDES A AND B

Early approaches to the synthesis of pederin concentrated on the individual synthesis of the two halves of the molecule[133,240,276,277,278], since it was proposed that these could be coupled at the amide linkage, or adjacent to it at C10[279]. The first successful total synthesis of pederin was reported in 1979[280] and 1982[90] by a Japanese group, Yanagiya and coworkers. A crucial factor in this synthesis was the novel construction of the central *N*-(1-

methoxyalkyl) amide bridge, involving the coupling of a carboxylic acid, including the left hand structural portion to C8 (activated *in situ* as the acyl chloride), with a methyl imidate, including the right hand portion to C10-NH, using triethylamine at room temperature (Scheme 8.1a). The acyl chloride was easily formed under very mild conditions by a reaction of the carboxylic acid with thionyl chloride and excess pyridine at room temperature, while the imidate was constructed from a C10 amide by treatment with trimethyloxonium tetrafluoroborate. The resulting methyl *N*-acyl imidates were reduced by sodium borohydride to generate the *N*-(1-methoxyalkyl) amide (Scheme 8.1a). During this synthesis[90] the hydroxyl groups were protected as benzoate esters and the exocyclic double bond was not generated until the penultimate step (by oxidation and elimination of a C4 alkyl phenyl selenium group), to counter acid instability problems[127,133,276]. Using this double bond protected substrate, kinetically controlled acid catalysed exchange reactions at C10 could be performed to optimise the yield of pederin over its thermodynamically favoured C10 epimer[127,130]. The full details of this synthesis were reported in 1988 by Matsuda, Matsumoto and coworkers[127].

Subsequent syntheses by Nakata, Oishi and coworkers[134,135] and by Willson and coworkers[128,129,252] depended to a large extent on these Matsumoto protocols. More recently, an alternative synthesis was reported by Willson[132], involving the novel coupling of a C6 metallated dihydropyran with an oxamate ester of the right hand portion (to C7) to generate the sensitive C6-C8 'masked tricarbonyl' system. This approach had the advantage of circumventing problems with the stability of the left hand side intermediates in the previous syntheses[90,129,132].

Recently, Kishi and coworkers[91] reported the total synthesis of mycalamides A and B, involving the coupling of isomeric C10 amines (having the entire right hand portion constructed) with the left hand side carboxylic

acid intermediate used in earlier syntheses of pederin. This total synthesis unambiguously established the absolute configuration of mycalamides A and B. It was also sufficiently flexible to allow for the future preparation of further mycalamide analogues.

**Scheme 8.1** Reaction sequences employed in the synthesis of pederin and a model compound (**8.3**).

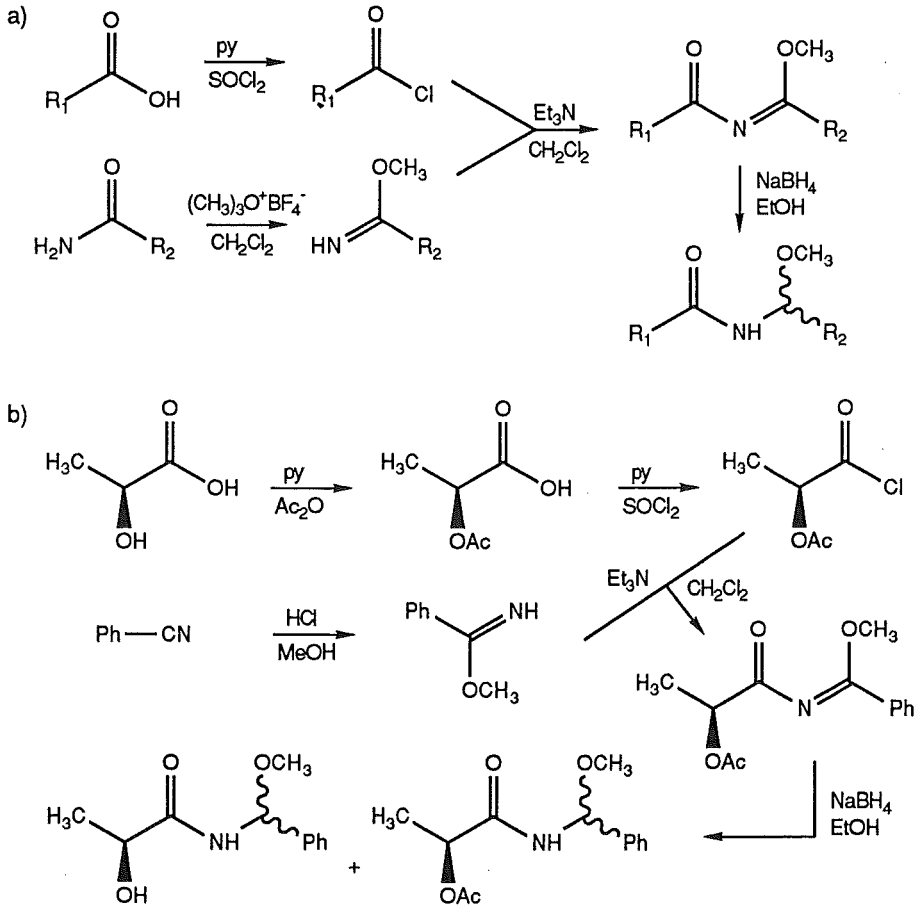


## 8.3.2 SELECTION OF A MODEL STRUCTURE

As indicated above, structure-activity correlations for the mycalamides A and B had established the importance of the central portion from C6 to C10 for the biological activity of these compounds. The original synthesis of pederin, involving the construction of the *N*-(1-methoxyalkyl) amide, led to the patenting of this synthesis of acylaminoacetals[281] (**8.1**) and of hydroxypropionyl-

aminoacetals[282] (**8.2**) as useful intermediates to pederin. The former patent description stated that this structure contributed to the physiological activity of pederin, and the second patent description claimed potent physiological activity for compounds of the form **8.2**, although this was not quantified. These hydroxypropionyl-aminoacetals (**8.2**) contained the structural features from C7 to C10 of pederin, so it was decided to synthesise and separate the isomers of one example of this class of compounds and determine the possible biological activities in our assay systems. The compound chosen for this study was **8.3**, whose synthesis was clearly described in the patent[282] and in the later Matsuda paper[127]. Note that the only other natural product containing similar structural features (C7-C10, with C10 having an OR group), was oxypinnatinine[283,284] (**8.4**), having no published biological activity data.

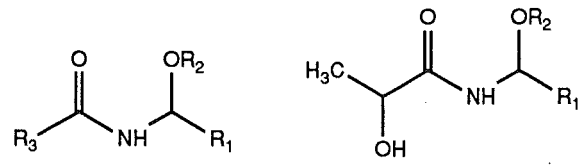


$R_1$-$R_3$=alkyl,aryl: (**8.1**) $R_1$=$R_2$=alkyl,aryl: (**8.2**)
$R_1$=Ph, $R_2$=$CH_3$: (**8.3**)

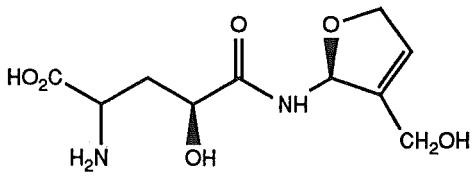


Oxypinnatinine (**8.4**)

## 8.3.3 SYNTHESIS OF N-(α-METHOXYBENZYL)-2-HYDROXY PROPIONAMIDE

A detailed account of the synthesis of the four diastereoisomers of this compound and their purification is presented in the Experimental section, so will be only briefly described here. The synthetic strategy has been illustrated in Scheme 8.1b, starting with benzonitrile and *S*-lactic acid (AR grade) in the

first instance. Unfortunately this grade of lactic acid was impure, containing other esters and anhydrides of lactic acid, but was still used for this initial study. Acetylation, using pyridine and acetic anhydride, gave the 2-acetyl derivative of *S*-lactic acid (**8.5**), containing minor amounts of pyridine and acetic acid, by $^1$H NMR spectroscopy (for NMR data see Experimental).

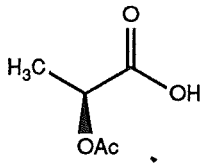


*S*-Lactic acid acetate (**8.5**)

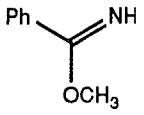


Imino ether (**8.6**)

The imino ether (**8.6**) was synthesised from benzonitrile, using acetyl chloride and excess dry methanol to generate anhydrous hydrochloric acid in situ, which was required to catalyse the addition of methanol across the C-N triple bond (Pinner synthesis[285]). The product was partially purified on Florisil, to give a sample which was at least 90% **8.6**, containing only traces of benzonitrile and methyl benzoate, by $^1$H and $^{13}$C NMR spectroscopy (see Experimental). Purification using silica gel gave a less pure sample having a new aromatic impurity which was not determined (it was not benzoic acid).

Crude *S*-lactic acid acetate (**8.5**) was converted into the acid chloride using thionyl chloride and pyridine, then this mixture reacted with the imino ether (**8.6**) in the presence of triethylamine to give the coupled *N*-acyl imino ether, which in turn was reduced using sodium borohydride to give the crude product mixture (Scheme 8.1b). This mixture contained the product diastereoisomers (**8.7**, **8.8**), their acetates (**8.9**, **8.10**), byproducts and reagent derived material by $^1$H NMR spectroscopy, so was initially purified by silica gel column chromatography. However, neither the two diastereoisomers (**8.7**, **8.8**), nor their acetates (**8.9**, **8.10**) were completely resolved by silica gel TLC. Preparative HPLC, using a chiral (*R*) phenyl urea column under

normal phase conditions, enabled a removal of impurities but gave no resolution of compounds **8.7** and **8.8**, and the yields appeared to be low. However, careful preparative silica gel TLC (developing the plate four times) of two fractions from the initial column chromatography above gave several fractions containing various ratios of **8.7** and **8.8**, including one that was at least 85% rich in one diastereoisomer and another of similar purity that was rich in the other. This work did not resolve the acetates of these compounds, but did purify a minor reaction product (**8.11**), having an *N*-acetyl group[281] in place of the *N*-(2-hydroxy propionyl) group[282], according to its $^{1}H$ NMR data (see Experimental). This compound would arise from the presence of small amounts of acetic acid in the crude lactic acid used for the coupling reaction.

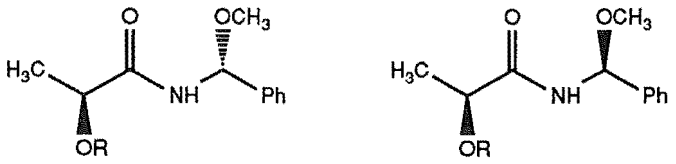


R=H: *SR*, *SS* Products (**8.7**, **8.8**)
R=Ac: *SR*, *SS* Product acetates (**8.9**, **8.10**)

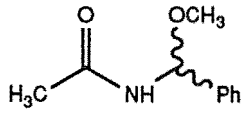


*N*-(α-Methoxybenzyl) acetamide (**8.11**)

### 8.3.3.2 CHARACTERISATION OF MAJOR PRODUCTS BY NMR AND MASS SPECTROSCOPIES

The $^{1}H$ and $^{13}C$ NMR data obtained for the two mostly separated diastereoisomers (**8.7** and **8.8**) have been listed in Table 8.1. (Data for the mixed acetates of these compounds are listed in the Experimetal section, being similar to these, except in the downfield shift of the α-proton resonances and characteristic shifts in the $^{13}C$ resonances, consistent with acetylation[98,117]). There was little difference in the $^{1}H$ NMR chemical shifts

for the two isomers. The largest differences occurred for the exchangeable proton resonances C2-OH and NH (around 0.1 ppm) and H2 (0.05 ppm). Similarly, the $^{13}C$ NMR chemical shifts were within 0.15 ppm for the two isomers.

NOE experiments were performed to investigate their solution conformations in an attempt to assign the stereochemistry at C5. Note that there was some conformational rigidity from C3 to C5, as in mycalamides A and B and pederin, since the amide bond would be in a *Z* conformation[107], and the NH and H5 protons were in an anti relationship from the magnitude of the observed coupling constant[98,102] (9.7 Hz). The NOE results (Table 8.2) were found to be similar for both isomers and did not help with the assignment of stereochemistry, since there were insufficient long range NOE interactions between substituents at C2 and C5. In any case, the likely conformational flexibility about the C2-C3 bond (HC-CO) would probably not allow a conclusive answer.

The structure of these diastereoisomers (**8.7** and **8.8**) was further supported by HREIMS results. A strong peak was observed at *m/z* 194, corresponding to a loss of $CH_3$ from the parent ion (adjacent to the α-hydroxy amide), while a base peak at *m/z* 121 was found, corresponding to an α-methoxy benzyl ion ($C_8H_9O$), along with a smaller ion at *m/z* 105, corresponding to a loss of $CH_4$ from the latter (to leave a benzoyl ion). The HREIMS spectrum of the mixed acetates (**8.9** and **8.10**) was also consistent with their structure, showing similar peaks at *m/z* 121 and 105, along with a strong peak at *m/z* 191, corresponding to a loss of acetic acid from the parent ion, and a weaker ion at *m/z* 220, corresponding to a loss of $CH_3O$ from the parent.

### 8.3.3.3 SYNTHESES USING OPTICALLY PURE LACTATE SALTS

Having successfully obtained two of the four isomers of **8.3**, it was then desirable to optimise the synthesis of all four by starting with the optically pure carboxylate salts, calcium L(+)-lactate and lithium D(-)-lactate. Therefore these salts were first acetylated, using the original reaction conditions, to give *S* lactic acid acetate (**8.5**) and *R* lactic acid acetate (**8.12**). The complete synthesis was then repeated for each, as before, except that the final sodium borohydride reduction step was performed on an ice cooled solution[127,282], rather than at room temperature, where the reaction was too vigorous. This modification had the result of giving much higher yields of the acetyl derivatives than in the original reaction. (Yields for the three reactions of purified acetates or hydroxy products ranged between 70-90%, with the latter reactions giving better overall yields, see Experimental).

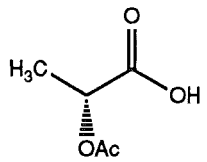


*R*-Lactic acid acetate (**8.12**)

The crude products obtained from both these latter syntheses were each subjected to a single stage of purification, using silica gel column chromatography, to give fractions containing mixtures of the acetates and/or hydroxy products. Note that the diastereoisomers derived from *R*-lactic acid are structures **8.13** and **8.14**, while their acetates are compounds **8.15** and **8.16**. These products were identical by HREIMS and $^1$H NMR spectroscopy to those compounds obtained from the first synthesis. Thus it remained only to submit these samples for biological testing.

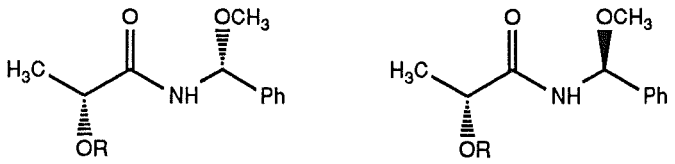

R=H: *RR*, *RS* Products (**8.13**, **8.14**)
R=Ac: *RR*, *RS* Product acetates (**8.15**, **8.16**)

## 8.3.4 BIOLOGICAL ASSAY RESULTS AND CONCLUSIONS

The crude reaction products from the first two syntheses showed very weak cytotoxicity in the P388 assay. However, this cytotoxicity was not associated with the diastereomeric products (**8.7**, **8.8**, **8.13**, **8.14**), nor with their acetates, but with some reagent derived material and other, more polar impurities. Thus none of the isomers of **8.3** had significant P388 antileukemic activity ($IC_{50}$ values greater than 125000 ng/ml). Similarly, no antiviral or cytotoxic response was observed in the antiviral assays for loadings of up to 80000 ng/disk. Therefore this compound did not seem to have any biological activity and was certainly not comparable to the mycalamides or pederin. It should be noted that this structure did not include an equivalent of the C6 acetal system, which did appear to be biologically important in these compounds. Thus there are certainly other possible structures to consider, which may be accessible using this mild synthetic route with more ambitious substrates. However, such investigations were beyond the objectives and time available for this research.

It is certainly possible that some simplification of the mycalamide and pederin structures could be achieved while retaining significant biological activity[4]. The production of more complex analogues may be readily achievable by small modifications to the existing synthetic routes to the natural products, as discussed above. The slight differences in the biological properties of pederin, mycalamides A and B and onnamide A (see Introduction) is sufficient evidence to suggest that such modifications may

provide compounds with even better therapeutic potential. It is hoped that the extensive structural modifications described in this present work, which have culminated in a large number of biological assay results and a better understanding of the chemical and conformational behaviour of these compounds, will provide some basis and stimulus for the ongoing study and development of such potential antitumour compounds in the future.

**Table 8.1** $^{1}H$ and $^{13}C$ NMR data[a] for compounds **8.7** and **8.8** (called 'isomers 1 and 2' since the stereochemistry at C5 was not defined).

| | $^{1}H$ NMR data | | | $^{13}C$ NMR data | |
|---|---|---|---|---|---|
| | Isomer 1 | Isomer 2 | | Isomer 1 | Isomer 2 |
| $CH_3$ | 1.46 (d, 6.9) | 1.48 (d, 6.8) | C1 | 21.29 | 21.42 |
| H2 | 4.32 (q, 6.9) | 4.27 (q, 6.8) | C2 | 68.39 | 68.51 |
| 2-OH | 2.56 (s) | 2.66 (s) | C3 | 174.52 | 174.61 |
| NH | 6.95 (d, 9.8) | 7.03 (d, 9.6) | C5 | 81.29 | 81.19 |
| H5 | 6.11 (d, 9.8) | 6.10 (d, 9.7) | 5-$OCH_3$ | 56.08 | 55.98 |
| 5-$OCH_3$ | 3.46 (s) | 3.44 (s) | Ph | 139.01 | 139.03 |
| Ph | 7.32-7.45 (m) | 7.32-7.43 (m) | | 128.67 | 128.65 |
| | | | | 128.64 | 128.61 |
| | | | | 125.84 | 125.84 |

[a]All data were recorded in $CDCl_3$, with chemical shifts in ppm relative to $CHCl_3$, δ7.25, or to $CDCl_3$, δ77.01 ppm (multiplicity, coupling constants in Hz).

**Table 8.2** $^{1}H$-$^{1}H$ NOE interactions[a] for compounds **8.7** and **8.8**.

| Compound | Signal(s) irradiated | Signals enhanced (% enhancement) |
|---|---|---|
| Isomer 1 | $CH_3$ | H2(5), NH(2) |
| (8.7 or 8.8) | H2 | $CH_3$(0.6), 2-OH(0.6), NH(1) |
| | 2-OH | H2(2), NH(1) |
| | H5 | 5-$OCH_3$(0.8), Ph(0.6) |
| | 5-$OCH_3$ | H5(3) |
| | NH | H2(1) |
| Isomer 2 | $CH_3$ | H2(6), NH(1), H5(0.2), 5-$OCH_3$(0.3) |
| (8.8 or 8.7) | H2 | $CH_3$(0.9), NH(1) |
| | 2-OH | $CH_3$(0.3), H2(3), NH(2), H5(0.3) |
| | H5 | $CH_3$(0.2), H2(0.3), 5-$OCH_3$(0.9), Ph(0.7) |
| | 5-$OCH_3$ | $CH_3$(0.5), H2(0.5), NH(1), H5(4), Ph(0.4) |
| | NH | $CH_3$(0.3), H2(2), 5-$OCH_3$(0.3) |

[a]All data were recorded in $CDCl_3$.

# EXPERIMENTAL

## GENERAL METHODS

Infrared (IR) spectra were recorded for $CHCl_3$ solutions or smears (film) on potassium bromide plates, using a Pye Unicam SP3-300 spectrometer. FTIR spectra were all recorded as smears using either a Perkin Elmer 1600 Series FTIR spectrometer, equipped with a Hewlett Packard Color Pro plotter, or a Bio-Rad Digilab Division FTS-40 FTIR spectrometer, equipped with a 3240-SPC data terminal, an NEC multisyncII screen and a KDC FPL-2000 plotter. Ultraviolet-Visible (UV) spectra were recorded as methanol solutions on a Varian DMS 100 UV/Visible spectrophotometer. Mass spectra were recorded on Finnegan 4500 (DCI/DEI), VG7070E or Jeol SX102 (high resolution) mass spectrometers (USA), or a Kratos MS80RFA mass spectrometer (UOC).

NMR spectra were recorded on a Varian XL300 spectrometer, operating at 300 MHz for $^1H$ and at 75 MHz for $^{13}C$ nuclei, except for 500 MHz $^1H$-detected HMQC or HMBC data, which were recorded on a VXR500S spectrometer. All samples for examination in $CDCl_3$ were normally prepared and stored in the presence of 0.1% pyridine to prevent acid catalysed decomposition[95,139]. Chemical shifts in this thesis have been expressed as parts per million (ppm) on the $\delta$ scale, relative to the following solvent reference peaks; $^1H$: $CHCl_3$ $\delta$7.25, $CHDCl_2$ $\delta$5.33, $CHD_2OD$ $\delta$3.30, $CHD_2SOCD_3$ $\delta$2.60, $C_6HD_5$ $\delta$7.27, or dioxan $\delta$3.70 (for spectra in $D_2O$) and $^{13}C$: $CHCl_3$ $\delta$77.01, $CD_2Cl_2$ $\delta$53.60, $CD_3OD$ $\delta$49.30, $CD_3SOCD_3$ $\delta$40.5, $C_6D_6$ $\delta$128.40 or dioxan $\delta$67.40 (for spectra in $D_2O$). The $^1H$ NMR resonances in this section are described as: chemical shift, assignment, multiplicity (s for singlet, d for doublet, t for triplet, q for quartet, m for multiplet),

coupling constant (in Hz). Difference NOE experiments were performed on non-degassed solutions in an arrayed experiment, with the decoupler offset 10000 Hz for the control experiment and then low power cycled over the multiplet peaks corresponding to the proton or protons being irradiated in the experiment[82]. A 1 s acquisition time (AT) was used, with a delay (D2) of 2 seconds. The reported percentage enhancements represented the increase in intensity of a particular resonance (independent of the power level used for irradiation or the degree of saturation obtained). All NOE and two-dimensional correlation experiments were performed using narrowed spectral windows. For NOE and COSY experiments this was typically δ0.5-8.5 ppm, but for HMQC or HMBC experiments the $^{1}H$ window was usually δ0.5-6.2 ppm and the $^{13}C$ window δ10-110 or 10-80 ppm. Typical acquisition parameters were used for COSY experiments (AT of 0.2 s, D1 of 1 s, pulse width (PW) = 0.5x P1 (45°), number of increments (NI) = 256), with zero-filling, pseudo-echo weighting functions, and symmetrisation used in the data processing. Acquisition parameters for HMQC experiments included AT's of 0.07-0.16 s and D1's of 0.7-1 s, with J1XH either 130 or 140 Hz, a JNXH of 140 Hz and a 'null' value of 0.4 s. For HMBC experiments similar AT and D1 values were used, but J1XH was 130 Hz and JNXH 8.3 Hz. Data were generally displayed in the absolute value mode. Molecular mechanics calculations, using standard MM2 parameters, were performed on a Vax computer, using a MODEL program, version KS 2.94[125].

Silica gel column chromatography was performed using Davisil, 35-70 μm, 170 Å, typically 200-300 mg in a pasteur pipette, using solvent gradients starting with mixtures of petroleum ether (PE) and ethyl acetate (EtOAc) and progressing to mixtures of ethyl acetate and ethanol (EtOH). Analytical and preparative silica gel TLC was performed on Merck DG P.K.60 $F_{254}$ plates, of 0.2 mm thickness, and reverse phase analytical TLC was performed on

Whatman $MKC_{18}F$ plates, of the same thickness. Visualisation of TLC plates containing mycalamide derivatives was achieved using an anisaldehyde dip reagent (0.1:1:100 by volume of anisaldehyde, concentrated sulphuric acid and glacial acetic acid) then heating at 120°C for 3-5 minutes. The yellow, orange or brown colour obtained for most derivatives (except cleavage fragments from the right hand portion which gave no colour, or those containing an oxazolidinone ring, which gave a blue colour) could be accentuated by iodine. In general, the mycalamides and derivatives gave no UV absorbance at $\lambda$=254 nm. Therefore, fully developed preparative TLC plates were visualised by removing a vertical strip of 2 mm width from the centre of the plate, visualising the strip with anisaldehyde reagent, then extrapolating the bands observed onto the remainder of the plate.

Reverse phase (C18) analytical and preparative HPLC was performed on a Shimadzu LC-4A instrument, equipped with a LKB Bromma 2142 Differential Refractometer (a refractive index recorder for semi-quantitative detection), using an Alltech Econosphere C18 column, of dimensions 250 mm x 4.6 mm and 5 $\mu$ particle size. A flow rate of 1 ml/min was generally used with the stated mixtures of methanol (AR grade, distilled and filtered) and water (deionised). Analytical and preparative normal phase HPLC (Chapter 8) was performed on the same instrument, using an Alltech Econosphere CN column, of dimensions 250 mm x 4.6 mm and 5 $\mu$ particle size, or a Supelcosil-LC-(*R*)-Urea chiral column of the same dimensions, and with UV detection ($\lambda$=254 nm). Solvents for this work were distilled and filtered (or further purified by standard procedures).

Microscale reactions were performed in either a 1 or 5 ml reactivial and stirred magnetically. (Hydrogenation reactions were performed using sealed microscale apparatus which permitted the entrance of a small flow of gas over the solution and contained an outlet tube vented into a beaker of water). All

technical grade solvents having boiling points less than 80°C were distilled prior to use, as were pyridine and acetic anhydride. Benzene and DMSO were AR grade, and the latter was usually predried over molecular sieves (type 4A). All other reagents were CP or AR grades and used without further purification, unless stated otherwise.

## BACKGROUND - ISOLATION AND CHARACTERISATION OF MYCALAMIDES A AND B[18,58]

The active *Mycale* sp. was recollected in January 1987 from the Otago Harbour (voucher specimen 87P1-1). Part of this collection (12.8 kg) was freeze-dried (3.9 kg) and extracted by blending with $CH_2Cl_2$ and $CH_3OH$ and filtering. The solvents were removed from the combined extracts to give an oil (409 g), having *in vitro* antiviral (AV) activity at 10 µg/disk, which was then partitioned between $CHCl_3$ and $H_2O$. Removal of the solvent from the organic fraction gave an oil (144 g, AV at 2.5 µg/disk), which was partitioned between 4:1 $CH_3OH$:$H_2O$ and $CCl_4$. The $CCl_4$ fraction was an oil (137 g, AV at 20 µg/disk), largely sterols. The major sterol was identified as 24-methylenecholesterol by its $^{13}C$ NMR signals. The $CH_3OH$:$H_2O$ fraction gave an oil (6.1 g, AV at 0.25 µg/disk), which was partitioned between 0.1 M aqueous NaOH and $CHCl_3$. The organic fraction was an oil (2.24 g, AV at 0.05 µg/disk), which was subjected to silica gel chromatography (45 g Davisil), developed in steps from $CH_2Cl_2$ to $CH_3OH$, to give a fraction (270 mg) containing mycalamide B (1:29 $CH_3OH$:$CH_2Cl_2$) and one (65 mg) containing mostly mycalamide A (1:9 $CH_3OH$:$CH_2Cl_2$). The fraction rich in mycalamide B was subjected to reverse phase liquid chromatography (RPLC) (2 g C18 material), developed in steps from 1:1 $CH_3OH$:$H_2O$ to $CH_3OH$. A fraction (20 mg), which eluted with 6:4 $CH_3OH$:$H_2O$, was mostly mycalamide B. This was

purified by further RPLC (Merck LOBAR RP18, 40-63 µm, 310 x 25 mm; 3 ml/min 3:1 MeOH.$H_2O$; refractive index detection). Mycalamide A was purified by similar RPLC steps.

Mycalamide A (**0.4**): an oil; $[\alpha]_D$ +34°, $[\alpha]_{365}$ +110° (*c* 0.2, $CHCl_3$); IR ($CHCl_3$) $\upsilon_{max}$ 3600-3200, 3420, 2950, 2900, 2860, 1680, 1380, 1100, 1085, 1065, 1020 $cm^{-1}$, (film) $\upsilon_{max}$ 3700-3100, 2960, 2890, 1690, 1540, 1470, 1390, 1100, 1080, 1040 $cm^{-1}$; $^1H$ and $^{13}C$ NMR data in Tables 1.1 and 1.3; HREIMS *m/z* 503.27220 ($M^+$, -1.7 ppm for $C_{24}H_{41}NO_{10}$), 471.24824 ($M^+$-$CH_3OH$, +3.0 ppm for $C_{23}H_{37}NO_9$); DCIMS ($NH_3$) *m/z* (%) 521 (13, $MNH_4^+$), 491 (34), 490 (31), 489 (100, $MNH_4^+$-$CH_3OH$), 472 (31, $MH^+$-$CH_3OH$), 316 (18), 288 (15), 272 (14), 260 (18); DCIMS ($ND_3$) *m/z* (%) 530 (22), 529 (66, $MND_4^+$), 528 (55), 527 (27), 498 (34), 497 (100, $MND_4^+$-$CH_3OH$), 496 (95), 495 (48); DCIMS ($CH_4$) *m/z* (%) 474 (16), 473 (34), 472 (100, $MH^+$-$CH_3OH$), 442 (14).

Mycalamide B (**0.5**): an oil; $[\alpha]_D$ +39° (*c* 0.2, $CHCl_3$); IR ($CHCl_3$) $\upsilon_{max}$ 3600-3200, 3375, 2935, 2900, 2850, 1680, 1380, 1090, 1070, 1025 $cm^{-1}$, (film) $\upsilon_{max}$ 3700-3150, 2985, 2950, 1690, 1535, 1460, 1390, 1100, 1075, 1035, 750 $cm^{-1}$; $^1H$ and $^{13}C$ NMR data in Tables 1.1 and 1.3; HREIMS *m/z* 485.26422 ($M^+$-$CH_3OH$, +3.5 ppm for $C_{24}H_{39}NO_9$); DCIMS ($NH_3$) *m/z* (%) 535 (7, $MNH_4^+$), 505 (28), 504 (38), 503 (100, $MNH_4^+$-$CH_3OH$), 488 (23), 487 (36), 486 (89, $MH^+$-$CH_3OH$); DCIMS ($ND_3$) *m/z* (%) 543 (5), 542 (14, $MND_4^+$), 541 (10), 513 (17), 512 (19), 511 (34), 510 (100, $MND_4^+$-$CH_3OH$), 509 (82), 508 (29), 493 (8), 492 (9), 491 (15), 490 (36, $MD^+$-$CH_3OH$), 489 (37), 488 (16); DCIMS ($CH_4$) *m/z* (%) 488 (16%), 487 (32%), 486 (100%, $MH^+$-$CH_3OH$), 456 (16%).

## WORK DESCRIBED IN CHAPTER 1

### 1.5 CHARACTERISATION OF PEDERIN DIBENZOATE (1.2) BY NMR SPECTROSCOPY

Pederin dibenzoate (**1.2**): an oil; $^{1}H$ NMR data in Table 1.7 except the following aromatic resonances, ($CDCl_3$) δ8.09 (dd, 1.5, 8.6), 8.03 (dd, 1.6, 8.6), 7.58 (m), 7.45 (t, 8.4) ppm and ($CD_3OD$) δ8.08 (dd, 1.5, 8.5), 8.05 (dd, 1.5, 8.6), 7.66 (dd, 1.5, 8.5), 7.63 (dd, 1.5, 8.5), 7.52 (t, 8.5) ppm; $^{13}C$ NMR data in Table 1.3 except the following aromatic resonances, ($CDCl_3$) δ133.50, 133.11, 130.29, 130.05, 129.56, 129.23, 128.51, 128.46 and ($CD_3OD$) δ135.07, 134.78, 131.84, 131.17, 130.86, 130.05, 130.01 ppm.

## WORK DESCRIBED IN CHAPTER 2

### 2.2.1 and 2.2.2 PREPARATION AND CHARACTERISATION OF TMS ETHERS

Mycalamide A (2.5 mg) was stirred with *N*, *O*-bis-trimethylsilyl acetamide (0.1 ml) in pyridine (0.1 ml) at room temperature overnight. $H_2O$ (0.3 ml) was added and the mixture extracted with $CH_2Cl_2$ (3x 0.2 ml). The solvent was removed and the crude organic products then subjected to silica gel column chromatography (200 mg Davisil), developed in steps from PE to EtOAc. A fraction (3 mg), which eluted with 4:1 PE:EtOAc, was pure mycalamide A tris-TMS ether (**2.1**).

**2.1**: an oil; $^{1}H$ and $^{13}C$ NMR data in Tables 2.1 and 2.2; HREIMS *m/z* 687.3651 ($M^{+}$-$CH_3OH$, -0.4 ppm for $C_{32}H_{61}NO_9Si_3$).

Mycalamide B (2.6 mg) was stirred with *N*, *O*-bis-trimethylsilyl acetamide (0.1 ml) in pyridine (0.1 ml) at room temperature overnight. $H_2O$ (0.3 ml) was added and the mixture extracted with $CH_2Cl_2$ (3x 0.2 ml). The

solvent was removed and the crude organic products then subjected to silica gel column chromatography (200 mg Davisil), developed in steps from PE to EtOAc. A fraction (3.1 mg), which eluted with 4:1 PE:EtOAc, was pure mycalamide B bis-TMS ether (**2.2**).

**2.2**: an oil, $^{1}H$ and $^{13}C$ NMR data in Tables 2.1 and 2.2; HREIMS *m/z* 629.3418 ($M^{+}$-$CH_3OH$, +0.5 ppm for $C_{30}H_{55}NO_9Si_2$).

Mycalamide B (2.0 mg) was dissolved in pyridine (0.1 ml) and cooled in ice. *N*, *O*-bis-trimethylsilyl acetamide (0.1 ml) was added and the reaction stirred in ice for 5 minutes. $H_2O$ (0.5 ml) was then added and the mixture extracted with $CH_2Cl_2$ (3x 0.2 ml). The solvent was removed and the crude organic products then subjected to silica gel column chromatography (200 mg Davisil), developed in steps from PE to EtOAc. A fraction (2.1 mg), which eluted with 2:1 PE:EtOAc, was pure mycalamide B 18-mono-TMS ether (**2.3**).

**2.3**: an oil; $^{1}H$ and $^{13}C$ NMR data in Tables 2.1 and 2.2; HREIMS *m/z* 557.3022 ($M^{+}$-$CH_3OH$, +0.4 ppm for $C_{27}H_{47}NO_9Si$).

Mycalamide A (1 mg) was dissolved in pyridine (0.1 ml) and cooled in ice. *N*, *O*-bis-trimethylsilyl acetamide (0.1 ml) was added and the reaction was stirred in ice for 4 minutes. $H_2O$ (0.5 ml) was then added and the mixture extracted with $CH_2Cl_2$ (3x 0.2 ml). The solvent was removed and the crude organic products then subjected to silica gel column chromatography (200 mg Davisil), developed in steps from PE to EtOAc. A fraction (1.2 mg), which eluted with 2:1 PE:EtOAc, was pure mycalamide A 17,18-bis-TMS ether (**2.4**).

**2.4**: an oil: $^{1}H$ NMR data in Table 2.1; HREIMS *m/z* 615.3263 ($M^{+}$-$CH_3OH$, +0.7 ppm for $C_{29}H_{53}NO_9Si_2$).

2.2.3 CLEAVAGE OF TMS ETHERS

Mycalamide A tris-TMS ether (**2.1**, 0.5 mg) was stirred with tetra-n-butyl ammonium fluoride (1 μl of a 1M solution) in THF (0.1 ml) at room temperature for 20 minutes. $H_2O$ (0.5 ml) was added and the mixture extracted with $CH_2Cl_2$ (3x 0.2 ml). The solvent was removed to give the crude organic product, which was almost pure mycalamide A by TLC and $^1H$ NMR spectroscopy.

2.2.4 PREPARATION AND CHARACTERISATION OF TBDMS ETHERS

Mycalamide A (1 mg), t-butyldimethylchlorosilane (8 mg), dimethyl-aminopyridine (1 mg) and triethylamine (5 μl) were stirred in pyridine (0.2 ml) at room temperature for 3 hours. $H_2O$ (0.5 ml) was added and the mixture extracted with $CH_2Cl_2$ (3x 0.3 ml). The solvent was removed and the crude organic product then subjected to silica gel column chromatography (200 mg Davisil), developed in steps from PE to EtOAc. A minor fraction (0.4 mg), which eluted with 4:1 PE:EtOAc, was pure mycalamide A 17,18-bis-TBDMS ether (**2.6**) while the major fraction (0.8 mg), which eluted with 2:1 PE:EtOAc, was pure mycalamide A 18-mono-TBDMS ether (**2.5**).

**2.5**: an oil; $^1H$ and $^{13}C$ NMR data in Tables 2.4 and 2.5; HRFABMS *m/z* 656.3214 ($MK^+$, -2.7 ppm for $C_{30}H_{55}NO_{10}SiK$).

Mycalamide A (2.6 mg), t-butyldimethylchlorosilane (~20mg), dimethyl-aminopyridine (2 mg) and triethylamine (30 μl) were stirred in pyridine (0.3 ml) at 60°C for 2 days. The solution was concentrated under nitrogen, then $H_2O$ (0.5 ml) was added and the mixture extracted with $CH_2Cl_2$ (3x 0.3 ml). The solvent was removed and the crude organic product then subjected to silica gel column chromatography (200 mg Davisil), developed in steps from PE to EtOAc. A minor fraction (1.5 mg), which eluted with 9:1 PE:EtOAc was mycalamide A tris-TBDMS ether (**2.7**), while the major fraction (2.5 mg), which

eluted with 3:1 PE:EtOAc, was pure mycalamide A 17,18-bis-TBDMS ether (**2.6**).

**2.6**: an oil; $^{1}H$ and $^{13}C$ NMR data in Tables 2.4 and 2.5; HRFABMS *m/z* 770.4145 ($MK^+$, +6.3 ppm for $C_{36}H_{69}NO_{10}Si_2K$).

**2.7**: an oil; $^{1}H$ and $^{13}C$ NMR data in Tables 2.4 and 2.5; HRFABMS *m/z* 814.5145 ($MH^+$-$CH_3OH$, +0.5 ppm for $C_{41}H_{80}NO_9Si_3$).

Mycalamide B (3 mg), t-butyldimethylchlorosilane (12 mg), dimethylaminopyridine (1 mg) and triethylamine (20 µl) were stirred in pyridine (0.2 ml) at room temperature for 20 hours. $H_2O$ (0.5 ml) was added and the mixture extracted with $CH_2Cl_2$ (3x 0.3 ml). The solvent was removed and the crude organic product then subjected to silica gel column chromatography (200 mg Davisil), developed in steps from PE to EtOH/EtOAc. The first fraction (1.5 mg), which eluted with 3:2 PE:EtOAc, was pure mycalamide B 18-mono-TBDMS ether (**2.8**), whereas the second fraction (1.7 mg), which eluted with 1:19 EtOH:EtOAc, was mycalamide B.

**2.8**: an oil; $^{1}H$ and $^{13}C$ NMR data in Tables 2.1 and 2.5; HRFABMS *m/z* 600.3535 ($MH^+$-$CH_3OH$, -5.4 ppm for $C_{30}H_{54}NO_9Si$).

Mycalamide B (2.8 mg), t-butyldimethylchlorosilane (25 mg), dimethylaminopyridine (6 mg) and triethylamine (40 µl) were stirred in pyridine (0.3 ml) at 80°C for 2 days. The solution was concentrated under nitrogen, then $H_2O$ (0.5 ml) was added and the mixture extracted with $CH_2Cl_2$ (3x 0.3 ml). The solvent was removed and the crude organic products then subjected to silica gel column chromatography (200 mg Davisil), developed in steps from PE to EtOAc. The MeOH soluble portion of the major fraction (2.5 mg), which eluted with 7:1 PE:EtOAc, was pure mycalamide B bis-TBDMS ether (**2.9**).

**2.9**: an oil; $^{1}H$ and $^{13}C$ NMR data in Tables 2.1 and 2.5; HRFABMS *m/z* 714.4383 ($MH^+$-$CH_3OH$, -6.9 ppm for $C_{36}H_{68}NO_9Si_2$).

## 2.3.1 PREPARATION AND CHARACTERISATION OF P-BROMOBENZOATE ESTERS

Mycalamide A (2.7 mg), p-bromobenzoyl chloride (5 mg) and triethylamine (4 μl) were stirred in $CH_2Cl_2$ (0.3 ml) at room temperature for 24 hours. The solvent was removed and the crude organic products subjected to silica gel column chromatography (200 mg Davisil), developed in steps from PE to EtOH/EtOAc. Two fractions, which eluted with 1:1 PE:EtOAc and EtOAc were a mixture of two products and unresolved reagent (TLC) so these were combined (4.2 mg). Preparative reverse phase HPLC (20% $H_2O$ in MeOH) gave two fractions (1.8 mg, 0.7 mg), which were pure mycalamide A 18-mono-p-bromobenzoate (**2.10**) and mycalamide A 7-mono-p-bromobenzoate (**2.11**), respectively.

**2.10**: an oil or white solid; UV ($CH_3OH$) $\lambda_{max}$ 244 nm (ε~5700); $^1H$ NMR data in Table 2.7; HRFABMS *m/z* 724.1709 ($MK^+$, -3.6 ppm for $C_{31}H_{44}{}^{79}BrNO_{11}K$).

**2.11**: an oil or white solid; UV ($CH_3OH$) $\lambda_{max}$ 245 nm (ε~6500); $^1H$ NMR data in Table 2.7; HRFABMS *m/z* 654.1914 ($MH^+$-$CH_3OH$, -0.2 ppm for $C_{30}H_{41}{}^{79}BrNO_{10}$).

Mycalamide A (5.0 mg), p-bromobenzoyl chloride (11 mg), dimethyl-aminopyridine (1 mg) and triethylamine (10 μl) were stirred in pyridine (0.4 ml) at 75°C overnight. The solution was concentrated under nitrogen, then $H_2O$ (0.4 ml) was added and the mixture extracted with $CH_2Cl_2$ (3x 0.4 ml). The solvent was removed to give the crude organic product (17 mg), which was a mixture of p-bromobenzoate esters and reagent (TLC). Preparative reverse phase HPLC (10% $H_2O$ in MeOH) gave four fractions (2 mg, 1 mg, 1.2 mg, 1.1 mg), which were pure mycalamide A 18-mono-p-bromobenzoate (**2.10**), mycalamide A 7,18-di-p-bromobenzoate (**2.12**), mycalamide A 17,18-di-p-bromobenzoate (**2.13**) and mycalamide A tri-p-bromobenzoate (**2.14**), respectively.

**2.12**: an oil or white solid; UV ($CH_3OH$) $\lambda_{max}$ 245 nm ($\varepsilon$~21000); $^1H$ NMR data in Table 2.7, $^{13}C$ NMR data in Table 2.2 except the following p-bromobenzoate resonances, ($CDCl_3$) δ165.72 and 164.77 (7- and 18-OCO), 131.82, 131.74, 131.50, 131.28, 131.14, 129.04, 128.73 and 128.17 (7- and 18-$OCOC_6H_4Br$) ppm; HRFABMS *m/z* 908.1109 ($MK^+$, +2.8 ppm for $C_{38}H_{47}{}^{79}Br^{81}BrNO_{12}K$).

**2.13**: an oil or white solid; $^1H$ NMR data in Table 2.7.

**2.14**: an oil or white solid; $^1H$ NMR data in Table 2.7; HRFABMS *m/z* 820.1175 ($MH^+$-$CH_3OH$-$C_6H_4{}^{79}BrCO_2H$, +2.2 ppm for $C_{37}H_{42}{}^{79}Br^{81}BrNO_{10}$), FABMS *m/z* (%) 1076 (5, $MNa^+$), 1074 (5, $MNa^+$), 1022 (14, $MNa^+$-$CH_3OH$), 1021 (8), 1020 (16, $MNa^+$-$CH_3OH$), 823 (27), 822 (51), 821 (37), 820 (100, $MH^+$-$CH_3OH$-$C_6H_4{}^{79}BrCO_2H$), 819 (22), 818 (50).

Mycalamide B (11 mg), p-bromobenzoyl chloride (26 mg), dimethylaminopyridine (2 mg), and triethylamine (20 μl) were stirred in pyridine (0.6 ml) at 55°C for one week. The solution was concentrated under nitrogen (to 0.1 ml), then $H_2O$ (0.3 ml) was added and the mixture extracted with $CH_2Cl_2$ (4x 0.4 ml). The solvent was removed to give the crude organic product (50 mg), which was a mixture of p-bromobenzoate esters and reagent (TLC). Preparative reverse phase HPLC (10% $H_2O$ in MeOH, then 18% $H_2O$ in MeOH) gave four fractions overall (1.2 mg, 0.8 mg, 5.2 mg, 2.4 mg), which were pure mycalamide B, mycalamide B 7-mono-p-bromobenzoate (**2.15**), mycalamide B 18-mono-p-bromobenzoate (**2.16**) and mycalamide B di-p-bromobenzoate (**2.17**), respectively.

**2.15**: an oil or white solid; $^1H$ NMR data in Table 2.4; HRFABMS *m/z* 738.1874 ($MK^+$, -2.4 ppm for $C_{32}H_{46}{}^{79}BrNO_{11}K$).

**2.16**: an oil or white solid; $^1H$ NMR data in Table 2.4, $^{13}C$ NMR data in Table 2.2 except the following p-bromobenzoate resonances, ($CDCl_3$) δ164.56

(18-OCO), 131.78, 131.14, 129.03 and 128.18 (18-$OCOC_6H_4Br$) ppm; HRFABMS *m/z* 722.2155 ($MNa^+$, +0.4 ppm for $C_{32}H_{46}{}^{79}BrNO_{11}Na$).

**2.17**: an oil or white solid; $^1H$ NMR data in Table 2.4, $^{13}C$ NMR data in Table 2.2 except the following p-bromobenzoate resonances, ($CDCl_3$) δ165.51, 164.71 (7- and 18-OCO), 131.91, 131.69, 131.41, 131.14, 129.16, 128.71, 128.15, 128.01 (7- and 18-$OCOC_6H_4Br$) ppm; HRFABMS *m/z* 852.1414 ($MH^+$-$CH_3OH$, -0.6 ppm for $C_{38}H_{46}{}^{79}Br^{81}BrNO_{11}$), DCIMS ($NH_3$) *m/z* (%) 872 (15), 871 (55), 870 (32), 869 (100, $MNH_4^+$-$CH_3OH$), 868 (16), 867 (51), 854 (17), 853 (8), 852 (52, $MH^+$-$CH_3OH$), 850 (18).

## 2.3.2 LARGE SCALE PREPARATION OF MYCALAMIDE B DI-P-BROMO-BENZOATE

Mycalamide B (19 mg), p-bromobenzoyl chloride (40 mg), dimethyl-aminopyridine (4 mg), and triethylamine (0.1 ml) were stirred in pyridine (0.5 ml) at 55°C for 1 day then at 70°C for 2 days. The solution was concentrated under nitrogen, then $H_2O$ (2 ml) was added and the mixture extracted with $CH_2Cl_2$ (4x 2 ml). The solvent was removed and the crude organic product then subjected to preparative silica gel TLC (developed in 2:1 PE:EtOAc). Two bands of silica were recovered and eluted with EtOAc, to give two fractions (6 mg, 15 mg), which were mycalamide B 18-mono-p-bromobenzoate (**2.16**) and pure mycalamide B di-p-bromobenzoate (**2.17**), respectively.

## 2.3.3 PREPARATION AND CHARACTERISATION OF ACETATE ESTERS

Mycalamide A (6.5 mg) was dissolved in pyridine (0.1 ml) and acetic anhydride (0.1 ml) and stirred at room temperature overnight. $H_2O$ (2 ml) was added and the mixture extracted with $CH_2Cl_2$ (3x 2 ml). The solvent was removed to give 8 mg of almost pure mycalamide A triacetate (**2.18**).

**2.18**: an oil; IR ($CHCl_3$) $\upsilon_{max}$ 3380, 2940, 2870, 1740, 1705, 1570, 1375, 1110, 1100, 1030 $cm^{-1}$, (film) $\upsilon_{max}$ 3370, 3070, 2954, 2925, 2855, 1741, 1678, 1588, 1522, 1463, 1368, 1230, 1145, 1034 $cm^{-1}$; $^1H$ and $^{13}C$ NMR data in Tables 2.7 and 2.2; HREIMS *m/z* 597.27536 ($M^+$-$CH_3OH$, -5.3 ppm for $C_{29}H_{43}NO_{12}$), DCIMS ($NH_3$) *m/z* (%) 647 (13, $MNH_4^+$), 617 (29), 616 (37), 615 (100, $MNH_4^+$-$CH_3OH$), 542 (35), 318 (42), 317 (44), 299 (30), 286 (58), 285 (41), 270 (28), 269 (60), 257 (30), DCIMS ($CH_4$) *m/z* (%) 598 (71, $MH^+$-$CH_3OH$), 538 (100, $MH^+$-$CH_3OH$-$CH_3CO_2H$), 299 (53), 269 (56), 240 (41), 208 (55).

Mycalamide A (3.7 mg) was dissolved in pyridine (0.1 ml) and acetic anhydride (0.1 ml) and stirred at room temperature for 4 hours. $H_2O$ (0.3 ml) was added and the mixture extracted with $CHCl_3$ (3x 0.3 ml). The solvent was removed and the crude organic product subjected to silica gel column chromatography (200 mg Davisil), developed in steps from PE to EtOAc. One fraction (0.7 mg) which eluted with EtOAc was a 1:1 mixture of mycalamide A triacetate (**2.18**) and, probably, mycalamide A 7,18-diacetate by $^1H$ NMR spectroscopy.

Mycalamide B (2.0 mg) was dissolved in pyridine (0.1 ml) and acetic anhydride (0.1 ml) and stirred at room temperature for 5 hours. $H_2O$ (0.5 ml) was added and the mixture extracted with $CHCl_3$ (3x 0.3 ml). The solvent was removed to give 2.5 mg of pure mycalamide B diacetate (**2.19**).

**2.19**: an oil; IR ($CHCl_3$) $\upsilon_{max}$ 3390, 2940, 2890, 1740, 1710, 1380, 1125, 1100, 1030, 910 $cm^{-1}$; $^1H$ and $^{13}C$ NMR data in Tables 2.8 and 2.9; HREIMS *m/z* 569.2848 ($M^+$-$CH_3OH$, +2.1 ppm for $C_{28}H_{43}NO_{11}$), HRFABMS *m/z* 624.2973 ($MNa^+$, -3.7 ppm for $C_{29}H_{47}NO_{12}Na$), DCIMS ($NH_3$) *m/z* (%) 619 (22, $MNH_4^+$), 589 (16), 588 (32), 587 (100, $MNH_4^+$-$CH_3OH$), 570 (25, $MH^+$-$CH_3OH$), 318 (19), 290 (25), 258 (62), 257 (26), 241 (45).

## 2.3.4 DEACETYLATION OF MYCALAMIDE A TRIACETATE AND MYCALAMIDE B DIACETATE

Mycalamide A triacetate (**2.18**, 0.5 mg) was stirred with potassium carbonate (0.2 mg) in 9:1 MeOH:$H_2O$ (0.2 ml) at room temperature for 2 hours. Silica gel TLC indicated complete hydrolysis to mycalamide A.

Mycalamide B diacetate (**2.19**, 2.2 mg) was stirred with potassium carbonate (0.3 mg) in 9:1 MeOH:$H_2O$ (0.3 ml) at room temperature for 12 hours. The solution was concentrated under nitrogen (to 0.1 ml), then $H_2O$ (0.5 ml) was added and the mixture extracted with $CH_2Cl_2$ (3x 0.4 ml). The solvent was removed to give 2 mg of about 90% mycalamide B by TLC and $^1H$ NMR spectroscopy, containing a small amount of a mycalamide B monoacetate.

Mycalamide B diacetate (**2.19**, 2.5 mg) was stirred with potassium carbonate (0.5 mg) in 9:1 MeOH:$H_2O$ (0.3 ml) at room temperature for 1 hour. $H_2O$ (2.5 ml) was added and the mixture extracted with $CH_2Cl_2$ (3x 2 ml). The solvent was removed and the crude organic products subjected to preparative silica gel TLC (developed in EtOAc). Two bands of silica were recovered ($R_f$=0.2 and 0.7) and eluted with 1:3 EtOH:EtOAc, to give two fractions (0.5 mg, 1.7 mg), which were pure mycalamide B and mycalamide B 18-monoacetate (**2.20**), respectively.

**2.20**: an oil; $^1H$ and $^{13}C$ NMR data in Tables 2.8 and 2.9; HREIMS *m/z* 527.2749 ($M^+$-$CH_3OH$, +3.6 ppm for $C_{26}H_{41}NO_{10}$), DCIMS ($NH_3$) *m/z* (%) 577 (1, $MNH_4^+$), 560 (1, $MH^+$), 547 (15), 546 (35), 545 (100, $MNH_4^+$-$CH_3OH$), 530 (16), 529 (27), 528 (88, $MH^+$-$CH_3OH$).

## 2.3.5 PREPARATION AND CHARACTERISATION OF MYCALAMIDE B 7-MONOACETATE

Mycalamide B 18-mono-TMS ether (**2.3**, 1.2 mg) was dissolved in pyridine (0.1 ml) and acetic anhydride (0.1 ml) and stirred for 3 hours at room temperature. $H_2O$ (0.4 ml) was added and the mixture extracted with $CH_2Cl_2$ (3x 0.3 ml). The solvent was removed to give the crude organic product (1.2 mg), which was a 3:1 mixture of mycalamide B 7-monoacetate (**2.21**) and mycalamide B diacetate (**2.19**) by TLC and $^1H$ NMR spectroscopy. This sample was then subjected to silica gel column chromatography (200 mg Davisil), developed in steps from PE to EtOAc. The major fraction (0.8 mg), which eluted with EtOAc, was pure mycalamide B 7-monoacetate (**2.21**).

**2.21**: an oil; $^1H$ and $^{13}C$ NMR data in Tables 2.8 and 2.9; HRFABMS *m/z* 528.2836 ($MH^+$-$CH_3OH$, +5.3 ppm for $C_{26}H_{42}NO_{10}$), DCIMS ($NH_3$) *m/z* (%) 577 (15, $MNH_4^+$), 547 (28), 546 (30), 545 (100, $MNH_4^+$-$CH_3OH$), 530 (10), 529 (11), 528 (34, $MH^+$-$CH_3OH$).

## 2.3.6 PREPARATION AND CHARACTERISATION OF OTHER ESTERS

Mycalamide A (2.8 mg) was dissolved in pyridine (0.1 ml) and propionic anhydride (0.1 ml) and stirred at room temperature overnight. $H_2O$ (0.4 ml) was added and the mixture extracted with $CHCl_3$ (3x 0.4 ml). The solvent was removed to give 3.7 mg of pure mycalamide A tripropanoate (**2.22**).

**2.22**: an oil; $^1H$ NMR data in Table 2.8, except the following propanoate resonances, ($CDCl_3$) δ2.50, 2.48 (7-$OCOCH_2$, 2xqd, 7.5, 16.5), 2.32 and 2.25 (17- and 18-$OCOCH_2$, 2xq, 7.5), 1.19, 1.12 and 1.07 (7-, 17- and 18-$OCOCH_2CH_3$), $^{13}C$ NMR data in Table 2.2, except the following propanoate resonances, ($CDCl_3$) δ173.95, 173.21 and 173.12 (7-, 17- and 18-OCO), 27.55, 27.46 and 27.34 (7-, 17- and 18-$OCOCH_2$), 9.11, 9.02 and 8.90 (7-, 17- and 18-$OCOCH_2CH_3$) ppm; HRFABMS *m/z* (%) 694.3356 ($MNa^+$,

-8.4 ppm for $C_{33}H_{53}NO_{13}Na$), DCIMS ($NH_3$) *m/z* (%) 689 (20, $MNH_4^+$), 657 (24, $MNH_4^+$-$CH_3OH$), 404 (23), 346 (52), 331 (44), 314 (28), 244 (85).

Mycalamide B (1.4 mg), methanesulphonyl chloride (1 µl) and triethylamine (3 µl) were stirred in pyridine (0.2 ml) at room temperature for 1 day, then at 40°C for 2 hours. The solution was concentrated under nitrogen (to 1 ml), then $H_2O$ (2 ml) was added and the mixture extracted with $CH_2Cl_2$ (3x 2 ml). The solvent was removed and the crude organic products subjected to preparative silica gel TLC (developed in EtOAc). Two bands of silica were recovered and eluted with 1:9 EtOH:EtOAc, to give two fractions (0.3 mg, 1.0 mg), which were mycalamide B and pure mycalamide B 18-monomesylate (**2.23**), respectively.

**2.23**: an oil; $^1H$ and $^{13}C$ NMR data in Tables 2.8 and 2.9; HRFABMS *m/z* 618.2576 ($MNa^+$, +2.6 ppm for $C_{26}H_{45}NO_{12}SNa$).

## 2.4.2 PREPARATION AND CHARACTERISATION OF *N,O*-METHYL DERIVATIVES

Mycalamide A (3 mg), powdered potassium hydroxide (3 mg) and methyl iodide (3 µl) were stirred in DMSO (0.2 ml) at room temperature for 4 hours. $H_2O$ (2 ml) was added and the mixture extracted with $CH_2Cl_2$ (3x 2 ml). The solvent was removed to give the crude organic product (3.5 mg), which was a mixture of at least two components (TLC). Preparative reverse phase HPLC (30% $H_2O$ in MeOH) gave two fractions (1.9 mg, 1 mg), which were pure 7-*O*-methyl, *N*-methyl mycalamide A (**2.24**) and a 4:1 mixture of 7,18-di-*O*-methyl, *N*-methyl mycalamide A (**2.25**) and 7,17-di-*O*-methyl, *N*-methyl mycalamide A (**2.27**), respectively.

**2.24**: an oil; $^1H$ and $^{13}C$ NMR data in Tables 2.10 and 2.11; HREIMS *m/z* 499.2798 ($M^+$-$CH_3OH$, +3.2 ppm for $C_{25}H_{41}NO_9$), DCIMS ($NH_3$) *m/z* (%) 549

(3, $MNH_4^+$), 519 (6), 518 (20), 517 (66, $MNH_4^+$-$CH_3OH$), 502 (10), 501 (29), 500 (100, $MH^+$-$CH_3OH$).

Mycalamide A (5.5 mg), powdered potassium hydroxide (14 mg) and methyl iodide (10 µl) were stirred in DMSO (0.3 ml) at room temperature for 3.5 hours. $H_2O$ was added (0.5 ml) and the mixture transferred onto a reverse phase pipette column (200 mg C18, equilibrated to $H_2O$), which was then flushed with $H_2O$ (6 ml) and eluted with MeOH (6 ml). The MeOH fraction was evaporated to dryness (5.5 mg), then subjected to preparative silica gel TLC (developed in EtOAc). Two bands of silica were recovered and eluted with 1:9 EtOH:EtOAc (4 ml) to give two fractions (1 mg, 3.5 mg), which were 7,18-di-*O*-methyl, *N*-methyl mycalamide A (**2.25**) and 7,17,18-tri-*O*-methyl, *N*-methyl mycalamide A (**2.26**), respectively.

**2.25**: an oil; $^1H$ and $^{13}C$ NMR data in Tables 2.10 and 2.11; HREIMS *m/z* 513.2928 ($M^+$-$CH_3OH$, -1.8 ppm for $C_{26}H_{43}NO_9$), DCIMS ($NH_3$) *m/z* (%) 563 (10, $MNH_4^+$), 533 (19), 532 (37), 531 (100, $MNH_4^+$-$CH_3OH$), 516 (17), 515 (32), 514 (95, $MH^+$-$CH_3OH$).

**2.26**: an oil; $^1H$ and $^{13}C$ NMR data in Tables 2.10 and 2.11; HREIMS *m/z* 527.3068 ($M^+$-$CH_3OH$, -5.1 ppm for $C_{27}H_{45}NO_9$), DCIMS ($NH_3$) *m/z* (%) 577 (1, $MNH_4^+$), 547 (4), 546 (6), 545 (19, $MNH_4^+$-$CH_3OH$), 531 (5), 530 (19), 529 (30), 528 (100, $MH^+$-$CH_3OH$).

Mycalamide B (2 mg), powdered potassium hydroxide (2 mg) and methyl iodide (2 µl) were stirred in DMSO (0.3 ml) at room temperature for 24 hours. $H_2O$ was added (0.5 ml) and the mixture extracted with $CH_2Cl_2$ (3x 0.3 ml). The solvent was removed to give the crude organic product (3 mg), which was a mixture of 2 components (TLC). Preparative reverse phase HPLC (30% $H_2O$ in MeOH) gave two fractions (1.2 mg, 0.6 mg), which were pure 7,17-di-*O*-methyl, *N*-methyl mycalamide A (**2.27**) and 7,17,18-tri-*O*-methyl, *N*-methyl mycalamide A (**2.26**), respectively.

**2.27**: an oil; $^{1}H$ and $^{13}C$ NMR data in Tables 2.10 and 2.11; HREIMS *m/z* 513.2945 ($M^{+}$-$CH_3OH$, +1.4 ppm for $C_{26}H_{43}NO_9$), DCIMS ($NH_3$) *m/z* (%) 563 (2, $MNH_4^{+}$), 533 (9), 531 (34, $MNH_4^{+}$-$CH_3OH$), 516 (25), 514 (100, $MH^{+}$-$CH_3OH$).

## 2.4.3 CONFORMATIONAL EXCHANGE OF 7,17,18-TRI-*O*-METHYL, *N*-METHYL MYCALAMIDE A

**2.26**: $^{1}H$ NMR data at 6°C, ($CDCl_3$) δ6.27 (H10, d, 9.8), 5.15 (10-OCH*R*, d, 6.7), 4.85 (10-OCH*S*, d, 6.7), 4.82 (4=CH*Z*, t, 1.9), 4.70 (4=CH*E*, t, 1.9), 4.26 (H7, s), 4.26 (H12, dd, 7.1, 10.4), 4.16 (H11, dd, 7.2, 9.9), 3.91 (H2, dq, 2.6, 6.5), 3.55 (13-$OCH_3$, s), 3.49 (H13, d, 10.5), 3.43 (7-$OCH_3$, s), 3.38 (H15, m), 3.29 (6-$OCH_3$, s), 3.20 (*N*-$CH_3$, s), 2.61 (H5a, dd, 1.9, 14.4), 2.26 (H5e, d, 14.4), 2.18 (H3, dq, 2.6, 7.1), 1.68 (H16, ddd, 1.1, 10.1, 14.0), 1.47 (H16, ddd, 3.3, 9.6, 14.0), 1.11 (2-$CH_3$, d, 6.6), 0.96 (14-$CH_3$*R*, s), 0.95 (3-$CH_3$, d, 7.0), 0.86 (14-$CH_3$*S*, s) ppm.

## 2.4.4 FURTHER METHYLATED DERIVATIVES

Mycalamide A (4 mg), powdered potassium hydroxide (7.2 mg) and methyl iodide (5 µl) were stirred in DMSO (0.3 ml) at room temperature for 20 hours, then at 40°C for 4 hours. $H_2O$ (0.5 ml) was added and the mixture transferred onto a reverse phase pipette column (200 mg C18, equilibrated to $H_2O$), which was then flushed with $H_2O$ (6 ml) and eluted with MeOH (6 ml). The MeOH fraction was evaporated to dryness (4.3 mg), then subjected to preparative silica gel TLC (developed in EtOAc). Three bands of silica were recovered and eluted with 1:9 EtOH:EtOAc (4 ml) to give three fractions (0.5 mg, 1.5 mg, 1 mg), which were 7,18-di-*O*-methyl, *N*-methyl mycalamide A (**2.25**), 7,17,18-tri-*O*-methyl, *N*-methyl mycalamide A (**2.26**) and 7*S*,17,18-tri-*O*-methyl, *N*-methyl mycalamide A (**2.28**), respectively.

**2.28**: an oil; $^{1}H$ and $^{13}C$ NMR data in Tables 2.10 and 2.11; HREIMS *m/z* 527.3078 ($M^{+}$-$CH_3OH$, -3.0 ppm for $C_{27}H_{45}NO_9$), DCIMS ($NH_3$) *m/z* (%) 577 (8, $MNH_4^{+}$), 547 (15), 546 (30), 545 (88, $MNH_4^{+}$-$CH_3OH$), 530 (19), 529 (37), 528 (100, $MH^{+}$-$CH_3OH$).

7,17-Di-*O*-methyl, *N*-methyl mycalamide A (**2.27**, 1.2 mg) was dissolved in a solution of sodium methoxide in MeOH (1M, 0.3 ml) and stirred at 90°C for three days. The solvent was removed and the residue partitioned in 1:1 $H_2O$:$CHCl_3$ (4 ml) and extracted in $CHCl_3$ (3x 1 ml). The solvent was removed and the crude organic product then subjected to silica gel column chromatography (200 mg Davisil), developed in steps from PE to EtOH/EtOAc. The major fraction (0.9 mg), which eluted with 1:19 EtOH:EtOAc, was a 1:3 mixture of starting material and its epimer at C7 by $^{1}H$ NMR spectroscopy. Further mixtures of the two epimers were combined (2 mg), reacted as above, then subjected to preparative silica gel TLC (developed twice in EtOAc). Two bands of silica were recovered and eluted with ethyl acetate to give two fractions (0.6 mg, 1.2 mg), which were 7,17-di-*O*-methyl, *N*-methyl mycalamide A (**2.27**) and 7*S*,17-di-*O*-methyl, *N*-methyl mycalamide A (**2.29**), respectively. **2.29**: an oil; $^{1}H$ and $^{13}C$ NMR data in Tables 2.10 and 2.11; HREIMS *m/z* 513.2960 ($M^{+}$-$CH_3OH$, +4.3 ppm for $C_{26}H_{43}NO_9$), DCIMS ($NH_3$) *m/z* (%) 563 (3, $MNH_4^{+}$), 533 (5), 532 (13), 531 (45, $MNH_4^{+}$-$CH_3OH$), 516 (14), 515 (28), 514 (100, $MH^{+}$-$CH_3OH$).

7-*O*-Methyl, *N*-methyl mycalamide A (**2.24**, 1.2mg) was dissolved in a solution of $NaOCD_3$ in $CD_3OD$ (3M, 0.3 ml) and stirred at 70°C for 2 days. The crude mixture was then subjected directly to preparative silica gel TLC (developed twice in 1:19 EtOH:EtOAc). Two bands of silica were recovered and eluted with 1:3 EtOH:EtOAc to give two fractions (0.4 mg, 0.7 mg), where the second (major) fraction was pure 7-deutero, 7*S*-*O*-Methyl, *N*-methyl mycalamide A (**2.30**).

**2.30**: an oil; $^1$H NMR data in Table 2.10; HREIMS *m/z* 500.2834 ($M^+$-$CH_3OH$, -2.0 ppm for $C_{25}H_{40}DNO_9$), DCIMS ($NH_3$) *m/z* (%) 550 (3, $MNH_4^+$), 520 (10), 518 (61, $MNH_4^+$-$CH_3OH$), 503 (23), 502 (9), 501 (100, $MH^+$-$CH_3OH$).

Mycalamide A (1.8 mg), anhydrous barium oxide (20 mg) and methyl iodide (6 µl) were stirred in DMSO (0.3 ml) at 60°C for 40 minutes. $H_2O$ (0.5 ml) was added and the mixture transferred onto a reverse phase pipette column (200 mg C18, equilibrated to $H_2O$), which was then flushed with $H_2O$ (6 ml) and eluted with MeOH (6 ml). The MeOH fraction was evaporated to dryness to give the crude organic product (1.5 mg) which was 7,17,18-tri-*O*-methyl, *N*-methyl mycalamide A (**2.26**) by TLC and $^1$H NMR spectroscopy.

Mycalamide B (1.1 mg), powdered potassium hydroxide (2 mg) and methyl iodide (0.8 µl) were stirred in DMSO (0.3 ml) at room temperature for 7 hours. $H_2O$ (0.4 ml) was added and the mixture extracted with $CH_2Cl_2$ (3x 0.3 ml). The solvent was removed to give the crude organic product (1.1 mg), which was a mixture of at least 2 components (TLC and $^1$H NMR spectroscopy). Preparative reverse phase HPLC (40% $H_2O$ in MeOH) gave two fractions (0.5 mg, 0.5 mg), where the first was possibly 7,17-di-*O*-methyl mycalamide A (**2.33**) and the second was pure 7,17-di-*O*-methyl, *N*-methyl mycalamide A (**2.27**) by $^1$H NMR spectroscopy.

### 2.4.5 PREPARATION AND CHARACTERISATION OF *O*-METHYL DERIVATIVES USING SILVER(I) OXIDE IN BENZENE

Mycalamide A (4.2 mg), silver(I) oxide (25 mg) and methyl iodide (8 µl) were stirred in benzene (0.3 ml) at 80°C for 3 days. The solution was then filtered over celite and the solvent removed to give the crude organic product (4.6 mg). Preparative silica gel TLC (developed in EtOAc) gave three fractions (0.5 mg, 1.2 mg, 2.0 mg), which were 7,17-di-*O*-methyl mycalamide A (**2.33**),

7,18-di-*O*-methyl mycalamide A (**2.32**) and 7,17,18-tri-*O*-methyl mycalamide A (**2.31**), respectively. (These were individually rechromatographed by preparative silica gel TLC to give the pure compounds).

**2.31**: an oil; $^{1}H$ and $^{13}C$ NMR data in Tables 2.12 and 2.14; HREIMS *m/z* 513.2916 ($M^{+}$-$CH_3OH$, -4.3 ppm for $C_{26}H_{43}NO_9$), DCIMS ($NH_3$) *m/z* (%) 563 (10, $MNH_4^{+}$), 533 (18), 532 (37), 531 (100, $MNH_4^{+}$-$CH_3OH$), 516 (11), 515 (22), 514 (74, $MH^{+}$-$CH_3OH$).

**2.32**: an oil; $^{1}H$ and $^{13}C$ NMR data in Tables 2.12 and 2.14; HREIMS *m/z* 499.2779 ($M^{+}$-$CH_3OH$, -0.6 ppm for $C_{25}H_{41}NO_9$), DCIMS ($NH_3$) *m/z* (%) 549 (7, $MNH_4^{+}$), 519 (22), 518 (30), 517 (100, $MNH_4^{+}$-$CH_3OH$), 502 (11), 501 (16), 500 (53, $MH^{+}$-$CH_3OH$).

Mycalamide A (7 mg), silver(I) oxide (55 mg) and methyl iodide (9 µl) were stirred in benzene (0.4 ml) in a sealed vial at 95°C for 1.5 hours. The solution was then filtered over celite and the solvent removed to give the crude organic product (7.3 mg). Preparative silica gel TLC (developed twice in 1:7 PE:EtOAc) gave four fractions (0.8 mg, 1.4 mg, 2.0 mg, 2.8 mg), which were mycalamide A, 7-*O*-methyl mycalamide A (**2.34**), 3:2 17-*O*-methyl mycalamide A:18-*O*-methyl mycalamide A (**2.35**), and pure 18-*O*-methyl mycalamide A (**2.35**), respectively. Subsequently, 7-*O*-methyl mycalamide A (**2.34**) was subjected to further preparative silica gel TLC (developed 3 times in 1:5 PE:EtOAc) to give the pure compound (1.2 mg).

**2.34**: an oil; $^{1}H$ and $^{13}C$ NMR data in Tables 2.12 and 2.14; HREIMS *m/z* 485.2618 ($M^{+}$-$CH_3OH$, -1.4 ppm for $C_{24}H_{39}NO_9$), DCIMS ($NH_3$) *m/z* (%) 535 (10, $MNH_4^{+}$), 505 (28), 504 (28), 503 (100, $MNH_4^{+}$-$CH_3OH$), 488 (12), 487 (9), 486 (30, $MH^{+}$-$CH_3OH$).

**2.35**: an oil; $^{1}H$ and $^{13}C$ NMR data in Tables 2.12 and 2.14; HREIMS *m/z* 485.2617 ($M^{+}$-$CH_3OH$, -1.6 ppm for $C_{24}H_{39}NO_9$), DCIMS ($NH_3$) *m/z* (%) 535

(16, $MNH_4^+$), 505 (24), 504 (33), 503 (100, $MNH_4^+$-$CH_3OH$), 487 (19), 486 (66, $MH^+$-$CH_3OH$).

Mycalamide B (6 mg), silver(I) oxide (40 mg) and methyl iodide (12 µl) were stirred in benzene (0.4 ml) in a sealed vial at 90°C for 2 hours. The solution was then filtered over celite and the solvent removed to give the crude organic product. Pyridine (0.1 ml) and acetic anhydride (0.1 ml) were added and the mixture stirred at room temperature for 16 hours. $H_2O$ (2.5 ml) was added and the mixture extracted with $CH_2Cl_2$ (3x 2 ml). The solvent was removed and the product subjected to preparative silica gel TLC (developed in 3:1 EtOAc:PE) to give three fractions (1.7 mg, 2.0 mg, 2.4 mg), which were pure 7,17-di-*O*-methyl mycalamide A 18-monoacetate (**2.37**), 17,18-di-*O*-methyl mycalamide A 7-monoacetate (**2.36**), and mycalamide B diacetate (**2.19**), respectively.

**2.36**: an oil; $^1H$ and $^{13}C$ NMR data in Tables 2.8 and 2.9; HREIMS *m/z* 541.2866 ($M^+$-$CH_3OH$, -3.9 ppm for $C_{27}H_{43}NO_{10}$), DCIMS ($NH_3$) *m/z* (%) 592 (10), 591 (32, $MNH_4^+$), 561 (26), 560 (33), 559 (100, $MNH_4^+$-$CH_3OH$), 544 (10), 543 (14), 542 (43, $MH^+$-$CH_3OH$).

**2.37**: an oil; $^1H$ and $^{13}C$ NMR data in Tables 2.8 and 2.9; HREIMS *m/z* 541.2881 ($M^+$-$CH_3OH$, -1.1 ppm for $C_{27}H_{43}NO_{10}$), DCIMS ($NH_3$) *m/z* (%) 591 (2, $MNH_4^+$), 562 (9), 561 (34), 560 (32), 559 (100, $MNH_4^+$-$CH_3OH$), 545 (11), 544 (36), 543 (30), 542 (99, $MH^+$-$CH_3OH$).

7,17-Di-*O*-methyl mycalamide A 18-monoacetate (**2.37**, 1.8 mg) was stirred with potassium carbonate (1.2 mg) in 9:1 MeOH:$H_2O$ (0.4 ml) at room temperature for 5 hours. The solution was concentrated under nitrogen (to 0.1 ml), then $H_2O$ (2.5 ml) was added and the mixture extracted with $CH_2Cl_2$ (3x 2 ml). The solvent was removed and the crude organic product then subjected to preparative silica gel TLC (developed twice in 1:5 PE:EtOAc) to give 1.2 mg of pure 7,17-di-*O*-methyl mycalamide A (**2.33**).

**2.33**: an oil; $^{1}H$ and $^{13}C$ NMR data in Tables 2.12 and 2.14; HREIMS *m/z* 499.2794 ($M^{+}$-$CH_3OH$, +2.6 ppm for $C_{25}H_{41}NO_9$), DCIMS ($NH_3$) *m/z* (%) 549 (6, $MNH_4^{+}$), 520 (4), 519 (20), 518 (40), 517 (100, $MNH_4^{+}$-$CH_3OH$), 502 (13), 501 (29), 500 (79, $MH^{+}$-$CH_3OH$).

17,18-Di-*O*-methyl mycalamide A 7-monoacetate (**2.36**, 2 mg) was stirred with potassium carbonate (0.4 mg) in 9:1 MeOH:$H_2O$ (0.4 ml) at room temperature for 1.5 hours. The solution was concentrated under nitrogen (to 0.1 ml), then $H_2O$ (2.5 ml) was added and the mixture extracted with $CH_2Cl_2$ (3x 2 ml). The solvent was removed to give 1.8 mg of pure 17,18-di-*O*-methyl mycalamide A (**2.38**).

**2.38**: an oil; $^{1}H$ and $^{13}C$ NMR data in Tables 2.12 and 2.14; HREIMS *m/z* 499.2773 ($M^{+}$-$CH_3OH$, -0.8 ppm for $C_{25}H_{41}NO_9$), DCIMS ($NH_3$) *m/z* (%) 549 (7, $MNH_4^{+}$), 520 (6), 519 (23), 518 (29), 517 (99, $MNH_4^{+}$-$CH_3OH$), 503 (5), 502 (19), 501 (29), 500 (100, $MH^{+}$-$CH_3OH$).

## 2.5.1-2.5.2 PREPARATION AND CHARACTERISATION OF BENZYL DERIVATIVES

Mycalamide A (5 mg), powdered potassium hydroxide (8 mg) and benzyl bromide (12 µl) were stirred in DMSO (0.3 ml) at room temperature for 3 minutes. $H_2O$ (2 ml) was added and the mixture extracted with $CH_2Cl_2$ (3x 2 ml). The solvent was removed to give the crude organic product (7.5 mg), which was a mixture of at least 4 components (TLC, HPLC). Preparative reverse phase HPLC (15% $H_2O$ in MeOH) gave four fractions (1 mg, 0.7 mg, 2 mg, 2 mg) but the third fraction was a mixture of the second component and another component (TLC). Preparative silica gel TLC (developed in 1:1 PE:EtOAc) and an appropriate combination of samples gave overall four pure products (1 mg, 1.3 mg, 1 mg, 2 mg), which were 7-*O*-benzyl mycalamide A (**2.39**), 7,18-di-*O*-benzyl mycalamide A (**2.40**), 7-*O*-benzyl, *N*-benzyl

mycalamide A (**2.41**) and 7,18-di-*O*-benzyl *N*-benzyl mycalamide A (**2.42**), respectively.

**2.39**: an oil; $^1$H NMR data in Table 2.15, $^{13}$C NMR data in Table 2.16 except the following aromatic resonances, ($CDCl_3$) δ128.55, 128.38 and 128.19 ppm; HREIMS *m/z* 561.2919 ($M^+$-$CH_3OH$, -3.4 ppm for $C_{30}H_{43}NO_9$), DCIMS ($NH_3$) *m/z* (%) 611 (7, $MNH_4^+$), 582 (8), 581 (26), 580 (34), 579 (100, $MNH_4^+$-$CH_3OH$), 564 (5), 563 (6), 562 (17, $MH^+$-$CH_3OH$).

**2.40**: an oil; $^1$H NMR data in Table 2.15, $^{13}$C NMR data in Table 2.16 except the following aromatic resonances, ($CDCl_3$) δ138.36, 137.15, 128.46, 128.41, 128.34, 128.07, 127.64 and 127.53 ppm; HRFABMS *m/z* 652.3510 ($MH^+$-$CH_3OH$, +3.7 ppm for $C_{37}H_{50}NO_9$), DCIMS ($NH_3$) *m/z* (%) 703 (7), 702 (12), 701 (28, $MNH_4^+$), 672 (9), 671 (27), 670 (41), 669 (100, $MNH_4^+$-$CH_3OH$), 654 (5), 653 (8), 652 (19, $MH^+$-$CH_3OH$).

**2.41**: an oil; $^1$H NMR data in Table 2.15; HRFABMS *m/z* 652.3486 ($MH^+$-$CH_3OH$, +2.8 ppm for $C_{37}H_{50}NO_9$), DCIMS ($NH_3$) *m/z* (%) 701 (12, $MNH_4^+$), 672 (17), 671 (46), 670 (44), 669 (100, $MNH_4^+$-$CH_3OH$), 654 (19), 653 (20), 652 (45, $MH^+$-$CH_3OH$).

**2.42**: an oil; $^1$H NMR data in Table 2.15, $^{13}$C NMR data in Table 2.16 except the following aromatic resonances, ($CDCl_3$) δ138.45, 128.68, 128.32, 128.15, 127.70, 127.60, 127.48, 127.35 and 126.95 ppm; HRFABMS *m/z* 742.3991 ($MH^+$-$CH_3OH$, +4.8 ppm for $C_{44}H_{56}NO_9$), DCIMS ($NH_3$) *m/z* (%) 791 (8, $MNH_4^+$), 761 (19), 760 (49), 759 (100, $MNH_4^+$-$CH_3OH$), 743 (13), 742 (24, $MH^+$-$CH_3OH$).

Mycalamide B (4.4 mg), powdered potassium hydroxide (7 mg) and benzyl bromide (8 μl) were stirred in DMSO (0.3 ml) at room temperature for 4 minutes. $H_2O$ (2 ml) was added and the mixture extracted with $CHCl_3$ (3x 2 ml). The solvent was removed and the crude organic product subjected to preparative silica gel TLC (developed in 1:1 PE:EtOAc). Three bands of silica

were recovered and eluted with EtOAc to give three fractions (1.8 mg, 0.8 mg, 0.9 mg), which were 7-*O*-benzyl mycalamide B (**2.43**), 7-*O*-benzyl, *N*-benzyl mycalamide B (**2.45**) and 7,18-di-*O*-benzyl mycalamide B (**2.44**), respectively.

**2.43**: an oil; $^{1}H$ NMR data in Table 2.17, $^{13}C$ NMR data in Table 2.16 except the following aromatic resonances, ($CDCl_3$) δ136.98, 128.57, 128.24 and 128.20 ppm; HRFABMS *m/z* 630.3202 ($MNa^+$, -8.3 ppm for $C_{32}H_{49}NO_{10}Na$), FABMS *m/z* (%) 631 (9), 630 (100, $MNa^+$), 598 (7, $MNa^+$-$CH_3OH$), 577 (8), 576 (20, $MH^+$-$CH_3OH$).

**2.44**: an oil; $^{1}H$ NMR data in Table 2.17, $^{13}C$ NMR data in Table 2.16 except the following aromatic resonances, ($CDCl_3$) δ138.58, 137.06, 128.51, 128.28, 128.10, 127.79 and 127.39 ppm; HRFABMS *m/z* 666.3647 ($MH^+$-$CH_3OH$, +0.8 ppm for $C_{38}H_{52}NO_9$), DCIMS ($NH_3$) *m/z* (%) 716 (9), 715 (19, $MNH_4^+$), 686 (10), 685 (28), 684 (45), 683 (100, $MNH_4^+$-$CH_3OH$), 668 (10), 667 (16), 666 (36, $MH^+$-$CH_3OH$).

**2.45**: an oil; $^{1}H$ NMR data in Table 2.17; HRFABMS *m/z* 666.3612 ($MH^+$-$CH_3OH$, -4.5 ppm for $C_{38}H_{52}NO_9$), DCIMS ($NH_3$) *m/z* (%) 715 (9, $MNH_4^+$), 686 (13), 685 (33), 684 (45), 683 (100, $MNH_4^+$-$CH_3OH$), 668 (22), 667 (27), 666 (63, $MH^+$-$CH_3OH$).

Mycalamide B (7 mg), powdered potassium hydroxide (22 mg) and benzyl bromide (26 μl) were stirred in DMSO (0.3 ml) at room temperature for 3 hours. $H_2O$ (2 ml) was added and the mixture transferred onto a reverse phase pipette column (200 mg C18, equilibrated to $H_2O$), which was then flushed with $H_2O$ (8 ml) and eluted with MeOH (6 ml). The MeOH fraction was evaporated to dryness, then subjected to preparative silica gel TLC (developed in 5:2 PE:EtOAc). Two bands of silica ($R_f$=0.6, 0.7) were recovered and eluted with EtOAc to give two fractions (2.2 mg, 5.2 mg), which were

7,8,18-tri-*O*-benzyl mycalamide B (**2.47**) and 7,18-di-*O*-benzyl, *N*-benzyl mycalamide B (**2.46**), respectively.

**2.46**: an oil; IR ($CHCl_3$) $\upsilon_{max}$ 3064, 3029, 2965, 2929, 2879, 2855, 1660, 1454, 1379, 1104, 1043, 1030 $cm^{-1}$; $^1H$ NMR data in Table 2.17, $^{13}C$ NMR data in Table 2.16 except the following aromatic resonances, ($CDCl_3$) δ139.01, 138.30, 138.17, 128.63, 128.28, 128.14, 127.88, 127.51, 127.26 and 126.67 ppm; HRFABMS *m/z* 756.4136 ($MH^+$-$CH_3OH$, +3.2 ppm for $C_{45}H_{58}NO_9$), DCIMS ($NH_3$) *m/z* (%) 805 (17, $MNH_4^+$), 775 (22), 774 (49), 773 (100, $MNH_4^+$-$CH_3OH$), 758 (8), 757 (18), 756 (35, $MH^+$-$CH_3OH$).

**2.47**: an oil; IR ($CHCl_3$) $\upsilon_{max}$ 3064, 3030, 2930, 2877, 1725, 1665, 1454, 1378, 1255, 1120, 1100, 1041, 1028, 997 $cm^{-1}$; $^1H$ NMR data in Table 2.17, $^{13}C$ NMR data in Table 2.16 except the following aromatic resonances, ($CDCl_3$) δ128.41, 128.34, 128.25, 128.01, 127.87, 127.69, 127.56 and 127.31 ppm; HRFABMS *m/z* 810.4231 ($MNa^+$, +4.7 ppm for $C_{46}H_{61}NO_{10}Na$), FABMS *m/z* (%) 826 (5, $MK^+$), 812 (8), 811 (25), 810 (48, $MNa^+$), 788 (5, $MH^+$) 757 (5), 756 (9, $MH^+$-$CH_3OH$).

## 2.5.2 CONFORMATIONAL EXCHANGE OF 7,18-DI-*O*-BENZYL, *N*-BENZYL MYCALAMIDE B

**2.46**: $^1H$ NMR data at -10°C, ($CDCl_3$) δ6.17 (H10, d, 8.2), 5.17 (10-OCH*R*, d, 6.6), 5.11 (*N*-CHPh, d, 17.6), 4.88 (10-OCH*S*, d, 6.6), 4.78 (4=CH*Z*, m), 4.66 (4=CH*E*, m), 4.63 (*N*-CHPh, d, 17.5), 4.56 (18-$OCH_2$Ph, s), 4.36 (7-OCHPh, d, 11.8), 4.24 (H12, dd, 6.9, 9.2), 4.19 (H7, s), 4.03 (H11, dd, 6.9, 8.3), 3.86 (H2, dq, 2.4, 6.4), 3.82 (7-OCHPh, d, 11.6), 3.75 (H18, dd, 1.3, 10.6), 3.58 (H18, dd, 2.3, 10.6), 3.52 (13-$OCH_3$, s), 3.45 (13'-$OCH_3$, s), 3.35 (17'-$OCH_3$, s), 3.32 (H13, d, 9.4), 3.26 (17-$OCH_3$, s), 3.17 (6'-$OCH_3$, s), 3.10 (H13', d, 9.8), 2.82 (6-$OCH_3$, s), 2.80 (H5a, d, 14.7), 2.38 (H5e', d, 14.8), 2.27 (H5e, d, 14.7), 2.17 (H3, dq, 2.4, 7.0), 1.90 (H16, m), 1.57 (H16, m), 1.15 (2-$CH_3$, d, 6.5), 1.09

(2'-$CH_3$, d, 6.5), 0.97 (3-$CH_3$, d, 7.0), 0.96 (14-$CH_3$*R*, s), 0.87 (3'-$CH_3$, d, 7.0), 0.84 (14-$CH_3$*S*, s), 0.83 (14'-$CH_3$*S*, s) ppm.

### 2.5.3 FURTHER ALKYLATIONS - REACTION OF MYCALAMIDE A WITH DDQ AND TRITYLATION ATTEMPTS

Mycalamide A (1 mg) was dissolved in $CDCl_3$ (0.6 ml), containing 0.1% pyridine, and placed in an NMR sample tube. 2,3-Dichloro-5,6-dicyanobenzoquinone (DDQ, 2 mg) was added and the sample monitored by $^1H$ NMR spectroscopy. Slow decomposition was observed over a period of several hours at room temperature.

Mycalamide A (1.9 mg), trityl chloride (4 mg), dimethylaminopyridine (0.1 mg) and triethylamine (2.5 µl) were stirred at room temperature for 24 hours. $H_2O$ (0.4 ml) was added and the mixture extracted with $CHCl_3$ (3x 0.4 ml). The solvent was removed to give the crude organic product but TLC and $^1H$ NMR spectroscopy indicated that substantial decomposition had occurred.

The reaction was repeated, but this time, after 1 day, no reaction was observed by TLC. A third reaction with pyridine as solvent also gave some decomposition but no other apparent reaction, and the use of DMF as solvent was equally unsuccessful.

## WORK DESCRIBED IN CHAPTER 3

### 3.2 ACID CATALYSED DECOMPOSITIONS

### 3.2.2 REACTIONS MONITORED BY HPLC

Mycalamide A (0.5 mg) was reacted with a solution of hydrochloric acid in 90% $H_2O$:MeOH (0.1M, 0.5 ml) at room temperature, monitoring by reverse

phase HPLC. After 4 hours there was a mixture of a more polar derivative (major) and unreacted mycalamide A.

This reaction was repeated on a larger scale (10-fold) for 1 hour, then dilute sodium hydroxide was added (until neutralised) and the solvent removed. The residue was extracted in $CHCl_3$, filtered over celite and the solvent removed, to give a mixture of pederolactone (**3.6**), mycalamide A and decomposition products ($^1$H NMR spectroscopy). This was subjected to silica gel column chromatography (200 mg Davisil), developed in steps from PE to EtOH/EtOAc. One fraction (1 mg), which eluted with 1:1 PE:EtOAc, was a crude sample of pederolactone (**3.6**), essentially free from mycalamide A, but with other alkyl impurities. Pederolactone could not be recovered from further silica gel column chromatography or preparative reverse phase HPLC.

**3.6**: an oil; FTIR (film) $\upsilon_{max}$ 2956, 2926, 2853, 1720, 1645, 1461, 1377, 1260, 1166, 1096, 1072, 1031 $cm^{-1}$; $^1$H NMR ($CDCl_3$) δ5.74 (H5, q, 1.5), 4.54 (H2, dq, 3.1, 6.6), 2.08 (H3, dq, 3.2, 7.2), 1.98 (4-$CH_3$, d, 1.5), 1.35 (2-$CH_3$, d, 6.6), 1.06 (3-$CH_3$, d, 7.2) ppm.

### 3.3.1 PREPARATION AND CHARACTERISATION OF PSEUDO-MYCALAMIDES A AND B

Mycalamide A (2.7 mg) was dissolved in $CH_2Cl_2$ (0.2 ml) and stirred with an aqueous solution of p-toluene sulphonic acid (0.05M, 0.2 ml) at room temperature for 4 hours. $H_2O$ (2 ml) was added and the mixture neutralised with dilute sodium hydroxide then extracted with $CH_2Cl_2$ (3x 2 ml). The solvent was removed to give 2.3 mg of pure pseudomycalamide A (**3.7**).

**3.7**: an oil; $^1$H and $^{13}$C NMR data in Tables 3.1 and 3.2; HREIMS *m/z* 471.2477 ($M^+$-$H_2O$, +1.9 ppm for $C_{23}H_{37}NO_9$), HRFABMS *m/z* 472.2560 ($MH^+$-$H_2O$, +2.8 ppm for $C_{23}H_{38}NO_9$), DCIMS ($NH_3$) *m/z* (%) 508 (27), 507

(100, $MNH_4^+$), 491 (34), 490 (26), 489 (72, $MNH_4^+$-$H_2O$), 474 (14), 473 (29), 472 (90, $MH^+$-$H_2O$).

Mycalamide B (5.5 mg) was dissolved in $CH_2Cl_2$ (0.5 ml) and stirred with an aqueous solution of p-toluene sulphonic acid (0.05M, 0.2 ml) at room temperature for 48 hours. The aqueous layer was removed and the organic layer washed with $H_2O$ (3x 0.3 ml). The mixture was then extracted with $CH_2Cl_2$ (3x 0.3 ml) and the solvent removed to give 5.1 mg of 90% pure pseudomycalamide B (**3.8**), containing a small amount of mycalamide B. Preparative reverse phase HPLC (20% $H_2O$ in MeOH) on a 1.2 mg subsample gave 0.9 mg of pseudomycalamide B (**3.8**).

**3.8**: an oil; $^1H$ and $^{13}C$ NMR data in Tables 3.1 and 3.2; HREIMS *m/z* 485.2614 ($M^+$-$H_2O$, -2.3 ppm for $C_{24}H_{39}NO_9$ ), HRFABMS *m/z* 486.2717 ($MH^+$-$H_2O$, +2.9 ppm for $C_{24}H_{40}NO_9$ ), DCIMS ($NH_3$) *m/z* (%) 522 (20), 521 (64, $MNH_4^+$), 504 (51, $MH^+$), 503 (72, $MNH_4^+$-$H_2O$), 487 (42), 486 (100, $MH^+$-$H_2O$).

### 3.3.5 REARRANGEMENT AND DECOMPOSITION OF PSEUDO-MYCALAMIDES

A sample of crude pseudomycalamide B (**3.8**, 3 mg), which had been in cold storage for several months, was found to contain a new component by TLC, so it was subjected to preparative silica gel TLC (developed twice in 1:9 PE:EtOAc). Three bands of silica were recovered and eluted with 1:4 EtOH:EtOAc to give three fractions (0.4 mg, 1.1 mg, 1.2 mg), which were mycalamide B and two identical mixtures of pseudomycalamide B (**3.8**) and, possibly, a C6 epimer of pseudomycalamide B.

### 3.3.6 METHANOLYSIS OF PSEUDOMYCALAMIDES A AND B

Pseudomycalamide A (**3.7**, 0.1 mg) was stirred with a solution of p-toluene sulphonic acid in methanol ($5x10^{-4}$M, 0.1 ml) at room temperature, monitoring by reverse phase HPLC. After 1 day, HPLC showed that there was no pseudomycalamide A present, but there was a single peak at the retention time of mycalamide A.

Pseudomycalamide B (**3.8**, 0.5 mg) was reacted under analogous conditions for 4 hours to give pure mycalamide B (TLC, HPLC).

### 3.4 1-3.4.3 ALKOXY EXCHANGE REACTIONS AT C6

Mycalamide A (1.1 mg) was reacted with a solution of trifluoroacetic acid in $CD_3OD$ (0.01M, 0.6 ml) in an NMR sample tube at room temperature overnight, to give almost pure 6-trideuteromethoxy mycalamide A (**3.9**).

**3.9**: an oil; HRFABMS *m/z* 529.2808 ($MNa^+$, -1.6 ppm for $C_{24}H_{38}D_3NO_{10}Na$), DCIMS ($NH_3$) *m/z* (%) 524 (16, $MNH_4^+$), 491 (14), 490 (22), 489 (81, $MNH_4^+$-$CD_3OH$), 472 (16, $MH^+$-$CD_3OH$), 278 (16), 245 (19), 244 (96).

Mycalamide A (1.3 mg) was stirred with a solution of trifluoroacetic acid in ethanol (0.01M, 0.5 ml) at room temperature overnight. The solution was neutralised and the solvent removed to give the crude organic product, which was a mixture of pseudomycalamide A (**3.7**), 6-ethoxy mycalamide A (**3.10**) and mycalamide A.

Mycalamide A (3.3 mg) was stirred with a solution of pyridinium p-toluene sulphonate in dry ethanol ($1x10^{-3}$M, 0.3 ml, dried over molecular sieves) at room temperature for 4 days. The solution was concentrated under nitrogen (to 0.1 ml), then dilute sodium hydroxide was added (2 ml, pH~9) and the mixture extracted in $CH_2Cl_2$ (3x 2 ml). The solvent was removed to give the crude organic product (3.2 mg), which was a mixture of unreacted mycalamide A and a less polar product (TLC, HPLC). Preparative reverse

phase HPLC (40% $H_2O$ in MeOH) gave two major fractions (1 mg, 2 mg), which were mycalamide A and 6-ethoxy mycalamide A (**3.10**) respectively. **3.10**: an oil; $^1H$ and $^{13}C$ NMR data in Tables 3.1 and 3.2; HRFABMS *m/z* 540.2785 ($MNa^+$, 0.0 ppm for $C_{25}H_{43}NO_{10}Na$), 472.2525 ($MH^+$-$CH_3CH_2OH$, -4.4 ppm for $C_{23}H_{38}NO_9$), DCIMS ($NH_3$) *m/z* (%) 535 (6, $MNH_4^+$), 491 (4), 490 (6), 489 (100, $MNH_4^+$-$CH_3CH_2OH$), 474 (5), 473 (5), 472 (65, $MH^+$-$CH_3CH_2OH$).

Mycalamide A (2.2 mg) was stirred with a solution of pyridinium p-toluene sulphonate in dry isopropyl alcohol ($1x10^{-3}$M, 0.3 ml, dried over molecular sieves) at room temperature for 16 hours, then at 55°C for 1 hour. The solution was concentrated under nitrogen (to 0.1 ml), then dilute sodium hydroxide was added (2 ml, pH~10) and the mixture extracted in $CH_2Cl_2$ (3x 2 ml). The solvent was removed to give the crude organic product (2 mg), which was a mixture of at least 4 components by $^1H$ NMR spectroscopy, including mycalamide A, pseudomycalamide A (**3.7**), pederolactone (**3.6**) and another compound. Preparative reverse phase HPLC (45% $H_2O$ in MeOH) gave two major fractions (0.5 mg, 0.7 mg), which were 5,6-dehydromethoxy mycalamide A (**3.11**) and mycalamide A, respectively.

### 3.4.5 BASE CATALYSED ELIMINATION

Mycalamide A (3.8 mg) was reacted with pyridine (10 µl) in DMSO (0.6 ml) in a sealed NMR sample tube at 150°C for 3 hours. $^1H$ NMR spectroscopy showed that the mixture consisted of about 90% 5,6-dehydromethoxy mycalamide A (**3.11**), with a small amount of unreacted mycalamide A and methanol. The sample was recovered with MeOH, then the solution concentrated under nitrogen, mixed with $H_2O$ (1 ml) and transferred onto a reverse phase pipette column (200 mg C18, equilibrated to $H_2O$). The column was flushed with $H_2O$ (5 ml), then eluted with MeOH (5 ml) and the latter

fraction evaporated to dryness, to give 3.6 mg of mostly 5,6-dehydromethoxy mycalamide A (**3.11**).

**3.11**: an oil; FTIR (film) $\upsilon_{max}$ 2960, 2926, 2855, 1679, 1600, 1529, 1454, 1385, 1266, 1194, 1109, 1074, 1031 $cm^{-1}$; $^{1}H$ and $^{13}C$ NMR data in Tables 3.1 and 3.2; HRFABMS *m/z* 510.2132 ($MK^+$, +5.3 ppm for $C_{23}H_{37}NO_9K$).

## 3.6 ACID CATALYSED DECOMPOSITIONS OF MYCALAMIDE A TRIACETATE

Mycalamide A triacetate (**2.18**, 5.5 mg) was reacted with a solution of trifluoroacetic acid in $CDCl_3$ (0.1M, 0.6 ml) in an NMR sample tube at room temperature for 5 days. The sample was recovered in $CH_2Cl_2$, then $H_2O$ (2 ml) was added and the mixture extracted in $CH_2Cl_2$ (3x 2 ml). The solvent was removed to give the crude organic product (5 mg). Preparative reverse phase HPLC (33% $H_2O$ in MeOH) gave three fractions (0.8 mg, 1 mg, 2.5 mg) which were mycalamide A triacetate (**2.18**), *E* neomycalamide A triacetate (**3.13**) and a mixture. The latter was further separated by HPLC (45% $H_2O$ in MeOH) to give two fractions (0.5 mg, 1 mg), which were an aldehyde fragment (**3.14**) and a mixture, respectively.

Mycalamide A triacetate (**2.18**, 8 mg) was dissolved in $CH_2Cl_2$ (2 ml) and stirred with an aqueous solution of p-toluene sulphonic acid (0.1M, 1 ml) in a sealed vial at 75°C for 24 hours, then at 85°C for 6 hours. Dilute sodium hydroxide was added until the mixture was neutralised, then the mixture extracted with $CH_2Cl_2$ (3x 2 ml). The solvent was removed and the crude organic products then subjected to preparative silica gel TLC (developed in 1:1 PE:EtOAc). Four bands of silica were recovered and eluted with EtOAc to give four fractions (3 mg, 1.2 mg, 1.5 mg, 0.8 mg), which were *E* neomycalamide A triacetate (**3.13**), mostly *Z* neomycalamide A triacetate (**3.12**) and two mixtures, respectively. Fraction 3 was therefore subjected to

preparative reverse phase HPLC (40% $H_2O$ in MeOH) to give three fractions (0.4 mg, 0.4 mg, 0.5 mg), which were mycalamide A triacetate (**2.18**), impure pseudomycalamide A triacetate (**3.15**) and 5,6-dehydromethoxy mycalamide A 17,18-diacetate (**3.16**), respectively. Fraction 4 was also subjected to preparative reverse phase HPLC (47% $H_2O$ in MeOH) to give two fractions (0.2 mg, 0.3 mg), which were a C11 lactone fragment (**3.17**) and a C10 aldehyde fragment (**3.14**), respectively.

**3.12**: an oil; FTIR (film) $\upsilon_{max}$ 3375, 2956, 2925, 2854, 1774, 1740, 1664, 1640, 1590, 1514, 1460, 1370, 1228, 1108, 1028, 800 $cm^{-1}$; $^1H$ NMR data in Table 3.6; HREIMS *m/z* 555.2682 ($M^+$-$CH_2CO$, +0.4 ppm for $C_{27}H_{41}NO_{11}$), HRFABMS *m/z* 598.2857 ($MH^+$, -0.9 ppm for $C_{29}H_{44}NO_{12}$).

**3.13**: an oil; FTIR (film) $\upsilon_{max}$ 3380, 2960, 2925, 2853, 1765, 1740, 1670, 1644, 1525, 1370, 1225, 1175, 1110, 1030 $cm^{-1}$; $^1H$ and $^{13}C$ NMR data in Tables 3.6 and 3.2; HRFABMS *m/z* 598.2862 ($MH^+$, -0.3 ppm for $C_{29}H_{44}NO_{12}$), DCIMS ($NH_3$) *m/z* (%) 616 (7), 615 (34, $MNH_4^+$), 600 (13), 599 (31), 598 (100, $MH^+$), 573 (28), 571 (18), 557 (24), 556 (66, $MH^+$-$CH_2CO$), 493 (8), 419 (35).

**3.14**: an oil; FTIR (film) $\upsilon_{max}$ 2963, 2926, 2854, 1741, 1700, 1637, 1450, 1372, 1230, 1093, 1044, 1027 $cm^{-1}$; $^1H$ NMR data in Table 3.6; DCIMS ($NH_3$) *m/z* (%) 348 (6), 347 (13), 346 (100, $MNH_4^+$), 315 (11), 314 (27, $MNH_4^+$-$CH_3OH$).

**3.16**: an oil; $^1H$ NMR data in Table 3.6; HRFABMS *m/z* 556.2765 ($MH^+$, +0.7 ppm for $C_{27}H_{42}NO_{11}$).

**3.17**: an oil; FTIR (film) $\upsilon_{max}$ 2960, 2925, 2853, 1740, 1720, 1665, 1614, 1455, 1371, 1229, 1095, 1031 $cm^{-1}$; $^1H$ NMR data in Table 3.6; HRFABMS *m/z* 353.0987 ($MK^+$, -4.4 ppm for $C_{15}H_{22}O_7K$).

### 3.6.6 NEOMYCALAMIDE A P-BROMOBENZOATES

Mycalamide A (11 mg), p-bromobenzoyl chloride (23 mg) and triethylamine (14 µl) were stirred in $CH_2Cl_2$ (0.3 ml) at room temperature for 24

hours. The solvent was removed to give the crude organic product which was a mixture of p-bromobenzoate esters and reagent (TLC). Preparative reverse phase HPLC (15% $H_2O$ in MeOH) gave five fractions (0.7 mg, 2.7 mg, 1.2 mg, 2.5 mg, 2.7 mg), which were mycalamide A 7-mono-p-bromobenzoate (**2.11**), mycalamide A 18-mono-p-bromobenzoate (**2.10**), a mixture of *E* and *Z* neomycalamide A 7,18-di-p-bromobenzoates (**3.19**, **3.18**), *Z* neomycalamide A 7,18-di-p-bromobenzoate (**3.18**) and mycalamide A 7,18-di-p-bromobenzoate (**2.12**), respectively. The *Z* isomer (**3.18**) was unstable in $CDCl_3$ solution, changing almost quantitatively overnight into the *E* isomer (**3.19**).

**3.18**: an oil or white solid; $^1H$ NMR ($CDCl_3$) δ7.99 and 7.91(7- and 18-$OCOC_6H_4Br$, 2xd, 8.5), 7.61 and 7.54 (7- and 18-$OCOC_6H_4Br$, 2xd, 8.6), 7.35 (H5, q, 1.5), 6.39 (NH9, d, 9.3), 5.94 (H10, t, 9.8), 5.18 (10-OCH*R*, d, 7.0), 4.86 (10-OCH*S*, d, 6.8), 4.23 ($H_2$18, m), 4.21 (H12, dd, 6.6, 10.5), 4.13 (H2, dq, 3.1, 6.5), 4.00 (H17, m), 3.86 (H11, dd, 6.7, 10.2), 3.56 (H15, dd, 2.3, 10.1), 3.56 (13-$OCH_3$, s), 3.51 (H13, d, 10.5), 2.01 (H3, dq, 2.8, 7.1), 1.92 (4-$CH_3$, d, 1.4), 1.70 (H16, m), 1.55 (H16, m), 1.07 (2-$CH_3$, d, 6.5), 0.96 (14-$CH_3$*R*, s), 0.87 (3-$CH_3$, d, 7.0), 0.86 (14-$CH_3$*S*, s) ppm.

**3.19**: an oil or white solid; UV ($CH_3OH$) $\lambda_{max}$ 245 nm (ε~23000), 285 nm (ε~7700); $^1H$ NMR ($CDCl_3$) δ8.09 (NH9, d, 9.0), 7.95 and 7.87 (7- and 18-$OCOC_6H_4Br$, 2xd, 8.6), 7.56 and 7.50 (7- and 18-$OCOC_6H_4Br$, 2xd, 8.6), 5.99 (H10, t, 9.7), 5.97 (H5, q, 1.5), 5.15 (10-OCH*R*, d, 6.8), 4.88 (10-OCH*S*, d, 7.0), 4.33 (H2, dq, 2.8, 6.4), 4.26 ($H_2$18, m), 4.25 (H12, m), 4.07 (H17, m), 3.89 (H11, dd, 6.7, 10.2), 3.67 (H15, broad d, 9.6), 3.55 (13-$OCH_3$, s), 3.48 (H13, d, 10.6), 2.06 (H3, dq, 2.8, 7.2), 1.83 (4-$CH_3$, d, 1.5), 1.70 (H16, m), 1.55 (H16, m), 1.41 (2-$CH_3$, d, 6.5), 0.99 (3-$CH_3$, d, 7.0), 0.95 (14-$CH_3$*R*, s), 0.89 (14-$CH_3$*S*, s) ppm; HRFABMS *m/z* 838.1307 ($MH^+$, +5.3 ppm for $C_{37}H_{43}{}^{79}Br^{81}BrNO_{11}$).

## WORK DESCRIBED IN CHAPTER 4

### 4.2.1 PREPARATION AND CHARACTERISATION OF DIHYDRO EPIMERS

Mycalamide A (5 mg) was stirred with Adams catalyst ($PtO_2$, 2 mg) in MeOH (0.8 ml) under hydrogen at room temperature (and atmospheric pressure) for 1 hour. The resulting solution was filtered over celite and the solvent removed to give the crude organic product (4.8 mg), which was a 2:1 mixture of the two dihydromycalamide A isomers at C4. Preparative reverse phase HPLC (35% $H_2O$ in MeOH) gave three fractions (0.9 mg, 1.3 mg, 1.9 mg), which were ~90% 4α-dihydro mycalamide A (**4.4**), a mixture and ~85% 4β-dihydro mycalamide A (**4.5**), respectively. Further HPLC of the combined second fraction and the residues gave three further fractions (0.5 mg, 0.5 mg, 0.6 mg) in the same manner to give overall yields of 1.4 mg 4α-dihydro mycalamide A (**4.4**) and 2.5 mg 4β-dihydro mycalamide A (**4.5**).

**4.4**: an oil; $^1H$ and $^{13}C$ NMR data in Tables 4.1 and 4.4; HRFABMS *m/z* 528.2751 ($MNa^+$, -6.4 ppm for $C_{24}H_{43}NO_{10}Na$).

**4.5**: an oil; $^1H$ and $^{13}C$ NMR data in Tables 4.1 and 4.4; HRFABMS *m/z* 528.2813 ($MNa^+$, +5.3 ppm for $C_{24}H_{43}NO_{10}Na$).

Mycalamide B (5.5 mg) was stirred with Adams catalyst ($PtO_2$, 3 mg) in MeOH (0.8 ml) under hydrogen at room temperature (and atmospheric pressure) for 1 hour. The resulting solution was filtered over celite and the solvent removed to give the crude organic product (5.5 mg), which was a 3:2 mixture of the two dihydromycalamide B isomers at C4. Preparative reverse phase HPLC (35% $H_2O$ in MeOH) gave three fractions (1.8 mg, 0.9 mg, 2.2 mg), which were ~90% 4α-dihydro mycalamide B (**4.6**), a mixture and ~90% 4β-dihydro mycalamide B (**4.7**), respectively. Further HPLC of the combined second fraction and the residues gave two further fractions (0.5 mg, 0.5 mg), which were a mixture and ~90% 4β-dihydro mycalamide B (**4.7**), respectively,

to give overall yields of 1.8 mg 4α-dihydro mycalamide B (**4.6**) and 2.7 mg 4β-dihydro mycalamide B (**4.7**).

**4.6**: an oil; $^{1}H$ and $^{13}C$ NMR data in Tables 4.1 and 4.4; HRFABMS *m/z* 510.2725 ($MNa^{+}$-$CH_3OH$, +9.1 ppm for $C_{24}H_{41}NO_9Na$).

**4.7**: an oil; $^{1}H$ and $^{13}C$ NMR data in Tables 4.1 and 4.4; HREIMS *m/z* 487.2765 ($M^{+}$-$CH_3OH$, -3.3 ppm for $C_{24}H_{41}NO_9$), DCIMS ($NH_3$) *m/z* (%) 537 (4, $MNH_4^{+}$), 507 (7), 506 (34), 505 (100, $MNH_4^{+}$-$CH_3OH$), 490 (6), 489 (27), 488 (90, $MH^{+}$-$CH_3OH$).

## 4.3 ACID CATALYSED HYDROLYSIS OF DIHYDRO EPIMERS

4α-Dihydro mycalamide A (**4.4**) was dissolved in $CDCl_3$ only (0.6 ml), for NMR studies, but hydrolysis occurred within minutes at room temperature to give 4α-dihydro pseudomycalamide A (**4.10**).

**4.10**: an oil; $^{1}H$ and $^{13}C$ NMR data in Tables 4.1 and 4.4; HRFABMS *m/z* 514.2655 ($MNa^{+}$, +5.2 ppm for $C_{23}H_{41}NO_{10}Na$), DCIMS ($NH_3$) *m/z* (%) 509 (9, $MNH_4^{+}$), 492 (36), 491 (83, $MNH_4^{+}$-$H_2O$), 474 (16, $MH^{+}$-$H_2O$), 292 (17), 262 (23).

4β-Dihydro mycalamide A (**4.5**) was dissolved in $CD_2Cl_2$ (0.6 ml) but hydrolysis occurred within minutes at room temperature to give mostly 4β-dihydro 6*S* pseudomycalamide A (**4.11**).

**4.11**: an oil; $^{1}H$ and $^{13}C$ NMR data in Tables 4.1 and 4.4; HRFABMS *m/z* 514.2585 ($MNa^{+}$, -8.4 ppm for $C_{23}H_{41}NO_{10}Na$).

### 4.4.1 HYDROGENATION OVER PALLADIUM ON CARBON

Mycalamide A (4.5 mg) was stirred with 10% palladium on carbon (4.5 mg) in MeOH (0.8 ml) under hydrogen at room temperature (and atmospheric pressure) for 5 hours. The resulting solution was filtered over celite and the solvent removed to give the crude organic product, which was a mixture of at

least 5 components (HPLC). Preparative reverse phase HPLC (40% $H_2O$ in MeOH) gave six fractions (0.7 mg, 0.5 mg, 0.7 mg, 0.8 mg, 0.4 mg, 0.9 mg), which were $\Delta^3$ mycalamide A (**4.12**), mycalamide A, mostly 4α-dihydro, 6-deoxy pseudomycalamide A (**4.13**), 4α-dihydro mycalamide A (**4.4**), a mixture and 4β-dihydro mycalamide A (**4.5**).

**4.12**: an oil; $^1H$ NMR data in Table 4.5; HRFABMS *m/z* 472.2548 ($MH^+$-$CH_3OH$, +0.3 ppm for $C_{23}H_{38}NO_9$).

**4.13**: an oil; $^1H$ and $^{13}C$ NMR data in Tables 4.5 and 4.4 (on larger sample - see below); HRFABMS *m/z* 476.2854 ($MH^+$, -1.1 ppm for $C_{23}H_{42}NO_9$).

4α-Dihydro, 6-deoxy pseudomycalamide A (**4.13**, 0.7 mg) was dissolved in pyridine (0.1 ml) and acetic anhydride (0.1 ml) and stirred at room temperature overnight. The solution was concentrated under nitrogen, then $H_2O$ (2 ml) was added and the mixture extracted with $CH_2Cl_2$ (2x 2 ml). The solvent was removed to give 0.8 mg of mostly 4α-dihydro, 6-deoxy pseudomycalamide A triacetate (**4.15**).

**4.15**: an oil; $^1H$ NMR data in Table 4.5.

### 4.5.1 HYDROGENATION OF 5,6-DEHYDROMETHOXY MYCALAMIDE A

5,6-Dehydromethoxy mycalamide A (**3.11**, 3.8 mg) was stirred with Adams catalyst ($PtO_2$, 4 mg) in MeOH (0.8 ml) under hydrogen at room temperature (and atmospheric pressure) for 8 hours. The resulting solution was filtered over celite and the solvent removed to give the crude organic product, which was a mixture of at least 5 components (HPLC). Preparative reverse phase HPLC (43% $H_2O$ in MeOH) gave five fractions (0.7 mg, 0.5 mg, 0.6 mg, 0.3 mg, 0.5 mg), which were 4α-dihydro, 5,6-dehydromethoxy mycalamide A (**4.16**), a mixture, 4α-dihydro, 6-deoxy pseudomycalamide A (**4.13**), mostly 4α-dihydro mycalamide A (**4.4**) and mostly 4β-dihydro mycalamide A (**4.5**), respectively.

**4.16**: an oil; $^1$H NMR data in Table 4.5; HRFABMS *m/z* 474.2721 ($MH^+$, +3.8 ppm for $C_{23}H_{40}NO_9$).

## 4.7 ATTEMPTS AT OTHER DOUBLE BOND REARRANGEMENTS

Mycalamide A (1 mg) was stirred with rhodium trichloride (0.5 mg) in EtOH (0.2 ml) at room temperature for 2 hours. The solvent was removed and the crude organic residue washed with $H_2O$ (2 ml) and extracted in $CH_2Cl_2$ (3x 2 ml). The solvent was removed to give the crude organic product, which was a mixture of a large number of products by silica gel TLC and $^1$H NMR spectroscopy indicated complete decomposition.

Mycalamide A (1 mg) was stirred with freshly prepared bis-benzonitrile palladium(II) chloride (1 mg) in benzene (0.5 ml) at room temperature for 3.5 hours. Silica gel TLC indicated decomposition, which was confirmed by $^1$H NMR spectroscopy on the material obtained after workup of the reaction.

### 4.9.1 PREPARATION AND CHARACTERISATION OF EPOXIDE ISOMERS

Mycalamide A (4.5 mg) and m-chloroperbenzoic acid (4.5 mg) were stirred in $CH_2Cl_2$ (0.3 ml) at room temperature for 1 day. The solvent was removed and the crude organic product subjected to preparative silica gel TLC (developed twice in 1:19 EtOH:EtOAc). Three bands of silica were recovered and eluted with 1:4 EtOH:EtOAc to give three fractions (1.8 mg, 0.6 mg, 1.7 mg), which were pure mycalamide A 4α-epoxide (**4.17**), mostly mycalamide A 4α-epoxide, and mycalamide A 4β-epoxide (**4.18**), respectively.

**4.17**: an oil; $^1$H and $^{13}$C NMR data in Tables 4.7 and 4.9; HRFABMS *m/z* 542.2594 ($MNa^+$, +3.1 ppm for $C_{24}H_{41}NO_{11}Na$), DCIMS ($NH_3$) *m/z* (%) 537 (10, $MNH_4^+$), 505 (22, $MNH_4^+$-$CH_3OH$), 488 (17, $MH^+$-$CH_3OH$), 487 (15), 335 (34), 262 (16), 231 (24), 230 (34).

**4.18**: an oil; $^{1}H$ and $^{13}C$ NMR data in Tables 4.7 and 4.9; HRFABMS *m/z* 542.2599 ($MNa^+$, +4.0 ppm for $C_{24}H_{41}NO_{11}Na$), DCIMS ($NH_3$) *m/z* (%) 537 (24, $MNH_4^+$), 505 (23, $MNH_4^+$-$CH_3OH$), 488 (15, $MH^+$-$CH_3OH$), 292 (22), 291 (34), 278 (23), 264 (31).

Mycalamide B (4.0 mg) and m-chloroperbenzoic acid (6 mg) were stirred in $CH_2Cl_2$ (0.3 ml) at room temperature for 20 hours. The solvent was removed and the crude organic product subjected to preparative silica gel TLC (developed twice in 1:19 EtOH:EtOAc). Two bands of silica were recovered and eluted with 1:4 EtOH:EtOAc to give two fractions (2.2 mg, 1.3 mg), which were pure mycalamide B 4α-epoxide (**4.19**) and mycalamide B 4β-epoxide (**4.20**), respectively.

**4.19**: an oil; $^{1}H$ and $^{13}C$ NMR data in Tables 4.7 and 4.9; HRFABMS *m/z* 556.2714 ($MNa^+$, -3.6 ppm for $C_{25}H_{43}NO_{11}Na$), DCIMS ($NH_3$) *m/z* (%) 551 (14, $MNH_4^+$), 519 (23, $MNH_4^+$-$CH_3OH$), 502 (36, $MH^+$-$CH_3OH$), 409 (12), 386 (15), 351 (15), 349 (15), 306 (23), 294 (22), 276 (20), 264 (80).

**4.20**: an oil; $^{1}H$ and $^{13}C$ NMR data in Tables 4.7 and 4.9; HRFABMS *m/z* 556.2756 ($MNa^+$, +4.0 ppm for $C_{25}H_{43}NO_{11}Na$), DCIMS ($NH_3$) *m/z* (%) 551 (17, $MNH_4^+$), 542 (16), 528 (50), 519 (32, $MNH_4^+$-$CH_3OH$), 503 (23), 502 (75, $MH^+$-$CH_3OH$), 408 (16), 406 (16), 400 (27), 391 (18), 386 (58), 373 (22), 372 (100).

## 4.10 OTHER DOUBLE BOND ADDITIONS

Mycalamide B (2.5 mg), potassium carbonate (8.5 mg) and ethyl chloroformate (4 μl) were stirred in benzene (0.3 ml) at room temperature for 20 hours. The solution was filtered over celite and the solvent removed to give the crude organic product (2.5 mg), which was then subjected to preparative silica gel TLC (developed in 3:2 PE:EtOAc). A single band of silica was

recovered and eluted with EtOAc to give 0.8 mg of 4',4-hydrochloro, 5,6-dehydromethoxy mycalamide B bis-ethylcarbonate (**4.21**).

**4.21**: an oil; $^1$H NMR data in Table 4.5.

Mycalamide A (1 mg) was reacted with a solution of bromine in $CCl_4$ (0.01M, 1 ml) at room temperature for 15 minutes. The solvent was removed to give the crude organic product which was a 1:1 mixture of mycalamide A and one major bromination product (TLC, $^1$H NMR spectroscopy).

The reaction was repeated with a more concentrated solution of bromine in $CCl_4$ (0.1M, 0.3 ml) at room temperature for 0.5 minutes, but this gave decomposition (TLC, $^1$H NMR spectroscopy). Similarly mycalamide A was reacted with a solution of bromine in 1:1 $CH_2Cl_2$:$CCl_4$ (0.02M, 0.3 ml), containing triethylamine (50 µl) at room temperature for 1 minute. The solvent was removed to give the crude organic product which was a mixture of several components (TLC), but $^1$H NMR spectroscopy indicated only decomposition.

## WORK DESCRIBED IN CHAPTER 5

### 5.2.2 INITIAL BASE CATALYSED REACTION STUDIES

Mycalamide A (0.2 mg) was stirred in a solution of sodium methoxide in MeOH (1M, 0.1 ml) at room temperature for 1 day. The reaction mixture was found to consist of at least one more polar component (HPLC) which gave a blue char on visualisation with anisaldehyde.

### 5.3.1 PREPARATION AND CHARACTERISATION OF MYCALAMIDE A OXAZOLIDINONES

Mycalamide A (3.8 mg) was stirred in a solution of sodium methoxide in MeOH (1M, 0.3 ml) at 50°C for 8 hours. The solvent was removed and the crude residue extracted with $CHCl_3$ (3x 1 ml) and filtered to give the crude

organic product (3.3 mg). Preparative reverse phase HPLC (45% $H_2O$ in MeOH) gave two fractions (1.0 mg, 1.3 mg), which were pure mycalamide A *cis* oxazolidinone (**5.2**) and mycalamide A *trans* oxazolidinone (**5.3**), respectively.

**5.2**: an oil; FTIR (film) $\upsilon_{max}$ 3700-3100, 3073, 2964, 2926, 2855, 1718, 1430, 1380, 1260, 1102, 1071, 1045, 1018, 800 $cm^{-1}$; $^1H$ and $^{13}C$ NMR data in Tables 5.1 and 5.2; HRFABMS *m/z* 496.2527 ($MNa^+$, +0.9 ppm for $C_{23}H_{39}NO_9Na$), DCIMS ($NH_3$) *m/z* (%) 491 (5, $MNH_4^+$), 461 (6), 460 (30), 459 (100, $MNH_4^+$-$CH_3OH$), 443 (17), 442 (63, $MH^+$-$CH_3OH$).

**5.3**: an oil; IR ($CHCl_3$) $\upsilon_{max}$ 3600-3200, 2920, 1715, 1600, 1400, 1100-1020 $cm^{-1}$; $^1H$ and $^{13}C$ NMR data in Tables 5.1 and 5.2; HRFABMS *m/z* 496.2539 ($MNa^+$, +3.3 ppm for $C_{23}H_{39}NO_9Na$), DCIMS ($NH_3$) *m/z* (%) 461 (6), 460 (29), 459 (100, $MNH_4^+$-$CH_3OH$), 443 (7), 442 (41, $MH^+$-$CH_3OH$).

## 5.4 FURTHER REACTIONS

Mycalamide A (0.2 mg) was stirred with barium oxide (9 mg) in DMSO (0.2 ml) at 50°C for 16 hours. $H_2O$ (0.5 ml) was added and the mixture transferred onto a reverse phase pipette column (200 mg C18, equilibrated to $H_2O$), which was then flushed with $H_2O$ (5 ml) and eluted with MeOH (6 ml). The MeOH fraction was evaporated to dryness to give the crude organic product, which was a 2:1 mixture of the two isomers, mycalamide A *cis* oxazolidinone (**5.2**) and mycalamide A *trans* oxazolidinone (**5.3**), respectively by HPLC and $^1H$ NMR spectroscopy.

Mycalamide A (1 mg) was stirred with powdered potassium hydroxide (3 mg) in DMSO (0.2 ml) at room temperature for 4 days. $H_2O$ (0.5 ml) was added and the mixture extracted with $CHCl_3$ (3x 0.3 ml). The solvent was removed to give the crude organic product which was mostly mycalamide A *cis* oxazolidinone (**5.2**).

Mycalamide A (1.5 mg) was stirred with powdered potassium hydroxide (7 mg) in DMSO (0.3 ml) at 80°C for 1 day, then at 105°C for 1 day. $H_2O$ (0.6 ml) was added and the mixture transferred onto a reverse phase pipette column (200 mg C18, equilibrated to $H_2O$), which was then flushed with $H_2O$ (5 ml) and eluted with MeOH (6 ml). The MeOH fraction was evaporated to dryness to give the crude organic product, which was mostly $\Delta^{4(5)}$ mycalamide A *cis* oxazolidinone (**5.6**).

**5.6**: an oil; HRFABMS *m/z* 442.2471 ($MH^+$-$CH_3OH$, +6.8 ppm for $C_{22}H_{36}NO_8$).

Mycalamide A (7 mg) was stirred in a solution of sodium hydroxide in 3:2 $H_2O$:MeOH (2M, 0.3 ml) at 55°C for 10 hours. The solution was concentrated (to 1 ml), then $H_2O$ (0.6 ml) was added. The mixture was transferred onto a reverse phase pipette column (200 mg C18, equilibrated to $H_2O$), which was then flushed with $H_2O$ (5 ml) and eluted with MeOH (5 ml). The MeOH fraction was evaporated to dryness to give the crude organic product, which was a mixture of at least 4 components (HPLC). Preparative reverse phase HPLC (45% $H_2O$ in MeOH) gave 4 fractions (1.4 mg, 1.8 mg, 0.7 mg, 0.8 mg), which were mycalamide A *cis* oxazolidinone (**5.2**), mycalamide A *trans* oxazolidinone (**5.3**), mostly 7*S* mycalamide A *trans* oxazolidinone (**5.8**) and mostly 7*S* mycalamide A *cis* oxazolidinone (**5.7**), respectively. Note that the latter two fractions contained up to 25% unresolved mycalamide A by FABMS and $^1H$ NMR spectroscopy.

**5.7**: an oil; $^1H$ NMR data in Table 5.1; HRFABMS *m/z* 442.2410 ($MH^+$-$CH_3OH$, -6.9 ppm for $C_{22}H_{36}NO_8$).

**5.8**: an oil; $^1H$ NMR data in Table 5.1; HRFABMS *m/z* 442.2430 ($MH^+$-$CH_3OH$, -2.4 ppm for $C_{22}H_{36}NO_8$).

Mycalamide B (2.5 mg) was stirred with powdered potassium hydroxide (5 mg) in DMSO (0.2 ml) at 40°C for 1 day. $H_2O$ (0.5 ml) was added and the

mixture extracted with $CHCl_3$ (3x 0.3 ml). The solvent was removed and the crude organic product subjected to preparative silica gel TLC (developed twice in 1:19 EtOH:EtOAc). Two bands of silica were recovered and eluted with 1:3 EtOH:EtOAc to give mycalamide B *cis* oxazolidinone (**5.9**) and mycalamide B *trans* oxazolidinone (**5.10**), respectively (although the latter fraction also contained traces of mycalamide B).

**5.9**: an oil; $^1H$ and $^{13}C$ NMR data in Tables 5.1 and 5.2; HRFABMS *m/z* 456.2587 ($MH^+$-$CH_3OH$, -2.3 ppm for $C_{23}H_{38}NO_8$).

**5.10**: an oil; $^1H$ NMR data in Table 5.1; HRFABMS *m/z* 510.26340 ($MNa^+$, -8.8 ppm for $C_{24}H_{41}NO_9Na$).

Mycalamide B (2.5 mg) was stirred in a solution of sodium methoxide in MeOH (1M, 0.3 ml) at room temperature for 1 day, then at 50°C for 1 day. The solvent was removed and the crude residue partitioned in 1:1 $CHCl_3$:$H_2O$ (5 ml), then extracted with $CHCl_3$ (3x 2 ml). The solvent was removed and the crude organic product subjected to preparative silica gel TLC (developed twice in 1:19 EtOH:EtOAc). Two bands of silica were recovered and eluted with 1:3 EtOH:EtOAc to give two fractions (1 mg, 1 mg), which were both mixtures, containing as major components mycalamide B *cis* oxazolidinone (**5.9**) and mycalamide B *trans* oxazolidinone (**5.10**), respectively.

## 5.5 REACTION MECHANISMS

Mycalamide A (1.5 mg) was stirred in a solution of sodium trideuteromethoxide in $CD_3OD$ (3M, 0.2 ml) at room temperature for 1 day, then at 50°C for 2 hours. The solvent was removed and the crude residue extracted with $CHCl_3$ (3x 1 ml). The solvent was removed to give the crude organic product which was a mixture of mycalamide A *cis* oxazolidinone (**5.2**), mycalamide A *trans* oxazolidinone (**5.3**) and minor products, but there was no incorporation of deuterium by $^1H$ NMR spectroscopy.

Mycalamide A *cis* oxazolidinone (**5.2**, 1 mg) was stirred in a solution of sodium trideuteromethoxide in $CD_3OD$ (4M, 0.4 ml) at 70°C for 2 hours. The solvent was removed and the crude residue extracted with $CHCl_3$ (3x 1 ml). This solution was filtered and the solvent removed to give the crude organic product, which was a mixture of mycalamide A *cis* oxazolidinone (**5.2**) and minor products. There was no mycalamide A *trans* oxazolidinone (**5.3**) present and no incorporation of deuterium.

Mycalamide A *trans* oxazolidinone (**5.3**, 1.7 mg) was stirred with powdered potassium hydroxide (10 mg) in DMSO (0.3 ml) at room temperature for 4 days. $H_2O$ (0.5 ml) was added and the mixture transferred onto a reverse phase pipette column (200 mg C18, equilibrated to $H_2O$), which was then flushed with $H_2O$ (8 ml) and eluted with MeOH (8 ml). The MeOH fraction was evaporated to dryness to give 1.3 mg of almost pure mycalamide A *trans* oxazolidinone (**5.3**).

Mycalamide A *trans* oxazolidinone (**5.3**, 1.3 mg) was stirred in a solution of sodium hydroxide in 40% $H_2O$/MeOH (1M, 0.4 ml) at 60°C for 1 day. The solution was concentrated under nitrogen (to 0.2 ml), then $H_2O$ (1 ml) was added and the mixture transferred onto a reverse phase pipette column (200 mg C18, equilibrated to $H_2O$), which was then flushed with $H_2O$ (6 ml) and eluted with MeOH (6 ml). The MeOH fraction was evaporated to dryness to give a mixture consisting of at least 60% mycalamide A *cis* oxazolidinone (**5.2**), with some decomposition.

## 5.6 ACID DECOMPOSITION

Mycalamide A *trans* oxazolidinone (**5.3**, 1.2 mg) in $CDCl_3$ only (0.6 ml) reacted overnight at 4°C to give *Z* neomycalamide A 10*S* oxazolidinone (**5.11**) cleanly. Similarly, mycalamide A *cis* oxazolidinone (**5.2**, 1 mg) in

$CDCl_3$ only (0.6 ml) reacted overnight at 4°C to give *Z* neomycalamide A 10*R* oxazolidinone (**5.12**) cleanly. These reactions could not be reproduced.

**5.11**: an oil; $^1H$ NMR ($CDCl_3$) δ8.06 (NH9, broad s), 6.94 (H5, q, 1.7), 5.86 (H10, d, 6.4), 4.16 (H2, dq, 2.9, 6.5), 4.05 (H12, dd, 6.1, 8.3), 3.98 (H11, t, 5.9), 3.91 (H17, m), 3.59 ($H_2$18, m), 3.59 (13-$OCH_3$, s), 3.54 (H15, m), 3.03 (H13, d, 8.2), 2.03 (H3, dq, 2.5, 7.2), 1.89 (4-$CH_3$, d, 1.3), 1.6-1.7 ($H_2$16, m), 1.32 (2-$CH_3$, d, 6.5), 1.00 (3-$CH_3$, d, 7.0), 1.00 (14-$CH_3$*R*, s), 0.87 (14-$CH_3$*S*, s) ppm.

**5.12**: an oil; $^1H$ NMR ($CDCl_3$) δ 6.89 (H5, q, 1.5), 6.54 (NH9, broad s), 5.86 (H10, d, 7.5), 4.15 (H2, dq, 2.8, 6.6), 4.01 (H12, dd, 7.2, 9.5), 3.95 (H17, m), 3.94 (H11, t, 7.4), 3.65 (H18, m), 3.63 (13-$OCH_3$, s), 3.60 (H18, dd, 5.2, 12.7), 3.6 (H15, m), 3.09 (H13, d, 9.5), 2.02 (H3, dq, 2.6, 7.3), 1.89 (4-$CH_3$, d, 1.6), 1.5-1.7 ($H_2$16, m), 1.35 (2-$CH_3$, d, 6.5), 1.01 (3-$CH_3$, d, 7.0), 0.96 (14-$CH_3$*R*, s), 0.88 (14-$CH_3$*S*, s) ppm.

## 5.7 ACETYLATION AND METHYLATION OF OXAZOLIDINONES

Mycalamide A *trans* oxazolidinone (**5.3**, 1.7 mg) was dissolved in pyridine (0.15 ml) and acetic anhydride (0.15 ml) and stirred at room temperature for 2 days. The solution was concentrated under nitrogen, then $H_2O$ (2 ml) was added and the mixture extracted with $CH_2Cl_2$ (3x 2 ml). The solvent was removed to give 1.8 mg of pure *N*-acetyl mycalamide A *trans* oxazolidinone 12,17,18-triacetate (**5.13**).

**5.13**: an oil; FTIR (film) $\upsilon_{max}$ 3075, 2968, 2925, 2850, 1745, 1715, 1657, 1438, 1373, 1295, 1264, 1228, 1144, 1094, 1047 $cm^{-1}$; $^1H$ and $^{13}C$ NMR data in Tables 5.9 and 5.2; HRFABMS *m/z* 664.2982 ($MNa^+$, +6.0 ppm for $C_{31}H_{47}NO_{13}Na$).

Mycalamide A *trans* oxazolidinone (**5.3**, 2 mg), powdered potassium hydroxide (12 mg) and methyl iodide (5 μl) were stirred in DMSO (0.3 ml) at 30°C for 20 hours. $H_2O$ (0.6 ml) was added and the mixture transferred onto a

reverse phase pipette column (200 mg C18, equilibrated to $H_2O$), which was then flushed with $H_2O$ (6 ml) and eluted with MeOH (6 ml). The MeOH fraction was evaporated to dryness to give the crude organic product (2.2 mg) which was then subjected to preparative silica gel TLC (developed in 5:2 EtOAc:PE). Three bands of silica were recovered and eluted with 3:1 $CH_2Cl_2$:MeOH to give three fractions (0.9 mg, 0.1 mg, 1.1 mg), which were 12,17,18-tri-*O*-methyl, *N*-methyl mycalamide A *trans* oxazolidinone (**5.14**), 12,17,18-tri-*O*-methyl, *N*-methyl 7*S* mycalamide A *trans* oxazolidinone (**5.16**), and 12,17,18-tri-*O*-methyl, *N*-methyl 7*S* mycalamide A *cis* oxazolidinone (**5.15**), respectively.

Mycalamide B (2.5 mg) and powdered potassium hydroxide (10 mg) were stirred in DMSO (0.3 ml) at room temperature overnight to give a mixture of mycalamide B *cis* and *trans* oxazolidinones (**5.9**, **5.10**) by TLC. Methyl iodide (4 µl) was added and the reaction stirred at room temperature for 1 day. $H_2O$ (0.5 ml) was added and the mixture transferred onto a reverse phase pipette column (200 mg C18, equilibrated to $H_2O$), which was then flushed with $H_2O$ (6 ml) and eluted with MeOH (6 ml). The MeOH fraction was evaporated to dryness to give the crude organic product (2.2 mg) which was then subjected to preparative silica gel TLC (developed in 5:2 EtOAc:PE). Three bands of silica were recovered and eluted with 1:5 EtOH:EtOAc to give three fractions (0.8 mg, 0.8 mg, 0.8 mg), which were mostly **5.14** (containing a small amount of 7,17,18-tri-*O*-methyl, *N*-methyl mycalamide A, **2.26**), pure **5.16**, and a mixture of **5.15** and another component. Preparative reverse phase HPLC (25% $H_2O$ in MeOH) gave two fractions (0.5 mg, 0.2 mg), which were **5.15** and 8,12,17,18-tetra-*O*-methyl mycalamide A *cis* oxazolidinone (**5.17**), respectively.

**5.14**: an oil; $^1H$ and $^{13}C$ NMR data in Tables 5.9 and 5.2; HRFABMS *m/z* 498.3067 ($MH^+$-$CH_3OH$, +0.1 ppm for $C_{26}H_{44}NO_8$).

**5.15**: an oil; $^{1}H$ and $^{13}C$ NMR data in Tables 5.9 and 5.2; HRFABMS *m/z* 568.2847 ($MK^+$, -7.1 ppm for $C_{27}H_{47}NO_9K$).

**5.16**: an oil; $^{1}H$ NMR data in Table 5.9; HRFABMS *m/z* 498.3083 ($MH^+$-$CH_3OH$, +3.3 ppm for $C_{26}H_{44}NO_8$).

**5.17**: an oil; $^{1}H$ NMR data in Table 5.9; HRFABMS *m/z* 498.3066 ($MH^+$-$CH_3OH$, -0.1 ppm for $C_{26}H_{44}NO_8$).

## WORK DESCRIBED IN CHAPTER 6

### 6.2 BASE CATALYSED REACTIONS OF *N*-ALKYL DERIVATIVES

7,18-Di-*O*-benzyl, *N*-benzyl mycalamide B (**2.46**, 5 mg) was stirred with powdered potassium hydroxide (6 mg) in DMSO (0.3 ml) at 60°C for 5 hours. $H_2O$ (0.6 ml) was added and the mixture transferred onto a reverse phase pipette column (200 mg C18, equilibrated to $H_2O$), which was then flushed with $H_2O$ (5 ml) and eluted with MeOH (5 ml). The MeOH fraction was evaporated to dryness to give the crude organic product, which was then subjected to preparative silica gel TLC (developed in 2:1 PE:EtOAc). Seven bands of silica were recovered and eluted with EtOAc, to give seven fractions (<0.5 mg, 1.5 mg, <0.5 mg, 1.8 mg, <0.5 mg, 1 mg, <0.5 mg), but all except fraction 4 contained only complex mixtures or alkyl impurities. Fraction 4 was a pure *N*-benzyl, *N*-formyl fragment (**6.1**).

**6.1**: an oil; FTIR (film) $\upsilon_{max}$ 3089, 3063, 3031, 2961, 2928, 2880, 2855, 2825, 1689, 1454, 1386, 1365, 1260, 1188, 1166, 1107, 1085, 1030 $cm^{-1}$; $^{1}H$ NMR data in Table 6.1, $^{13}C$ NMR data in Table 6.3 except the following aromatic resonances, ($CDCl_3$) δ128.76, 128.44, 128.31, 128.26, 128.21, 127.95, 127.85, 127.65, 127.58, 127.39, 127.23 ppm; HRCIMS ($C_4H_{10}$) *m/z* 514.2802 ($MH^+$, -0.5 ppm for $C_{29}H_{40}NO_7$).

Mycalamide B (3.6 mg), powdered potassium hydroxide (6 mg) and methyl iodide (4 μl) were stirred in DMSO (0.2 ml) at room temperature for one day to give 7,17,18-tri-*O*-methyl, *N*-methyl mycalamide A (**2.26**) by TLC. Powdered potassium hydroxide (2 mg) was added and the mixture stirred at 70°C for 5 hours. $H_2O$ (0.5 ml) was added and the mixture extracted with $CHCl_3$ (3x 0.3 ml). The solvent was removed to give 1.8 mg of a pure *N*-methyl *N*-formyl fragment (**6.2**).

**6.2**: an oil; IR ($CHCl_3$) $\upsilon_{max}$ 2900, 2860, 1680, 1600, 1380, 1080-1020 $cm^{-1}$; $^1H$ and $^{13}C$ NMR data in Tables 6.1 and 6.3; HRCIMS ($C_4H_{10}$) *m/z* 362.2179 ($MH^+$, +0.1 ppm for $C_{17}H_{32}NO_7$).

## 6.3 BASE CATALYSED REACTIONS OF 7-*O*-BENZYL DERIVATIVES

7-*O*-Benzyl mycalamide A (**2.39**, 2 mg) was stirred with barium oxide (11 mg) in DMSO (0.3 ml) at 60°C for 4 hours, then at 75°C for 4 hours. $H_2O$ (0.5 ml) was added and the mixture transferred onto a reverse phase pipette column (200 mg C18, equilibrated to $H_2O$), which was then flushed with $H_2O$ (6 ml) and eluted with MeOH (6 ml). The MeOH fraction was evaporated to dryness to give the crude organic product, which was then subjected to preparative silica gel TLC (developed in EtOAc). Two bands of silica were recovered and eluted with 1:9 EtOH:EtOAc to give two fractions (0.8 mg, 0.8 mg), which were 7-*O*-benzyl mycalamide A (**2.39**) and 7-*O*-benzyl 10*R* mycalamide A (**6.3**), respectively.

**6.3**: an oil; $^1H$ NMR data in Table 6.4, $^{13}C$ NMR data in Table 6.5 except the following aromatic resonances, ($CDCl_3$) δ137.26, 128.49, 128.38, 127.98 ppm; HREIMS *m/z* 561.3149 ($M^+$-$CH_3OH$, 0.0 ppm for $C_{30}H_{43}NO_9$), DCIMS ($NH_3$) *m/z* (%) 611 (2, $MNH_4^+$), 594 (3, $MH^+$), 582 (9), 581 (26), 580 (28), 579 (80, $MNH_4^+$-$CH_3OH$), 565 (12), 564 (37), 563 (33), 562 (100, $MH^+$-$CH_3OH$).

Mycalamide A (6 mg), barium oxide (26 mg) and benzyl bromide (10 μl) were stirred in DMSO (0.3 ml) at 60°C for 2 hours. $H_2O$ was added (0.5 ml) and the mixture transferred onto a reverse phase pipette column (200 mg C18, equilibrated to $H_2O$), which was then flushed with $H_2O$ (8 ml), then eluted with MeOH (6 ml). The resulting MeOH fraction was evaporated to dryness, then this crude organic product was subjected to preparative silica gel TLC (1:2 PE:EtOAc). Four bands of silica were recovered and eluted with EtOAc to give four fractions (1 mg, 1 mg, 1.5 mg, 1.5 mg), which were 7-*O*-benzyl mycalamide A (**2.39**), 7-*O*-benzyl 10*R* mycalamide A (**6.3**), 7,18-di-*O*-benzyl 10*R* mycalamide A (**6.4**) and 7,18-di-*O*-benzyl mycalamide A (**2.40**), respectively.

**6.4**: an oil; $^1H$ NMR data in Table 6.4, $^{13}C$ NMR data in Table 6.5 except the following aromatic resonances, ($CDCl_3$) δ137.31, 128.53, 128.40, 128.33, 127.89, 127.72, 127.66 ppm; HRFABMS *m/z* 652.3495 ($MH^+$-$CH_3OH$, +1.4 ppm for $C_{37}H_{50}NO_9$), DCIMS ($NH_3$) *m/z* (%) 701 (4, $MNH_4^+$), 672 (5), 671 (18), 670 (42), 669 (100, $MNH_4^+$-$CH_3OH$), 654 (11), 653 (21), 652 (53, $MH^+$-$CH_3OH$).

7-*O*-Benzyl mycalamide A (**2.39**, 2 mg) was stirred in a solution of sodium methoxide in MeOD (1.5M, 0.4 ml) at 60°C for 2.5 hours. The solvent was removed and the crude residue partitioned in 1:1 $CHCl_3$:$H_2O$ (5 ml), then extracted in $CHCl_3$ (3x 2 ml). The solvent was removed to give the crude organic product, which was a mixture of at least eight components (HPLC). Preparative reverse phase HPLC gave eight fractions (0.2 mg, 0.4 mg, 0.3 mg, 0.3 mg, 0.2 mg, 0.1 mg, 0.1 mg, 0.1 mg), which were 7-deutero, 7-*O*-benzyl, *Z* $\Delta^{10}$, 10-deformyl mycalamide A (**6.5**), 7-deutero, 7-*O*-benzyl, 10*R*-*O*-methyl mycalamide A (**6.6**), a 2:1 mixture of 7-deutero, 7-*O*-benzyl, 10*S*-*O*-methyl mycalamide A (**6.8**) and 7-deutero, 7-*O*-benzyl mycalamide A (**6.7**), 7-deutero, 7*S*-*O*-benzyl 10*R*-*O*-methyl mycalamide A (**6.9**), 7-deutero,

7-*O*-benzyl 10*R* mycalamide A (**6.10**), 7-deutero, 7*S*-*O*-benzyl mycalamide A (**6.11**), 7-deutero, 7*S*-*O*-benzyl 10*S*-*O*-methyl mycalamide A (**6.12**) and 7-deutero, 7*S*-*O*-benzyl 10*R* mycalamide A (**6.13**), respectively.

**6.5**: an oil; $^1$H NMR data in Table 6.7; HRFABMS *m/z* 603.2770 ($MK^+$, -4.0 ppm for $C_{30}H_{44}DNO_9K$).

**6.6**: an oil; $^1$H NMR data in Table 6.7; HRFABMS *m/z* 635.3059 ($MK^+$, +0.4 ppm for $C_{31}H_{48}DNO_{10}K$).

**6.7**: an oil; HRFABMS *m/z* 633.2890 ($MK^+$, -1.5 ppm for $C_{31}H_{46}DNO_{10}K$).

**6.8**: an oil; $^1$H NMR data in Table 6.7; HRFABMS *m/z* 635.3023 ($MK^+$, -5.2 ppm for $C_{31}H_{48}DNO_{10}K$).

**6.9**: an oil; $^1$H NMR data in Table 6.7; HRFABMS *m/z* 635.3111 ($MK^+$, +8.9 ppm for $C_{31}H_{48}DNO_{10}K$).

**6.11**: an oil; $^1$H NMR data in Table 6.7; HRFABMS *m/z* 617.3203 ($MNa^+$, +6.9 ppm for $C_{31}H_{46}DNO_{10}Na$).

**6.12**: an oil; $^1$H NMR data in Table 6.7.

**6.13**: an oil; $^1$H NMR data in Table 6.7.

7-*O*-Benzyl mycalamide A (**2.39**, 1 mg) was stirred with sodium methoxide in MeOH (1M, 0.3 ml) at 70°C for 2 hours. The solvent was removed and the crude residue partitioned in 1:1 $CHCl_3$:$H_2O$ (5 ml), then extracted in $CHCl_3$ (3x 2 ml). The solvent was removed to give the crude organic product, which was a mixture of several components, as above (TLC, $^1$H NMR spectroscopy).

Mycalamide A (4 mg), barium oxide (20 mg) and benzyl bromide (9 µl) were stirred in DMSO (0.3 ml) at 65°C overnight. Barium oxide (10 mg) was then added and the reaction stirred at 80°C overnight. $H_2O$ (0.6 ml) was added and the mixture transferred onto a reverse phase pipette column (200 mg C18, equilibrated to $H_2O$), which was then flushed with $H_2O$ (7 ml) and eluted with MeOH (7 ml). The MeOH fraction was evaporated to dryness to

give the crude organic product, which was a mixture of 2 major components (HPLC). Preparative reverse phase HPLC (25% $H_2O$ in MeOH) gave two fractions (1 mg, 1 mg), which were 7-*O*-benzyl pederamide (**6.14**) and 7*S*-*O*-benzyl pederamide (**6.15**), respectively.

**6.14**: an oil; FTIR (film) $\upsilon_{max}$ 3700-3100, (3464, 3338, 3203), 3070, 3031, 2972, 2927, 2855, 1685, 1607, 1490, 1455, 1379, 1325, 1228, 1146, 1102, 1075, 1048, 1015, 876, 740, 700 $cm^{-1}$; $^1H$ NMR data in Table 6.4, $^{13}C$ NMR data in Table 6.5 except the following aromatic resonances, ($CDCl_3$) δ137.06, 128.48, 128.44, 128.09 ppm; HREIMS *m/z* 319.1788 ($M^+$, +1.6 ppm for $C_{18}H_{25}NO_4$), 287.1536 ($M^+$-$CH_3OH$, +4.9 ppm for $C_{17}H_{21}NO_4$).

**6.15**: an oil; FTIR (film) $\upsilon_{max}$ 3700-3100, (3474, 3360), 3069, 3031, 2972, 2922, 2851, 1686, 1587, 1456, 1378, 1325, 1231, 1144, 1077, 1041, 1028, 892, 791, 735, 698 $cm^{-1}$; $^1H$ NMR data in Table 6.4, $^{13}C$ NMR data in Table 6.5 except the following aromatic resonances, ($CDCl_3$) δ128.48, 128.01 ppm; HREIMS *m/z* 319.1797 ($M^+$, +4.1 ppm for $C_{18}H_{25}NO_4$), 287.1518 ($M^+$-$CH_3OH$, -1.4 ppm for $C_{17}H_{21}NO_4$).

## 6.4 REACTION OF MYCALAMIDE A WITH SODIUM AZIDE

Mycalamide A (6 mg) was stirred with sodium azide (26 mg) in DMSO (0.3 ml) at 135°C for 4 days. $H_2O$ (0.6 ml) was added and the mixture transferred onto a reverse phase pipette column (200 mg C18, equilibrated to $H_2O$), which was then flushed with $H_2O$ (6 ml) and eluted with MeOH (6 ml). The MeOH fraction was evaporated to dryness and the crude organic products subjected to preparative silica gel TLC (developed twice in EtOAc). Six bands of silica were recovered and eluted with 1:3 EtOH:EtOAc to give six fractions (0.4 mg, 2.8 mg, 0.7 mg, 0.7 mg, 1.0 mg, 0.2 mg), which were 11*R* mycalamide A *trans* oxazolidinone (**6.20**), *Z* $\Delta^{10}$ 10-deformyl mycalamide A (**6.16**), a mixture consisting of mycalamide A and mycalamide A *cis* and *trans*

oxazolidinones (**5.2**, **5.3**), two more mixtures and crude pederamide (**3.4**), respectively. Preparative reverse phase HPLC (35% $H_2O$ in MeOH) on TLC fraction 4 gave three fractions (0.1 mg, 0.2 mg, 0.3 mg), which were mycalamide A *trans* oxazolidinone (**5.3**), $\Delta^{11}$ mycalamide A *trans* oxazolidinone (**6.21**) and 10*R* mycalamide A (**6.17**), respectively. Preparative reverse phase HPLC (45% $H_2O$ in MeOH) on TLC fraction 5 gave three fractions (0.2 mg, 0.3 mg, 0.4 mg), which were mycalamide A *trans* oxazolidinone (**5.3**), *E* $\Delta^{10}$ 10-deformyl mycalamide A (**6.19**) and 10*R* mycalamide A (**6.17**), respectively.

**6.16**: an oil; FTIR (film) $\upsilon_{max}$ 3600-3100, (3400), 3073, 2971, 2929, 2855, 1670, 1512, 1380, 1295, 1228, 1092, 1074, 1043, 1015, 910, 880, 735, 704 $cm^{-1}$, IR ($CHCl_3$) $\upsilon_{max}$ 3600-3300, 2900, 1670, 1380, 1080-1020, 905 $cm^{-1}$; $^1H$ and $^{13}C$ NMR data in Tables 6.8 and 6.9; HRFABMS *m/z* 442.2444 ($MH^+$-$CH_3OH$, +0.8 ppm for $C_{22}H_{36}NO_8$).

**6.17**: an oil; FTIR (film) $\upsilon_{max}$ 3600-3100, (3357), 2923, 2853, 1688, 1531, 1460, 1380, 1197, 1140, 1099, 1075, 1035, 1018 $cm^{-1}$; $^1H$ and $^{13}C$ NMR data in Tables 6.8 and 6.9; HRFABMS *m/z* 542.2339 ($MK^+$, -5.2 ppm for $C_{24}H_{41}NO_{10}K$).

(PURIFICATION AND CHARACTERISATION OF 10*R* MYCALAMIDE B)

Mycalamide B reacted with sodium methoxide in MeOH, as described in Section 5.4, and preparative TLC gave two fractions which were mixtures. In particular, fraction 2 (1 mg) contained mycalamide B *trans* oxazolidinone (**5.10**) and a second significant component ($^1H$ NMR spectroscopy). Preparative reverse phase HPLC (25% $H_2O$ in MeOH) gave three fractions (0.6 mg, 0.1 mg, 0.2 mg), which were a mixture of mycalamide B *trans* oxazolidinone (**5.10**) and its C7 epimer, a mixture and pure 10*R* mycalamide B (**6.18**), respectively.

**6.18**: an oil; $^1$H NMR data in Table 6.8; HRFABMS *m/z* 556.2562 ($MK^+$, +6.9 ppm for $C_{25}H_{43}NO_{10}K$).

**6.19**: an oil; $^1$H NMR data in Table 6.8.

**6.20**: an oil; $^1$H NMR data in Table 6.11; HRFABMS *m/z* 512.2248 ($MK^+$, -2.7 ppm for $C_{23}H_{39}NO_9K$).

**6.21**: an oil; $^1$H NMR data in Table 6.11; HRFABMS *m/z* 494.2194 ($MK^+$, +7.7 ppm for $C_{23}H_{37}NO_8K$).

*Z* $\Delta^{10}$, 10-Deformyl mycalamide A (**6.16**, 2 mg) was stirred with sodium azide (23 mg) in DMSO (0.3 ml) at 90°C for 6 days. $H_2O$ (0.5 ml) was added and the solution transferred onto a reverse phase pipette column (200 mg C18, equilibrated to $H_2O$), which was then flushed with $H_2O$ (6 ml) and eluted with MeOH (6 ml). The MeOH fraction was evaporated to dryness and the crude organic product then subjected to preparative silica gel TLC (developed twice in EtOAc). Three bands of silica were recovered and eluted with 1:4 EtOH:EtOAc to give three fractions (0.2 mg, 0.5 mg, 0.6 mg), which were an unknown mycalamide A oxazolidinone derivative, *Z* $\Delta^{10}$, 10-deformyl mycalamide A (**6.16**) and pure pederamide (**3.4**), respectively.

**3.4**: an oil; FTIR (film) $\upsilon_{max}$ 3484, 3358 (br), 3068, 2979, 2914, 2851, 1683, 1573, 1417, 1375, 1323, 1230, 1139, 1124, 1103, 1071, 1039, 1015, 999, 886 $cm^{-1}$; $^1$H and $^{13}$C NMR data in Tables 6.4 and 6.9; HREIMS *m/z* 197.1049 ($M^+$-$CH_3OH$, -1.6 ppm for $C_{10}H_{15}NO_3$), EIMS *m/z* (%) 197 (32), 155 (71), 153 (76), 151 (80), 143 (77), 134 (57), 123 (55), 109 (33), 107 (21), 96 (22), 95 (100), 93 (23), 91 (22), 81 (78), CIMS ($NH_3$) *m/z* (%) 199 (11), 198 (100, $MH^+$-$CH_3OH$), 180 (22), 155 (83), 153 (57), 152 (36), 134 (40), 125 (16), 123 (49), 109 (17), 96 (18), 95 (47), 81 (34).

## 6.5.1 REACTION OF MYCALAMIDE A WITH SODIUM BOROHYDRIDE

Mycalamide A (6 mg) was stirred with sodium borohydride (24 mg) in DMSO (0.3 ml) at 130°C for 2 days. $H_2O$ (0.6 ml) and formaldehyde (40%, 0.2 ml) were added (the latter to destroy excess sodium borohydride), then the mixture was transferred onto a reverse phase pipette column (200 mg C18, equilibrated to $H_2O$), which was then flushed with $H_2O$ (6 ml) and eluted with MeOH (6 ml). The MeOH fraction was evaporated to dryness and the crude organic product (10 mg) then subjected to preparative silica gel TLC (developed twice in 1:25 EtOH:EtOAc). Five bands of silica were recovered and eluted with 1:3 EtOH:EtOAc to give five fractions (0.9 mg, 0.3 mg, 1.2 mg, 1.2 mg, 1 mg), which were 10,12-*O*-dihydro mycalamide A (**6.22**), $\Delta^{4(5)}$ mycalamide A *trans* oxazolidinone (**6.23**), a mixture of mycalamide A and mycalamide A *cis* oxazolidinone (**5.2**), a mixture of mycalamide A and mycalamide A *trans* oxazolidinone (**5.3**) and mycalamide A *trans* oxazolidinone (**5.3**), respectively.

**6.22**: an oil; FTIR (film) $\upsilon_{max}$ 3700-3100, 2961, 2925, 2874, 1660, 1548, 1458, 1382, 1262, 1101, 1073, 1044, 1014, 735 $cm^{-1}$; $^1H$ and $^{13}C$ NMR data in Tables 6.8 and 6.9; HRFABMS *m/z* 444.2614 ($MH^+$-$CH_3OH$, +3.8 ppm for $C_{22}H_{38}NO_8$).

**6.23**: an oil; $^1H$ NMR data in Table 6.11; HRFABMS *m/z* 442.2426 ($MH^+$-$CH_3OH$, -3.3 ppm for $C_{22}H_{36}NO_8$).

Mycalamide A (1 mg) was stirred with sodium borohydride (1.5 mg) in EtOH (0.3 ml) for 4 hours at room temperature. No reaction was observed by TLC or $^1H$ NMR spectroscopy of the product obtained after standard workup procedures.

6.5.1.3 REDUCTION ATTEMPTS USING LITHIUM ALUMINIUM HYDRIDE

Mycalamide A (1 mg) was stirred with lithium aluminium hydride (0.3 mg) in dry THF (0.8 ml) at reflux temperature for 4 hours. The resulting solution was filtered over celite and the solvent removed to give the crude organic product, which was unreacted mycalamide A by TLC and $^1$H NMR spectroscopy.

Mycalamide A (1 mg) was stirred with lithium aluminium hydride (5 mg) in dry THF (0.5 ml) in a sealed vial at 70°C for 2 days. The resulting solution was filtered over celite, washing with $CH_2Cl_2$. The solvent was removed to give the crude organic product, a mixture of at least 4 components by TLC, so this was then subjected to preparative silica gel TLC (developed in EtOAc). Four bands of silica were recovered and eluted with 1:9 EtOH:EtOAc to give four fractions (0.1 mg, 0.3 mg, 0.1 mg, 0.2 mg), where fraction 2 was mycalamide A, but the remaining fractions had decomposed by TLC and $^1$H NMR spectroscopy.

6.5.2.1 REACTION OF MYCALAMIDE A WITH BARIUM OXIDE IN BENZENE

Mycalamide A (3 mg) was stirred with barium oxide (20 mg) in benzene (0.4 ml) in a sealed vial at 100°C for 20 hours. The solvent was removed and the crude residue partitioned in 1:1 $CHCl_3$:$H_2O$ (5 ml), then extracted in $CHCl_3$ (3x 2 ml). The solvents were removed to give two fractions (1 mg, 14 mg), representing organic and water soluble material respectively, but the former was a mixture (TLC, $^1$H NMR spectroscopy). Preparative reverse phase HPLC on this organic fraction (32% $H_2O$ in MeOH) gave two new fractions (0.5 mg, 0.3 mg), which were a mixture of mycalamide A and another component, and pure 10*R* mycalamide A (**6.17**), respectively. HPLC fraction 1 was then subjected to preparative silica gel TLC (developed twice in EtOAc) to give two further fractions (0.2 mg, 0.2 mg), which were mycalamide A and 7*S*

mycalamide A (**6.24**), respectively. The water soluble fraction above consisted of inorganic barium salts and the barium salt of a C7 carboxylate fragment (**6.25**).

**6.24**: an oil; $^{1}H$ NMR data in Table 6.7; FABMS *m/z* (%) 473 (3), 472 (8, $MH^{+}$-$CH_3OH$), 460 (10), 391 (15), 355 (10), 308 (24), 307 (83), 289 (65).

**6.25**: a salt; $^{1}H$ and $^{13}C$ NMR data in Tables 6.7 and 6.9; HRFABMS (-ve ion) *m/z* 199.0970 ($M^{-}$, -3.0 ppm for $C_{10}H_{15}O_4$).

Mycalamide A (3 mg) was stirred with barium oxide (20 mg) in benzene (0.3 ml) at 80°C for 2 hours. The solvent was removed and the crude residue partitioned in 1:1 $CHCl_3$:$H_2O$ (4 ml), then extracted in $CHCl_3$ (3x 2 ml). The solvents were removed to give two fractions (1.9 mg, 10 mg), representing organic and water soluble material respectively, as above. The crude organic fraction was a mixture of mycalamide A and at least 2 minor components, so it was subjected to preparative silica gel TLC (developed twice in EtOAc). Three bands of silica were recovered and eluted with 1:5 MeOH:$CH_2Cl_2$ to give three fractions (1.1 mg, 0.1 mg, 0.4 mg), which were mycalamide A, impure 7*S* mycalamide A (**6.24**) and a mixture of two unknown derivatives, possibly C7 ketones. The water soluble fraction above consisted of inorganic barium salts, the barium salt of a C7 carboxylate fragment (**6.25**) and a mixture of at least two minor mycalamide fragments derived from the right hand portion of the molecule.

The C7 carboxylate fragment (**6.25**, 0.5 mg), barium oxide (6 mg) and methyl iodide (3 µl) were stirred in DMSO (0.3 ml) at 70°C for 3 days. $H_2O$ (0.5 ml) was added and the mixture transferred onto a reverse phase pipette column (200 mg C18, equilibrated to $H_2O$), which was then flushed with $H_2O$ (8 ml) and eluted with MeOH (8 ml). The solvent was removed from the latter fraction to give the crude product which was a complex mixture by $^{1}H$ NMR spectroscopy.

## WORK DESCRIBED IN CHAPTER 7

### 7.2.1 OXIDATION OF MYCALAMIDE B WITH PYRIDINIUM DICHROMATE

Reagent preparation: Chromium trioxide (1 g) was dissolved in $H_2O$ (1 ml) and cooled in ice. Pyridine (0.8 ml) was added slowly, then acetone (4 ml) and the mixture set aside in a freezer for 2 hours. The orange crystals of pyridinium dichromate were collected by vacuum filtration, washed with acetone and dried under vacuum (1.5 g).

Mycalamide B (1.5 mg) was stirred with pyridinium dichromate (3.4 mg) in $CH_2Cl_2$ (0.3 ml) at room temperature for 3 days, then at 50°C for 1 hour. The resulting solution was filtered over celite and the solvent removed to give the crude organic product, which was a mixture of several components by TLC and $^1H$ NMR spectroscopy, including pederolactone (**3.6**), mycalamide B and other oxidation products. These were either not resolved or had decomposed by reverse phase HPLC and TLC, so this was abandoned.

### 7.2.2 REACTION OF MYCALAMIDE B WITH A RUTHENIUM(II) COMPLEX

Mycalamide B (3.5 mg), potassium carbonate (6 mg) and tris-triphenylphosphine ruthenium(II) chloride (12 mg) were stirred in dry benzene (0.4 ml, dried over molecular sieves) at 60°C for 7 hours. The solvent was removed and the crude residue subjected to preliminary silica gel column chromatography (200 mg Davisil), eluting with EtOAc. The solvent was removed to give the crude organic product (13 mg), which was then subjected to preparative silica gel TLC (developed in 1:1 PE:EtOAc). Five bands of silica were recovered and eluted with EtOAc to give five fractions (1-5) (1 mg, 8 mg, 2 mg, 0.5 mg, 1 mg), which were, a mixture of reagent derived material and mycalamide B, a mixture of reagent derived material and minor oxidation products, a mixture of two oxidation products, and two

mixtures of reagent derived material only, respectively. TLC fraction 3 was further purified by preparative reverse phase HPLC (35% $H_2O$ in MeOH) to give four fractions (0.4 mg, 0.5 mg, 0.5 mg, 0.3 mg), which were, reagent derived, *E* $\Delta^{16}$ 18-normycalamide B (**7.3**), *Z* $\Delta^{16}$ 18-normycalamide B (**7.4**) and an unknown derivative, respectively. TLC fraction 2 was also further purified, using the same HPLC system, to give four fractions (0.1 mg, 0.3 mg, 4 mg, 3 mg), which were 18-normycalamide A 17-aldehyde (**7.5**) and three complex mixtures, respectively.

**7.3**: an oil; FTIR (film) $\upsilon_{max}$ 3500-3200, (3353), 3065, 2954, 2921, 2849, 1678, 1656, 1529, 1462, 1438, 1378, 1261, 1102, 1072, 1031, 1012 $cm^{-1}$; $^1H$ and $^{13}C$ NMR data in Tables 7.1 and 7.3; HRFABMS *m/z* 454.2410 ($MH^+$-$CH_3OH$, -6.8 ppm for $C_{23}H_{36}NO_8$).

**7.4**: an oil; $^1H$ NMR data in Table 7.1; HRFABMS *m/z* 454.2401 ($MH^+$-$CH_3OH$, -8.7 ppm for $C_{23}H_{36}NO_8$).

### 7.3.1 REACTION OF MYCALAMIDE A WITH A RUTHENIUM(II) COMPLEX

Mycalamide A (3.5 mg) was stirred with tris-triphenylphosphine ruthenium(II) chloride (5 mg) in benzene (0.5 ml) at room temperature for 2 days. The solvent was removed and the crude products subjected to silica gel column chromatography (200 mg Davisil), developed in steps from PE to EtOAc. The major two fractions (6 mg combined), which eluted with 1:1 PE:EtOAc and EtOAc, were mixtures of reagent derived material and 18-normycalamide A 17-aldehyde (**7.5**), while a minor fraction (1.5 mg), which eluted in 1:19 EtOH:EtOAc, was a mixture of reagent derived material and mycalamide A.

Mycalamide A (3.7 mg), potassium carbonate (4.2 mg) and tris-triphenylphosphine ruthenium(II) chloride (14 mg) were stirred in benzene (0.3 ml) at 50°C for 2 hours. The solvent was removed and the crude residue

subjected to preliminary silica gel column chromatography (200 mg Davisil), eluting with EtOAc, then 1:9 EtOH:EtOAc, to give two fractions (11 mg, 3 mg), which were a mixture of reagent derived material and oxidation products, and a mixture of reagent derived material and mycalamide A, respectively. Fraction 1 was then subjected to preparative silica gel TLC (developed in EtOAc) to give one major fraction (9 mg), which was a complex mixture of reagent derived material and mycalamide A oxidation products in low yield.

### 7.3.2 REACTIONS WITH LEAD TETRAACETATE

Mycalamide B (2.3 mg) was stirred with lead tetraacetate (~8 mg) in pyridine (0.2 ml) and benzene (0.2 ml) at 30°C for 18 hours. The solution was concentrated (to 0.1 ml), then $H_2O$ (2 ml) was added and the mixture extracted with $CH_2Cl_2$ (3x 2 ml). The solvent was removed to give the crude organic product, which was unreacted mycalamide B.

Mycalamide A (4 mg) was stirred with lead tetraacetate (10 mg) in pyridine (0.2 ml) and benzene (0.2 ml) at room temperature for 1.5 hours. The solution was concentrated (to 0.1 ml), then $H_2O$ (2 ml) was added and the mixture extracted with $CH_2Cl_2$ (3x 2 ml). This extract was filtered and the solvent removed to give 3.8 mg of pure 18-normycalamide A 17-aldehyde (**7.5**).

**7.5**: an oil; FTIR (film) $\upsilon_{max}$ 3600-3100 (3350), 3065, 2968, 2924, 2852, 1725, 1678, 1527, 1454, 1380, 1260, 1100, 1033, 798, 734 $cm^{-1}$; $^1H$ and $^{13}C$ NMR data in Tables 7.1 and 7.3; HRFABMS *m/z* 440.2305 ($MH^+$-$CH_3OH$, +4.8 ppm for $C_{22}H_{34}NO_8$).

**7.6**: $^1H$ and $^{13}C$ NMR data in Tables 7.1 and 7.3.

## 7.4 REACTIONS OF 18-NORMYCALAMIDE A 17-ALDEHYDE

18-Normycalamide A 17-aldehyde (**7.5**, 1.5 mg) was stirred with sodium borohydride (1.2 mg) in MeOH (0.3 ml) at room temperature for 15 minutes. The solution was concentrated (to 0.1 ml), then $H_2O$ (2 ml) was added and the mixture extracted with $CH_2Cl_2$ (3x 2 ml). The solvent was removed to give 1.5 mg of pure 18-normycalamide A (**7.7**).

**7.7**: an oil; FTIR (film) $\upsilon_{max}$ 3600-3100 (3348), 3072, 2969, 2928, 2882, 1676, 1529, 1453, 1382, 1263, 1107, 1074, 1035 $cm^{-1}$; $^1H$ and $^{13}C$ NMR data in Tables 7.1 and 7.3; HRFABMS *m/z* 442.2426 ($MH^+$-$CH_3OH$, -3.4 ppm for $C_{22}H_{36}NO_8$).

18-Normycalamide A 17-aldehyde (**7.5**, 0.8 mg) was stirred with sodium metabisulphite (4 mg) in 1:1 $H_2O$:MeOH (0.4 ml) at room temperature for 16 hours, then at 50°C for 1.5 hours. The solvent was removed to give the crude product, which was a mixture of decomposition products by TLC and $^1H$ NMR spectroscopy.

## WORK DESCRIBED IN CHAPTER 8

### SYNTHESIS OF $PhC(OCH_3)=NH$

Benzonitrile (PhCN, 7.5 ml, 7 g) and dry MeOH (7 ml, 5.5 g) were sealed in a flask under nitrogen and cooled in ice. Acetyl chloride (6.5 ml, 7.2 g) was added and the solution stirred at 4°C for 14 hours. The resulting mixture was poured into aqueous sodium carbonate (5%, 200 ml), and this solution stirred for 5 minutes, then extracted with $CH_2Cl_2$ (3x 200 ml). The solvent was removed to give the crude organic product (7.46 g), which was a mixture of $PhC(OCH_3)=NH$ (**8.6**) and unreacted PhCN. Chromatography in two portions on Florisil (60 g), developed in $CH_2Cl_2$, gave 0.9 g pure PhCN

and 1.2 g 90% $PhC(OCH_3)=NH$ (**8.6**) (containing traces of $PhCOOCH_3$ and PhCN), with the remainder representing combined mixtures (5.3 g). The latter fraction was then subjected to silica gel column chromatography (60 g Davisil), developed in steps from $CH_2Cl_2$ to $MeOH/CH_2Cl_2$. Two fractions (3.1 g, 0.8 g), which eluted with $CH_2Cl_2$, were pure PhCN, and a mixture, respectively, while a third fraction (1.2 g), which eluted with 1:9 $MeOH:CH_2Cl_2$, was at least 80% pure $PhC(OCH_3)=NH$ (**8.6**), containing small amounts of $PhCOOCH_3$ and another phenyl component (not benzoic acid). Thus the overall purified yield of $PhC(OCH_3)=NH$ (**8.6**) was approximately 35%.

$PhC(OCH_3)=NH$ (**8.6**): an oil; $^1H$ NMR ($CDCl_3$) δ7.71 (Ph, broad d, 7.0), 7.41 (Ph, m), 3.91 ($OCH_3$, s) ppm, $^{13}C$ NMR ($CDCl_3$) δ168.20 (C=N), 132.52, 130.75, 128.33 and 126.59 (Ph), 53.29 ($OCH_3$) ppm.

SYNTHESIS OF *S*-LACTIC ACID ACETATE (CRUDE)

*S*-Lactic acid (AR grade, ~80%, 316 mg) was heated with $H_2O$ (100 µl) at 70°C for 30 minutes to remove anhydrides. The solution was then concentrated under nitrogen and pumped under vacuum for 5 minutes to give the crude starting material (240 mg). Pyridine (1 ml) and acetic anhydride (1 ml) were added and the mixture allowed to stand at room temperature for 1 day. This solution was then concentrated under nitrogen (to 0.5 ml), then partitioned in 1:1 $CHCl_3:H_2O$ (10 ml) and extracted with $CHCl_3$ (3x 6 ml). The solvent was removed under nitrogen and the sample pumped under vacuum to give 215 mg of viscous liquid, which was mostly *S*-lactic acid acetate (**8.5**), containing no more than 26 mg of pyridine and 17 mg of acetic acid by $^1H$ NMR spectroscopy.

*S*-Lactic acid acetate (**8.5**): a viscous liquid; $^1H$ NMR ($CDCl_3$) δ5.10 (CH, q, 7.1), 2.13 ($OCOCH_3$, s), 1.52 ($CH_3$, d, 7.1) ppm, $^{13}C$ NMR ($CDCl_3$) δ170.48 (C=O), 68.65 (CH), 20.72 ($COCH_3$), 16.92 ($CH_3$) ppm.

SYNTHESIS OF (*SR*, *SS*)-$CH_3CHOH(C{=}O)NHCH(OCH_3)Ph$

*S*-Lactic acid acetate (**8.5**, 215 mg crude, 1 mole equiv.) was dissolved in pyridine (300 µl) and $CH_2Cl_2$ (1 ml) and sealed under nitrogen. Thionyl chloride (140 µl, 1.5 mole equiv.) was added and the mixture stirred for 10 minutes at room temperature. To this was added a solution of 90% $PhC(OCH_3){=}NH$ (**8.6**, 135 mg, 0.7 mole equiv.), triethylamine (215 µl) and $CH_2Cl_2$ (0.1 ml) and the resulting mixture was stirred at room temperature for 70 minutes. This solution was concentrated under nitrogen (to 0.5 ml) and reacted with a suspension of sodium borohydride (600 mg) in EtOH (5 ml) for 10 minutes. The reaction was quenched with brine (150 ml) then this mixture extracted with $CHCl_3$ (3x 100 ml). The solvent was removed to give 270 mg of a crude organic product, which was then subjected to silica gel column chromatography (3 g Davisil), developed in steps from $CH_2Cl_2$ to MeOH/$CHCl_3$, in two portions and the results combined. One fraction (76 mg), which eluted with $CHCl_3$, was an approximately 3:1 mixture of the two diastereomeric products (**8.7**, **8.8**) and their acetates (**8.9**, **8.10**), while a second fraction (63 mg), which eluted with 1:19 MeOH:$CHCl_3$, was a 2:1 mixture of the two diastereomeric products only (**8.7**, **8.8**). Thus the overall yield of **8.7** and **8.8** was about 63%, with a further 9% yield of the acetates **8.9** and **8.10**.

These fractions were further analysed and purified by preparative TLC and HPLC. Firstly, a subsample of Fraction 2 (15 mg) was subjected to preparative normal phase HPLC (55% EtOAc in Hexane), using a chiral (*R*) phenyl urea column, to give two major fractions (6 mg, 3 mg), which were a mixture of the two diastereomeric products (**8.7**, **8.8**), and mostly an unknown phenyl derivative, respectively. Secondly, preparative silica gel TLC (developed four times in $CHCl_3$) on a subsample of Fraction 1 (30 mg) gave seven fractions (7 mg, 7 mg, 2 mg, 3 mg, 2 mg, 3 mg, 0.5 mg), which were a

1:1 mixture of the two diastereomeric products (**8.7**, **8.8**), a 1:6 mixture of the two diastereomeric products (**8.7**, **8.8**), a mixture of one product diastereomer and an *N*-acetyl compound (**8.11**), this *N*-acetyl compound (**8.11**), and three mixtures of the diastereomeric product acetates (**8.9**, **8.10**). Finally, preparative silica gel TLC (developed four times in $CHCl_3$) on a subsample of Fraction 2 (15 mg) gave five fractions (5 mg, 5 mg, 2.5 mg, 1 mg, 0.5 mg), of which the first four fractions were approximately 9:1, 6:1, 3:1 and 1:4 mixtures of the diastereomeric products (**8.7**, **8.8**) respectively, but the fifth fraction consisted only of impurities.

*N*-Acetyl compound (**8.11**): an oil; $^1H$ NMR ($CDCl_3$) δ7.37 (Ph, m), 6.11 (CH, d, 9.5), 5.92 (NH, broad d, 9.5), 3.46 ($OCH_3$, s), 2.05 ($OCOCH_3$, s) ppm.

Diastereomeric products (**8.7**, **8.8**): oils; $^1H$ and $^{13}C$ NMR data in Table 8.1; HREIMS *m/z* 194.0820 ($M^+$-$CH_3$, +1.5 ppm for $C_{10}H_{12}NO_3$), EIMS *m/z* (%) 195 (8), 194 (59), 178 (8), 177 (12), 176 (17), 133 (8), 122 (19), 121 (100), 106 (21), 105 (33), 104 (22), 91 (13), 78 (10), 77 (32)

Mixed diastereomeric product acetates (**8.9**, **8.10**): an oil; $^1H$ NMR ($CDCl_3$) δ7.38 (Ph, m), 6.51 (NH, broad d, 9.6), 6.15 and 6.14 (H5, 2xd, 9.6), 5.23 and 5.19 (H2, 2xq, 6.9), 3.47 and 3.45 (5-$OCH_3$, 2xs), 2.10 and 2.07 ($OCOCH_3$, 2xs), 1.52 and 1.49 ($CH_3$, 2xd, 6.8) ppm, $^{13}C$ NMR ($CDCl_3$) δ170.84, 170.80 (C=O), 169.46, 169.43 (C3), 138.94, 138.91, 128.64, 128.59, 125.77 and 125.74 (Ph), 81.04 (C5), 70.62, 70.55 (C2), 56.20, 56.12 (5-$OCH_3$), 20.99, 20.96 ($COCH_3$), 17.91, 17.88 ($CH_3$) ppm; HREIMS *m/z* 220.0972 ($M^+$-$CH_3O$, -0.9 ppm for $C_{12}H_{14}NO_3$), EIMS *m/z* (%) 220 (10), 192 (21), 191 (83), 190 (41), 176 (13), 162 (14), 159 (11), 136 (49), 132 (62), 131 (19), 122 (42), 121 (100), 115 (30), 106 (73), 105 (75), 104 (46), 91 (34), 87 (78), 78 (23), 77 (81).

SYNTHESIS OF *S*-LACTIC ACID ACETATE

Calcium L(+)-lactate (352 mg) was slurried with acetic anhydride (1 ml) and pyridine (1 ml) for 3 minutes at room temperature, until crystallisation occurred, then allowed to stand for 10 minutes. $H_2O$ (8 ml) was added and the solution extracted with $CHCl_3$ (3x 6 ml). The solvent was removed under nitrogen and the sample pumped under vacuum to give 165 mg of viscous liquid, which was mostly *S*-lactic acid acetate (**8.5**), containing no more than 28 mg of pyridine and 9 mg of acetic acid by $^1H$ NMR spectroscopy.
*S*-Lactic acid acetate (**8.5**): a viscous liquid; $^1H$ NMR ($CDCl_3$) δ5.09 (CH, q, 7.1), 2.11 ($OCOCH_3$, s), 1.50 ($CH_3$, d, 7.2) ppm, $^{13}C$ NMR ($CDCl_3$) δ174.94, 170.60 (C=O), 68.85 (CH), 20.70 ($COCH_3$), 16.97 ($CH_3$) ppm.

SYNTHESIS OF (*SR*, *SS*)-$CH_3CHOH(C{=}O)NHCH(OCH_3)Ph$

*S*-Lactic acid acetate (**8.5**, 165 mg crude) was dissolved in pyridine (280 µl) and $CH_2Cl_2$ (1 ml) and sealed under nitrogen. Thionyl chloride (123 µl) was added and the mixture stirred for 10 minutes at room temperature. To this was added a solution of 90% $PhC(OCH_3){=}NH$ (**8.6**, 118 mg), triethylamine (187 µl) and $CH_2Cl_2$ (0.1 ml) and the resulting mixture was stirred at room temperature for 70 minutes. This solution was concentrated under nitrogen (to 1 ml), cooled in ice, and reacted with a suspension of sodium borohydride (500 mg) in EtOH (5 ml) for 30 minutes. The reaction was quenched with brine (50 ml) then this mixture extracted with $CHCl_3$ (3x 50 ml). The solvent was removed to give 285 mg of a crude organic product, which was then subjected to silica gel column chromatography (10 g Davisil), developed in steps from $CH_2Cl_2$ to MeOH/$CHCl_3$. Three fractions (60 mg combined), which eluted with $CHCl_3$, were all mixtures of the diastereomeric product acetates (**8.9**, **8.10**), while two further fractions (46 mg, 30 mg), which also eluted with $CHCl_3$, were an impure mixture of the diastereomeric acetates

(**8.9**, **8.10**), and a 1:1 mixture of the diastereomeric products (**8.7**, **8.8**), respectively. A sixth fraction (10 mg), which eluted with 1% MeOH/$CHCl_3$, was a 9:1 mixture of the two diastereomeric products (**8.7**, **8.8**). ($^1H$ and $^{13}C$ NMR spectroscopy and mass spectroscopy results as above). Thus the overall yield of acetates **8.9** and **8.10** was about 53%, with a 24% yield of **8.7** and **8.8**.

SYNTHESIS OF *R*-LACTIC ACID ACETATE

Lithium D(-)-lactate (100 mg) was stirred with acetic anhydride (1 ml) and pyridine (1 ml) for 18 hours at room temperature. $H_2O$ (8 ml) was added and the mixture extracted with $CHCl_3$ (4x 7 ml). The aqueous portion was also acidified and reextracted. The solvent was removed from this combined extract under nitrogen and the sample pumped under vacuum to give 94 mg of viscous liquid, which was mostly *R*-lactic acid acetate (**8.12**), containing no more than 14 mg of pyridine and 5 mg of acetic acid by $^1H$ NMR spectroscopy. *R*-Lactic acid acetate (**8.12**): a viscous liquid; $^1H$ NMR ($CDCl_3$) δ5.10 (CH, q, 7.1), 2.12 ($OCOCH_3$, s), 1.52 ($CH_3$, d, 7.2) ppm.

SYNTHESIS OF (*RR*, *RS*)-$CH_3CHOH(C{=}O)NHCH(OCH_3)Ph$

*R*-Lactic acid acetate (**8.12**, 94 mg crude) was dissolved in pyridine (160 µl) and $CH_2Cl_2$ (1 ml) and sealed under nitrogen. Thionyl chloride (71 µl) was added and the mixture stirred for 20 minutes at room temperature. To this was added a solution of 90% $PhC(OCH_3){=}NH$ (**8.6**, 70 mg), triethylamine (110 µl) and $CH_2Cl_2$ (0.1 ml) and the resulting mixture was stirred at room temperature for 80 minutes. This solution was concentrated under nitrogen (to 1 ml), cooled in ice, and reacted with a suspension of sodium borohydride (300 mg) in EtOH (3 ml) for 4 hours. The reaction was quenched with brine (50 ml) then this mixture extracted with $CHCl_3$ (3x 50 ml). The solvent was removed to give 165 mg of a crude organic product, which was then subjected

to silica gel column chromatography (10 g Davisil), developed in steps from $CH_2Cl_2$ to MeOH/$CHCl_3$. Two fractions (22 mg, 60 mg), which eluted with $CHCl_3$, were both mixtures of the diastereomeric product acetates (**8.15**, **8.16**) and a third fraction (15 mg), which also eluted with $CHCl_3$, was a 1:3 mixture of these acetates and the diastereomeric products (**8.13**, **8.14**). A fourth fraction (4 mg), which eluted with 1% MeOH/$CHCl_3$, was a 4:1 mixture of the two diastereomeric products only (**8.13**, **8.14**). ($^1H$ and $^{13}C$ NMR spectroscopy results were almost identical to those for the products from *S*-lactic acid). Thus the overall yield of acetates **8.15** and **8.16** was about 73%, with a 15 % yield of **8.13** and **8.14**.

Mixed diastereomeric products (**8.13**, **8.14**): an oil; HREIMS *m/z* 194.0816 ($M^+$-$CH_3$, -0.7 ppm for $C_{10}H_{12}NO_3$), EIMS *m/z* (%) 195 (6), 194 (49), 178 (7), 177 (11), 176 (16), 133 (8), 122 (15), 121 (100), 106 (21), 105 (38), 104 (20), 91 (11), 78 (10), 77 (27).

Mixed diastereomeric product acetates (**8.15**, **8.16**): an oil; HREIMS *m/z* 220.0977 ($M^+$-$CH_3O$, +1.7 ppm for $C_{12}H_{14}NO_3$), EIMS *m/z* (%) 220 (4), 192 (9), 191 (57), 190 (15), 179 (4), 176 (6), 162 (6), 159 (5), 136 (14), 133 (4), 132 (22), 122 (12), 121 (100), 115 (8), 106 (23), 105 (24), 104 (13), 91 (10), 87 (27), 78 (6), 77 (28), 73 (6).

# REFERENCES


1. Ferguson, L. N. *Chem. Soc. Rev.* **1975**, *4*, 289.
2. Albert, A. *Selective Toxicity*, 7th ed.; Chapman and Hall Ltd.: London, 1985; pp 3-20.
3. Albert, A. *Selective Toxicity*, 7th ed.; Chapman and Hall Ltd.: London, 1985; pp 206-237.
4. Albert, A. *Selective Toxicity*, 7th ed.; Chapman and Hall Ltd: London, 1985; pp 271-281.
5. Copp, B. R. Ph. D. Thesis; University of Canterbury, 1989; pp 3-8.
6. Munro, M. H. G.; Blunt, J. W.; Barns, G.; Battershill, C, N.; Lake, R. J.; Perry, N. B. *Pure Appl. Chem.* **1989**, *61*, 529.
7. Faulkner, D. J. *Nat. Prod. Rep.* **1984**, *1*, 251.
8. Faulkner, D. J. *Nat. Prod. Rep.* **1984**, *1*, 551.
9. Faulkner, D. J. *Nat. Prod. Rep.* **1986**, *3*, 1.
10. Faulkner, D. J. *Nat. Prod. Rep.* **1987**, *4*, 539.
11. Faulkner, D. J. *Nat. Prod. Rep.* **1988**, *5*, 613.
12. Faulkner, D. J. *Nat. Prod. Rep.* **1990**, *7*, 269.
13. Munro, M. H. G.; Luibrand, R. T.; Blunt, J. W. in *Biorganic Marine Chemistry*, edited by P. J. Scheuer; Springer-Verlag: Berlin, 1987; Vol. 1, pp 93-176.
14. World Health Organisation *Rapid Laboratory Techniques for the Diagnosis of Viral Infections*; WHO: Geneva, Switzerland, 1981; pp 6, 17-25. (Technical Reports Series 661)
15. Albert, A. *Selective Toxicity*, 7th ed.; Chapman and Hall Ltd.: London, 1985; pp 21-55.
16. Albert, A. *Selective Toxicity*, 7th ed.; Chapman and Hall Ltd.: London, 1985; pp 491-509.

17. Blunt, J. W.; Munro, M. H. G.; Battershill, C.N.; Copp, B. R.; McCombs, J. D.; Perry, N. B.; Prinsep, M.; Thompson, A. M. *New J. Chem.* **1990**, *14*, 761.

18. Perry, N. B.; Blunt, J. W.; Munro, M. H. G.; Pannell, L. K. *J. Am. Chem. Soc.* **1988**, *110*, 4850.

19. Perry, N. B.; Blunt, J. W.; Munro, M. H. G.; Thompson, A. M. *J. Org. Chem.* **1990**, *55*, 223.

20. Corriero, G.; Madaio, A.; Mayol, L.; Piccialli, V.; Sica, D. *Tetrahedron* **1989**, *45*, 277.

21. Kato, Y.; Fusetani, N.; Matsunaga, S.; Hashimoto, K. *Tetrahedron Lett.* **1985**, *26*, 3483.

22. Fusetani, N.; Yasumuro, K.; Matsunaga, S.; Hashimoto, K. *Tetrahedron Lett.* **1989**, *30*, 2809.

23. Capon, R. J.; MacLeod, J. K. *Tetrahedron* **1985**, *41*, 3391.

24. Capon, R. J.; MacLeod, J. K. *J. Nat. Prod.* **1987**, *50*, 225.

25. Stonik, V. A.; Makar'eva, T. N.; Antanov, A. S.; Elyakov, G. B. *Khim. Prir. Soedin.* **1981**, 104.

26. Dr. P. T. Northcote, personal communication.

27. Cardani, C.; Ghiringhelli, D.; Mondelli, R.; Quilico, A. *Tetrahedron Lett.* **1965**, 2537.

28. Cardani, C.; Ghiringhelli, D.; Quilico, A.; Selva, A. *Tetrahedron Lett.* **1967**, 4023.

29. Societa Farmaceutici Italia Brit. 932,875, July 31 1963. (CA59:11194f)

30. Quilico, A.; Cardani, C.; Ghiringhelli, D.; Pavan, M. *Chim. Ind.* **1961**, *43*, 1434.

31. Sakemi, S.; Ichiba, T.; Kohmoto, S.; Saucy, G.; Higa, T. *J. Am. Chem. Soc.* **1988**, *110*, 4851.

32. Anon. *Chem. Br.* **1982**, *18*, 696.

33. Pavan, M.; Bo, G. *Physiol. Comparata et Oecol.* **1953**, *3*, 307.

34. Furusaki, A.; Watanabe, T. *Tetrahedron Lett.* **1968**, 6301.

35. Pavan, M. *Atti. Accad. Nazl. Ital. Entomol. Rend.* **1962**, *10*, 119.

36. Leigheb, G.; Moroni, P.; Pavan, M. *Chron. Derm.* **1983**, *14*, 357.

37. Pavan, M. *Chron. Derm.* **1983**, *14*, 301.

38. Boggio, P.; Davalli, R.; Leigheb, G.; Moroni, P.; Pavan, M. *Chron. Derm.* **1985**, *16*, 249.

39. Brega, A.; Falaschi, A.; De Carli, L.; Pavan, M. *J. Cell Biol.* **1968**, *36*, 485.

40. Soldati, M.; Fioretti, A.; Ghione, M. *Experientia* **1966**, *22*, 176.

41. Sentein, P. *Caryologia*, **1975**, *28*, 163.

42. Jacobs-Lorena, M.; Brega, A.; Baglioni, C. *Biochim. Biophys. Acta* **1971**, *240*, 263.

43. Carrasco, L.; Vazquez, D. *J. Antibiotics* **1972**, *25*, 732.

44. Barbacid, M.; Fresno, M.; Vazquez, D. *J. Antibiotics* **1975**, *28*, 453.

45. Carrasco, L.; Battaner, E.; Vazquez, D. *Methods Enzymol.* **1974**, *30*, 282.

46. Vazquez, D. *Inhibitors of Protein Biosynthesis*; Springer-Verlag: Berlin, 1979; pp 1-14.

47. Vazquez, D. *Inhibitors of Protein Biosynthesis*; Springer-Verlag: Berlin, 1979; pp 155-163.

48. Stryer, L. *Biochemistry*; W. H. Freeman and Co.: San Francisco, 1975; pp 675-6.

49. Albert, A. *Selective Toxicity*, 7th ed.; Chapman and Hall Ltd.: London, 1985; pp 143-7, 198-9.

50. Baglioni, C.; Jacobs-Lorena, M.; Meade, H. *Biochim. Biophys. Acta* **1972**, *277*, 188.

51. Carrasco, L.; Fernandez-Puentes, C.; Vazquez, D. *Mol. Cell. Biochem.* **1976**, *10*, 97.

52. Jimenez, A.; Carrasco, L.; Vazquez, D. *Biochemistry* **1977**, *16*, 4727.

53. Grollman, A. P.; Jarkovsky, Z. in *Antibiotics Vol III: Mechanism of Action of Antimicrobial and Antitumor Agents*, edited by J. W. Corcoran and F. E. Hahn; Springer-Verlag: Berlin, 1975; pp 420-435.

54. Levine, M. R.; Dancis, J.; Pavan, M.; Cox, R. P. *Pediat. Res.* **1974**, *8*, 606.

55. Carollo-Cusimano, T. *Acta Embr. Exp.* **1979**, 335.

56. Bernocchi, G.; Garagna, S.; Manfredi-Romanini, M. G.; Arrigoni, E.; Benzi, G.; Pavan, M. *Chron. Derm.* **1983**, *14*, 353.

57. Burres, N. S.; Clement, J. J. *Cancer Res.* **1989**, *49*, 2935.

58. Dr. N. B. Perry, personal communication.

59. Jennings, L., Christchurch Hospital Board, personal communication.

60. Stryer, L. *Biochemistry*; W. H. Freeman and Co.: San Francisco, 1975; pp 726-7.

61. Ogawara, H.; Higashi, K.; Perry, N. B. *Comp. Biochim. Biophys.* **1991** (in press).

62. Ogawara, H.; Hasumi, Y.; Higashi, K.; Ishii, Y.; Saito, T.; Watanabe, S.; Suzuki, K.; Kobori, M.; Tanaka, K.; Akiyama, T. *J. Antibiotics* **1989**, *42*, 1530.

63. Tanaka, H.; Kuroda, A.; Manusawa, H.; Hatanaka, H.; Kino, T.; Goto, T.; Hashimoto, M. *J. Am. Chem. Soc.* **1990**, *109*, 5031.

64. Rosen, M. K.; Standaert, R. F.; Galat, A.; Nakatsuka, M.; Schreiber, S. L. *Science* **1990**, *248*, 863.

65. Albers, M. W.; Walsh, C. T.; Schreiber, S. L. *J. Org. Chem.* **1990**, *55*, 4984.

66. Harding, M. W.; Galat, A.; Uehling, D. E.; Schreiber, S. L. *Nature* **1989**, *341*, 758.

67. Heischkeil, R. *Z. Tropenmed. Parasitol.* **1973**, *24*, 505. (CA80:115961h)

68. Munro, M. H. G.; Perry, N. B.; Blunt, J. W. Eur. Pat. Appl. EP 289203, 2 Nov 1988. (CA110:88610x)

69. Blunt, J. W.; Munro, M. H. G.; Perry, N. B.; Thompson, A. M. U. S. US 4868204, 19 Sep 1989. (CA113:114949y)

70. Kessler, H. *Angew. Chem. Int. Ed. Eng.* **1982**, 512.

71. Kaminski, J. J.; Puchalski, C.; Solomon, D. M.; Rizvi, R. K.; Conn, D. J.; Elliott, A. J.; Lovey, R. G.; Guzik, H.; Chiu, P. J. S.; Long, J. F.; McPhail, A. T. *J. Med. Chem.* **1989**, *32*, 1686.

72. Loosli, H.; Kessler, H.; Oschkinat, H.; Weber, H.; Petcher, T. J.; Widmer, A. *Helv. Chim. Acta* **1985**, *68*, 682.

73. Issaq, H. J.; Muschik, G. M. *Int. Lab.* **1988**, 18.

74. Deeg, M.; Hagenmaier, H.; Kretschmer, A. *J. Antibiotics* **1987**, *40*, 320.

75. van den Brook, L. A. G. M.; Lazaro, E.; Zylicz, Z.; Fennis, P. J.; Missler, F. A. N.; Lelieveld, P.; Garzotto, M.; Wagener, D. J. T.; Ballesta, J. P. G.; Ottenheijm, H. C. J. *J. Med. Chem.* **1989**, *32*, 2002.

76. Flowers, H. M in *The Chemistry of the Hydroxyl Group*, edited by S. Patai; Interscience: London, 1971; pp 1001-1015.

77. Ferrier, R. J.; Collins, P. M. *Monosaccharide Chemistry*; Penguin Books Ltd.: England, 1972; pp 184-195.

78. Greene, T. W. *Protective Groups in Organic Synthesis*; J. Wiley and Sons: New York, 1981; pp 10-86.

79. Findlay, J. A.; Radics, L. *Can. J. Chem* **1980**, *58*, 579.

80. Bax, A.; Freeman, R. *J. Magn. Reson.* **1981**, *44*, 542.

81. Bax, A.; Freeman, R.; Morris, G. *J. Magn. Reson.* **1981**, *42*, 164.

82. Kinns, M.; Sanders, J. K. M. *J. Magn. Reson.* **1984**, *56*, 518.

83. Perry, N. B.; Blunt, J. W.; Munro, M. H. G. *Magn. Reson. Chem.* **1989**, *27*, 624.

84. Perry, N. B.; Blunt, J. W.; Munro, M. H. G.; Thompson, A. M. (manuscript yet to be submitted for publication).

85. Muller, L. *J. Am. Chem. Soc.* **1979**, *101*, 4481.

86. Bax, A.; Summers, M. F. *J. Am. Chem. Soc.* **1986**, *108*, 2093.

87. Martin, G. E.; Zektzer, A. S. *Magn. Reson. Chem.* **1988**, *26*, 631.

88. Bax, A.; Morris, G. A. *J. Magn. Reson.* **1981**, *42*, 501.

89. Reynolds, W. F.; Hughes, D. W.; Perpick-Dumont, M. *J. Magn. Reson.* **1985**, *63*, 413.

90. Matsuda, F.; Yanagiya, M.; Matsumoto, T. *Tetrahedron Lett.* **1982**, *23*, 4043.

91. Hong, C. Y.; Kishi, Y. *J. Org. Chem.* **1990**, *55*, 4242.

92. Veber, D. F.; Holly, F. W.; Nutt, R. F.; Bergstrand, S. J.; Brady, S. F.; Hirschmann, R.; Glitzer, M. S.; Saperstein, R. *Nature* **1979**, *280*, 512.

93. Bonamartini Corradi, A.; Mangia, A.; Nardelli, M.; Pelizzi, G. *Gazz. Chim. Ital.* **1971**, *101*, 591.

94. Cardani, C.; Ghiringhelli, D.; Mondelli, R.; Quilico, A. *Gazz. Chim. Ital.* **1966**, *96*, 3.

95. Matsumoto, T.; Tsutsui, S.; Yanagiya, M.; Yasuda, S.; Maeno, S.; Kawashima, J.; Ueta, A.; Murakami, M. *Bull. Chem. Soc. Japan* **1964**, *37*, 1892.

96. Silverstein, R. M.; Bassler, G. C.; Morrill, T. C. *Spectrometric Identification of Organic Compounds*, 4th ed.; J. Wiley and Sons: New York, 1981; pp 106-127.

97. Selva, A. *Gazz. Chim. Ital.* **1968**, *98*, 1464.

98. Silverstein, R. M.; Bassler, G. C.; Morrill, T. C. *Spectrometric Identification of Organic Compounds*, 4th ed.; J. Wiley and Sons: New York, 1981; pp 188-210.

99. Wagner, G. *J. Magn. Reson.* **1983**, *55*, 151.

100. IUPAC Commission on the Nomenclature of Organic Chemistry *Pure Appl. Chem.* **1976**, *45*, 13.

101. Silverstein, R. M.; Bassler, G. C.; Morrill, T. C. *Spectrometric Identification of Organic Compounds*, 4th ed.; J. Wiley and Sons: New York, 1981; pp 220-237.

102. Sternhell, S. *Quart. Rev. Chem. Soc.* **1969**, *23*, 236.

103. Haasnoot, C. A. G.; de Leeuw, F. A. M. M.; Altona, C. *Tetrahedron* **1980**, *36*, 2783.

104. Jackman, L. M.; Sternhell, S. *Applications of Nuclear Magnetic Resonance Spectroscopy in Organic Chemistry*, 2nd ed.; Pergamon Press Ltd.: Oxford, 1969; pp 316-344.

105. Booth, H.; Khedhair, K. A.; Readshaw, S. A. *Tetrahedron* **1987**, *43*, 4699.

106. Ferrier, R. J.; Collins, P. M. *Monosaccharide Chemistry*; Penguin Books Ltd.: England, 1972; pp 32-49.

107. Robin, M. B.; Bovey, F. A.; Basch, H. in *The Chemistry of Amides*, edited by J. Zabicky (S. Patai series editor); Interscience: New York, 1970; pp 1-37.

108. Bystrov, V. F.; Ivanov, V. T.; Portnova, S. L.; Balashova, T. A.; Ovchinnikov, Y. A. *Tetrahedron* **1973**, *29*, 873.

109. Mattinen, J.; Pihlaja, K.; Czombos, J.; Bartok, M. *Tetrahedron* **1987**, *43*, 2761.

110. Ferrier, R. J.; Collins, P. M. *Monosaccharide Chemistry*; Penguin Books Ltd.: England, 1972; pp 214-221.

111. Swaelens, G.; Anteunis, M. *Tetrahedron Lett.* **1970**, 561.

112. Cahn, R. S.; Ingold, C.; Prelog, V. *Angew. Chem. Int. Ed. Eng.* **1966**, *5*, 385.

113. Bhatti, A. K.; Anteunis, M. *Tetrahedron Lett.* **1973**, 71.

114. Dalling, D. K.; Grant, D. M.; Johnson, L. F. *J. Am. Chem. Soc.* **1971**, *93*, 3678.

115. Blunt, J. W.; Coxon, J. M.; Lindley, N. B.; Lane, G. A. *Aust. J. Chem.* **1976**, *29*, 967.

116. Wu, T.; Goekjian, P. G.; Kishi, Y. *J. Org. Chem.* **1987**, *52*, 4819.

117. Silverstein, R. M.; Bassler, G. C.; Morrill, T. C. *Spectrometric Identification of Organic Compounds*, 4th ed.; J. Wiley and Sons: New York, 1981; pp 258-272.

118. Stothers, J. B. *Carbon-13 NMR Spectroscopy*, (Organic Chemistry: A Series of Monographs, Vol. 24, edited by A. T. Blomquist and H. Wasserman); Academic Press: New York, 1972; pp 144-151, 295-301.

119. Eliel, E. L.; Manoharan, M.; Pietrusiewicz, R. M.; Hargrave, K. D. *Org. Magn. Reson.* **1983**, *21*, 94.

120. Dalling, D. K.; Grant, D. M. *J. Am. Chem. Soc.* **1972**, *94*, 5318.

121. Stothers, J. B. *Carbon-13 NMR Spectroscopy*, (Organic Chemistry: A Series of Monographs, Vol. 24, edited by A. T. Blomquist and H. Wasserman); Academic Press: New York, 1972; pp 420-3.

122. Cohen, N. C.; Blaney, J. M.; Humblet, C.; Gund, P.; Barry, D. C. *J. Med. Chem.* **1990**, *33*, 885.

123. Jackman, L. M.; Sternhell, S. *Applications of Nuclear Magnetic Resonance Spectroscopy in Organic Chemistry*, 2nd ed.; Pergamon Press Ltd.: Oxford, 1969; pp 61-95.

124. Howard, A. E.; Kollman, P. A. *J. Med. Chem.* **1988**, *31*, 1669.

125. A copy of the extensively rewritten MODEL program of C. Still (version KS 2.94) was provided by Professor Kosta Steliou of the University of Montreal.

126. Matsumoto, T.; Yanagiya, M.; Maeno, S.; Yasuda, S. *Tetrahedron Lett.* **1968**, 6297.

127. Matsuda, F.; Tomiyoshi, N.; Yanagiya, M.; Matsumoto, T. *Tetrahedron* **1988**, *44*, 7063.

128. Willson, T. M.; Kocienski, P.; Jarowicki, K.; Isaac, K.; Hitchcock, P. M.; Faller, A.; Campbell, S. F. *Tetrahedron* **1990**, *46*, 1767.

129. Willson, T.; Kocienski, P.; Faller, A.; Campbell, S. *J. Chem. Soc. Chem. Commun.* **1987**, 106.

130. Matsuda, F.; Tomiyoshi, N.; Yanagiya, M.; Matsumoto, T. *Tetrahedron Lett.* **1983**, *24*, 1277.

131. Greene, T. W. *Protective Groups in Organic Synthesis*; J. Wiley and Sons: New York, 1981; pp 1-9.

132. Jarowicki, K.; Kocienski, P.; Marczak, S.; Willson, T. *Tetrahedron Lett.* **1990**, *31*, 3433.

133. Adams, M. A.; Duggan, A. J.; Smolanoff, J.; Meinwald, J. *J. Am. Chem. Soc.* **1979**, *101*, 5364.

134. Nakata, T.; Nagao, S.; Mori, N.; Oishi, T. *Tetrahedron Lett.* **1985**, *26*, 6461.

135. Nakata, T.; Nagao, S.; Oishi, T. *Tetrahedron Lett.* **1985**, *26*, 6465.

136. Corey, E. J.; Venkateswarlu, A. *J. Am. Chem. Soc.* **1972**, *94*, 6190.

137. Hurst, D. T.; McInnes, A. G. *Can. J. Chem.* **1965**, *43*, 2004.

138. Greene, T. W. *Protective Groups in Organic Synthesis*; J. Wiley and Sons: New York, 1981; pp 296-314.

139. Chapman, A. T. *J. Am. Chem. Soc.* **1935**, *57*, 419.

140. March, J. *Advanced Organic Chemistry*, 3rd ed.; J. Wiley and Sons: New York, 1985; pp 298-321.

141. March, J. *Advanced Organic Chemistry*, 3rd ed.; J. Wiley and Sons: New York, 1985; pp 256-262.

142. Chaudhary, S. K.; Hernandez, O. *Tetrahedron Lett.* **1979**, 99.

143. Scriven, E. F. V. *Chem. Soc. Rev.* **1983**, *12*, 129.

144. Calvo, K. C. *J. Am. Chem. Soc.* **1985**, *107*, 3690.

145. Schneider, H.; Hoppen, V. *J. Org. Chem.* **1978**, *43*, 3866.

146. March, J. *Advanced Organic Chemistry*, 3rd ed.; J. Wiley and Sons: New York, 1985; pp 290-295.

147. Ferrier, R. J.; Collins, P. M. *Monosaccharide Chemistry*; Penguin Books Ltd.: England, 1972; pp 108-115, 124, 140.

148. Duddeck, H. *Org. Magn. Reson.* **1975**, *7*, 151.

149. Merz, A. *Angew. Chem. Int. Ed. Eng.* **1973**, *12*, 846.

150. Wallenfels, K.; Bechtler, G.; Kuhn, R.; Trischmann, H.; Egge, H. *Angew. Chem. Int. Ed. Eng.* **1963**, *2*, 515.

151. Johnstone, R. A. W.; Rose, M. E. *Tetrahedron*, **1979**, *35*, 2169.

152. Ley, S. V.; Neuhaus, D.; Williams, D. J. *Tetrahedron Lett.* **1982**, *23*, 1207.

153. Parker, A. J. *Chem. Rev.* **1969**, *69*, 1.

154. March, J. *Advanced Organic Chemistry*, 3rd ed.; J. Wiley and Sons: New York, 1985; pp 527-9.

155. Shafer, J. A. in *The Chemistry of Amides*, edited by J. Zabicky (S. Patai series editor); Interscience: New York, 1970; pp 697-705.

156. Challis, B. C.; Challis, J. A. in *The Chemistry of Amides*, edited by J. Zabicky (S. Patai series editor); Interscience: New York, 1970; pp 731-757.

157. Hopkins, G. C.; Jonak, J. P.; Minnemeyer, H. J.; Tieckelmann H. *J. Org. Chem.* **1987**, *32*, 4040.

158. March, J. *Advanced Organic Chemistry*, 3rd ed.; J. Wiley and Sons: New York, 1985; pp 263-5, 517.

159. Oikawa, Y.; Yoshioka, T.; Yonemitsu, O. *Tetrahedron Lett.* **1982**, *23*, 885.

160. Jackman, L. M.; Sternhell, S. *Applications of Nuclear Magnetic Resonance Spectroscopy in Organic Chemistry*, 2nd ed.; Pergamon Press Ltd.: Oxford, 1969; pp 270-279.

161. Walker, D.; Hiebert, J. D. *Chem. Rev.* **1967**, *67*, 153.

162. Chaudhary, S. K.; Hernandez, O. *Tetrahedron Lett.* **1979**, 95.

163. Wratten, S. J.; Meinwald, J. *Tetrahedron Lett.* **1980**, *21*, 3163.

164. Cardani, C.; Ghiringhelli, D.; Mondelli, R.; Selva, A. *Gazz. Chim. Ital.* **1973**, *103*, 247.

165. Cardani, C.; Ghiringhelli, D.; Mondelli, R.; Pavan, M.; Quilico, A. *Ann. Soc. Entomol. France* **1965**, *1*, 813.

166. Cardani, C.; Fuganti, C.; Ghiringhelli, D. *Gazz. Chim. Ital.* **1968**, *98*, 474.

167. Miyashita, N.; Yoshikoshi, A.; Grieco, P. A. *J. Org. Chem.* **1977**, *42*, 3772.

168. Seebach, D.; Chow, H.; Jackson, R. F. W.; Lowson, K.; Sutter, M. A.; Thaisrivongs, S.; Zimmermann, J. *J. Am. Chem. Soc.* **1985**, *107*, 5292.

169. Baker, G. H.; Brown, P. J.; Dorgan, R. J. J.; Everett, J. R.; Ley, S. V.; Slawin, A. M. Z.; Williams, D. J. *Tetrahedron Lett.* **1987**, *28*, 5565.

170. Ferrier, R. J.; Collins, P. M. *Monosaccharide Chemistry*; Penguin Books Ltd.: England, 1972; pp 50-72.

171. Cordes, E. H.; Bull, H. G. *Chem. Rev.* **1974**, *74*, 581.

172. March, J. *Advanced Organic Chemistry*, 3rd ed.; J. Wiley and Sons: New York, 1985; pp 329-32.

173. Sterzycki, R. *Synthesis* **1979**, 724.

174. Marshall, J. A.; Conrow, R. E. *J. Am. Chem. Soc.* **1983**, *105*, 5679.

175. Polonsky, J.; Beloeil, J.; Prange, T.; Pascard, C.; Jacquemin, H.; Donnelly, D. M. X.; Kenny, P. T. M. *Tetrahedron*, **1983**, *39*, 2647.

176. March, J. *Advanced Organic Chemistry*, 3rd ed.; J. Wiley and Sons: New York, 1985; pp 873-896.

177. March, J. *Advanced Organic Chemistry*, 3rd ed.; J. Wiley and Sons: New York, 1985; pp 234-6.

178. Dauben, W. G.; Michno, D. M. *J. Am. Chem. Soc.* **1981**, *103*, 2284.

179. Kemp, D. S.; Vellaccio, F. *Organic Chemistry*; Worth Publishers, Inc.: New York, 1980; pp 850-1.

180. Societa Farmaceutici Italia Brit. 1,078,049, 2 Aug 1967. (CA68:95687v)

181. Societa Farmaceutici Italia Brit. 1,113,829, 15 May 1968. (CA69:33079k)

182. IUPAC Commission on the Nomenclature of Organic Chemistry *Pure Appl. Chem.* **1972**, *31*, 285.

183. Rylander, P. N. *Hydrogenation Methods*; Academic Press: London, 1985; pp 29-52.

184. Rylander, P. N. *Hydrogenation Methods*; Academic Press: London, 1985; pp 4-11.

185. Rylander, P. N. *Catalytic Hydrogenation over Platinum Metals*; Academic Press: London, 1967; pp 91-107.

186. Briggs, A. J.; Glenn, R.; Jones, P. G.; Kirby, A. J.; Ramaswamy, P. *J. Am. Chem. Soc.* **1984**, *106*, 6200.

187. Kruse, C. G.; Jonkers, F. L.; Dert, V.; van der Gen, A. *Rec. Trav. Chim. Pays-Bas* **1979**, *98*, 371.

188. Kotsuki, H.; Ushio, Y.; Yoshimura, N.; Ochi, M. *J. Org. Chem.* **1987**, *52*, 2594.

189. Tsunoda, T.; Suzuki, M.; Noyori, R. *Tetrahedron Lett.* **1979**, 4679.

190. Eliel, E. L.; Nowak, B. E.; Daignault, R. A.; Badding, V. G. *J. Org. Chem.* **1965**, *30*, 2441.

191. Rylander, P. N. *Hydrogenation Methods*; Academic Press: London, 1985; pp 165-168.

192. March, J. *Advanced Organic Chemistry*, 3rd ed.; J. Wiley and Sons: New York, 1985; pp 691-9.

193. Cocker, W.; Shannon, P. V. R.; Staniland, P. A. *J. Chem. Soc. C* **1966**, 41.

194. Davies, N. R. *Rev. Pure Appl. Chem.* **1967**, *17*, 83.

195. March, J. *Advanced Organic Chemistry*, 3rd ed.; J. Wiley and Sons: New York, 1985; pp 389-394.

196. March, J. *Advanced Organic Chemistry*, 3rd ed.; J. Wiley and Sons: New York, 1985; pp 524-7.

197. Harrod, J. F.; Chalk, A. J. *J. Am. Chem. Soc.* **1966**, *88*, 3491.

198. March, J. *Advanced Organic Chemistry*, 3rd ed.; J. Wiley and Sons: New York, 1985; pp 735-7.

199. Andrews, L. J. T.; Coxon, J. M.; Hartshorn, M. P. *J. Org. Chem.* **1969**, *34*, 1126.

200. Grant, P. K.; Weavers, R. T. *Tetrahedron* **1974**, *30*, 2385.

201. Bastard, J.; Duc, D. K.; Fetizon, M.; Francis, M. J.; Grant, P. K.; Weavers, R. T.; Kaneko, C.; Baddeley, G. V.; Bernassau, J.; Burfitt, I. R.; Wovkulich, P. M.; Wenkert, E. *J. Nat. Prod.* **1984**, 47, 592.

202. Berti, G. in *Topics in Stereochemistry*, edited by N. L. Allinger and E. L. Eliel; Interscience (J. Wiley and Sons): New York, 1973; Vol. 7, pp 118-162.

203. Fieser, L. F.; Fieser, M. *Reagents for Organic Synthesis*; J. Wiley and Sons: New York, 1967; Vol. 1, pp 364-7.

204. Fieser, M.; Fieser, L. F. *Reagents for Organic Synthesis*; J. Wiley and Sons: New York, 1974; Vol. 4, p 228.

205. Kemp, D. S.; Vellaccio, F. *Organic Chemistry*; Worth Publishers, Inc.: New York, 1980; pp 261.

206. Wolinsky, J.; Novak, R. W.; Erickson, K. L. *J. Org. Chem.* **1969**, *34*, 490.

207. Wicha, J.; Zorecki, A. *Tetrahedron Lett.* **1974**, 3059.

208. Pilgram, K.; Pollard, G. E. *J. Heterocycl. Chem.* **1977**, *14*, 1029.

209. Deavenport, D. L.; Harrison, C. H.; Rathburn, D. W. *Org. Magn. Reson.* **1973**, *5*, 285.

210. Bowman, R. E.; Campbell, A.; Tanner, E. M. *J. Chem. Soc.* **1963**, 692.

211. Cort, L. A.; Stewart, R. A. *J. Chem. Soc. C* **1971**, 1386.

212. Baron, M.; Hollis, D. P. *Rec. Trav. Chim. Pays-Bas* **1965**, *84*, 1109.

213. A copy of a program for the analysis of MODEL files was provided by D. Q. McDonald of the University of Canterbury.

214. Saunders, M.; Houk, K. N.; Wu, Y.; Still, W. C.; Lipton, M.; Chang, G.; Guida, W. C. *J. Am. Chem. Soc.* **1990**, *112*, 1419.

215. Lopez-Herrera, F. J.; Pino-Gonzalez, M. S.; Planas-Ruiz, F. *Tetrahedron Asymmetry* **1990**, *1*, 465.

216. Chang, G.; Guida, W. C.; Still, W. C. *J. Am. Chem. Soc.* **1989**, *111*, 4379.

217. Cornforth, J. W. in *Heterocyclic Compounds*, edited by R. C. Elderfield; J. Wiley and Sons: New York, 1957; Vol. 5, pp 402-3.

218. Bishop, D. C.; Bowman, R. E.; Campbell, A.; Jones, W. A. *J. Chem. Soc.* **1963**, 2381.

219. Homer, R. B.; Johnson, C. D. in *The Chemistry of Amides*, edited by J. Zabicky (S. Patai series editor); Interscience: New York, 1970; pp 187-191, 238-240.

220. Firestone, R. A.; Reinhold, D. F.; Gaines, W. A.; Chemerda, J. M.; Sletzinger, M. *J. Org. Chem.* **1968**, *33*, 1213.

221. Boyd, G. V. in *Comprehensive Heterocyclic Chemistry*, edited by A. R. Katritzky and C. W. Rees; Pergamon Press: Oxford, 1984; Vol 6, p 213.

222. Ionescu, M.; Makkay, C. *Stud. Univ. Babes-Bolyai, Ser. Chem.* **1966**, *11*, 115.

223. Ionescu, M.; Makkay, C. *Stud. Univ. Babes-Bolyai, Ser. Chem.* **1968**, *13*, 89.

224. Ionescu, M.; Makkay, C. *Stud. Univ. Babes-Bolyai, Ser. Chem.* **1968**, *13*, 5.

225. Ionescu, M.; Makkay, C. *Rev. Roum. Chim.* **1970**, *15*, 265.

226. Ionescu, M.; Makkay, C. *Stud. Univ. Babes-Bolyai, Ser. Chem.* **1971**, *16*, 61.

227. Ferrier, R. J.; Collins, P. M. *Monosaccharide Chemistry*; Penguin Books Ltd.: England, 1972; p 75.

228. Registry file, CAS ONLINE search.

229. Kernan, M. R.; Molinski, T. F.; Faulkner, D. J. *J. Org. Chem.* **1988**, *53*, 5014-20.

230. Kemp, D. S.; Vellaccio, F. *Organic Chemistry*; Worth Publishers, Inc.: New York, 1980; pp 879-890.

231. Kemp, D. S.; Vellaccio, F. *Organic Chemistry*; Worth Publishers, Inc.: New York, 1980; pp 1141, 1149.

232. Kemp, D. S.; Vellaccio, F. *Organic Chemistry*; Worth Publishers, Inc.: New York, 1980; pp 839-844, 859-861.

233. Ferrier, R. J.; Collins, P. M. *Monosaccharide Chemistry*; Penguin Books Ltd.: England, 1972; pp 88-93, 173-183.

234. Eisele, G.; Simchen, G. *Synthesis* **1978**, 757.

235. Kapnang, H.; Charles, G. *Tetrahedron Lett.* **1983**, *24*, 1597.

236. Barluenga, J.; Bayon, A. M.; Campos, P.; Asensio, G.; Gonzalez-Nunez, E.; Molina, Y. *J. Chem. Soc. Perkins Trans. 1* **1988**, 1631.

237. Hurd, C. D. *J. Chem. Educ.* **1966**, *43*, 527.

238. Kemp, D. S.; Vellaccio, F. *Organic Chemistry*; Worth Publishers, Inc.: New York, 1980; pp 283-306.

239. March, J. *Advanced Organic Chemistry*, 3rd ed.; J. Wiley and Sons: New York, 1985; pp 1117-9.

240. Tsuzuki, K.; Watanabe, T.; Yanagiya, M.; Matsumoto, T. *Tetrahedron Lett.* **1976**, 4745.

241. March, J. *Advanced Organic Chemistry*, 3rd ed.; J. Wiley and Sons: New York, 1985; pp 796-8.

242. March, J. *Advanced Organic Chemistry*, 3rd ed.; J. Wiley and Sons: New York, 1985; pp 784-6.

243. Parker, A. J. *Quart. Rev. Chem. Soc.* **1962**, *16*, 163.

244. Isono, F.; Inukai, M.; Takahashi, S.; Haneishi, T. *J. Antibiotics* **1989**, *42*, 667.

245. Chen, R. H.; Buko, A. M.; Whittern, D. N.; McAlpine, J. B. *J. Antibiotics* **1989**, *42*, 512.

246. March, J. *Advanced Organic Chemistry*, 3rd ed.; J. Wiley and Sons: New York, 1985; pp 664-681, 684-5.

247. Hutchins, R. O.; Kandasamy, D.; Dux III, F.; Maryanoff, C. A.; Rotstein, D.; Goldsmith, B.; Burgoyne, W.; Cistone, F.; Dalessandro, J.; Puglis, J. *J. Org. Chem.* **1978**, *43*, 2259.

248. Abraham, R. J.; Loftus, P. *Proton and Carbon-13 NMR Spectroscopy*; Heydon: London, 1978; pp 42-45.

249. Pfeffer, P. E.; Silbert, L. S. *J. Org. Chem.* **1976**, *41*, 1373.

250. March, J. *Advanced Organic Chemistry*, 3rd ed.; J. Wiley and Sons: New York, 1985; pp 932-4.

251. March, J. *Advanced Organic Chemistry*, 3rd ed.; J. Wiley and Sons: New York, 1985; pp 1076-7.

252. Willson, T. M.; Kocienski, P.; Jarowicki, K.; Isaac, K.; Faller, A.; Campbell, S. F.; Borner, J. *Tetrahedron* **1990**, *46*, 1757.

253. Mancuso, A. J.; Swern, D. *Synthesis* **1981**, 165.

254. March, J. *Advanced Organic Chemistry*, 3rd ed.; J. Wiley and Sons: New York, 1985; pp 1057-60.

255. Corey, E. J.; Schmidt, G. *Tetrahedron Lett.* **1979**, 399.

256. Sharpless, K. B.; Akashi. K.; Oshima, K. *Tetrahedron Lett.* **1976**, 2503.

257. Partch, R. E. *Tetrahedron Lett.* **1964**, 3071.

258. Ferrier, R. J.; Collins, P. M. *Monosaccharide Chemistry*; Penguin Books Ltd: England, 1972; pp 82-87, 162-6, 223-5.

259. March, J. *Advanced Organic Chemistry*, 3rd ed.; J. Wiley and Sons: New York, 1985; pp 1081-83.

260. Ueno, Y.; Okawara, M. *Tetrahedron Lett.* **1976**, 4597.

261. Tomioka, H.; Oshima, K.; Nozaki, H. *Tetrahedron Lett.* **1982**, *23*, 539.

262. Jung, M. E.; Brown, R. W. *Tetrahedron Lett.* **1978**, 2771.

263. Fried, J.; Sih, J. C. *Tetrahedron Lett.* **1973**, 3899.

264. Tomioka, H.; Takai, K.; Oshima, K.; Nozaki, H. *Tetrahedron Lett.* **1981**, *22*, 1605.

265. Regen, S. L. *J. Org. Chem.* **1974**, *39*, 260.

266. Sasson, Y.; Rempel, G. L. *Tetrahedron Lett.* **1974**, 3221.

267. Hallman, P. S.; McGarvey, B. R.; Wilkinson, G. *J. Chem. Soc. A* **1968**, 3143.

268. Chatt, J.; Shaw, B. L.; Field, A. E. *J. Chem. Soc.* **1964**, 3466.

269. March, J. *Advanced Organic Chemistry*, 3rd ed.; J. Wiley and Sons: New York, 1985; pp 655-6.

270. March, J. *Advanced Organic Chemistry*, 3rd ed.; J. Wiley and Sons: New York, 1985; pp 1063-5.

271. Morrison, R. T.; Boyd, R. N. *Organic Chemistry*, 3rd ed.; Allyn and Bacon Inc.: Boston, 1973; pp 628-43, 740-1.

272. Greene, T. W. *Protective Groups in Organic Synthesis*; J. Wiley and Sons: New York, 1981; pp 114-128.

273. Lane, C. F. *Synthesis* **1975**, 135.

274. March, J. *Advanced Organic Chemistry*, 3rd ed.; J. Wiley and Sons: New York, 1985; pp 629-31.

275. Kempf, D. J.; de Lara, E.; Stein, H. H.; Cohen, J.; Egor, D. A.; Plattner, J. J. *J. Med. Chem.* **1990**, *33*, 371.

276. Isaac, K.; Kocienski, P.; Campbell, S. *J. Chem. Soc. Chem. Commun.* **1983**, 249.

277. Yanagiya, M.; Matsuda, F.; Hasegawa, K.; Matsumoto, T. *Tetrahedron Lett.* **1982**, *23*, 4039.

278. Isaac, K.; Kocienski, P. *J. Chem. Soc. Chem. Commun.* **1982**, 460.

279. Meinwald, J. *Pure Appl. Chem.* **1977**, *49*, 1275.

280. Yanagiya, M.; Tsuzuki, K.; Watanabe, T.; Nakajima, Y.; Matsuda, F.; Hasegawa, K.; Matsumoto, T. *Koen Yoshishu-Tennen Yuki Kagobutsu Toronkai 22nd.* **1979**, 635.

281. Matsumoto, T.; Yanagiya, M.; Tsuzuki, K.; Watanabe, T.; Nakajima, Y. Jpn. Kokai Tokkyo Koho 79,145,609, 14 Nov 1979. (CA92:146456z)

282. Mitsubishi Chemical Industries Co. Ltd. Jpn. Kokai Tokkyo Koho 80 53,252, 18 Apr 1980. (CA93:185793x)

283. Grove, M. D.; Weisleder, D.; Daxenbichler, M. E. *Tetrahedron* **1973**, *29*, 2715.

284. Kruger, G. J.; du Plessis, L. M.; Grobbelaar, N. *J. S. Afr. Chem. Inst.* **1976**, *29*, 24.

285. March, J. *Advanced Organic Chemistry*, 3rd ed.; J. Wiley and Sons: New York, 1985; pp 792-3.

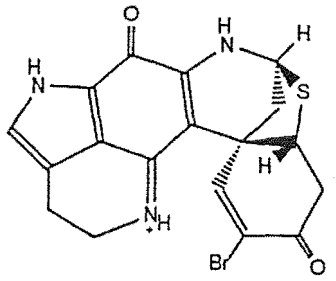

Discorhabdin A (**0.1**)

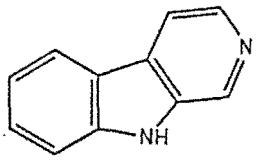

β-Carboline (**0.2**)

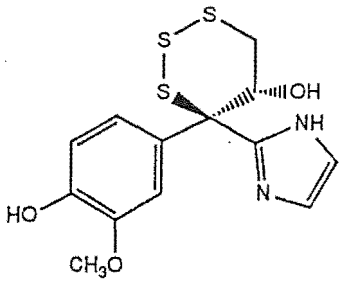

Trithiane A (**0.3**)

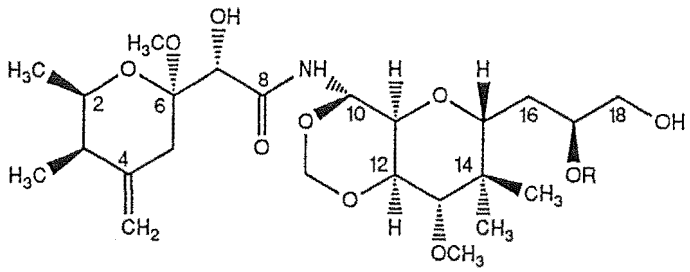

R=H: Mycalamide A (**0.4**)

R=$CH_3$: Mycalamide B (**0.5**)

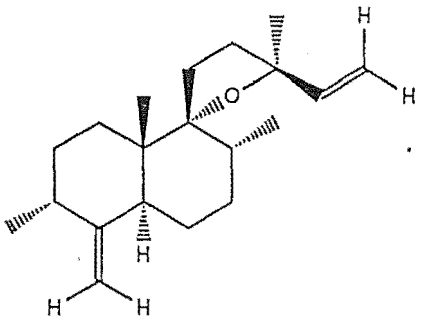

Rotalin A (**0.6**)

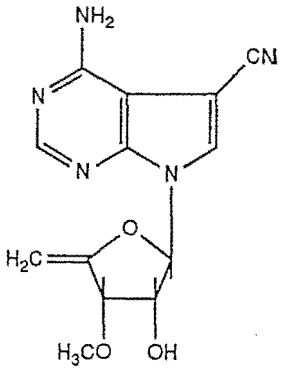

Mycalisine A (**0.7**)

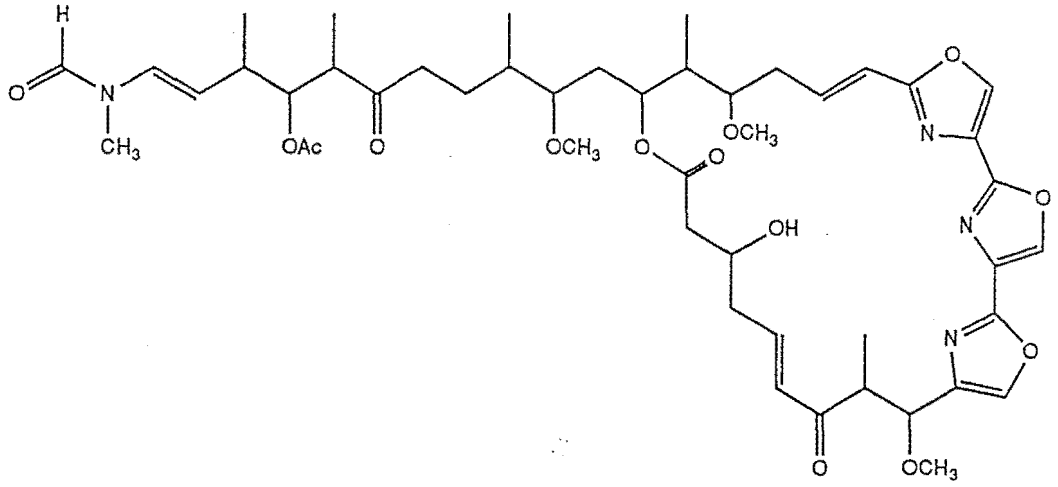

Mycalolide A (**0.8**)

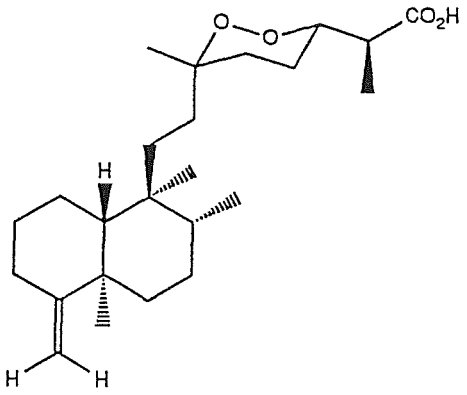


Cyclic peroxide (**0.9**)

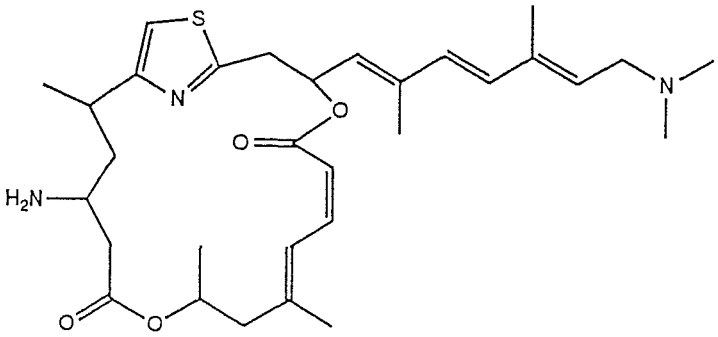


Pateamine (**0.10**)

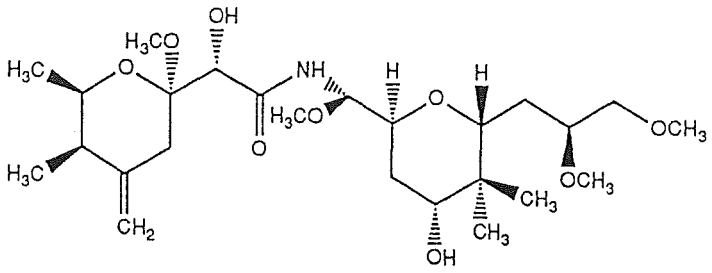


Pederin (**0.11**)

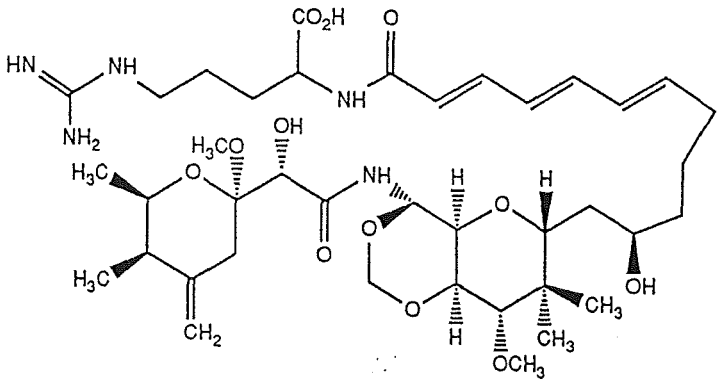


Onnamide A (**0.12**)

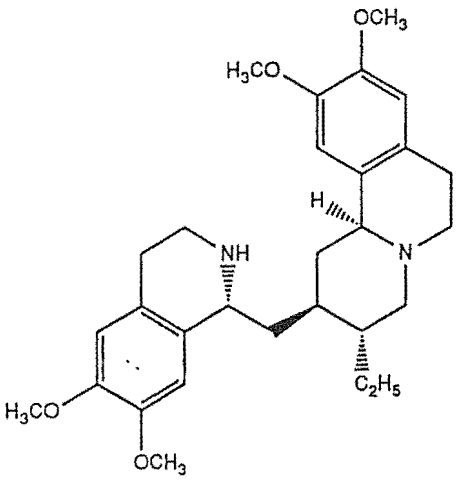

Emetine (**0.13**)

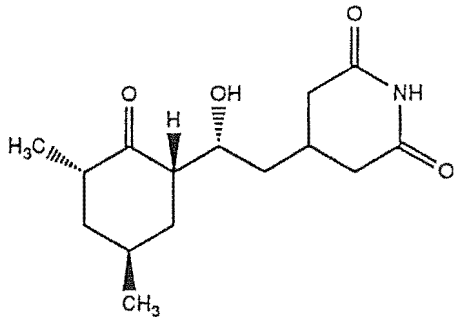

Cycloheximide (**0.14**)

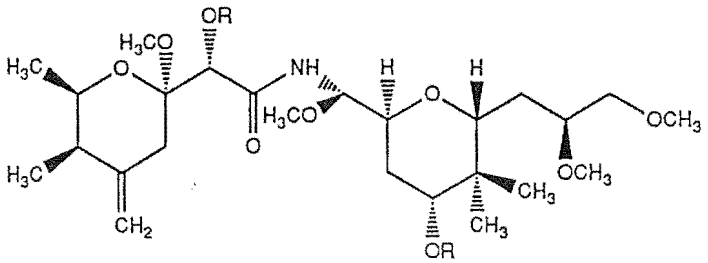

R=$COC_6H_4Br$: Pederin di-p-bromobenzoate (**1.1**)

R=$COC_6H_5$: Pederin dibenzoate (**1.2**)

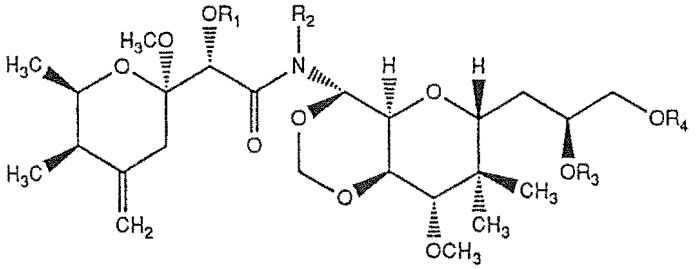

$R_1$=$R_3$=$R_4$=$Si(CH_3)_3$, $R_2$=H: Mycalamide A tris-TMS ether (**2.1**)

$R_1$=$R_4$=$Si(CH_3)_3$, $R_2$=H, $R_3$=$CH_3$: Mycalamide B bis-TMS ether (**2.2**)

$R_1$=$R_2$=H, $R_3$=$CH_3$, $R_4$=$Si(CH_3)_3$: Mycalamide B 18-mono-TMS ether (**2.3**)

$R_1$=$R_2$=H, $R_3$=$R_4$=$Si(CH_3)_3$: Mycalamide A 17,18-bis-TMS ether (**2.4**)

$R_1$=$R_2$=$R_3$=H, $R_4$=$Si(CH_3)_2C(CH_3)_3$: Myc.A 18-mono-TBDMS ether (**2.5**)

$R_1$=$R_2$=H, $R_3$=$R_4$=$Si(CH_3)_2C(CH_3)_3$: Myc.A 17,18-bis-TBDMS ether (**2.6**)

$R_1$=$R_3$=$R_4$=$Si(CH_3)_2C(CH_3)_3$, $R_2$=H: Mycalamide A tris-TBDMS ether (**2.7**)

$R_1$=$R_2$=H, $R_3$=$CH_3$, $R_4$=$Si(CH_3)_2C(CH_3)_3$: Myc.B 18-mono-TBDMS... (**2.8**)

$R_1$=$R_4$=$Si(CH_3)_2C(CH_3)_3$, $R_2$=H, $R_3$=$CH_3$: Myc.B bis-TBDMS ether (**2.9**)

$R_1$=$R_2$=$R_3$=H, $R_4$=$COC_6H_4Br$: Myc.A 18-mono-p-bromobenzoate (**2.10**)

$R_1$=$COC_6H_4Br$, $R_2$=$R_3$=$R_4$=H: Myc.A 7-mono-p-bromobenzoate (**2.11**)

$R_1$=$R_4$=$COC_6H_4Br$, $R_2$=$R_3$=H: Myc.A 7,18-di-p-bromobenzoate (**2.12**)

$R_1$=$R_2$=H, $R_3$=$R_4$=$COC_6H_4Br$: Myc.A 17,18-di-p-bromobenzoate (**2.13**)
$R_1$=$R_3$=$R_4$=$COC_6H_4Br$, $R_2$=H: Mycalamide A tri-p-bromobenzoate (**2.14**)
$R_1$=$COC_6H_4Br$, $R_2$=$R_4$=H, $R_3$=$CH_3$: Myc.B 7-mono-p-bromobenzoate (**2.15**)
$R_1$=$R_2$=H, $R_3$=$CH_3$, $R_4$=$COC_6H_4Br$: Myc.B 18-mono-p-bromobenzoate (**2.16**)
$R_1$=$R_4$=$COC_6H_4Br$, $R_2$=H, $R_3$=$CH_3$: Myc.B di-p-bromobenzoate (**2.17**)
$R_1$=$R_3$=$R_4$=$COCH_3$, $R_2$=H: Mycalamide A triacetate (**2.18**)
$R_1$=$R_4$=$COCH_3$, $R_2$=H, $R_3$=$CH_3$: Mycalamide B diacetate (**2.19**)
$R_1$=$R_2$=H, $R_3$=$CH_3$, $R_4$=$COCH_3$: Mycalamide B 18-monoacetate (**2.20**)
$R_1$=$COCH_3$, $R_2$=$R_4$=H, $R_3$=$CH_3$: Mycalamide B 7-monoacetate (**2.21**)
$R_1$=$R_3$=$R_4$=$COCH_2CH_3$, $R_2$=H: Mycalamide A tripropanoate (**2.22**)
$R_1$=$R_2$=H, $R_3$=$CH_3$, $R_4$=$SO_2CH_3$: Mycalamide B 18-monomesylate (**2.23**)
$R_1$=$R_2$=$CH_3$, $R_3$=$R_4$=H: 7-*O*-Methyl, *N*-methyl mycalamide A (**2.24**)
$R_1$=$R_2$=$R_4$=$CH_3$, $R_3$=H: 7,18-di-*O*-Methyl, *N*-methyl mycalamide A (**2.25**)
$R_1$=$R_2$=$R_3$=$R_4$=$CH_3$: 7,17,18-tri-*O*-Methyl, *N*-methyl mycalamide A (**2.26**)
$R_1$=$R_2$=$R_3$=$CH_3$, $R_4$=H: 7,17-di-*O*-Methyl, *N*-methyl mycalamide A (**2.27**)
$R_1$=$R_3$=$R_4$=$CH_3$, $R_2$=H: 7,17,18-tri-*O*-Methyl mycalamide A (**2.31**)
$R_1$=$R_4$=$CH_3$, $R_2$=$R_3$=H: 7,18-di-*O*-Methyl mycalamide A (**2.32**)
$R_1$=$R_3$=$CH_3$, $R_2$=$R_4$=H: 7,17-di-*O*-Methyl mycalamide A (**2.33**)
$R_1$=$CH_3$, $R_2$=$R_3$=$R_4$=H: 7-*O*-Methyl mycalamide A (**2.34**)
$R_1$=$R_2$=$R_3$=H, $R_4$=$CH_3$: 18-*O*-Methyl mycalamide A (**2.35**)
$R_1$=$COCH_3$, $R_2$=H, $R_3$=$R_4$=$CH_3$: 17,18-di-*O*-Methyl myc.A 7-monoacet. (**2.36**)
$R_1$=$R_3$=$CH_3$, $R_2$=H, $R_4$=$COCH_3$: 7,17-di-*O*-Methyl myc.A 18-monoacet. (**2.37**)
$R_1$=$R_2$=H, $R_3$=$R_4$=$CH_3$: 17,18-di-*O*-Methyl mycalamide A (**2.38**)
$R_1$=$CH_2Ph$, $R_2$=$R_3$=$R_4$=H: 7-*O*-Benzyl mycalamide A (**2.39**)
$R_1$=$R_4$=$CH_2Ph$, $R_2$=$R_3$=H: 7,18-di-*O*-Benzyl mycalamide A (**2.40**)
$R_1$=$R_2$=$CH_2Ph$, $R_3$=$R_4$=H: 7,18-di-*O*-Benzyl mycalamide A (**2.41**)
$R_1$=$R_2$=$R_4$=$CH_2Ph$, $R_3$=H: 7,18-di-*O*-Benzyl, *N*-benzyl mycalamide A (**2.42**)
$R_1$=$CH_2Ph$, $R_2$=$R_4$=H, $R_3$=$CH_3$: 7-*O*-Benzyl mycalamide B (**2.43**)
$R_1$=$R_4$=$CH_2Ph$, $R_2$=H, $R_3$=$CH_3$: 7,18-di-*O*-Benzyl mycalamide B (**2.44**)
$R_1$=$R_2$=$CH_2Ph$, $R_3$=$CH_3$, $R_4$=H: 7-*O*-Benzyl, *N*-benzyl mycalamide B (**2.45**)
$R_1$=$R_2$=$R_4$=$CH_2Ph$, $R_3$=$CH_3$: 7,18-di-*O*-Benzyl, *N*-benzyl myc.B (**2.46**)

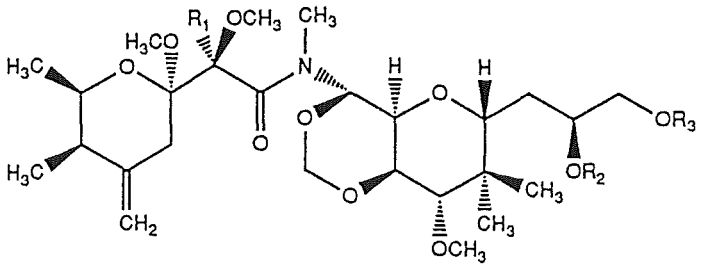

$R_1$=H, $R_2$=$R_3$=$CH_3$: 7*S*,17,18-tri-*O*-Methyl *N*-methyl mycalamide A (**2.28**)
$R_1$=$R_3$=H, $R_2$=$CH_3$: 7*S*,17-di-*O*-Methyl *N*-methyl mycalamide A (**2.29**)
$R_1$=D, $R_2$=$R_3$=H: 7-Deutero, 7*S*-*O*-methyl *N*-methyl mycalamide A (**2.30**)

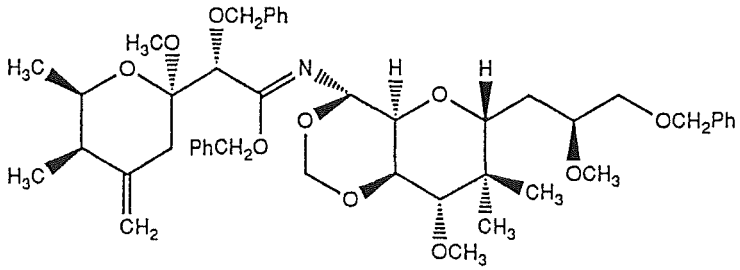

7,8,18-tri-*O*-Benzyl mycalamide B (**2.47**)

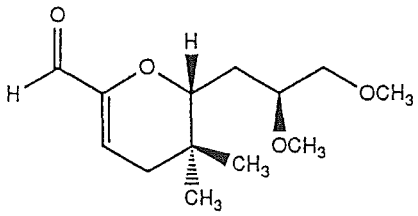

Pederenal (**3.1**)

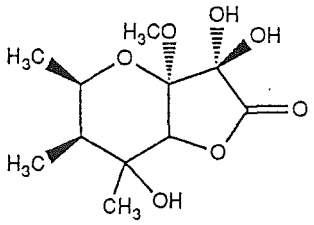

Pederinolactone (**3.2**)

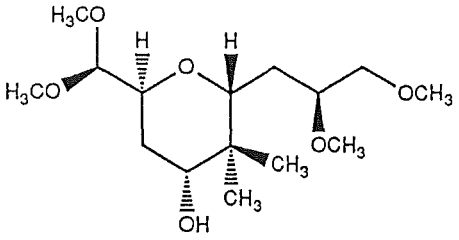

Meropederinacetal (**3.3**)

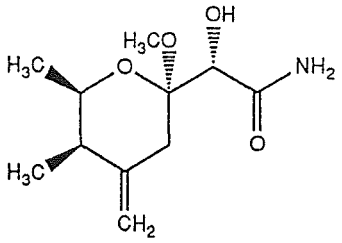

Pederamide (**3.4**)

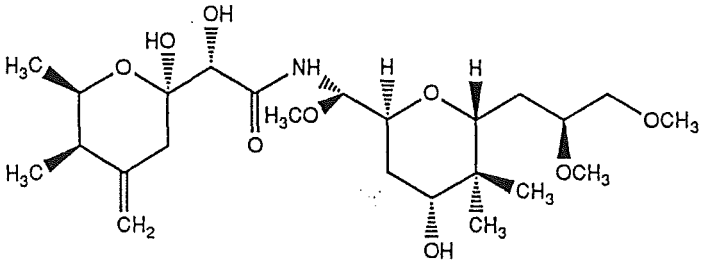

Pseudopederin (**3.5**)

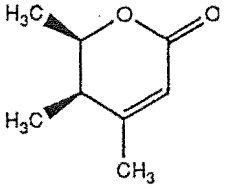

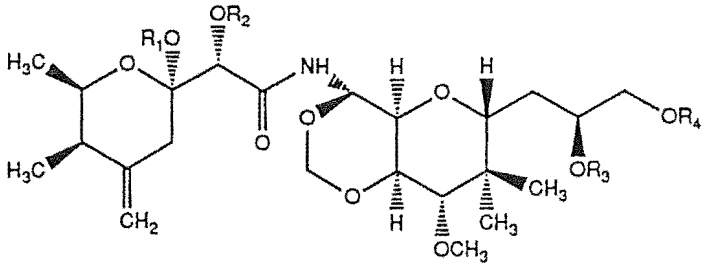

Pederolactone (**3.6**) $R_1=R_2=R_3=R_4=H$: Pseudomycalamide A (**3.7**)

$R_1=R_2=R_4=H$, $R_3=CH_3$: Pseudomycalamide B (**3.8**)

$R_1=CD_3$, $R_2=R_3=R_4=H$: 6-Trideuteromethoxy A (**3.9**)

$R_1=CH_2CH_3$, $R_2=R_3=R_4=H$: 6-Ethoxy myc.A (**3.10**)

$R_1=H$, $R_2=R_3=R_4=COCH_3$: Pseudo A triacetate (**3.15**)

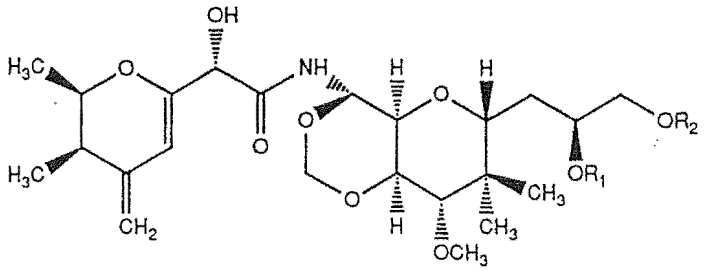

$R_1=R_2=H$: 5,6-Dehydromethoxy mycalamide A (**3.11**)

$R_1=R_2=COCH_3$: 5,6-Dehydromethoxy A 17,18-diacetate (**3.16**)

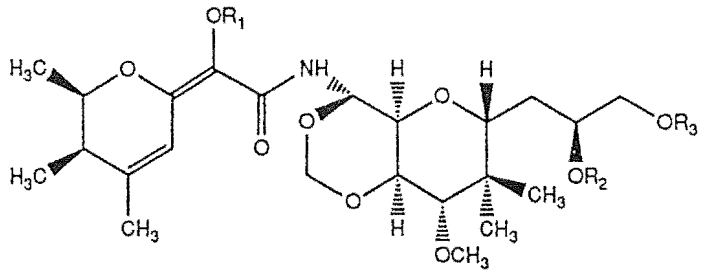

$R_1=R_2=R_3=COCH_3$: *Z* Neomycalamide A triacetate (**3.12**)

$R_1=R_3=COC_6H_4Br$, $R_2=H$: *Z* Neomyc.A 7,18-di-p-bromobenzoate (**3.18**)

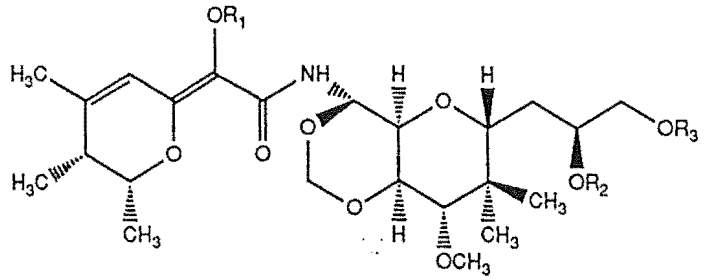

$R_1=R_2=R_3=COCH_3$: *E* Neomycalamide A triacetate (**3.13**)

$R_1=R_3=COC_6H_4Br$, $R_2=H$: *E* Neomyc.A 7,18-di-p-bromobenzoate (**3.19**)

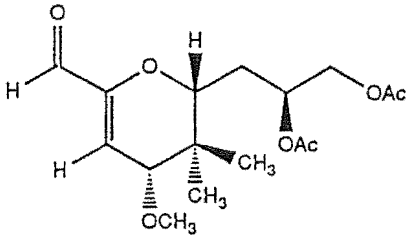

10-Aldehyde fragment (**3.14**)

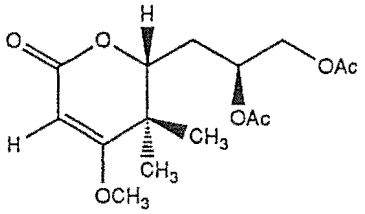

11-Lactone fragment (**3.17**)

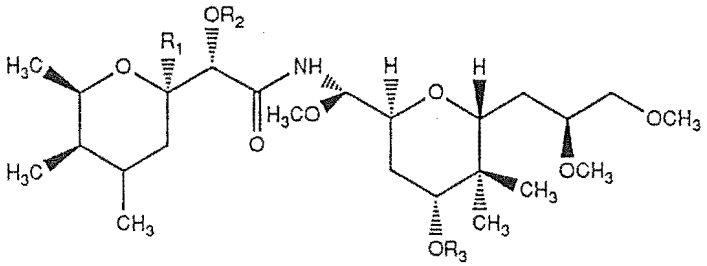

$R_1$=$OCH_3$, $R_2$=$R_3$=H: Dihydro pederin (**4.1**)

$R_1$=OH, $R_2$=$R_3$=H: Dihydro pseudopederin (**4.2**)

$R_1$=H, $R_2$=$R_3$=H: Dihydro deoxy pseudopederin (**4.3**)

$R_1$=$OCH_3$, $R_2$=$R_3$=Ac: Dihydro pederin diacetate (**4.8**)

$R_1$=H, $R_2$=$R_3$=Ac: Dihydro deoxy pseudopederin diacetate (**4.14**)

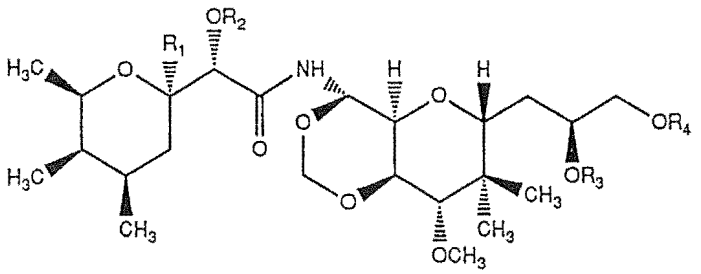

$R_1$=$OCH_3$, $R_2$=$R_3$=$R_4$=H: 4α-Dihydro mycalamide A (**4.4**)

$R_1$=$OCH_3$, $R_2$=$R_4$=H, $R_3$=$CH_3$: 4α-Dihydro mycalamide B (**4.6**)

$R_1$=OH, $R_2$=$R_3$=$R_4$=H: 4α-Dihydro pseudomycalamide A (**4.10**)

$R_1$=H, $R_2$=$R_3$=$R_4$=H: 4α-Dihydro, 6-deoxy pseudomycalamide A (**4.13**)

$R_1$=H, $R_2$=$R_3$=$R_4$=Ac: 4α-Dihydro, 6-deoxy pseudomyc.A triacetate (**4.15**)

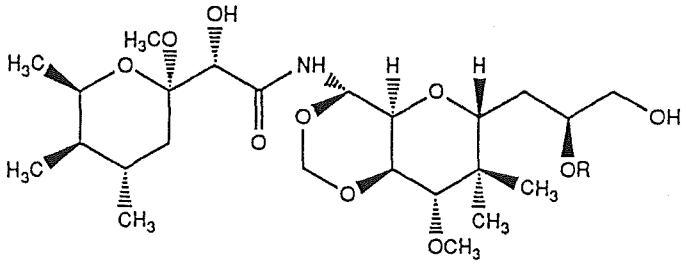

R=H: 4β-Dihydro mycalamide A (**4.5**)

R=$CH_3$: 4β-Dihydro mycalamide B (**4.7**)

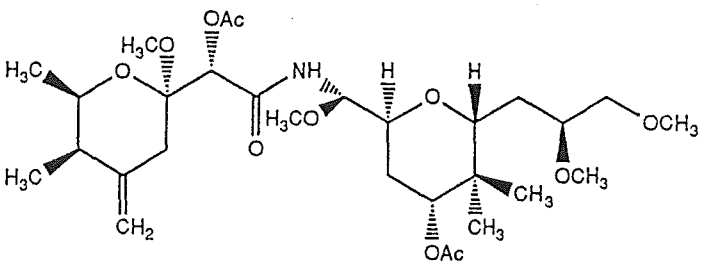

Pederin diacetate (**4.9**)

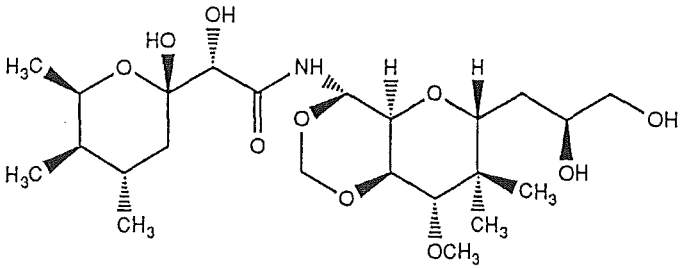

4β-Dihydro 6*S* pseudomycalamide A (**4.11**)

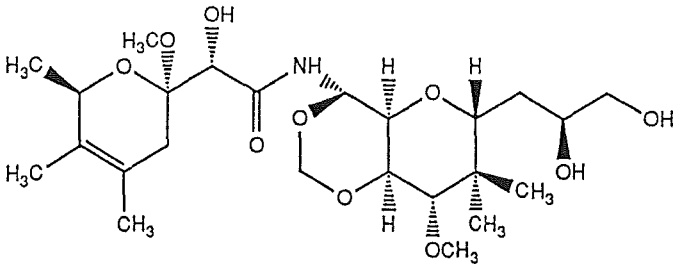

$\Delta^3$ Mycalamide A (**4.12**)

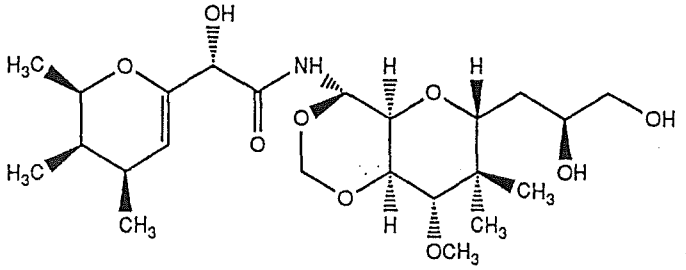

4α-Dihydro, 5,6-dehydromethoxy mycalamide A (**4.16**)

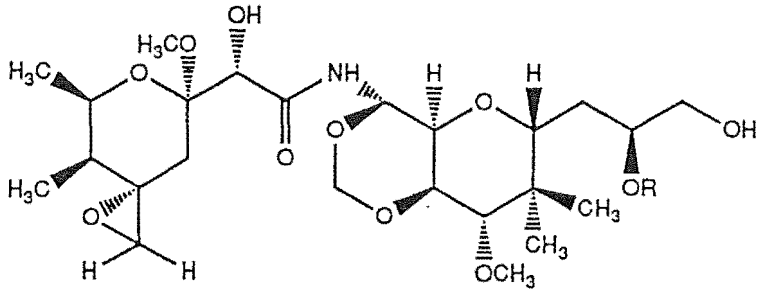

R=H: Mycalamide A 4α-epoxide (**4.17**)

R=$CH_3$: Mycalamide B 4α-epoxide (**4.19**)

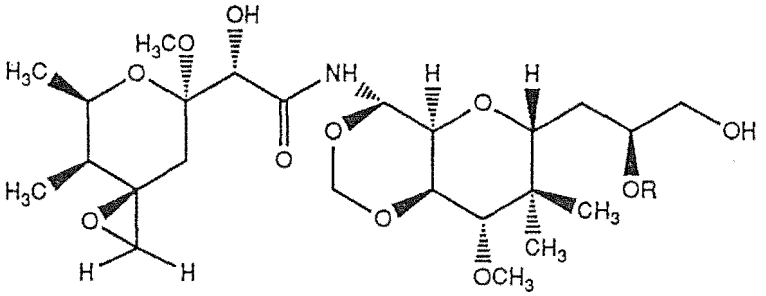

R=H: Mycalamide A 4β-epoxide (**4.18**)

R=$CH_3$: Mycalamide B 4β-epoxide (**4.20**)

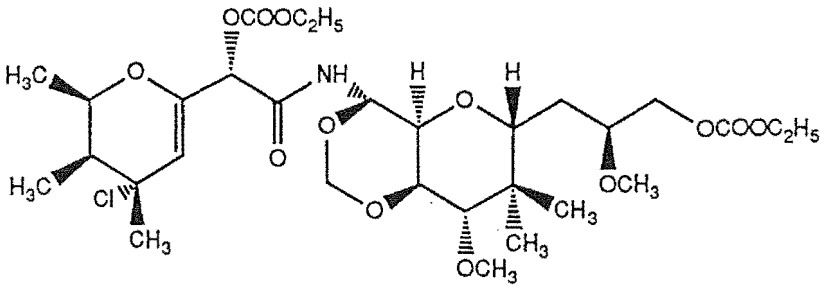

4-Hydrochloro, 5,6-dehydromethoxy mycalamide B bis-ethylcarbonate (**4.21**)

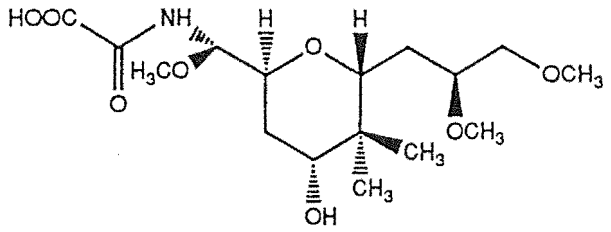

Meropederoic acid (**5.1**)

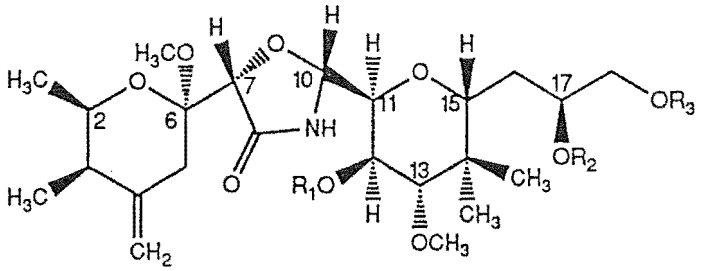

$R_1$=$R_2$=$R_3$=H: Mycalamide A *cis* oxazolidinone (**5.2**)

$R_1$=$R_3$=H, $R_2$=$CH_3$: Mycalamide B *cis* oxazolidinone (**5.9**)

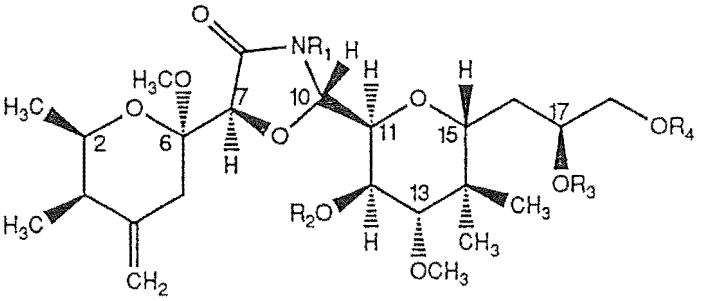

$R_1$=$R_2$=$R_3$=$R_4$=H: Mycalamide A *trans* oxazolidinone (**5.3**)

$R_1$=$R_2$=$R_4$=H, $R_3$=$CH_3$: Mycalamide B *trans* oxazolidinone (**5.10**)

$R_1$=$R_2$=$R_3$=$R_4$=$COCH_3$: *N*-Acetyl myc.A *trans* oxazolidinone triacetate (**5.13**)

$R_1$=$R_2$=$R_3$=$R_4$=$CH_3$: 12,17,18-tri-*O*-Methyl, *N*-methyl myc.A *trans* oxaz.(**5.14**)

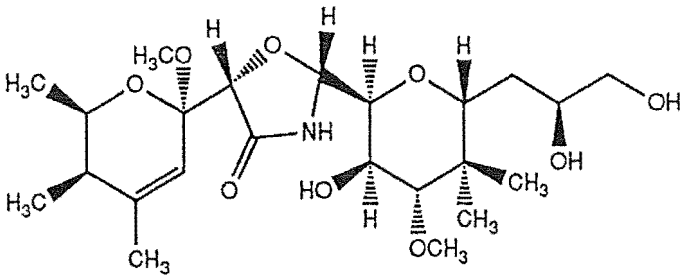

$\Delta^{4(5)}$ Mycalamide A *cis* oxazolidinone (**5.6**)

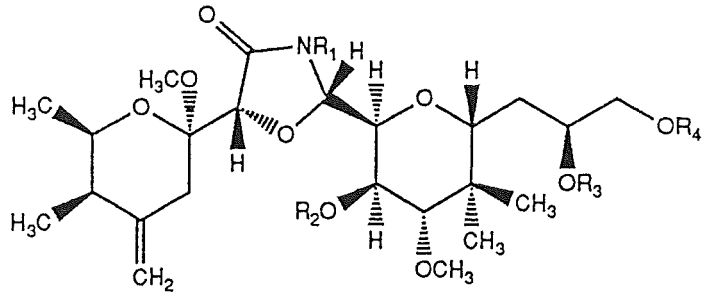

$R_1$=$R_2$=$R_3$=$R_4$=H: 7*S* Mycalamide A *cis* oxazolidinone (**5.7**)

$R_1$=$R_2$=$R_3$=$R_4$=$CH_3$: 12,17,18-tri-*O*-Methyl, *N*-methyl 7*S* A *cis* oxazo.(**5.15**)

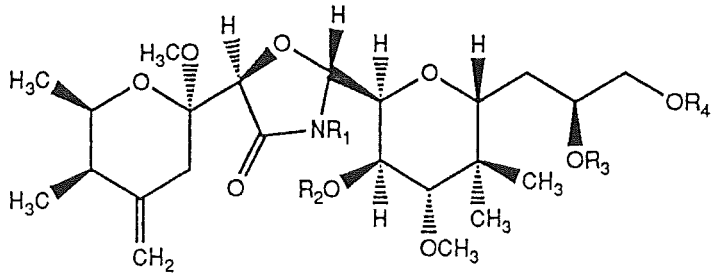

$R_1$=$R_2$=$R_3$=$R_4$=H: 7*S* Mycalamide A *trans* oxazolidinone (**5.8**)

$R_1$=$R_2$=$R_3$=$R_4$=$CH_3$: 12,17,18-tri-*O*-Methyl, *N*-methyl 7*S* A *trans* oxazo.(**5.16**)

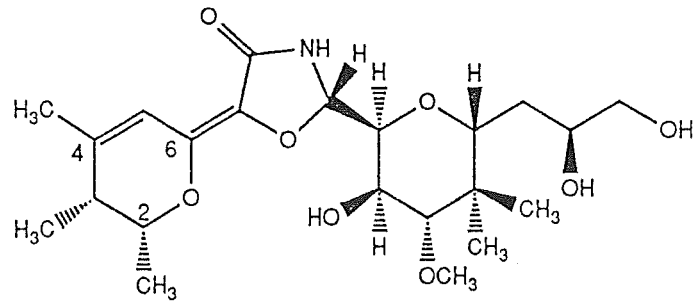

10*S* Neomycalamide A oxazolidinone (**5.11**)

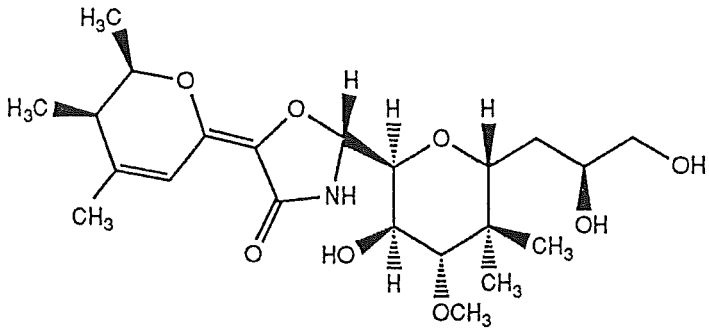

10*R* Neomycalamide A oxazolidinone (**5.12**)

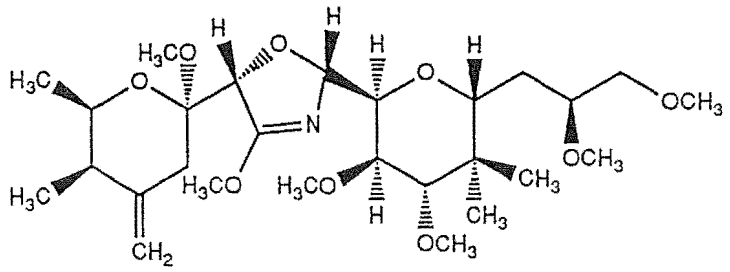

8,12,17,18-tetra-*O*-Methyl, mycalamide A *cis* oxazolidinone (**5.17**)

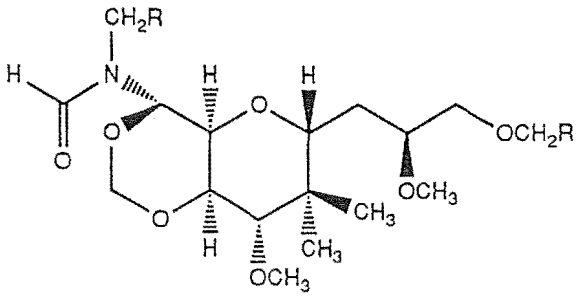

R=Ph: *N*-Benzyl, *N*-formyl fragment (**6.1**)

R=H: *N*-Methyl, *N*-formyl fragment (**6.2**)

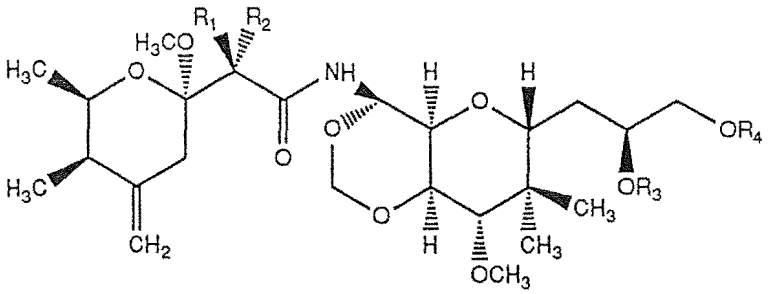

$R_1$=$R_3$=$R_4$=H, $R_2$=$OCH_2Ph$: 7-*O*-Benzyl 10*R* mycalamide A (**6.3**)

$R_1$=$R_3$=H, $R_2$=$OCH_2Ph$, $R_4$=$CH_2Ph$: 7,18-di-*O*-Benzyl 10*R* myc.A (**6.4**)

$R_1$=D, $R_2$=$OCH_2Ph$, $R_3$=$R_4$=H: 7-Deutero, 7-*O*-benzyl 10*R* myc.A (**6.10**)

$R_1$=$OCH_2Ph$, $R_2$=D, $R_3$=$R_4$=H: 7-Deutero, 7*S*-*O*-benzyl 10*R* myc.A (**6.13**)

$R_1$=$R_3$=$R_4$=H, $R_2$=OH: 10*R* Mycalamide A (**6.17**)

$R_1$=$R_4$=H, $R_2$=OH, $R_3$=$CH_3$: 10*R* Mycalamide B (**6.18**)

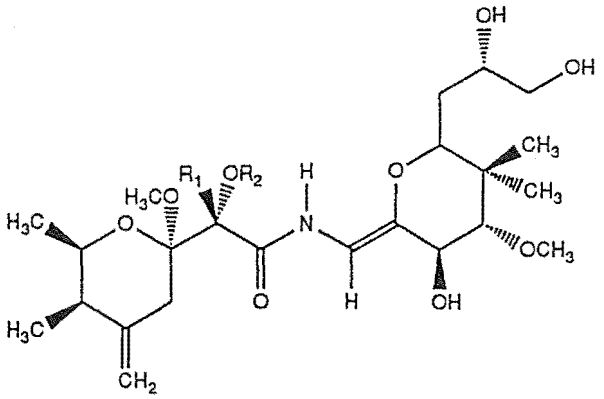

$R_1$=D, $R_2$=$CH_2Ph$: 7-Deutero, 7-*O*-benzyl, $Z\Delta^{10}$ 10-deformyl myc.A (**6.5**)
$R_1$=$R_2$=H: $Z\Delta^{10}$ 10-Deformyl mycalamide A (**6.16**)

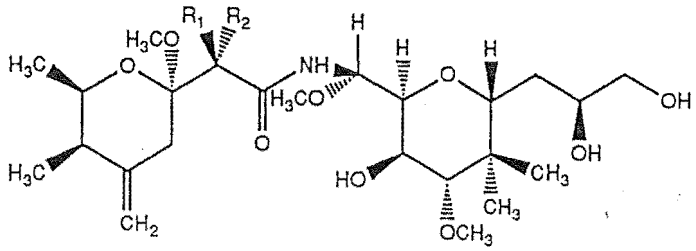

$R_1$=D, $R_2$=$OCH_2Ph$: 7-Deutero, 7-*O*-benzyl, 10*R*-*O*-methyl myc.A (**6.6**)
$R_1$=$OCH_2Ph$, $R_2$=D: 7-Deutero, 7*S*-*O*-benzyl, 10*R*-*O*-methyl myc.A (**6.9**)

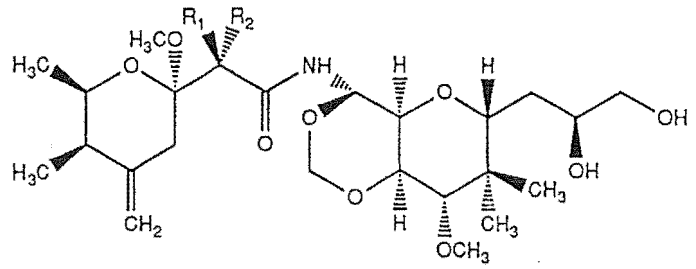

$R_1$=D, $R_2$=$OCH_2Ph$: 7-Deutero, 7-*O*-benzyl mycalamide A (**6.7**)
$R_1$=$OCH_2Ph$, $R_2$=D: 7-Deutero, 7*S*-*O*-benzyl mycalamide A (**6.11**)
$R_1$=OH, $R_2$=H: 7*S* Mycalamide A (**6.24**)

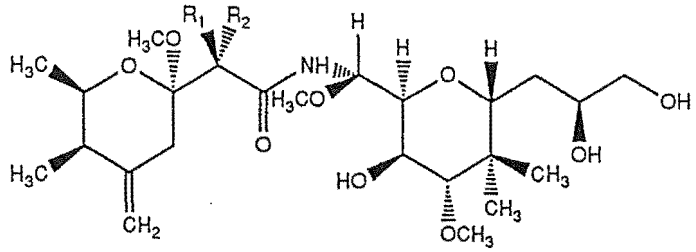

$R_1$=D, $R_2$=$OCH_2Ph$: 7-Deutero, 7-*O*-benzyl, 10*S*-*O*-methyl myc.A (**6.8**)
$R_1$=$OCH_2Ph$, $R_2$=D: 7-Deutero, 7*S*-*O*-benzyl, 10*S*-*O*-methyl myc.A (**6.12**)

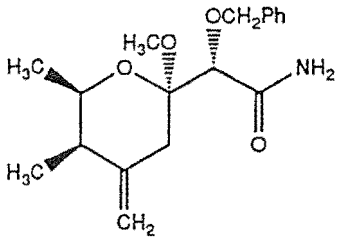

7-*O*-Benzyl pederamide (**6.14**)

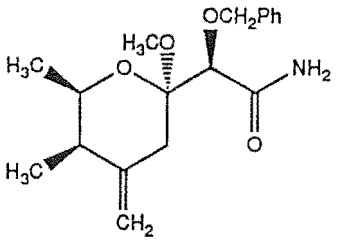

7*S*-*O*-Benzyl pederamide (**6.15**)

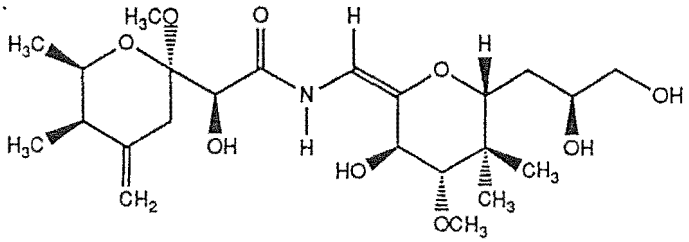

*E* $\Delta^{10}$ 10-Deformyl mycalamide A (**6.19**)

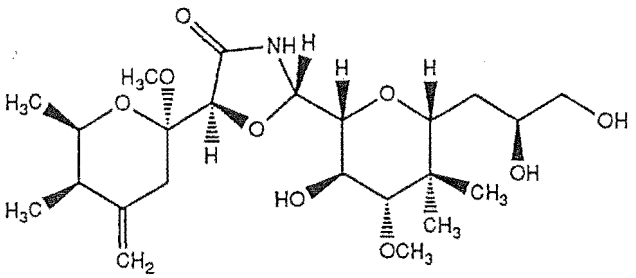

11*R* Mycalamide A *trans* oxazolidinone (**6.20**)

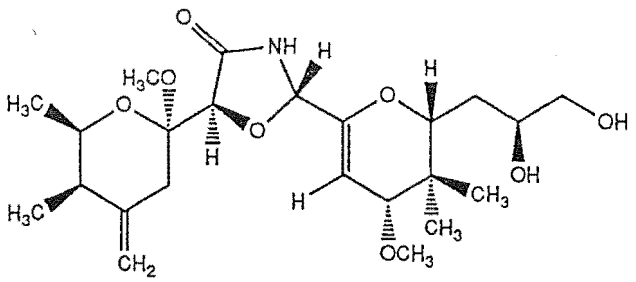

$\Delta^{11}$ Mycalamide A *trans* oxazolidinone (**6.21**)

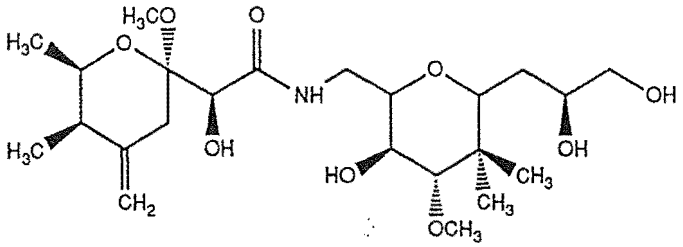

10,12-*O*-Dihydro mycalamide A (**6.22**)

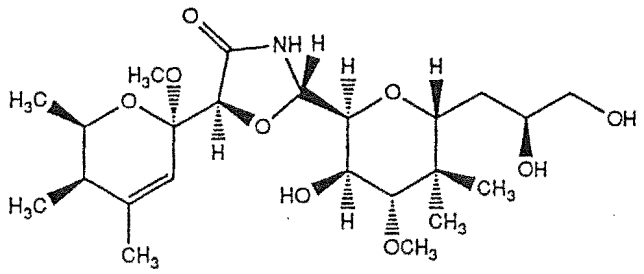

$\Delta^{4(5)}$ Mycalamide A *trans* oxazolidinone (**6.23**)

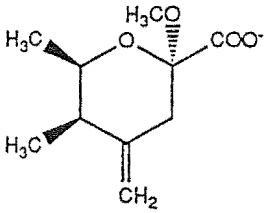

7-Carboxylate fragment (**6.25**)

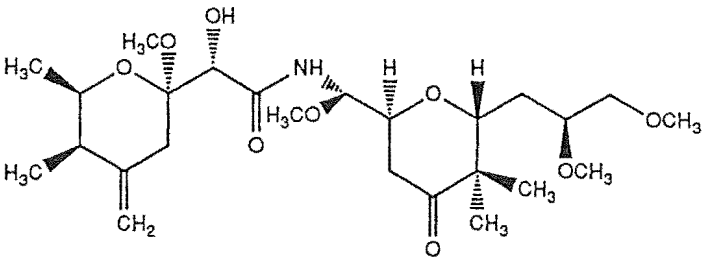

Pederone (**7.1**)

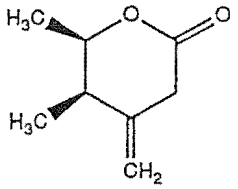

Isopederolactone (**7.2**)

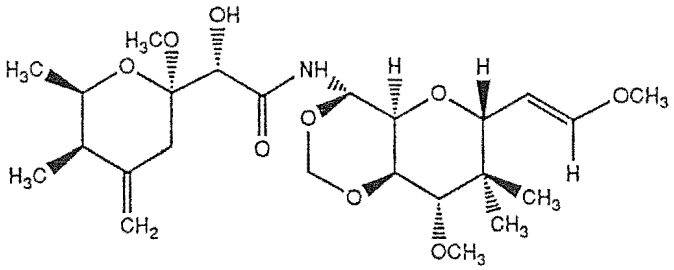

*E* $\Delta^{16}$ 18-Normycalamide B (**7.3**)

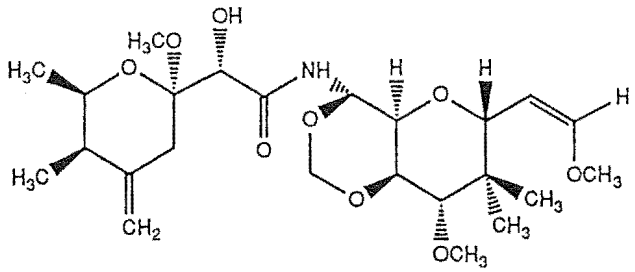

*Z* $\Delta^{16}$ 18-Normycalamide B (**7.4**)

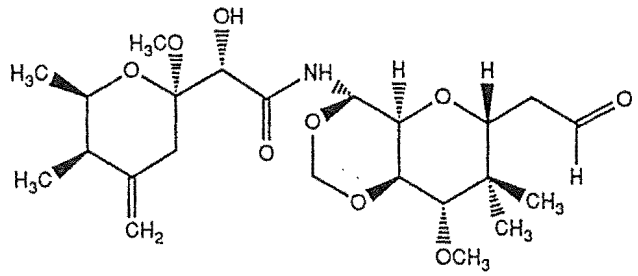

18-Normycalamide A 17-aldehyde (**7.5**)

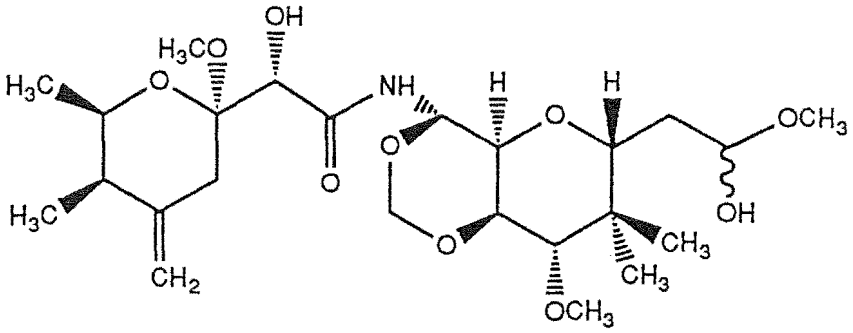

18-Normycalamide A 17-aldehyde hemiacetals (**7.6**)

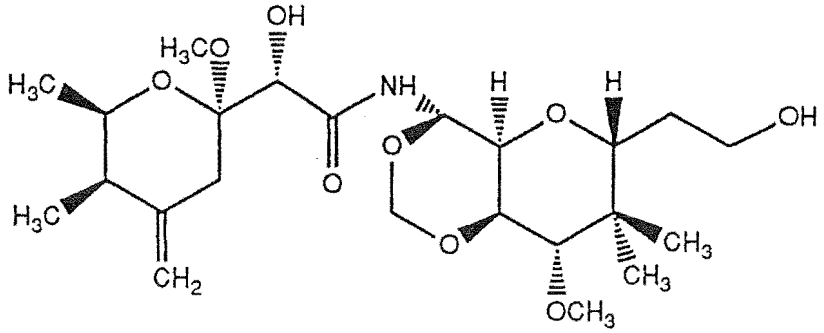

18-Normycalamide A (**7.7**)

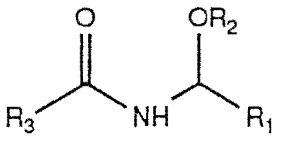

$R_1$-$R_3$=alkyl,aryl: (**8.1**)

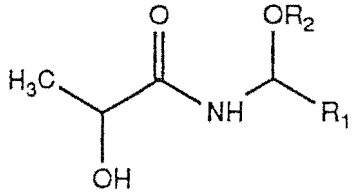

$R_1$=$R_2$=alkyl,aryl: (**8.2**)

$R_1$=Ph, $R_2$=$CH_3$: (**8.3**)

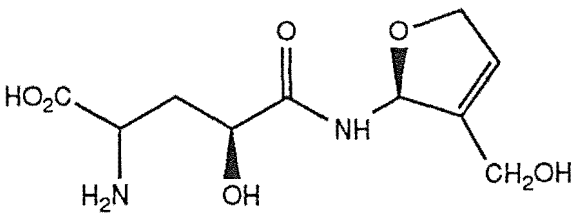

Oxypinnatinine (**8.4**)

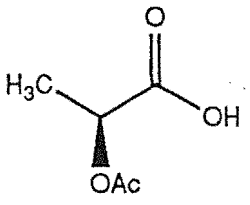

*S*-Lactic acid acetate (**8.5**)

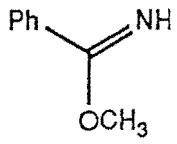

Imino ether (**8.6**)

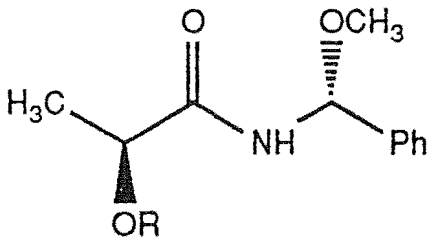


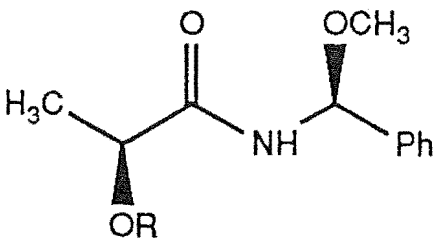


R=H: *SR*, *SS* Products (**8.7**, **8.8**)

R=Ac: *SR*, *SS* Product acetates (**8.9**, **8.10**)

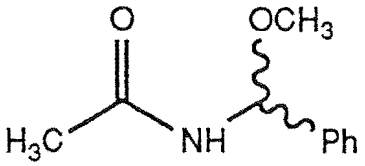


*N*-(α-Methoxybenzyl) acetamide (**8.11**)

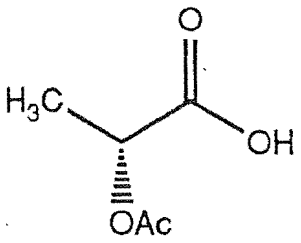


*R*-Lactic acid acetate (**8.12**)

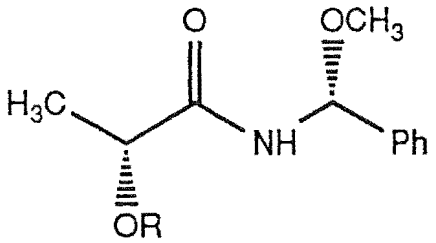


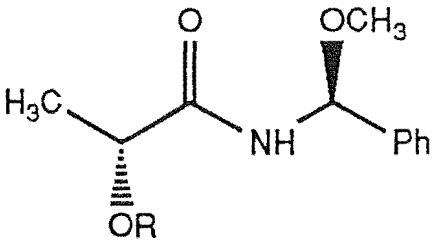


R=H: *RR*, *RS* Products (**8.13**, **8.14**)

R=Ac: *RR*, *RS* Product acetates (**8.15**, **8.16**)